Taphonomy and palaeoecology of benthic macroinvertebrates from the Agua de la Mula Member of the Agrio Formation, Neuquén Basin (Neuquén province, Argentina): sequence stratigraphic significance

349 pages, 11 plates, 27 figures, 12 tables

Dissertation zur Erlangung des
naturwissenschaftlichen Doktorgrades
der Bayerischen Julius-Maximilians-Universität Würzburg

vorgelegt von

FERNANDO ARCHUBY

aus

La Plata, Argentinien

Würzburg, Juli 2009

To my parents, César and Liliana.

Index

Taphonomy and palaeoecology of benthic macroinvertebrates from the Agua de la Mula Member of the Agrio Formation, Neuquén Basin (Neuquén province, Argentina): sequence stratigraphic significance

Fernando Archuby[1]

[1]Institut für Paläontologie der Universität Würzburg

Abstract.

The taphonomic and paleoecologic aspects of the Upper Hauterivian to Lower Barremian Agua de la Mula Member of the Agrio Formation (Neuquén Basin, Argentina) were studied in the frame of the sequence stratigraphic paradigm. The Agua de la Mula Member, a ca. 600 m thick succession of highly cyclic marine sediments was surveyed at two localities. Detailed bed-by-bed sedimentologic, stratigraphic, ichnologic, taphonomic and paleoecologic data collection allowed a precise paleoenvironmental, stratigraphic, taphonomic and synecologic interpretation, in a controlled sequence stratigraphic framework.

The main architectural stratigraphic component is the Starvation-Dilution Sequence, interpreted as a the effect of a sixth-order, Milankovitch precession-driven cycle. Dilution hemisequences are siliciclastic-dominated and show evidence of depth changes. Starvation hemisequences show a diverse variation of mixed carbonate-siliciclastic facies that is linked to sequence stratigraphy.

Ammonite-based biostratigraphy was revised and new knowledge proposed. The stratigraphic framework was improved by combining biostratigraphy, sequence stratigraphy and event stratigraphy. Nine main sequences were described, linked to other stratigraphic markers and correlated with other sequence stratigraphic charts.

Several orders of cyclicity were inferred. Third- and fourth-order sequences are the major sequences, not subordinated to higher hierarchies (lower order). Precession, obliquity, and short and long eccentricity cycles of the Milankovitch band are proposed. Among the different sequence stratigraphic models the transgression-regression model fits the majority of the sequences described in this work. The depositional-sequence model could be applied only to the first third-order sequence, in which the true sequence boundary is identifiable. Starvation-dilution sequences, however, are composed by to components that are not completely explained by those models. Starvation hemisequences developed in intermediate to deep settings record the

transgressive phase as well as the earLy regressive one without visible stratigraphic boundaries.

112 samples with 22,572 individuals were grouped into fifteen fossil associations and one assemblage that reflect the interaction of different factors: age, position in major, medium and starvation dilution sequences and, linked to sequence stratigraphy, depth, oxygen availability, rate of terrigenous input, water agitation, and substrate conditions. Temporary possible reduction in oxygen content is inferred based on all sources of available evidence. Organic buildups are briefly described and their development interpreted in terms of the sequence stratigraphic framework. Vertical patterns of replacement of fossil associations are described and related to sequence stratigraphy.

Five types of skeletal concentrations represent the diversity of coquinas decribed in this study. Type 1, 2, 4 and 5 correspond to starvation hemisequences deposited in progressively shallower settings, from basin to inner ramp. Type 3 is embedded into dilution hemisequences and inferred to be linked to shell bed type I of Kidwell (1985). Types 1 and 2 correspond to transgression, maximum flooding and early regression without distinction. Type 4A as well as Type 5 are interpreted as onlap shell beds (Kidwell 1991a) or early TST shell beds (Fürsich and Pandey 2003). Type 4B corresponds to the MFZ shell bed (Fürsich and Pandey 2003) or mid-cycle shell bed (Abbott 1997), while Type 4C to the downlap shell bed (Kidwell 1991a).

Time-averaging of shell beds was assessed with precision as the time involved in the deposition of the starvation hemisequences could be inferred. All shell beds comprise within-habitat assemblages forming within a few thousand years, with little environmental condensation.

The fossilization of the marine calcareous shells is modelled as a series of steps called windows: environmental, destructional, burial and diagenetic. The “diagenetic window” is the most relevant. Connected to this it is proposed that carbonate dissolution is the primary control on the development of shell beds, as has been proposed before (Fürsich 1982; Fürsich and Pandey 2003).

The interpretative power resulting from combining several lines of evidence, e.g., facies analysis, sequence stratigraphy, biostratigraphy, trace fossil analysis, paleoecology and taphonomy, and unravelling their multiple relationships, are the most relevant conclusions of this study.

1. Introduction

One of the most obvious features of the stratigraphic record is the uneven distribution of fossil material. Calcium carbonate shells constitute relevant components of sediments deposited in most marine siliciclastic environments, where they preserve usually in shell beds more frequently than isolated (Kidwell 1986a). Models for the formation of fossil concentrations stress in the relationship of rate of sedimentation and hard-part input (Kidwell 1986a; Kidwell and Bosence 1991; Tomasovych et al. 2006) or on the variables that drive the processes of concentration (Fürsich and Oschmann 1993). The role of diagenetic dissolution as a barrier to the preservation of fossils and hence as a primary factor for the formation of skeletal accumulations was also modelized (Fürsich 1982; Fürsich and Pandey 2003b). The onset of the sequence stratigraphy leaded to the development of models that relate the different types of skeletal concentrations to particular positions into sedimentary sequences (Abbott 1997; Abbott 1998; Fürsich et al. 1991; Fürsich and Pandey 2003; Kidwell 1991a; Kidwell 1991b). The sequence stratigraphic model predicts changes in sedimentation rates and turbulence from eustatic sea-level changes, and can also predict the positions in which sindepositional and diagenetic dissolution cannot cope with completely erase calcium carbonate shells from the fossil record (Fürsich and Pandey 2003).

The hypotheses of this work is that the factors leading the formation of skeletal concentrations, i.e. turbulence, rates of sediment and hard-part input and diagenetic dissolution, are subordinated to the development of sequences. Since that, if the sequence stratigraphic model can be applied, regardless of which type of sequence is used (sedimentary, genetic or transgressive-regressive), there is a great potential for the interpretation of the genesis of the skeletal accumulations. Conversely, when sediments other than bioclasts do not yield enough information for the sequence stratigraphic interpretation, shell beds constitute invaluable evidence for the assembly of the model. As was indicated by Fürsich (1995), shell concentrations have been primarily viewed as products, in which palaeoecological information is preserved as distorted relics.

This apparent disadvantage is more than compensated by the information on depositional environments and on the depositional history, which make shell concentrations ideal geological tools.

The general purpose of this dissertation is to characterize and interpret the genesis of the different types of skeletal concentrations left in the deposition of sedimentary sequences of the highly cyclic and fossiliferous marine sediments of the Agua de La Mula Member, Agrio Formation (Neuquén Basin, Argentina) of Late Hauterivian to Early Barremian age. The individual goals represent:

- The development of a detailed facies analysis in order to obtain a reliable sequence stratigraphic scheme.
- The taphonomic and paleoecologic characterization of several different types of skeletal concentrations, their location into sedimentary sequences and their interpretation from the view of the sequence stratigraphic model.
- The evaluation of the predictive power of the sequence stratigraphic model with respect to the position and features of the shell beds.
- To contrast available models for the genesis of skeletal concentrations.
- To assess the degree of time averaging of the fossil assemblages and their reliability as evidence of the life in the geological past.
- To contribute to the synecology of the Lower Cretaceous of South America.

Very little information exists concerning the sequence stratigraphic context of benthic faunas and skeletal concentrations, a remarkable exception being the work done by Abbott (Abbott 1997; Abbott 1998; Abbott and Carter 1997). Thus, the potential of the contribution of palaeoecology and taphonomy for the analysis of cycles is far from fully explored.

2. Geological setting

The Neuquén Basin is located on the eastern side of the Andes of Argentina and Chile, between a latitude of 32° and 40°S (Text-Fig. 1) (Howell et al. 2005). It extends for approximately 700 km from north to south and more than 400 km from west to east. The basin contains a Late Triassic to Cenozoic sedimentary succession comprising continental and marine siliciclastic, carbonate, and evaporitic deposits, which are at least 7 km thick and cover an area of over 160,000 km^2 (Vergani et al. 1995).

The basin has been characterised as a back-arc basin placed east of the Andean magmatic arc, which developed because of the subduction of the Nazca Plate below the South American Plate (Text-Fig. 2). It is limited by cratonic areas to the northeast (Sierra Pintada System) and southeast (North Patagonian Massif). Two main regions are recognized: westward, the strongly deformed Andean area, and south-eastward, the Neuquén Embayment (Spalletti et al. 2001b). While in the Neuquén Embayment the Mesozoic sedimentary record is in the subsurface, in the Andean area it crops out as a series of N-S-oriented fold and thrusts belts (Aconcagua, Malargüe, and Agrio) (Howell et al. 2005).

During the Jurassic and the Early Cretaceous the basin developed a steeply dipping, active subduction zone, and the associated evolution of a magmatic arc along the western margin led to back-arc subsidence within the Neuquén Basin (Howell et al. 2005). The tectonic setting during this time has been characterized as dominated by a steady and slow subsidence (Legarreta and Gulisano 1989; Legarreta et al. 1993; Legarreta and Uliana 1991; Mitchum and Uliana 1985; Spalletti et al. 2001a; Spalletti et al. 2001b). Vergani et al. (1995) showed that the infilling of the basin is punctuated by several unconformities that reflect intermittent subsidence, as well as several episodes of structural inversion. They point out that the Lower Cretaceous Mendoza-Rayoso succession is punctuated by several unconformities that define the stacking pattern of multiple transgressive-regressive sequences, reflecting intermittent subsidence and eustatic processes.

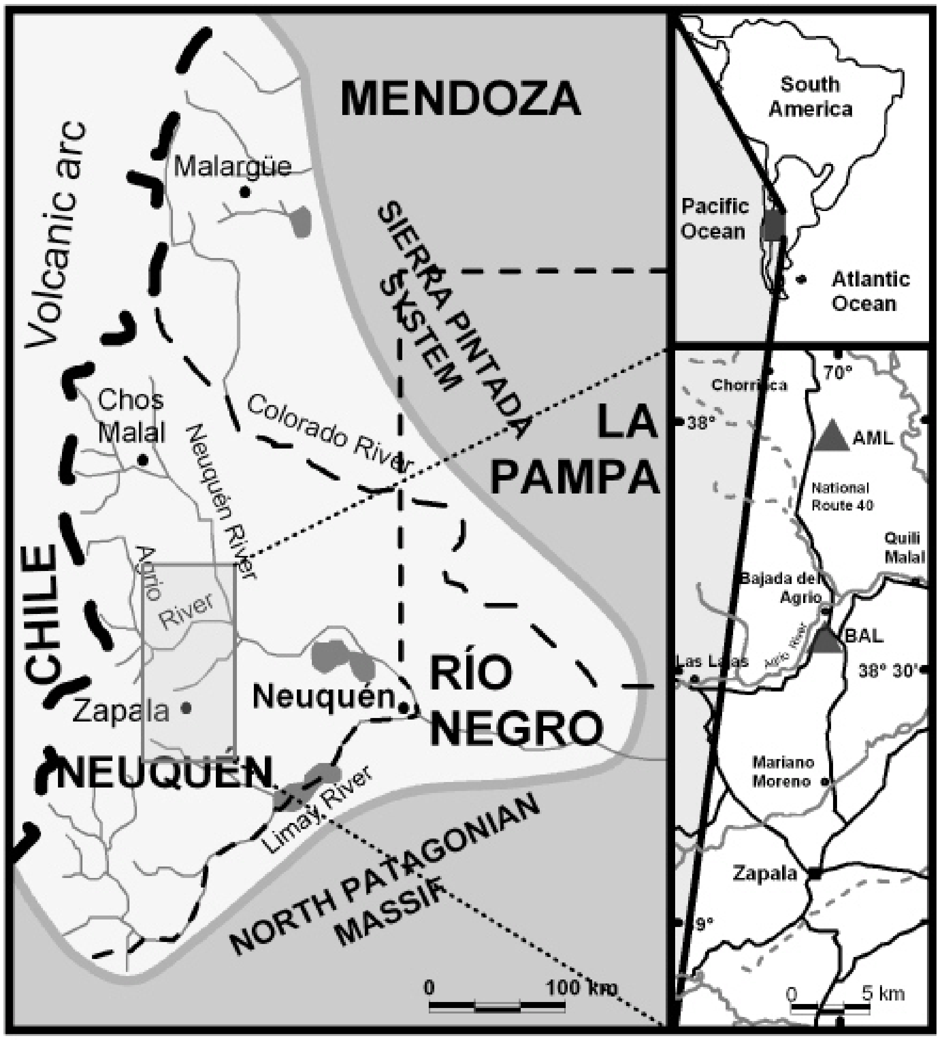

Text-Fig. 1: Geographic position of the Neuquén Basin

The Jurassic and Cretaceous fill of the Neuquén Basin, predominantly marine, consists of thick and widespread successions deposited during a protracted thermal subsidence and regional back-arc extension. They include a complex series of transgressive-regressive cycles of different magnitude, controlled by the combined effects of changes in subsidence rates, local uplift, and eustatic sea-level oscillations (Howell et al. 2005; Sagasti 2001). The main sources of sediments were the foreland (i.e. Sierra Pintada System from the east and North Patagonian Massif from the south (Legarreta and Gulisano 1989). Although the Andean magmatic arc was completely developed, by the time of deposition of the section studied here the Neuquén Basin was connected to the west with the Pacific Ocean through gaps in the volcanic arc (Spalletti et al. 2000). Uplift and inversion of the Andes during Cretaceous finally isolated the basin from the marine realm and, with further compression, it evolved from a back-arc into a foreland basin (Veiga et al. 2005).

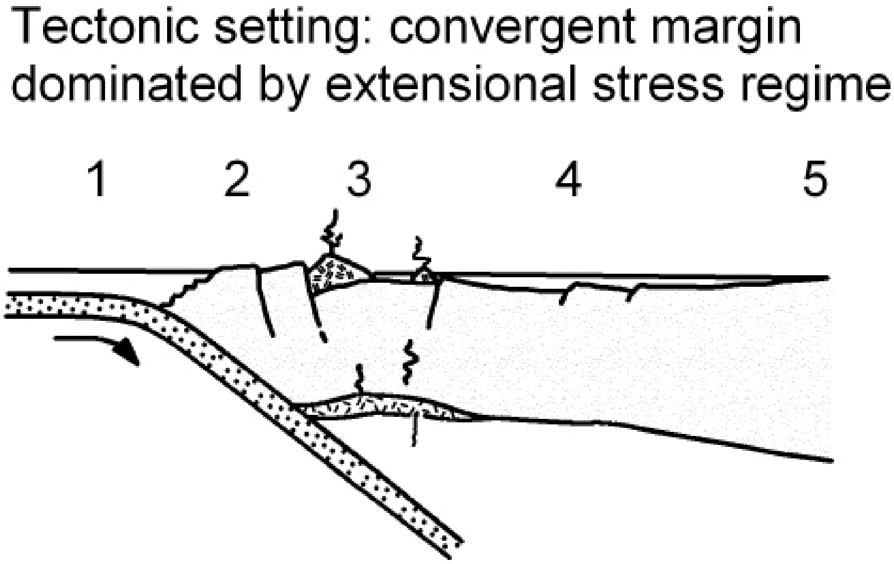

Text-Fig. 2: Schematic diagram across the Pacific margin of Gondwanaland. Not to scale. (Modified from Legarreta and Uliana 1991). 1: Minor accretionary wedge (or tectonic erosion). 2: Ridged forearc. 3: Magmatically active half-graben or graben depressions. 4: Backarc basin under extension and strike-slip conditions. 5: Continental interior (foreland).

Lithostratigraphy: the Agrio Formation

The Agrio Formation is widely exposed along the Fold and Thrust Agrio Belt in the Andean sector of the Neuquén Basin. It extends from the vicinity of La Mala Dormida in southern Mendoza southwards to Catán Lil, a few kilometers to the south of Cerro Marucho in southern Neuquén. To the west, the boundary of present-day outcrops coincides with the foothills of the Andes; (Text-Fig. 1). Towards the eastern and southern margins of the basin, the marine rocks of the Agrio Formation interfinger with the Centenario Formation. The formation overlies marine deposits of the Mulichinco Formation and is covered discordantly by siliciclastic, carbonate, and evaporitic rocks of the Huitrín Formation (Text-Fig. 3).

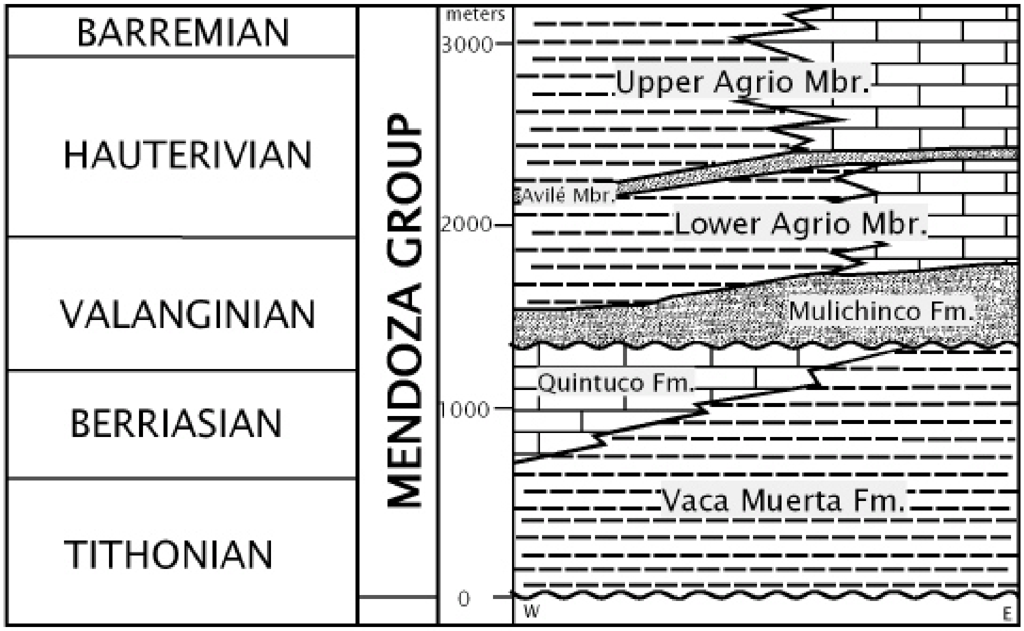

Text-Fig. 3: Schematic stratigraphic section of the Mendoza Group (modified from Aguirre Urreta and Rawson 1997).

The unit was first named by Weaver (1931) for a thick succession of marine shales overlying the Mulichinco Formation. Weaver divided the Agrio Formation into lower and upper divisions separated by a thin but laterally persistent unit, the Avilé Sandstone. The three lithostratigraphic elements are considered members. The Pilmatué (lower) Member (Leanza et al. 2001) is composed of up to 600 m of marine shales and mudstones associated with thin sandstone beds and carbonates (wackestones and packstones) (Aguirre Urreta and Rawson 1997). The middle unit, the Avilé Member, consists of up to 100 m thick sandstones with fine conglomerates and subordinated mudrocks interpreted as aeolian and arid fluvial deposits. It represents a major drop in sea level across the basin (Veiga et al. 2002). The Agua de la Mula (upper) Member (AMMb) is a marine succession, up to 1000 m thick, composed of shales, mudstones, sandstones and bioclastic carbonates (Spalletti et al. 2001b). Leanza (2003) placed the Chorreado Member, previously considered as a Hutrinian unit, in the Agrio Formation.

Biostratigraphy

The Agrio Formation contains an abundant ammonite fauna of Valanginian to Barremian age (Aguirre Urreta and Rawson 1997). Until the nineties of the last century, the whole succession was divided into five biozones (Gerth 1925; Leanza 1945; Leanza 1981, 2003; Riccardi 1988). Since that, four biozones based on ammonites were defined for the Agua de la Mula Member. They are, from base to top, the *Spitidiscus riccardii* zone of late Early Hauterivian age (Aguirre Urreta 1995; Aguirre Urreta et al. 1993; Leanza and Wiedmann 1992), the *Crioceratites schlagintweiti* and *Crioceratites diamantensis* zones in the Early and latest Hauterivian, respectively (Aguirre Urreta and Rawson 1993), and the *Paraspiticeras groeberi* zoneof Early Barremian age (Aguirre Urreta and Rawson 1993). This information and the equivalent Western Mediterranean zonation are compiled in Text-Fig. 4. Recently, Aguirre Urreta et al. (Aguirre Urreta et al. 2005) proposed that the *Paraspiticeras groeberi* biozone might have began in the youngest part of the Hauterivian.

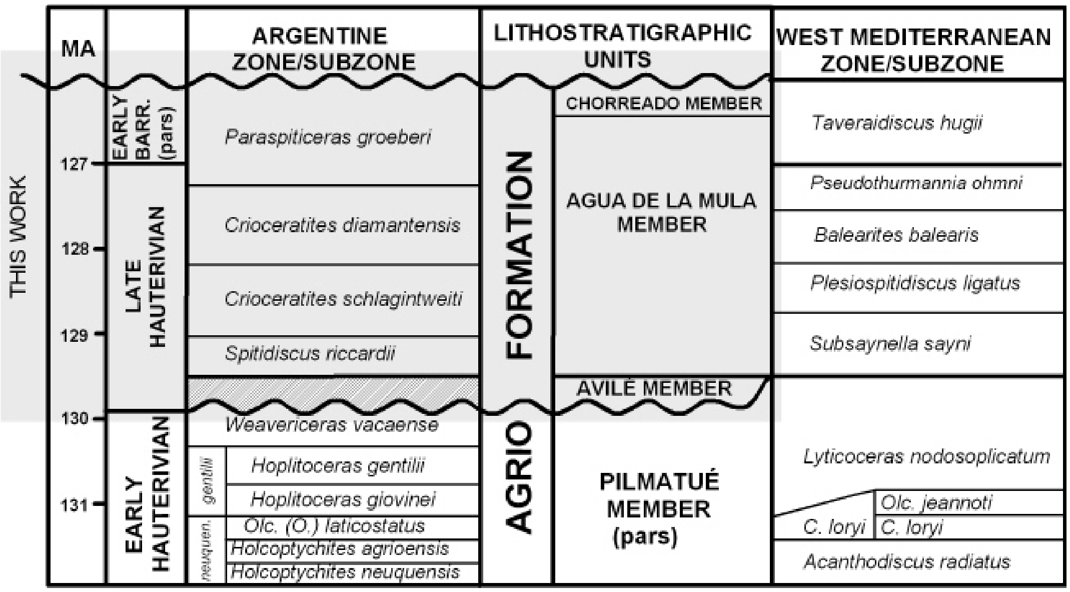

Text-Fig. 4: Previous knowledge on the ammonite biostratigraphy of the Hauterivian-Lower Barremian of the Neuquén Basin, and standard West Mediterranean zonation (modified after Aguirre Urreta and Rawson 1997 and Aguirre Urreta et al. 2005)

Sequence stratigraphy

Various authors carried out sequence stratigraphic studies in the Neuquén Basin. Legarreta and Gulisano (1989) applied sequence stratigraphic tools to study the upper Triassic to lower Tertiary sedimentary succession of the basin. Legarreta and Uliana (1991) developed a detailed study of the Jurassic and Cretaceous marine oscillations of the basin and tried to relate them with the 'global' sea-level chart of Haq et al. (1987). Legarreta et al. (1993) dealt with the Jurassic and Cretaceous sequences in the Mendoza province. Mitchum and Uliana (1985) studied carbonate depositional sequences of upper Jurassic and lower Cretaceous age. Spalletti et al. (2000) investigated the Tithonian-early Berriasian succession in the southern part of the Neuquén province. The Agua de La Mula Member of the Agrio Formation was investigated in the northern Neuquén Basin (Spalletti et al. 2001b), and near the town of Bajada del Agrio in the center of the same province (Spalletti et al. 2001a). Sagasti (2001) dealt with sedimentological and stratigraphic aspects of the Agrio Formation in the Mendoza province, where deep, basinal to outer ramp sediments predominate.

Legarreta and Gulisano (1989) proposed three supersequences named Lower, Middle, and Upper supersequence for the Jurassic-Cretaceous basin fill, which are more or less equivalent to the "Jurassic", Andean, and Riograndic cycles of Groeber (1946). The Middle Supersequence is equivalent to the lithostratigraphic unit Mendoza Group (Tithonian - Barremian). It was in turn divided into three mesosequences: Lower, Middle and Upper Mendoza mesosequences (Text-Fig. 5). These three mesosequences begin with continental and/or marginal marine sedimentary packages, deposited in the central part of the basin (Legarreta and Gulisano 1989). The Agua de la Mula and Avilé members of the Agrio Formation are interpreted as a second order sedimentary sequence (Upper Mendoza Mesosequence, Legarreta and Gulisano 1989). The Avilé Sandstone appears in most of the Neuquén Basin (Spalletti et al. 2001b). According to Legarreta and Gulisano (1989), Legarreta and Uliana (1991) and Legarreta et al. (1993), it represents deposition during a major drop in relative sea level. This unit is interpreted as a lowstand systems tract (LST) (Legarreta and Gulisano 1989; Legarreta and Uliana 1991; Legarreta et al. 1993; Veiga et al. 2002; Veiga and Vergani 1993). The overlying Agua de la Mula Member of the Agrio Formation shows the re-establishment of marine conditions, which persisted until the end of the Upper Mendoza Mesosequence.

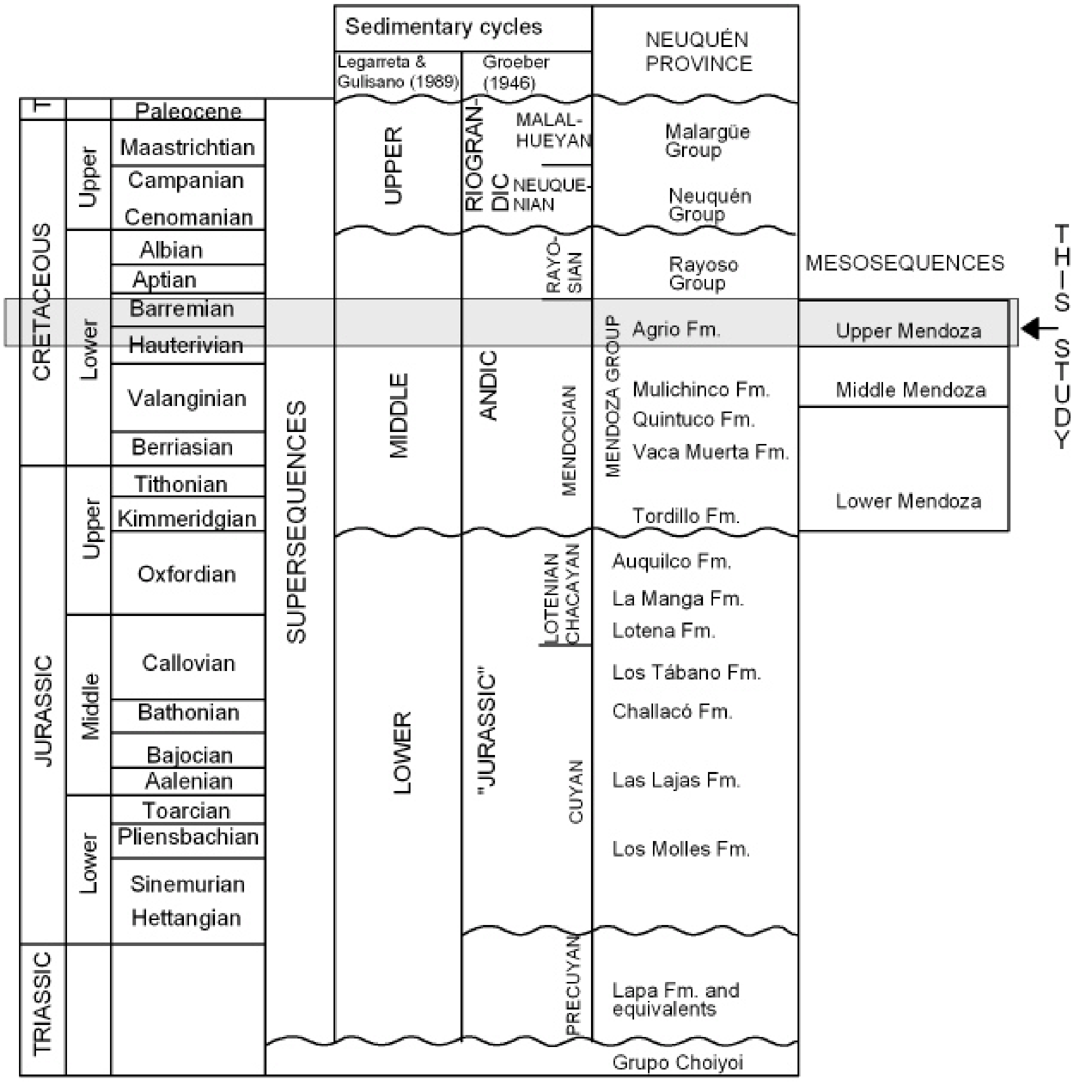

Text-Fig. 5. Stratigraphic chart of the Neuquén Basin. Modified after Groeber (1946), Legarreta and Gulisano (1989), and Sagasti (2001).

Legarreta and Uliana (1991) report "…at least two short episodes of shallowing that caused the exposure of the shelf and abrupt basinward shift of the clastic depositional fringe" punctuated the widespread shelfal accumulation of the Agua de la Mula Member. This statement points to the presence of (at least) three (third-order) sedimentary sequences for the section under study. Spalletti et al. (2001b) also found, in a distal (basinal to outer ramp) setting in the northern Neuquén Basin, three main (third-order) sequences. Legarreta et al. (1993) proposed the presence of at least eight third-order sequences for the Agua de la Mula Member of the Agrio Formation in the southern part of Mendoza province. Sagasti (2000) found in deep basinal environments of the southern Mendoza province five groups of bedding couplets, interpreted as the distal expression of five third-order sequences. Subsequently, the same author considered the five sequences to correspond to fourth-order sea-level changes, based on the estimated duration of each (Sagasti 2001).

Spalletti et al. (2001a; 2001b) recognised the presence of high-order sequences (or high-frequency cycles) in the Agua de la Mula Member of the Agrio Formation, in the areas of Loma La Torre (northern part of Neuquén province) and Bajada del Agrio (central part of the province). For these authors, the high-frequency cycles are particularly well developed in the highstand systems tracts (HST) of third-order sequences. Sagasti (2001) reported similar results. Sagasti (2000) described the development of bedding couplets for the unit in the Mendoza province. Orbital forcing Milankovitch cyclicity was claimed to explain the cycle origin for the Agua de la Mula Member (Sagasti 2000; Sagasti 2001; Spalletti et al. 1990; Spalletti et al. 2001a; Spalletti et al. 2001b).

3. Materials and methods

Field work

During spring and autumn of 2002, 2003, and 2004 the Agua de la Mula Member of the Agrio Formation was studied in detail at two localities (Text-Fig. 1). The first section, Bajada del Agrio (BAL) (S 38° 03'; W 70° 02'), is situated 64 km north of the town Zapala on National Road 40. The other one, Agua de la Mula (AML) (S 38° 26'; W 70° 04'), is located 104 km north of Zapala and around 3 km to the east of the national road

Outcrops in Bajada del Agrio are almost complete and continuous for several hundreds of meters. The ammonite fauna is abundant and present in most of the profile, which allows a good biostratigraphic control. Outcrops in Agua de la Mula are generally poorer. Apart from some portions of the section that are not exposed, the upper 100-150 m are faulted and were not surveyed.

Field work involved detailed measuring of sections including: type of lithology, sedimentary structures, bioturbation including trace fossils, and observations of taphonomic features of shell concentrations. The latter included proportion of articulated shells, preservation in life position, degree of fragmentation, degree of abrasion, bioerosion, and encrustation, and orientation of shells in plan-view and in cross-section. In addition, all sedimentological attributes were recorded at a 1:100 scale.

Faunal content

Benthic macroinvertebrates were studied bed by bed. Wherever possible, the benthic fauna was counted to allow statistical treatment. Taxonomic identifications were made up to the generic and specific level in almost all cases. There are several gastropod and bivalve taxa as yet undescribed (see Appendix A and chapter 8 for more detailed information). Cephalopods (ammonites and nautiloids) are numerically important in several shell beds. They were not included in the quantitative analysis because of their nektonic nature. Serpulids are numerically relevant in some assemblages. Bryozoans and agglutinating-encrusting foraminifers are common in certain beds.

All skeletal concentrations and faunal remains in fossil poor beds were described. Shell packing was evaluated in the field and from samples. Shell packing was classified according to Kidwell’s (Kidwell and Holland 1991) classification for coarse bioclastic fabrics. A further refinement was used: the category “densely packed” was divided into skeletal or bioclast-supported, and matrix-supported. Matrixes of the matrix-supported category include any kind of non-skeletal material, like mud or sand. “Densely-packed, matrix-supported” fabric is equivalent to the Kidwell’s “dense/loose” borderline fabric.

In some specific cases, different kinds of taphonomic variables were quantitatively evaluated. Features counted were: (a) life position/articulation, (b) fragmentation, (c) encrustation, (d) borings and (e) corrasion. Borings and encrustation were evaluated with a semi-quantitative scale: absence, low (less of 25% of the shell area), high (around 50%) and very high (above 75 %). Corrasion was measured as low, medium and high.

Different degrees of lithification imposed problems to the evenness of recording the taxonomic composition and taphonomic signatures of the fauna. For instance, well-lithified early transgressive shoreface deposits did not allow unbiased taxonomic counts as many thin-shelled bivalves can hardly be identified in vertical sections of the beds. In turn, boundaries between different parts of starvation deposits (e.g. lower and middle) are usually not sharp and thus counts may not always belong to a particular horizon with certainty. Biased counts were discarded. For counts that were not clearly biased sedimentological and stratigraphic characteristics of the shell beds were registered with the aim of re-evaluating any bias in the laboratory.

Encrusting foraminifers, bryozoans, and serpulids were counted per shell encrusted (one shell encrusted = 1 count), regardless the amount of surface covered. In turn, each foraminifer buildup was assigned one count. Reworked fragments of scleractinian coral colonies were counted as fragments of colonies (each fragment = one count). Small scleractinian colonies found attached to concretions or shells were counted individually. Serpulids were separated in morphological groups, related to the main anatomical features of the tubes (diameter, ornamentation, length, and track). Tubes of *Parsimonia antiquata* were counted separately because these thick-tubed polychates could be easily recognized. Colonies of *Sarcinella occidentalis* were also easy to recognize and were counted per branch. Each bivalve valve was counted individually. Left and right valves were counted separately when important morphological differences were found between them (e.g. oysters). In general, only moderately complete shells were counted in order to avoid over-counting individuals.

Trace fossils

Trace fossils were described and photographed in the field as well as collected and studied in the laboratory. The name *Spongeliomorpha suevica* was preferred to *Thalassinoides suevicus*, following Fürsich (1973), despite the ongoing debate about this group of Y-shaped trace fossils (Schlirf 2000). Based on Schlirf (2000), the name *Bolonia lata* was preferred for horizontal, non-branching, straight, tapering, bilobed traces, with median furrow and a heart-shaped cross-section, composed by biserial pads, and preserved as epireliefs (Schlirf 2003b; Schlirf 2005). This description fits very well the specimens found in this work (Pl. 1, Fig. 5). Spalletti et al. (2001a) named similar trace fossils observed at a locality close to the BAL section *Scolicia*. Apertures of subvertical, lined tubes of around 10 mm in diameter were named *Skolithos*. Their fill is similar to the host rock, i.e. bioturbated fine-grained sandstone. The walls are lined with fine silt-sized mud. The vertical expression of these circular cross-sections was partially observed as en exception (Pl. 2, Fig. 2). It could not be properly described and the actual morphology of the burrow is not known. Openings of vertical burrows, 0.5 cm in diameter, without lining, and filled with a different (finer) sediment were found in fine-grained cross-laminated sandstones within marginal marine (?) facies at the top of the Avilé Member. Again, the vertical expression of the burrows was not seen. This trace has been referred to *Skolithos* with much doubt. Bedding planes were rarely available for study because the dip of the strata was less than 15° at AML and 23° at BAL, and also due to the usual poor lithification of the rocks that comprise the majority of the sections. This fact imposes a problem for the recognition of trace fossils.

Data analysis

Taxonomic counts of the benthic macrofauna were treated statistically by applying cluster analysis to the identified samples. The database was previously standardised to percentages to avoid the biasing effect of different sample sizes and then transformed with the square root function to reduce the effect of dominant species. The resemblance matrix was calculated with the Bray-Curtis similarity coefficient. Benthic associations were recognized, described, and interpreted based on their diversity, trophic composition, and life habit composition. Statistical comparisons are described afterwards.

Abbreviations used in the text

AMMb: Agua de la Mula Member of the Agrio Formation
AF: Agrio Formation
BAL: Bajada del Agrio locality
AML: Agua de la Mula locality

S/D-S: Starvation/Dilution Sequence
S-HS: Starvation Hemisequence
D-HS: Dilution Hemisequence
SB: Sequence Boundary
FSST: Falling Stage Systems Tract
LST: Lowstand Systems Tract
TS: Transgressive Surface
TST: Transgressive Systems Tract
RST: Regressive Systems Tract
MFZ: Maximum Flooding Zone
HST: Highstand Systems Tract
DSAM: Depositional Sequence Agua de La Mula
SBAM: Sequence Boundary Agua de La Mula

4. The sections

The Agua de la Mula Member is sandwiched between two continental lithostratigraphic units that represent important regressive events during which the basin was above sea level: the Avilé Member below and the Huitrín Formation above (Text-Fig. 3; Pl. 3, Fig. 5). The unit is well defined in the study area. It overlies the Avilé Member in a concordant but sharp and abrupt way. At the locality of Agua de la Mula, sandy calcareous argillaceous shales overlie the medium- to coarse-grained sandstones of the Avilé Member. At Bajada del Agrio, the marly shales of the upper member cover fine-grained sandstones and siltstones with ripple cross-lamination and desiccation cracks, deposited on top of the fluvial sandstones of the Avilé Member. At the same locality, the top of the unit is well marked by a surface of erosion underlain by a marine oolitic and bioclastic grainstone bed, and is overlain by fluvial coarse-grained sandstones (Troncoso Member) of the Huitrín Formation, covered in turn by a gypsum layer of the same unit (Pl. 3, Fig. 6). As mentioned above, the upper 150 meters are poorly exposed at Agua de la Mula locality and therefore were not included in the thesis.

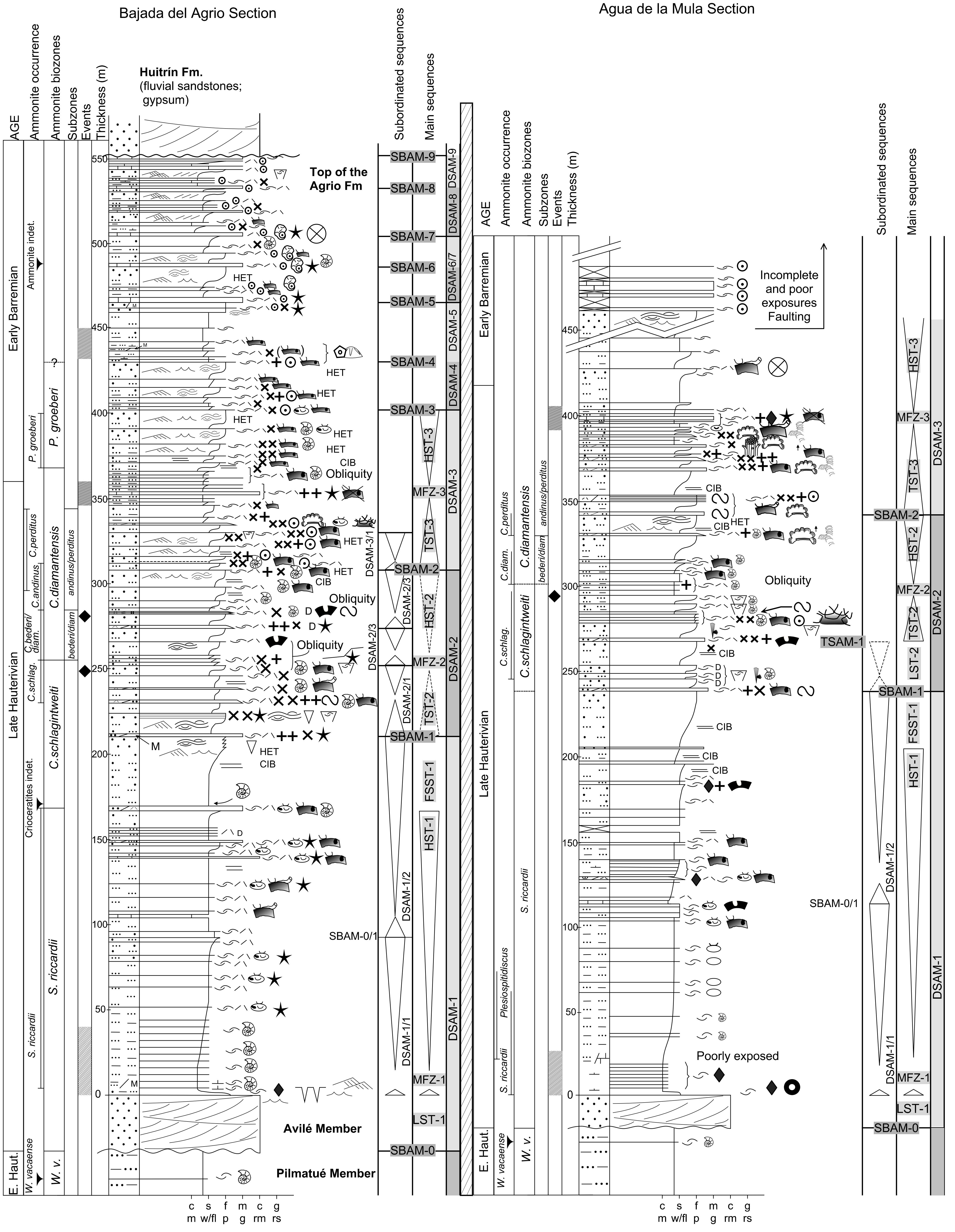

Text-Fig. 6. Legend. For other symbols see legend in appendix figure 3.

▽ Skeletal concentration on top of dilution hemisequence

▽ Sixth order sequence without starvation hemisequence

★ Amalgamation of sequences

∾ Stacking of incomplete cycles (truncation)

Encrustation and bioerosion

W. v.: *Weavericeras vacaense*

▨ Anoxic event

◆ Occurrence of uncoiled ammonites

Plate 1. Legend. For other symbols see legend in appendix figure 3.

▽ Skeletal concentration on top of dilution hemisequence
▽ Sixth order sequence without starvation hemisequence
★ Amalgamation of sequences
∾ Stacking of incomplete cycles (truncation)
Encrustation and bioerosion
W. v.: *Weavericeras vacaense*

▨ Anoxic event
◆ Occurrence of uncoiled ammonites

Bajada del Agrio

The Agua de la Mula Member at the Bajada del Agrio (BAL) section is completely exposed (Text-Fig. 6). The Avilé Member is an almost 10 m thick medium- to coarse-grained sandstone unit with trough cross-stratification. Its erosional base represents a second-order sequence boundary (Pl. 3, Fig. 5). Ten meters below the base of the Avilé Sandstone, intercalated into siliciclastic mudstones of the Pilmatué Member, a thin shell-bed appears, containing the ammonite *Weavericeras vacaense* of Early Hauterivian age. On top of the Avilé Member at BAL, there is a 1 m thick transitional set of beds with fine- to medium-grained sandstones with desiccation cracks and vertical burrows. These beds are sharply overlain by offshore marls and marly clays. The section can be subdivided into four segments. The first 165 m are dominated by dark, fine-grained siliciclastic sediments (clay to silt) with thin intercalated shell-beds, showing a long-term subtle progradational pattern. Abundant ammonites indicate an earliest Late Hauterivian age for these beds. Between 165 and 210 m, there is a strongly progradational sedimentary package that ends with an important erosional surface. The third segment comprises a thick sedimentary pile characterised by numerous short sixth-order sequences (Pl. 6, Fig. 8), each of them composed of a basal starved shell-rich hemisequence usually overlying a surface of erosion, and a siliciclastic-dominated and markedly progradational upper part. Bundles of these short sequences compose sequences of different hierarchies. Facies typically fluctuate in the shortest sequences from offshore to shoreface settings. Starved portions of these sequences have thick and complex shell beds with abundant and well preserved fossil invertebrates. Crioceratitid ammonites of Late Hauterivian age are abundant in these shell beds. On top of this third segment, *Paraspiticeras groeberi* of latest Hauterivian-Early Barremian age was recorded. Siliciclastic input was low to moderate during the deposition of this part of the section. In the fourth segment, although short sequences are present, sedimentary trends are characterised by higher hierarchy sequences of fifth or fourth order. Only on top of these sequences, progradational patterns are present and siliciclastic facies reach shallow settings. Transgressive beds consist of pure limestones, and coral patch reefs are present. Siliciclastic input was here at its lowest level.

Agua de la Mula

The Agua de la Mula locality (AML) is situated 40 km north of BAL, approximately 5 km east of the National Route 40. The contacts between the Pilmatué, Avilé, and Agua de la Mula members are very well exposed, as are the first 20 m of the latter (Text-Fig. 6 Pl. 5). From there onwards, outcrops show some gaps or poorly exposed segments for approximately 150 m. From 170 to 450 m the section is fairly well exposed. However, the inclination of the beds is low (*ca*. 13º) which makes it difficult to observe some sedimentological features. Above 450 m, the section at AML is strongly faulted and was not measured. The section at AML can be subdivided in a similar way as in the case of the BAL section. The lowermost part bears early Late Hauterivian ammonites. Fine-grained siliciclastic rocks with thin intercalations of shell beds dominate. The second part is well exposed and less developed with respect to BAL. The features of the third segment are similar to those described for BAL. The fourth segment of BAL is very poorly exposed at AML, although thick oolitic and bioclastic grainstone beds and coral reefs indicate similar depositional environments.

Two features distinguish the sections. First, the section at Agua de la Mula was deposited in a more basinward position compared to Bajada del Agrio. Facies at AML represent deeper sedimentary environments compared with BAL at equivalent positions. Thick successions of nearshore sandstones at the top of major regressive cycles, observed in AML, are lacking in BAL, probably because of erosion or non-deposition due to sediment bypassing. These features coincide with the assumed palaeogeographic position of the sections in the basin. The second aspect that differentiates AML from BAL is the higher amount of terrigenous sediment in most of the section, indicating a higher extrabasinal input and/or higher availability of accommodation space.

Results

5. *Facies analysis*

The deposition of the Agua de la Mula Member took place in a back-arc basin under steady thermal subsidence. The depositional system proposed for the unit is a gently sloping open marine ramp (Legarreta et al. 1993; Legarreta and Uliana 1991). Subsidence remained approximately constant and was not a relevant factor controlling the development of the sedimentary succession (Spalletti et al. 2000). The basin was connected with the Pacific Ocean to the west, even when the magmatic arc was completely developed (Spalletti et al. 2001b). On a ramp, shallow water sediments pass gradually offshore into deeper water, and there is no major break in slope (Tucker 1985). Ramp facies reflect the protracted offshore energy gradients, which are a consequence of gradual changes in water-depth (Burchette and Wright 1992).

The studied sections consist entirely of marine siliciclastic, carbonate, and mixed siliciclastic-carbonate sediments and rocks, ranging from clays and claystones to fine-grained sandstones among the siliciclastic ones, mudstones to grainstones and rudstones among the limestones, and a wide spectrum of mixtures of these two rock types. Siliciclastic rocks dominate the unit and, among them, the fine-grained fraction is more common. Pure carbonate rocks are the least represented type. Fine-grained limestones are found in condensed beds near the base of the unit, and otherwise intercalated between fine-grained siliciclastic sediments. Coarse-grained pure limestones are found exclusively towards the top of the unit, where the shallowest facies are present.

Mixed siliciclastic and carbonate rocks are relatively common and rank second in frequency. Mount (1985) defined this kind of rocks as characterized by the presence of at least 10% of any of the two kinds of components, siliciclastics or carbonate. The classification proposed by Mount considers two end members for the siliciclastic particles, clay (mud in this study) and sand, and two for the carbonate particles, micrite and allochems. In this scheme, micrite includes particles smaller than 20μm, while allochems comprise ooids, intraclasts, bioclasts, shells and peloids, all detrital carbonate particles larger than 20μm.

As has already been pointed out in the literature, a distinctive feature of the Agua de la Mula Member is its cyclicity (Spalletti et al. 2001b). Apart from the third-order sequences described in sequence stratigraphic studies (Legarreta and Gulisano 1989; Legarreta et al. 1993; Legarreta and Uliana 1991), sedimentary sequences of at least three other orders were described for the same unit in different locations (Sagasti 2000; Sagasti 2001; Spalletti, Del Valle, and Kielbowicz 1990; Spalletti et al. 2001a). This is the main characteristic of the unit at outcrop scale and represents the structure, in which the facies and their successions are organized.

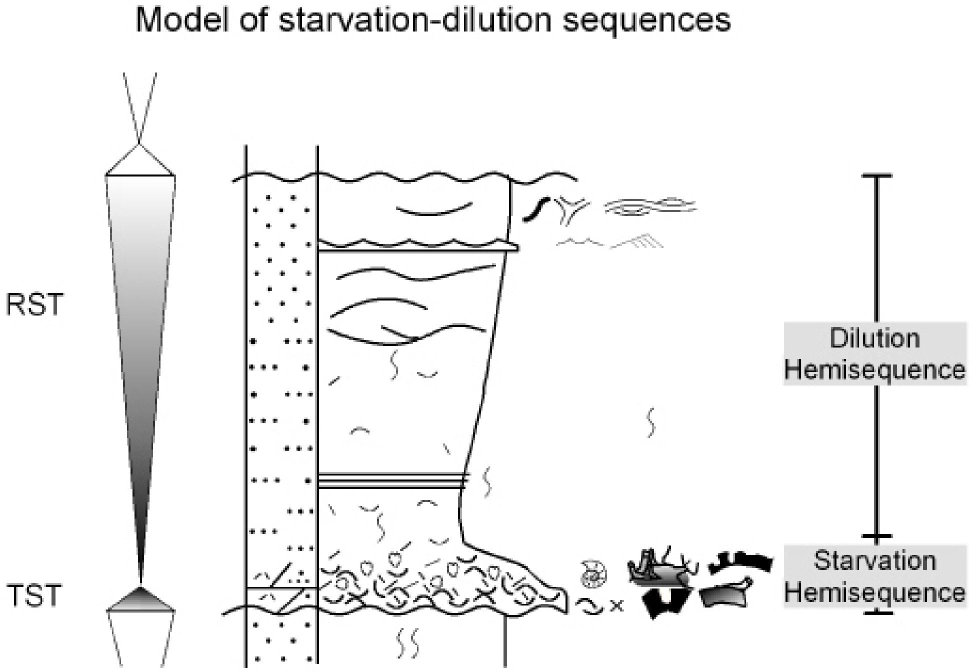

Text-Fig. 7: Model of starvation-dilution sequences. TST: Transgressive Systems Tract; RST: Regressive Systems Tract. For other symbols see Appendix-Fig. 3.

In the field, the characteristic feature that clearly stands out is the presence of relatively thin, tabular beds, extending throughout the outcrops, with evidence of sedimentary condensation (Pl. 6, Fig. 8). They are dominated by carbonate components and contain mollusc-rich skeletal concentrations. A deepening upward trend is often evident from base to top within these layers. These beds alternate with thicker siliciclastic packages usually showing coarsening- and shallowing-upward facies successions, and lack fossil remains or, if present, they are scattered and preserved as moulds. These two kinds of deposits alternate in couplets that are equivalent to parasequences. In this work the lower package is identified as **starvation hemi-sequence** (S-HS; with skeletal concentrations, autigenic glauconite, rich in iron, and with evidence of a long residence time of the skeletal remains on the sea floor), which is essentially though not completely transgressive in nature. The upper package is termed **dilution hemi-sequence** (D-HS; with no or rare shelly material partially or completely dissolved), and is regressive. Likewise, I propose the term **starvation/dilution sequence** (S/D-S) for the couplet of starvation and dilution hemi-sequences. In Text-Fig. 7 a model for starvation/dilution sequences is presented.

The entire member shows the alternation of starvation and dilution hemi-sequences. However, the features of these two types of hemi-sequences change throughout the sections, following long-term changes in depth and rate of terrigenous input. The character of dilution hemi-sequences changes according to bathymetry and sedimentation rate, giving rise to different patterns of aggradation and progradation. In turn, the starvation hemi-sequences show a great diversity with respect to composition, ranging from siliciclastic to fully carbonate, passing through a wide spectrum of mixed types. In well developed starvation hemi-sequences, deposited at intermediate depth, it is possible to distinguish three parts termed from base to top lower, middle and upper parts of starvation hemi-sequences. Similarly, skeletal concentrations corresponding to the three levels are named as lower starvation shell-bed, mid-starvation shell-bed and upper-starvation shell bed. As will be seen later, mid-starvation shell-beds correspond stratigraphically to the mid-cycle condensed shell-beds of Abbott (1997). However, in the usual case the starvation hemi-sequences are thin and environmentally condensed, which makes them less accurate bathymetric indicators than the dilution hemi-sequences. The stratigraphic composition of starvation/dilution sequences is discussed at the end of chapter 6 (Stratigraphy). The stratigraphy of starvation hemisequences is analysed in chapter 10 (Discussion).

Methods

A refined facies analysis was performed in order to get reliable bathymetric indicators, a requisite to develop a trustable sequence stratigraphic scheme (Flügel 2004). Deepening and shallowing trends used to build the sequence stratigraphic scheme are mainly based on siliciclastic facies corresponding to dilution hemi-sequences. As most of this study relates to the fossil content of the starvation hemi-sequences, using data coming from other sources for the bathymetric interpretation prevents circular reasoning. Apart from bathymetry, facies analysis is also used to evaluate the rate of sedimentation. Finally, other useful environmental variables related to depth and rate of sedimentation, such as firmness of the substrate, availability of oxygen, and nutrients, were also investigated.

Siliciclastic rocks were described in the field, with the exception of some particular beds, which were sampled and studied in the lab. Almost all mixed and carbonate rocks were sampled, and from them more than 200 polished slabs and more than 70 thin-sections were made. Each sample was studied under a binocular microscope. For thin-sections and polished slabs the relative importance of sand and allochems (discriminated in different components when possible) were semi-quantitatively estimated using charts (Flügel 1982). Mud proportion was calculated by subtracting sand and allochems from the total. The nature of the mixed muds, i.e., siliciclastic- or carbonate-dominated, was established with less accuracy, as lime mud cannot be easily discriminated from siliciclastic mud in polished slabs or thin-sections. In most cases, the presence of coarse silt particles was detected. In the case of finer-grained matrices, the proportion of carbonate mud was evaluated by applying a drop of diluted (10%) hydrochloric acid (HCl). The reaction was classified in low, medium and high and these three levels were considered to reflect the proportion of lime mud in the matrix.

For the compositional analysis, fossils were included to estimate the proportion of carbonate material. The size of the taxa contributing to skeletal concentrations ranges from the less than 5 mm large *Disparilia elongata* and *Corbulomima bodenbenderi* to the almost 20 cm long *Cucullaea gabrielis* and *Steimannella vacaensis*. In this way, it does not seem practical to place a boundary between bioclasts and shells at 2 mm as has been proposed by Kidwell and Holland (1991). If applied, this boundary would imply that a weakly reworked shell of a small bivalve broken into two halves, whose taxonomic origin can still be reconstructed, is a bioclast, while thick and resistant fragments of large bivalves are counted as shells, even after having suffered extensive transport, breakage, and erosion.

Shell packing was classified according to Kidwell and Holland's (Kidwell and Holland 1991) classification for coarse bioclastic fabrics. A further refinement was used: the category "densely packed" was divided into skeletal or bioclast-supported, and matrix-supported. Matrixes of the matrix-supported category include any kind of non-skeletal material, like mud or sand. "Densely-packed, matrix-supported" fabric is equivalent to the Kidwell and Holland's "dense/loose" borderline fabric.

Mixed rocks were classified according to Mounts's classification (Mount 1985), that involves a binary process with a series of yes/no questions about the composition and texture of the sample. Firstly, the sample has to be identified as mixed in composition. This means that each of the antithetic components has to represent more than 10% of the volume. Then it has to be decided whether the rock is dominated by carbonate or siliciclastic components. In any of the two cases, the end member that dominates (micrite vs. allochem or mud vs. sand) gives the second and main part of the rock name. Afterwards, the dominating end-member of the antithetic component has to be identified, which gives the first name of the rock. Eight hypothetical categories result, four of them dominated by carbonate: sandy allochem limestone, muddy allochem limestone, sandy micrite, and muddy micrite; and the other four dominated by siliciclastic grains: allochemic sandstone, micritic sandstone, allochemic mudrock and micritic mudrock. The term "mudrock" was used to refer to siliciclastic mudstones. "Mudstone" alone refers to limestones dominated by micrite and with less than 10% carbonate grains (Dunham 1962).

In the course of the work, this classification scheme was refined. For instance, silt/silty instead of mud/muddy was used when the fine siliciclastic component was clearly dominated by silt. In addition, the main kind of carbonate particles among the allochems was added to the name (e.g. silty bioclastic allochemic limestone replaced muddy allochemic limestone). The term “marl” was used instead of the corresponding terminology for mixed rocks (muddy micrite or micritic mudrock).

A problem arose in the facies analysis because differences between the various mixed and carbonate facies are usually minor, and there is often a gradation from one to the other. For instance, “micritic mudrock” facies are common at the base of the BAL section, and are replaced by marl in the same stratigraphic position in the more distal AML section. A relatively minor increase in shell density turns a muddy allochemic limestone (MB1) with a densely packed matrix-supported skeletal concentration into a muddy rudstone (LRm). A minor increase in shell density turns a bioturbated fine-grained sandstone into the mixed rock “allochemic sandstone”. The categories created from lithological descriptions may give rise to boundaries between facies that result in classifying them in different facies association, although they may not differ much in terms of their genesis. The use of different schemes for facies classification in the same analysis, i.e. textural and compositional, should be avoided whenever possible.

Content of glauconite and iron was assessed with a simple semi-quantitative scale: absent, low and high. Highest levels of glauconite rarely reached more than 5 % in thin-sections/polished slabs. The “low” category implies a few grains per field with x12 magnification. High levels of iron are present in the matrix of sandy transgressive beds in the vicinity of major sequence boundaries. Low levels of iron consist of replacements of shells, ooids and other carbonate grains, usually in low proportions. Both, iron and glauconite are evidence of long periods of terrigenous starvation (Fürsich and Pandey 2003; Odin and Matter 1981).

For the environmental interpretation of the facies, different strategies were followed. Siliciclastic facies interpretation relies on grain size and physical and biogenic sedimentary structures. Abundant literature on siliciclastic facies analysis and trace fossil analysis (Einsele et al. 1991; Frey and Seilacher 1980; Fürsich 1975; Fürsich 1998; Pemberton et al. 1992; Reading 1996; Reineck and Singh 1980; Reineck and Wunderlich 1968; Seilacher 1967; Walker and James 1992), and studies specifically developed for the lithostratigraphic unit under study (Spalletti et al. 2001b) and even the same locality (Spalletti et al. 2001a) allow a more or less precise facies interpretation. Carbonate facies were also studied with the help of specialized literature (Burchette and Wright 1992; Flügel 1982; Flügel 2004; Wright and Burchette 1996). For mixed rocks, in contrast, fewer studies exist. These rocks were formerly considered simply as impure siliciclastic or carbonate rocks. As a result, mixed rocks were interpreted in this study using both siliciclastic and carbonate facies information, with particular emphasis on skeletal concentrations, which represent an important part of them. Besides, mixed rocks share many features with limestones and criteria to interpret limestones are also useful for mixed facies.

Mixed rocks develop almost invariantly in condensed beds, formed under low terrigenous input. Reworking and bioturbation resulted in heterogeneous rocks lacking sedimentary structures and exhibiting very poorly sorting. Terrigenous input was evaluated from the relative amounts of sand and mud vs. carbonate particles. Depth, in turn, was assessed from grain size, sedimentary structures, presence/absence of fine matrix and density of bioclasts (clast-supported versus matrix-supported).

The shelly nature of most of the starved deposits is the result of storm action (storm-wave concentrations, proximal and distal tempestites *sensu* Fürsich and Oschmann (1993). During storm weather there is a net offshore movement of sediments by means of downwelling, offshore directed bottom flows (Nummedal 1991), whose product are so-called tempestites. Tempestites are recognized from bimodal sorting of complete shells and comminuted shell debris, mixture of epifaunal and infaunal elements, random orientation, floatstone and packstone matrix between the shells, usually low levels of abrasion, bioerosion and encrustation, as well as high degrees of completeness and articulation (Flügel 2004).

Bimodal size sorting consists of shell fragments of thin-shelled species plus better-preserved larger shells. This pattern indicates the input of shell hash formed above wave base by means of tempestites, with the addition of autochthonous or parautochthonous shells (Fürsich and Oschmann 1993). However, at least some of the small elements may also represent autochthonous skeletal fragments. It is thus not possible to clearly distinguish between allochthonous, autochthonous, and parautochthonous shell fragments at least in some cases.

Thickness, grain size, and proportion of mud may be indications of distality of tempestites, allowing to distinguish between proximal (thicker and coarser) and distal (thinner and finer) tempestites (Flügel 2004; Fürsich and Oschmann 1993). Besides, distal tempestites are rarer, better preserved and more biogenic in composition (Seilacher and Aigner 1991).

The original tempestite signature may be wiped out by bioturbation (Seilacher and Aigner 1991). In addition, the lack of lithification of most of the shell beds made it difficult to recognize structures and textures of tempestites. Moreover, most of the starvation-hemi-sequences are very thin, which makes recognition of tempestite patterns difficult. Individual tempestites are rare in the sections analysed here and, in their place, starvation hemi-sequences developed that comprise several amalgamated storm-flow deposits.

Several features supply information on the rate of terrigenous input. Autigenic glauconite and iron are known to form under low rates of sedimentation (Flügel 2004; Odin and Matter 1981). The presence of shell beds in siliciclastic sequences indicates early diagenetic processes that usually occurs during periods of starvation, otherwise, shells usually dissolve (Fürsich 1982; Fürsich and Pandey 2003). Relative abundance of micrite and other carbonate particles as well as evidence of a long residence time of shells on the sea floor also point to low rates of terrigenous input.

The homoclinal ramp model (Burchette and Wright 1992) distinguishes between inner, middle and outer ramp, and basin. In the following, I will briefly describe the features expected for each subdivision separately for siliciclastic, shell-poor facies, and mixed and carbonate shell-rich facies. The inner ramp corresponds to depths above the fair-weather wave-base, and is equivalent to the nearshore zone. Inner ramp deposits typically consist of oolitic or bioclastic shoal, barrier and back-barrier sediments (Burchette and Wright 1992). Shoal deposits commonly form sheet-like grainstone units. In this work, the most proximal inner ramp facies correspond to the shoreface. Constant agitation by normal waves precludes deposition of mud, either siliciclastic or carbonate. Winnowing, abrasion, and bioerosion are the main processes affecting grains. In the realm of siliciclastic deposition, clean, fine-grained sandstones with variable types of sedimentary structures can be expected. Mixed rocks of the inner ramp are sandy allochemic limestones and allochemic sandstones. Allochems may be in-situ formed ooids, broken and worn bioclasts, large and thick shells, and lithoclasts. Thin shells would easily be broken and reduced to small bioclasts while large ones were able to resist destruction by waves. Typical high-energy limestones are oolitic and bioclastic grainstones. Organic buildups may consist of biostromes and small patch reefs.

Middle ramp deposits consist of variable carbonate sediments deposited between fair-weather and storm wave-base, and are equivalent to the offshore transition zone. They reflect varying degrees of storm influence depending on water depth and the depth of wave base (Burchette and Wright 1992; Flügel 2004). Among siliciclastic facies, alternations of sand and mud deposition such as heterolithic or coarsely interlayered bedding (see Reineck and Singh 1980), as well as bioturbated sandy siltstones and silty sandstone facies can be expected. Mixed rocks and limestones likely have an important content of allochems that originated in the inner ramp and were deposited in offshore environments by storm-induced flows. Autochthonous shells also occur.

The outer ramp is a zone where argillaceous carbonates and terrigenous mud dominate. Only the most severe storms affect the sea floor and so evidence of wave reworking is sparse. Instead, thin distal tempestites composed of parautochthonous and autochthonous shells are expected.

Burchette and Wright (1992) characterized the basinal environment by the absence of coarse tempestites, lack of wave reworking, and depths below the pycnocline. In this study, the boundary between outer ramp and basin is defined as the depth below which there is little or no evidence of storm-induced flows. Depth of FWWB or SWB or the deepest reach of tempestites is relative rather than absolute, as it varies with factors such as the intensity of storms.

Facies and facies associations

The following facies and facies associations are based mainly on lithological aspects. Taphonomic and other palaeontological features were regarded as of secondary importance. Species composition of the fossil concentrations, not included in this analysis, is dealt with in the chapter 8.

Three main groups of facies and facies associations are distinguished: (a) siliciclastic, (b) mixed, and (c) carbonate. The first group comprises facies and facies associations linked to regressive phases of short sequences (i.e. dilution hemi-sequences) and is dominated by deposition of terrigenous siliciclastic material, while the second and third group include a wide variety of rocks in terms of composition that share a condensed nature. Groups (b) and (c) represent the starvation part of starvation/dilution hemi-sequences.

Pervasive bioturbation and lack of lithification, widespread in both sections, are characteristic features of the unit. Well-developed sedimentary structures are restricted to upper offshore and shoreface facies, which are in turn also well lithified. Only starved deposits developed above and just below the fair-weather wave-base are lithified.

Table 1 lists the various facies and facies associations, together with their interpretation.

Table 1. Synthesis of facies and their interpretation.

Facies association	Facies	Description (lithological features and sedimentary structures)	Sequence stratigraphic position	Interpretation
Siliciclastic rocks				
1. Mudrocks (S-C, S-SC, S-AS and S-S)	1.1.Shell-poor mudrocks	Dark massive bioturbated claystones to siltstones. Fissile. Rarely thin-bedded or laminated. Scattered shells and shell fragments.	D-HS of major late TST, MFZ and early HST. Early D-HS.	Outer ramp to basin. Moderate terrigenous input. Dysaerobic but no evidence of prolonged anoxia.
	1.2.Shell-rich mudrocks	Bioturbated siltstones and argillaceous siltstones. Disperse shell beds. Gradual contacts.	Complete S-HS in major late TST or early HST.	Outer ramp to basin. Low terrigenous input.
2. Mud-sandstone mixtures	2.1.Coarsely interlayered bedding (S-CIB)	Alternating coarser (fine-gr. ss) and finer (mud) layers. Sand layers increasing in frequency and thickness of upwards. Traces: *Gyrochorte*, *Planolites*, *Chondrites*, *Treptichnus*, and *Paleophycus*.	Middle to late HST of 1st and 2nd major sedimentary sequences.	Outer to inner ramp. High terrigenous input. Availability of accommodation space.
	2.2.Heterolithic stratification (S-HET)	Intercalations of coarse- (lenticular or tabular fine-gr. ss) and fine-grained beds. Coarse layers with ripple cross-lamination and oscillation ripples. Abundant and diverse trace fossils.	Late major and intermediate HST, close to SB. Middle to upper parts of D-HS.	Autocyclic variations in wave regime. Close to the FWWB (lower shoreface). High terrigenous input.
	2.3.Bioturbated sand-mud mixtures (S-SaS, S-SiS)	Highly bioturbated sandy siltstones to silty fine sandstones, usually inserted in coarsening-upward facies successions. Trace fossils rare: *Planolites*, *Palaeophycus*, *Spongeliomorpha suevica*.	Widespread throughout the sections except in late HSTs or deep settings. Lower to upper D-HSs.	Deposition in offshore settings. Moderate rates of sedimentation. Totally bioturbated.

	2.4.Very poorly sorted sandy mudstones (S-SaS) to muddy fine sandstones (S-SiS)	Bioturbated and heterogeneous mixtures of very fine- to medium-grained sand, silt and clay, micrite and bioclasts. Rare.	Lower part of S/D-Ss close to the base of 3rd order SB.	Mixing of inner to outer ramp sediments. Fast transgression, low sedimentation rate, bioturbation.
3. Very fine- to fine-grained sandstones	3.1. Fine-grained sandstones with hummocky cross stratification (S-FS-H and S-FS-AH)	Well lithified fine-grained sandstones with hummocky cross-stratification, as interbedded (lenticular) or amalgamated (tabular) bodies. Trace fossils rare (*Spongeliomorpha suevica*, *Planolites*, *Paleophycus*).	Upper parts of D-HSs in middle to late major or intermediate HST.	Deposits generated by storm waves in the middle to lower inner ramp.
	3.2. Fine-grained sandstones with medium-scale symmetrical wave ripples and ripple lamination (S-FS-W)	Lenticular or tabular beds with symmetrical wave ripples. Trace fossils common and well preserved (*Bolonia lata, Chondrites*, *Bergaueria*, *Gyrochorte,* and *Palaeophycus*).	Middle to upper parts of D-HSs in middle to late major or intermediate HST.	Storm-generated deposits in middle ramp settings.
	3.3. Highly bioturbated fine-grained sandstones (S-FS)	Bioturbated very fine- to fine-grained sandstones. Glauconite, micrite, and occasionally low density shell concentrations. Trace fossils rare (*Skolithos, Planolites, Palaeophycus, Spongeliomorpha suevica, Chondrites* and *Diplocraterion*).	Top of D-HSs in early TST and late HST.	Inner (to middle) ramp deposits. Low rate of sedimentation due to toplap condensation.
	3.4. Fine grained sandstones with cross- stratification (S-FS-C)	Well sorted fine-grained sandstones with large-scale tabular cross-bedding. Asymmetric climbing ripples on top.I.	Middle and upper part of D-HSs in the last 50 m of the section.	Offshore sand bars.
	3.5. - Very fine- to coarse-grained sandstones with desiccation cracks, climbing ripples and small channels	Desiccation cracks. *Planolites*? and *Skolithos*?. Alternations of very fine-grained sandstones with trough cross-lamination and rib-and-furrow pattern on top, and parallel laminated coarse siltstones.	Only one occurrence at the base of the section in BAL	Back ramp.

Facies association	**Facies**	**Description (lithological features and sedimentary structures)**	**Stratigraphic position**	**Interpretation**
Mixed rocks				
4. Fine-grained dominated, allochem-poor mixed rocks	4.1. Marlstones (Ma)	Poorly lithified bioturbated dark-grey to orange-coloured marl and marlstone. Intercalations of thin shell-beds (shell-rich floatstones-LF-R) in AML.	Complete dilution HSs in the vicinity of major MFZs.	D HS deposited in basinal environments during major late TST, MFZ and early HST. Sedimentation rate low. Lowered oxygen levels close to the sediment-water interface.
	4.2. Micritic mudrocks (MC1)	Dark, fissile, bioturbated and poorly lithified clays and siliciclastic muds with subordinated micrite. Common intercalations of shell beds (S-HS).	Complete D-HSs in the vicinity of major MFZ.	
	4.3. Muddy micrite (MA1)	Orange-coloured, highly bioturbated muddy carbonate mudstones. Very rare.	Whole dilution HSs in the vicinity of major MFZs.	
5. Fine-grained dominated allochem-rich mixed rocks		Thin planar strata with diffuse contacts containing low density skeletal concentrations in fine-grained matrix. Highly bioturbated. Trace fossils rare (*Chondrites*?; predatory borings: *Oichnus simplex* and *O. ovalis*; *Meandropolydora* and Cirripedian borings in carbonate concretions).	Complete S-HSs in deep settings or latest part of S-HS at intermediate depths.	Deposition below storm wave-base (Ma-R and MC1-R) or within the reach of distal tempestites (Ma-B-R and MC2-R).
	5.1. Shell-rich marls (Ma-R) and bioclastic shell-rich marls (Ma-B-R)	5 to 20 cm thick disperse to loosely packed skeletal concentrations in a marly matrix. Benthic fossils excellently (Ma-R) to well (Ma-B-R) preserved.	Whole starvation HSs of major late TST, MFZ and early HST.	Basinal environments. High density shell hash in bioclastic shell-rich marls represent outer ramp distal tempestites.
	5.2. Shell-rich micritic mudrocks (MC1-R)	Dispersed to loosely packed skeletal concentrations in mixed matrix dominated by fine-grained siliciclastics . Benthic fossils excellently preserved.	Complete starvation HSs of major late TST, MFZ and early HST.	Deposition in basinal environments, below the reach of distal tempestites.

	5.3. Allochemic mudrocks (MC2-R)	Loosely packed skeletal concentrations into a fine-grained siliciclastic matrix (type a) and silty and sandy matrix (type b). Foraminiferal buildups may be very abundant. *Caulostrepsis*, rare *Entobia* and cirripedian borings.	Complete S-HS of early major HST (type a) or top of complex S-HS in middle part of major TST and HST (type b).	Outer ramp. High density shell fragments represent distal tempestites.
6. Sandy and silty micrites (MA2)	6. Sandy and silty micrites (MA2)	Well lithified massive beds of sandy or silty micrite. Contacts sharp. Low densities of skeletal remains, completely micritized or as moulds. Glauconite.	S-HSs into intermediate 3^{rd} order HSTs.	Condensed deposits developed in offshore settings. Shells lost by dissolution and micritization.
7. Coarse-grained dominated allochem-rich sediments	7.1. Muddy allochemic limestones (MB1)	Poorly sorted mixtures of shells, shell fragments, ooids, echinoderm ossicles, micrite and some siliciclastic mud and sand grains. Bioturbated. Micritization low. Subfacies (a): complete S-HS at intermediate depths. Reworked concretions. Subfacies(b): close to the top of fining-upward sequences within particular S-HSs. Large and thick shells. Abundant encrusting agglutinating foraminifers building small nodules.	Subfacies (a): complete S-HSs in lower to middle HST, MFZ. Subfacies (b): middle major HST and TST at intermediate depths.	Deposition of condensed deposits in low energy settings, (lower middle to outer ramp). Tempestites brought sand, ooids, shell hash and other grains from the inner ramp. Permanent low deposition of mud facilitated the early burial of shells and the development of foraminiferal buildiups.
	7.2. Sandy allochemic limestones (MB2)	Heterogeneous mixtures of coarse sediments dominated by shells, shell fragments, ooids and some fine sand grains. Autigenic glauconite. High density skeletal concentrations. Highly bioturbated (*Planolites*, *Palaeophycus*, *Spongeliomorpha suevica* and unidentified burrows). High levels of bioerosion (*Gastrochaenolites*, *Trypanites*, *Entobia*, cirripedian borings). Micritization usually very important, particularly at mid-starvation horizons.	Lower to middle starvation deposits in late TST and early HST.	Condensed deposits of lower inner to upper middle ramp. Basal lag and early transgressive sediments deposited above fair-weather wave-base (high shell destruction). Mid-starvation horizon, deposited in the middle ramp, related to maximum flooding in S/D-sequences.

	7.3. Micritic sandstones (MD1)	Poorly sorted fine-grained sand and micrite, with subordinated bioclasts, shells, ooids and silt. Abundant iron replacements. Autigenic glauconite. Burrows occur (*Planolites*, *Palaeophycus* and unidentified burrows; *Spongeliomorpha suevica* , *Arenicolites* ?). Shells absent or in loosely to densely packed, matrix-supported concentrations.	Top of coarsening-upward D-HSs, in early TST or late HST (type a); S-HSs in high energy early TST (type b) or intermediate energy in various stratigraphic settings (type c).	Toplap or onlap condensation in high energy (mostly inner ramp) late major HST and early TST, or intermediate energy middle to outer ramp.
	7.4. Allochemic sandstones (MD2)	Bioturbated mixtures of poorly sorted very fine- to fine-grained sandstones with subordinated shells, shell fragments, echinoderm ossicles and ooids. Autigenic glauconite and iron. Strongly bioturbated (*Planolites*), rare trough? Cross- stratification. Bioerosion abundant (*Gastrochaenolites*, *Meandropolydora*, *Trypanites*, *Caulostrepsis*).	Always at the base of S-HS underlain by erosional transgressive surfaces. Near major SB.	High-energy deposits corresponding to the inner ramp, above fair-weather wave-base.

Facies association	**Facies**	**Description (lithological features and sedimentary structures)**	**Stratigraphic position**	**Interpretation**
Carbonate rocks				
8. Fine-grained limestones	8.1. Mudstones (LM) and wackestones (LW)	Rare, thin, tabular beds wackestones or mudstones. Grains, when present consist of bioclasts. Siliciclastic mud may be present. Massive.	Complete or parts of S-HSs in early TST.	Outer ramp to basin. High terrigenous starvation.
	8.2. Floatstones (LF)	Rocks with <10% siliciclastic material and >10% of allochems larger than 2 mm in a micritic matrix. Echinoderm ossicles, ooids, lithoclasts and faecal pellets. Autigenic glauconite and iron. Well preserved fossil assemblages at MFZ and in tempestitic shell beds at shallower settings. Burrows rare. Borings occur (*Oichnus simplex*, *O. ovalis*, cirripedian borings, and *Entobia*).	Part or complete S-HSs in different stratigraphic positions (major late TST, MFZ and HST).	Outer ramp to basinal shell-rich skeletal concentrations in a micritic matrix. Starvation. Skeletal concentrations of biogenic and/or physical origin (distal tempestites).

9. Coarse-grained limestones	9.1. Packstones (LP) and grainstones (LG)	Bio-packstones with some ooids. Micritic matrix. Lithoclasts. Beds thin and heterogeneous. Bioturbation and micritization of skeletal components high. Well sorted oo-grainstones with highly abraded bioclasts. Lithoclasts rare.	Starvation HSs of middle (packstones) to late (grainstones) major HST.	Packstones deposited in the middle ramp. Coarse material derived from the inner ramp supplied by storm surges. Grainstones correspond to inner ramp, high-energy deposits.
	9.2. Micritic rudstones (LRm)	Shells, shell fragments, nodular foraminiferal buildups and ooids. Low-energy LRm: thin planar strata, with densely packed, moderately well sorted shell beds. Shells disarticulated, horizontally oriented, and little abraded or broken. Iron content low to high. High-energy LRm: thin, coarse, planar beds, densely to loosely packed coquinas supported by a muddy micritic matrix. Nodular foraminiferal buildups. Sorting poor and sometimes bimodal. Autigenic glauconite. Micritization and bioerosion higher than in the other subfacies.	Complete S-HSs near MFZs (low-energy LRm). Whole or partial S-HSs in middle positions of major and intermediate TST and HST (high energy LRm).	Low-energy LRm deposited in the outer ramp. High-energy muddy-LRm corresponds to the middle to outer ramp.

Siliciclastic facies and facies associations

This facies group ranges from claystones to fine-grained sandstones and can be subdivided as follows:

1. Mudrock facies association

1.1. Shell-poor (siliciclastic) mudrocks (S-C, S-SC, S-AS, and S-S)

Thick, dark, massive bioturbated claystones, silty claystones, bioturbated dark-grey argillaceous siltstones, and bioturbated or bedded greyish to greenish silt comprise this facies (Pl. 4, Fig. 7). Lithification is poor.

Physical sedimentary structures are restricted to rare and poorly developed short segments with parallel lamination. Fissility is common mainly in claystones. Pervasive bioturbation is the rule. Apart from some small unidentified burrows trace fossil are rare. Partially dissolved shells and moulds of small, commonly disarticulated bivalves and gastropods are relatively common throughout this facies. Silt and argillaceous silt usually contain scattered echinoderm bioclasts that are locally abundant.

Mudrock appears at the base of dilution hemi-sequences, usually conformably overlain by coarser grained facies (e.g., facies association 2). In many instances, shell-rich starvation hemi-sequences are intercalated between this facies type. Lower contacts are usually sharp when overlying starvation hemi-sequences. Tops grade into shallower facies or are sharp and sometimes erosional when giving way to starvation hemi-sequences.

This facies occurs at maximum flooding zones of high-hierarchy sequences and at the base of the majority of the dilution hemi-sequences. In the last 150 m of the member, in which limestones are more common, dilution hemi-sequences consist mainly of mudrock almost without changes in grain size. This facies association shares its position with the micritic (siliciclastic) mudrock facies (MC1), deposited under similar conditions but with less terrigenous influx. Altogether, the mudrock is the most common facies association, reaching thicknesses of up to 25 m.

Interpretation. This facies represents low energy environments, in offshore position, below storm wave base (i.e., outer ramp to basin). Evidence is the fine-grained nature of the sediment, the lack of sedimentary structures, and the absence of other intercalations indicating shallower positions. The lack of skeletal concentrations indicate a moderate terrigenous input. Considerable amounts of organic matter accumulated with the fine-grained sediment. Anoxia is not evident from the features of this facies, considering that even the most fine-grained and darkest claystones are highly bioturbated and contain an autochthonous benthic fauna.

1.2. Shell-rich (siliciclastic) mudrocks

This facies is composed of bioturbated fossil-rich siltstones and argillaceous siltstones. The well-preserved fauna occurs in dispersed concentrations in thin, tabular beds. The matrix is similar to that in the strata below and above. Contacts are gradual. This facies is uncommon and occurs in major late TST or early HST.

Interpretation. This facies is considered as representing starvation hemi-sequences and was deposited in offshore environments under a low sedimentation rate, which allowed the benthic fauna to become concentrated. The energy level was very low because the bivalves are usually articulated and the degree of fragmentation is low. The concentration process was driven by the high rate of shell production and preservation, compared to the terrigenous input. These starvation hemi-sequences exhibit fewer signs of condensation than others. An outer ramp to basinal environment is assumed for this facies.

2. Mixed mud-/sandstone facies association

This facies association includes three subtypes: coarsely interlayered mud-/sandstone bedding, heterolithic stratified beds and bioturbated sandy-silt to silty-fine-grained sandstone, all of them sharing the presence of mud and sand. The first two are types of alternating bedding (sensu Reineck and Singh 1980), while the last one probably is their bioturbated equivalent.

2.1. Coarsely interlayered mud-/sandstone bedding (S-CIB)

This facies is composed of alternating coarser and finer-grained layers, which are usually a few millimetres to a few centimetres thick. Coarser layers consist of very fine- to fine-grained, well sorted sandstone, while finer beds are bioturbated mudstones. Stratification is always horizontal and lower contacts of the sand layers are sharp. The finer-grained layers, when thickly developed, show parallel stratification and sometimes poorly preserved parallel lamination. Body fossils are completely absent. This style of stratification was described as coarsely interlayered bedding (CIB) by Reineck and Singh (1980). CIB is a characteristic feature in the HST of the first and second major sedimentary sequences that show relatively high sedimentation rates (Pl. 5, Figs. 1-3). Based on grain size of each of the two layers involved, five types of CIB were defined in this study. Type (1) (S-CIB1) reaches thicknesses of up to 7 m and consists of less than 1 cm thick coarser beds of sandy siltstone, and several cm thick layers of mudstone or siltstone (finer layer). This type overlies bioturbated siltstones, sandy siltstones, or starved deposits corresponding to starvation hemi-sequences, and may be overlain by silty sandstones or CIB2. In type (2) (S-CIB2) coarse and fine layers are similar to type 1 but are of equivalent thickness. Thicknesses of S-CIB2 packages are less than 3 m. The packages overlie siltstones, silty fine-grainedsandstones or CIB1 and are capped by silty fine-grained sandstones, CIB3, CIB4 or bioturbated fine-grained sandstones. The coarse layers of type (3) (S-CIB3) are thin, flat, fine-grained sandstones, or occasionally silty sandstone, up to 1 cm thick. Finer-grained layers consist of thicker beds of siltstone (rarely sandy siltstone) that dominate this type, and may show poorly developed lamination. Within a package, the distance between two sand layers decreases up-section and their thickness increases. CIB3 usually rests on siltstones or, less commonly, sandy siltstones, reaches a thickness of up to 3 m, and grades upwards into CIB4, bioturbated silty fine-grained sandstones, and rarely heterolithic wavy beds (S-HET2). S-CIB3 appears in late HST of major and intermediate sedimentary sequences. Close to the latest part of the HST of the first major sequence, once in each section, CIB3 packages reach thicknesses of more than 20 m. The coarser- and finer-grained layers of CIB4 and 5 have similar composition as CIB3. CIB4 always follows CIB3 and is invariantly succeeded by CIB5. This subfacies reaches a thickness of 11 m and is intercalated into coarsening-/shallowing-upward facies successions close to third-order HST. Cross-lamination, *Gyrochorte* and *Planolites* are common features of CIB4. Thin levels of fine-grained sandstone with rippled bedding planes and ripple cross-lamination (facies S-FS-W) may be intercalated. CIB5 usually rests on CIB4 and is overlain by bioturbated fine-grained sandstone. Less commonly it overlies bioturbated silty sandstones and is followed by beds with wavy heterolithic stratification, or is capped by an erosional surface representing the top of a dilution-hemi-sequence. Thicknesses range from 1 to 5 m. Fine-grained sandstone layers with ripple-cross lamination and hummocky cross-stratification are intercalated. Associated trace fossils are *Chondrites*, *Gyrochorte*, *Treptichnus*, *Planolites,* and *Palaeophycus*. *Bolonia lata* was found on S-FS-W intercalated between CIB5. Shells are rare, an exception being an articulated specimen of *Steinmanella vacaensis* and fragments of *Inoceramus*. CIB5 occurs almost without exception in the latest part of third- or fourth-order HST, just below major or intermediate sequence boundaries, in the first two third-order sequences.

Contacts between the various types of CIB are completely gradual. As a rule, coarse layers become closer and thicker upward, giving rise to the next type of CIB. Grain size commonly also increases upward. Lower contacts are usually gradual. Upper contacts are gradual except when this facies represents the top of starvation-dilution sequences. In these cases, the facies is capped by an erosional or sharp, transgressive surface. A common feature of CIB is the intercalation of lenses and layers of very fine- to fine-grained sandstone with ripple lamination and surfaces with symmetrical ripples, typical of heterolithic stratification. However, the dominating stratification style is clearly coarsely interlayered bedding.

Interpretation. The preservation of this style of sedimentation indicates high sedimentation rates as well as plenty of accommodation space. The absence of body fossils does not indicate that the habitat was unsuitable for the benthic fauna, as there is no evidence of oxygen deficiency, departure from normal salinity or of any other alteration. Instead, synsedimentary and/or early diagenetic dissolution of shells appear likely.

Sandy layers can be interpreted as the result of storm surges, i.e. tempestites. Together with the interbedded bioturbated mud, they represent deposits of the storm-influenced shelf. The succession of subfacies marked by an increase in grain size, thickness, and dominance of sand layers probably reflects a trend towards greater proximality (Fürsich and Pandey 2003).

Facies S-CIB 1 to 5 were deposited in progressively shallower environments from the outer ramp (marked by the first tempestites) to the middle or even inner ramp, close to the FWWB. The presence of S-FS-W facies indicates the action of storm waves and its onset the lower boundary of the middle ramp (the storm wave base). Close to the upper boundary of the middle ramp the tops of the sand layers show oscillation ripples and hummocky cross-stratification becomes frequent. Heterolithic stratification and bioturbated fine-grained sandstones replace coarsely interlayered bedding up-section. Intercalation of heterolithic stratification indicates an inner ramp setting for the deposition of CIB-5 type.

CIB facies is present in diluted hemi-sequences that developed under high rates of terrigenous sedimentation, in the middle to late parts of HST. In particular dilution hemi-sequences CIB facies is located in middle to upper positions.

2.2. Heterolithic stratified beds (S-HET)

Heterolithic stratified beds consists of an alternation of coarser and finer beds, made of fine- to very fine-grained sandstones with ripple cross-lamination, and siltstone or mudrock, respectively (Pl. 5, Fig. 4). The sandstones show ripples with a wavelength of less than 10 cm and amplitude of 1-2 cm. The ripples are symmetric and show straight and sinuous crests in plan view. Bioturbation is usually moderate to high in sandstone beds and high in mudrocks. Based on the proportion of sand and mud three kinds of heterolithic bedding were recognised following Reineck and Wunderlich (1968) and Reineck and Singh (1980). The lenticular type (S-HET-1) consists of lenses of fine sand within bioturbated mudrocks or siltstones, with thicknesses between 1-3 m. This facies usually rests on bioturbated siltstones and is capped by wavy-type heterolithic facies (S-HET-2), and rarely by erosional surfaces marking the top of S/D hemi-sequences. Intercalations of facies FS-W, FS-H and of bioturbated fine-grained sandstones are rare. *Gyrochorte*, *Lockeia,* and *Chondrites*? were found in the sandy lenses of this subfacies. Beds with wavy stratification (S-HET-2) consist of equal quantities of sand and mud and usually occur inbetween HET-1 and HET-3 (or flaser type bedding). It is rarely underlain by silty sandstones or CIB 3 or 4, and is overlain in one case by bioturbated fine-grained sandstone and in a second case by the following starvation-hemi-sequence. This subfacies reaches a maximum thickness of 6 m. Lenticular and tabular intercalations of facies FS-W as well as lenses of fine-grained sandstone with hummocky cross-stratification are common. Trace fossils are diverse and comprise, in decreasing abundance, *Gyrochorte*, *Planolites*, *Bergaueria*, *Protovirgularia*, *Spongeliomorpha suevica*, *Lockeia siliquaria*, *Phycodes*, *Treptichnus*, *Teichichnus*, *Chondrites*, *Bolonia lata*, *Taenidium*, and unidentified burrows. Beds with flaser stratification (S-HET-3) are 1-3 m thick, overlie wavy bedding and are covered by erosional surfaces marking the top of starvation/dilution-sequences, which usually coincide with important sequence boundaries. Common intercalations are tabular fine-grained sandstone beds with medium-scale wave ripple surfaces (facies FS-W), lenses with hummocky cross-stratification and amalgamated hummocks. Trace fossils in HET-3 are similar to HET-2 but less abundant. Heterolithic stratification occurs mainly close to the top of HST of high-hierarchy sedimentary sequences, when shallow environments prograded towards the basin. In dilution hemi-sequences, heterolithic stratification occupies middle to upper parts. Despite its low frequency, this facies is particularly important as it shows progradational trends close to sequence boundaries.

Interpretation. Heterolithic stratification developed in shallow subtidal settings, under relatively high input of siliciclastics. From a bathymetric point of view, the deposits formed near the fair-weather wave-base. Sand/mud alternation is the result of autocyclic variations in wave-regime. The ripples formed under the influence of shallow oscillatory waves in the lower shoreface (Harms et al. 1982; Spalletti et al. 2001b).

2.3. Bioturbated sandy siltstones (S-SiS) and silty fine-grained sandstones (S-SaS)

This facies comprises highly bioturbated massive beds ranging from sandy siltstones to silty very fine- to fine-grained sandstones with thicknesses between 1 and 7 m, exceptionally reaching 11 m. It is widespread throughout the sections with the exception of segments in which deep facies dominate, and close to the top of major HSTs, where this facies is replaced by the other two facies of the association (i.e., S-HET and S-CIB). The two subfacies are usually inserted into a succession beginning with siltstones (S-S), followed by sandy siltstones (S-SaS), silty sandstones (S-SiS), and bioturbated fine-grained sandstones (S-FS) on top. However, many variations of this succession exist, e.g., the succession may start with S-SaS or with S-SiS, or may finish with S-SaS or S-SiS. Trace fossils are rare, comprising poorly developed horizontal burrows such as *Planolites* and *Palaeophycus*, and *Spongeliomorpha suevica.*. *S. suevica* occurs when this facies is directly overlain by S/D-S. The galleries are usually filled with shelly material similar to the matrix found in the transgressive bed above, and hence the trace maker made their burrows while the sedimentation rate was very low. Other features of this facies are: lenses of fine-grained, cross-laminated sandstone, tabular fine-grained sandstone beds with medium-scale wave ripples (S-FS-W), and lenses with hummocky cross-stratification.

In some cases, the density of bioclasts and shells is higher than expected giving place to “dispersed concentrations” *sensu* Kidwell and Holland (1991). Shells belong to small bivalves and gastropods such as *Disparilia elongata, Corbulomima bodenbenderi*, *Grammatodon securis,* and *Promathilda* sp.

Interpretation. This facies is interpreted as the bioturbated product of the other two facies in this association. Relatively low sedimentation rates allowed the benthic fauna to completely destroy the physical sedimentary structures. This is corroborated by the replacement of this facies by the other two in positions closer to the top of major HST, in which faster progradation and a high rate of terrigenous sedimentation is expected. This facies was deposited in offshore settings, the silty sandstones closer to the fair-weather wave-base, and the sandy silts basinward of the former.

2.4. Very poorly sorted sandy mudrocks to muddy fine-grained sandstones

This very rare facies consists of bioturbated and heterogeneous beds with mixtures of very fine- to medium-sized sand grains, silt and clay, micrite, and bioclasts. This highly heterogeneous facies appears at the lower part of starvation/dilution sequences close to the base of major sequence boundaries, and particularly at the base of the section at both localities.

Interpretation. The main feature of this facies is its highly heterogeneous nature, involving very different grain sizes. This is the result of mixing of fine-grained transgressive deposits with the underlying sandstones of the regressive phase. Transgression was probably fast. Mixing was possibly due to bioturbation that acted during extensive periods of low rates of sedimentation.

3. Very fine- to fine-grained sandstone facies association

3.1. Fine-grained sandstones with hummocky cross-stratification (S-FS-H and S-FS-AH)

Fine-grained sandstone beds with low-angle cross-lamination and typical hummocky cross-stratification occur in two ways: (a) as lenticular beds interbedded between other facies (S-FS-H), or (b) as amalgamated tabular units (S-FS-AH). This kind of stratification occurs more commonly at levels within the sections where shallow facies and high rates of sedimentation prevail, i.e. in middle to late major and intermediate HST. Type (a) usually appears intercalated between the sand-dominated heterolithic and coarsely interlayered facies, between bioturbated fine-grained sandstones and silty sandstones, and occasionally between mudrocks. Amalgamated HCS occurs in sand-dominated S-CIB or S-HET facies and on top of dilution-hemi-sequences. When both types are present in the same dilution-hemi-sequence, the second type overlies the first one, indicating that the amalgamated units were deposited in shallower water. Thicknesses may reach a few metres for beds with amalgamated hummocks, but usually are less than 40 cm thick. Trace fossils are rare in this facies and consist of a few *Palaeophycus* and *Planolites* on top and *Spongeliomorpha* at the contact between beds with amalgamated hummocks and overlying transgressive strata.

Interpretation. Hummocky cross-stratified sediments are interpreted as deposits of storm waves (Dott and Bourgeois 1982; Duke 1985) and thus were deposited above storm wave base and most probably below fair-weather wave-base (i.e. on the middle ramp). Both types of occurrences found in this study can be assigned to the interbedded and amalgamated associations described in the literature (see for instance Duke 1985). Amalgamated hummocks were deposited in shallower facies than the interbedded variation. Hummocky cross-stratification is not a good environmental indicator, as this structure was described from delta, estuarine, beach, and tidal flat environments (Klein and Marsaglia 1987). In shoreface settings these structures have a low preservation potential due to reworking by fair-weather waves and tides (Duke 1987). Besides, depth of deposition cannot be precisely stated as it highly depends on storm energy. From the sedimentary context, in which this facies was found, a middle ramp position can be envisaged for the interbedded hummockies and middle to lower inner ramp for the amalgamated structures.

3.2. Fine-grained sandstones with medium-scale symmetric wave ripples and ripple lamination

This facies consists of lenticular or tabular beds, usually thin (5 to 10 cm), made of fine-grained sandstones with symmetric ripples. Ripple wavelength is up to 20 cm and crests are sinuous. This facies is interbedded between facies HET-2, HET-3, CIB-4, CIB-5, and bioturbated fine-grained sandstones and becomes common close to the top of major and intermediate HST. Common trace fossils are *Bolonia lata* and *Chondrites*, less frequent are *Bergaueria*, *Gyrochorte*, *Palaeophycus,* and some unidentified burrows.

Interpretation. Fine-grained sandstones with medium-scale symmetric ripples were considered by Spalletti et al. (2001b) as produced by storm-induced low-energy regime orbital or oscillatory flows, deposited either at greater depth or under lower energy than the hummocky cross-stratified beds, and this interpretation is adopted here. Spalletti et al. (2001a) described the same facies for a section of the AMMb placed very close to BAL. A middle ramp position is proposed for this facies.

3.3. Highly bioturbated fine-grained sandstones (S-FS)

This facies consists of massive beds of poorly sorted, sometimes silty, and pervasively bioturbated fine-grained sandstones, often glauconite-bearing, micritic or both, as well as with shell concentrations. Thicknesses never exceed a few meters and the frequency of occurrence of this facies is moderate. In general, these highly bioturbated fine-grained sandstones overlie silty sandstones, and less commonly beds with CIB or HET stratification, invariably with gradual lower contacts. The top is always sharp and in many cases erosional. This facies is usually overlain by transgressive surfaces bordering two successive starvation/dilution-sequences. In half of the occurrences, there is no starvation hemi-sequence above the transgressive surface, while in the other half there is a variably developed bed characterized by the presence of skeletal concentrations. Despite the very high bioturbation that characterises this facies, trace fossils are neither abundant nor diverse. *Skolithos* and *Arenicolites* may be locally abundant (Pl. 2, Figs. 2, 4), *Planolites* and *Palaeophycus* are common, and *Spongeliomorpha suevica* (Pl. 2, Fig. 3) and *Chondrites*? are rarer. Several unidentified simple burrows were also found in this facies. Among them ill-defined vertically oriented burrows, 5-10 mm thick, with walls lined with dark mud, are common. Ammonites, when present, occur on top.

A particular case of this facies are the fossil-rich, bioturbated, fine-grained sandstones (S-FS-R), which are more common at AML than at BAL.

Disperse to loosely-packed shell concentrations contain shells of originally calcitic composition such as *Pinna robinaldina*, serpulids (originally high-Mg-calcite), and gryphaeid oysters (originally low-Mg-calcite) or internal moulds of other taxa, such as *Panopea neocomiensis*, *P*. *dupiniana*, and Veneridae sp. indet 2. In *Pinna robinaldina* only the outer, low-Mg-calcitic layer is preserved. Common features of most of these skeletal concentrations are: a nearly complete lack of encrustation and bioerosion, low species richness, and a high proportion of both, infaunal taxa (e.g., *Panopea neocomiensis*) and the semi-infaunal *Pinna robinaldina* articulated and in life position. In some beds, serpulids of variable morphologies are common but not attached to any shell or shell fragment (in fact, there are generally no bioclasts in this facies).

Interpretation. There are several indications of a low sedimentation rate, which governed the deposition of this facies: (a) the completely bioturbated sediment, (b) the common development of skeletal concentrations, (c) the high amount of micrite, and (d) the presence of autigenic glauconite. I interpret this facies as shoreface sandstones, which subsequently became completely bioturbated. Because of the absence of sedimentary structures, the environmental interpretation of this facies cannot go further. A shoreface setting is supported by the frequent position of this facies above sand-dominated CIB and HET in the same dilution hemi-sequence. Very poorly sorted and silty variations of this facies could be the bioturbated result of sand-dominated alternating bedding such as CIB or HET. The net rate of sedimentation was low probably due to bypassing, providing time for the benthic fauna to completely erase any primary sedimentary structures. In cases, in which there is no starvation hemi-sequence above, the top of these beds can be interpreted as a flooding surface, i.e. a transgressive surface, because it is connected with a distinct drop in grain size. Shells were probably dissolved synsedimentarily or early on during diagenesis. Fossil-rich, bioturbated, fine-grained sandstones impose different constraints on the interpretation of the depositional environment. Permanent agitation by fair-weather waves does not match the widespread occurrence of the semi-infaunal *Pinna robinalina* and the infaunal *Panopea neocomiensis*, both usually articulated and in life position. These sandstone levels could have been deposited in a shoreface setting but the colonization by the benthic community took place later on, when as a result of transgression the sea floor occupied a greater depth. Autocyclic processes cannot be ruled out. Shell concentrations are dominated by mineralogically more stable calcitic elements such as pinnids (only the outer layer), serpulids, and oysters.

In one case, this facies appears as series of three 20 to 30 cm thick planar beds intercalated between sandy siltstones, with large *Spongeliomorpha suevica*, *Diplocraterion saxicavum*? and other not identified thick-walled burrows connecting two sandy levels (BAL section at 395 m; Appendix Fig. 1; Pl. 2, Figs. 6-8). These levels are interpreted as proximal tempestites that exported sand and trace makers from the inner ramp offshore.

3.4. Fine-grained sandstones with cross-stratification (S-FS-C)

Well-sorted fine-grained sandstones with large-scale tabular cross bedding occur in packages up to 4 m thick in the last 50 m of section BAL (Pl. 3, Fig. 1). Asymmetric climbing ripples with 4 cm wave length and a few mm in height, may occur close to the top of these units. Climbing ripple cross-lamination can be observed in vertical sections (Pl. 5, Fig. 8). These sandstone bodies occur either between finer-grained sediments in the middle or on top of starvation/dilution sequences. Base and top are sharp and possibly erosional. Thin packages of thinly laminated coarse siltstones to very fine-grained sandstones, usually with cross-lamination, alternate with the sandstones.

Interpretation. These sand bodies possibly represent off shore sand bars (Spalletti 1980).

3.5. Very fine- to coarse-grained sandstones with desiccation cracks, climbing ripples, and small channels

Between the fluvial, medium- to coarse-grained trough cross-bedded sandstones of the Avilé Member and the first marine beds of the Agua de la Mula Member, a series of transitional facies with various features crop out in the BAL section. The complete thickness is less than 2 m. Three levels with desiccation cracks of two sizes are well developed (Pl. 4, Figs. 4-5). The larger desiccation cracks are close to the last fluvial beds of the Avilé Member, while the smaller ones occur a few centimetres above. Bioturbation is represented by bed-parallel burrows and by cross-sections of probably vertical tubes (Pl. 6, Fig. 2). Less than 1 m above, there are alternations of very fine-grained sandstones with trough cross-lamination and a rib-and-furrow pattern on top (Pl. 4, Fig. 6), and parallel-laminated coarse siltstones. Towards the top of this set of beds thin strata of very fine-grained sandstones with symmetric small wave ripples with sinuous to straight crests occur. Small channels filled with medium- to coarse-grained sandstone cut the levels with small ripples (Pl. 6, Fig. 3).

Interpretation. Thin, very fine- to fine-grained sandstone beds with small ripples on top, cut by channels filled with medium- to coarse-grained sandstones are interpreted as deposited in the intertidal (foreshore) zone (Spalletti 1980) (although the size of the channels described here is very small). These strata are interpreted as deposited in the upper part of the inner ramp, e.g. the back ramp.

Condensed facies

Condensed facies comprise mixed (siliciclastic and carbonate) and limestone facies. Mixed rocks (sensu Mount 1985) and limestones characterize segments of the sections with low terrigenous input. This scenario is common in the starved hemi-sequences of S/D sequences, but also in dilution hemi-sequences developed under very low terrigenous input (i.e. in major early TST and MFZ). A wide spectrum of mixed rocks is present in the studied unit. Besides, carbonate rocks are usually impure containing variable amounts of siliciclastic components. Thus, there is a gradation in the amount of siliciclastic material between mixed rocks and limestones. For that reason, mixed rocks and limestones share many features and a similar genesis. For the limestones, Dunham's textural classification (Dunham 1962), plus its expansion (following Embry and Klovan 1971; see also Flügel 2004, chapter 8) was used. When clearly identifiable, microspar was considered as micrite for the purpose of the classification.

Burrows are poorly represented in these condensed rocks. Among them, *Spongeliomorpha suevica* is situated just below sequence boundaries and filled with the shelly material of the transgressive bed above. Burrows probably representing *Skolithos* cross transgressive beds. *Planolites* and other horizontal burrows are less obvious and appear only in beds with low shell density.

Carbonate material consists mainly of shells, shell fragments and micrite. Subordinate components are ooids, lithoclasts, echinoderm ossicles, and foraminiferal buildups. These components may reach exceptionally high percentages at particular levels. Shells come from the autochthonous or parautochthonous epi- and endobenthic macrofauna. Less common are nektonic ammonites and nautiloids. Micrite has probably been produced by the accumulation and disintegration of calcareous nannoplankton, as well as from the biodegradation of skeletal grains accumulating on the sea floor. As pointed out by Flügel (2004; p: 40) many modern high latitude carbonate muds are bioerosional and result from maceration of shells.

Mixed facies and facies associations

4. Fine-grained dominated, allochem-poor mixed facies association

This facies association comprises poorly lithified, fissile dark rocks, composed mainly of micrite, siliciclastic mud, and mixtures of both, and lacking dense skeletal concentrations. All facies of the association occur close to maximum flooding zones of major to intermediate sedimentary sequences, especially in the first few metres of the unit in both sections. Deposition took place at great depth, during long-term terrigenous starvation. Short-term pulses of starvation produced skeletal concentrations with a micritic matrix. Sedimentary structures are usually absent, as are well defined trace fossils. These facies only rarely show grain-size trends (i.e., minor sedimentary sequences), but are commonly inserted in more extensive shallowing-upward facies successions. Shells and shell fragments may occasionally occur as dispersed concentrations. The benthic fauna consists mainly of small bivalves such as *Disparilia elongata*, *Corbulomima bodenbenderi*, *Mesomiltha argentina,* *Mesomiltha.* sp. A, scaphopods, and small gastropods. Shells are partially dissolved or represented by moulds. Bivalve shells are usually complete and often articulated. Due to their more condensed nature, shell-rich marls (Ma-R) and shell-rich micritic mudrocks (MC1-R) were included in the facies association 5.

4.1. Marlstones (Ma)

This facies consists of poorly lithified, bioturbated dark-grey to orange-coloured marls and marlstones, which may contain some small shells and/or bioclasts in very low densities. Thicknesses range from 0.1 to 4 m. Regular intercalations of thin, regularly intercalated shell-beds (shell-rich floatstones -LF-R) are common in the AML section, where the marlstone facies is more widespread. This facies is moderately common in the vicinity of major MFZ.

4.2. Micritic mudrocks (MC1)

Dark, fissile, micritic mudrocks comprise clays and siliciclastic muds with subordinate micrite. This common facies usually occurs as a few dm- to m-thick beds. Bioturbation is high and lithification poor. Trace fossils are absent with the exception of tiny burrows (Ø <1 mm) with variable orientation. As in the case of the marlstone facies, thin intercalations of starvation-HS with skeletal concentrations are common. Micritic mudrocks of starvation/dilution sequences usually do not show trends in grain size but represent the whole dilution hemi-sequence. This facies exceptionally grades into argillaceous siltstones or siltstones. MC1 facies occurs very commonly in or close to high hierarchy MFZ.

4.3. Muddy micrite (MA1)

This rare facies consists of thin (<50 cm) beds of muddy carbonate mudstones (muddy micrite -MA1- in the mixed facies terminology) which are usually orange-coloured and highly bioturbated. Occasionally, ill-defined burrows are present. MA1 occurs at great depths and close to maximum flooding zones of major sedimentary sequences. In two cases, dispersed skeletal concentrations occur.

Interpretation. Marlstones (Ma) and micritic mudrocks (MC1) represent the dilution hemi-sequences of starvation/dilution sequences. At the base of the succession in the AML section, under general very low terrigenous input, alternations of marlstones (Ma) are developed as dilution hemi-sequences and shell-rich floatstones (LF-R) as starvation hemi-sequences, in the fashion of marl-limestone couplets. At equivalent levels in the less distal BAL section, the dilution hemi-sequences are composed of micritic mudrocks (MC1) while the starvation hemi-sequences are shell-rich marlstones (MA-R). There is a relatively higher proportion of carbonate mud at the base of the unit in the AML section with respect to the BAL section, which may be related to the more distal position of the first locality. The difference between dilution and starvation hemi-sequences lies in the relative amount of carbonate components i.e. micrite and bioclasts, and is a relative rather than an absolute feature. In the rest of the succession above the first 50 m, however, the input of terrigenous sediment seems to be higher in AML than in BAL. For instance, in the maximum flooding zone after the third major sequence boundary, the dilution hemi-sequences are compose of argillaceous siltstones in AML, and micritic mudrocks (MC1) in BAL. This may also imply a change in the rate of terrigenous input in AML from base to top. There are no indications in the literature about shifts in terrigenous input along the deposition of the unit. Main sources of terrigenous sediments are assumed to lie in the south and east (Legarreta and Gulisano 1989), which partially but not completely fits the observations made in this study.

All the facies of this association were deposited in deep, offshore environments, well below storm wave-base, in an outer ramp to basinal position. The shells of he intercalated starvation hemi-sequences do not show evidence of transport. This supports deposition in rather basinal settings, deeper than the reach of the most distal tempestites. The bioturbation and the dispersed shells of benthic molluscs indicate that there was always sufficient oxygen to support some benthic fauna. However, the usually dark colour and organic-rich nature point to some oxygen deficiency close to the sediment-water interface. The abundance of deposit-feeding molluscs and, in particular, the presence of two lucinid species of the genus *Mesomiltha*, presumed to have been well adapted to live in oxygen-poor sediments, support the idea of lowered oxygen levels and high accumulation of organic matter on the bottom during the deposition of these facies.

5. Dominantly fine-grained, allochem-rich, mixed facies association

This facies association comprises all rocks of mixed nature, rich in shells and small bioclasts and dominated by either siliciclastic, carbonate or mixed siliciclastic-carbonate dark and fissile mudstone. Beds are thin, with gradual contacts and without grain-size trends. The outstanding feature of this facies association is the very good preservation of the benthic fauna. The fossils occur in loosely packed shell concentrations. Specimens are small, usually articulated, and often in life position. Infaunal bivalves such as *Mesomiltha argentina*, *Mesomiltha*. sp. A, *Corbulomima bodenbenderi* as well as epifaunal and infaunal gastropods and scaphopods are usually complete, and their delicate ornamentation is very well preserved. The small epifaunal bivalve *Grammatodon securis* occurs in growth position and is well preserved but usually flattened in a dorso-ventral direction. Ammonites are abundant but flattened and fractured. These facies are present in both sections close to MFZ. However, they are better developed and more abundant in BAL. At the base of this section, the matrix is marly (Ma-R facies). Up-section, the matrix turns into less carbonate-rich micritic mudrocks (MC1-R facies). Still higher up, shell concentrations show stronger evidence of physical concentration, replacement of some bivalve species and an increase in the abundance of cementing serpulids and oysters, giving way to the allochemic mudrock facies (MC2-R). Physical sedimentary structures are lacking probably due to bioturbation. Trace fossils are rare, represented only by ill-defined, few mm-thick, horizontal, simple burrows and scarce, even thinner burrows with variable orientation (*Chondrites*?). Bioerosion is usually low, restricted to gastropod-like drill holes on lucinid bivalves (*Oichnus simplex*), rare octopus drill holes (*Oichnus ovalis*) and crab attacks on gastropod apertures. In one case, exhumed early diagenetic concretions had been bored by polychaetes (*Meandropolydora*) and cirripedians.

5.1. Shell-rich marls (Ma-R) and bioclastic shell-rich marls (Ma-B-R)

Shell-rich marls (Ma-R) consist of dispersed to loosely packed skeletal concentrations with a marly matrix. Shell fragments are scarce in the Ma-R. Bioclastic shell-rich marls (Ma-B-R), in turn, are composed of loosely packed skeletal concentrations with a bioclastic, marly matrix. The main difference between the two subfacies is the lower preservation quality of the fauna and the higher abundance of shell fragments in the Ma-B-R subfacies. This facies occurs in thin, up to 20 cm thick, planar beds with diffuse contacts with the overlying and underlying dark micritic mudrocks (MC1) or argillaceous siltstones (S-AS). The marly matrix gives a light-grey hue to the exposures of these sediments when weathered. Shell-rich marls are common close to the base of the succession in the BAL section. In AML, the bioclastic shell-rich marlstones occur at 130 m above the base, at the base of a fourth-order TST.

5.2. Shell-rich micritic mudrocks (MC1-R)

Shell-rich micritic mudrocks occur as thin, planar beds intercalated between siliciclastic mudrocks. Minor changes with respect to Ma-R facies define this facies. These differences are the less micritic matrix, some minor species replacements in the benthic fauna, the absence of ammonites from 30 m upward, and the presence of early diagenetic carbonate concretions. MC1-R appears at 18 m in the BAL section and replaces the facies Ma-R in the position of the starvation hemi-sequences. Up-section, MC1-R is replaced by MB1 facies.

5.3. Allochemic mudrocks (MC2-R)

This facies occurs in two ways: (a) as thin, planar beds of up to 20 cm, intercalated between fine-grained sediments, and (b) at the top of more complex starvation hemi-sequences (i.e., late starvation deposits). Lithologically, the facies consists of loosely packed shell concentrations in an argillaceous silt to fine silt matrix. This facies is intercalated between dark, fissile siltstones or argillaceous siltstones. Reworked early diagenetic concretions are very rare in this facies. Occasionally MC2-R type (a) occurs close to MFZ of intermediate (4th or 5th order) sequences. In these cases, the matrix is silt to sandy silt. Type (b) often has a coarser, silty to silty- sandy matrix and occurs at the top of starvation hemi-sequences, above facies MB1, within a muddier and less bioclastic upward trend. In some cases, foraminiferal buildups are important in this facies (see facies MB1 for a more detailed description). Shells in late starvation beds are rarely bored by *Caulostrepsis*, cirripedian pouches and *Entobia*, as well as by microborers.

Interpretation. The shell-rich marlstones (Ma-R), bioclastic marlstones (Ma-B-R), shell-rich micritic mudrocks (MC1-R) and type (a) allochemic mudrocks (MC2-R) represent starvation hemi-sequences of starvation/dilution sequences. This is evident from the higher proportion of carbonate mud in the matrix with respect to the sediments below and above, and the presence of in-situ shell concentrations absent in contiguous beds. The fine-grained nature of the facies in this association indicates deposition beyond the reach of fair-weather waves. Low-density concentrations of a fairly well preserved benthic fauna precludes (frequent) physical disturbance from tempestites or storm waves. Benthic fauna accumulated as a product of combined low net sedimentation (and hence relatively high shell production), and high preservation potential due to pore waters supersaturated with respect to calcium carbonate. The shell concentrations close to the base of the succession were deposited in an outer ramp or, more likely, basinal environment, certainly below storm wave base. Evidence is the excellent preservation of the fauna and the low density of the concentrations, which look mostly biogenic in nature. Shells in the deepest facies almost completely lack microborings. This may be related to the exclusion of endolithic algae below the photic zone. However, as there are several other organisms producing microborings, which do not depend on light, differences in this feature can also be explained by a low residence time on the sea floor. In the latter case, shells have never became exhumed and exposed to the activity of microborers. High turbidity related to assumed eutrophy for most of the time span represented by the section might have reduced the penetration depth of light. Facies MC2-R higher up has a higher proportion of shell fragments, lower percentage of articulated bivalves, and a higher proportion of encrusting fauna, all of which indicate physical reworking that generated disarticulation, breakage, sea-floor exposition, and some hard substrate for attachment of cementing biota. Another directed change in the sections is the progressive decrease of the relative abundance of deposit-feeders and subsequent increase of suspension-feeders usually associated with more agitated waters. At equivalent positions at the base of the succession, starvation hemi-sequences are composed of bioclastic floatstones in AML and bioclastic marlstones in BAL. The AML section was deposited in a more distal position and probably experienced less terrigenous input. As a result, the proportion of carbonate mud is higher in the AML section than in the BAL section, leading to the development of limestones. Up-section, the bioclastic marls are replaced in BAL by allochemic mudrocks, reflecting the increase of terrigenous input at the beginning of the HST. Facies MC2 type (b) is rarer than type (a). It was deposited in outer ramp to basinal environments but in a different stratigraphic position than the other subfacies. Facies MC2 type (b) represents the topmost part of starvation hemi-sequences developed at relatively great depth (e.g., at 283m in BAL, at 351m and 372m in AML).

6. Sandy and silty micrite (MA2) facies association

Three beds of sandy to sandy-silty micrite occur in BAL at 150 m. They are massive, yellowish to grey, well lithified, ca. 30 cm thick, and lack trace fossils. Sand grains are sub-angular and poorly sorted, ranging from very fine- to medium-grained. Skeletal remains are present in low densities. They are disarticulated and usually represented by their moulds or their micritized ghosts in thin-sections. Original calcitic shells are present as such. Occasionally, glauconitic grains are present. The three occurrences of this facies are intercalated in a coarsening-upward succession of siltstone to silty sandstone, in the middle part of a third-order HST. There is also an up-section increase in shell density from one MA2 bed to the next. Sandy and silty micrites share lithological features with facies association 4, but their position in the section and genesis seem to be completely different.

Interpretation. Sandy and silty micrites (MA2) are considered starvation hemi-sequences due to their higher carbonate content as well as to the presence of glauconite. Depth of deposition can hardly be deduced due to the lack of sedimentary structures or other sources of evidence. An offshore position below fair-weather wave-base can be assumed for the deposition of this facies. The scarcity of skeletal remains contrasts with other starved hemi-sequences. Possibly part of the fossil content in this facies was dissolved. This is supported by the high degree of micritization observed in the skeletal remains. The high degree of destruction of the skeletal remains, in contrast with what is found in shell beds with mixed or siliciclastic matrices, is corroborated by the findings of Kidwell et al. (2005) that shell loss by means of bioerosion and dissolution is higher in carbonate sea floors.

A similar genesis can be envisaged for silty and sandy floatstones and mudstones scattered throughout the sections, which exhibit dispersed to loosely packed skeletal concentrations and high levels of micritization.

7. Dominantly coarse-grained allochem-rich facies association

This facies association includes allochem- and sand-dominated mixed rocks. All of them are coarse-grained, contain skeletal concentrations exhibiting variable influence of sedimentological and biostratinomic processes, and abundant evidence of sediment starvation and environmental condensation. All facies in this association are placed in the starved part of starvation hemi-sequences.

7.1. Allochem-dominated mixed facies

7.1.1. Muddy allochemic limestones (MB1)

Muddy allochemic limestones are poorly sorted mixtures of shells, shell fragments, ooids, echinoderm ossicles and micrite, and subordinate siliciclastic mud and fine-grained sand. This facies is very common but never thick. Beds are tabular with thicknesses of usually a few decimetres although they may reach 2 m. Bioturbation is high and mechanical sedimentary structures are absent. The usually poorly lithified facies MB1 contains loosely to densely packed, occasionally clast-supported skeletal concentrations. Burrows are rare and restricted to simple horizontal tubes (*Palaeophycus*? and other unidentified burrows), *Spongeliomorpha suevica*, and rare very small burrows with variable orientations (*Chondrites*?). Due to the shelly nature of this facies, borings are more abundant and diverse than burrows. However, macroborings as well as microborings are less common than in other facies of this association.

This facies may represent (a) the complete starvation hemi-sequence of a S/D-sequence or (b) part of it. The first case occurs as thin beds at intermediate depths, in lower HST position, usually without erosional base, although base and top are distinct. Subfacies (a) is common close the base of the sections in the first 3rd order sedimentary sequence and occurs scattered near the MFZ of other sequences. Subfacies (b) of MB1 overlies coarse-sandy allochemic limestones or bioclastic allochemic sandstones, and is usually overlain by bioclastic mudrocks (MC2) within a succession of decreasing sand and increasing siliciclastic mud. Type (b) occurs also at intermediate depths that is, far from important sequence boundaries, but in a shallower position than type (a). While type (a) does not show trends in grain size and/or composition, type (b) is part of fining-upward successions and corresponds to upper starvation deposits. Shells in type (a) are smaller and accumulated in lower energy environments. The size of the shells depends on the species in the assemblages and is not related to physical sorting. Borings are usually of a small size. They include *Oichnus simplex*, and microborings. Larger borings such as *Gastrochaenolites*, *Trypanites*, and other unidentified borings are restricted to exhumed concretions or the large shells of *Aetostreon* sp. A common feature of MB1 type (a) is the presence of aligned, flat, early diagenetic concretions, containing dispersed to loosely packed shell concentrations. In many cases, the concretions are reworked, bored (*Gastrochaenolites*, *Trypanites*, and microborings) and encrustated with serpulids, small (*Ceratostreon*) and large (*Aetostreon*) gryphaeid oysters, crinoid holdfasts, bryozoans, and small colonies of scleractinian corals. Some of the concretions are bored and/or encrusted on both sides (Pl 1, Fig. 6).

Additional features of this subfacies are the subordinate presence of iron and pyrite replacing shells, and the scarce nautiloid *Cymatoceras perstriatum*.

Common features of MB1 type (b) are the presence of glauconite and iron in low amounts. Occasionally, echinoderm ossicles occur in high densities, as do ooids with nuclei consisting of fine quartz grains, bioclasts, or glauconite and which are occasionally replaced by iron. Borings are usually rare or absent. They consist of cirripedian pouches, *Entobia*, *Caulostrepsis*, *Trypanites*, and *Meandropolydora*, in addition to *Gastrochaenolites* in big shells. Micritization is generally low. *Spongeliomorpha suevica* is common at some MB1 levels, some decimetres below major sequence boundaries. Despite some rare oysters and serpulids encrusting shells, the main encrusting element in this facies is the agglutinating foraminifer *Placopsilina* sp. (see Chapter 7 for more details).

The outstanding feature of subfacies MB1 type (b) is the concentration of small nodules of the encrusting foraminifer *Placopsilina* sp. (Barnard). The concentrations reach a thickness of up to 2 m. These accumulations are more common in the AML section, where they give way to particularly thickly developed late stages of starvation hemi-sequences (e.g., AML section at 345 m, 350 m, 366 m, 371 m and 382 m; BAL section at 333 m). In most cases, the nodules are small, semiglobular, and grew on small bioclasts. In some cases, there is a mix of nodules and bigger lumps consisting of bioclasts fixed by the foraminifers and mud trapped inbetween. Such constructions are not restricted to this facies but are also present in other bioclast-rich siliciclastic mud such as MB2, MC2, muddy floatstones, and rudstones. However, it is in facies MB1 where they are best developed.

Closely related to this facies are muddy limestones (floatstones or micritic rudstones), which represent simply the less muddy versions of MB1.

Interpretation. This facies was deposited under low energy conditions, from just below the storm wave-base to below the fair-weather wave-base, i.e. the lower-middle to outer ramp. The mud was deposited out of suspension and episodically removed by the action of storms. Storms also carried some sand, glauconite, shell hash and ooids from shallower inner ramp environments. The benthic fauna was sometimes exhumed, disarticulated, bioeroded and encrusted. However, intensity and frequency of storms was usually not high enough to preclude the sedimentation of mud and/or cause the total reworking of the shells. The substrate was suitable for the development of an abundant and variably diverse fauna composed mainly of shallow infaunal, semi-infaunal and epifaunal bivalves plus gastropods, rare serpulids and abundant foraminifers. These elements, plus the non-skeletonized benthic taxa, completely churned the substrate and eliminated the sedimentary structures. Everything points to conditions of relative terrigenous starvation: the presence of shell beds, glauconite, iron replacement, and micritization of shells. However, for MB1 type (b) the sedimentation rate does not seem to have been very low. Evidence of this is the widespread presence of mud and the common absence of encrustation from serpulids and oysters. Permanent sedimentation of mud did not allow the larvae of encrusters to settle on the bottom. The foraminifers appear to have had different ecological requirements, needing sand and silt grains and small bioclasts to build their skeletons.

Type (a) corresponds to complete starvation hemi-sequences during whose development sea level changes did not cause distinct depth/environmental changes. Conversely, facies MB1 type (b) represents only a part of starvation hemi-sequences and is thus less time-averaged.

7.1.2. Sandy allochemic limestones (MB2)

Sandy allochemic limestones are heterogeneous mixtures of sediments dominated by shells, shell fragments, and sometimes ooids, with subordinate fine quartz grains. At early TST of major sedimentary sequences, this facies may have abundant ooids. In these cases, ooid density is higher in early rather than middle starvation deposits. Diverse amounts of siliciclastic mud and micrite can also occur. Autigenic glauconite is present in low to high amounts. Ammonites are abundant in this facies at middle starvation position. Beds of this facies usually have a thickness of a few decimetres. Skeletal remains reach high densities in this facies, equivalent to densely packed, matrix- or clast-supported concentrations.

Facies MB2 is placed at the base of most of the starvation/dilution sequences developed in major late HST and early TST. However, starvation/dilution sequences close above and below major sequence boundaries begin with bioclastic or micritic fine-grained sandstones (i.e. facies MD2 or MD2). When both, sandy allochemic sandstones (MB2) and allochemic (bioclastic) sandstones (MD2) co-occur in the same starvation-hemi-sequence, the second underlies the first. Lower contact is erosional when placed at the base the starvation/dilution sequences and gradual when it overlies the bioclastic sandstones facies (MD2). There is often a temporal trend in this facies: the lower part is sandier and shells are heavily worn and broken. The facies becomes less sandy and richer in bioclasts upward, and articulated bivalves and better-preserved shells are common at the top. There is also an increase in the amount of micrite and sometimes also of siliciclastic mud.

The top of this facies, e.g. the previously defined mid-starvation horizon, is distinctive but its contacts are gradual. It consists of a level with a higher density of well-preserved bivalve shells, many of them articulated. Ammonites usually reach high densities only at this level. There is an increase in the proportion of siliciclastic mud, which progressively gives way to muddy allochemic limestones (facies MB1) of the upper starvation bed. At this horizon the highest levels of encrustation and autigenic glauconite occur. The mid-starvation horizon is usually composed of facies MB2. However, in some cases it reaches a very high density of bioclasts and becomes a limestone, e.g. a bioclastic floatstone or micritic rudstone.

The sediment is completely bioturbated. Burrows are rarely preserved. They consist mainly of *Palaeophycus*, *Planolites*, and unidentified burrows of different diameters. *Spongeliomorpha suevica* occurs just below starvation/dilution-sequence boundaries, in major or medium late HST (i.e. high-energy, middle to inner ramp environments). The Y-shaped burrows are filled with bioclastic material. Ill defined, more or less vertical burrows occur at the sequence boundary of some starvation/dilution sequences. In this case, bioturbation blurred the bounding surface. Bioclastic lenses some decimetres below, within the siliciclastic facies, may represent burrow systems (BAL section at 367 m above base). Bioerosion is generally high. Micritization is usually very important, though the main destructive process at the base of beds with this facies is breakage due to high water energy. In basal shell beds shells are bored (e.g., *Gastrochaenolites*, *Trypanites*, *Entobia* and some cirripedian borings). In many instances, the outer layers of the shells are lost because of abrasion and the internal boxwork of *Entobia* is seen. In shells in mid-starvation position, *Gastrochaenolites* is less abundant and restricted to large shells such as *Myochoncha transatlantica,* and *Trypanites* and *Entobia* become more frequent. Microborings and general micritization become relevant features at mid-starvation positions.

Skeletal remains at the base of MB2 consist of large and sturdy shells that are usually disarticulated and broken. There are abundant shell fragments of thinner-shelled species, but also deep burrowing bivalves such as *Panopea dupiniana* and *Pholadomya gigantea* in life position, and some delicate complete shells. Encrustation by gryphaeid oysters and serpulids may be locally important, but is usually low. Size range and species diversity increases towards the mid-starvation position. There, encrustation reaches high levels. (For an in-depth discussion on taphonomic patterns, see chapter 8.) Agglutinating foraminifers encrust shells to a moderate to high degree, particularly at mid-starvation level. Bryozoan colonies occur in low amounts. Small patches of the serpulid *Parsimonia antiquata* and/or the gryphaeid oyster *Ceratostreon* sp. occur precisely at the level of mid-starvation. These buildups grew on big ammonites or large semi-infaunal bivalves such as *Myoconcha transatlantica*. In the AML section at 281 m above the base, a large serpulid and oyster buildup 1 m high and at least 50 m wide (Pl. 7, Fig. 1) is situated at the mid-starvation position. In the BAL section at 332 m above the base, abundant and large oyster patches up to 1 m in diameter occur at the base of the starvation hemi-sequence. The buildups grew on *Steinmanella vacaensis* shells that were exhumed when the top of the underlying dilution hemi-sequence was eroded. *S. vacaensis* shells are disarticulated and heavily bored (*Gastrochaenolites* and *Trypanites*). At 374 m above base in the BAL section, branches of *Sarcinella occidentalis* buildups are abundant, partly in vertical position and partly horizontally. High densities of ammonites occur in this facies also at the mid-starvation point.

Occasionally reworked (encrusted and bored) early diagenetic concretions occur. At 142 m above base in the BAL, patchy dissolution affected the sediment in a starvation hemi-sequence. In parts of the bed, only calcitic shells are found in a poorly lithified marly matrix, while in other parts a fully cemented, thick bed with a high density of both, calcitic and aragonitic shells occurs. (For a deeper discussion on dissolution patterns see chapter 8.)

Interpretation. Sandy allochemic limestones (MB2) represent condensed deposits generated under low input of terrigenous sediments. Evidence of this is: the presence of shell beds and glauconite, the occurrence of iron replacements, and high levels of encrustation and borings. As such, these condensed beds correspond to the early and middle part of starvation hemi-sequences. The lack to low proportion of mud indicates deposition above or immediately below fair-weather wave-base, in inner to middle ramp environments. Ooids, shells, and shell fragments came from shallower shoreface environments, probably transported by storm-induced currents. Fair-weather and storm waves permanently removed fine-grained sediment and reworked the benthic fauna. These high-energy processes fragmented small shells, most of which became dissolved. The more resistant thick shells became exposed and then bored and encrusted. This setting operated for a considerable time span leading to the concentration of shells as well as to the mixing of faunas of different ages and of different taphonomic signatures. Towards the end of the transgression (i.e. at the top of the mid-starvation level) shells accumulated in great densities producing a significant habitat change. The substrate became more appropriate for semi-infaunal and epifaunal elements and was no longer suitable for most infaunal bivalves. Energy decreased and fair-weather waves hardly reached the bottom. Terrigenous input was at a minimum during the maximum transgression. Under these conditions the mid-starvation deposits developed. Due to bioturbation, sand grains, bioclasts, ooids, and mud became mixed. As a result, no sedimentary structures are preserved.

From a stratigraphic point of view, facies MB2 represents transgressive lags (Kidwell 1991b) or a part of it, condensed onlap deposits (Kidwell 1991b) and so-called mid-cycle condensed shell beds (Abbott 1997). The first two elements correspond to the lower starvation deposits described above, while the third corresponds to the middle one. Usually, there are no relevant lithological differences between lower and middle starvation deposits. Differences exist mainly in taphonomic features. Transgressive lags are the result of shoreface erosion (ravinement process) during transgression after regression left the sea floor sub-aerially exposed or at very shallow depths. A characteristic feature of lags is the dominance of large and thick shells, which became exhumed during erosion and survived despite the high water energy and the intense bioerosion. The fate of thinner shells differed as they were easily broken and dissolved (Fürsich and Pandey 2003). The outcome of this process is a fossil assemblage enriched in thick-shelled species, and taxonomically biased. Onlap condensed deposits represent early transgressive deposition not related to erosion of previous deposits. While in lags old shells pre-dating the transgressive erosion dominate, in condensed onlap deposits new shells prevail, accumulating after the transgressive erosion. Onlap condensed deposits are exposed to constant wave agitation and low sedimentation rate and thus may develop taphonomic features similar to those of transgressive lags. In this study the distinction of these two elements is not clear. Shells pre-dating the transgressive erosion, when present, probably became mixed with newer ones. One species suspected of coming from older HST deposits is *Steinmanella vacaensis*. *S. vacaensis* occurs articulated and usually in life position in mudrocks and sandy siltstones of dilution hemi-sequences. It is also a common element close to the base of some lower starvation shell beds, where it appears disarticulated and usually bored and encrusted. In section BAL at 332 m above base, *Ceratostreon* buildups grew on disarticulated shells of *S. vacaensis.* This is a clear example of psalimpsest shells becoming incorporated in the sediments above the transgressive surface. Conversely, *Myoconcha transatlantica* is a thick-shelled species with a semi-infaunal sessile life habit that appears also in early starvation beds. Shelly, stable substrates, rather than sandy substrates subject to high rates of sedimentation have been the proper habitat of this species.

7.2. Sand-dominated mixed facies

7.2.1. Micritic sandstones (MD1)

Micritic fine-grained sandstones are mainly composed of poorly sorted sand grains and micrite. Micrite may be partially or completely recrystallized (neomorphism). It never reaches high proportions. Bioclasts, complete shells, ooids and silt are also present. Concentrations of iron are usually high, while autigenic glauconite reaches medium to high levels. Frequency is moderate to low, and thickness ranges from 0.1 to 1 m, exceptionally 3 m.

Facies MD1 beds is often completely massive with the exception of hummocky cross-stratification occasionally observed on top of some beds. Traces are present in low frequencies. *Planolites*, *Palaeophycus* and other unidentified burrows are relatively common, while possible openings of *Arenicolites* and tiny burrows considered as *Chondrites* are rare. In some cases, *Spongeliomorpha suevica* occur crossing erosional surfaces bounding two starvation/dilution sequences.

This facies occurs at different positions in the sections and in variable sequence stratigraphic settings. As a result, three different types can be distinguished: (a) at the top of coarsening-upward dilution hemi-sequences with high levels of glauconite and some ooids, (b) in high-energy environments subject to parts of or complete starvation hemi-sequences, and (c) in moderate-energy environments of the same setting. Facies MD1 in the lower part of starvation hemi-sequences corresponds to type (b). It is overlain by muddy allochemic limestones (MB2 facies), and rarely by muddy bioclastic floatstones (L-F) or bioclastic mudrocks (MC2). Type (c) usually has higher proportions of siliciclastic mud and micrite, and less glauconite and iron.

Facies MD1 as part of starvation hemi-sequences contains dispersed to densely packed, matrix-supported skeletal concentrations. In high-energy MD1 (type b), skeletal remains are mainly disarticulated and exhibit signs of physical reworking (breakage and abrasion), in an iron-rich matrix. There is a size bias towards large and thick shells. Bioerosion is high in these settings (Pl. 3, Fig. 3), with *Gastrochaenolites, Trypanites, Entobia,* cirripedian pouches and other borings. Encrustation is usually moderate to low, despite isolated small serpulid patch reefs. Conversely, in MD1 characteristic of medium-energy both, bioerosion and encrustation are usually low, while micritization may be high. Ammonites occur on top of micritic sandstones in starvation hemi-sequences and may reach high densities in MD1 of medium-energy. Micritic sandstones placed at the top of dilution hemi-sequences do not contain skeletal concentrations.

Interpretation. Occurrences of this facies seem to have different origins. A feature shared by all micritic sandstones is their condensed nature, evidenced by the presence of iron, autigenic glauconite, the complete bioturbated fabric, and skeletal concentrations. Another common element of this facies is the presence of micrite and micritized bioclasts. This, plus some evidence of partial lack of original aragonitic skeletal remains, points to selective removal of the benthic fauna by micritization and dissolution. This process lowered the proportion of bioclasts as well as increased the amount of micrite in the matrix.

In high-energy MD1 (type b), the unexpectedly high content of micrite is interpreted as due to micritization and/or physical destruction of carbonate shells. These examples were deposited in the inner ramp, under constant wave agitation. Medium-energy MD1 beds (type C), in turn, often with significant amounts of silt (i.e. micritic silty sandstones), were deposited below fair-weather wave-base, on the middle to outer ramp. Examples of micritic sandstones at the top of dilution hemi-sequences (type a), in middle to late HST, are considered as having formed by means of toplap condensation (low net accumulation due to bypassing of sediment while clinoforms prograded), in high-energy settings such as the inner ramp. High levels of bioturbation and the lack of sedimentary structures preclude a more accurate environmental interpretation of this subfacies. Several features shared between type (a) micritic sandstones and highly bioturbated fine-grained sandstones (facies S-FS) indicate a similar origin.

High-energy micritic sandstones form thick beds with particularly high levels of iron in the first starvation bed above the first 3rd order sequence boundary in both sections. Shell beds enriched in large, thick-shelled species support its interpretation as lag and/or condensed onlap deposits (sensu early TST shell-bed of Fürsich and Pandey 2003; Kidwell 1991a).

The micritic sandstone facies in the BAL section at 462 m above base represents a special case. This transgressive bed is 6 m thick and probably represents the base of a fourth or fifth order sedimentary sequence. The base of this bed is a loosely packed, 20 cm thick shell bed with an oolitic and bioclastic packstone matrix. Immediately above and separated by a sharp surface there is an approximately 3 m thick orange-coloured micritic sandstone, which is overlain by a light-grey bio-oo-grainstone of similar thickness, with a shell concentration on top. Branching burrows with a diameter of 10-20 cm mark the “contact” between these two lithologies (Pl. 6, Fig. 1). Below the contact between the micritic sandstone bed and the grainstone, the galleries are filled with the oolitic grainstone of the upper bed. There is an upward increase in the density of grainstone-filled galleries, up to the contact, above which the oolitic grainstone dominates over the micritic sandstone. At this level, galleries are filled with micritic sandstone and the dominant sediment is oolitic grainstone. A plausible interpretation for this pattern would be the action of benthic bioturbators, which mixed the sediments from above and below an important surface. However, the bioturbator would have taken micritic sand from below to fill the galleries above the “contact” which looks like an unexpected behaviour. Another, more likely interpretation would involve several not-recorded changes in sedimentation. In some cases only the fill of burrows were preserved and are the only evidence of a particular sedimentation episode, the corresponding layer having been eroded subsequently.

7.2.2. Allochemic sandstones (MD2)

Allochemic sandstones are bioturbated mixtures of usually poorly sorted, very fine- to fine-grained sandstones with some shells, shell fragments, echinoderm ossicles, and ooids. Micrite and siliciclastic mud can also participate. Autigenic glauconite and iron usually reach high levels. Although quite abundant, facies MD2 rarely exceeds 40 cm in thickness.

Bioturbation is complete. Rare, doubtful and poorly preserved trough? cross-stratification, inferred from the orientation of shells is the only physical sedimentary structure found in this facies. Bioturbation consists of occasional *Planolites* and other poorly preserved, mostly horizontal, simple burrows. Bioerosion is usually very high and characterized by borings such as *Gastrochaenolites*, *Meandropolydora*, *Trypanites*, *Caulostrepsis*, *Entobia*, cirripedian borings, and microborings. The bored substrate consists mainly of shells.

Allochemic sandstones are always found at the base of starvation hemi-sequences. This facies is typically underlain by an erosional surface corresponding to a minor sequence boundary (= transgressive surface). The allochemic sandstones grade upwards into sandy allochemic facies (MB2) becoming shellier and less sandy. Facies MD2 is located very close to important sequence boundaries, either below or above.

The skeletal concentrations in this facies are densely packed, but the rock is supported by the sandy matrix. As in the case of facies MB2, which usually overlies this facies, shells in MD2 show evidence of high physical reworking, i.e. disarticulation, abrasion, breakage, and size sorting. Large and thick shells that are usually bored dominate the assemblages. Encrustation by oysters and/or serpulids may be locally abundant. Faunal content and taphonomic features are similar to facies MB2 to which this facies is closely related. Occasionally, the serpulid *Parsimonia antiquata* forms small buildups or occurs reworked in great abundance. Ammonites may be locally present.

Signs of strong micritization and dissolution characterize some occurrences of MD2. These beds are not fully lithified and occur at greater depth than expected for this facies. These examples may have been deposited as sandy allochemic limestones (facies MB2), which were further modified during diagenesis.

Close to the third major sequence boundary in BAL (at 391 and 401 m above base), this facies contains pebbles composed of fine-grained sandstone with cross-lamination which exhibit borings of *Gastrochaenolites* and *Trypanites* and which are encrusted by small oysters, serpulids and bryozoans. These pebbles clearly represent the reworked topmost part of the underlying dilution hemi-sequence.

Interpretation. Allochemic (bioclastic) fine-grained sandstones (MD2 facies) were deposited in high-energy environments, above fair-weather wave-base, on the inner ramp. They represent the earliest facies of the starvation hemi-sequence in which it appears. During deposition of these rocks, fair- and storm-weather waves acted on the sea floor precluding sedimentation of fine-grained material. During the advance of the transgression, shoreface erosion reworked the top of the former dilution hemi-sequence. The reworked pebbles described above are clear evidence of the ravinement process. Destruction of the thin faunal elements in the high-energy environment resulted in mechanical sorting in favour of large and thick shells. Activity of infaunal organisms erased sedimentary structures as well as mixed sediments, thus producing the heterogeneous and highly bioturbated fabric.

Judging from their relative positions, and according to Walther's law, the allochemic sandstones seems to have been deposited in more proximal environments than the sandy allochemic limestone facies. This reasoning is based on the fact that MD2 regularly underlies MB2 with gradual contacts.

Carbonate facies and facies associations

Limestones are the least represented rock type in the sections. Limestone facies were separated in two categories, fine-grained and coarse-grained limestones, following the descriptive criteria adopted for this analysis. Genetically, two types of limestones can be distinguished: (a) those accumulating as high-density skeletal concentrations in a mixed or siliciclastic matrix (micrite, siliciclastic mud and sand) and (b) those forming during complete starvation of terrigenous sediments as accumulation of shells, shell fragments, ooids, lithoclasts, and micrite. The first type comprises floatstones and micritic rudstones. It is closely related to mixed rocks and represents starvation hemi-sequences in a siliciclastic/mixed ramp setting. Moderate to low density of skeletal remains in a mixed matrix would generate a mixed rock and not a limestone. The second type comprises mudstones, wackestones, packstones and grainstones. These "pure" limestones occur in most of the starvation hemi-sequences deposited in the last 150 m of the section and seem to be also related to a change to a more arid climate. The main difference between both types is in the matrix: with siliciclastic grains in the first type and without them in the second.

8. Fine-grained limestone facies association

8.1. Mudstones (LM-R) and wackestones (LW-R)

This facies comprises limestones supported by micrite and with rare (wackestones) or very rare to absent (mudstones) allochems, and with few components larger than 2 mm. In one case, a wackestone bed contains a dispersed skeletal concentration. Grains, when present, consist of bioclasts. Siliciclastic mud may be present. Bioturbation is high, represented by poorly defined, unlined burrows whose fill differs from the matrix (*Planolites*).

The facies is very rare. It appears either close to the base of the section, where a fast transgression took place or, at 450 m above the base in BAL, in a fairly deep ramp setting, commonly intercalated between fine-grained siliciclastics. Thickness ranges from 20 to 70 cm. Beds are planar with sharp but not erosional contacts.

Interpretation. These rare facies comprise thin beds of micrite-dominated rocks, which are usually orange-coloured and highly bioturbated. High amounts of micrite and lack of siliciclastic mud indicate lack of terrigenous input. According to their position in the sections and to their fine-grained nature, these facies were deposited below storm wave-base, in outer ramp to basinal environments.

8.2. Floatstones (LF-R)

Shell-rich floatstones comprise a wide variety of rocks in terms of components. They include all rocks with less than 10% siliciclastic material, more than 10% of allochems larger than 2 mm, and with a micritic matrix. Similar rocks but more densely packed and bioclast-supported are considered as micritic rudstones. Contribution of sand and siliciclastic mud is variable. Allochems are usually mollusc and serpulid shells and shell fragments. Ooids may be abundant in particular beds. Echinoderm ossicles are common and locally abundant. Ooids are either tangential or more commonly completely micritized and usually superficial, i.e. the cortex diameter is smaller than that of the nucleus (Flügel 2004). Ooid nuclei are composed of bioclasts, glauconite, and less commonly sand grains and lithoclasts (intraclasts), and may be replaced by iron or recrystallized. Autigenic glauconite and iron-rich matrix generally are rare but at particular levels may be abundant. Microbial crusts, intraclasts and pellets are less represented. In the BAL section at 109 m above the base, there is a floatstone bed rich in medium-sized angular potassium feldspar grains of probable volcanic origin. Beds are tabular with a thickness of commonly less than 30 cm.

Except in a few cases, shell-rich floatstones characterize starvation hemi-sequences in high hierarchy late transgressive, maximum flooding and early highstand settings. Two main types of floatstones are present: those developed in low-energy/deep environments equivalent to the type I of Plumley's Energy Index Classification (i.e., with minimum water agitation) (see Flügel 2004 pp. 591-593) and the rest, which show more or less abundant skeletal remains with signs of transport. The last type partially coincides with type II of the above-mentioned classification, e.g. deposition in alternately agitated and quiet water. At the parasequence scale, floatstones may comprise the whole starvation hemi-sequence or only part of it.

The shell-rich floatstones are always bioturbated. In the examples deposited at intermediate depths inhomogeneities in the distribution of the bioclasts resembles sometimes the presence of amalgamated tempestites. However, clear evidence is lacking probably due to bioturbation and the limited thickness of the strata. Trace fossils are not evident at the outcrop, but in thin-sections, simple, unlined burrows of different sizes are abundant. Micritization is usually pervasive and sometimes erases shells so that they are only visible with a careful study of the microfacies. At the base of the AML section, shell-rich floatstone beds contain abundant predatory drill holes of probable gastropod origin in the shells of the small lucinid bivalve "*Mesomiltha*" *argentina*. Small gastropods in the same assemblage exhibit *Oichnus ovalis* and signs of probable crab attacks at their apertures. Other borings such as cirripedian pouches and *Entobia* are rare and occur in shallower settings.

Shells and shell fragments are concentrated in loosely packed to densely packed but matrix-supported shell beds. Skeletal remains range in size from small shell fragments to complete valves. Encrusting agglutinating forams, gryphaeid oysters and serpulids are moderately common and only locally abundant.

Interpretation. Shell-rich floatstones occur at different stratigraphic positions, because this facies comprises all dispersed, loosely packed and densely packed, matrix-supported skeletal concentrations with micritic matrix, regardless of the nature of the shell-producing species. LF-R strata are condensed deposits and developed in starvation hemi-sequences. Floatstones form characteristically in outer ramp to basinal environments. In shallower settings, allochem-supported fabrics are expected.

In the AML section, shell-rich argillaceous floatstones occur at the very beginning of the succession, in the context of a major MFZ. These floatstones share their genetic origin with facies Ma-R and MC1-R of facies association 5. All of them were deposited in basinal settings, mostly beyond the reach of physical disturbing agents. The fauna is very well preserved with respect to articulation, percentage of individuals in life position, absence of abrasion, and negligible levels of encrustation.

Other floatstones show evidence of physical disturbance. In these cases, micritization is high and seems to be an important destructive process that attacked aragonitic shells more than calcitic ones. The accumulation of small bioclasts was probably due to storm surges. Tempestite evidence is bimodal size sorting (small broken shell fragments and complete or even articulated shells), articulated bivalves with their commissure plane horizontal (i.e. exhumed and quickly reburied), and low levels of encrustation that indicate a short residence time on the sea floor. Intraclasts represent resedimented limestone particles probably produced by exceptionally strong storm waves.

Ooids included in the floatstones formed in higher-energy inner-ramp settings and were transported to deeper environments by storm-induced currents.

Towards the top of the member in the BAL section, bioclastic and ooid-rich floatstones (occasionally micritic rudstones) containing partially dissolved *Isognomon* may represent lagoonal deposits.

8.3. Coral patch reefs (LReefs)

At 503 m above the base of the BAL section small coral patch-reefs with a texture ranging from floatstones to micritic rudstones, a diameter of a few metres, and a height of less than 3 m occur (Pl. 6, Fig. 5). In the patches, different kinds of colonial corals are usually broken, heavily bored, and not in growth position. The accompanying fauna consists of sponges, serpulids, bryozoans, and oysters. Tabular and domal growth forms dominate at the base of the buildups and are replaced by bulbous and branching colonies in most of the remaining reef. Bioerosion becomes very prominent towards the top of the patches, characterized by *Gastrochaenolites*, *Entobia*, and *Trypanites*. Inbetween the patches mollusc shells are concentrated in low densities in a micritic matrix. Occasionally small delicate branching monospecific bush-shaped colonies, a few decimetres in diameter, occur in growth position some metres above the rest of the reef. In the Agua de la Mula section, larger coral patches were observed at similar stratigraphic positions.

Interpretation. The coral patch-reefs of the BAL section probably developed at middle ramp position. The dominating micritic matrix and the low density of skeletal remains speak against an inner ramp setting as proposed by Lazo (2005). Besides, these buildups developed above oolitic and bioclastic grainstones of the lower shoreface in a late TST setting that according to Walther’s law suggests a deeper environment. These colonies grew under very low to absent terrigenous input, in minor to medium or major MFZ. This is the only widespread coral reef-building phase within the whole succession. For a more detailed discussion of the environmental context of these reefs, see the section “Organic Buildups” in Chapter 8.

9. Coarse limestones facies association

9.1. Packstones (LP) and grainstones (LG)

Packstones are rare within the sections because shells and shell fragments are commonly larger than 2 mm. Most micrite-rich, shell-supported rocks were thus included in the micritic rudstone facies (LRm). Likewise, grainstones are absent up to about 460 m. In the last 150 m of the BAL section (in AML this part of the unit was not studied), where limestones are common and dominate the sedimentation during terrigenous starvation, oolitic and bioclastic grainstones and packstones as well as intermediate textures become more common. Intermediate textures refer to heterogeneous beds that show both grainstone and packstone textures.

The dominant components of these facies are ooids and/or bioclasts. Grainstones are usually composed of ooids and some highly abraded (rounded) bioclasts. Packstones are characterized by better-preserved shells. The packstone matrix is usually microsparitic considered here as recrystallized from micrite. Intraclasts are common to abundant especially in the packstones. Intraclast matrix and grains are similar to the ones found in the host rock but the orientation of the bioclasts differs. Microbial crusts are rarely found. Ooids are usually simple, superficial or normal. Compound ooids may occur. Nuclei can be quartz grains, bioclasts or glauconite. Micritization is always complete and iron replacement is common. Ooid diameter is close to 0.5 mm but may reach 0.9 mm. Oolitic grainstones are usually associated with larger, thinly coated grains.

Thickness of grainstone beds range from a few decimetres to a few metres. Packstones are thinner, usually less than 1 m. Despite some rare relics of cross-stratification in the grainstones, physical sedimentary structures are usually absent. Bioturbation is high in both facies, and particularly evident in the very heterogeneous packstones. Sorting ranges from poor to good in the LG facies and poor to very poor in the packstones. Trace fossils are in general rare. Small burrow systems were detected in packstones, and simple, horizontal, a few to 10 mm thick burrows with an infilling differing from the host rock, identified as *Planolites,* are common. Well-developed galleries of *Spongeliomorpha suevica* occur below erosional contacts between siliciclastic and carbonate facies, which, in some cases, correspond to packstones or grainstones. In the BAL section, at 462 m above the base, thick galleries are developed (see facies MD1). Microborings are common.

Packstones and grainstones usually represent the whole starvation hemi-sequence. Grainstones overlie fine-grained sandstones bounded by an erosion surface. In some cases, there are erosional surfaces in grainstones, associated with shell concentrations and lithoclasts. Packstones are intercalated between finer-grained siliciclastic sediments.

Grainstones may contain loosely packed shell concentrations consisting mainly of *Pterotrigonia coihuicoensis* and some *Isognomon* near the top of the section. Shells are usually disarticulated, broken and abraded. Small bioclasts are heavily worn, well rounded, and sometimes thinly coated or forming the nucleus of ooids. Packstones exhibit bimodal size sorting, with small bioclasts and ooids supporting the rock, and rare larger shells forming dispersed to loosely packed concentrations. Rarely, sharp-based levels with higher concentration of bioclasts occur in packstone beds. Small serpulid buildups grew in this facies. Micritization is high. Lithification is complete. Shells and bioclasts do not show preferred orientation patterns.

Interpretation. The oolitic and bioclastic grainstones and packstones represent shallow marine carbonates forming during starvation hemi-sequences. Grainstones were deposited in the inner ramp, above the fair-weather wave-base (Burchette and Wright 1992) under high-energy conditions, during late stages of intermediate or major highstand systems tracts. The formation of ooids and the generally high abrasion and breakage of the bioclasts suggests deposition within the shoreface. Packstones were deposited at greater depth, below the fair-weather wave-base or close to it, based on the presence of micrite and the better preservation of the fauna. Bimodal size sorting of bioclasts and chaotic orientation of shells indicate deposition as amalgamated proximal tempestites, which were later mixed by burrowing organisms. Storm-induced currents transported ooids from the high-energy inner ramp to the offshore. An upper? middle ramp position is proposed for this facies. In both cases, low accumulation rates caused high levels of bioturbation that erased the sedimentary structures. Micritization and probably dissolution reduced the shell density in the packstone facies. Ooid nuclei change up-section from quartz grains to bioclasts, indicating long-term starvation. Erosional surfaces within grainstones and grainstone/packstones are associated with discrete shell concentrations and may indicate the amalgamation of S/D sequences.

9.2. Micritic rudstones (LRm)

The term micritic rudstone refers to limestones supported by shells larger than 2 mm and with a micritic matrix. Components are poorly sorted shells and shell fragments, semi-globular foraminiferal buildups, and subordinated ooids.

Facies LRm developed in two different settings. Low-energy LRm appears in the MFZ of the third 3rd order sedimentary sequence, between the *diamantensis* and the *groeberi* ammonite zones, and less frequently at other levels. Occurrences are usually thin, i.e. less than 20 cm thick, but may reach almost 3 m. In the latter case, less shelly (muddier) levels are intercalated. Shell packing is very dense. Shells are delicate and small, and belong mainly to small bivalves such as *Corbulomima bodenbenderi, Mesomiltha* spp., *Disparilia elongata*, and astartids, whereas gastropods, oysters, and serpulids are rare. Occasionally abundant echinoderm ossicles occur. Valves are usually horizontally oriented, fragmented and little to moderately abraded. Microborings and micritization are rare to common, although occasionally some bioclasts may be highly micritized. Pyrite replacing shells is a common feature in most beds. Macroborings are rare to absent and restricted to few *Entobia* and *Gastrochaenolites* on *Cucullaea gabrielis* shells. The matrix is micrite or microsparite. Iron may reach high levels in the matrix. These shell beds represent complete starvation hemi-sequences and do not show textural trends from base to top. No physical sedimentary structures were found nor were discrete trace fossils.

High-energy (muddy) LRm occurs in starvation hemi-sequences developed in the middle part of major and intermediate TST or HST. LRm comprise complete starvation hemi-sequences as well as just the lower or upper part of them. In some cases, LRm partly consists of densely packed accumulations of foraminifer nodules (see facies MB1), together with tempestitic deposits of shells and small bioclasts. Thickness ranges from a few decimetres up to a maximum of 1 m. Particular features of this subfacies are the presence of siliciclastic mud in the matrix, the presence of autigenic glauconite in low to high amounts, usually low but occasionally high degrees of encrustation (foraminifers, oysters, and serpulids), rare high abundance of ammonites, moderate levels of iron, occasional presence of pyrite and phosphate replacing shells, and a very high proportion of echinoderm ossicles at particular levels. High levels of bioerosion are due to microborings. Macroborings (*Gastrochaenolites, Entobia, Trypanites,* cirripedian borings, *Caulostrepsis* and rare *Oichnus simplex*) are rarer, reaching high levels only in a few beds. Orientation of shells is usually chaotic, the fabric is heterogeneous, bimodal sorting is not always the rule. Burrows were not seen except a few poorly defined, simple, horizontal tubes and a bed crowded with *Planolites* at its base. The benthic macrofauna is diverse and variable. It consists of small to large infaunal, semi-infaunal, and epifaunal bivalves, as well as small gastropods and serpulids. Serpulids may form small patches.

Interpretation. Low-energy micritic mudstones were deposited at depths greater than the other subfacies. Shells bear little evidence of reworking or exposure on the sea floor, which indicates rapid deposition and/or little or no winnowing. The species that compose the shell concentrations are the same that are present in facies 4 and 5, which accumulated in deep settings. This facies is here interpreted to represent amalgamated distal tempestites that accumulated over a long period. Between storms mud accumulated at very low rates and small shallow-infaunal and some epifaunal bivalves colonized the substrate. Storm surges periodically swept the bottom and buried both, autochthonous and parautochthonous shells. These shell beds represent starvation hemi-sequences. Their condensed nature with respect to the sediments below and above is supported by (1), intercalation within less starved siliciclastic facies, (2) presence of skeletal concentrations, and (3) presence of an iron-rich matrix. When thickly developed, this facies may comprise more than one starvation/dilution sequence amalgamated due to considerably reduced terrigenous input in deep environments. The low-energy LRm facies was deposited on the outer ramp, within the reach of only distal tempestites.

It is worthwhile to point out that there is one occurrence of thickly developed low-energy LRm in each section at an equivalent position (i.e., similar distance from the base, same ammonite biozone and same position with respect to intermediate and major sequence boundaries). I interpret this MFZ as the Neuquén Basin equivalent of the Faraoni event (for more information see chapter on stratigraphy).

The high-energy, muddy, micritic rudstones reflect a depositional environment similar to that of the related facies MB1 i.e., low energy conditions, a position below the fair-weather wave-base to just below the storm wave-base (lower middle to outer ramp). The mud settled out from suspension and was episodically removed by storm waves and currents. Terrigenous input was low. High levels of encrustation and microborings may indicate that shells were repeatedly exposed probably due to winnowing.

The high-energy muddy micritic rudstones were deposited at depths greater than the packstones. This is evident from the higher proportion of mud, the better preservation of shells and shell fragments, and their position within depositional sequences.

Facies successions

Sedimentation of the marine succession of the Agua de la Mula Member was driven by different types of cyclicity. In this study, I argue that this cyclicity was governed by climatic changes that influenced sedimentation by eustatic sea-level changes, changes in the rate of terrigenous input or most probably both. Facies successions are hence closely related to the development of these cycles and to the interaction between the different types of cyclicity. The dominating feature of the sections are the so-called starvation/dilution sequences, which are the product of the shortest cyclicity identified and interpreted as reflecting the precession cycles of the Milankovich band (for further discussion see chapter on stratigraphy). The obvious shallowing trend from base to top of the Agua de la Mula Member is best explained as due to the infilling of the basin or to a lowering of the subsidence rate. This, plus a progressively lower terrigenous input towards the top and the effects of the interaction of different hierarchies of cycles, is probably the reason why different parts of a sedimentary sequence (e.g. early HST or late TST) are not represented by characteristic re-occurring facies.

Major trends

A tendency to lower terrigenous input up-section is evident. In the lower half of the sections, nearly up to the end of the Hauterivian, starved hemi-sequences are predominantly siliciclastic even in relatively deep middle to outer ramp facies. Above the major MFZ in the uppermost Hauterivian, thick siliciclastic facies successions are rarer and restricted to middle or major HSTs, and starvation hemi-sequences are mostly limestones (floatstones, packstones, micritic rudstones and oolitic grainstones).

Trends in alternating bedding

Whereas coarsely interlayered bedding dominates HSTs in the lower half of the sections, heterolithic stratification replaces it in the upper part. The same pattern is observed in particular dilution hemi-sequences, where the succession begins with coarsely interlayered bedding and grades into heterolithic rocks (see for example section AML at 340 m in Appendix-Fig. 2). In section BAL at 215 m (Appendix-Fig. 1) flat-bedded sandy layers (coarsely interlayered bedding type 5) are intercalated between rocks with wavy type heterolithic bedding. The opposite pattern is also present, i.e. coarsely interlayered bedding as main sedimentary structures with intercalations of heterolithic stratification. Coarsely interlayered bedding represents outer to middle or even inner ramp tempestites. Heterolithic stratification, in turn, was deposited close to the fair-weather wave-base in the upper middle to lower inner ramp. The change from coarsely interlayered bedding to heterolithic bedding thus indicates a shallowing trend. Coarsely interlayered bedding is the common stratification pattern under high sedimentation rates and sufficient accommodation space, while heterolithic stratification replaces the former when accommodation space was reduced (or created at lower rate), that is, close to the top of the second third-order highstand systems tract.

Discussion

Depositional model

The depositional model proposed for the Agua de la Mula Member is an open marine ramp (Legarreta et al. 1993; Legarreta and Uliana 1991) developed under supposedly fairly constant subsidence (Spalletti et al. 2001b). Storm deposits are abundant throughout the sections and allow to define the succession as a storm-dominated ramp. Other features of the basin are discussed in the following sections.

Restricted versus open marine ramp

It has been proposed that, despite the complete development of a volcanic arc to the west during Late Jurassic and Early Cretaceous times, the Neuquén Basin was connected with the Pacific Ocean (Spalletti et al. 2000; Spalletti et al. 2001b). Additional evidence about the partial isolation of the basin can be inferred from the benthic macrofauna. Partial or complete isolation may cause environmental parameters to differ from normal marine ones. Such modified habitats influence life and should be reflected in the faunal composition. Lowered salinity can be caused by high input of freshwater and restricted connections with the open sea. Conversely, low freshwater input and poor connections may induce hypersaline conditions provided a warm to arid climate prevailed. Several benthic groups do not tolerate lowered salinities. In Agua de la Mula Member stenohaline species such as echinoderms, corals, and bryozoans are common throughout the sections. Besides, there are no evaporitic sediments. All this precludes marked departures from normal marine salinity in the Neuquén Basin between the uppermost lower Hauterivian and the lower Barremian. Enclosed seas may have restricted water circulation and thus oxygen stratification leading to accumulation of organic matter in the sediment. Nutrients may also be high in enclosed settings. Although dark shales are a common feature of the member, indicating high levels of organic matter, the presence of benthic fauna throughout the sections and the absence of laminated shales indicate that, if present, strongly lowered oxygen levels or anoxia above the sediment-water interface were restricted to very short time periods. For some periods, nutrient supply seems to have been high, as shown by the spread of opportunistic strategies demonstrated by oyster and serpulid buildups. Another indication of high nutrient levels is the almost complete lack of typical oligotrophic and autotrophic communities such as coral reefs.

Homoclinal ramp versus distally steepened ramp

The difference between the BAL and AML sections in terms of accommodation space and bathymetry can be explained as the product of a shelf break. However, the total lack of gravitational deposits such as turbidites and slumps preclude this possibility. With a slope gradient of one degree, each kilometre in a basinward direction lowers the sea floor by 17 metres. This means that, in theory, the 40 km that separate the BAL from the AML section may represent a depth difference of up to 700 m. This figure may be lowered assuming a lower angle and a shorter distance considering that the depocenter was probably not in the prolongation of a line line linking both sections. Nevertheless, distinct bathymetric differences can be explained simply by differences in the distance from the shore, without the need of a slope break. Based on the seismic analysis of supposed homoclinal ramps, Burchette and Wright (1992) expressed doubts that homoclinal ramps in the strictest sense exist. The authors concluded that ramps are actually seldom homoclinal but possess subtle slope geometries that reflect the ramp environments.

Mixed ramp versus carbonate ramp

The Agua de la Mula Member was interpreted as a mixed siliciclastic and carbonate ramp (Spalletti et al. 2001a; Spalletti et al. 2001b). Mixed sedimentation refers to alternations of periods during which siliciclastic and carbonate sediments were deposited, to contemporaneous deposition of both types regionally separated, or to syndepositional mixtures of both kinds of sediments in the same bed. In the Agua de la Mula Member, it depends on the position within the sections whether the environment can be characterized as a siliciclastic, mixed or carbonate ramp. Boundaries are, as expected, not sharp but gradational and somewhat arbitrary.

Siliciclastic ramp. The first approximately 250 m in the BAL section and the first 300 m in the AML section were deposited on a siliciclastic ramp. This part extends from the base of the section up to some metres above the first 3rd order sequence boundary and comprises the *Spitidiscus riccardii* and the lower part of the *Crioceratites schlagintweiti* biozones (lowermost to middle Upper Hauterivian). In this part of the succession, starvation/dilution (sixth order) sequences are usually thick, dilution hemi-sequences show strong progradational facies successions in late HSTs, and starvation hemi-sequences are sand- or silt-dominated.

Mixed and siliciclastic ramp. This type of ramp is represented by the sediments deposited between 250-400 m in the BAL section and 300-450 m in the AML section. It includes the upper part of the *Crioceratites schlagintweiti* biozone, and the *Crioceratites diamantensis* and *Paraspiticeras groeberi* biozones (middle Upper Hauterivian and Early Barremian). Parasequences (i.e. starvation/dilution sequences) are shorter and bioclast-dominated mixed facies are very common in starvation hemi-sequences. At late HST positions, shallow starvation hemi-sequences consist of mixtures of sand and bioclasts. In TSTs of shallow settings, ooids are an important proportion of the allochems. Stacking of several starvation hemi-sequences without the respective dilution hemi-sequences indicates phases of enhanced terrigenous starvation. Starvation hemi-sequences immediately above and below the third major MFZ are chiefly composed of carbonate particles. This may be linked with an important transgression, probably related to the Faraoni anoxic event. TSTs and RSTs of major and intermediate hierarchy are retrogradational and progradational respectively. Foraminiferal constructions are typical of starvation hemi-sequences in mixed ramps. Apart from the shell concentrations at the base of the Agua de la Mula Member, it is in the mixed ramp that the preservation of the benthic fauna is best.

Carbonate-Siliciclastic ramp. In about the last 150 m, already in the Barremian, terrigenous input seems to have been sufficiently low so that poorly developed dilution hemi-sequences composed of siliciclastic mudrocks and marlstones, and fully carbonate starvation hemi-sequences became established. Dilution hemi-sequences developed as progradational facies successions and reached shallow depth only in major or middle RSTs. Starvation hemi-sequences in early TSTs following major or middle sequence boundaries are composed of oolitic and bioclastic grainstones of shoreface origin. Middle and outer ramp starvation deposits are represented mainly by packstones, micritic rudstones, floatstones, and rare mudstones and wackestones. Occasionally, mixed facies occur. This closely fits the carbonate ramp model.

The lowered terrigenous input was probably due to an arid climate but was accentuated during major transgressions and maximum flooding periods. Starvation hemi-sequences in these parts of the sections consist solely of carbonate, while dilution ones are represented by relatively thin, bioturbated muddy siliciclastic facies almost without trends in grain size. Only during late RST of intermediate or major sequences, the sedimentation rate was high enough to fill the basin margins and generate progradational patterns such as those observed in the BAL section. This interplay between climate-generated changes in sedimentation and changes due to eustatic sea-level changes is evident throughout the section.

Burchette and Wright (1992) indicate that in some basins, ramp sedimentation and progradation appears to have been facilitated by terrigenous muds which infilled most of the available accommodation space and so allowed shallow-water ramps to prograde. This model coincides with the features described for the Agua de la Mula Member. Carbonate ramps in such settings may form the marginal portions of large-scale basinward-thickening siliciclastic or mixed carbonate-siliciclastic wedges.

Many features indicate that deposition of the carbonates occurred under cool water conditions (Table 2). Non-tropical carbonate shelf sediments are primarily controlled by bottom currents, which distribute the bioclastic sediments over extended areas (Flügel 2004). The results are homoclinal ramps, developing in low- energy, and distally steepened ramps in high-energy environments.

There have been certain periods in which ramps dominated over other types of carbonate platforms. These periods alternate with others, which are characterized by the widespread development of reef complexes. Although this pattern is poorly understood (Burchette and Wright 1992), one possible explanation is that factors such as major extinctions, oceanographic changes (e.g. eutrophication) or climatic changes may have been responsible for the exclusion of frame-building organisms from shallow water environments and may have favoured the massive oolite production which characterizes the ramp-dominated time intervals. Eutrophic conditions inferred for the Neuquén Basin during the deposition of the Agua de la Mula Member seem to be a plausible explanation for the lack of well-developed reef complexes. This pattern fits the global dominance of carbonate ramps observed for the early Cretaceous.

From a genetic point of view, different kinds of sediment mixing can be recognized in the Agua de la Mula Member. In siliciclastic regimes, mixed rocks result from relatively high shell input and preservation during phases of low siliciclastic sedimentation that characterizes starvation periods. In this case, sand- or silt-dominated mixed rocks are the most common facies in starvation hemi-sequences in shallow subtidal environments. Allochems consist merely of shells and shell fragments. In deeper settings, mixed sediments are dominated by bioclasts, autochthonous or transported by storms. Siliciclastic and carbonate mud, settling from suspension constitute the matrix. At levels dominated by mixed sedimentation carbonate production was higher than siliciclastic input. Shallow-water starved facies consist usually of mixtures of sand and bioclasts. Ooids represent an important part of starvation hemi-sequences during early major and intermediate transgressions, under combined high water energy and low terrigenous input. Ooids were probably produced on the inner ramp and transported offshore by means of storm-induced currents. At MFZ, very low input of terrigenous sediments produced muddy limestones. Nevertheless, sand and/or siliciclastic mud are commonly important components of starved hemi-sequences. Foraminiferal constructions contributed significantly to the development of some thick starvation hemi-sequences. The previously defined carbonate-siliciclastic ramp developed as alternation of the two settings. The former developed under the starved conditions of the starvation hemi-sequences, while the latter corresponds to the dilution hemi-sequences.

Table 2. Main features of warm- versus cool-water carbonates observed in modern tropical (warm) and non-tropical (cool and cold) carbonates. Only features, which were observed in this study, were included in this chart. Crosses indicate coincidence with Agua de la Mula Member data. Based on Flügel (2004, p: 35).

Features	Tropical carbonates		Non-tropical carbonates		Carbonate facies in this study
Environment	Platform; shelf		Open shelf; ramp	X	ramp
Terrigenous input	Low		Low to high	X	intermediate to high
Geometry of buildups	Attached and isolated platforms with marginal rims		Homoclinal and distally steepened ramps	X	Homoclinal? ramp
Salinity	Normal to hypersaline	X	Normal to reduced	X	Normal
Carbonate saturation	Supersaturated to saturated		Saturated to undersaturated	X	Undersaturated
Accumulation rates	50 to 1000 cm/1000 a		1-10 cm/1000 a	X	Very low
Reefs	Common to abundant		Rare to absent	X	small coral patch reefs at a single level
Algal mats	Common		Absent	X	Absent
Biodegradation	Common to abundant		Abundant to strong	X	Strong
Ooids	Common	X	Absent		Present in inner ramp facies
Aggregate grains	Common	(X)	Absent		Rare, only in grainstone facies
Peloids	Common		Rare to absent	X	Absent
Intra-/lithoclasts	Common	X	Rare to common	X	Rare to common
Calcareous red algae	Common to abundant		Abundant		Absent
Rhodoids	Common		Abundant		Absent

Calcareous green algae	Abundant		Very rare		Absent
Stromatolites	Common to abundant		Rare		Absent
Zooxanthellate corals	Abundant		Rare	X	Rare
Benthic foraminifera	Common, high diversity		Abundant, low diversity	(X)	Moderately abundant, low diversity
Bryozoans	Rare to common	X	Abundant		Rare to common
Bivalves	Common and diverse		Abundant and diverse	X	Abundant and diverse
Serpulid worms	Rare to common		Common	X	Abundant
Echinoderms	Common		Abundant	X	Abundant
Association with non-carbonate grains	Rare		Rare to abundant	X	Abundant
Glauconite	Rare		Common	X	Common
Biogenic silica	Rare		Rare to common		Absent
Low-Mg calcite	Rare to common	(X)	Common to abundant	X	Common to abundant
High-Mg calcite	Abundant	X	Abundant to common	(X)	Abundant
Aragonite	Abundant	(X)	Rare		Common (original aragonite)
Early sea bed lithification	Common to abundant		Less common	X	Rare

6. Stratigraphy

6.1. Lithostratigraphy

The Jurassic-Cretaceous infilling of the Neuquén basin was divided into three supersequences named Lower, Middle and Upper (Legarreta and Gulisano 1989). The Middle Supersequence is equivalent to the lithostratigraphic unit Mendoza Group (Tithonian - Early Barremian). It was in turn divided into three mesosequences: Lower, Middle and Upper Mendoza mesosequences (Text-Fig. 5). These three mesosequences begin with continental and/or marginal marine sedimentary packages, deposited in the inner portion of the basin (Legarreta and Gulisano 1989). The Agua de la Mula Member of the Agrio Formation together with the Avilé Member are interpreted as a second order sedimentary sequence (Upper Mendoza Mesosequence, Legarreta and Gulisano 1989). The Avilé Sandstone appears in most of the Neuquén Basin (Weaver 1931). It represents deposition during a major drop in relative sea level and is interpreted as a lowstand systems tract (Legarreta and Gulisano 1989; Legarreta and Uliana 1991; Legarreta et al. 1993; Veiga and Vergani 1993; Veiga et al. 2002). The overlying Agua de la Mula Member of the Agrio Formation shows the re-establishment of marine conditions, which persisted until the end of the Upper Mendoza Mesosequence.

6.2. Biostratigraphy

Background knowledge

The Agua de la Mula Member of the Agrio Formation contains four ammonite biozones, i.e. from base to top the *Spitidiscus riccardii* Zone of early Late Hauterivian age (Aguirre Urreta 1995; Aguirre Urreta et al. 2005; Leanza and Wiedmann 1992); the *Crioceratites schlagintweiti* and *Crioceratites diamantensis* zones of the early to late Late Hauterivian, respectively (Aguirre Urreta and Rawson 1993); and the *Paraspiticeras groeberi* Zone of latest Hauterivian to early Barremian age (Aguirre Urreta and Rawson 1993; Aguirre Urreta et al. 2005). Background knowledge of the Hauterivian-Barremian ammonite biozonation of the Neuquén Basin and West Mediterranean are summarized in Text-Fig. 4.

With the objective of improving the stratigraphic knowledge of the Agua de la Mula Member, the ammonite fauna has been sampled in both sections. Besides, an intensive bed-by-bed survey has been carefully carried out in BAL, were there is a continuous outcrop of the section. Ammonites were taken to the lab for preparation and identification. The ammonite occurrences, biozones and biozone thicknesses are described and compared with other biostratigraphic schemes in Text-Fig. 8.

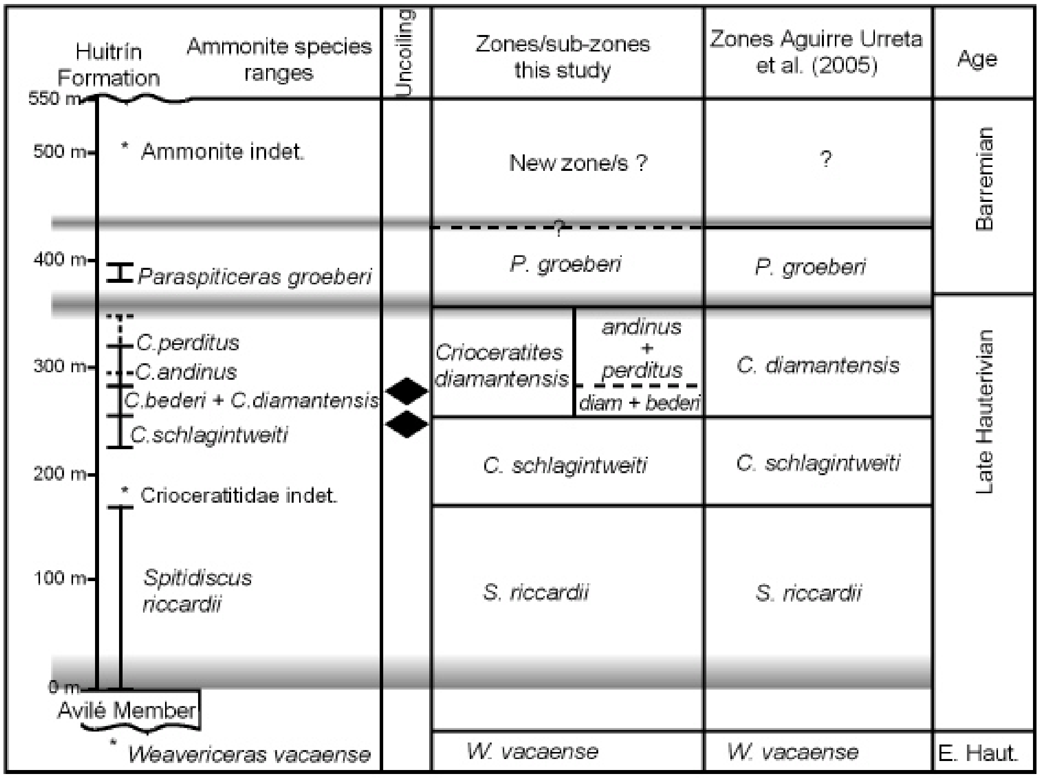

Text-Fig. 8. Ammonite occurrences in section BAL, biozones, and comparison with previous biostratigraphic schemes. Shaded areas represent anoxic events. Rhombs indicate the occurrence of uncoiled ammonites. Bajada del Agrio Section.

Results

Weavericeras vacaense Zone.

A thin shell-bed with a ferruginous bioclastic matrix containing several well-preserved specimens of *Weavericeras vacaense* Weaver, was found in the Pilmatué Member, 10 m below the Avilé Member. This species indicates a late Early Hauterivian age for the topmost portion of the Pilmatué Member (Aguirre Urreta et al. 2005). This biozone ends with the erosional base of the fluvial sandstones of the Avilé Member (Coihuequican Unconformity of Leanza et al. 2006).

Spitidiscus riccardii Zone

Several specimens of *Spitidiscus riccardii* Leanza and Wiedmann were found in the Agua de la Mula Member in both sections, indicating an earliest

Late Hauterivian age of the basal part of this member (Aguirre Urreta et al. 2005). In the BAL section, this biozone extends up to 166 m above the Avilé Member. The first occurrence coincides with the first level of fossil concentration of the unit. These ammonites normally occur flattened or, less commonly, in three dimensions, usually as fragments of whorls, but also as almost complete specimens. In the AML section, specimens of *S. riccardii* have been found from the base of the unit up to 140 meters. Some fragments found at this locality show weak ornamentation between widely developed constrictions, displaying features close to *Plesiospitidiscus gutierrezi* Leanza and Wiedmann, which has also been assigned to this biozone. No vertical patterns were detected between these two species. However, the poor representation of *P. gutierrezi* does not allow discarding this possibility.

Crioceratites schlagintweiti Zone

This biozone was defined by Aguirre Urreta and Rawson (1993) for the occurrence of the crioceratitid species *Crioceratites schlagintweiti* Giovine and *C. apricus* Giovine, assigned to an early Late Hauterivian age. Aguirre Urreta and Rawson (1997) defined the base of this zone as the first appearance of crioceratitid ammonites. In the BAL section, 170 m above the base there is a juvenile ammonite whorl with well-developed radial ribs that do not change throughout the shell. This specimen has been identified, with doubt, as Crioceratitidae indet., and its appearance marks the base of the *C. schlagintweiti* zone in BAL. It is worth mentioning that the last occurrence of *S. riccardii* specimens is four meters below the first appearance of crioceratitid remains, making the contact between these two biozones very sharp at this locality.

Two different types of specimens of *C. schlagintweiti* have been found. Type A resembles in ornamentation descriptions and figures made by Giovine (1950), but the shell is larger (sometimes more than 30 cm of diameter) and not uncoiled. Type B fully coincides with the original description of the species. *C. schlagintweiti* type A is abundant in both sections. In BAL, it was observed 225 to 255 m from the base. Type B, however, is lacking in Bajada del Agrio and rare in Agua de la Mula, where it occurs together with type A. The top of this biozone is indicated by the first occurrence of *C. diamantensis* of the homonymous zone. *C. apricus* has not been observed in any of the sections.

Crioceratites diamantensis Zone

According to Aguirre Urreta et al. (2005), this biozone comprises the beds above the *C. schlagintweiti* Zone and is characterized by the presence of the crioceratitid ammonite *C. diamantensis*, which can occur together with *C. andinus*. In the BAL section *C. diamantensis* and *C. andinus* occur between 255 and 347 m from the base. The first appearance of *C. diamantensis* is few meters above the last appearance of *C. schlagintweiti,* forming a sharp contact. Two biosubzones have been recognized: Between 255 and 283 m *C. diamantensis* and *C. bederi* (sensu Gerth, 1925) occur together and are replaced up-section by *C. andinus* and *C. perditus,* species which extend upwards to the end of the zone. It is worth noting the presence of uncoiled shells of *C. bederi* at the top of the lower subzone. This fact indicates the presence of two events of uncoiling, one in the C. *schlagintweiti* Zone and a second in the *C. diamantensis* Zone. In the AML section specimens of both, *C. diamantensis* and *C. perditus* have been collected.

Paraspiticeras groeberi Zone

Two beds with abundant fragments of *Paraspiticeras groeberi* have been found between 381 m and 392 m from the base in BAL. This ammonite species has not been recorded in AML, where the section is incomplete and beds of this biozone probably could not been sampled.

Level with ammonite indet.

In BAL there are almost not ammonites from 392 m up to the top of the section. The exception consists on a specimen of a probably new species collected at 499 m. The taxonomic determination of this specimen will probably improve the knowledge of the age of the unit because of its stratigraphic position. Aguirre Urreta et al. (2005) also mentioned the finding of a new species around this level. These authors describe a not yet studied open-coiled ammonite species, which differs from the aforementioned specimen.

Discussion

The *Spitidiscus ricardii* Zone is well developed, and its lower and upper boundaries are sharp. The age of this biozone is inferred as earliest Late Hauterivian (Aguirre Urreta et al. 2005), based on the similarity with species of the Mediterranean region. In this study, the base of the biozone coincides with the erosional surface below the Avilé Member. The first 2.1 m lack ammonites in BAL. They consist of unfossiliferous marginal marine facies and a barren level of sandy and silty clays with early diagenetic calcareous concretions containing very scarce molluscan fossils but no ammonites. These 2.1 meters are assigned to the *S. riccardii* Zone considering the stratigraphic continuity between the top of the Avilé Member and the first appearance of *Spitidiscus*. The erosional surface at the base of the Avilé Member is a second-order sequence boundary termed the Coihuequican Unconformity (Leanza et al. 2006), that represents an important amount of time. It seems therefore sensible to consider the Avilé Member genetically linked with the overlying Agua de la Mula Member and not with the underlying Pilmatué Member. In this sense, the Avilé Member is here assigned to the *Spitidiscus* Zone and, hence, to the earliest Late Hauterivian ammonite biozone of the Neuquén Basin.

The *C. schlagintweiti* Zone has been linked to Mid-Hauterivian ammonites of the Mediterranean region based on the uncoiled nature of the shells (Aguirre Urreta and Rawson 1997). In the present study, open-coiled shells were found in this as well as in the *C. diamantensis* biozone, which opens a question as to the criteria of correlation between regions. Ammonites of the *C. diamantensis* biozone are correlated with latest Hauterivian forms of the Mediterranean region because of the more compressed and involute nature of the shells, observed in *Pseudothurmannia* (Aguirre Urreta and Rawson 1997; Aguirre Urreta et al. 2005). In the present study, these features were found in *C. andinus* and *C. perditus* both characterizing the upper biosubzone. In this way, the correlation with the *Plesiospitidiscus ligatus* Zone of the Mediterranean region is proposed to extend up to the top of the *C. diamantensis*/*C. bederi* biosubzone. *Paraspiticeras groeberi*, provisionally dated as Early Barremian

(Aguirre Urreta and Rawson 1993; Aguirre Urreta et al. 2005), is now more confidently placed at the base of this stage after detection of the possible expression of the uppermost Hauterivian Faraoni Event (for more information see section 6.3, Anoxic events). The upper third of the section at BAL is poor in ammonites and thus exhibits a less trustable biostratigraphic zonation.

Our knowledge of the ammonite biostratigraphy of the Agua de la Mula Member is not quite satisfactory. The basal biozone exhibits a yet not understood succession of *Spitidiscus* species. There is also confusion about the systematics of the crioceratitid species that compose the second and third biozones. The upper third of the section yielded only two ammonite specimens, which have not yet been studied. Correlation with the West Mediterranean Province and hence the age of each biozone is still in flux.

Conclusions

- Bed-by-bed sampling employed in the Bajada del Agrio section allowed to build a scheme of the vertical distribution of ammonite biozones, their thicknesses, and their relationship with other stratigraphic indicators (i.e. major sedimentary sequences and sequence boundaries and inferred anoxic events). The second and third features and their linkage with ammonite biozones are useful stratigraphic tools, although yet not fully explored for this unit.
- The ammonite biostratigraphy of the Agua de la Mula Member of the Agrio Formation is more complex than previous studies indicate (Aguirre Urreta and Rawson 1997; Aguirre Urreta et al. 2005). Besides, crioceratitid systematics is in need of revision as has been already stated by (Aguirre Urreta and Rawson 1997). However, these two problems are beyond the scope of this dissertation.
- The *Spitidiscus riccardii* Zone can probably be separated into two biosubzones based on the appearance of shells that resemble *Plesiospitidiscus gutierriezi*.
- *Crioceratites schlaginweiti* specimens coinciding with Giovine’s (1950) descriptions, are rare in the Agua de la Mula section and absent in Bajada del Agrio. This biozone is well represented by large specimens that, although

regularly coiled, share all other morphological features with the original description of *C. schlagintweiti*.

- The finding of uncoiled specimens of *C. bederi* as low as in the *C. diamantensis* Zone suggests that previous correlations of the *C. schlagintweiti* Zone by Aguirre Urreta and Rawson (1997) with the mid-Hauterivian uncoiled crioceratitid ammonites of Europe should be revisited. Uncoiling occurs at least in two different biozones in the section at Bajada del Agrio.
- The *P. groeberi* Zone is now more confidently placed in the upermost Hauterivian – lowermost Barremian stage as it is developed immediately above the inferred uppermost Hauterivian Faraoni Event expression in the Neuquén Basin.
- The upper third of the section has a very limited occurrence of ammonites. However, these more than 100 m of sediments probably involved a significant amount of time and deserve a more intensive study in the future.

6.3. Anoxic events

Exceptional transgressions of global extent caused worldwide floodings that combined with local factors, deposited organic-rich sediments synchronically in different parts of the world. These “global anoxic events” are the result of large-scale transgressions that left thick and widespread black shales. The anoxic events are useful stratigraphic references as well as indicators of marine source rocks. The combination of dysoxic-anoxic conditions and sediment starvation (i.e. good preservation of marine organic matter and low siliciclastic dilution) favoured the widespread deposition of organic-rich facies during the transgressive intervals of the Agrio Formation (Legarreta and Uliana 1991; Tyson et al. 2005; Uliana and Legarreta 1993). This unit includes organic-rich and bituminous black-shale facies (Leanza 1981) that contributed to the ‘Agrio’ petroleum system that has a cumulative production of over 164 million barrels of oil (Tyson et al. 2005).

Important packages of bituminous black-shales occur at two levels in the sections studied here. The first one is situated 15 to 20 m from the base of the unit in both sections. It is characterized by well-developed black, dark-bluish and dark-grey marls, micritic clays and micritic silty clays. Ammonites and benthic fauna occur scattered or in loosely packed shell-beds interpreted as the sediment-starved lower portion of orbitally induced precession cycles (see below). The ammonites belong to the genus *Spitidiscus,* indicating an earliest Late Hauterivian age. The preservation of the fossils is excellent and there are little or not indications of physical disturbance i.e., the sediments were deposited well below the storm wave base (for more information see facies 5.1-3 and 8.2 in chapter 5). The sediments are always bioturbated, although discrete trace fossils are rare (e.g., *Chondrites*). The benthic macrofauna consists of a diverse group of small, chiefly epifaunal and semi-infaunal bivalves and gastropods. Shallow infaunal bivalves are rare. There are two species of relatively deep infaunal lucinid bivalves. Recent lucinids are known to be well adapted to thrive in poorly oxygenated environments. These benthic molluscs obtain nutrients from endosymbiotic chemo-autotrophic, sulphide-oxidizing bacteria: While the body rests in anoxic sediments rich in hydrogen sulphide, the siphon and a mucus-tube connect with the more oxygenated sediment-water interface (Reid and Brand 1986). This organic-rich set of beds has already been recognised in the literature and designed as the “Spitidiscus black shale” (Tyson et al. 2005). It was proposed that these sediments were deposited under anoxic to dysoxic conditions (Spalletti et al. 2001b; Tyson et al. 2005). However, bioturbation and presence of benthic macrofauna indicate that the so-called “Spitidiscus black shale” probably did not experience total oxygen depletion at the sediment-water interface at any time. Instead, dysoxia and anoxia a few centimetres below the sediment-water interface can be deduced from the organic-rich nature of the sediments, the scarcity of infaunal species and the presence of lucinid bivalves, adapted to thrive under such conditions.

Between 349 and 353 m from the base in BAL and 395 to 400 in AML there is a distinct alternation of dark-grey and black mudrocks and marly mudrocks, and medium to thick, densely-packed shell-beds. This package represents the third major (third-order) maximum flooding zone. (MFZ-3. See Text-Fig. 6). The shell beds are composed mainly of shells and shell fragments of small molluscs (bivalves and gastropods) in densely-packed, bioclast-supported rocks (facies 9.2., low-energy micritic rudstones). This facies is developed as particularly thick beds once in each section: almost 1 m in BAL

(351 m from the base) and 2.5 m in AML (396-398 m from the base). The low-energy micritic rudstones are interpreted here as amalgamated distal tempestites that accumulated over a long period, on the outer ramp. The interpretation of this set of beds as a distinct flooding event relies on two lines of arguments. Firstly, considering that the general trend of the unit is towards a progressive infill of the basin, this set of beds was deposited at a greater depth than the previous MFZ. Secondly, the same facies occurs in both sections at equivalent positions, even though sedimentation below and above these beds differed between the two localities. These facts suggest the occurrence of a wide-spread phenomenon proposed here as the Neuquén basin's equivalent of the "Faraoni Level" (Cecca et al. 1994). The "Faraoni Level" is the first widely known dysoxic event in the European Cretaceous, whose Neuquén Basin equivalent had not yet been found (Tyson et al. 2005). It ranks among the seven significant excursions in the carbon cycle during the Cretaceous (Ogg et al. 2004). This MFZ occurs between the *C. diamantensis* and the *P. groeberi* biozones, in a 43-m-thick package of beds without well-preserved ammonites. If correctly identified, this event would indicate the top of the Hauterivian better than the ammonite biozones.

Other occurrences of dark mudrocks are found at the maximum flooding position of sequences in the last 150 m, for instance, at 432 to 450 m from the base in BAL (the equivalent part of the section is not properly exposed in AML). In this case, micritic mudrocks and marls alternate with fine-grained limestones. However, these occurrences are less conspicuous and their precise age is not known because of the poor ammonite record.

6.4. Sequence stratigraphy

During the Jurassic and Early Cretaceous the Neuquén Basin passed through a sag evolutionary stage, behaving as a marginal basin (Mitchum and Uliana 1985). From the upper Jurassic (Kimmeridgian) to the upper Cretaceous, the basin experienced a thermal subsidence evidenced by the geometry of the mesosequences as well as their internal stacking pattern, which shows subtle facies changes (Legarreta and Gulisano 1989). Zapata and Folguera (2005) and Ramos (1977) indicate that during this period the Neuquén Basin was a back-arc basin strongly affected by tectonic and eustatic sea-level changes due to a narrow connection with the ocean towards the northwest (Text-Fig. 2). As the Neuquén Basin experienced a relatively simple thermal sag mode of subsidence, a low gradient depositional ramp developed in which the nature and extent of the facies were strongly influenced by variations in global sea level (Legarreta and Uliana 1991).

Most published information indicate that the Agua de la Mula Member was deposited in a tectonic setting characterised by a steady and slow subsidence (Legarreta and Gulisano 1989; Legarreta et al. 1993; Legarreta and Uliana 1991; Mitchum and Uliana 1985; Spalletti et al. 2001a; Spalletti et al. 2001b). Vergani et al. (1995) in turn, indicate that the Lower Cretaceous Mendoza-Rayoso succession is punctuated by several unconformities that define the stacking pattern of multiple transgressive-regressive sequences, reflecting intermittent subsidence and eustatic processes. In summary, while several authors support the dominance of eustatic sea-level changes on tectonics to explain most of the Lower Cretaceous sedimentary record of the Neuquén Basin, and in particular of the unit under study (see references above), others give tectonics a more important role.

There is no agreement on the number of third-order sequences that compose the Agua de la Mula Member. Many authors described three third-order (major) sedimentary sequences for the unit (Legarreta and Gulisano 1989; Legarreta and Uliana 1991; Spalletti et al. 2001b). Legarreta and Uliana (1991) report at least two short episodes of shallowing that caused exposure of the shelf and abrupt basinward shift of the siliciclastic fringe punctuated the widespread shelfal accumulation of the Agua de la Mula Member. Legarreta et al. (1993) recognised at least eight (third-order) sequences for the Agua de la Mula Member of the Agrio Formation in the southern part of Mendoza province (fig. 2 in the cited article). Sagasti (2000) found, in a deep basinal setting of southern Mendoza, five groups of bedding couplets, which were interpreted as the distal expression of five major sequences [third-order in Sagasti (2000); fourth-order in Sagasti (2001)].

The Agua de la Mula Member of the central Neuquén province has four segments that can be easily recognised from their sedimentological, stratigraphic and palaeontological features (see Chapter 4 for a description of the sections). They probably fit with the three third-order sequences described in the literature (Legarreta and Gulisano 1989; Legarreta and Uliana 1991; Spalletti et al. 2001b) in the following way: The first two parts mentioned here correspond to the first sedimentary sequence of the literature. The third and fourth in turn coincide with second- and third-order sequences, respectively. However, based on detailed investigations a different scheme is proposed here.

The studied unit exhibits a very cyclic pattern, which can be followed throughout the sections. Lowest hierarchy (i.e. highest order) sequences develop in a wide variety of ways. In most cases, the sequences are composed by a starved lower hemisequence followed by a usually thicker, bioclast-poor and siliciclastic-dominated upper portion. These sequences have been previously named in this study “Starvation/Dilution Sequences” or S/D sequences (see Chapter 5: Facies Analysis and Text-Fig. 7; for a discussion about S/D sequences see the end of this chapter). Spalletti et al. (2001a; 2001b) recognised the presence of low hierarchy sequences (or high-frequency cycles) in the Agua de la Mula Member in the areas of Loma La Torre, south of Pampa Tril (in the north of the Neuquén province) and at Bajada del Agrio (central part of the same province). For these authors, the high-frequency cycles are particularly well developed in the highstand systems tracts of third-order sequences. Sagasti (2000; 2001) describes the development of bedding couplets for the same unit in the Mendoza province. Orbital forcing of Milankovitch cyclicity was used to explain the cycle origin in several articles (Sagasti 2000; Sagasti 2001; Spalletti et al. 1990; Spalletti et al. 2001a; Spalletti et al. 2001b).

Multiple-order cyclicity is evident troughout the sections. Sequences in these cases have been more properly described as composed by sequence sets instead of systems tracts (like in Coe and Church 2003). In this way, high hierarchy sequences are composed by transgressive, highstand, etc sequence sets. However, whether sequences are composed of parasequences or minor sequences is irrelevant as the features that define the sedimentary product of each portion of a relative sea-level change curve are the stacking patterns of sedimentary packages, and their position with respect to important surfaces. Consequently, systems tracts are named here as in classical sequence stratigraphic jargon.

Main sequences

Based on the stacking patterns of the starvation/dilution sequences, the studied unit has been subdivided into three main sedimentary sequences, and an upper fourth portion whose internal structure cannot unambiguously be subdivided into conformable sedimentary packages. In this study, main sequences are defined as those that define the major retrogradational/ progradational patterns built by the S/D sequences. These sedimentary packages were interpreted as either third or fourth order, considering the amount of S/D sequences involved, their thicknesses, and their position with respect to ammonite biozones. There is not exact correspondence between former sequence stratigraphic schemes (Legarreta and Gulisano 1989) and the diagram described here. Consequently, sedimentary sequences and their boundaries of the Agua de la Mula Member were named:

- Main sequences: Depositional Sequence Agua de la Mula, plus a correlative number (e.g. DSAM-1).
- Main sequence boundaries: Sequence Boundary Agua de la Mula, plus a number (e.g. SBAM-1).
- Sequences nested into other higher hierarchy sequences – fourth-order into third order – with an additional number after the main sequence to which they belong (e.g. DSAM-1/1).
- Sequence boundaries of these subordinated sequences after the main sequence boundary below it (e.g. SBAM-0/1).

Similar nomenclature has been used for the maximum flooding zones, and systems tracts. In Text-Fig. 9 a scheme of main and subordinated sedimentary sequences is shown, together with ammonite biozones and other stratigraphic markers. Text-Fig. 10 shows the inferred correlations between Neuquén Basin and European sedimentary sequences.

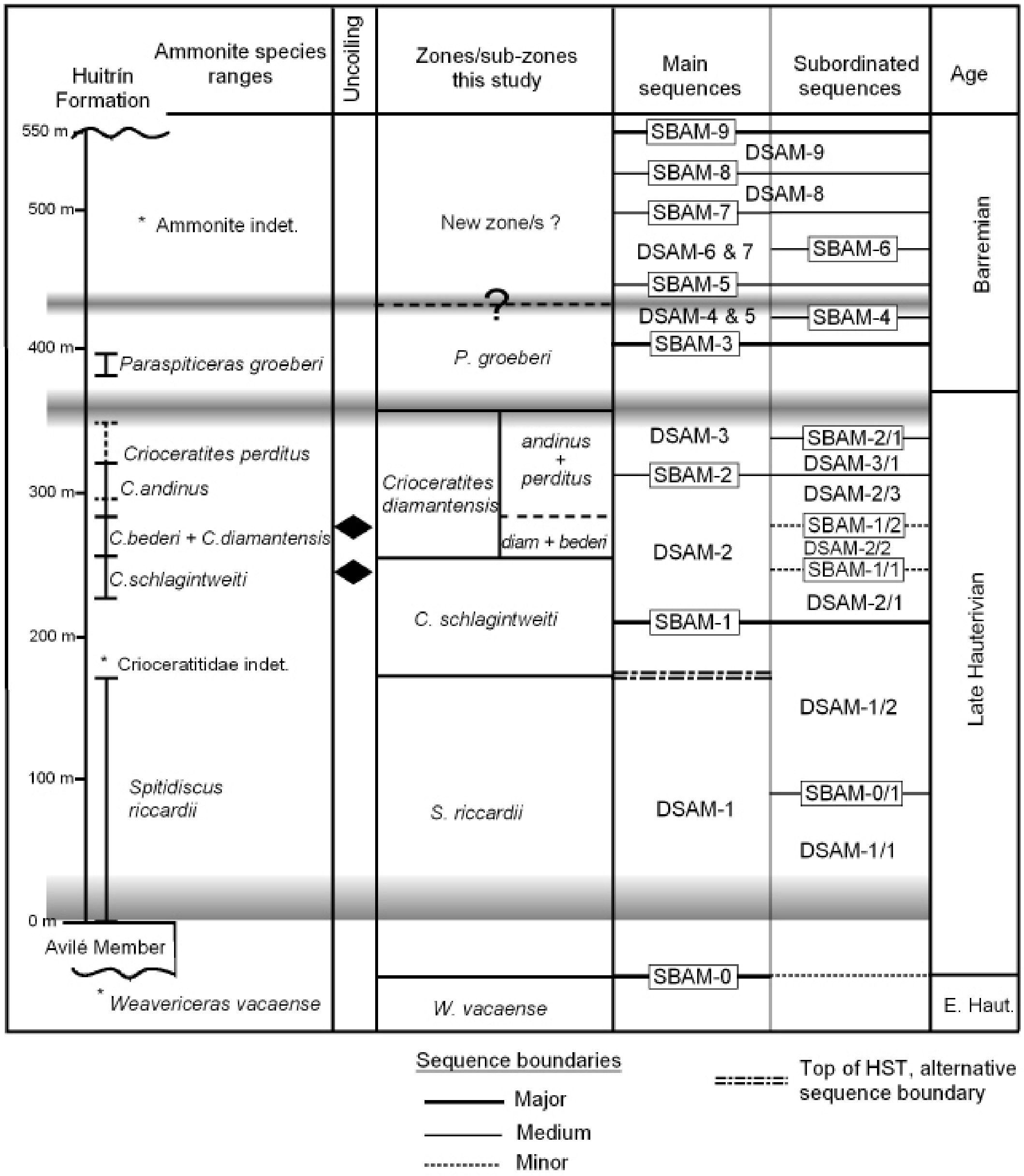

Text-Fig. 9. Sequences, sequence boundaries, ammonite occurrences, and biozones of the investigated section. Shaded areas represent anoxic events. Rhombus indicate the occurrence of uncoiled ammonites. Bajada del Agrio Section.

All, even minor, facies changes were considered in order to identify progradational, aggradational and retrogradational sets. These, in turn, have been used to interpret which part of the base level curve the sedimentary package was linked with. Sequences were considered as major after fulfilling three criteria: (1) clearly detectable changes in facies trends (e.g. progradation to retrogradation) through key surfaces such as sequence boundaries or maximum flooding; (2) important facies contrasts in sequences in terms of depth; and (3) a relevant amount of time involved in the development of the sequence. According to the sedimentary sequence model (Van Wagoner et al. 1988) sequence boundaries are composite surfaces consisting of the sub-aerial unconformity and its marine correlative conformity. The correlative conformity was afterwards placed at the end of the falling stage systems tract, i.e., at the end of base level fall (Hunt and Tucker 1992). Maximum flooding periods do not necessarily leave a surface but a zone (i.e. Maximum Flooding Zone or MFZ). In a homoclinal ramp setting, which was the situation in which the Agua de la Mula Member was deposited, sharp boundaries are not expected between the different regressive systems tracts (i.e. between HST- FSST and FSST-LST) in medial to distal positions. Hence, the sedimentary-sequence model boundary would be problematical to detect and the only detectable boundary would represent the top of the progradational sedimentary packages, i.e. the Maximum Regressive Surface, equivalent to the transgressive surface. Therefore, at least in some cases, the progradational packages can only be considered as regressive systems tracts. This coincides with the transgressive-regressive (T-R) sequence model of Embry (1993) that responds to the transgressive-regressive curve (Catuneanu 2002).

Sedimentary sequences and sequence boundaries have been dated with ammonites. However, the recent literature on Valanginian-Hauterivian biostratigraphy of the Neuquén Basin (Aguirre Urreta 1993; Aguirre Urreta 1995; Aguirre Urreta et al. 1993; Aguirre Urreta and Rawson 1993; Aguirre Urreta and Rawson 1997; Aguirre Urreta et al. 2005, and references cited in these articles), although having considerably improved the biostratigraphic scheme, demonstrates that the latter is still in flux (e.g., the different opinions concerning correlation). Besides, the systematics of crioceratitid species, on which two of the four biozones are based, awaits revision (Aguirre Urreta and Rawson 1997). Finally, the uppermost biozone described (*Paraspiticeras groeberi* Zone) is provisionally placed in the Lower Barremian (Aguirre Urreta et al. 2005), and in the upper third of the unit ammonites are rare and have not yet been studied.

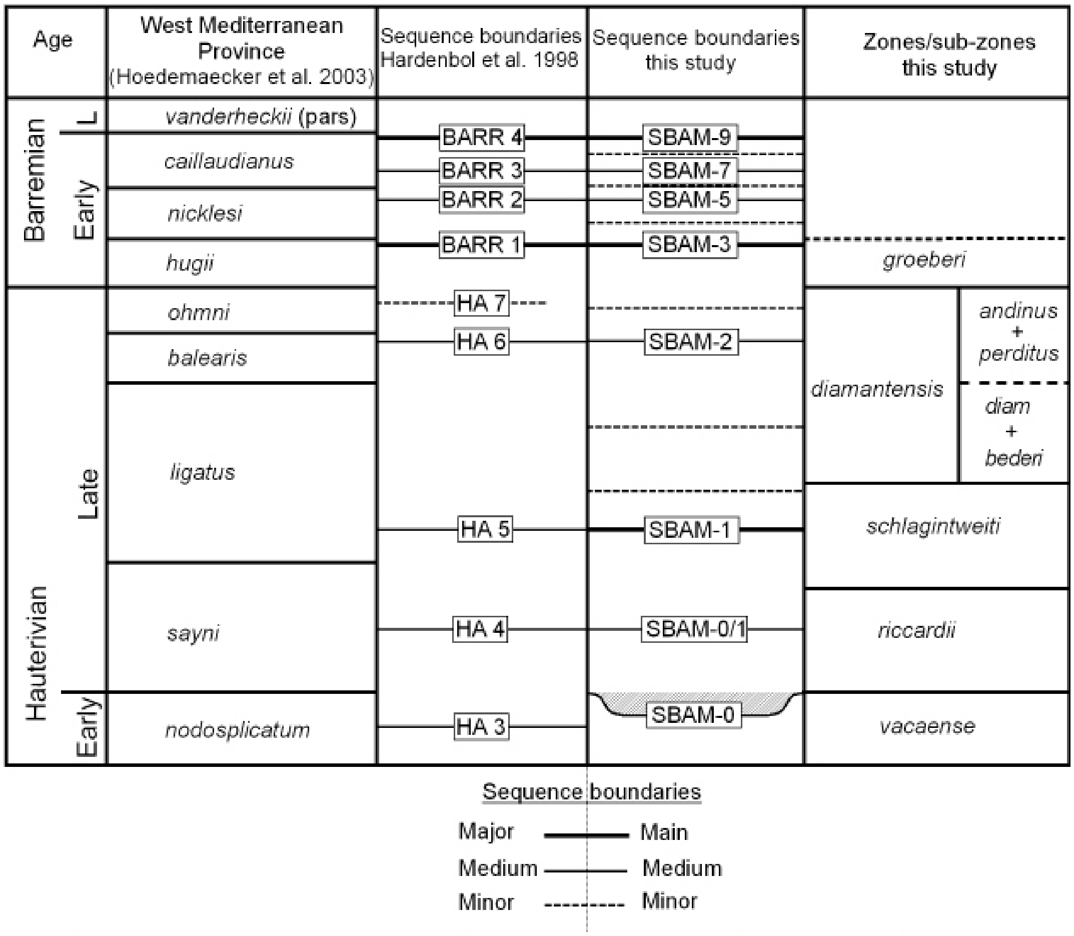

Text-Fig. 10. Sequence boundaries of the studied stratigraphic interval and correlation with the West Mediterranean Province. Major, medium and minor sequences are equivalent to third, fourth and fifth order, respectively in this study. Minor sequences are not labelled.

The section at Agua de la Mula is thicker and has a higher number of sixth-order sequences composed only by dilution hemisequences. This was interpreted as a consequence of higher terrigenous input at this locality (Lazo 2004). However, this explanation is in contrast with the widespread accepted model indicating that the main source of sediments was the foreland, i.e. the Sierra Pintada System in the east and the North Patagonian Massif in the south (Legarreta and Gulisano 1989). A more feasible explanation is that the more distal position of Agua de la Mula allowed sediments to continue accumulating while the basin margins in more proximal positions had already become completely filled (i.e. BAL section).

First Depositional Sequence (DSAM-1)

DSAM-1 begins with the sequence boundary below the Avilé Member (SBAM-0) and finishes at 210 m (BAL) and 269 m (AML) above the base, at the position of the SBAM-1 (Text-Fig. 6). The SBAM-0 in the area surveyed in this study represents the subaerial unconformity (Coihuequican Unconformity of Leanza et al. 2006). Ten metres below the boundary there is a conspicuous level with *Weavericeras vacaense* of latest Early Hauterivian age. Few meters above the Avilé Member, the ammonite *Spitidiscus riccardii* indicates the earliest Late Hauterivian. Consequently, the SBAM-0 is placed close to the boundary between Early and Late Hauterivian. In both sections, the transition from the fluvial sandstones of the Avilé Member to the deep marine argillaceous sandy micrite and marls (AML) and muddy micrites (BAL) is abrupt. This maximum regressive surface (i.e. transgressive surface) is separated from SBAM-0 by the lowstand deposits of the Avilé Member. In this case, the depositional sequence can be differentiated from the T-R sequence, as it is possible to distinguish between the subaerial unconformity and the maximum regressive surface. In Bajada del Agrio there is a less than 2-m-thick package of transitional back-ramp sandstones at the top of the Avilé Member.

The DSAM-1 can be subdivided into two fourth-order sequences (DSAM-1/1 and 2) indicated by two thick sets of progradational piles of S/D sequences. DSAM-1 and the fourth-order sequences nested into it are highly asymmetric in nature, characterized by very short TSTs and thicker RSTs. The first ca. 15 m of DSAM-1 are characterized by an aggradation of basinal mixes of clay and micrite, punctuated by thin tabular levels of skeletal concentrations. These facies are the deepest recorded for the sequence and the unit, and are interpreted as the MFZ of the DSAM-1. From 15 m to 105 m (BAL) and 115 m (AML) there is a gentle progradational pattern from bioturbated silty clays to argillaceous silts, silts and sandy silts, more or less regularly interrupted by thin, tabular skeletal concentrations that represent the starvation hemisequences of S/D sequences. The skeletal remains show a worse state of preservation and shell beds more evidence of physical destruction up-section. At the top of this progradational set there is a short, minor retrogradation, followed by a conspicuous, although thin (ca. 1 m), tabular bed rich in micrite, which is easily recognisable from its orange colour. The progradational set of beds is interpreted as a fourthorder regressive systems tract (RST), probably composed by sediments originated during the highstand, fall and early rise in base level. The top of this sequence (SBAM-0/1) probably represents the top of the LST, i.e., the maximum regressive surface, and is placed into the *S. riccardii* Zone of early Late Hauterivian age. SBAM-0/1 is a T/R-type sequence boundary. The complete fourth-order sequence (DSAM-1/1) developed in an offshore setting (basin to middle ramp) and this may be the reason why there are not distinct facies contrasts. The finer and more calcareous beds deposited above it are interpreted as the TST and maximum flooding surface of the following fourth-order sequence (DSAM-1/2). The RST of the DSAM-1/2 consists of a gentle progradational pattern up to 165 m (in BAL) and 185 m (in AML) characterized by a moderate to low sedimentation rate (high degree of bioturbation of dilution hemisequences), and a strongly progradational upper portion. Starvation hemisequences are thicker and were deposited in progressively shallower environments (middle to inner ramp) as evidenced by taphonomic features of the benthic fossils. The relevant characteristics of the top part of the DSAM-1 are the faster progradation with respect to the sediments below and the high rate of siliciclastic sedimentation, with the development of coarsely interlayered and heterolithic bedding, and hummocky and amalgamated hummocky cross-stratification towards the top of the section. In BAL this fast-prograding package is a single coarsening- and shallowing-upward set of beds, although internal cyclicity is apparent in the repeated occurrence of amalgamated hummocky tabular beds. The lower portion of the regressive part of DSAM-1/2 is considered as the HST-1 and belongs to the *S. riccardii* Zone. The upper, highly prograding one represents the FSST of both, the fourth- and the third-order sequences. This unit yielded a single remain of a juvenile crioceratitid shell at its base and has been included into the *Crioceratites schlagintweiti* Zone of the middle Late Hauterivian. In this way, the top of the DSAM-1 (and DSAM-1/2) represents the sequence boundary-2, or SBAM-1, placed in the *C. schlagintweiti* Zone. This surface represents the subaerial unconformity and the ravinement surface. LST deposits are absent in this case.

The uppermost 80-90 m of the DSAM-1 have a different configuration at AML (see Text-Fig. 6 and Appendix-Figure 2). The first 50 m show a clear coarsening- and shallowing-upward trend, high sedimentation rate, and the development of coarsely interlayered bedding like in BAL but reaching less shallow settings. In the last 40 m there are four S/D sequences that show a rather aggradational stacking pattern. The basal one has a well-developed starvation hemisequence on an erosional surface, with a thick and complex shell-bed deposited on the inner ramp. The other three S/D sequences are composed only by the dilution hemisequences, a feature that is rare throughout the sections. The last of these four S/D sequences is thicker and shows a higher sedimentation rate evidenced by the development and preservation of a coarsely interlayered bedding facies with a shallowing-upward trend capped by bioturbated fine-grained sandstones. Another feature of these S/D sequences is the common occurrence of *C. schlagintweiti* type A (see section 6.2: Biostratigraphy) on top of the dilution hemisequences. I interpret the first 50 m to represent the FSST-1 and as equivalent of the FSST-1 of BAL. The following 40 m may be either the topmost part of the RST (FSST) that was not deposited in BAL because of the lack of accommodation space, or the LST. In the first case, the SBAM-1 would coincide with the transgressive surface and the interpretation would be the same for both sections. In the second, conversely, the sequence boundary would be separated from the maximum regressive surface by the presence of the LST. In this case, the SBAM-1 would have to be placed close to the boundary between the *S. riccardii* and *C. schlagintweiti* biozones, i.e. in the early to middle Late Hauterivian (the biostratigraphic control in AML is less precise than in BAL). These interpretations are somehow speculative and should be tested by measuring several other sections in different parts of the basin. For both sections, a more conservative but less explicative interpretation would consider that the whole regressive package represents the HST and FSST, and the LST were deposited basinward. Regardless the complexity of the upper portion of the DSAM-1, the erosional transgressive surface (ravinement) is a more trustable sedimentary surface for correlations due to the clear change towards a retrogradational stacking pattern above it in both sections, and the development of a thick, sand-dominated and highly ferruginous transgressive bed immediately overlying the surface. In both sections, this surface is placed into the *C. schlagintweiti* Zone. For this situation, it is easier and more unequivocal and practical to use T/R sequences instead of depositional sequences, as was indicated by Embry (1993).

Second Depositional Sequence (DSAM-2)

DSAM-2 is a 96 m (BAL) and 74 m (AML) thick package bounded by SBAM-1 of middle and the SBAM-2 of late Late Hauterivian age (C. *andinus* /C. *perditus* subzones of the C. *diamantensis* Zone). Two systems tracts of equivalent thicknesses can be recognised, a lower TST and an upper RST, the last probably consisting chiefly of the HST. Additionally, the lower 30 m of the sequence in AML are interpreted as the LST-2. Three subordinated depositional sequences compose the DSAM-2 (DSAM-2/1 to 3). A fourth sequence was probably truncated at the base of DSAM-2. This complex pattern of fourth-order sequences is only evident in the BAL section. The TST-2 typically shows a retrogradational stacking pattern of S/D sequences. Up-section there is a tendency to more distal facies in the dilution hemisequences, from shoreface sandstones to offshore bioturbated siltstones (BAL) and argillaceous siltstones (AML). At the base of the systems tract there are S/D sequences without the starvation hemisequence and truncation (more than one S/D sequence represented only by the starvation hemisequence). Close to the maximum flooding zone dilution-hemisequences have less clear or no coarsening/shallowing-upwards trends, and the S/D sequences are shorter, indicating greater distality and reduced sedimentation rate. The MFZ-2 consists of three short S/D sequences characterized by thin starvation hemisequences with plenty of ammonites. The last occurrence of *C. schlagintweiti* and the first of *C. diamantensis* and *C. bederi* is at the MFZ and, hence, also the change from the second to the third ammonite biozone. The HST is represented by a progradational stacking pattern altered by the occurrence of a fourth-order depositional sequence (DSAM-2/3). Dilution hemisequences range from offshore bioturbated mudrocks and siltstones to lowershoreface sand-dominated heterolithic and hummocky stratification, as well as bioturbated fine-grained sandstones and amalgamated hummockies (in BAL). Starvation hemisequences are usually developed as thick, complex shell-beds, in some cases with a very well preserved benthic fauna. At the position of the MFZ of the DSAM-2/3 the *C. diamantensis* /*C. bederi* subzone is replaced by the *C. andinus* /*C. perditus* subzone. Last *C. bederi* specimens are uncoiled, indicating the second occurrence of uncoiling ammonites in the unit. The SBAM-2 occurs at 306 m (BAL) and 343 m (AML) above the base, in the *C. andinus* /*C. perditus* subzone of the *C. diamantensis* Zone, i.e., late Late Hauterivian. It is interpreted as the subaerial unconformity reworked after the onset of the following transgression. This means that it also represents the transgressive surface. If so, FSST and LST would have been deposited in a more basinal position.

Third Depositional Sequence (DSAM-3)

DSAM-3 measures 95 m in BAL and more than 90 m in AML. The base is represented by an erosional transgressive surface that coincides with the SBAM-2 of late Late Hauterivian age (*C. andinus* /*C. perditus* Subzone of the *C. diamantensis* Zone). The top is the SBAM-3 which is placed above the beginning of the *Paraspiticeras groeberi* Zone, provisionally dated as Early Barremian (Aguirre Urreta and Rawson 1993; Aguirre Urreta et al. 2005). A transgressive systems tract and a highstand systems tract of similar thicknesses compose the depositional sequence DSAM-3. Both systems tracts show strong retrogradational and progradational stacking patterns of S/D sequences, respectively and a conspicuous maximum flooding zone (MFZ-3) interpreted as the possible expression of the Faraoni AOE (see Anoxic Events above). High-frequency sequences (fifth-order) are more or less evident, probably overprinted by the significant deepening related to the Faraoni Event. The section at AML is strongly faulted and poorly exposed a few meters above the MFZ-3 and this upper part was not studied. TST-3 develops between 306 m and 351 m at BAL and 343 m to 396 m at AML, almost completely in the latest Late Hauterivian *C. andinus* /*C. perditus* Subzone. Facies in dilution hemisequences of the early TST-3 consist of bioturbated fine-grained sandstones, hummocky cross-stratification and coarsely interlayered bedding, reflecting lower shoreface and upper offshore (i.e. inner and middle ramp) depositional environments. Characteristic late TST-3 sediments are bioturbated micritic silty clays and argillaceous siltstones, reflecting both, deep depositional settings (outer ramp) and generalized starvation. At BAL, at the early part of the TST there is a well-developed fourth-order sequence composed by four S/D sequences that clearly have a lower retrogradational TST and upper progradational RST. Thickly developed starvation hemisequences usually with a complex set of shell concentrations are another feature of the early TST-3. In AML this systems tract has a different configuration: fourth-order sequences are not unambiguously developed. The outstanding feature of the TST-3 in AML is the stacking of several starvation hemisequences without the respective dilution hemisequences, indicating phases of enhanced terrigenous starvation (see Appendix- Fig.2, AML section, 343-353 m from the base and Pl. 7, Fig. 2). MFZ-3 is a conspicuous feature of the unit at both sections. It consists on an alternation of short, bioturbated and muddy dilution hemisequences intercalated with variably thick starvation hemisequences composed of a homogeneous, densely-packed bioclast-supported shell bed (low-energy micritic rudstones facies). The starvation hemicycle in the middle of the MFZ reaches almost 1 m in thickness in BAL and more than 2 m in AML. Regardless the differences of TST-3 between sections, MFZ-3 has very similar facies at both localities, with a comparable development. This fact makes this maximum flooding zone a useful stratigraphic feature for correlation and a plausible expression of the Faraoni AOE.

The HST-3 is only partially exposed at AML. Nevertheless, its lower part shows a progradational trend. At BAL there is a distinct coarsening- and shallowing-upward trend up-section, together with the marked increment in the thickness of the S/D sequences. Dilution hemisequences range from offshore micritic mudrocks to lower shoreface bioturbated fine-grained sandstones with hummockies and ripple cross-lamination. Specimens of *Paraspiticeras groeberi* occur in the middle part of the HST. Although the age of this species is doubtful, it is reasonable to regard the beds containing *P. groeberi* as Early Barremian in age, provided it is placed above the expression of the Faraoni Event of latest Hauterivian age (Ogg et al. 2004), without any kind of unconformity inbetween.

The early HST-3 at BAL is characterized by an alternation of two kinds of cycles (see Appendix- Fig. 1, BAL section, 352 m to 365 m above the base): main (normal) S/D sequences with the dilution hemisequence showing a more or less pronounced coarsening-upward trend, and whose starvation hemisequences are mainly bioclastic limestones. The second (minor) kind of cycle consists of thin intercalations of shell beds, one per dilution hemicycle of the main S/D sequences. These shell beds are homogeneous, have a micritic and muddy matrix and are characterized by very well preserved, mainly disarticulated bivalves, gastropods, and scaphopods, in contrast with the less well preserved fauna in the starvation hemisequences of the main S/D sequences. The minor cycles are interpreted as subordinated (minor) starvation hemisequences that formed during deposition of the main dilution hemisequence. It is proposed here that these cycle couplets represent the expression of orbital cycles of obliquity (for a detailed discussion see the section on High Frequency Cycles in this chapter).

SBAM-3 of Early Barremian age represents an erosional surface on top of a coarsening- and shallowing-upward stacking of S/D sequences. It is interpreted as the subaerial unconformity, placed on top of the HST.

Upper part of the member

The upper 150 m of the Agua de la Mula Member, above the SBAM-3, exhibit a different and distinct stacking pattern of S/D sequences. It is not possible to divide this segment of the unit into the systems tracts of a single sequence. Instead, six sedimentary packages can be recognized, interpreted as sedimentary sequences (DSAM-4 to 9). These sequences can, in turn, be grouped into three segments, the boundaries placed at the position of thickly developed oolitic grainstones (SBAM-5 and 7), which indicate important events of shallowing of the basin. There are no ammonites in these beds with the exception of a single specimen, not yet described, collected from the uppermost part of the member at BAL, and some fragments of a another species mentioned in the literature (Aguirre Urreta et al. 2005). In the next section, the age of the last 150 m of the unit will be assessed after correlating it with the global/European charts of sea-level change.

Facies differences in each of the six sequences are more drastic than in the older sequences of the unit. For instance, the facies in the second sequence (DSAM-5) change from micritic fissile argillaceous siltstones to a 2-m-thick bed of shoreface origin with amalgamated hummockies at top of the regressive package, and a several-metres-thick bio-oo-grainstone, in only five S/D sequences. Facies analysis suggests that there was low terrigenous input for the last 150 m. Consequently, facies belts were narrower in a more or less sediment-filled basin. Only during late stages of regression of intermediate or major sequences, sedimentation rate was high enough to fill the basin margins and generate progradational patterns like those observed in the BAL section. From the facies differences, taken as a proxy of the magnitude of the base level change, these sequences should be considered as of third order. However, they are composed of a maximum of nine S/D sequences, which suggests that they involve little time, less than expected for a major sequence. An alternative interpretation would imply the erosion or non-deposition of many of the cycles due to the lack of accommodation space. For the purpose of this study, all these sequences will be considered as of fourth-order (but named as main sequences, DSAM-4 to 9), and other possible interpretations will be discussed.

Three meters above the SBAM-3 there is a conspicuous starvation hemisequence deposited on an inner ramp setting. Its sandy matrix, iron content, and the highly abraded nature of the large and thick-shelled dominating benthic fauna indicate deposition under high-energy conditions. All these features are shared with the first bed above the transgressive surfaces of DSAM-1 and 2. This bed (named BA 94, see profile in App.-Fig. 1) is probably the first starvation hemisequence above the TS-4 below.

The DSAM-4 to 7 have more or less well developed lower retrogradational and upper progradational packages, identified as TSTs and RSTs, respectively. Sequence boundaries are transgressive (ravinement) surfaces. Whether these sequence boundaries represent the top of the HST, FSST or LST remains unclear. MFZs are not clearly developed. Starvation hemisequences close to MFZs are matrix-rich fine-grained bioclastic limestones (mudstones, wackestones, packstones, and floatstones), while closer to sequence boundaries coarser textures (grainstones and micritic rudstones) are common. Shells in fine-grained bioclastic limestones show different sizes and low quality of preservation due to high degrees of micritization. Shells in grainstones are highly abraded and rounded. Starvation hemisequences deposited in segments with high proportion of terrigenous sediments are usually mixed rocks and contain well-preserved benthic fossils.

SBAM-5 and 7 underlie thick packages of upper shoreface bio-oo grainstones and probably represent higher hierarchy (third-order) sequence boundaries that separate two inferred third-order sequences, each composed by two fourth-order sequences (DSAM-4 and 5, and DSAM-6 and 7). The uppermost 50 m were provisionally subdivided into two sedimentary sequences (DSAM-8 and 9), with the boundary placed below a moderately thick bio-oo-grainstone bed at 526 m above the base. These sequences cannot be subdivided into systems tracts as facies in dilution hemisequences do not show any kind of trend.

Correlations with global and European sea-level charts

Sedimentary sequences described above were compared with global and European sequence stratigraphic charts (Haq et al. 1987; Hardenbol et al. 1998) in order to establish correlations between sequences, sequence boundaries, and maximum flooding surfaces. A detailed scheme of the sedimentary sequences of the Agua de la Mula Member is presented in Text-Figure 9. In Text-Figure 10 the main sequences recognised in the member are compared with the detailed sequence chronostratigraphic chart of Hardenbol et al. (1998). As it does not make sense to correlate the abundant high-frequency sequence boundaries described in this study, only third- and occasionally fourth-order sequence boundaries have been used for correlation purposes.

Early Hauterivian

SBAM-0 is placed at the base of the section between the *vacaense* and *spitidiscus* biozones. It is probably equivalent to the sequence boundary HA3 of latest Early Hauterivian age (*Lyticoceras nodosoplicatum* Zone). However, although both sequence boundaries coincide in time, SBAM-0 represents one of the major sea-level falls in the history of the basin, a feature that does not fully correspond to the 'medium' nature of HA3. As has been mentioned before, SBAM-0 may represent a tectonically driven base-level fall or an eustatic, tectonically enhanced (uplift) fall. The sequence boundary of Haq et al. (1987) at the base of the third-order sequence 2.5 does not coincide with SBAM-0, as the former is placed at the base of the *L. nodosoplicatum* Zone, i.e. it is older than the latter.

Late Hauterivian

The Late Hauterivian sequence boundaries HA4 to 6 coincide with the three main sequence boundaries described in this study for the same time segment: SBAM-0/1, SBAM-1, and SBAM-2, respectively. There are two more sequence boundaries between SBAM-1 and 2 (SBAM-1/1 and 2). These SBs separate three fourth-order sequences that are of lower hierarchy than DSAM-2 and have no equivalents in the published charts. SBAM-2/1 marks the top of a short eccentricity cycle (see below). As such, it represents a minor sequence boundary. It may coincide with the minor boundary HA7 of Hardenbol et al. (1998) but with uncertainty. The major maximum flooding surface coinciding with the Faraoni Event and placed in the *ohmni* Biozone of the European basins has its equivalent in the MFZ-2 of the Neuquén Basin.

The two medium sequence boundaries proposed by Haq et al. (1987) for the Late Hauterivian may correspond to SBAM-0 and SBAM-2. If so, SBAM-1 would not have a global equivalent. Conversely, if SBAM-1 were placed at the top of the HST (at 165 m in BAL and at 185 m in AML) and not on top of the FSST, it would belong to the *riccardii* Biozone, and would correlate with the oldest Late Hauterivian sequence boundary of Haq et al. (Haq et al. 1987). In this case, the two main Hauterivian sequences boundaries of the Neuquén Basin would have equivalents in the sequence stratigraphic chart of Haq et al. (1987).

Barremian

SBAM-3, occurring in the *groeberi* Biozone is a relevant third-order sequence boundary that reliably correlates with the major sequence boundary BARR 1 of the European Basins. It represents the first sequence boundary above the Faraoni Event (see section 6.3. of this chapter). From SBAM-3 to the top of the unit there is not biostratigraphic control (see Aguirre Urreta and Rawson 1997; Aguirre Urreta et al. 2005). Therefore, published sequence boundaries can be used as references to date the Barremian marine sediments of the Neuquén Basin, until the biostratigraphy of this part of the succession is better understood. In this way, sequence boundaries SBAM-5, 7 and 9 correlate with boundaries BARR 2, 3, and 4. SBAM-9 that represents the top of the unit, is a eustatically driven major drop in base level overlain by fluvial and evaporitic sediments of the Huitrín Formation (Leanza 2003). It is correlated with the major sequence boundary BARR 4 of Hardenbol et al. (1998). The Early Barremian major MFS of the *caillaudianus* Zone in the chart of Hardenbol et al. (1998) has not an unequivocal equivalent in the Neuquén Basin. The sequence boundary of Haq et al. (1987) below sequence 3.3 is inferred to correspond to the oldest Barremian sequence boundary SBAM-3 . If the other two Barremian sequence boundaries of the chart (at the base of sequences 3.4 and 3.5) were correlated with the main boundaries SBAM-5 and 7 described here, then SBAM-9 would have to be placed already in the Aptian. This option does not seem to be justified, although it has been suggested in sequence chronostratigraphic charts previously published for the Neuquén Basin (Legarreta and Gulisano 1989; Legarreta et al. 1993). The first interpretation, shown in Text-Fig. 10, is supported in this work. A better understanding of the ammonite biostratigraphy of this part of the succession will solve this problem.

High-frequency sequences

The development of complex sedimentary patterns, product of the interaction between cyclic sea-level changes of several different orders of magnitude, becomes most apparent in outcrop-based, high-resolution sequence-stratigraphy. The interactions among multiple orders of sea-level oscillations can be additive or substractive and, ultimately, determine the actual rate of sea-level change (MacNaughton et al. 1997). Such sedimentary successions have been extensively studied in carbonates where complex arrangements of nested sequences of different hierarchies have been well demonstrated (e.g.Wilmsen 2003). In siliciclastic settings they have only recently been systematically investigated (MacNaughton et al. 1997), examples being Mitchum and Van Wagoner (1991), MacNaughton et al. (1997) and, for the Agrio Formation, Spalletti et al. (1990; 2001a) and Sagasti (2001).

Nested sequences of third- to sixth-order are evident throughout the succession at both sections. The Avilé and Agua de la Mula members of the Agrio Formation are interpreted as a second-order sedimentary sequence, the Upper Mendoza Mesosequence (Legarreta and Gulisano 1989). It has been subdivided into third-order sequences, although their number and stratigraphic position have not been unequivocally defined. If the cycles are analysed from the lowest to the highest hierarchical level, four types of sequences are recognised: (1) S/D sequences, interpreted as Milankovitch precession cycles. (2) Bundles of around five S/D sequences considered as short-eccentricity cycles of the Milankovitch band. (3) Groups of short-eccentricity cycles, although less clearly defined, lump together to form possible long-eccentricity cycles. (4) At certain levels in the rock succession, couples of S/D sequences show a zigzagging facies trend behaviour, interpreted here as the response to obliquity cycles.

The combined effects of two of these cyclicities can have additive or subtractive effects. The simultaneous action of more than two cyclicities may produce highly complex, not easily interpretable patterns. The position with respect to coastline and depth seem to be crucial when dealing with multiple-order sequence patterns. In both, deep and shallow settings, multiple order cyclicities are expected to be poorly expressed or not developed at all. In deep settings, a complete succession will be preserved, but facies contrasts are commonly too subtle to distinguish different orders of cyclicities. Techniques other than facies analysis (resistivity, gamma ray, and sonic logs) were used to study the same succession from a drill hole in a basinal position, in the southern Mendoza province (Spalletti et al. 1990). These authors found four hierarchical rhythmicities that they interpreted as due to precession and three eccentricity cycles of different periodicity. Sedimentary packages deposited mainly in shallow environments are dominated by processes of erosion and non-deposition during sequence boundary development, and consequently the loss of evidences can be expected.

(1) Sixth-order starvation/dilution sequences and Milankovitch's precession cycles

The starvation/dilution sequences (S/D-Ss) are the lowest hierarchy sequences recognizable in the field (Text-Fig. 7). They show a wide variety of types regarding their different features, e.g. presence/absence and thickness of each of the two hemisequences, kind of sediments, sedimentary structures, trace fossils, taphonomic features of macrofossils, and the occurrence of amalgamation or the stacking of incomplete sequences (Appendix-Figs. 1-2). A simple calculation based on the 5.4 My estimated for the unit from the base of Upper Hauterivian to the top of the Lower Barremian (ages taken from Ogg et al. 2004), results in a figure between 38,000 and 43,000 years for each of the 127 to 141 S/D sequences identified. The figure, close to 40 ky, is an overestimation if the time periods not represented by sediments are taken into account. In a sedimentary sequence, i.e. the product of a cyclic base level change, more than half of the time corresponds to the deposition of falling stage and lowstand systems tracts that are usually not deposited together with highstand and transgressive systems tracts. Moreover, part of the sequences can be expected to be lost by subaerial or submarine erosion during falling and lowstand of the base level, and during the subsequent ravinement process. Therefore, these cycles are inferred to represent the sedimentary product of the ca. 20 ky precession cycle of the Milankovitch band. Besides, the S/D sequences are commonly found in groups of around five, a pattern described as "precession-eccentricity syndrome" taken as an evidence of both, the precession and the ca. 100 ky, short-eccentricity cycles of the Milankovitch band (Gale 1998).

The characteristics of the sixth-order sequences differ throughout the sections. The majority of the sequences consist of a basal, terrigenous-starved *starvation hemisequence* and an upper, terrigenous-rich *dilution hemisequence*.

S/D sequences are considered here as caused by base-level changes, mainly driven by eustatic cyclic sea level changes (see next section for a discussion about genetic aspects of S/D sequences). In some examples starvation hemisequences are absent, while in others they are the only component. In the remaining examples that represent the majority, both hemisequences are present.

Most of the S/D sequences in offshore settings are complete. In these cases, the two components can be interpreted as a basal transgressive and an upper regressive systems tracts. Due to the poor thickness and the little time involved in the development of these sixth-order sequences, a distinction between highstand, falling stage, and lowstand systems tracts, if more than one is present, cannot be not expected. Depth changes during the regression did not significantly modify the sedimentary environment in which the sequences were built. Under this scenario, the eustatic sea-level change produced two simple alternating signals; terrigenous sediment starvation during the transgression and terrigenous sediment dilution during the regression. The sequence boundary, which underlies the starvation hemisequence, is always sharp but usually not erosional. It represents the onset of the starved conditions, coinciding with the beginning of the transgression, i.e. it would be equivalent to the maximum regressive surface and the transgressive surface. The top of the starvation hemisequence does not necessarily coincide with the top of the transgression, as will be described in the next section. In these settings, there are not signs of a maximum flooding zone.

Starvation/dilution sequences deposited in environments that are more proximal have different characteristics. The top of the regressive systems tract consists of facies that are shallower than the storm-weather wave-base (facies associations 2 and 3). The sequence boundary is usually erosional and the early starvation facies are coarse-grained mixed carbonate-siliciclastic rocks or limestones (see Pl. 6, fig. 7). The sequence boundary coincides with the transgressive surface and the maximum regressive surface. However, the top of the maximum regressive surface does not necessarily represent the top of the LST, FSST or HST. The first two could have been deposited in a more basinward position and became preserved, or be partially or completely removed by the onset of the following transgression (ravinement). Part of the upper part of the RST is expected to have been removed between the sea level fall and the ravinement. A horizon with maximum degree of starvation, taken as maximum flooding zone, is present in some of these S/D sequences. It is noteworthy that the positions of these MFZs do not coincide with the top of the starvation hemisequences. Instead, they are in the middle. The top of the starvation hemisequence is indicated by a gradual change from bioclastic-rich mudrock to a siliciclastic rock without fossils.

The sequence boundary of sixth-order sequences coincides with the transgressive surface. It is placed at the base of the starvation hemisequence and is easily recognizable in almost all cases throughout the sections. Conversely, the boundary between starvation and dilution hemisequences has different meanings according to the depth at which the sequence developed. At intermediate depths, the maximum flooding surface, i.e. the top of the transgressive systems tract, is pinpointed in the middle of the starvation hemisequence. Starvation hemisequences are, hence, not full equivalents of transgressive systems tracts. A similar situation is inferred for sequences in deeper settings, where the usually simple homogeneous starvation hemisequence does not have a surface indicating maximum flooding. Starvation hemisequences in shallow settings are interpreted as fully transgressive and are equivalent to TST. Dilution hemisequences are inferred to be composed by sediments deposited during different segments of the sea-level curve, depending on depth. They are usually not strict equivalents of the highstand systems tract. Small (i.e. lower hierarchy) sequences such as S/D ones exhibit fewer features for dividing them into systems tracts and are thus not suitable to be interpreted in terms of models that were built for higher sequences (third-order or higher). In Text-Fig. 11 A-C, three sixth-order sequences developed in distal to proximal positions are shown, together with the components, surfaces and the interpretation of the position of systems tracts.

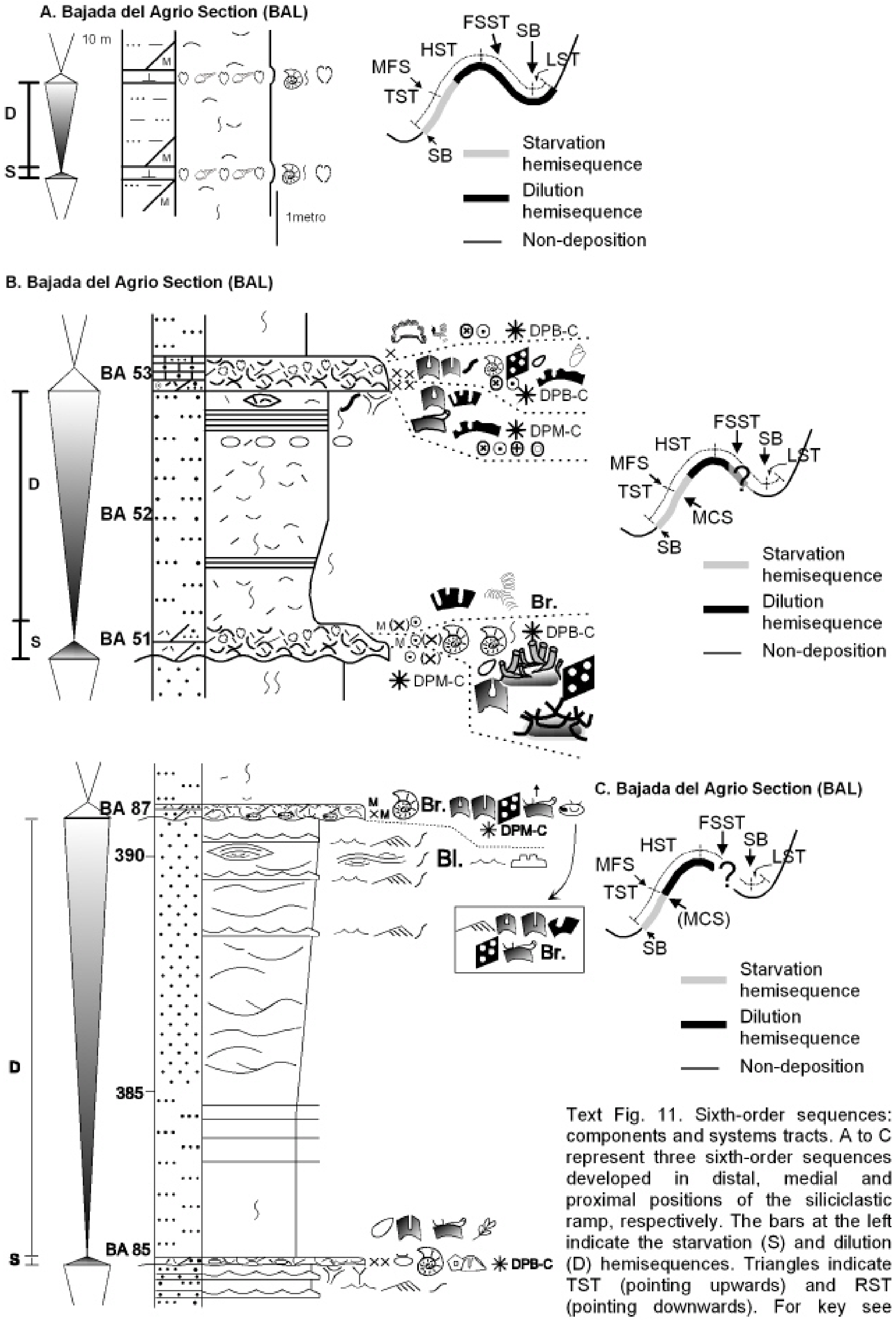

Text Fig. 11. Sixth-order sequences: components and systems tracts. A to C represent three sixth-order sequences developed in distal, medial and proximal positions of the siliciclastic ramp, respectively. The bars at the left indicate the starvation (S) and dilution (D) hemisequences. Triangles indicate TST (pointing upwards) and RST (pointing downwards). For key see Appendix-Fig. 3.

(2) Fifth-order sequences: Milankovitch short-eccentricity cycles

At several positions in both sections bundles of four to six S/D sequences lump together in packages that, with different configurations, are interpreted as sequences. These sequences are inferred to indicate the ~100 ky short eccentricity cycles of the Milankovitch band, and expected to be composed by around five 20 ky precession cycles. However, due to erosion during sea level fall and other stratigraphic "noise" a figure between three and eight is probable (Fischer 1986b). Four types of eccentricity cycles were detected in the present study.

Sedimentological cycles type 1. Composed of lower retrogradational and upper progradational stacking of S/D sequences. The stacking patterns are recognised from the facies in the dilution hemisequences. This type of eccentricity cycle is common in DSAM-2 and 3. Examples include BAL 276-306 m, 306-328 m (Text-Fig. 12), 328-346 m and -AML 239-269 m, 269-288 m, 288-313 m and 313-343 m (Text-Fig. 6; Appendix-Figs. 1-2). In some cases, enhanced starvation related with fifth- or fourth-order cyclicity caused the stacking of two or more starvation hemisequences, almost completely lacking sediments of the dilution component. Examples are BAL at 225 m and 282 m, and AML at 239, 280, 343 and 350 m (Text-Fig. 6; Appendix-Figs. 1-2; Pl. 7, Fig. 2). The amalgamation of starvation hemisequences, also related with phases of enhanced starvation and/or reworking has been detected in several S/D sequences (App.-Figs. 1 and 2). Amalgamation is inferred from different stratigraphic and taphonomic features, for instance thickly developed starvation hemisequences, internal surfaces of erosion and the presence of concretions formed early on during the diagenesis that are bored and encrusted by serpulids and oysters. However, none of the features used for inferring amalgamation is conclusive.

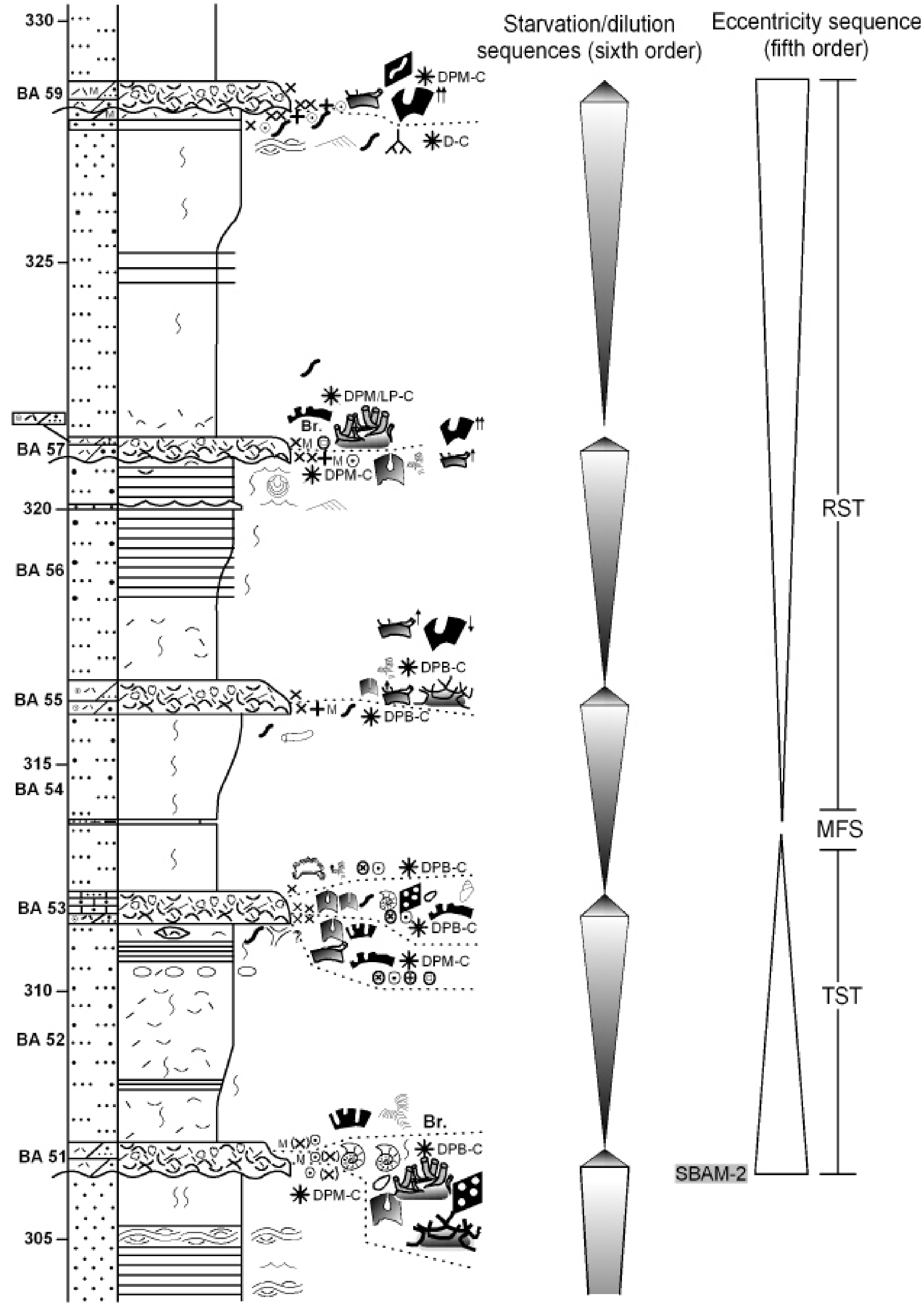

Text-Fig. 12. An example of fifth-order sequences: short-eccentricity cycles of the Milankovitch band. Section BAL at 304-330 m

Sedimentological cycles type 2. These cycles are similar to type 1 with the exception that sequence boundaries are clearly marked by an erosional surface separating siliciclastic shoreface facies below from calcareous shoreface facies above. The main evidence of cyclicity is a strong progradation of siliciclastic facies at the end of the sequence, into a generalized terrigenous starvation. Examples are BAL at 403-431 m, 466-486 m, and 486-503 m (App.-Fig. 1).

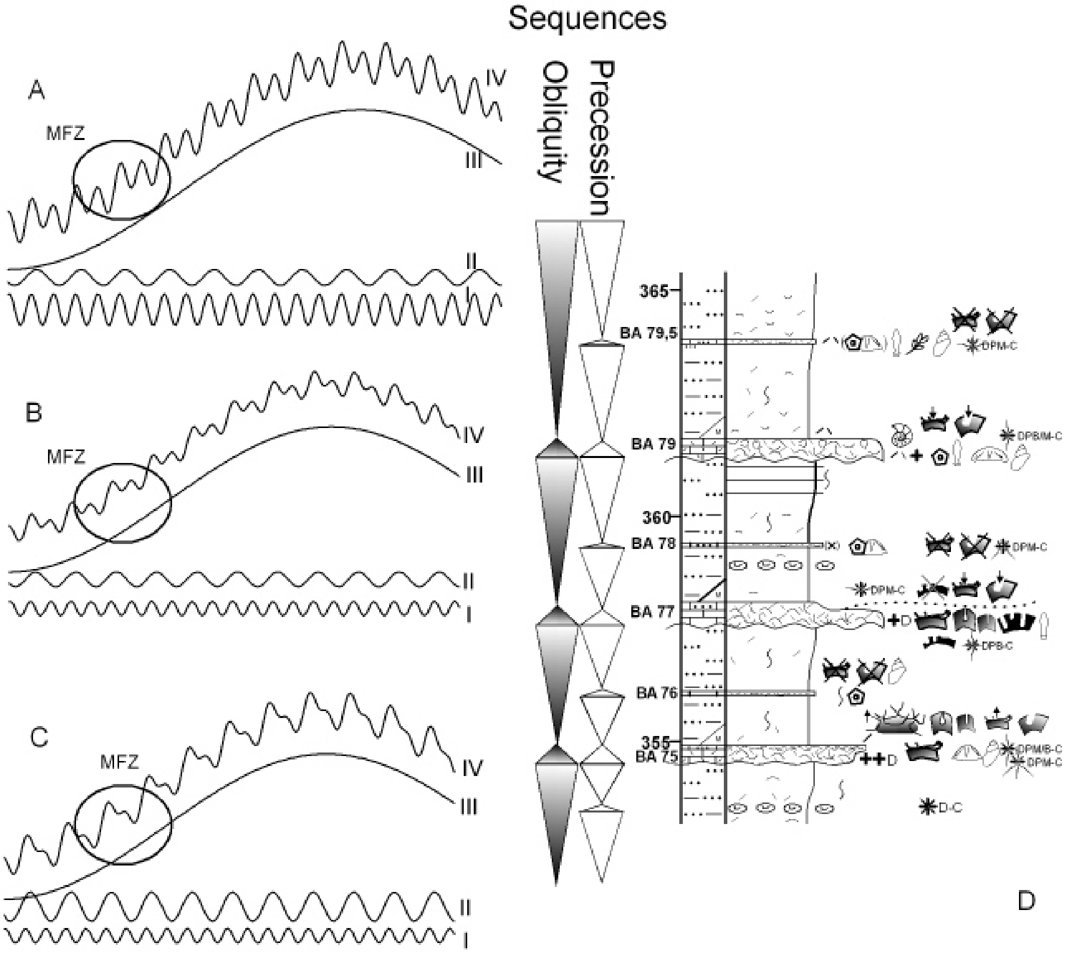

Text-Fig. 13. Models of sea-level change used to explain possible Milankovich obliquity cycles. Curve I, II and III represent precession, obliquity and a major cycle. Curve IV is the sum of curves I, II and III, and represents the actual eustatic sea-level change of the model. **A** The intensity (amplitude) of precession is two times that of obliquity. **B** Precession and obliquity have the same intensity. **C** Obliquity intensity is two times that of precession. **D**, BAL section from 353 to 365 m where obliquity can be clearly seen.

Taphonomic cycles type 1. Taphonomic cycles type 1 consist of groups of two or more "normal" sixth-order sequences with thin starvation hemisequences containing skeletal concentrations with weakly reworked shells that alternate with a sequence containing a single, usually thicker bed with stronger evidence of erosion and reworking. These thick starvation beds usually enclose concretions formed early on during diagenesis, with evidence of having been exhumed and reworked (encrustations and borings occurring on both sides). An interpretation of the thick beds is the amalgamation of two or more cycles by means of erosion and little or no deposition during a period of particularly high starvation. None of the dilution hemisequences shows facies trends. The bundles of S/D sequences of two types are interpreted as proper sequences and, taking into account the number sixth-order units involved, they are interpreted to correspond to short eccentricity cycles of the Milankovitch band. The monotonous succession of basinal to outer ramp, “normal” S/D sequences, characterized by the alternation of periods of starvation and non-starvation but without marked depth changes, is interrupted by a period in which base-level fall was large enough to bring the sear floor within the storm wave-base. During this period, distal tempestites supplied broken bioclasts and storm waves swept the sea floor increasing the firmness of the substrate by exhuming concretions and shells that enabled hard-bottom dwellers to settle. Examples are AML 15-150 m and BAL 40-140 m (Text-Fig. 6; Appendix-Figs. 1-2).

Taphonomic cycles type 2. This type is represented by a single example observed in BAL between 142 and 166 m. The cyclicity is evident from features of the fossil content in the starvation hemisequences of sixth-order sequences. The basal starvation hemisequence is a thick bed with a densely packed skeletal concentration deposited on the middle ramp. Diagenetic dissolution is patchily present. The starvation hemisequences of the following four S/D sequences consist of weakly developed micrite-rich mixed carbonate-siliciclastic levels (marls or micritic silts/sands). The fossil content of these levels increases up-section, from disperse to loosely-packed concentrations. Part of the fossil content in the micrite-rich levels is thought to have been dissolved. This is supported by the high degree of micritization of the skeletal remains. The high degree of destruction of the skeletal remains, in contrast with what is found in shell beds with mixed or siliciclastic matrices, is corroborated by the findings of Kidwell et al. (2005) that shell loss by means of bioerosion and dissolution is higher in carbonate settings.

Fifth order sequences are composed of a lower TST and an upper RST. It is not possible to discriminate between the different components of the RST. It is also not sensible to assume that in all cases the RST consists only of the HST. Consequently, the transgressive-regressive sequence model fits the fifth order sequences better. The sequence boundary is the top of the RST, equivalent to the transgressive surface. The maximum flooding zone represents the limit between the two systems tracts, TST and RST, which usually lacks distinguishable features.

(3) Long-eccentricity cycles of the Milankovitch band

DSAM-2 at BAL contains 18 sixth-order sequences (precession cycles), which can be sorted into three fifth-order ones (short-eccentricity cycles) and a probable incomplete sequence at the base (Text-Fig. 6; Appendix-Figs. 1-2). The evidence strongly suggests that DSAM-2 is the sedimentary response to the long-eccentricity 400 ky orbital Milankovitch cyclicity. In a hierarchical scheme, DSAM-2 would correspond to a fourth-order sequence, although in this study it is not subordinate to any third-order sequence and hence considered as a “main” sequence. DSAM-3 is composed by 23 sixth-order sequences that cannot be unequivocally sorted into fifth-order sequences, with the exception of the basal DSAM-3/1. This sequence is also considered as the product of a long-eccentricity Milankovitch cycle. DSAM-1/1 and 2 are subordinate to the main (third order) sequence DSAM-1, and considered as of fourth-order. These two fourth-order sequences cannot be linked to any of the cyclicities in the Milankovitch band.

(4) Obliquity couplets

Close to MFZ-2 and 3 (BAL) and MFZ-2 (AML), a distinct pattern of alternation of sixth-order sequences indicates a different sort of cyclicity. It consists of normal S/D sequences (i.e. starvation component and dilution hemisequence consisting of a more or less distinct coarsening-upward facies succession) that have a very thin tabular calcareous bed intercalated. This bed is interpreted as the starvation hemisequence linked to a different cycle. It is thinner than the other starved bed, and the shelly content shows little evidence of physical destruction or exposure on the sea floor. The phenomenon can be clearly observed in the BAL section from 353 to 390 m. Other examples are BAL 250-290 m and 330-350 m; and AML 295-330 m (Text-Fig. 6; Appendix-Figs. 1-2). Both types of starvation hemisequences have different faunal contents that cluster in different benthic fossil associations. For instance, in the BAL section from 353 to 390 m, thin beds contain the fossil association P (Veneridae sp. 2- *Panopea neocomiensis*) that characterize outer ramp settings into the mixed-ramp, with availability of organic matter on the sea floor and low energy. Thick beds in turn contain middle ramp, moderate energy associations J, L and K (for more information see Sinecology in Chapter 8). I interpret that every two sixth-order (i.e. precession) sequences, an augmentation of the eustatic signal of the precession frequency is produced. This cycle pattern, which is in phase with the precession signal, causes the setting to become significantly shallower so that coarsening-upward trends are possible. In the same way, starvation hemisequences are thicker and the fauna carries evidence of stronger physical damage. This situation is only possible at positions where the “normal” precession signal needs an augmentation to generate a shallowing that has sedimentological relevance, i.e., that shifts the sea floor from basinal settings to the outer or middle ramp. The frequency of this phenomenon, i.e. once every two precession cycles indicates the presence of a 40 ky cyclicity interpreted here as obliquity signal of the Milankovitch band. At major MFZs none of the two intensities would make a relevant change in depth and only the “signals of starvation” would leave a sedimentary fingerprint. At late major HSTs every precession cycle would leave a similar signal. An alternative interpretation for the latter implies the progressive tendency of the cycles to be out of phase resulting in a pattern with multiple cycles (three in this case; two of precession and one of obliquity). Out-of-phase obliquity cycles could have a weak signal and may not be recognizable under the higher sedimentation rate governing the late major HST. If the intensity of the obliquity signal were higher than that of the precession signal, at late highstand positions there would be only one signal, driven by the obliquity frequency. In Text-Fig. 13 a hypothetical sea-level curve illustrates the phenomenon described above. In this Text-Fig., three situations are considered in relation to the relative magnitude of the precession and obliquity signals. Considering that the majority of the starvation-dilution sequences described in this work are interpreted as caused by the precession signal, it seems parsimonious to infer that precession signal is stronger than obliquity and then only in some cases the combination of both signals can have a detectable effect (Text-Fig. 13 A).

Discussion

Main sedimentary sequences are well developed in the Agua de la Mula Member. However, patterns of stacking of the sixth-order sequences that compose the systems tracts are somehow blurred by the development of high frequency sequences nested into them, the non- recording of sediments by erosion and/or non-deposition, and the latest Hauterivian major transgression probably related to the Faraoni Event. For instance, the DSAM-2 has three MFZs, of which the middle one was regarded as recording a third-order cyclicity because it marks the general change from retrogradation to progradation throughout the whole sequence. However, the remaining MFZs are almost of equivalent magnitude. Other dissimilarities with the expected pattern of a sedimentary sequence are explained by the occurrence of multiple out-of-phase cycles. An example, and an alternative explanation for the deposition of the top of DSAM-1 in AML (already discussed above), may be the occurrence of a short-eccentricity cycle close to the top of the rise in the relative sea-level curve. The relative sea-level rise of the subordinate curve would have caused a minor retrogradational or aggradational pattern within a general progradational stacking of S/D sequences. Conversely, if cycles were in phase, normal (i.e. upward prograding), late HST would be expected. Examples of multiple in-phase cycles would be the top of DSAM-2 and 3. Text-Fig. 14 represents a hypothetical curve of relative sea-level rise modified by the addition of four different cyclicities not completely in phase as well as by the effect of subsidence. In this Text-Figure the two cases described above have been identified. Out-of-phase cycles do not fit models that show low hierarchy sequences nested into higher hierarchy ones (Catuneanu 2002). However, if the intensity of the higher hierarchy cycles exceeds in most that of the other ones, a nested pattern could be expected, as the sedimentary effect of the minor cycles would be irrelevant at sequence boundaries and MFZs.

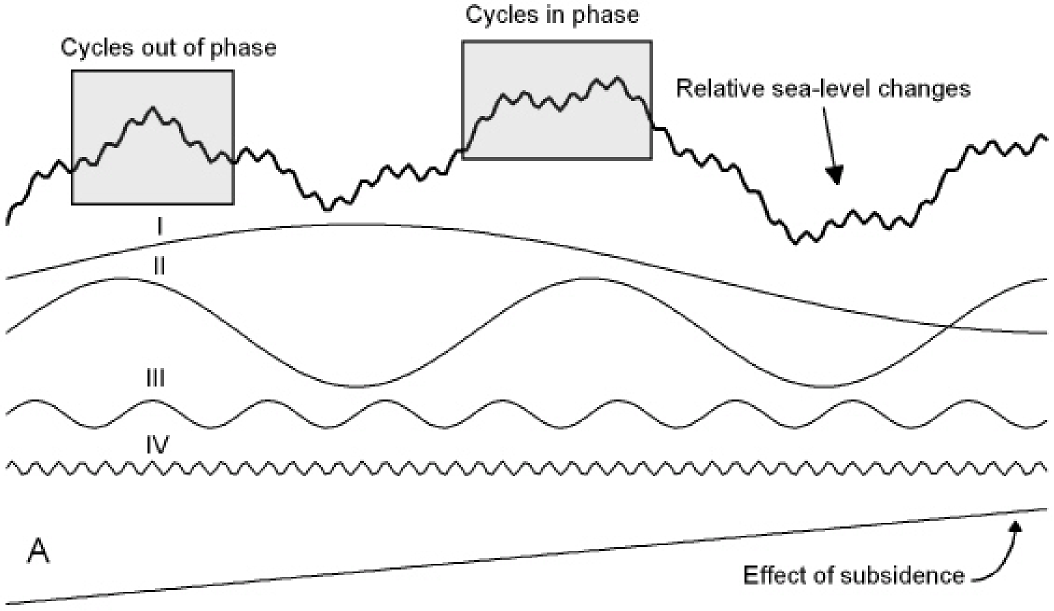

Text-Fig. 14. Hypothetical relative sea-level curve as a function of four cyclic functions and a constant subsidence (linear function). The relative sea-level curve is the result of the sum of the curves I to IV and the effect of subsidence. Curves I to IV are constructed from sinus functions. There are nearly three cycles of curve II into curve I, four of curve III into curve II and five of curve IV into curve III. Curves were built in a way that they are not always in phase. Curves I and II have a similar effect (amplitude). Amplitude of curve III is half that of curves I and II while curve IV is two times shorter than III.

DSAM-1/1 is subordinate to the main, third-order cycle DSAM-1, and thus considered of fourth-order level. However, if numbers of sixth-order sequences and time involved are considered, DSAM-1/1 could well be a third-order cycle, albeit ill developed because of having formed while water depth was great and/or accommodation space was created fast. The second and third main sequences (DSAM-2 and 3) are shorter and composed of fewer S/D sequences when compared with the basal DSAM-1. DSAM-2 is actually composed by the stacking of three or four subordinate sequences that, in turn, are composed of five to seven S/D sequences, a total of 18 in the BAL section. DSAM-1/1 probably involves more time as it is composed of more than 30 S/D sequences.

The Avilé Member is a tabular sandstone body mainly composed of fluvial sediments, intercalated between offshore mudrocks (Pl. 3, Fig. 5). It has been interpreted as a lowstand wedge produced by a major relative sea-level drop that almost completely exposed the entire basin (Legarreta and Gulisano 1989; Veiga et al. 2002). The surface below the Avilé Member is considered to represent a second-order sequence-boundary that marks the base of the Upper Mendoza Mesosequence. Nonetheless, the passage from the underlying offshore mudrocks of the Pilmatué Member to the fluvial and marginal marine facies of the Avilé Member is sudden. This and also the sharp upper contact with the basinal shales of the Agua de la Mula Member, almost without any signs of transgressive deposits inbetween, may indicate that this sea-level fall was tectonically enhanced.

Sequence stratigraphic charts of the Neuquén Basin for the Hauterivian-Barremian have been published in Legarreta (1989) and Legarreta et al. (1993). Legarreta and Gulisano (1989) mention three sequences for the investigated segment, named Ms1 to 3, whose age was based on ammonite biozones or, when not possible, on the sequence stratigraphic chart of Haq et al. (1987). However, in the cited work there are is no explicit correlation between sequences and ammonite biozones, and/or Haq's sequences Thus it is not possible to establish correlations with the sedimentary packages described here. Nevertheless, the three sequences mentioned by Legarreta and Gulisano (1989) may correspond to the three segments mentioned in Chapter 4. In this case, the boundaries defining the sequences would correlate with SBAM-1 and 3. Legarreta et al. (1993) briefly describe the presence of nine sedimentary sequences for the Agua de la Mula Member in its northern outcrop area. The sequences and their correlation with ammonite biozones are not presented with the exception of a simplified chart that considers only two biozones for the whole unit: *C. andinus* that is equivalent to the *S. ricardii, C. schlagintweiti* and *C. diamantensis* zones, and *P. groeberi*, the equivalent of the current homonymous zone. The beds up to the top of the unit appear as "in review". The sequence chronostratigraphic chart built in this dissertation agrees with the chart of Legarreta et al. (1993) in some important aspects. First of all, there are also nine main sequences in this study, if all non-subordinate packages are considered, regardless of their hierarchy. Secondly, sequence boundaries are largely equivalent: Legarreta et al. (1993) place two sequence boundaries below the *P. groeberi* Zone that can correlate with SBAM-1 and 2; two more within the *P. groeberi* Zone would correspond with SBAM-3 and 4 and, finally, five more sequence boundaries above this biozone (DSAM-5 to 9). Legarreta et al. (1993) place the top of the AMMb already in the Albian, probably based on correlation with the sequence chart of Haq et al. (1987). Recent biostratigraphic articles (Aguirre Urreta and Rawson 1997; Aguirre Urreta et al. 2005) tend to consider that the youngest sediments of the member as Early Barremian, although authors show no evidence in support of this hypothesis.

Origin of high frequency sequences

According to the Milankovitch theory external climatic forcing results from changes in the orbital parameters of the Earth's path around the Sun which affect the amount of solar radiation received at the top of the atmosphere (Berger and Loutre 1989). The Milankovitch-related eustatic sea-level changes are known to be produced by means of changes in the volume of water in the ocean. This happens, in first place, through growth and decay of continental ice sheets, and subordinately through other processes such as desiccation and inundation of marginal seas, thermal expansion and contraction of sea water, and variation in ground water and lake storage (Miller et al. 2005). The global nature of these sea-level changes have really only been proven for the Quaternary and much of the Neogene where the oxygen-isotope record is good (Coe and Church 2003).

During the Cretaceous, the world was in a greenhouse stage. Continental ice sheets were supposed to be almost or completely absent and, accordingly, high-amplitude short-term glacio-eustatic oscillations have been exceptional (Skelton 2003). The origin of these short cycles during this period remains *unclear*, although orbitally forced climatic cyclicity, acting on sediment supply and periodic climatic warming (producing thermal expansion and some melting of polar ice), is one possibility (Skelton 2003). Miller et al. (2005) described that several processes other than melting or growing of ice sheets (e.g., thermal expansion and contraction of sea-water, variation in continent-bound water, and desiccation and inundation of marginal seas) can cause variations of the water volume responsible for eustatic sea-level changes of 5-10 m. Moreover, these authors consider that ephemeral ice sheets existed for geologically short intervals also during warm periods, based on the finding of high amplitudes and rates of eustatic change, for the Late Cretaceous to Eocene greenhouse world. Accordingly, the occurrence of eustatic changes of sea level due to climatic (Milankovitch) cycles has been assumed for most of the Phanerozoic, even for periods during which continental ice was less developed.

The sequence stratigraphic model for siliciclastic systems predicts two main kinds of deposits: transgressive, terrigenous-starved sediments during fast sea-level rise, and regressive, terrigenous-rich packages for the rest of the curve. Regressive packages can be further subdivided into highstand, falling stage, and lowstand systems tracts, although in many instances this subdivision is not possible and hence only two systems tracts can be differentiated: transgressive and regressive (Catuneanu 2002). Transgressive systems tract comprise the sediments deposited during a period, in which the accommodation space created by the rise in sea level grows faster than it is consumed by the input of sediment from the continent. Consequently, sediments of basinal character are deposited progressively coastward and very little or no terrigenous material enters deeper settings. Regressive systems tract sediments consist of dominantly terrigenous grains entering the sea by rivers, and deposited in progressively basin-ward settings. This situation occurs in three parts of the base level curve: (1) after the transgression, when the input of terrigenous sediments consumes accommodation space faster than it is created by the rise in base level (normal regression during the highstand systems tract); (2) during the fall in base level (forced regression, falling stage systems tract), and (3), during the early rise in base level, when the rise is not fast enough to produce a transgression (normal regression, lowstand systems tract).

The genesis of high-frequency sedimentary sequences can be explained, excluding eustasy as a cause, by the action of orbitally-forced climatic changes on sediment supply (for instance productivity and dilution cycles; Gale 1998; Sagasti 2005) or sediment-transport rate and carbonate productivity. For example, Sagasti (2000; 2001; 2005) describes cycles of precession, obliquity, and eccentricity of the Milankovitch band in the Agua de la Mula Member as generated by climatic changes producing dilution cycles. According to this model, with a more or less constant production of carbonate, warm-temperate (wet) periods would increase weathering of rocks on the continent and thus the amount of clay reaching the basin. Arid (cold) periods, in turn, would reduce the supply of terrigenous sediments to the basin allowing the dominance of carbonates (Sagasti 2005).

In order to link orbitally-driven climatic changes with sedimentary cycles in siliciclastic systems, a coincidence between warmer (or cooler) with corresponding either more arid or humid conditions has to be assumed, regardless of which one is associated with which. As a result, arid periods would deprive the basin of terrigenous sediments and, in case there is subsidence, transgressive-like packages are deposited. When the climate is more humid, more sediment reaches the shelf margin and, if the accommodation space is used up by sediment input being faster than subsidence, there is progradation and deposition of regressive-type sediments. To explain the origin of early transgressive lag deposits that rework the top of the previous sequence, an increase in water energy has to be added to the model at the beginning of the transgression.

Nevertheless, from the evidence of this study, it looks simpler to consider that the main factor shaping the high-frequency sedimentary sequences of the Agua de La Mula Member were the cyclic changes in sea-level caused by the effect of the climate on the eustatic level. The other processes described above might also be involved, the relative magnitude of each one remains, however, unknown. For these reasons, and bearing in mind this disclaimer of certitude, the eustatic model is adopted here as the main cause for the origin of high-frequency cycles.

In sequences completely developed in offshore settings, effects of changes in water depth are negligible, and the record is composed simply by the products of the starved (transgressive) and the diluted (regressive) periods. At the other extreme of the depth range, starvation hemisequences show both, starvation and a deepening-upward trend, while dilution hemisequences develop a coarsening and shallowing pattern up-section. The presence of a basal subaerial (?) or marine erosional surface and a lag bed above in many starvation/dilution sequences indicates that a significant period of erosion took place and hence, eustasy becomes the main cause driving the development of these sequences.

Sixth-order sequences: components, systems tracts, and sequence stratigraphic models

Sixth-order sequences or *starvation/dilution sequences* described in this study are characterized by two main components: basal starvation and upper dilution hemisequences (see introduction of Chapter 5 and Text-Fig. 7). These two packages are easily recognizable from their sedimentary features, in particular the composition: in starvation hemisequences, the density of carbonate particles, especially macrofossils, is higher than in dilution hemisequences. The basal surface of the starvation hemisequence is more often sharp than gradual, and occasionally erosional. Its upper surface can be gradual or sharp, with similar frequencies (for various examples of S/D sequences see Appendix-Figs. 1-2). The two components and bounding surfaces of the starvation/dilution sequences cannot be directly ascribed to any of the systems tracts of the depositional sequence model (like in Catuneanu 2002), nor to the transgressive-regressive model (like in Embry 1993). Even when all sixth-order sequences are interpreted as the response to the same sort of phenomenon, i.e. the orbitally-driven precession cycles of the Milankovitch band, they differ with respect to facies and facies trends in relation to the depth at which these cycles developed and with respect to their position within the sequence hierarchy. Besides, according to their position within the sequence hierarchy not only the facies changes but also the stratigraphic significance of each two hemisequences. For instance, in sixth-order sequences developed in shallow settings close to the top of major regressions (usually late HST), no sediments are inferred to be deposited during the period represented by the fall in sea level (FSST) and lowstand (LST) following the highstand (HST) packages. Instead, erosional processes with or without subaerial exposure, leave a surface of erosion which is enhanced by the ensuing ravinement. Short sequences formed at greater water depth, i.e. late major TSTs, major MFZs and early major HSTs, are not topped by a surface of erosion. RSTs are expected to consist of sediments deposited during the late rise to the early rise of the following cycle of sea level change (i.e. HST, FSST and LST). Bounding surfaces between the HST, FSST, and LST of sixth-order sequences, if they existed, could not be detected in this study. Accordingly, dilution hemisequences of sixth-order sequences are interpreted to contain sediments deposited mainly related to highstands in shallow environments, but all along highstand, falling sea level and lowstand in deep settings. Gradation from one to the other of these two end members exists (see Text-Fig. 11).

The surface at the base of the starvation hemisequence is considered as the sequence boundary. It is equivalent in all types of starvation/dilution sequences studied here and represents the transgressive surface. This surface coincides with the sequence boundary of the transgressive-regressive model. The depositional-sequence model originally placed the boundary between sequences at the maximum of the sea-level curve (end of sea level rise). The boundary was subsequently moved to the minimum of the same curve (equivalent to the end of the sea level fall, Hunt and Tucker 1992). The low hierarchy sixth-order sequences of the Agua de la Mula Member have short and simple dilution hemisequences which cannot be subdivided into components. Therefore, the surface that separates FSST from LST, i.e. the sequence boundary, cannot be identified in these sixth-order sequences.

Starvation hemisequences of both, deep and shallow settings are thin, environmentally condensed simple homogeneous beds. In contrast, at intermediate depths, these sixth-order sequences are thick and complex. Basal starvation hemisequences are inferred to represent high-energy, early transgressive deposits, usually composed of coarse, mixed carbonate-siliciclastic rocks, i.e. mixtures of fine sand, small bioclasts, and physically altered, usually disarticulated shells. The mid-starvation horizon is distinct but its contacts are gradual. It consists of a level with a higher density of well-preserved bivalve shells, many of them articulated. Ammonites usually reach high densities only at this level. At this horizon the highest levels of encrustation and autigenic glauconite occur. The mid-starvation horizon is usually composed of carbonate-dominated, coarse, mixed carbonate-siliciclastic facies. From the mid-starvation horizon upwards, there is an increment in the proportion of siliciclastic mud, which progressively gives way to muddier facies of the upper starvation bed. The upper starvation bed is characterized by a fining-upward trend, with decreasing density of shells and increasing siliciclastic mud content. It is worth mentioning that in all cases, in which the mid-starvation horizon was found, it was invariably in contact with the early transgressive shell-bed. This pattern differs from the findings of Spalletti et al. (2001a) for the same unit at a locality very close to the BAL section. These authors described strongly progradational sedimentary sequences interpreted as short-eccentricity Milankovitch cycles that contain, in their lower part, a thin shell-bed considered as MFZ. The MFZ beds are detached from the early TST beds. The same or equivalent sequences were analysed in this study (DSAM-4 to 7). Thin beds, usually more than one, intercalated within the RST of these sequences are interpreted here as starvation hemisequences of precessionally-driven sixth-order sequences. It is quite likely that, under certain circumstances, a poorly exposed complex pattern of cycles of different orders is interpreted as a single sequence, and a lower hierarchy sequence mistakenly considered as a MFZ.

Starvation/dilution (sixth order) sequences: interpretation.

The position of the boundary between transgression and regression in the starvation-dilution sequences is a debatable matter. Evidence in favour of placing the end of transgression at the middle level of the starvation hemisequences (i.e. the mid-starvation horizon or MSH) is more abundant and convincing, and this is the interpretation adopted here. The evidence includes:

- the position of MSH on top of reliable transgressive deposits;
- the highly starved nature of the MSH indicated by highest levels of encrustation and glauconite, highest densities of bioclasts and lowest levels of terrigenous sediments;
- the change from highly starved to a succession in which the mud content increases upward through the MSH, indicating the onset of terrigenous input after maximum starvation;
- the occurrence of buildups of oysters and serpulids situated precisely at the level of the mid-cycle;

- the highest frequency of ammonite shells that also indicates low sedimentation rates.

Above the MSH, different features indicate a change in the sedimentary regime, such as

- low levels of encrustation, despite occasionally highly abundant agglutinating foraminifers or small oysters;
- very low degrees of boring that indicates a low residence time of the shells on the sea-floor, i.e. comparatively high sedimentation rates;
- higher levels of articulation and shells in growth position;
- high degree of micritization from the base of the transgression to the top of the so-called mid-cycle shell-bed. Above this level, together with the progressive increment in the proportion of siliciclastic mud, shells are less altered by microborings and micritization, indicating a shorter residence time on the sea floor.

A horizon or bed indicating higher starvation is never present at the contact of starvation and dilution hemisequences, what excludes the possibility of placing the MFS at this position. The contact between the shell-rich top of the starvation hemisequence and the base of the following dilution hemisequence is, instead, often gradual. Sediments become gradually richer in siliciclastic mud and poorer in shells and bioclasts. In some cases, there is a thin bed close to the top of the starvation hemisequence making it more or less sharp. This situation co-occurs with well-developed MSHs in the same cycle. A possible interpretation of these sharp contacts is the occurrence of a stronger storm period that was responsible for the accumulation of the hard parts. In Text-Fig. 7 a schematic starvation/dilution sequence with the model proposed in this work is presented.

A different view on the processes assumes a higher position for the boundary between transgressive and regressive beds (i.e. between starvation and dilution hemisequences). There is a general fining-upward trend from base to top of the starvation hemisequences. Thus, a decrease in the energy level from the early to the late starvation deposits can be inferred. It is plausible to interpret the middle starvation deposit as recording the passage from inner to middle ramp (i.e. through the fair-weather wave-base, from shoreface to offshore). In this case, lower “starvation-sediments” (early transgression) were deposited above or close to the fair-weather wave-base. Normal waves prevented the deposition of mud and caused the high physical alteration of the benthic fauna. The upper “starvation” sediments were deposited below this depth, where only strong storm-induced currents reached the bottom causing merely some winnowing of the shells. The mid-starvation deposits would then have formed at the transition from shoreface to offshore positions. At such sedimentary setting, mud was deposited during periods of fair weather conditions, while storm waves and storm-induced currents removed part of it, concentrated the benthic fauna, and deposited some fine sand. The onset of the deposition of siliciclastic mud does not indicate the beginning of terrigenous input after transgression started (i.e. the early HST), but the transition from the permanently reworked shoreface to the episodically altered offshore sea floor. However, if the mid-starvation hemisequence shell-bed (i.e. mid-cycle shell bed) were facies-related, i.e. the deposits originated during the passage from shoreface to offshore environments, and were not the product of the highly starved conditions typical of MFZ, the starvation hemisequences whose base formed already below fair-weather wave-base should not contain a mid-cycle shell bed. Nonetheless, this is not true of many of these short sixth-order sequences. Examples exist in which the base of the starvation hemisequence is represented by middle to outer ramp facies (i.e. below fair-weather wave-base) and there is a well developed mid-cycle-type shell bed (e.g., Appendix-Fig. 1, at BAL 226 m, 312 m, and Appendix-Fig. 2, at AML 129 m, 306 m, 352 m). Then, the evidence rejects this second view, in favor of the model in which the boundary between starvation and dilution hemisequences does not coincide with the maximum flooding, but is placed above it.

According to the model adopted here, starvation hemisequences completely formed in quiet intermediate to deep settings can encompass sediments deposited from the beginning of the transgression to the early part of the regression (Text-Fig. 11 A). These starvation hemisequences do not correspond to the transgressive systems tract. Therefore, the corresponding dilution hemisequence does not correspond to the regressive systems tract. It encompasses instead sediments deposited during the remaining part of the sea-level cycle (i.e., latest rise, fall and early rise). Starvation/dilution sequences developed in shallow environments (Text-Fig. 11 C) would be composed of a lower TST sensu stricto, and a dilution hemisequence probably roughly equivalent to HST and certainly equivalent to RST.

7. Trace fossils

Trace fossil assemblages are well known to represent excellent tools for reconstructing ancient environments (Fürsich 1998). Single ichnotaxa instead are rarely of use for this purpose (Schlirf 2003a). This is partly because many ichnotaxa are present in a number of facies representing different paleoenvironments (e.g., the eurybathic *Palaeophycus*). Other examples of non-strict correspondence between trace fossils and environment are for instance the “excursions” of traces after particular conditions (Föllmi and Grimm 1990). Fürsich (1998) showed that *Thalassinoides* and *Ophiomorpha* burrows in sandstone beds (interpreted as tempestites) occurring at depths greater than expected actually were produced by crustaceans that lived in shallower environments and were transported offshore by storm flows. It is known that a single trace producer may be tolerant of a wide spectrum of environmental conditions. Besides, trace makers may not be contemporaneous with the sediments in which they left their traces. An example of the latter are borings on hardgrounds which originated after long periods of sediment starvation.

Most sediments of the Agua de la Mula Member at the sections studied here are highly bioturbated. However, trace fossils are common only at certain levels and rare in most parts of the sections. Different factors are responsible for this pattern, one of the most important is that most facies represent unconsolidated offshore siliciclastic muds. It is well known that the distribution of trace fossils depends largely on sedimentary facies and that preservation is usually best in sandstones and in sandstone/mudstone alternations (Seilacher 1967). Sandstones account for less than 5% of the thickness of the succession at the BAL section. Furthermore, facies representing shallow, upper offshore to shoreface settings comprise 13% of the same section. It is thus not possible to carry out an extensive ichnologic analysis, on which an environmental reconstruction can be based. Consequently, the opposite strategy is followed here: Trace fossils are analyzed with the help of a sedimentological-based interpretation of the environment.

I interpret the absence of physical and biogenic sedimentary structures as due to the activity of the benthic fauna combined with low rates of sedimentation. Under a low sedimentation rate, the permanent activity of the benthic fauna results in a completely bioturbated sediment without recognizable individual trace fossils (Fürsich 1975). It is worthwhile to stress that even in the black shales at the base of the succession the sediments are completely bioturbated. Therefore, there are no signs of long-term anoxia for the Agua de la Mula Member in the sections AML and BAL.

Trace fossils have more chances of being preserved when there are substrate changes (i.e. alternations of different sediments) (Fürsich 1975). This is the case where heterolithic bedding (S-HET) is developed and fine-grained sandstones beds with wave ripples (S-FS W facies), that are intercalated between facies S-HET. These two facies contain the highest diversity and abundance of trace fossils in the Agua de la Mula Member. Lower shoreface fine-grained sandstones have lower abundance and diversity of burrows compared with the heterolithic facies. Deep offshore facies exhibit a very low diversity and abundance of traces, despite their bioturbated nature. In densely packed shell beds, bioturbation is rare, but bioerosion is prominent. During the development of starved deposits, corresponding to transgressions, densely packed skeletal concentrations precluded the penetration of the substrate and thus excluded the common high-energy traces. As was already pointed out by Fürsich (1975), argillaceous substrates as well as coarse shelly ones have low abundance of traces.

In the Agua de la Mula Member, traces interpreted to have been produced by suspension-feeders such as *Skolithos* or *Arenicolites* are common only in sediments deposited in high-energy shoreface environments. Traces occurring in the proximal offshore heterolithic facies are the product of deposit-feeders, microcarnivores, rare suspension-feeders and of other feeding types (see Table 3 for a list of trace fossils and their inferred feeding habits). The highest diversity and abundance of traces, despite the preservational and observational biases, occurs in environments of intermediate energy, suitable for both, suspension-and deposit-feeders.

Table 3. Feeding habits of trace fossils of unconsolidated substrates found in this study (based on Fürsich (1974; 1975) and Schlirf (2000; 2003a; 2005).

Suspension-feeders	Deposit- feeders	Other feeding types
Skolithos	Gyrochorte	*Treptichnus* (2) (farmer)
Arenicolites	Chondrites (1)	*Bolonia lata* (detritus feeders, scavengers)
Diplocraterion	Planolites	
	Phycodes	*Bergaueria* (microcarnivores)
	Teichichnus	
	Taenidium	
	Treptichnus (2)	

Ichnotaxa of equivocal feeding habit: *Lockeia siliquaria, Protovirgularia, Spongeliomorpha suevica, Palaeophycus*

(1) *Chondrites* is also considered a chemichnion.

(2) *Treptichnus* is interpreted as reflecting farming, but a deposit-feeding mode of life cannot be ruled out.

In this study, four groups of ichnofossils (ichnoassemblages) can be distinguished from the co-occurrence of the component ichnospecies. They correlate with some of the lithofacies described above.

(A) The first ichnoassemblage is of low diversity and occurs in highly bioturbated shoreface sandstones (facies S-FS). Inferred shoreface position and numerical dominance of suspension-feeders are features that partially coincide with Seilacher’s Skolithos ichnofacies (Seilacher 1967). However, high levels of bioturbation and the presence of ichnotaxa typical of more stable and less agitated settings such as *Palaeophycus*, *Treptichnus* and *Chondrites* do not correspond to the characteristic high energy and unstable substrate conditions of the ichnofacies. A low sedimentation rate is supported by the common presence of autigenic glauconite. All these features point to the co-occurrence of non-contemporaneous traces, those associated with the environment in which the sediments were deposited (*Skolithos*, *Arenicolites*?, Pl. 2, Figs. 2 and 4) and those that were produced when more stable conditions prevailed, probably associated with flooding after the onset of transgression (e.g. *Chondrites*, Pl. 2, Fig. 1).

(B) In the second ichnoassemblage, diverse traces developed in heterolithic sediments and related facies. They can be accommodated within the Cruziana ichnofacies (Seilacher 1967). Similar observations were already made for sediments at the top of the BAL section (Spalletti et al. 2001a). Traces are preserved in sandstone beds either as hyporeliefs (e.g., *Bergaueria, Lockeia siliquaria*, *Phycodes, Treptichnus*, *Teichichnus*) or as epireliefs (*Bolonia lata*, *Planolites*, *Chondrites* and indeterminable burrows), and rarely as full reliefs (Pl. 1, Figs. 1-5; Pl. 2, Figs. 1, 5; Pl. 6, Fig. 6 and Pl. 4, Figs. 1-2). A similar pattern was found by Fürsich et al. (2005) in Upper Triassic sediments of east-central Iran. In many cases, ripple cross-lamination and aggrading ripples, usually in phase, are associated with the trace fossils. This pattern indicates episodes of rapid sedimentation and reworking of sand that allowed the preservation of the lamination. The trace makers had time to subsequently bioturbate the sediment while the mud layer slowly aggraded.

(C) Fine-grained sediments interpreted as belonging to outer ramp and basinal settings contain very few recognizable trace fossils, merely *Chondrites* and other ill-defined burrows. This may be due to the thorough reworking of the sediment by the benthic fauna, to low chances of preservation, or both. However, the only trace found in this facies, *Chondrites* fits the environmental interpretation of the facies as representing a low energy, organic-rich, soft substrate. *Chondrites* was found on top of fine-grained sandstone within wavy heterolithic bedded facies and particularly in fine-grained ripple-laminated sandstones (Pl. 2, Fig 1). *Chondrites* is considered the trace of a chemosymbiotic organism (Bromley and Ekdale 1984) that required access to both, oxygen and hydrogen sulphide, and/or a deposit-feeder. The lithofacies analysis indicates that the sediment hosting *Chondrites* was deposited in upper offshore to lower shoreface environments. The redox boundary probably was close to the sediment-water interface. Poorly preeserved *Chondrites* also occur in deeper settings as well as in other parts of the section.

(D) High-density skeletal concentrations of the early and middle parts of starvation-hemisequences probably precluded the activity of infauna. In fact, burrows are rare in the facies types found at the base of the cycles (mostly facies MB2, MD1, MD2). Nevertheless, the lack of sedimentary structures expected for tempestites invokes the action of bioturbators. Traces of these beds fit with Trypanites ichnofacies (Frey and Seilacher 1980) that develops in consolidated substrates. It is noteworthy that hardgrounds did not develop in the sections and that this ichnofacies formed mainly on shelly substrates in the Agua de la Mula Member. Borings occur also in reworked pebbles, which are common in offshore shell beds of both sections. In the majority of the cases, these carbonate concretions resulted from early diagenetic lithification, followed by exhumation so that they could become intensively bored. (Pl. 1, Figs. 6-7). Nestling taxa (cryptoendoliths) are well seen in most *Gastrochaenolites* borings (Pl. 1, Fig. 8).

There is a zonation of boring types and density from early to late starvation deposits (starvation hemisequences). Early and middle starvation deposits are interpreted here as developed during the early transgression and mid-cycle respectively. Late starvation deposits, in turn, are considered as belonging to the early part of the following HST. Early starvation deposits developed in the inner ramp, under constant water agitation. The lower part usually includes lag material, reworked from the former sequence during the process of ravinement. Middle starvation deposits were formed while sedimentation of terrigenous was at a minimum and corresponds to the MFZ of the S/D cycle. Late starvation deposits formed mostly in the outer ramp, below the storm-weather wave base. Its main difference is the presence of siliciclastic mud.

In high-energy, early starvation deposits large and thick shells show both, high density of large holes and high degrees of abrasion. Borings belong mainly to *Gastrochaenolites* and *Trypanites*. *Entobia* systems can be detected after careful examination. This pattern of bioerosion fits very well the Entobia Ichnosubfacies (Bromley 1994) of the Trypanites Ichnofacies. This ichnosubfacies is characterized by the development of deep-seated bioeroders, sponges and bivalves (Bromley 1994). Pioneer colonizers that occupy the shallowest tiers become eliminated due to the action of the other borers and the abrasive action of waves. This ichnosubfacies occurs in the early starvation deposits of some starvation/dilution sequences, in sandy allochemic limestones (MB2), allochemic sandstones (MD2), and micritic sandstones (MD1). Environmental conditions inferred from the sediments are very low terrigenous input related to the transgression of a shoreline and landward migration of depositional systems; high water energy because of the position above or close to the fair-weather wave-base; reduced deposition of mud, which is kept in suspension by waves and currents and deposited further offshore. All these features resulted in shells exposed on the sea floor for a considerable time, which allowed the development of the Entobia Ichnosubfacies. A high density of *Gastrochaenolites* is common in many early starvation beds, interpreted as deposited in the nearshore or proximal offshore zone (inner and upper middle ramp). Crowded and dominating *Gastrochaenolites* is regarded as an indication of very shallow water (Bromley 1994).

Skeletal remains deposited in deeper environments, particularly in cases in which they represent late starvation deposits are less bioeroded. Outer shell layers are usually micritized and microborings are evident. *Entobia*, cirripedian borings and *Caulostrepsis* are present in low abundances. At first sight this ichnoassemblage fits Bromley's (1994) Gnathichnus Ichnosubfacies. These offshore deposits formed in two different stratigraphic settings, both characterized by low rates of terrigenous input. The first one represent complete starvation hemisequences deposited in middle to outer ramp environments. Large and deep borings (*Gastrochaenolites*, *Trypanites,* and *Meandropolydora*) are rare and occur almost exclusively in exhumed carbonate concretions and big shells of *Aetostreon*. The absence of the typical Entobia Ichnosubfacies may be due to both, lack of substrates thick enough for the emplacement of the bioeroders as well as the low frequency of high-energy events, which removed mud that had settled on the shells below the fair-weather wave-base. The second case comprises late starvation deposits on top of starvation-hemisequences, in which a medium-sized fauna is common and large specimens of *Myoconcha transatlantica* and *Cucullaea gabrielis* also occur. Elements of the Entobia Ichnosubfacies are almost completely absent. Deposition of mud between storms and rapid burial by tempestites reduced the chances of establishing well-developed endolithic communities. This leads to the development of only shallow tiers of bioeroders of the Gnathichnus Ichnosubfacies.

However, data from this study does not completely fit Bromley's (1994) model of depth-related ichnosubfacies interpretation. In that model the Gnathichnus Ichnosubfacies corresponds to the basin floor where bioerosion is short-termed and upper tiers of bioerosion are preserved by sudden burial. The Entobia Ichnosubfacies, in turn, is characteristic of the rocky shore and bypassed rocky margins of the basin. The second ichnosubfacies holds true for the shallow, high-energy, terrigenous-starved early transgressive deposits described in this work, the first one seems to be controversial. Bioerosion in shells deposited in offshore settings apparently depends not only on depth but also on the position within sedimentary sequences which, in turn, governs the rate of sedimentation. Moreover, the development of the Entobia Ichnosubfacies is governed by the availability of large pieces of hard substrate for the settling of the macroboring fauna. The Gnathichnus Ichnosubfacies developed in terrigenous, basal starvation-hemisequences completely deposited in the middle to outer ramp, in shells of small molluscs dominating the benthic communities. However, when thick shells of the gryphaeid *Aetostreon* and/or large carbonate concretions are available, elements of the "rocky shore subfacies" occur. Shells hosted in similar facies but occurring in the upper part of starvation-hemisequences exhibit bioerosion that is more typical of Gnathichnus Ichnosubfacies. In this case, deposition of terrigenous mud of the early HST already began and the concentration of the shells is mainly due to the action of tempestites and storm waves. Below wave base, mud is constantly being deposited at least in small amounts and more or less frequently removed by the action of storm waves. Tempestites also contribute to burial of skeletal remains that are then no longer available for the bioeroders. According to

Bromley (1994), the presence of well developed bioerosion sculpture is good evidence that no sediment was deposited for a considerable period of time. Only small amounts of sediment are necessary to kill off an endolithic community. This explains why high levels of bioerosion are present mainly in beds deposited in shallow environments during transgressions, in which wave and current energy precluded mud of being deposited.

In carbonate settings represented by bioclastic wackestones, floatstones, packstones and micritic rudstones, and the mixed sandy and silty micrites (facies MA2), levels of shell destruction are higher than expected. Many examples of these facies were deposited under negligible terrigenous input. Micritization as well as *Entobia*, *Trypanites* and other borings reach very high concentrations. There is an enrichment in calcitic shells. In thin-sections, aragonitic shells usually appear completely micritized. The higher degree of bioerosion found in these beds can be related to the lower proportion of terrigenous mud in their matrix. The probability of being buried and thus escaping bioerosion is reduced with low input of mud. The destructive processes that acted on the shells reach a magnitude that is similar to other cases that were deposited in more agitated environments, under higher input of terrigenous sediments. Kidwell et al. (2005), in a comparative study, found that destructive processes act faster on shells in carbonate substrates than in siliciclastic ones. This is supported by the observations made in this study.

Stratigraphic changes in bioerosion are evident in starvation-hemisequences, which record changes in sea level from shoreface to offshore. Some starvation-hemisequences deposited in high-energy settings consist only of early and middle parts. In these cases, they only contain borings of the Entobia Ichnosubfacies. There are also examples in which the whole starvation-hemisequence developed below the fair-weather wave-base and only the Gnathichnus Ichnosubfacies is developed.

Spongeliomorpha suevica usually occurs in siliciclastic muds or sandstones as a positive hyporelief, crossing transgressive surfaces of high frequency cycles (see Pl. 6, Fig. 4 and Pl. 4, Fig. 3). *Planolites* may also occur in a similar fashion. *S. suevica* usually forms a regular or irregular horizontal maze. This ichnospecies is considered characteristic of relatively low energy settings in a cohesive sediment in which additional stabilization of the burrow wall is not necessary (Schlirf 2003a). In the Agua de la Mula Member *S. suevica* occurs usually just below transgressive surfaces, on the top of dilution hemisequences in which a low sedimentation rate is expected to produce a firm substrate, although facies containing the burrows as well as those overlying them usually indicate moderate to high energy conditions of the upper middle to inner ramp. Even though traces occur in the siliciclastic sediments below the sequence boundary, their fill is clearly derived form the transgressive bed above it. This means that the galleries were constructed during the deposition of the S-HS or even afterwards. The relationship of *S. suevica* with early transgressive deposits was already mentioned in the literature (Fürsich 1998; Fürsich et al. 1991).

The occurrence of large regular mazes of *Spongeliomorpha suevica* and specimens of *Diplocraterion saxicava*?, and other unidentified thick-walled burrows in and between tempestitic sandstone beds (see facies analysis, 3.3. Facies S-FS), may represent the transport of shoreface sediments and their traces into an offshore setting. The sandy levels are intercalated between offshore, middle-ramp sandy siltstones, into a monotonous coarsening-upward facies succession. Base and top are rather sharp. There are no sedimentary structures or fossils preserved. The traces appear both, connecting two beds like *D. saxicava* and unidentified burrows (Pl. 2, Figs. 7-8) or at their bases (*Spongeliomorpha suevica*; Pl. 2, Fig. 6). These traces are extremely rare in the rest of the section where offshore sediments dominate. The trace makers were transported offshore and forced to begin their activities in an unfavourable environment. Although they started to excavate their burrows, the population did not become established (Bromley and Ekdale 1984; Fürsich 1998).

8. *The benthic macrofauna*

In the course of four field trips to both localities, almost 24,000 specimens were counted among the 118 shell beds studied. This information was complemented with sedimentological, taphonomic and ichnological observations. After cleaning the database -elimination of biased samples- 112 samples with 22,572 individuals were incorporated to the multivariate analysis.

In the case of bivalves, the number of individuals was obtained by summing up articulated specimens and number of right or left valves, whichever was larger. Serpulid tubes were grouped into four categories, two of them are based on the diameter of the tube: small (2 mm or less, usually less than 1 mm) and medium (2 to 5 mm); the other two are already recognized taxa: *Parsimonia* (larger than 5 mm) and *Sarcinella* (colonial serpulids with very thin tubes that grow in branches). Scaphopods occur usually fragmented as a result of recent weathering phenomena. In bulk samples taken to the lab fractured individuals usually separate into several fragments and the same process can be detected in the field. Therefore, scaphopods were quantitatively evaluated as one count per cm of tube. This strategy leads to a minor (negligible) overestimation of the abundance of the group. The list of the taxa included in the multivariate analysis together with their life habits is found in Table 4.

Table 4. Faunal list and life habits. For more information se Appendix A. E: epifauna; I: infauna; SI: semi-infauna; Pr: patch-reef builder; b: byssate; fr: free-living; m: mobile; c: cemented; bo: boring; sh: shallow infaunal; d: deep infaunal; Ca: carnivorous; S: suspension feeding; H: herbivorous/detritus feeding; D: deposit feeding; Mc: microcarnivorous; Ch: chemosymbiotic.

	Mode of life	Feeding habits
FORAMINIFERIDA		
Placopsilina sp.	Ec	D
SCLERACTINIA		
Scleractinia sp. A	Ec	Mc
Scleractinia spp. indet.	Ec,Pr	Mc
ECHINOIDEA (Irregularia)		
aff. *Pygaster gerthi* (Weaver, 1931)	SI	D
Holectypus cf. *H. planatus* (Roemer var. *numismalis* Gabb in Weaver, 1931)	SI	D
Holectypus sp.	SI	D
ECHINOIDEA (Regularia)		
Regularia sp. indet. A	Em	H
CRINOIDEA		
Crinoidea ossicles	Ec	S
SERPULIDAE		
Parsimonia cf. *P. antiquata* (J. de C. Sowerby, 1829)	Ec,Pr	S
Sarcinella occidentalis (Leanza and Castellaro, 1955)	Ec,Pr	S
Small-sized serpulids	Ec	S
Medium-sized serpulids	Ec	S
SCAPHOPODA		

Dentalium sp.	SI	D
GASTROPODA		
Trochidae		
Trochidae sp. A	Em	H
Trochidae? sp. B	Em	H
Cerithiidae		
Cerithium sp. A	Em	H
Cerithium sp. B	Em	H
Procerithiidae		
Rhabdocolpus sp. A	Em	H
Rhabdocolpus sp. B	Em	H
Pseudomelaniidae		
Poasia sp. A	Em	H
Poasia sp. B	Em	H
Poasia sp. C	Em	H
Aporrhaidae		
Protohemichenopus neuquensis (Camacho, 1953)	Ish	S
Dimorphosoma sp.	Ish	S
Aporrhaidae sp. B	Ish	S
Ampullospiridae		
Pictavia sp. A	I	Ca/H
Pictavia sp. B	I	Ca/H
Epitoniidae		
Confusiscala sp.	Em	H
Mathildidae		
Bathraspira sp. A cf. *B. neocomiensis* (d'Orbigny, 1843)	Em	H
Bathraspira sp. B	Em	H
Bathraspira? sp. C	Em	H
Ringiculidae		
Ringinella sp. A	Em	H
Ringinella sp. B	Em	H
Acteonidae		
Tornatellaea sp.	Em	H
BIVALVIA		
Nuculidae		
Paleonucula sp.	Im	D
Arcidae		
Barbatia (*Barbatia*) sp. A	Eb	S
Cucullaeidae		
Cucullaea gabrielis (Leymerie, 1842)	I	S
Parallelodontidae		
Grammatodon securis (Leymerie, 1842)	Eb	S
Grammatodon (*G.*) sp.	Eb	S
Grammatodontinae sp. A	Eb	S
Grammatodontinae sp. B	Eb	S
Mytilidae		
Mytilinae sp. A	Eb	S
Crenellinae sp. A	SIb	S
Crenellinae sp. B	SIb	S

Modiolus cf. *M. ligeriensis* (d'Orbigny, 1943)	SIb	S
Modiolus cf. *M. subsimplex* (d'Orbigny, 1844)	SIb	S
Pinnidae		
Pinna robinaldina (d'Orbigny, 1844)	SIb	S
Pinnidae sp.	SIb	S
Bakevelliidae		
Gervillaria alatior (Imlay, 1940)	Eb	S
Gervillella aviculoides (J. Sowerby, 1814)	SIb	S
Bakevelliidae sp. aff. *Cuneigervillia* sp.	SIb	S
Pterioida sp. A		S
Inoceramidae		
Inoceramus sp. aff. *I. curacoensis* (Weaver, 1931)	Eb	S
Inoceramus sp. *B*	Eb	S
Isognomonidae		
Isognomon (I.) lotenoensis (Weaver, 1931)	Eb	S
Isognomon sp. A	Eb	S
Pectinidae		
Mimachlamys robinaldina (d'Orbigny, 1847)	Eb	S
"*Chlamys*" *puzoziana* (Matheron, 1842)	Eb/fr	S
"*Pecten*" *vacaensis* (Weaver, 1931)	Eb/fr	S
cf. *Eopecten covuncoensis* (Weaver, 1931)	Eb/fr	S
Pectinidae sp. A	Eb/fr	S
Anomiidae		
Anomiidae sp.	Eb	S
Limidae		
aff. *Acesta* sp.	Eb/fr	S
aff. *Pseudolimea* sp.	Eb/fr	S
Gryphaeidae		
Aetostreon sp. aff. *A. latissimum* (Defrance, 1821)	Efr	S
Ceratostreon minos (Coquand, 1869)	Ec,Pr	S
Gryphaeostrea sp. 1	Ec	S
Gryphaeostrea sp. 2	Ec	S
Exogyrinae sp.	Ec	S
Ostreidae		
Lophinae sp. A	Ec	S
Lophinae sp. B	Ec	S
Trigoniidae		
Myophorella (Haidaia) volkheimeri (Leanza and Garate, 1987)	Ish	S
Myophorella (Promyophorella) garatei (Leanza, 1981)	Ish	S
Steinmanella (Transitrigonia) raimondii (Lisson, 1930)	SI	S
Steinmanella (Macrotrigonia) vacaensis (Weaver, 1931)	SI	S
Rutitrigonia agrioensis (Weaver, 1931)	Ish	S
Pterotrigonia (Rinetrigonia) coihuicoensis (Weaver, 1931)	Ish	S
Pterotrigonia (Rinetrigonia) sp. A aff. *P. coihuicoensis* (Weaver, 1931)	Ish	S
Lucinidae		
Mesomiltha? *argentina* (Behrendsen, 1891)	Id	S/Ch
Mesomiltha? sp. A	Id	S/Ch

Lucina corbisoides (d’Orbigny, 1845)	Id	S/Ch
Lucina neuquensis (Haupt, 1907)	Id	S/Ch
Lucinidae sp. A	Id	S/Ch
Permophoridae		
Myoconcha transatlantica (Burckhardt, 1900)	Slb	S
Astartidae		
Eriphyla argentina (Burkhardt, 1900)	Ish	S
Disparilia elongata (d’Orbigny, 1843)	Ish	S
Neocrassina (Coelastarte?*)* sp.	Ish	S
Astartidae sp. A	Ish	S
Cardiidae		
Protocardia sp.	Ish	S
Solecurtidae		
Solecurtus? neuquensis (cf. *S. neuquensis* Weaver, 1931)	Id	??
Ptychomyidae		
Ptychomya sp A (cf. *P. koeneni* Behrendsen, 1892)	Ish/Sl	S
Ptychomya sp. B	Ish	S
Arcticidae		
Arcticidae sp.	Ish	S
"Cyprina" (?)	Ish	S
Veneridae		
Veneridae sp. 1	Ish	S
Veneridae sp. 2	Ish	S
Veneridae sp. 3	Ish	S
Corbulidae		
Corbulomima bodenbenderi (cf. *Corbula bodenbenderi* Behrendsen, 1892)	Ish	S
Corbulidae sp. A	Ish	S
Corbulidae sp. B	Ish	S
Hiatellidae		
Panopea gurgitis (Brongniart, 1822)	Id	S
Panopea dupiniana (d’Orbigny, 1843)	Id	S
Heterodonta sp. A	Ish	S
Heterodonta sp. B	Ish	S
Heterodonta sp. C	Ish	S
Pholadomyidae		
Pholadomya gigantea (J. de C. Sowerby, 1836)	Id	S
Machomya? sp.	Id	S
Bryozoa spp. A to D	Ec	S

For the multivariate analysis samples with high frequencies of serpulids and/or oysters were incorporated twice, once with all the specimens counted originally in the same bed, and a second time without specimens in buildups. This was done for two reasons: in many cases the buildups represent volumetrically little of the assemblage but are numerically very important due to small size and crowding of individuals. Besides, the gryphaeid *Ceratostreon* buildups in some cases have clearly grown after the deposition of what constitutes the rest of the assemblage, and would represent the relics of a different community. However, this is not so clear in other cases and the strategy adopted here is to perform the analysis considering both possibilities. This strategy was adopted only to build the dendrogram. Statistics of the fossil benthic associations were calculated including every sample only once. Without exceptions samples with and without specimens in buildups clustered together, indicating that although numerically relevant, these species are not crucial for the structure of the benthic associations resulting from the cluster analysis. In two cases it was obvious that the oyster/serpulid accumulation was stratigraphically separated from underlaying beds. For these examples, a third count was included exclusively with specimens from the buildups.

Taxonomic counts of the benthic macrofauna were treated statistically by applying cluster analysis to the samples. The database was previously standardised to percentages to avoid the biasing effect of different sample sizes and then transformed with the square root function to reduce the effect of dominant species. The resemblance matrix was calculated with the Bray-Curtis similarity coefficient (Legendre and Legendre 1983). The cut-off level used to define associations was not fixed. The procedure utilized consisted in defining groups biologically consistent with the highest similarity (see Fürsich et al. 2004).

The groupings that resulted from the cluster analysis were considered as (fossil) benthic associations and assemblages (in the case of single sample clusters). Benthic associations were recognized, described, and interpreted based on their diversity, trophic composition, and life habit composition. The associations were described in terms of the mean percentages of the fossil species across the different samples that compose the grouping. Although the median is a better measure of central tendency for data in percentages, it was preferred to calculate the arithmetic means (averages) instead. This decision relies on the fact that in the case of heterogeneous groupings, some species that are more or less relevant in some samples but absent in more than half of them have medians = 0 although arithmetic means can be significantly higher.

Autoecological remarks

Life habits in terms of relationship with sediment-water interface and feeding habits are listed in Table 4. In Appendix A the taxa included in the multivariate analysis are listed, with a brief description and a discussion on possible taxonomical affinities of problematic and/or yet not described species. Although the scope of this dissertation does not comprehend autoecologic analysis, a few examples are discussed here.

- *Placopsilina*

Recent foraminifera feed upon phytoplankton and zooplankton (Dodd and Stanton 1981) and organic matter. Benthic foraminifers swallow the food particles they capture with the pseudopodia (thread-like extensions of the ectoplasm). *Placopsilina* sp. are considered here deposit feeders. Modern agglutinated foraminifera such as *Placopsilina* are especially common in low-salinity, relatively low-temperature bays and estuaries if compared with the distribution of species with calcareous tests. They are also relatively more abundant in deep waters and at high latitudes (Dodd and Stanton 1981). Although with some uncertainty, this distribution pattern was related to the solubility of $CaCO_3$ in water (Greiner 1969). Agglutinated tests tend to be more common in waters undersaturated with respect to $CaCO_3$. In the Agua de la Mula Member, there is no reason to suspect reduction of salinity for the beds in which these organisms are relatively abundant. Their occurrence above the maximum flooding zone of some precession sequences, in muddy allochemic limestones or allochemic mudrocks (facies MB1 and MC2-R, Chapter 5) indicates that they are related to an increased rate of terrigenous input.

- Semi-infaunality

Steinmanella vacaensis, *Ptychomya koeneni* and *Myoconcha transatlantica* are considered with a semi-infaunal life habit in this work, based on encrustation and boring patterns. Semi-infaunality was already proposed for *Steinmanella* (Villamil et al. 1998), although considered statistically not significant (Lazo 2004). The few specimens of *S. vacaensis* preserved well enough to contrast Villamil's hypothesis showed epibionts, such as agglutinating foraminifers and oysters, occupying the posterior end of the shell. This evidence indicates a semi-infaunal life position for *Steinmanella vacaensis*. *Ptychomya koeneni* commonly occurs with one-third of the posterior end of both valves completely encrusted by the foraminifer *Placopsilina* sp. *Placopsilina* sp. leaves the commissure free, indicating a life-life interaction. *Myoconcha transatlantica* very often shows a similar pattern. In this case, both valves carry a proper oyster or serpulid-oyster buildup that extends over half of each valve, normally above the carena, and stops at the commissure.

- Gastropods

With the exception of the shallow infaunal, suspension-feeder aporrhaeids and the possibly infaunal, carnivorous ampullospirids (see below), gastropods included in this analysis were grouped as epifaunal detritus-feeders, because it is no possible to distinguish whether they fed on live or dead plant, on animal material or were omnivorous (Fürsich et al. 2001). However, from the paleoecologic evidence, a detritivorous feeding can be proposed for some species. Those gastropods found in sediments at the base of the sections belong to the fossil benthic association A, characterized by reduced levels of oxygen, at least below the sediment-water interface. Nevertheless, high degrees of anoxia are not supported. Diversity of association A is intermediate while evenness is high. High evenness indicates the absence of opportunistic species and a more or less stable environment. Diversity is moderate probably due to the difficulties to develop suspension feeding, and the probable anoxia below the sediment/water interface that prevented colonization by infaunal elements. A consequence of these inferences is the mode of life of the small gastropods that dominate benthic association A: mainly *Bathraspira* sp. A and *Bathraspira*? sp. C. An epifaunal mode of life is inferred for these gastropods from the low oxygen levels of the sediment. The suspected high amount of deposited organic matter, plus the deposition below the photic zone supported by the rarity of microborings and the inferred depth, indicate that these species most probably were epifaunal deposit feeders, that fed on organic matter, and not grazers.

- *Pictavia* sp.

Fossil ampullospirid gastropods were considered the ancestors of the Naticidae and hence infaunal predators that could potentially drill the shell of their prey to feed on it. It was recently proposed, based on protoconch morphology, that naticids and ampullospirids are not related (Bandel 1999). Besides, the finding of a Recent ampullospirid species grazing on algae was considered an arguable evidence to propose that the whole group shares the herbivorous mode of feeding (Kase and Ishikawa 2003a; Kase and Ishikawa 2003b; Leighton and Aronowsky 2003). The coexistence of *Pictavia* sp. A and *Mesomiltha argentina*, the latter with predatory drill-holes, in the same beds, suggests that the former most likely was the predator of the latter. This speculation leads to infer an infaunal predatory mode of life for these gastropods. *Pictavia* would have to tolerate the reduced oxygenation inferred for the dark basinal fine-grained sediments holding the fossils.

Synecology

Community analysis: Fossil associations

From the cluster analysis fifteen groupings and a single sample were distinguished, with variable paleoecologic significance (Text-Fig. 15). Table 5 provides a synthesis of statistical information of the associations. Average sample size, species richness, diversity, and evenness indexes per association/assemblage are depicted in Text-Fig. 16 A-D. Table 6 sums up information on fossil benthic assemblages and associations. The list of the main contributing species of each benthic association is presented in Table 7. Diversity is described in terms of species richness (number of species, S), Shannon-Wienner diversity index (H') and an evenness index (E). E represents the ratio between maximum and actual H' diversity multiplied by 100: E=H'/Hmax*100, where Hmax is the maximal diversity which could occur, if all species collected were equally abundant. Association diversity indices were calculated as the average of the indices of each sample. Diversity measures were arbitrarily categorized as low ($S<8$; $H'<1.0$; $E<60\%$), medium ($8 \leq S \geq 16$; $1.0 \leq H' \geq 2.0$; $60\% \leq E \geq 70\%$) and high ($S > 16$; $H' > 2.0$; $E > 70\%$). In

Appendices D and E details of information samples are given. Finally, in Text-Figs. 13A-D information on fossil benthic associations in terms of taxonomic groups, modes of life, substrate preferences and feeding is synthesized.

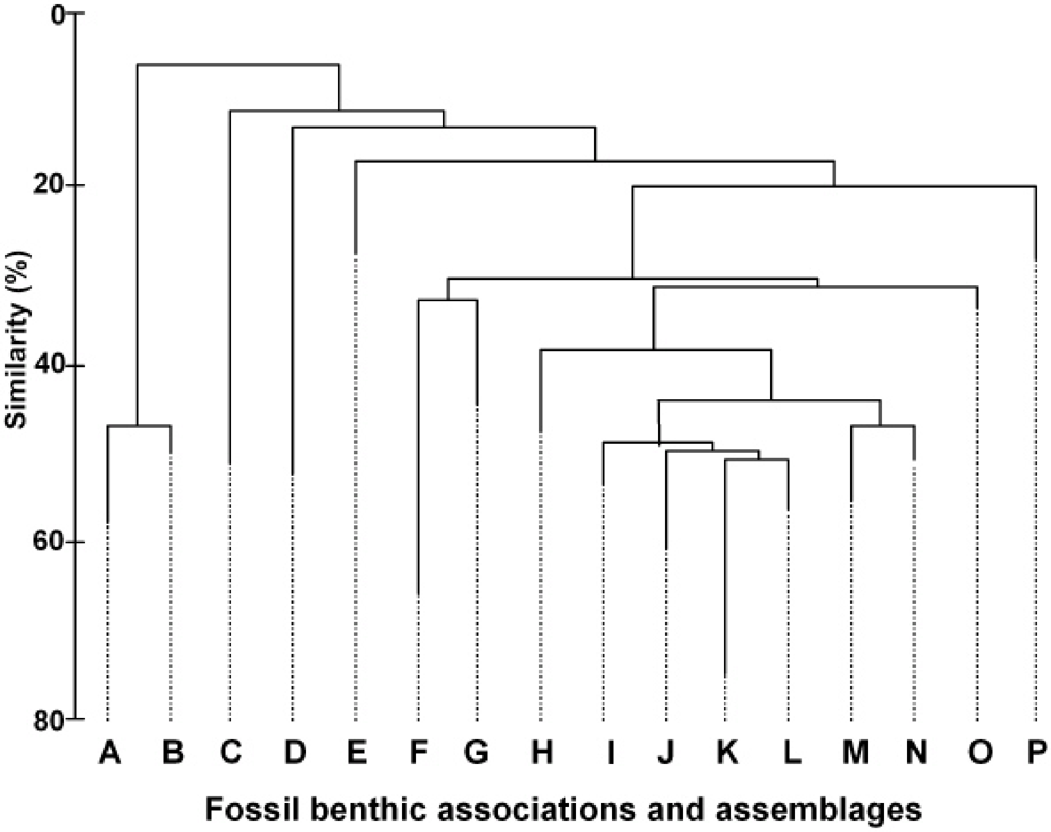

Text-Fig. 15. Dendrogram of the cluster analysis with associations and assemblages.

- **Fossil Association A: *Bathraspira* spp. – *Mesomiltha argentina***

This association is the result of the clustering of 25 samples that comprise 4,128 individuals spread across 27 species. Average species richness (S=9) and diversity (H'=1.57) are intermediate, although evenness is high (71.57%). All samples clustered in this association come from the first 56 m of the section in Bajada del Agrio that correspond to the TST, MFZ and early HST of the first major depositional sequences (DSAM-1), in the earliest Late Hauterivian *Spitidiscus riccardii* Zone (see Text-Fig. 6).

Shell beds of this association consist of loosely-packed skeletal concentrations found in thin (less than one cm) strata with a fine-grained marly or micritic matrix. The shell beds represent complete starvation hemisequences.

These beds are intercalated between a more or less monotonous succession of dark, fissile, bituminous marls, marly (micritic) mudrocks and argillaceous mudstones. The sediments are always bioturbated although trace fossils are rare (e.g. *Chondrites*). The environment inferred for these facies is outer ramp to basin, characterized by little or no water agitation, a steady but low rate of terrigenous input, reduced oxygen levels, and organic matter accumulating on the sea floor. Strata containing association A shell beds are relatively more condensed than sediments below and above, as is shown by the higher micrite content and the concentration of shells. These beds are simple and homogeneous.

Fossil ass.	Nr. of samples	N	S	S (min-max)	H'(e)	E
A	25	165	9	6-16	1.57	71.57
B	8	237	11	6-16	1.41	60.85
C	3	94	6	(1) 4-8	0.78	47.54
D	2	378	22	20-24	2.16	70.02
E	18	113	14	(2) 6-23	1.70	67.94
F*	1	308	9	9	1.45	65.96
G	7	175	7	3-13	0.97	55.70
H	2	211	23	22-23	2.22	71.40
I	11	319	13	10-16	1.91	74.75
J	3	174	15	10-21	1.80	67.70
K	3	239	13	12-14	1.34	53.55
L	14	254	17	12-21	1.88	67.39
M	7	387	21	17-23	2.29	75.61
N	7	323	17	11-26	2.04	74.57
O	5	179	10	7-13	1.70	73.67
P	9	155	10	4-16	1.45	68.35

Table 5. Synthesis of statistics of benthic fossil associations and assemblages. N, average sample size; S, average species richness; S (min-max), minimum and maximum species richness per sample; H'(e), Shannon-Wiener's diversity index, based on natural logarithms; E, evenness index. Values in brackets correspond to possibly biased samples. *benthic fossil assemblage.

Species in this association are small-sized. Bivalves appear more often articulated than not, and usually in life position. The preservation of the fossils is excellent and there are little or not indications of physical disturbance i.e., the sediments were deposited below storm wave-base (for more information see facies 5.1-3 and 8.2 in chapter 5). Infaunal bivalves such as *Mesomiltha argentina* as well as epifaunal and infaunal gastropods and scaphopods are usually complete, and their delicate ornamentation is very well preserved. Shells of the ampullospirid gastropod *Pictavia* sp. A were found with remains of the original colour patterns. The small epifaunal bivalve *Grammatodon securis* occurs in growth position and is well preserved but usually flattened in a dorso-ventral direction. Ammonites are abundant but flattened and fractured. Higher up, shell beds show weak evidence of physical concentration, replacement of some mollusc species and an increase in the abundance of cementing serpulids and oysters, giving way to the fossil association E. Physical sedimentary structures are lacking probably due to bioturbation. Trace fossils are rare, represented only by ill defined, few mm-thick, horizontal, simple burrows and scarce, even thinner burrows with variable orientation (*Chondrites*?). Bioerosion is usually very low, restricted to gastropod-like drill holes (*Oichnus simplex*) on lucinid bivalves, rare octopus drill holes (*Oichnus ovalis*) and crab attacks on gastropod apertures. Microborings are rare or absent indicating that the shells were deposited below the photic zone.

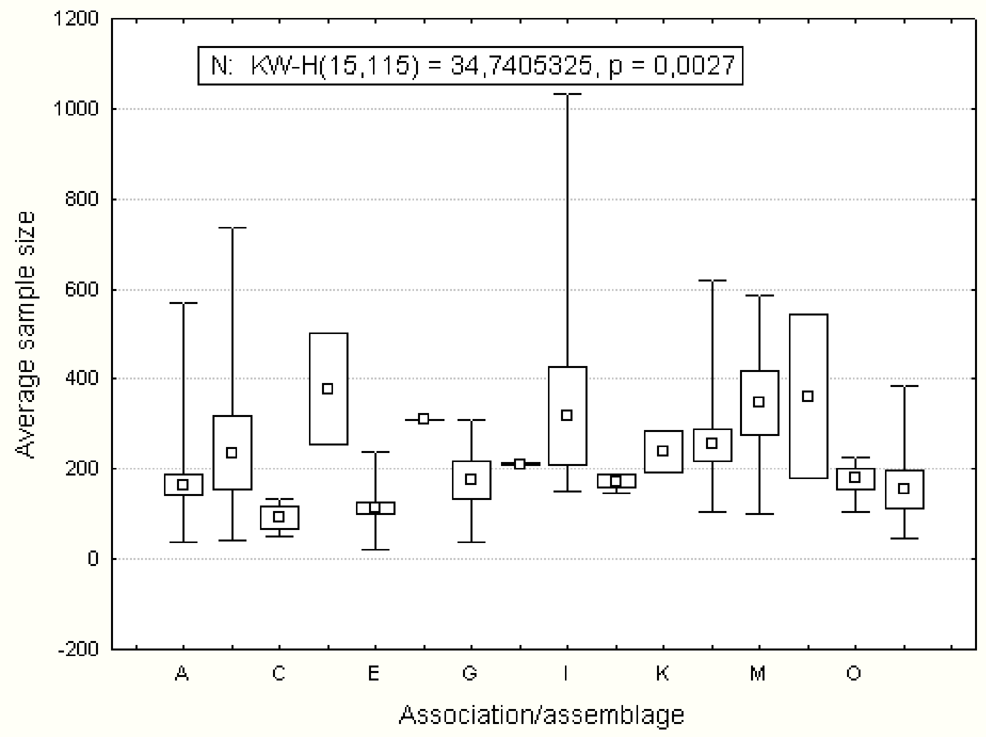

Text-Figure 16A. Box and whisker plot diagrams showing average sample sizes of benthic associations/assemblage.

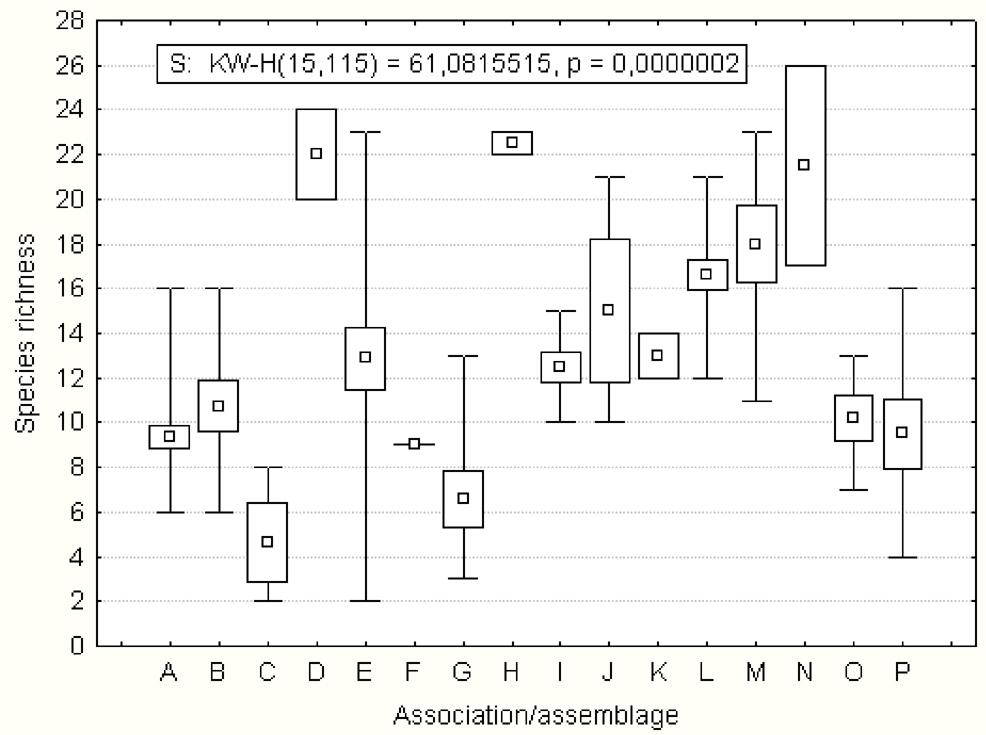

Text-Figure 16B. Box and whisker plot diagrams showing species richnesses of benthic associations/assemblage.

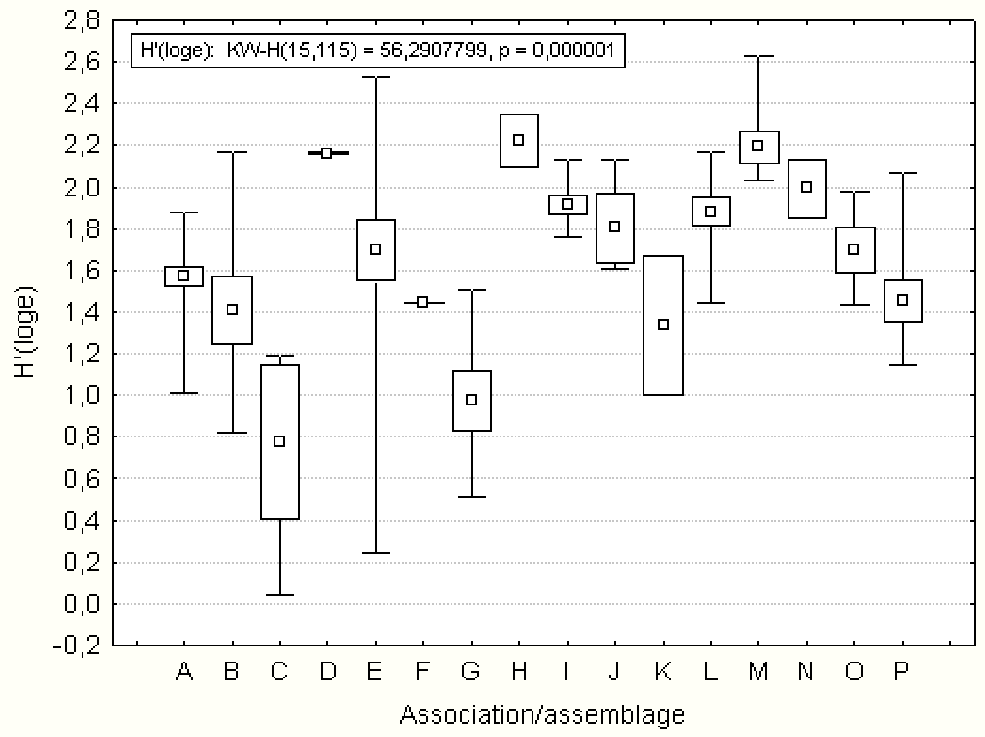

Text-Figure 16C. Box and whisker plot diagrams showing Shannon's diversity indices of benthic associations/assemblage.

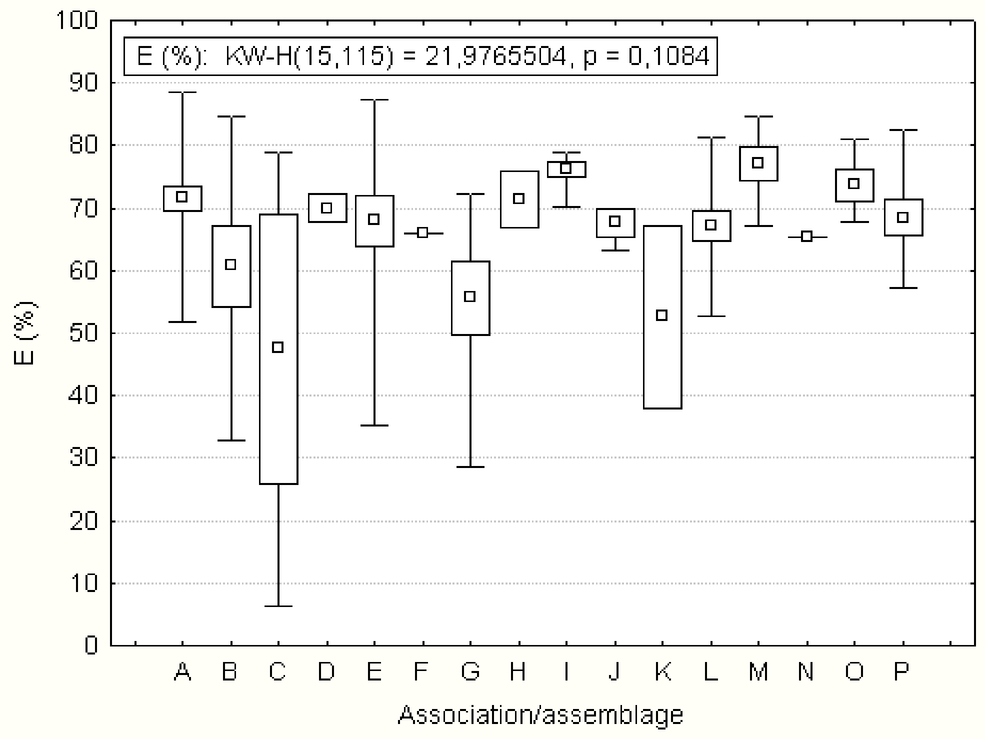

Text-Figure 16D. Box and whisker plot diagrams showing eveness indices of benthic associations/assemblage.

The benthic macrofauna consists of a diverse group of small chiefly epifaunal and semi-infaunal bivalves and gastropods. Dominating species are the gastropods *Bathraspira* sp. A (36.61%) and sp. C (20.80%), the lucinid bivalve *Mesomiltha argentina* (16.65%) and the aporrhaeid *Protohemichenopus* sp. (12.78%). Epifaunal species dominate with almost 70%. Semi-infaunality is represented by a single scaphopod species accounting for 0.73% of the association. Six species of small shallow infaunal bivalves account for only 0.87%. Shallow infaunal aporrhaeid gastropods represent 12.8%. The lucinid *Mesomiltha argentina* is the only relatively deep infaunal species of the association (15.56%). Only 12% of the specimens are related to hard substrates, either cementing or byssally attached. A quarter of the individuals were suspension feeders (aporrhaeid gastropods, bivalves and serpulids). The association is dominated by herbivorous/detritus-feeding gastropods (57.73%) and the chemosymbiotic *M. argentina*.

Discussion

The *Bathraspira* spp. – *Mesomiltha argentina* association lived in a quiet, deep setting, with high availability of organic matter and reduction of oxygen level (dysoxia) close to the sediment-water interface. The excellent preservation of the fauna (e.g. almost 100% of bivalves are articulated), the fine-grained nature of the sediment and the reduced availability of hard substrates (shells, carbonate concretions), inferred from the low abundance of encrusting species, indicate that the bottom was only exceptionally if ever exposed to physical disturbance. The dominance of detritus/deposit-feeders points to low energy conditions and plenty of particulate organic matter on the sea-floor.

The abundance of *Mesomiltha argentina*, presumed to have been well adapted to live in oxygen-poor sediments, supports the idea of lowered oxygen levels for the facies holding association A. Recent lucinid bivalves are known to be well adapted to thrive in low-oxygen environments. These benthic molluscs obtain nutrients from endosymbiotic sulphide-oxidizing bacteria: while the body rests in anoxic sediments rich in hydrogen sulphide, the siphon and a mucus-tube connect with the more oxygenated sediment-water interface (Reid and

Brand 1986). The sediments, in which this association was deposited, were characterized as anoxic to dysoxic (Spalletti et al. 2001b; Tyson et al. 2005). In this work, the evidence (i.e. bioturbation, presence of benthic macrofauna) indicates that the so-called “Spitidiscus” black shale did not probably experience oxygen depletion at any time. Instead, dysoxia and anoxia a few centimetres below the sediment-water interface can be deduced from the organic-rich nature of the sediments, the scarcity of infaunal species and the presence of lucinid bivalves, adapted to live in anoxic sediments. The presence of abundance of predatory drill holes in *M. argentina* specimens in this association poses a question on the oxygen levels of sediments: the predator needed to be able to cope with lowered oxygen so as to find the prey, drill the hole and consume the soft tissues. It is intriguing whether the possible predator, the ampullospirid gastropod *Pictavia* sp. A was adapted to this.

The *Bathraspira* spp. – *Mesomiltha argentina* association represents the first biological colonization that took place after the very fast transgression that drowned the basin, following the regression that deposited the continental sandstones of the Avilé Member. It is present along the MFZ and early HST of the first major depositional sequence (DSAM-1). These strata are characterized by an aggradation of basinal to outer ramp sediments, punctuated by thin levels with evidence of starvation where the shell beds are found. In turn, each shell bed represents the period of starvation of a particular starvation/dilution (sixth order) sequence, that is interpreted to have happened during the transgression and beginning of the regression. Fossils accumulated passively; infaunal individuals remained buried after death, while epifaunal ones were little encrusted or bored. The habitat was not suitable for the settlement of high densities of hard-substrate fauna probably due to the little abundance of hard parts of the seafloor.

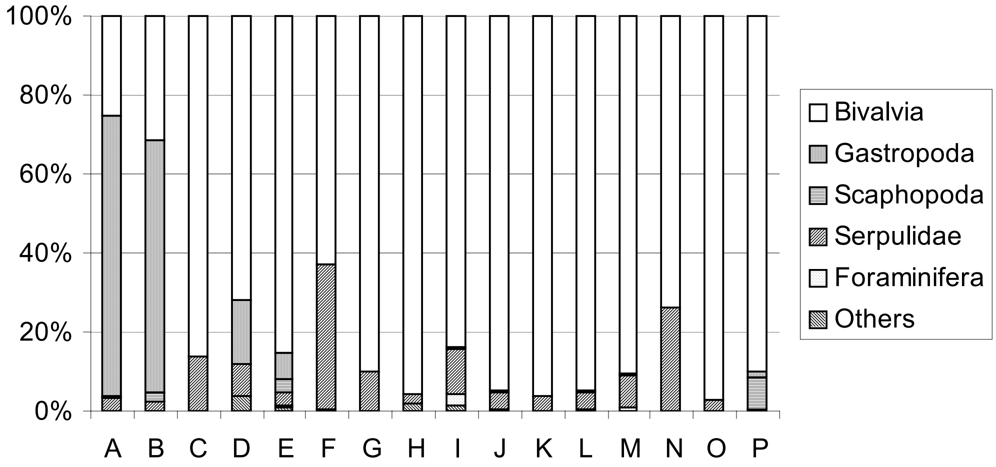

Text-Figure 17A. Fossil associations per major taxonomic groups.

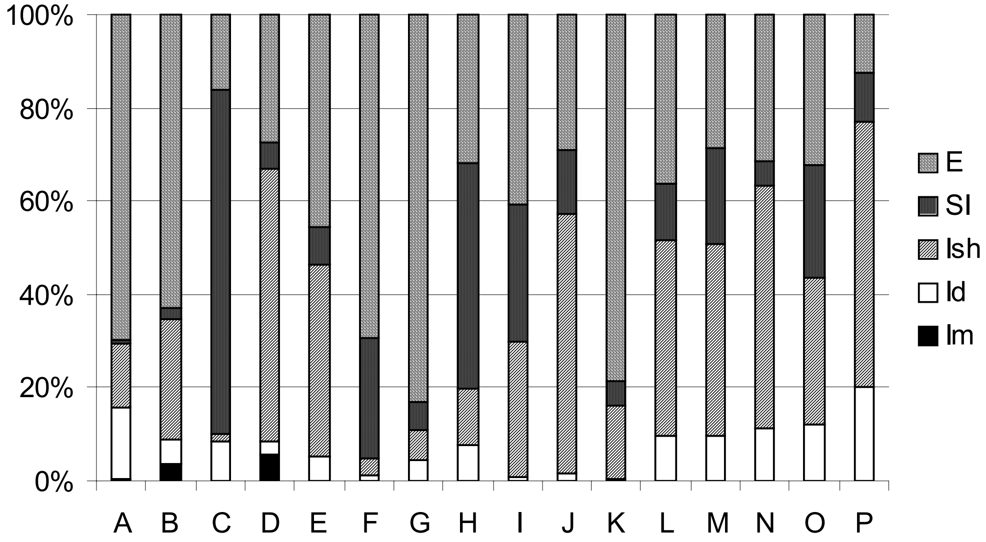

Text-Fig. 17 B. Life habits of fossil associations with respect to substrate. E: epifaunal; SI: semi-infaunal; Ish: shallow infaunal; Id: deep infaunal; Im: infaunal mobile.

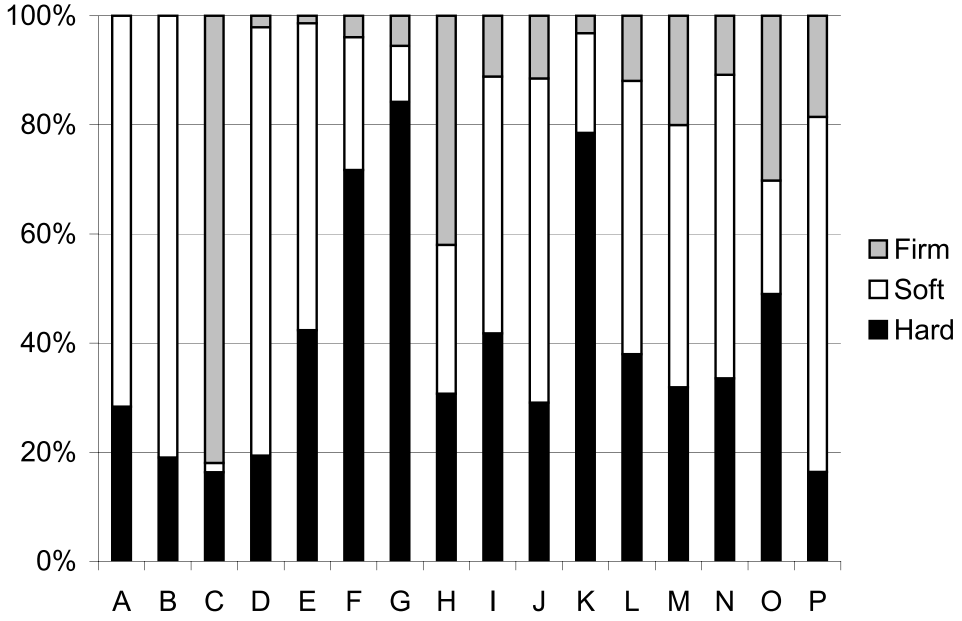

Text-Fig. 17 C. Life habits of fossil associations in terms of type of substrate inhabited.

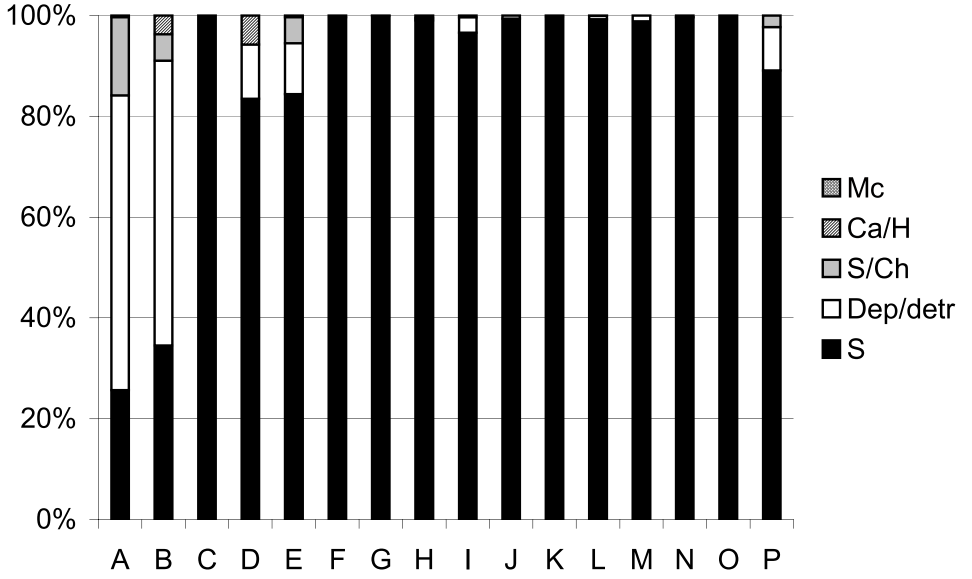

Text-Fig. 17 D. Life habits of fossil associations in terms of feeding types. Mc: microcarnivores; Ca/H: carnivores, less probably herbivores; S/Ch: suspension-feeders and chemosymbionts; Dep/detr: deposit/detritus-feeders; S: suspension-feeders.

Benthic association/assemblage	**Depth range**	**Stratigraphic context**			**Dominant species (trophic nucleus)**	**Diversity**
		Small scale (starvation dilution sequences)	**Large scale (medium and major sequences)**	**Ammonite biozones**		
A: *Bathraspira* spp. – *Mesomiltha argentina.*	(Outer ramp to) basin	Whole starvation hemisequence	TST, MFZ and early HST	S. riccardii	*Bathraspira* sp. A, *Bathraspira*? sp. C, *Mesomiltha argentina*, *Protohemichenopus* sp.	Moderate
B: *Bathraspira* sp. C – *Corbulomima bodenbenderi.*	Outer ramp (to basin)	Whole starvation hemisequence	Middle HST	S. riccardii	*Bathraspira*? sp. C, *Corbulomima* "*bodenbenderi*", *Protohemichenopus* sp., *Mesomiltha argentina*, *Grammatodon securis*	Moderate
C: *Pinna robinaldina* in dilution hemisequences	Middle to outer ramp	Late dilution hemisequence (late starvation hemisequence)	LST (early TST)	C. schlagintweiti	*Pinna robinaldina*, Serpulidae small	Low
D: *Pterotrigonia* sp. A – Gastropods.	Middle to outer ramp	Whole starvation hemisequence	MFZ	P. groeberi or younger	*Pterotrigonia* sp. A, Serpulidae small, *Pictavia* sp. B, *Poasia* sp. B, *Ceratostreon* sp., Arcticidae sp., *Myophorella volkheimeri*, Briozoa sp. B, *Ptychomya* sp. B, *Steinmanella vacaensis*	High
E: *Aetostreon* sp.- *Disparilia elongata*	Middle to outer ramp	Whole starvation hemisequence	Middle to late HST	S. riccardii (C. schlagintweiti, C. diamantensis)	*Aetostreon* sp., *Disparilia elongata*, *Mesomiltha* sp. A, Veneridae sp. 2, *Rhabdocolpus* sp. A, Veneridae sp. 1, *Ceratostreon* sp., *Dentallium* ?, *Eriphyla argentina*, *Myophorella volkheimeri*, Serpulidae small	Moderate
F: *Parsimonia antiquata* – *Ceratostreon* sp. - *Steinmanella vacaensis*	Inner to middle ramp	Early starvation hemisequence	Late HST	C. diamantensis	*Parsimonia antiquata*, *Ceratostreon* sp., *Steinmanella vacaensis*	Moderate
G: *Ceratostreon minos.*	Middle to outer ramp	Middle starvation	TST	C. schlagintweiti, C.	*Ceratostreon* sp., *Parsimonia antiquata*, *Ptychomya* sp. A, *Panopea neocomiensis*, Serpulidae	Low

Benthic association/assemblage	**Depth range**	**Stratigraphic context**			**Dominant species (trophic nucleus)**	**Diversity**
		Small scale (starvation dilution sequences)	**Large scale (medium and major sequences)**	**Ammonite biozones**		
				diamantensis, P. groeberi	middle	
H: *Myoconcha transatlantica*	Inner to middle ramp	Early starvation hemisequence	Early TST	P. groeberi	*Myoconcha transatlantica*, *Ceratostreon* sp., *Ptychomya* sp. A, Arcticidae sp., *Steinmanella vacaensis*, *Panopea dupiniana*, *Isognomon lotenoensis*, Serpulidae small, *Mimachlamys robinaldina*	High
I: *Ceratostreon* - *Eriphyla* – *Ptychomya.*	Middle ramp	Middle starvation	Late TST, early HST	C. diamantensis	*Ceratostreon* sp., *Eriphyla argentina*, *Ptychomya* sp. A, *Myoconcha transatlantica*, Serpulidae middle, Serpulidae small	Moderate
J: *Pterotrigonia coihuicoensis*	Middle ramp	Early-middle starvation hemisequence	Middle HST	P. groeberi	*Pterotrigonia coihuicoensis, Ceratostreon* sp., *Isognomon lotenoensis, Myoconcha transatlantica, Eriphyla argentina*	Moderate
K: *Ceratostreon* – *Eriphyla* with aragonite dissolution.	Middle to outer ramp	Whole starvation hemisequence	Early HST	No ammonites (Early Barremian)	*Ceratostreon* sp., *Eriphyla argentina, Mimachlamys robinaldina, "Pecten" vacaensis*	Moderate
L: *Ceratostreon* – *Pterotrigonia* – *Eriphyla*	(Inner to) Middle ramp	Middle to late starvation hemisequence	Early-middle TST, middle-late HST	C. diamantensis, P. groeberi	*Ceratostreon* sp., *Pterotrigonia coihuicoensis, Eriphyla argentina, Ptychomya* sp. A, *Panopea dupiniana*, Serpulidae small, *Pholadomya gigantea*	Moderate
M: *Eriphyla* – *Ceratostreon* – *Ptychomya*	Middle to outer ramp	Middle to late starvation hemisequence	Late TST, early HST	C. schlagintweiti, C. diamantensis	*Eriphyla argentina, Ceratostreon* sp., *Ptychomya* sp. A, *Panopea dupiniana, Myophorella volkheimeri, Gervillella aviculoides, Parsimonia antiquata*, Veneridae sp. 3,	High

Benthic association/assemblage	**Depth range**	**Stratigraphic context**			**Dominant species (trophic nucleus)**	**Diversity**
		Small scale (starvation dilution sequences)	**Large scale (medium and major sequences)**	**Ammonite biozones**		
					Veneridae sp. 2	
N: Veneridae sp. 3 – *Panopea dupiniana*	Middle to outer ramp	Whole starvation hemisequence	MFZ	C. schlagintweiti	Veneridae sp. 3, Serpulidae middle, *Panopea dupiniana*, Veneridae sp. 2, *Myophorella volkheimeri, Ptychomya* sp. A, *Disparilia elongata, Parsimonia antiquata, Cucullaea gabrielis*	High
O: *Cucullaea gabrielis* – *Gervillella aviculoides* – *Aetostreon* sp.	Inner ramp	Early starvation hemisequence	Early TST, late HST, LST	C. schlagintweiti, C. diamantensis	*Cucullaea gabrielis, Gervillella aviculoides, Aetostreon* sp., *Panopea dupiniana, Eriphyla argentina, Ceratostreon* sp., "*Pecten*" *vacaensis, Steinmanella vacaensis, Mimachlamys robinaldina*	Moderate
P: Veneridae sp. 2 – *Panopea necomiensis*	(Middle to) outer ramp	Whole starvation hemisequence	Late TST, early HST	C. schlagintweiti, C. diamantensis (P. groeberi?)	Veneridae sp. 2, *Panopea neocomiensis, Ceratostreon* sp., *Dentallium*?, *Panopea dupiniana Cucullaea gabrielis*, Arcticidae sp., *Corbulomima* "*bodenbenderi*"	Moderate

Table 6. Synthesis of fossil benthic associations and assemblages.

The association represents the almost undisturbed relics of the shelled part of a benthic community living in an organic-rich soft bottom with little or not water energy. The degree of time-averaging of these shell beds is inferred to be moderate, like in the case of the “within-habitat assemblages” of Kidwell and Bosence (1991). Although each one represents a complete starvation hemisequence that lasted for at least a few thousand years (from the beginning of the transgression up to the early part of the next regression of a 20,000 thousand years cycle) little environmental change is envisaged to have happened during the period involved. Hence, little environmental condensation and high fidelity is inferred for the association.

- **Fossil Association B: *Bathraspira* sp. C – *Corbulomima bodenbenderi***

1,895 specimens in eight samples compose this association. Diversity (S=11, H’=1.41) and evenness (E=60.85%) are intermediate and vary to some extent between samples. The association totals 26 species, although only five belong to the trophic nucleus. It was sampled from 56 to 75 m in the BAL section and at equivalent positions in AML, in the earliest Late Hauterivian *Spitidiscus riccardii* Zone. These sediments belong to the middle HST of DSAM-1, more specifically represent the late RST of the subordinated fourth order DSAM-1/1, and overlie sediments holding the benthic association A.

The gastropod *Bathraspira* sp. C dominates the association with 52.37%, replacing *Bathraspira* sp. A (0.3%), the most abundant species in the benthic association A. The very small corbulid *Corbulomima bodenbenderi* (14%) is the second most abundant species. The trophic nucleus is completed with the aporrhaid *Protohemichenopus* sp. (5.81), the lucinid *Mesomiltha argentina* (5.24), and *Grammatodon securis* (4.85). Epifauna (62.8%) dominates over infauna (34.76%), which reaches slightly higher percentages than in association A (29.5%). Detritus/deposit-feeders represent 56.54% of the individuals. Compared with association A there is a small increase in the percentage of deposit-feeding scaphopods (0.72 to 2.44%), a moderate increase in the percentage of suspension-feeders (25.65 to 34.52%) and a decrease in chemosymbiotic lucinids from 15.56 to 5.24%.

Table 7. Trophic nuclei of benthic associations. A%: accumulated percentage.

Benthic association A	**%**	**A %**	**Rank**
Bathraspira sp. A	36,61	36,61	1
Bathraspira? sp. C	20,8	57,41	2
Mesomiltha argentina	15,56	72,96	3
Protohemichenopus sp.	12,78	85,74	4

Benthic association B	**%**	**A %**	**Rank**
Bathraspira? sp. C	52,37	52,37	1
Corbulomima "bodenbenderi"	14,02	66,39	2
Protohemichenopus sp.	5,81	72,19	3
Mesomiltha argentina	5,24	77,43	4
Grammatodon securis	4,45	81,88	5

Benthic association C	**%**	**A %**	**Rank**
Pinna robinaldina	73,47	73,47	1
Serpulidae small	13,61	87,07	2

Benthic association D	**%**	**A %**	**Rank**
Pterotrigonia sp. A	40,93	40,93	1
Serpulidae small	7,73	48,66	2
Pictavia sp. B	5,59	54,25	3
Poasia sp. B	5,59	59,84	4
Ceratostreon sp.	4,92	64,76	5
Arcticidae sp.	3,45	68,21	6
Myophorella volkheimeri	3,35	71,56	7
Bryozoa sp. B	3,27	74,82	8
Ptychomya sp. B	3,19	78,01	9
Steinmanella vacaensis	3,06	81,07	10

Benthic association E	**%**	**A %**	**Rank**
Aetostreon sp.	26,07	26,07	1
Disparilia elongata	21	47,07	2
Mesomiltha sp. A	4,71	51,77	3
Veneridae sp. 2	4,7	56,47	4
Rhabdocolpus sp. A	4,58	61,05	5
Veneridae sp. 1	4,1	65,15	6
Ceratostreon sp.	3,96	69,11	7
Dentalium ?	3,53	72,64	8
Eriphyla argentina	3,28	75,92	9
Myophorella volkheimeri	3,21	79,13	10
Serpulidae small	3,13	82,26	11

Benthic assemblage F	**%**	**A %**	**Rank**
Parsimonia antiquata	36,69	36,69	1
Ceratostreon sp.	32,14	68,83	2
Steinmanella vacaensis	21,43	90,26	3

Benthic association G	**%**	**A %**	**Rank**
Ceratostreon sp.	69,26	69,26	1
Parsimonia antiquata	4,42	73,68	2
Ptychomya sp. A	3,02	76,7	3
Panopea neocomiensis	2,97	79,68	4
Serpulidae middle	2,9	82,58	5

Benthic association H	**%**	**A %**	**Rank**
Myoconcha transatlantica	30,89	30,89	1
Ceratostreon sp.	17,01	47,89	2
Ptychomya sp. A	10,05	57,94	3
Arcticidae sp.	5,52	63,46	4
Steinmanella vacaensis	4,54	68	5
Panopea dupiniana	4,48	72,48	6
Isognomon lotenoensis	3,31	75,79	7
Serpulidae small	2,4	78,19	8
Mimachlamys robinaldina	2,35	80,54	9

Benthic association I	**%**	**A %**	**Rank**
Ceratostreon sp.	23,81	23,81	1
Eriphyla argentina	19,91	43,72	2
Ptychomya sp. A	18,47	62,19	3
Myoconcha transatlantica	9,84	72,03	4
Serpulidae middle	5,25	77,28	5
Serpulidae small	5,05	82,33	6

Benthic association J	**%**	**A %**	**Rank**
Pterotrigonia coihuicoensis	44,64	44,64	1
Ceratostreon sp.	12,83	57,47	2
Isognomon lotenoensis	9,65	67,12	3
Myoconcha transatlantica	8,85	75,97	4
Eriphyla argentina	6,71	82,68	5

Benthic association K	**%**	**A %**	**Rank**
Ceratostreon sp.	64,14	64,14	1
Eriphyla argentina	11,48	75,62	2
Mimachlamys robinaldina	4,33	79,95	3
"Pecten" vacaensis	3,75	83,7	4

Benthic association L	**%**	**A %**	**Rank**
Ceratostreon sp.	29,7	29,7	1
Pterotrigonia coihuicoensis	22,04	51,73	2
Eriphyla argentina	12,99	64,73	3
Ptychomya sp. A	6,24	70,97	4
Panopea dupiniana	3,7	74,67	5
Serpulidae small	3,16	77,82	6
Pholadomya gigantea	2,72	80,55	7

Table 7. (cont.)

Benthic association M	**%**	**A %**	**Rank**
Eriphyla argentina	19,19	19,19	1
Ceratostreon sp.	17,52	36,71	2
Ptychomya sp. A	9,27	45,98	3
Panopea dupiniana	6,6	52,58	4
Myophorella volkheimeri	6,48	59,07	5
Gervillella aviculoides	6,34	65,4	6
Parsimonia antiquata	5,46	70,86	7
Veneridae sp. 3	4,98	75,84	8
Veneridae sp. 2	4,68	80,52	9

Benthic association O	**%**	**A %**	**Rank**
Cucullaea gabrielis	16,59	16,59	1
Gervillella aviculoides	12,01	28,6	2
Aetostreon sp.	10,25	38,85	3
Panopea dupiniana	10,2	49,05	4
Eriphyla argentina	9,35	58,4	5
Ceratostreon sp.	7,98	66,38	6
"Pecten" vacaensis	5,66	72,04	7
Steinmanella vacaensis	5,38	77,42	8
Mimachlamys robinaldina	4,62	82,04	9

Benthic association N	**%**	**A %**	**Rank**
Veneridae sp. 3	29,15	29,15	1
Serpulidae middle	22,47	51,62	2
Panopea dupiniana	7,65	59,27	3
Veneridae sp. 2	6,1	65,37	4
Myophorella volkheimeri	4,16	69,53	5
Ptychomya sp. A	4,06	73,59	6
Disparilia elongata	3,33	76,92	7
Parsimonia antiquata	2,76	79,68	8
Cucullaea gabrielis	2,58	82,26	9

Benthic association P	**%**	**A %**	**Rank**
Veneridae sp. 2	35,48	35,48	1
Panopea neocomiensis	12,9	48,39	2
Ceratostreon sp.	10,44	58,82	3
Dentalium ?	8,38	67,21	4
Panopea dupiniana	4,88	72,09	5
Cucullaea gabrielis	3,96	76,05	6
Arcticidae sp.	3,02	79,07	7
Corbulomima "bodenbenderi"	2,89	81,96	8

Shell beds of this association are found in silty to sandy-silty allochemic limestones, intercalated into a steady but slow progradational succession of facies. The environment inferred for these sediments is the outer ramp, i.e., below storm-wave base but within the reach of distal tempestites and weak bottom currents. The beds containing the shell concentrations included in this association are interpreted as the starved portions of starvation/dilution sequences. The beds are thin, exceptionally more than 20 cm thick. Bed contacts are usually sharp. There are little indications of vertical changes in these beds, exceptions being the occurrence of relatively higher abundances of *M. argentina* and *Dentalium* sp. on top of some shell beds, embedded in finer and darker sediments. Shell packing is usually dense but matrix-supported. Shells are found in two modes, broken and unrecognizable fragments, or complete, bivalves usually are articulated. Microborings are common. Other types of bioerosion, such as *Meandropolydora*, cirripedian borings and predatory drill holes on *M. argentina* occur, although not abundantly. A feature common to beds of this association is the presence of early diagenetic carbonate concretions that in same cases became exhumed and encrusted by oysters and small serpulids. Patchy lithification occurs frequently in shell beds of this association. When early lithification happened a good picture of the biofabric can be seen. Where not, the matrix looks marly and only relatively large and/or only calcitic shells are detected.

Discussion

Samples containing the *Bathraspira* sp. C – *Corbulomima bodenbenderi* association samples come from the sediments immediately above those containing the *Bathraspira* spp. – *Mesomiltha argentina* association. Both benthic associations cluster together with relatively high similarity (Text-Fig. 15). The former, however, was deposited in slightly shallower settings, under higher sedimentation rates and within the reach of distal tempestites. The presence of exhumed concretions formed during early diagenesis, although little bored and encrusted, suggests that the bottom currents winnowed the sea floor, exposed the lithified portions of the beds and concentrated the fauna. The diagenetic "window", i.e., the conditions under which most of the shelled fauna is preserved, occurred only patchily during the starved period of sixth order sequences.

Association B was deposited in deep tranquil waters, with high abundance of organic matter. If compared with association A, the *Bathraspira* sp. C – *Corbulomima bodenbenderi* association differs very little with respect to life and feeding habits, with a minor increase in infaunal species, and an increase in the percentage of suspension-feeders on the expense of deposit/detritus-feeders and chemosymbionts. Conversely, there is an important change in the proportion of gastropod species between benthic associations A and B. While the former is dominated by *Bathraspira* sp. A (36.61%), in the latter *Bathraspira* sp. C is the most abundant taxon (52.37%). The autoecological differences between both gastropod species, which possibly reflect habitat differentiation, are not evident from the morphology of their shells.

Although not drastical, changes in faunal composition with respect to association A seem to correlate with the environmental changes driven by the development of the first major depositional sequence of the unit (DSAM-1), e.g. higher terrigenous input, higher physical stress, and shallowing. This is evident from sedimentological (higher shell density, presence of reworked concretions), taphonomic (higher levels of microborings, fragmentation and disarticulation) and paleoecological data (increase of suspension-feeders and infaunal elements with respect to chemosymbionts).

Benthic association B was sampled in shell beds that represent the starvation hemisequence of sixth order sequences, i.e., represent condensed sediments with respect to sediments below and above. The occurrence of *Dentalium* sp. and articulated specimens of *M. argentina* on top of some beds indicates a possible vertical pattern of environmental change, probably deepening, within the starvation hemisequences. This vertical change is not evident in the majority of the beds. Time averaging is moderate. Minor environmental condensation probably characterizes the samples of this association. Evidence of this are the variable diversity values that range from low to high among samples. Samples included in this association were deposited during the development of the HST-1 and include the remains of communities that lived on the outer ramp (middle HST-1). However, basinal (or middle ramp) influence is not discarded as the association was deposited close to the boundaries of both facies belts.

- **Fossil Association C: *Pinna robinaldina***

Fossil benthic association C is composed of three samples with 282 specimens. It has the lowest diversity and evenness values of all associations (S=6, H'=0.78, E=47%). Eight taxa belong to the association, of which only two constitute the trophic nucleus, *Pinna robinaldina* and small serpulids.

All samples composing the association come from beds that belong to the *C. schlagintweiti* biozone, immediately above SBAM-1. Sample M45 comes from the BAL section and was retrieved from a sandy-silty bioclastic allochemic limestone bed. It overlies the first shell bed after the sequence boundary. Samples M101 and M102, taken from the AML section, were found in a different sedimentological and stratigraphic context, although share with M45 the position close above SBAM-1. These samples come from fossil-rich, bioturbated, fine-grained sandstones (S-FS-R facies, see Chapter 5 for more information) that represent the top of the few starvation/dilution sequences that lack the starvation hemisequence. These beds were deposited in the context of the lowstand systems tract of the second major sequence of the unit (LST-2), that lacks in the BAL section. Other bioturbated sandstone beds with similar fossil content exist but were not surveyed.

The semi-infaunal bivalve *Pinna robinaldina* (73.47%) dominates the association. Together with small serpulids (13.61%) it forms the trophic nucleus. Two other species have percentages above 1: the small deep burrowing *Panopea neocomiensis* (7.82%) and the reclining oyster *Aetostreon* sp. (2.72%). The association is completed by rare *Myophorella volkheimeri*, *Eriphyla argentina*, *Panopea dupiniana* and Veneridae sp. 2. Suspension-feeders constitute 100% of the association. Semi-infaunal bivalves dominate (73.47%) followed by epifaunal serpulids and oysters (16.33%), deep infaunal *Panopea* (8.50%) and shallow infaunal bivalves (1.70%). The majority of the individuals prefered firm (81.97%) or hard (16.33%) substrates.

Shell concentrations of benthic association C are disperse to loosely packed, contain shells of originally calcitic composition such as *Pinna robinaldina*, serpulids (originally high-Mg-calcite), and gryphaeid oysters (originally low-Mg-calcite) or internal moulds of taxa with originally aragonitic shell such as *Panopea neocomiensis*, *P. dupiniana*, and Veneridae sp. indet 2. In *Pinna robinaldina* specimens only the outer, low-Mg-calcite layer is preserved. The strong dominance of species with original calcitic shell (89.80%) over aragonitic ones (10.20%) is remarkable. Association C has the highest percentages of calcitic fossils if compared with other associations/assemblages. Average calcitic content through all associations is 41%, the median 35% (minimum 4%, maximum 89.8%). Common features of most of these skeletal concentrations are a nearly complete absence of encrustation and bioerosion, low species richness, and a high proportion of infaunal taxa (e.g., *Panopea neocomiensis*) and of the semi-infaunal *Pinna robinaldina,* both articulated and in life position. In some beds, serpulids of variable morphologies are common but not attached to any shell or shell fragment (in fact, there are generally no bioclasts in this facies).

Discussion

The *Pinna robinaldina* association is the only association that was completely sampled from dilution hemisequences. From the sedimentologic evidence, the communities lived in firm, stable substrates, which were exposed on the sea floor long enough to become completely bioturbated. The lack of sedimentary structures does not match permanent agitation by fair-weather waves. Similarly, taphonomic information, i.e. the widespread occurrence of the semi-infaunal *Pinna robinaldina* and the infaunal *Panopea neocomiensis*, both usually articulated and in life position, agrees with a calm environment. The sediments could have been deposited in a shoreface setting but the colonization by the benthic community took place later on when, as a result of transgression, the sea floor occupied a greater depth. Shell concentrations are dominated by mineralogically more stable calcitic elements such as pinnids, serpulids, and oysters. This probably points to some sort of selective dissolution of a fraction of the originally aragonitic shells, and would suggest a bias.

Association C does not show signs of environmental condensation. Time averaging is probably low although some condensation is evident. The communities probably lived during the transgression phases of sixth order sequences, although no sediments were deposited during this period.

- **Fossil Association D: *Pterotrigonia* sp. A – Gastropods**

The *Pterotrigonia* sp. A – Gastropods association is the result of the grouping of two samples with 755 specimens. Diversity (S=22, H'=2.16) and evenness (E=70%) are high. Among the 31 species found in these samples, ten are present in the trophic nucleus. Both samples come from the BAL section at 498 m (sample M92) and 505 m (sample M93, respectively. Similar fauna was observed in the AML section at equivalent stratigraphic position.

The samples composing this association are the youngest surveyed in this study. No ammonites are described from equivalent strata, although the level is certainly Lower Barremian or higher. Sample M92 comes from a bed placed in the MFZ position of the DSAM-7, and M93 from the probable MFZ of DSAM-8. Strata holding M92 and M93 are classified as sandy bioclastic allochemic limestones (MB2, Chapter 5), and sandy bio-oo-floatstones (LF-R, Chapter 5) respectively. Both constitute complete starvation hemisequences in which no internal stratigraphic subdivisions are evident. The beds are tabular and sharp-based, and are preceded and followed by fine-grained siliciclastic facies. Terrigenous starvation is evident from the relatively higher carbonate content and from the presence of authigenic glauconite grains and iron replacement. These types of facies formed in the middle to outer ramp, certainly below the fair-weather wave-base. The major sedimentary sequences at that position of the unit were characterized as a carbonate ramp in which coarse-grained siliciclastic sediments are common only on top of major HSTs (for more information see discussion in Chapter 5).

Among the species counted in this association 13, that account for more than 64% of the abundance were not recorded in older strata. 16% of the association are gastropods (9 species). The association is dominated by the small trigonid bivalve *Pterotrigonia* sp. A (40.93%). Bivalves represent more than 70%, serpulids 7.93%, bryozoans 3.27% of the fauna. Shallow infaunal species (58.45%) dominate over epifauna (27.56%), semi-infauna (5.64%), infaunal mobile taxa (5.59%), and deep infaunal species (2.76%). Suspension-feeders constitute most of the association (81.21%), followed by deposit/detritus-feeders (10.44%) and the probably carnivorous ampullospirids (5.59%). The preservation of the fauna is rather good: more than 15% of the bivalves are articulated, corrasion does not represent an important taphonomic destructive factor, borings are rare, and a bit more than 16% of the shells are encrusted.

Discussion

Association D represents a moderately within-habitat time-averaged relic of the hard parts of a benthic community. Diversity is enhanced probably due to time-averaging and some taphonomic feedback. Environmental condensation is low as there is no sign that indicates distinct depth changes during the deposition of the beds. Shells accumulated progressively under low terrigenous input conditions. Storms sporadically concentrated and disarticulated the shells, and imported shell fragments from shallower settings by means of tempestites. The taxonomic composition of association D, in which several species are exclusively represented, is a consequence of faunal replacement related to the time involved, evolution and environmental changes. The younger of the two beds containing association D is placed in the depositional sequence 4 (DSAM-4), while shell beds in this association come from DSAM-7 and 8. These sediments are conservatively considered as Early Barremian. However, if correlation is made based on sequence boundaries, the top of the Agrio Formation could be as young as Albian. Evolution also contributed with species that are apparently closely related to species found in the rest of unit (e.g., *Pterotrigonia* sp. A and *P Pterotrigonia coihuicoensis*; *Ptychomya* sp. A, and *Ptychomya* sp., cf. *P. koeneni* respectively). Detailed studies are needed to elucidate these relationships.

The high diversity values are a consequence of an environment suitable for the settling of several guilds rather than an artifact of the clustering of several different samples. An oligotrophic regime is envisaged for this association. Time-averaging also played a role in enhancing diversity, as samples composing association D represent complete starvation hemisequences. This means that early and late transgression and early highstand are condensed in a single bed.

Most marine carbonate systems develop under oligotrophic regimes in which there is little particulate organic matter available. These oligotrophic ecosystems are usually characterized by high levels of biodiversity if there are not other stress factors (e.g. reduced salinity, low oxygen availability, soupy substrate). Conversely, high availability of organic matter on a well oxygenated eutrophic seafloor favours colonization by opportunistic species, resulting in a low diversity biocoenosis. This last case is exemplified by the *Ceratostreon minos* association (see below), in which the opportunistic gryphaeid oyster *C. minos* and the large serpulid *Parsimonia antiquata* formed buildups that occupied most of the bottom. Judging from the ecological evidence, the diverse and abundant gastropods found in the oligotrophic benthic association D, are better interpreted as algae browsers rather than detritus-feeders.

- **Fossil Association E: *Aetostreon* sp. - *Disparilia elongata***

The *Aetostreon* sp. - *Disparilia elongata* association is composed of 2,026 specimens in 18 samples. Diversity and evenness have intermediate values (S=14, H’=1.70, E=68%). Diversity values among the different samples exhibit remarkable differences. There are 51 species in this association, 11 of which constitute the trophic nucleus.

The majority and most representative samples of this association come from the middle and late stages of the major HST-1, and span the whole RST of the subordinated DSAM-1/1 (Text-Fig. 6). These beds are the highest levels of the *Spitidiscus riccardii* Zone. Benthic association E supersedes association B, continuing the shallowing-upward trend that began at the base of the unit with association A. Samples M47, M73, and M100 are atypical. Sample M100 is composed of two species, *Aetostreon* sp. (>90%) and *Pinna robinaldina*, and probably exhibit some diagenetic bias as originally aragonitic shells are absent. The nature of samples M47 and M73 is discussed below.

Bivalves (85.45%) dominate the association, followed by gastropods (6.46%), scaphopods (3.53%), and serpulids (3.28%). Echinoids, foraminifers, scleractinian corals, and bryozoans complete the association. Epifauna (45.74%) and shallow infauna (41.29%) are more or less equally abundant. The semi-infaunal life habit (7.69%) is represented by the detritus-feeders scaphopod *Dentalium* and the irregular echinoid *Pygaster gerthi*, and the suspension-feeder *Ptychomya* sp. The deep infaunal mode of life is mainly represented by *Mesomiltha* sp. A and two more lucinid species. 84.44% of the specimens are suspension-feeders. Deposit/detritus-feeders reach 10%, chemosymbionts 5.24%, and microcarnivores 0.28%.

Beds that contain skeletal concentrations of association E are vertically homogeneous and sharp-based starvation hemisequences (exceptions are described below). Sedimentary facies typical of this association are bioclast-dominated muddy or sandy to muddy mixed rocks, or muddy bioclast-rich fine-grained limestones (floatstones or low-energy micritic rudstones). Shell beds are loosely to densely packed. Shells are usually disarticulated. Two sizes of bioclasts are present: complete and fragmented shells and unrecognizable shell fragments. Microborings are common. Macroborings (*Gastrocheanolites*, *Trypanites* and *Meandropolydora*) are rare to abundant on *Aetostreon* shells and carbonate concretions. Several beds contain reworked calcareous concretions of early diagenetic origin, variably bored (mainly *Gastrocheanolites* and *Trypanites*) and encrusted by *Aetostreon*, corals, *Ceratostreon*, and small and medium serpulids (Pl. 1, figs. 6 and 7).

Aetostreon sp. aff. *A. latissimum* Defrance, 1821 is with 26% the most abundant species in association E. It is a reclining gryphaeid oyster described in different units of the Neocomian of the Neuquén Basin (Lazo 2004; Schwarz et al. 2001; Weaver 1931). It has wide morphological and size variability. Its small attachment area (Pl. 10, Fig. 1a) with respect to the size of the shell indicates that the species lived attached to a hard substrate during the first stages of growth. With size increasing, the attachment area became too small to support the whole shell and the individual rested freely on the sea floor. It is absent in three samples (M47, M73 and M96). M47 was sampled from the late starvation portion of a sixth order sequence deposited higher up in the section, in the TST-2. It overlies shell beds containing benthic association M, typical of a shallower facies. M73 is a sample that comes from a bed close below the major MFZ-3. It clusters with association E because of its high abundance of *Disparilia elongata*. M96 is one of the few samples taken from dilution hemisequences. It lacks species living on hard substrates as a consequence of a relatively higher rate of sedimentation. This sample is interesting as it not condensed at all, although it clusters with condensed shell beds of starvation hemisequences deposited immediately above it (see AML section in appendix-figure 2, M96 from 185 m; M97 and 98 from bed "AM55", 186 m from the base). *D. elongata* (21%), *Mesomiltha* sp. A (4.71%), Veneridae sp. 2 (4.70%) and Veneridae sp. 1 (4.10%), are species diagnostic of this association. There are also species typical of associations A and B, such as *Rhabdocolpus* sp. A (4.58%), *Dentalium* sp. (3.53%), *Corbulomima bodenbenderi* (2.35%), *Gryphaeostrea* sp. 2 (1.89%), *Grammatodon securis* (1.23%), and others.

Samples M41 and M43 correspond to the base of a complex shell bed situated at 166 m above the Avilé Member in section BAL. This basal shell bed has a different composition compared with the overlying concentration, sampled as M42 and also included in this association. The basal shell bed is dominated by disarticulated shells of the shallow infaunal bivalves Veneridae sp. 1 and 2, followed by *D. elongata*. M42, in turn, is widely dominated by *Aetostreon* sp. The basal shell bed is interpreted as a reworked and physically concentrated relic of the top of the underlying RST, and can be considered as a transgressive lag. Conversely, M42 was deposited during the maximum flooding and is dominated by species that make use of available hard substrates for settling.

Discussion

Aetostreon sp.- *Disparilia elongata* association represents the remains of a group of heterogeneous taphocoenoses deposited from the upper outer to the middle ramp, mostly above storm wave-base and certainly below fair-weather wave-base. During deposition of dilution hemisequences an association dominated by the shallow infaunal astartid *Disparilia elongata* and Veneridae sp. 1 and 2 dominated. During times of starvation hemisequences, the sea floor was relatively rich in shells, shell fragments, and carbonate concretions, a setting that induced the colonization of species making use of hard substrates, such as *Aetostreon*, *Ceratostreon*, and serpulids. However, according to the position in the sedimentary sequence (late major HST) the sedimentation rate was high and water agitation not high enough nor permanent to uncover sufficiently abundant hard substrate for a massive colonization by encrusters. Instead, scarce islands of hard substrate were available. A fauna typical of dilution-hemisequence probably partly coexisted with colonizers of the starvation period. Storm waves helped in creating new hard substrates for the encrusting fauna. Storm flows brought shell hash from shallower environments.

The association is dominated by suspension-feeders. Detritus/deposit-feeding gastropods and scaphopods represent more than 10% of the association and indicate that the bottom was rich in particulate organic matter. The chemosymbiotic lucinids, inhabitant of anoxic sediments, are also an important part of the association. The presence of more than 15% of non-suspension feeders is a consequence of the position of the beds containing this association in deep offshore settings. The two feeding types probably coexisted in time. Another possibility is that every bed is a mixture of different communities that inhabited the bottom during the development of each starvation hemisequence. The small thickness of these beds did not allow a stratigraphical distinction between communities of the lower (shallower) early starvation hemisequence and upper (deeper) middle to late starvation hemisequence. An exception to this is a complex bed deposited at 129 m in section AML (Appendix-Fig. 2, 129 m, “AM 45” bed). In this bed, the lower part is a muddy bioclastic allochemic limestone with abundant carbonate concretions and rich in *Aetostreon* sp., both bored and encrusted. Sample M95 of Association E is from this bed. The upper portion contains a higher abundance of the chemosymbiotic *Mesomiltha* sp. A and the deposit-feeder *Dentalium* sp. (no sample was taken there). Such a differentiation is not possible in the rest of the beds. Time-averaging of samples in association E is thus moderate. Some kind of environmental condensation occurred, although this phenomenon did not shape significantly the composition of the assemblages.

- **Fossil Assemblage F: *Parsimonia antiquata* – *Ceratostreon* sp. - *Steinmanella vacaensis***

This assemblage is composed of sample M111P. It is derived from a well-lithified bioclastic fine-grained sandstone bed (MD2 facies, in Chapter 5), deposited on the inner ramp, above the fair-weather wave-base (or just below it). The bed containing this assemblage represents the base of the starvation hemisequence of the last starvation/dilution sequence of depositional sequence 2 (DSAM-2). It was deposited in a high-energy environment. The majority of the bivalves are disarticulated and out of life position (95%), and belong to the largest and thickest-shelled species. With few exceptions (two *Cucullaea gabrielis* and one *Gervillella aviculoides*) articulated specimens belong to *S. vacaensis*. *S. vacaensis* usually appears in butterfly position (with opened but still articulated valves) and usually is not encrusted. Micro- and macroborings are abundant.

The assemblage is composed of 308 specimens distributed among nine species. Diversity and evenness show intermediate values (S=9, H’=1.45, E=66%). Only three species constitute the trophic nucleus. Bivalves (63%) dominate over serpulids (36.7%); foraminifers represent less than 1 %. Epifaunal cemented specimens such as the large serpulid *Parsimonia antiquata* and the gryphaeid oyster *Ceratostreon* sp., represent almost 70%. The majority of these epifaunal species are found in small clusters. Following in abundance are semi-infaunal (25.97%), and shallow-infaunal (3.57%) large and thick-shelled bivalves e.g., *Steinmanella vacaensis*, *Cucullaea gabrielis*, and

Gervillella aviculoides, and the deep infaunal *Panopea neocomiensis* (1.30%). More than 99% of the assemblage consists of suspension-feeders.

Discussion

Fossil assemblage F represents the relict of a community that lived in a high-energy setting, above the fair-weather wave-base. At least some of the large shells were unearthed from the underlying RST. They are heavily worn, fragmented, bored, and encrusted. The assemblage is composed almost exclusively of large and thick-shelled infaunal and semi-infaunal species and cementing oysters and serpulids. Smaller, thinner shells were probably broken and became unrecognizable fragments or were dissolved. Encrusting fauna colonized the stable hard substrates offered by large shells, constructing small buildups on them.

The abundant shells and shell fragments of this assemblage are characterized by disarticulation, fragmentation and pervasive encrustation and borings. However, *S. vacaensis* is frequently found articulated with closed valves or in butterfly position, in these cases without borings or encrustation. This shows that *S. vacaensis* lived in this high-energy shoreface environment. However, *S. vacaensis* was also found in offshore muddy settings of both, starvation and dilution hemisequences. This indicates that this species was eurytopic at least with respect to depth. The time involved in the deposition of assemblage F is shorter than in most other associations: the bed represents only the base of a starvation hemisequence. However, the probable mix of faunas of the late RST with those living in the TST suggests some sort of environmental condensation.

• Fossil Association G: *Ceratostreon minos*

Seven samples constitute this association, comprising 1,226 specimens. It is characterized by low levels of diversity (S=7, H'=0.97) and evenness (E=55.7%). The trophic nucleus consists of only five of the 25 species that integrate the association. Shell beds of the *Ceratostreon minos* association occupy different positions in the major third depositional sequence (DSAM-3) and close to the base of DSAM-4 in section BAL, and in DSAM-2 in section AML. Some samples represent oyster-serpulid buildups overlying other types of shell beds. The other examples are beds in which *C. minos* buildups on ammonites, nautiloids or other large shells represent the majority of the preserved fauna. In all cases this association was sampled from beds in which enhanced starvation, associated with fourth, fifth or third-order cyclicity can be expected.

Ceratostreon minos (69.26%) dominates the association and all samples composing it. This species is the only one present in all samples. Small, medium and large serpulids are also abundant in some samples. Small, cementing, patch-reef constructors represent the main life habit (79%). Together with epi-byssate species (3.55%), the epifauna reaches 82.94%. Semi-infaunal (5%), shallow infaunal (6.44%), and deep infaunal (4.62%) bivalves complete the association. More that 99% of individuals in association G are suspension-feeders.

The *C. minos* association consists of small, high-density patches of oysters and or serpulids on large shells. In two cases, buildups appear at the position of maximum flooding/minimum terrigenous input in starvation/dilution sequences (e.g. M58R and M105R). Patches are usually few tens of cm of diameter, mimicking the shape of the shells they cement (usually large crioceratitid ammonites), while fossils in the neighbourwood remain almost without encrustations. This is the case of sample M58R (section BAL, at 306 m), as well as of samples belonging to other associations (e.g. associations H to M). In sample M105R (section AML, at 281 m), a more than 50 m long oyster/serpulid reef developed (Pl. 7, Fig. 1). The reef grew on the shell bed of the maximum flooding zone of the sixth order sequence. In its thickest part the bioconstruction reaches almost one meter. The base is dominated by the large serpulid *Parsimonia antiquata*, which up section is progressively replaced by *C. minos*. *P. antiquata* colonised shells lying on the sea floor and, after few cm of horizontal growth, continued growing in an upright direction (Scrutton 1975). This species is more often found in aggregations of several tubes than alone. The top of the reef is dominated by *Ceratostron*. Further away from the centre, the reef becomes composed by patches that progressively diminish in size. The furthest patches are dominated by *P. antiquata*, which is replaced by *Ceratostron* towards the centre.

Discussion

The *Ceratostreon minos* association results from the clustering of samples in which this gryphaeid oyster represents the majority of the assemblage, in the form of small to large patch reefs. In the case of large buildups, the serpulid *Parsimonia antiquata* constitutes the pioneer species that first colonised the hard bottom, which was then overgrown by *Ceratostreon*. Other samples with high abundance of *Ceratostreon* forming buildups are found in associations H to M.

The dominance of species that need hard substrates to settle and of suspension-feeders indicate that this association was deposited in settings governed by low sedimentation rates and whithin the reach of currents or waves. This coincides with the position of *Ceratostreon* association in parts of sequences in which a high degree of starvation is expected. The low diversity and evenness may be due to a factor that made the environment suitable for a population explosion of *Ceratostreon*. The high density of shells probably prevented colonization by infaunal elements. Other limiting factors such as oxygen depletion or changes of salinity are not supported by the evidence. *Ceratostreon minos* probably experienced high population growth after exploiting a particularly suitable combination of ecologic factors: high availability of hard substrates and abundant organic particles in suspension. However, these two conditions are rather opposite: high input of particulate food needs relatively high rate of terrigenous input, while high availability of hard substrates in offshore settings implies sediment starvation. A possible explanation is the formation in contact of highly starved sediments (below) with the onset of the early part of the following regression. Selective dissolution of originally aragonitic shells cannot be discarded as an explanation for the low levels of diversity.

- **Fossil Association H: *Myoconcha transatlantica***

This association is composed of two samples that total 421 specimens. It exhibits very high diversity and evenness values (S=23, H’=2.22, E=71.40%). The trophic nucleus consists of nine species and the whole association of 32. Both samples come from the starvation hemisequences of two contiguous sixth order sequences a few meters above the major sequence boundary SBAM-3. No ammonites were collected from these beds, which are situates above the last record of *Paraspiticeras groeberi*. The age is most probably Early Barremian.

The facies of these shell beds are sandy bioclastic allochemic limestones (MB2 facies). Autigenic glauconite is common in sediments of both samples, while ooids with nuclei of sand and glauconite grains nuclei characterize the sediments of sample M90, deposited closer to the SBAM-4 and hence in a higher energy setting. Beds have erosional bases and gradual tops. MB2 facies is interpreted as condensed deposits generated under low input of terrigenous sediments, above or immediately below fair-weather wave-base, on inner to middle ramp environments.

Bivalves represent almost 96% of the association. The remaining specimens are distributed among serpulids, bryozoans, scleractinian corals, crinoids, and echinoids. The most common life habit is the semi-infaunal one (48.57%), represented by byssate (33.50%) and free living species (15.07%). Epifaunal species represent 31.70%; they are either cemented (21.30%) or byssate (10.39%). Shallow infaunal species account for 12%, deep infaunal ones for 7.77%. More than 98% of the specimens of association H are suspension-feeders. The rest consists of the deposit-feeding irregular echinoid *Holectypus planatus* and of microcarnivorous scleractinian corals.

The sediment is completely bioturbated. Burrows are rarely preserved. *Spongeliomorpha suevica* occurs just below the sequence boundary of M90. The Y-shaped burrows are filled with bioclastic material. Bioerosion is high. Micritization is usually a very important feature, although the main destructive process is breakage. Shells are normally bored with ichnotaxa of the Entobia Ichnosubfacies (e.g., *Gastrochaenolites*, *Trypanites*, *Entobia* and some cirripedian borings). In many instances, the outer layers of the shells are lost because of abrasion and the internal boxwork of *Entobia* is seen. Skeletal remains at the base of beds with association H consist of large and sturdy shells that are usually disarticulated and broken. There are abundant shell fragments of thinner-shelled species, but also deep burrowing bivalves such as *Panopea dupiniana* and *Pholadomya gigantea* in life position, as well as some delicate complete shells. Encrustation by gryphaeid oysters and serpulids may be locally important, particularly on disarticulated shells of *S. vacaensis*. *M. transatlantica* occurs both, disarticulated and heavily bored, and articulated and little bioeroded.

Discussion

The *M. transatlantica* association occurs in beds, in which mixing of older elements from underlying regressive beds (transgressive lag), as well as a bias against fragile species due to the effect of high energy on the community during the transgressive phase is expected. Transgressive lags are the result of shoreface erosion (ravinement process) during a transgression, after the regression that operated immediately before left the sea floor subaerially exposed or at very shallow depths. A characteristic feature of lags is the dominance of large and thick shells, which become exhumed during erosion and survive despite the high water energy and the intense bioerosion. The fate of thinner shells differs as they are easily broken and dissolved (Fürsich and Pandey 2003). The outcome of this process is a fossil assemblage enriched in thick-shelled species and taxonomically biased. Onlap condensed deposits represent early transgressive deposition not related to erosion of previous deposits. While in lags old shells pre-dating the transgressive erosion dominate, in condensed onlap deposits new shells prevail, accumulating after the transgressive erosion. Onlap condensed deposits are exposed to constant wave agitation and low net sedimentation and thus may develop taphonomic features similar to those of transgressive lags. However, a clear distinction of these two elements is not expected. Shells pre-dating the transgressive erosion, when present, probably became mixed with newer ones.

Lag material in association H seems to be restricted to few species, especially some shells of *S. vacaensis* that occur disarticulated and heavily encrusted and bored at the base of the beds. Specimens of the same species occur articulated and usually in life position in mudrocks and sandy siltstones of dilution hemi-sequences but never in the same bed. Instead, the most abundant species in the association, *Myoconcha transatlantica*, is large and very thick-shelled with a semi-infaunal byssate life habit that occurs articulated in early as well as middle starvation beds. Shelly, stable substrates, rather than sandy substrates subject to high rates of sedimentation were the proper habitat of this species. Large size probably allowed specimens of *M. transatlantica* to cope with the high-energy conditions. The majority of the remaining species are also well fitted to live in sediment-starved environments. All the evidence indicates that association H represents a moderately time-averaged early transgressive (onlap) community, with a moderate degree of environmental condensation. A small proportion of the association probably comes from older, regressive sediments. Late transgressive (middle starvation) communities probably contributed also some shells. This period was probably not registered in the record because of the very low input of sediments. No clear distinction was detected between early and middle starvation deposits in the beds containing association H. Starvation and high levels of water agitation provided a firm, shell-rich and mud-poor bottom, suitable for epifaunal, semi-infaunal and deep infaunal suspension-feeders that form the bulk of the association. Environmental condensation mixed communities ranging from the shoreface to the upper offshore. The main taphonomic bias that influenced this association was the physical destruction of fragile shells, which led to an enrichment of large and thick-shelled species.

- **Fossil Association I: *Ceratostreon - Eriphyla – Ptychomya***

The *Eriphyla – Ptychomya – Ceratostreon* association is composed of eight samples which total 2,555 specimens spread across 31 species, six of them in the trophic nucleus. Diversity is moderate (S=13, H'=1.91) and evenness is high (E=74.75%). All samples composing the association are restricted to the *Andinus/Perditus* Subzone of the *C. diamantensis* Zone of the latest Hauterivian age (see section 2 in chapter 6 and Text-Fig. 6). The association occurs in muddy or sandy-muddy allochemic bioclastic limestones, inferred to have been deposited in middle ramp settings, below fair-weather wave-base. Ooids are common and may equal bioclasts in abundance. Autigenic glauconite is common to abundant. Iron replacing shells is a common feature of these beds. Coquinas are densely-packed. Encrustation by serpulids, oysters and agglutinating foraminifers is high. Shells commonly exhibits microborings and micritization. Macroborings such as *Gastrochaenolites*, *Entobia* and *Trypanites* (Entobia Ichnosubfacies) are often abundant. In samples 67, 68 and 112P foraminifers buildups are common to abundant. Shell beds of benthic association I occur in starvation hemisequences. The majority of samples comes from mid to late starvation shell beds (i.e. maximum flooding and early regression).

The association is dominated by bivalves (83.84%), followed by serpulids (11.57%), foraminifers (3.06%) and other taxa (1.53%). Life habits are more or less equally distributed among epifaunal (40.73%), semi-infaunal (29.54%) and shallow infaunal (28.98%) species. Suspension-feeding constitutes the main feeding strategy (96.58%), followed by the inferred deposit-feeder *Placopsilina* sp. (3%). The chemosymbiotic *Mesomiltha* sp. A is rare (0.36%). This species is present only in an atypical sample of this association, the level of which is very close to the major MFZ-3 (sample M72, BAL section, 351 m). Articulation degrees are intermediate to high. Life position is rare to common depending on the sample and life habit (shallow infaunal and semi-infaunal burrowers).

Discussion

The *Eriphyla – Ptychomya – Ceratostreon* association represents the relict of a benthic community that characterizes middle to late starvation deposits. In the middle positions epifaunal and semi-infaunal species are more abundant than in late starvation portions, where shallow infaunal bivalves dominate. Unfortunately the stratigraphic condensation typical of these starved deposits makes it difficult to differentiate between the three parts of starvation hemisequences, and most samples are composed of a mix of faunal elements.

The environment is characterized by a low input of terrigenous sediments, normal values of dissolved oxygen, moderate depth, below but usually close to the fair-weather wave-base, and of moderate water agitation. The substrate was firm but not hard, evidenced by the abundance of shallow infaunal or semi-infaunal species such as *Eriphyla argentina* and *Ptychomya* sp. A. Byssate semi-infaunal taxa made use of the abundant shells and shell fragments to settle. Storm waves periodically swept the bottom, eroding and concentrating valves, and increasing the number of disarticulated and fragmented shells. In samples that include faunal elements of higher energy, early starvation regimes, the degree of disarticulation is higher and large macroborings are more abundant. Storm-induced currents introduced inner ramp ooids and shell hash. Samples composed totally or partially by late starvation shells usually have higher proportions of burrowing species such as *Ptychomya* sp. A. These late starvation sediments were deposited well below fair-weather wave-base. Terrigenous mud input was still low. The moderate to high diversity levels indicate a general lack of stress factors such as salinity fluctuations, high input of sediment, high water energy, and reduced oxygen. Besides, life habits are quite diverse and tiering is well developed. Beds of similar age, in which early starvation sediments were deposited in high-energy inner ramp settings, clustered with other associations or assemblages (e.g. association L., assemblage F). Environmental condensation and time-averaging were minor.

- **Fossil Association J: *Pterotrigonia coihuicoensis***

This association is composed of three samples collected from the same bed at different places in section BAL. The three samples total 522 specimens in 27 species, five of which belong to the trophic nucleus. Diversity and evenness are moderate (S=15, H'=1.8, E=67.7%). The bed was sampled in section BAL at 361 m above base. It is a complex starvation hemisequence placed ten meters above the major MFZ-3. MFZ-3 is considered as the probable expression of the Global Faraoni Anoxic Event. The bed contains the first occurrence of the ammonite *Paraspiticeras groeberi* and therefore belongs to the biozone of the same name of earliest Barremian age.

The whole bed is more than 50 cm thick. There is a basal starvation shell bed characterized by a relatively high degree of disarticulation. The mid starvation shell bed has a higher proportion of epifaunal and semi-infaunal species. The facies of the bed is the micritic and muddy rudstones, deposited in the middle ramp, below the fair weather wave base.

Association J is mainly composed of bivalves that represent almost 95% of the individuals followed by serpulids (4.15%), echinoids (spines), crinoids (ossicles), bryozoans, and gastropods. Shallow infaunal bivalves dominate the association (55.86%), whereas epifaunal elements account for only 29.17%.

Semi-infaunal species follow with 13.45%. There is a single deep-infaunal species *Panopea neocomiensis* with 1.52%. More than 99% of the specimens of this association are suspension-feeders.

Discussion

Association J is set apart from other associations beacause of its high percentage of *Pterotrigonia coihuicoensis*. It was deposited on the middle ramp, during the early to middle starvation period of a sixth order sequence. Terrigenous input was very low. Fine-grained sedimentation occurred in the form of micrite.

The *Pterotrigonia coihuicoensis* association represents the first undoubtful Barremian middle-ramp benthic community relict surveyed in this study. Some species appear in this association for the first time probably due to the faunal replacement after the major MFZ-3. This is perhaps the reason why diversity is intermediate even when the deposits holding this association were sedimented in relatively high-energy settings, under very low burial rate.

• Fossil Association K: *Ceratostreon – Eriphyla* with aragonite dissolution

The two samples that were grouped to compose this association come from the same bed, which is characterized by patchy lithification. One of the samples (M74P) was counted in a place where the bed was little lithified and aragonitic shells were represented by ill-defined, not identifiable moulds, suggesting a possible dissolution bias. The other count (M75) was made in a place where the bed was fully lithified. The samples account for 477 specimens in 17 species, four of which constitute the trophic nucleus. Diversity is moderate in terms of species richness (S=13) and Shannon's' index (H'=1.34), while evenness is low (E=53.55%) due to the high dominance of *Ceratostreon* shells. Sample M74P includes several small oyster patch-reefs.

Association K was sampled from a bed that constitutes a starvation hemisequence in itself, with little vertical change. The facies is a bioclast-dominated micritic rudstone (LRm) deposited on the middle to outer ramp under highly reduced terrigenous input. The bed occurs in a part of the section where no ammonites were found. It is most probably of earliest Barremian age because of its position above the inferred latest Hauterivian expression of the Global Faraoni Anoxic Event and its proximity to the first appearance of *P. groeberi*.

The association is chiefly composed of bivalves (96%) and serpulids (3.62%), with minor contribution of echinoids and gastropods. Epifaunal species (78.54%) dominate over shallow infaunal (15.63%), semi-infaunal (5.29%) and deep infaunal ones (0.53%). Among epifaunal components, cemented species dominate over byssate taxa. Suspension-feeders constitute more than 99% of the fauna. Disarticulation is generally high (slightly less than 96%) as well as breakage. Borings are widespread, large ones such as *Gastrochaenolites* on the few large shells available (e.g. *M. transatlantica*) and *Entobia* on pectinids and shallow infaunal species. Encrustation by small serpulids and *Ceratostreon* sp. is generally high and reaches a peak towards the top of the bed, where high-density buildups are common.

Discussion

One of the outstanding features of association K is its development under much reduced terrigenous input, evidenced by the calcareous nature of the rock. The communities that contributed to this association suffered reworking and concentration by storm waves, supply of shell hash from shallower settings by means of storm-induced currents, and by the process of taphonomic feedback. The bottom was probably firstly colonized by shallow infaunal bivalves such as *E. argentina, P. coihuicoensis* and *Ptychomya* sp. A, but these elements were replaced by epifaunal pectinids, *M. transatlantica*, cementing oysters and serpulids. In a last stage the gryphaeid oyster *Ceratostreon* sp. developed small buildups. Deep infaunal bivalves had little chances of settling in a very dense shelly substrate.

Patchy lithification was possibly one cause for the moderate to low diversity of this bed. Prefferential dissolution of aragonitic shells in the poorly lithified part of the bed may have enhanced the relative importance of calcitic shells. The “aragonite-rich” sample (M75) has a higher amount of aragonitic shells than the other sample. These differences were found statistically significant (2x2 contingency tables with Yates correction, M75-M74P, X^2= 29.74, p= 0.000). The difference is still significant if small *Ceratostreon* patch reefs are excluded (2x2 contingency tables with Yates correction, M75-M74, X^2= 7.51, p= 0.006). The “fully aragonitic” (M75) count has higher scores of Shannon’s diversity and evenness than the “calcitic enriched” bed (see Table 8). Species richness is higher in M74P, although this can be due to larger sample size.

Table 8. Comparison of diversity between poorly cemented parts of the bed with a dominance of calcitic taxa and well cemented parts with higher percentage of aragonitic taxa. (association K). S: species richness; N sample size; H’: Shannon-Wienner diversity index; E: evenness index.

Sample	**S**	**N**	**H'(loge)**	**E**
M74P (poorly cemented)	14	283	1,00	38,00%
M75 (well cemented)	12	194	1,67	67,15%

Benthic association K characterizes offshore, middle ramp bottoms subject to high terrigenous starvation and moderate water energy. Infaunal species are less abundant than semi-infaunal and epifaunal ones, which ar better adapted to live on shelly substrates. Deposit-feeders were excluded because of the lack of organic matter on the sea floor, due to the very low terrigenous input or to the relatively high water energy. Environmental condensation due to depth changes driven by eustatic sea-level fluctuations does not seem to have been important. Taphonomic feedback probably increased diversity. Patchy dissolution altered counts in favor of originally calcitic shells. The low burial rate reduced the preservation potential of thin shells, imposing another likely bias. This bed differs from others because of its high proportion of hard substrate taxa. Besides, it is situated just above the major MFZ-3, interpreted as expression of the Faraoni Event. This event is related to a major transgression that probably brought larvae of new species from the open ocean, which contributed to the composition of association K.

- **Fossil Association L: *Ceratostreon – Pterotrigonia – Eriphyla***

Fossil association L is the result of the grouping of thirteen samples with 3,302 specimens, spread across 44 species, seven of them in the trophic nucleus. Species richness is high (S=17) while Shannon's diversity and evenness are moderate (H'= 1.88, E=67.39%). All samples of association L come from section BAL, between 307 and 391 m above from the base. These sediments contain ammonites from two contiguous biozones, top of *C. diamantensis* Zone (*C. andinus*/*C. perditus* subzone) and base of the *P. groeberi* Zone, and accumulated all along the third major depositional sequence (DSAM-3), except for the beds close to MFZ-3.

The main facies is sandy to muddy, bioclastic, allochemic limestone, occasionally the association occurs in sandy, bioclastic, allochemic limestone, or muddy to sandy, micritic rudstones. Ooids with nuclei of sand or glauconite grains are common to abundant, although subordinated to bioclasts. Autigenic glauconite is always abundant. Shell beds of association L normally occur in middle to late starvation sediments (MFZ to early RST) of sixth order sequences (Pl. 3, Fig. 8). These short cycles usually exhibit sharp or erosional base and the early starvation sediments represent shoreface facies. Some samples were taken from strata in which distinction among the different parts of the starvation hemisequence could not be recognised.

The association is mainly composed of bivalves (94.72%). Serpulids (4.23%) occur in more than half of the samples. Gastropods (0.36%), bryozoans (0.35%), and foraminifers (0.25%) are rare. Echinoderms are very rare. Life habits are more or less evenly distributed among shallow-infaunal (41.83%), epifaunal (35.98%), semi-infaunal (12.14%), and deep-infaunal species (9.47%). There are four different deep-infaunal species. Suspension-feeders dominate the association with 97.75%. The remaining trophic groups are rare deposit/detritus-feeders and chemosymbionts.

Taphonomic signatures vary depending on the position in the starvation hemisequence at which the sample was taken and on the inferred depth. Articulation is moderate to low. Micritization and macroborings are average to very abundant. Encrustation is always abundant. Small oysters and serpulids constructed small buildups (Pl. 3, Fig. 7). At least two clear examples of transgressive lags materials were detected in samples that belong to this association. Sample M87 (starvation hemisequence, section BAL, at 391 m) contains concretions composed of fine-grained, ripple-bedded sandstones that are bored by *Trypanites* and encrusted by oysters. Similar facies are observed on top of the underlying regressive sediments. In samples M65 and M66 (both from the base of a starvation hemisequence, section BAL at 334 m), *Ceratostreon* sp. buildups developed on disarticulated *Steinmanella vacaensis* shells. These shells are considered to belong to specimens that lived during the regression of the preceding sixth order sequence. The shells and the sediments of the base of the sequence would then constitute a lag.

Discussion

Communities that constitute this association grew on a firm substrate, in which shells were an important fraction of the sediment. Infaunal species typical of starved beds such as *Pterotrigonia coihuicoensis*, *Eriphyla argentina* and *Ptychomya* sp. A were well adapted to burrow into these sediments. Four different species of deep infaunal bivalves document that the sediments were firm but still loose enough for these bivalves to settle. Typically several tiers of suspension-feeders are represented in this association. Conversely, deposit/detritus-feeders are almost absent, probably due to the low input of organic mater and/or it was kept in suspension. The association characterizes lower inner to middle ramp settings. Terrigenous input was low due to the transgressive setting. A setting like this is inferred to have occurred in middle to early late-starvation hemicycles, as well in early starvation sediments that developed below fair-weather wave-base. Fair-weather and storm waves reworked, concentrated and disarticulated shells. The availability of hard substrates on the seafloor (large shells and carbonate concretions) was utilized by epifaunal species, the shells of which in turn increased the abundance of hard material on the bottom. Taphonomic feedback acted in combination with the progressive reduction in the rate of terrigenous input towards the horizon of maximum starvation.

- **Fossil Association M: *Eriphyla – Ceratostreon – Ptychomya***

This association is composed of seven samples with 2,438 specimens and 37 species, nine of them in the trophic nucleus. Diversity and evenness reach high values (S=18, H'=2.19, E=77.07%). Samples clustering in this association come from the *C. schlagintweiti* biozone and *C. diamantensis / C. bederi* subzone of the *C. diamantensis* biozone of middle Late Hauterivian age. These sediments belong to the major TST-2.

Typically, facies containing the association M are mixed muddy and/or sandy, bioclast-dominated rocks and sandy limestones, and occur in mid-cycle to early regression position of starvation/dilution sequences (middle to late starvation deposits). These assemblages formed in middle to outer ramp settings, during maximum starvation and beginning of the following regression. They are underlain by higher energy inner to middle ramp sediments. Samples M48 and M51 were retrieved from starved, internally homogeneous beds inferred to have been deposited completely in the middle to outer ramp.

The *Eriphyla – Ceratostreon – Ptychomya* association is mainly composed of bivalves (90.36%) and serpulids (8.35%), with minor contributions of foraminifers (0.81%), gastropods (0.31%), and scaphopods (0.07%). With the exception of infaunal mobile species, all types of life habits are represented in this association. Shallow-infaunal species (41.18%) dominate over epifaunal ones (28.47%), followed by semi-infaunal (20.56%) and deep-infaunal bivalves (9.78%). 98.26% of association M are suspension-feeders. The remaining faunal elements are either deposit-feeders (0.88%) or herbivores/deposit-feeders (0.26%).

Skeletal concentrations of association M are densely packed, and bioclast- or matrix-supported. Encrustation reaches high levels particularly at the maximum starvation horizon (or in mid-starvation sediments), in which *Ceratostreon* and *Parsimonia* buildups are common. Borings are also common and the shells are usually micritized. Fragmentation is moderate. Bivalve shells are more often articulated than not, and less than half of articulated individuals occur in life position. Deep-infaunal bivalves are commonly found in life position. Large semi-infaunal bivalves such as *Gervillella aviculoides* or *Cucullaea gabrielis* remain usually in growth position. Articulated specimens of *Eriphyla* and *Ptychomya* are commonly found in high densities, little bored and encrusted but not in life position.

Discussion

The *Eriphyla – Ceratostreon – Ptychomya* association characterizes maximum flooding levels of precession cycles (i.e. middle starvation deposits) that were deposited during the development of a major TST (TST-2). Communities that contributed to this association lived below the fair-weather wave-base (i.e. middle to outer ramp), under low terrigenous input, in a firm substrate rich in shells and shell fragments. Low energy, little risk of sudden burial, normal oxygen levels and stability contributed to the development of highly diverse communities. The substrate, although with high density of hard parts, also supported a diverse association of semi- and shallow-infaunal bivalves, and three species of deep-infaunal bivalves. Diversity values were probably pushed up by environmental condensation as faunas of the maximum flooding zone and of the early RST are mixed in the same bed: communities developed under maximum starvation mixed with those that developed when the terrigenous mud of the following regression restarted. The mixing was probably caused by storm waves.

The availability of patchy hard substrates allowed the development of numerous epi- and endobionts. This phenomenon is referred to as taphonomic feedback. The substrate was, however, loose enough for infaunal elements such as *Eriphyla* and semi-infaunal burrowers such as *Ptychomya* to reach high densities.

Environmental condensation played only a minor role in association M. Communities that lived during the maximum flooding became mixed with the less starved ones that developed at the beginning of the following regression. Time averaging was thus moderate to minor.

• Fossil Association N: Veneridae sp. 3 – *Panopea dupiniana*

Two samples, M49P and M50, compose this association that accounts for 723 specimens spread across 30 species, of which nine belong to the trophic nucleus. Species richness and Shannon's diversity are high (S=22, H’=2), while evenness exhibits intermediate values (E=65.39%). Both samples are placed in the major MFZ-2, at the top of the middle Late Hauterivian *C. schlagintweiti* biozone. Facies are middle to outer ramp mixtures of sand, mud and micrite with evidence of sediment starvation. Strata are simple, homogeneous and sharp-based, and constitute a complete starvation hemisequence. Sample M49P was deposited in a shallower setting than sample M50, probably in the middle ramp, within the reach of storm waves. Sample M50, instead, shows little evidence of physical reworking, and lacks indications of other stress factors associated with increase water depth such as reduced oxygenation.

Bivalves dominate the association (73.94%). Serpulids follow with 25.97%, and are particularly abundant in M49P, where they built small patches on large ammonites, nautiloids and bivalves. Shallow-infaunal bivalves (51.61%) dominate over epifaunal species (31.05%), deep-infaunal (11.06%) and semi-infaunal (5.45%) taxa. More than 98% of the specimens in this association are suspension-feeders.

Epifauna is rare and occurs mainly on large *Cucullaea gabrielis* and some nautiloids. Percentages of articulated specimens and those preserved in life position are high, mainly among deep-infaunal elements, such as *P. dupiniana*. Fragmentation is moderate. Altogether the evidence indicates low levels of reworking because of more depth. Ammonites occur in high densities. Macroborings are present mainly on *C. gabrielis*. Micritization is widespread.

Discussion.

The Veneridae sp. 3 – *Panopea dupiniana* association represents the fossilized hard parts of Late Hauterivian communities living in stable, firm substrates, under low energy conditions and reduced terrigenous input. Large shells of ammonites, nautiloids, and bivalves such as *C. gabrielis* served as substrate for serpulids and oysters, which constructed small buildups.

Time averaging is moderate based on the time involved in the deposition of the fauna as it comprises the whole starvation hemisequence. Environmental condensation is inferred to be low in this case: the whole starvation hemicycle seems to have been deposited under similar environmental conditions, i.e. below fair-weather wave-base in stable, well aerated, firm substrates. Evidence of this is the rarity of deposit-feeders, the high levels of diversity, and the representation of different tiers of bivalves.

- **Fossil Association O: *Cucullaea gabrielis* – *Gervillella aviculoides* – *Aetostreon* sp.**

Association O is the result of the clustering of five samples with 894 specimens distributed across 20 species, nine of them in the trophic nucleus. Diversity is moderate (S=10, H'=1.70), while evenness is high (E=73.67%). All samples come from DSAM-2 of Late Hauterivian age. The counts were made in early starvation deposits characterized by micritic or bioclastic fine-grained sandstones (facies MD1 and MD2), all of them deposited in the inner ramp, under constant wave agitation. In micritic sandstones, the micritization process seems to have erased part of the shells. Iron impregnation and glauconite grains are abundant in these beds.

Association O is composed of bivalves that strongly dominate (97.06%) and secondarily serpulids (2.94%). Life habits are more or less evenly distributed amongst epifauna (32.41%), shallow infauna (31.65%), semi-infaunal (24.01%) and deep infauna (11.93%). All specimens of this association are suspension-feeders.

Large, thick-shelled species dominate the association: *Cucullaea gabrielis, Gervillella aviculoides*, and *Aetostreon* sp. Specimens in life position are rare and restricted to deep infaunal *Panopea dupiniana* and few specimens of *Cucullaea gabrielis* and *Gervillella aviculoides*. Instead, degrees of disarticulation and fragmentation are high in absolute terms and also in relation to shell beds deposited in less shallow settings. In beds with association O that represent the base of complex starvation hemisequences faunal elements are significantly less well preserved in terms of bioerosion, disarticulation and fragmentation, when compared with those deposited in overlying middle and late starvation strata. Encrustation is not as relevant as in shell beds sampled from deeper facies.

Discussion

Samples of association O represent the relics of communities that lived in bottoms that suffered permanent water agitation. In addition, elements of communities that colonized these shoreface sediments later on during the transgression, became mixed with them due to sediment starvation. The high energy caused the destruction of most of the small and/or thin-shelled fauna, which is more abundant in other associations. Dissolution probably biased the samples in favor of thick-shelled species. This inference correlates with the deposition of these shell beds in segments of the sedimentary column characterized by a high rate of terrigenous input, due to the development of sequences of higher hierarchy.

In complex starvation hemisequences beds containing association O occur at the base, underlain by an erosional surface. The first few decimeters of these starvation hemisequences were deposited in the inner ramp. In other cases there are no middle or upper-starvation-like sediments. In these cases, however, middle ramp, maximum flooding faunal elements such as *Gervillella aviculoides* may have colonized the seafloor and became mixed with the inner ramp community.

The complete absence of deposit-feeding species correlates with the high energy environment. Abundant large borings of the Entobia ichnosubfacies also support a shallow-water environment.

Communities that compose benthic association O lived in the inner to upper middle ramp during starved periods but under general high terrigenous input. The thanatocoenoses lost most fragile shells by means of physical and chemical destruction. Besides, it cannot be excluded that these large species fitted the habitat better, and this enrichment may be at least partially primary. There is no evidence of allochthonous lag components: all species that are heavily worn are also represented by relatively well preserved specimens.

All shell beds that compose association O represent complete or parts of starvation hemisequences, which involve at least a few thousand of years. This implies some degree of time averaging. Environmental condensation was minor, associated with the possible colonization of middle ramp communities on the inner ramp sea floor.

- **Fossil Association P: Veneridae sp. 2 – *Panopea necomiensis***

This association is composed of eight samples with 1,236 specimens. It has 34 species, eight of them form the trophic nucleus. Diversity and evenness are moderate (S=10, H'=1.45, E=68.35%). Samples of the association occur in or close to major and middle MFZs (MFZ-2 in both sections, MFZ-3 in BAL), in the latest Hauterivian sediments of the sections. Facies are fine-grained mixed limestone-siliciclastics or fine-grained limestones, deposited in the middle to outer ramp. Strata are homogeneous, usually sharp based and, in most cases, intercalated into a shallowing-upward dilution hemisequence of a higher hierarchy cyclicity, inferred as the expression of the obliquity cycles of the Milankovitch band.

The Veneridae sp. 2 – *Panopea neocomiensis* association is composed of bivalves (89.90%), scaphopods (8.38%), gastropods (1.42%), foraminifers (0.23%) and rare bryozoans and serpulids. The small bivalve Veneridae sp. 2 dominates the association (35.48%) followed by the medium-sized deep-infaunal *P. neocomiensis* (12.90%). The association contains some species typical of associations A and B, indicating a relatively deep setting. Shallow infaunal species represent more than a half of the specimens (56.9%). Deep-infaunal (20.05%), epifaunal (12.45%) and semi-infaunal (10.60%) species also contribute. 65% of the species are well adapted to unconsolidated substrates. Suspension-feeders dominate association P (89.12%). However, deposit-feeders (8.61%) and chemosymbiotic lucinids (2.27%) contribute appreciably.

Shell beds of association P are often thin and densely, less often loosely packed. Specimens in life position are rare. The degree of articulation is moderate. Encrustation and borings are moderate to very rare, depending on the bed surveyed. Microborings are rare in a few beds, common in the rest.

Discussion

Association P constitutes the mineralized remains of benthic communities that lived at the end of the Hauterivian period, on relatively sediment-starved bottoms. Input of terrigenous mud was low. In some cases storm waves and/or bottom currents concentrated the shells that were available for the boring and encrusting fauna that colonized the sea floor. The occurrence of abundant deposit-feeders indicates the availability of organic matter on the bottom as well as a low energy regime. The presence of chemosymbiotic lucinids also points to oxygen deficiency, at least some cm below the sediment-water interface.

The Veneridae sp. 2 – *Panopea necomiensis* association is characterized by a moderate degree of time-averaging. Strata containing skeletal concentrations of the association represent the whole starvation hemisequence, i.e. a few thousand years. As the habitat did not change much during the development of the starvation hemicycle the degree of environmental condensation is not high. The moderate level of diversity may be due to some reduction of the oxygen level close below the sediment-water interface, which precluded the colonization by large, deep-infaunal species such as *Panopea dupiniana* or *Pholadomya gigantea*.

Discussion

The fossil concentrations studied here are the result of long-term processes that operated during hundreds or thousands of years. However, the taxonomic composition of the shell beds differ from one another indicating that even when all fossil assemblages are time-averaged they average a limited number of communities and roughly characterize the different environments in which these communities lived during the Early Cretaceous. The benthic associations and the assemblage defined in this work reflect the interaction of different factors, the most important being age, position in major, medium and sixth order (starvation/dilution) sequences and, relation to sequence stratigraphic position, depth, oxygen availability, rate of terrigenous input, water agitation, and substrate conditions, in particular density of hard parts on the seafloor.

The first major division of the dendrogram (Text-Fig. 15) separates associations A and B. These associations are restricted to the *S. riccardii* biozone. Besides, they yield signs of oxygen deficiency, connected to their position in the MFZ and early HST of the first major sedimentary sequence. Time-averaging was moderate and environmental condensation negligible.

In the second major division, association C forms an isolated cluster. It is represented by a particular grouping of species preserved in dilution hemisequences, in the context of the unique sediments identified as a major lowstand systems tract (LST-2). Low degree of time-averaging, hardly any environmental condensation, and likely selective dissolution processes lowered the diversity of this association.

The next branching of the dendrogram, benthic association D is the only that is placed well above the last occurrence of *P. groeberi*, more than 80 m above the previous fossiliferous bed, with several medium to major sedimentary sequences in between. Association D is inferred to be Barremian or younger. In this way, the samples composing the association are different at least partly as a consequence of its younger age. At least two species of this association are probably derived from species present in older sediments (*Ptychomya* sp. B from *Ptychomya* sp. A aff. *P. koeneni*; and *Pterotrigonia* sp. A from *P. coihuicoensis*). Besides, benthic association D is the only association occurring in what is considered a mixed carbonate-siliciclastic ramp (for more information see Discussion of Chapter 5).

The following association (E) is also isolated. It comes mainly from sediments of the *S. riccardii* biozone and overlies beds containing association B without overlap. It was deposited during the first major HST (HST-1) under generally elevated levels of terrigenous input. Characteristically, association D is heterogeneous in terms of faunal composition. During starvation hemisequences sedimented in this period, the seafloor was characterized by only few small hard parts and by a low energy regime. Encrustation and boring, and accumulation of shells on the bottom were rare, and taphonomic feedback did not play a major role. During dilution hemisequences, carbonate skeletal elements were usually dissolved.

The remaining groupings mainly belong to the Schlagintweiti, Diamantensis and Groeberi biozones and occur on a mixed-siliciclastic ramp (in the sense of the discussion in Chapter 5).

Association P was sampled from middle to outer ramp beds. Low water energy, reduced levels of oxygen below the sediment-water interface and availability of organic matter on the sea floor characterize this association. Hard substrates were rare. This association differs from association E in terms of faunal composition, although the environment of deposition looks similar. However, association P is younger, was deposited mixed-siliciclastic ramp (see discussion of Chapter 5 for more information), and under a reduced general input of terrigenous sediment.

Associations M and N constitute a grouping characterized by high levels of diversity. A wide variety of guilds is represented in these typical outer to middle ramp community relicts. Characteristically, samples of these associations come from late starvation deposits, les common from middle starvation deposits developed in middle to outer ramp settings, or in outer ramp homogeneous starvation hemisequences. In all these cases, the beds with associations M and N are placed in major late TSTs, MFZs or early HSTs. The high species diversity is interpreted as the consequence of a combination of factors, among which deposition in calm and fully aerated waters, and a habitat suitable for different modes of life (burrowing, semi-infaunal attachment, encrustating and boring) appear to have been most relevant.

Benthic associations I, J, K and L represent middle ramp communities, studied mainly from middle to late starvation beds. Water energy was not a limiting factor for colonization but strong enough to concentrate shells and produce a high density of hard substrates. A combination of infaunal species apparently well adapted to live in shelly sediments such as *Eriphyla argentina* and *Pterotrigonia coihuicoensis*, epifaunal gryphaeid oysters, pectinids, isognomids and serpulids, and the semi-infaunal *Myoconcha transatlantica* and *Ptychomya* sp. A characterize the communities of this grouping. The high density of hard parts probably limited the development of infauna, while small, fragile shells were removed by the moderate to high water energy.

The outstanding feature of assemblage F and association G is the development of small to large buildups constructed by large serpulids, small gryphaeid oysters or both. Samples of association G were found in the mid-starvation position (mid-cycle beds), while assemblage F was retrieved from a early starvation bed in a shoreface setting. In most cases, these communities developed under enhanced sediment starvation due to the influence of higher hierarchy cycles.

Associations O and H differen in having been deposited in high-energy settings, above the fair-weather wave-base or just below. All beds containing samples of these associations are very close to major sequence boundaries. The samples occur at the base of starvation-dilution hemisequences, in the context of onlap. In some cases, lag material, product of ravinement processes can be detected. Bias against small fragile shells is evident.

Oxygen deficiency

Deep bottoms, with little or no water circulation and with a relatively high input of organic matter are usually characterized by low levels of oxygen. Ecosystems with this type of restriction are usually characterized by species that tolerate oxygen reduction, and a low species richness. A consequence of anoxia close to the sediment-water interface is the exclusion of infaunal species. Oxygen-poor environments are inferred in this study in sediments deposited after exceptional transgressions, which combined with local factors, led to accummulations of organic-rich sediments. The combination of dysoxic-anoxic conditions and sediment starvation (i.e. good preservation of marine organic matter and low siliciclastic dilution) favoured the widespread deposition of organic-rich facies during the transgressive intervals of the Agrio Formation (Legarreta and Uliana 1991; Tyson et al. 2005; Uliana and Legarreta 1993).

In the upper water column the oxygen is taken up through exchange with the atmosphere and, all through the photic zone, its content is increased by photosynthesis. Oxygen is consumed during respiration and oxidation processes. Below the photic zone, oxygen is not replenished by photosynthesis but is consumed by organic respiration and microbial degradation of organic material (Brenchley and Harper 1998). In deep waters, oxygen levels depend on water circulation. High organic production as in upwelling areas can drastically decrease oxygen level.

Important packages of bituminous black-shales occur at two positions at least in the sections studied here. The first one is found in the lower 15 to 20 m of the unit in both sections. It is characterized by well-developed black, dark-bluish and dark-grey marls, micritic clays and micritic silty clays. This organic-rich set of beds has already been recognised in the literature and designated as “Spitidiscus” black shale (Tyson et al. 2005). It was proposed that these sediments were deposited under anoxic to dysoxic conditions (Spalletti et al. 2001b; Tyson et al. 2005). Evidence (i.e. bioturbation, presence of benthic macrofauna) put forth in the present study indicates that the so-called "Spitidiscus" black shale probably did not experience oxygen depletion at any time. Instead, dysoxia and anoxia a few centimetres below the sediment-water interface can be deduced from the organic-rich nature of the sediments, the scarcity of infaunal species and the presence of lucinid bivalves, adapted to live in anoxic sediments.

Ammonites and benthic fauna occur scattered or in loosely packed shell-beds interpreted as the sediment-starved lower portion of orbitally induced precession cycles. The ammonites belong to the genus *Spitidiscus* and correspond to the earliest Late Hauterivian. The preservation of fossils is excellent and there is little or no indication of physical disturbance i.e., the sediments were deposited below storm wave-base (for more information see facies 5.1-3 and 8.2 in Chapter 5). The benthic fauna sampled from these beds belong to the benthic association A. The sediments are always bioturbated although trace fossils are rare (e.g. *Chondrites*). The benthic macrofauna consists of a diverse group of small, chiefly epifaunal and semi-infaunal gastropods and bivalves. Shallow infaunal bivalves are rare. There is one species of deep infaunal lucinid bivalve, *Mesomiltha*? *argentina* whose shells are very small, rarely longer than one cm. This means that even when they are considered as deep infaunal they could not live more than a few cm below the sediment-water interface. Recent lucinid bivalves are known to be well adapted to thrive in low-oxygen environments. These benthic molluscs obtain nutrients from endosymbiotic sulphide-oxidizing bacteria they farm ino the gills: while the body rests in anoxic sediments rich in hydrogen sulphide, the siphon and a mucus-tube connect with the more oxygenated sediment-water interface (Reid and Brand 1986).

The presence and abundance of the lucinid *Mesomiltha*? *argentina* can be related to anoxia at least some centimetres below the sediment-water interface. This assumption is supported by the fact that the lucinid is the only deep burrower species of the benthic fossil association A (i.e. other deep burrowers were precluded from colonising the bottom due to its lack of oxygen).

Apart from feeding on the bacteria they farm, Recent lucinids eat also suspended food. However, in low energy settings suspension-feeders are virtually excluded as they are strongly dependant on turbulence or currents for their food intake (Fürsich 1975). The basinal environments in which *M.*? *argentina* lived was too calm to keep food particles in suspension. One possibility is that even when for most of the time oxic conditions existed above the substrate, oxygen was lacking just below the sediment-water interface, where the lucinid lived. However, predatory drill holes were abundantly found in these bivalves, indicating that at least at times the sediment was suitable for the penetration and drilling activity of infaunal ampullospirid gastropods, not adapted to anoxia as known to date. From all sources of information, it is unlikely that the substrate was anoxic and the gastropods could thrive under such conditions. *M. argentina* specimens collected from the deepest shell beds of the section are smaller and completely lack drill holes. Small size may be related to lower metabolism because of reduced availability of oxygen that may have completely excluded predators.

Paleoecologic evidence does not support a high degree of anoxia. The diversity of association A is intermediate while evenness is high. High evenness indicates the absence of opportunistic species and a more or less stable environment. Diversity is moderate probably due to the difficulties of suspension-feeders to become established, and the likely anoxia below the sediment/water interface that prevented colonization by infaunal elements. These inferences provide information on the mode of life of the small gastropods that dominate association A, mainly *Bathraspira* sp. A and *Bathraspira*? sp. C. Based on the low oxygen levels of the sediment an epifaunal mode of life is inferred for these gastropods. The assumed high amount of deposited organic matter, plus deposition below the photic zone which is supported by the rarity of microborings and the depth, indicate that these species most probably were epifaunal deposit-feeders that fed on organic matter, and not grazers.

Organic buildups

Oyster, oyster/serpulid, serpulid, foraminifer and coral reefs occur at different positions in the two sections studied here and represent different settings. A common factor to all them is the availability of hard substrates, related to a reduced rate of sedimentation. Conversely, availability of nutrients, depth and water agitation varied among the different examples.

- Oysters and/or serpulid buildups at mid-starvation position

Small patches of *Parsimonia antiquata*, *Sarcinella occidentalis* and other serpulid species, and/or the gryphaeid oyster *Ceratostreon* sp. occur widespread at the level of mid-starvation. Typically, *Ceratostreon* and *P. antiquata* buildups are found associated, even in the same patch or in the same bed. These buildups grew on big ammonites or large semi-infaunal bivalves such as *Myoconcha transatlantica*. Accumulations are due to gregarious behaviour. These patch reefs range in size from a few cm to one meter, exceptionally they are larger. Some of the several examples found are mentioned below. In section BAL at 306 m above the base, *Ceratostreon* and serpulid buildups are very common and grow on every large crioceratitid ammonite shell found in the mid-starvation horizon. At 368 and 374 m above base in the BAL section, branches of *Sarcinella occidentalis* buildups are abundant, partly growing vertically and partly horizontally. High densities of ammonites occur in this facies also at the mid-starvation point. In sample M105R (section AML at 281 m), a more than 50 m long oyster/serpulid reef grew on top of the maximum flooding shell bed of the sixth order sequence (Pl. 7, Fig. 1 and association G). These accumulations are part of benthic associations E, G, I, K, L, M and P, and are associated with the Schlagitweiti, Diamantensis and Groeberi biozones, comprising most of the Late Hauterivian and part of the Early Barremian.

Parsimonia antiquata is the pioneer species that first colonized the hard bottom, which was then overgrown by *Ceratostreon*. *P. antiquata* colonized relatively small shell fragments by growing horizontally and changed the growth direction to vertical at their end (Scrutton 1975). Subsequent generations can grow on the first colonizers. In this way, the serpulid increases the availability of hard substrate for other encrusters to settle.

Starvation and hence hard substrate availability, is the rule of almost all the shell beds in this study. However, buildups are well developed only at certain levels, indicating the presence of particular conditions. Small-sized accumulations (a few cm, few oysters or serpulid tubes) are very common in starvation hemisequences, especially in the mid-starvation horizon. This is particularly true of sequences in which high-energy facies characterize the lower early starvation hemisequences (onlap beds). Medium-sized buildups (i.e. a few decimeters, hundreds of specimens) are supported mainly by large crioceratitid ammonites, and secondarily by large bivalves such as *Myoconcha transatlantica* and *Cucullaea gabrielis*. Oysters and serpulids also encrust smaller shells in the same beds although not forming accumulations. Rocks around buildups contain sand, mud and mostly articulated shells, indicating that in the case of medium-sized constructions starvation was not extreme and the substrate was still soft enough for the infauna, which restricted the proliferation of large oysters/serpulid accumulations. In this case the limiting factor was the availability of large pieces of hard substrate.

There is one large oyster/serpulid reef (sample M105R, mentioned above and described in association G) and a few other intermediate cases that reach meter-size dimensions. These epifaunal accumulations clearly overlie mid-starvation hemisequence shell beds, and are not restricted to large shells. Instead, these large accumulations rest on the whole densely packed early transgression shell bed. Diversity and evenness are characteristically low. High density of the shells pre-dating the settling of the reef builders probably prevented colonization by infaunal elements. There is no indication that other factors limited the diversity, such as oxygen depletion or departures from normal marine salinity. *Ceratostreon* and serpulids probably experienced high population growth after exploiting a particularly suitable combination of ecologic factors: high availability of hard substrates and abundant organic particles in suspension. However, these two conditions are rather opposite: high input of particulate food requires relatively much terrigenous input, while high availability of hard substrates in offshore settings implies sediment starvation. A possible explanation is the deposition at the contact of highly starved oligotrophic transgressive sediments rich in hard substrates (below) with the onset of the early part of the following regression that brought high amounts of nutrients from the continent turning the environment more eutrophic. This last phenomenon did not produce large accumulations at every mid-starvation horizon probably due to the lack of large, stable pieces of hard substrates for the encrusting fauna, a high-energy (shoreface) setting inappropriate for the development of small oyster accumulations, or low energy conditions (below storm wave base) so that food particles were not kept in suspension (Text-Fig. 18).

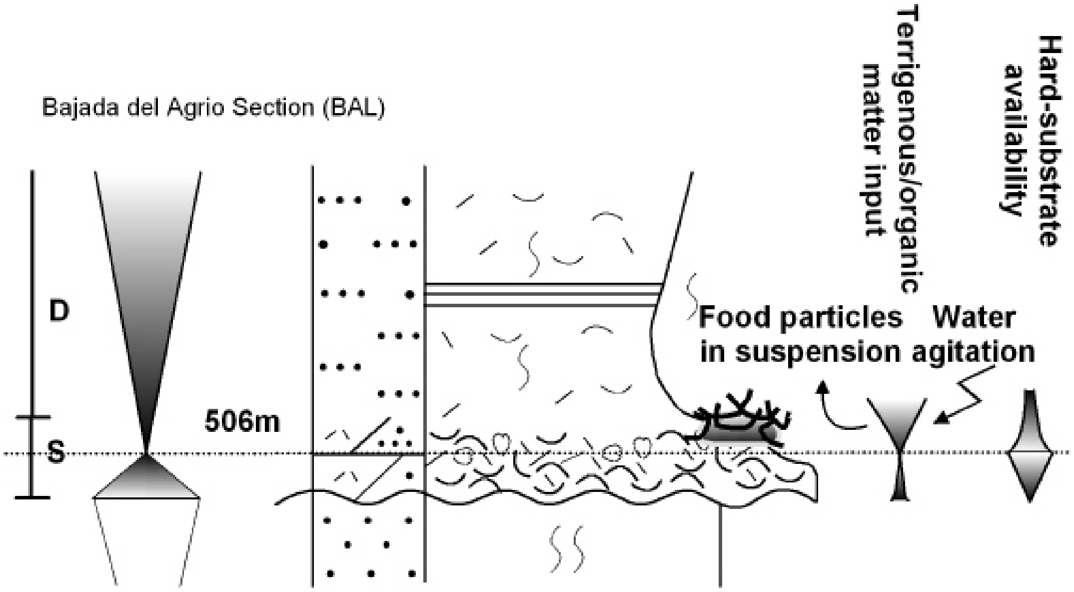

Text-Fig. 18. Model for the development of oyster-serpulid buildups. For key of symbols see Appendix-Fig. 3.

Neocomian oyster and serpulid patch reefs (*sensu lato*) of the Neuquén Basin were classically interpreted as having grown under reduced salinity conditions (Damborenea et al. 1979; Lazo 2004). However, careful observation of the sedimentologic, paleoecologic and stratigraphic evidence associated with equivalent buildups studied here, as well as observations of the buildups of the Valanginian Middle Member of the Mulichinco Formation made by the author, completely preclude that salinity departed from normal marine values during the growth of these biocoenoeses. Thus, it is proposed here that at least some of the Neocomian gryphaeid oysters and/or serpulid buildups of the Neuquén

Basin developed under fully marine conditions. The factors that favoured the population explosions of oysters and serpulids were probably the high availability of stable hard substrates and nutrients at the contact between transgression and regression.

- Oysters and serpulids at early-starvation position.

A different setting in which *Ceratostreon* and *P. antiquata* patch reefs were found is at the base of starvation hemisequences. This is the case in samples M65 and 66 (association L, section BAL at 332 m) and M111P (assemblage F, section AML at 329 m). In these two samples, abundant and large oyster patches up to 1 m in diameter occur at the base of the starvation hemi-sequence. The buildups grew on *Steinmanella vacaensis* shells that were exhumed when the top of the underlying dilution hemi-sequence was eroded. *S. vacaensis* shells are disarticulated and heavily bored (*Gastrochaenolites* and *Trypanites*). In this example, the buildups developed during or immediately after the onlap of the starvation/dilution sequence.

- Agglutinating foraminifers

Agglutinating foraminifers identified as *Placopsilina* sp. commonly encrust shells in most middle to late starvation deposits deposited in middle to outer ramp settings (Pl. 8, Figs. 1-3). High water energy apparently limits the growth of these protozoans, while they are rare in deep facies. The test of *Placopsilina* sp. consists of siliciclastic silt to very fine sand grains cemented by a calcareous matrix. These foraminifers needed sand- and silt-sized grains to build their skeletons. *Placopsilina* sp. built small constructions at some levels, usually in high densities, originating tabular accummulations, always in the late starvation hemisequence. These accumulations are common in muddy and sandy allochemic limestones of low to moderate water energy, allochemic mudrocks and muddy floatstones, and muddy micritic rudstones. Characteristically they develop in the mixed-siliciclastic ramp system of Chapter 5. Conversely, they are absent in the upper 150 m of the formation, where the depositional environment was characterized as a carbonate-siliciclastic ramp (see depositional model section in Chapter 5).

The accumulations of small *Placopsilina* sp. nodules are up to 2 m thick. These accumulations are more common in the AML section, where they give way to particularly thickly developed late stages of starvation hemi-sequences (e.g., section AML at 345 m, 350 m, 366 m, 371 m and 382 m; section BAL at 333 m). In most cases, the nodules are small, semiglobular, and grew on small bioclasts (Pl. 8, fig. 3). In some cases, there is a mix of nodules and bigger lumps consisting of bioclasts fixed by the foraminifers and mud trapped in between. *Placopsilina* sp. was able to encrust available hard substrates during the middle to late starvation hemisequences. Dense encrustations (Pl. 8, fig. 2) are common in upper (late) parts of starvation hemisequences, in facies dominated by terrigenous mud deposition. Important accumulations of *Placopsilina* sp. buildups (nodules) typically occur at late stages of starvation hemisequences, already in the regressive systems tract of the starvation/dilution sequence. Moderate mud input and low energy, and hence high availability of nutrients on the seafloor seem to have played a role in the growth of these constructions.

- Corals.

Small coral patch reefs with a texture ranging from floatstones to micritic rudstones, a diameter of a few metres, and a height of less than 3 m occur at 503 m in the section BAL (Pl. 6, Fig 5; Facies 8.3, chapter 5). In the patches, the different colonial corals are usually broken, heavily bored, and not in growth position. The accompanying fauna consists of sponges, serpulids, bryozoans, and oysters. Tabular and domal growth forms dominate at the base of the buildups and are replaced by bulbous and branching colonies in most of the remaining reef. Bioerosion becomes very prominent towards the top of the patches, characterized by *Gastrochaenolites*, *Entobia*, and *Trypanites*. Occasionally small, delicate branching, bush-shaped colonies, a few decimetres in diameter, occur in growth position in the same bed. In the Agua de la Mula section, larger coral patches were observed at the equivalent stratigraphic position.

The coral patch reefs of the BAL section probably developed at middle ramp position. The dominating micritic matrix and the low density of skeletal remains speak against an inner ramp setting as was proposed by Lazo (2005). Besides, these buildups developed above oolitic and bioclastic grainstones of the lower shoreface (early TST), in a late TST that according to Walther's law suggests a deeper environment. These colonies grew under very low to absent terrigenous input, in medium or major MFZ. This is the only widespread coral reef-building phase within the whole succession. Isolated buildups in ramp depositional systems are known to develop mainly during the transgressive and early highstand systems tracts, when sediment input to the offshore environment is minimal. They are typical features of mid- and outer-ramp environments (Burchette and Wright 1992).

Eutrophic conditions, inferred for the Neuquén Basin during the deposition of the Agua de la Mula Member, seem to be a plausible explanation for the lack of well-developed reef complexes. This pattern fits the global dominance of carbonate ramps observed for the Early Cretaceous. For some periods, nutrient supply seems to have been especially high, as shown by the spread of opportunistic strategies demonstrated by oyster, serpulid and foraminifer buildups. The almost complete lack of typical oligotrophic and autotrophic communities such as coral reefs (the reefs described above being the exception) represents another indication of high nutrient levels that prevailed in the Neuquén Basin during deposition the Agua de la Mula Member. Only at the top of the unit, when the basin was almost completely filled the depositional system turned into a carbonate ramp on which a coral patch-reef complex developed.

Vertical patterns of faunal replacement

Several examples of benthic faunal replacement have been observed, most of them correlated with the sedimentary sequences. There are long-term faunal trends evident along major sedimentary sequences as well as short-term ones, observed in single starvation hemisequences. Long-term trends are modified by subordinated sequences that formed smaller-scale stratigraphic patterns within major ones. In some cases in short-term faunal replacement, relevant faunal changes are detected from base to top of a particular starvation hemisequence. Then, long-term patterns are not faithfully recorded when the different starvation hemisequences are sampled at different positions, a methodological problem that is sometimes unavoidable.

Along the first major sedimentary sequence (DSAM-1), association A, typical of oxygen-reduced bottoms rich in organic matter, is replaced by association B, which grew in shallower settings. Association B in turn is replaced by association E. The succession of associations A-B-E follows a shallowing-upward trend related to HST-1, which lacks unconformities. The typical high-energy association that is found after the SBAM-1 is association O.

In DSAM-2 of section BAL, the succession of associations O-M-N-M-P-M-I mimics first deepening and then shallowing. Inner ramp association O is followed by middle ramp association M, which alternates with outer ramp associations N and P, and returns to the middle ramp associations M and I. DSAM-2 is characterized by the development of three subordinated sequences that shape the general sedimentologic pattern. Therefore, the retrograding-prograding pattern expected for the sequence is somehow blurred by the lower hierarchy sequences. This may explain why the succession of benthic associations does not fully meet the expectations.

DSAM-3 also shows a benthic faunal pattern that follows the deepening-shallowing pattern of the sequence. Early TST is characterized by the presence of association L that gives place to association I. Towards the late stage of the transgression outer to middle ramp associations P and E occur. In the early RST of DSAM-3 there is an alternation of middle and outer ramp associations in the following way: K-P-J-P-L-P-L-L-L-L. The alternation consists of the development of two types of sixth order sequences, shown by the regular change between thicker, higher-energy starvation hemisequences and thinner, lower-energy ones. This pattern was interpreted as the expression of cycles of obliquity (for more information see the high frequency cycles section in Chapter 6). The high-energy starvation hemisequences document a trend from the middle/outer (associations K and J) to inner/middle ramp fauna (association L). The low-energy starvation hemisequences are characterized by association P. There is a subtle faunal change of samples belonging to association P following the shallowing-upward trend of the regressive systems tract of DSAM-3. The change consists of a reduction of species typical of deep facies and benthic associations A and B such as *Dentalium* sp., *Corbulomima bodenbenderi*, *Disparilia elongata*, and *Mesomiltha argentina*.

In the fifth order DSAM-3/1 a subtle pattern of faunal replacement can be observed. The inner to middle ramp association L characterizes early transgressive systems tract and late regressive systems tract shell beds, while around the maximum flooding zone the samples belong to the middle (to outer) ramp association I. The relationship between associations L and I is also supported by an example, in which association L is replaced by association I in a starvation hemisequence (section BAL at 334 m).

Other examples of short-term faunal replacement give extra support to the interpretations developed above. In section BAL at 276 m above the base, a single starvation hemisequence contains inner ramp association O at its base and middle/outer ramp association M above. Close to MFZ-3 (section BAL at 351 m) the middle ramp association I is overlain by the middle to outer ramp association E. In section AML at 239 m, association O is replaced by the middle to outer ramp association I, although there is some stratigraphic complexity that does not allow to directly interpret the faunal replacement. At 330 m inner ramp association F is replaced by middle ramp association I.

9 *Taphonomy*

Calcareous shells constitute relevant components of sediments deposited in most marine siliciclastic environments, where they are preserved in shell beds more commonly than isolated (Kidwell 1986a). Models for the formation of fossil concentrations stress the relationship of rate of sedimentation and hard-part input (Kidwell 1985, 1986; Kidwell and Bosence 1991; Tomasovych et al. 2006) or the variables that drive the processes of concentration (Fürsich and Oschmann 1993). The role of diagenetic dissolution as a barrier to the preservation of fossils and hence as a primary factor for the formation of skeletal accumulations was also considered as a relevant taphonomic factor (Fürsich 1982; Fürsich and Pandey 2003). Shell concentrations have been primarily viewed as products, in which paleoecological information is preserved as distorted relics. This apparent disadvantage is more than compensated by the information on depositional environments and on the depositional history, which make shell concentrations ideal geological tools (Fürsich 1995).

The onset of the sequence stratigraphy led to the development of models that relate the different types of skeletal concentrations to particular positions within sedimentary sequences (Abbott 1997, 1998; Fürsich et al. 1991; Fürsich and Pandey 2003; Kidwell 1991a and b; Kondo et al. 1998). The sequence stratigraphic model predicts changes in sedimentation rates and turbulence levels from eustatic sea-level changes, and can also predict the positions in which synsedimentary and diagenetic dissolution cannot completely erase calcium carbonate shells from the fossil record (Fürsich and Pandey 2003).

It is worth noting that the factors associated with the genesis of skeletal concentrations, i.e. turbulence (destruction rate), rates of sediment and hard-part input and diagenetic dissolution are subordinated to processes that are responsible for the development of sedimentary sequences. Therefore, whenever the sequence stratigraphic model can be applied, regardless of which type of sequence is used (sedimentary, genetic or transgressive-regressive), there is a great potential for interpreting the genesis of the skeletal accumulations, and predicting paleoecological and taphonomic aspects of shell concentrations. Conversely, when sediments other than bioclasts do not yield enough information for the sequence stratigraphic interpretation, shell beds may provide invaluable evidence for construction of the sequence stratigraphic model.

In Text-Fig. 19 A to C a siliciclastic sedimentary sequence model is presented with the expected positions of condensed deposits. Four types of condensed deposits are expected, that coincide with the positions at which time lines join: onlap, backlap, downlap and toplap. The position of the coastline at the beginning of the cycle, as well as the time involved in the deposition of the sequence are relevant factors that modify the final product, as was shown by Kondo et al. (1998).

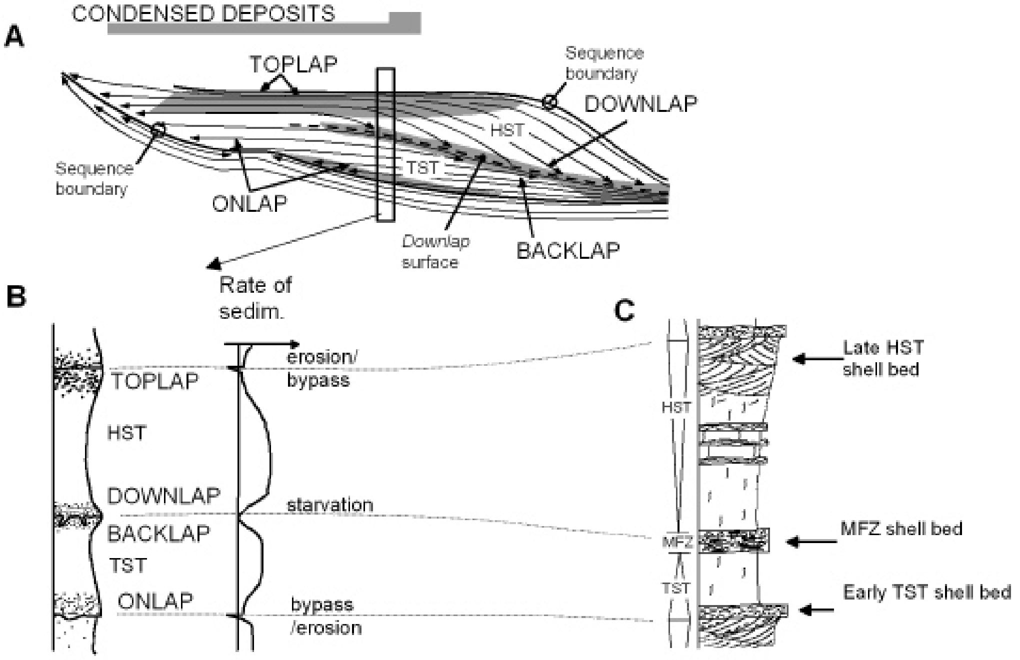

Text-Fig. 19. A. Expected positions of condensed deposits (after Kidwell, 1991a). **B**. Hypothetic section based on Fig. A (after Kidwell, 1991a). **C**. Sedimentary sequence with shell beds in the Jurassic of Kachchh, India (Fürsich and Pandey, 2003).

Sediments in the Agua de la Mula Member are of two kinds: siliciclastic-dominated (dilution hemisequences) and condensed (limestones or mixed siliciclastic-carbonate, i.e. starvation hemisequences). Siliciclastic facies are barren or have only scarce remains of partially dissolved shells. Very exceptionally skeletal concentrations are found on top of dilution hemisequences in siliciclastic facies. In turn, condensed facies usually contain abundant fossil invertebrates. The primary absence of marine shelly fauna in the siliciclastic sediments can be discarded. There are no indications of departures from normal marine conditions with respect to salinity or oxygen content for any part of the section. The presence of autochthonous and parautochthonous skeletal concentrations of starvation hemisequences, full of shells of marine benthic fauna, intercalated within dilution hemisequences, and the generalized bioturbated nature of these barren siliciclastic sediments are both evidence of the primary presence of benthic fauna that was secondarily eliminated by dissolution. Fossil-rich (starvation hemisequences) and fossil-poor (dilution hemisequences) strata are qualitatively different, both as repositories of paleontological information and as settings for biotic interactions (Kidwell 1985).

The majority of the skeletal concentrations in the Agua de La Mula Member of the Agrio Formation are restricted to the base of the starvation/dilution (sixth order) sequences, i.e. they occur in the condensed part of these cycles and are, hence, condensed. These sixth order sequences are linked to the precession cycles of the Milankovich band, involving ca. 20 ka each. The starvation period is only the period during which sea level rises very fast. During fast rising of sea level the coast migrates landward and the deposition of terrigenous sediments shifts progressively farther from the center of the basin. Accommodation space is created faster than it is filled with terrigenous sediments, the basin is starved, and these conditions favour the formation of shell concentrations. The stratigraphic significance of the different parts of a starvation/dilution sequence changes according to the position of the coastline at the beginning of the cycle, as was already discussed in Section 6.4 above, and shown in Text-Fig. 11 (see also Kondo et al. 1998).

Skeletal concentrations in starvation hemisequences are always more or less amalgamated. Thin shell pavements, single tempestites, etc, are completely absent. Shells belong mainly to molluscs, secondarily to serpulid polychaetes, and subordinately to foraminifers, bryozoans, scleractinian corals, echinoderms, and rare crustaceans. Among the molluscs, the bivalves are far the most abundant element. Gastropods are abundant in particular beds. Ammonites and scaphopods are third in rank abundance.

Types of skeletal concentrations

Based on taphonomic and taxonomic features of the fossils, as well as on stratigraphic and sedimentologic observations, the skeletal concentrations of the Agua de la Mula section were classified into five types. These types are interpreted in terms of the available models that relate shell beds to their position in sedimentary sequences (see Text-Fig. 20). Equivalent interpretations of the genesis of the shell bed types based on other models are presented in Text-Fig. 21. These shell bed types represent the variation of what can be observed in the field. However, intermediate cases are common. Skeletal concentrations that could not be evaluated taphonomically or paleoecologycally because of the lack of reasonably preserved shells, were excluded from this classification. This is the case of bio-oo-grainstones or beds in which shells were unrecognisable because of fragmentation and erosion.

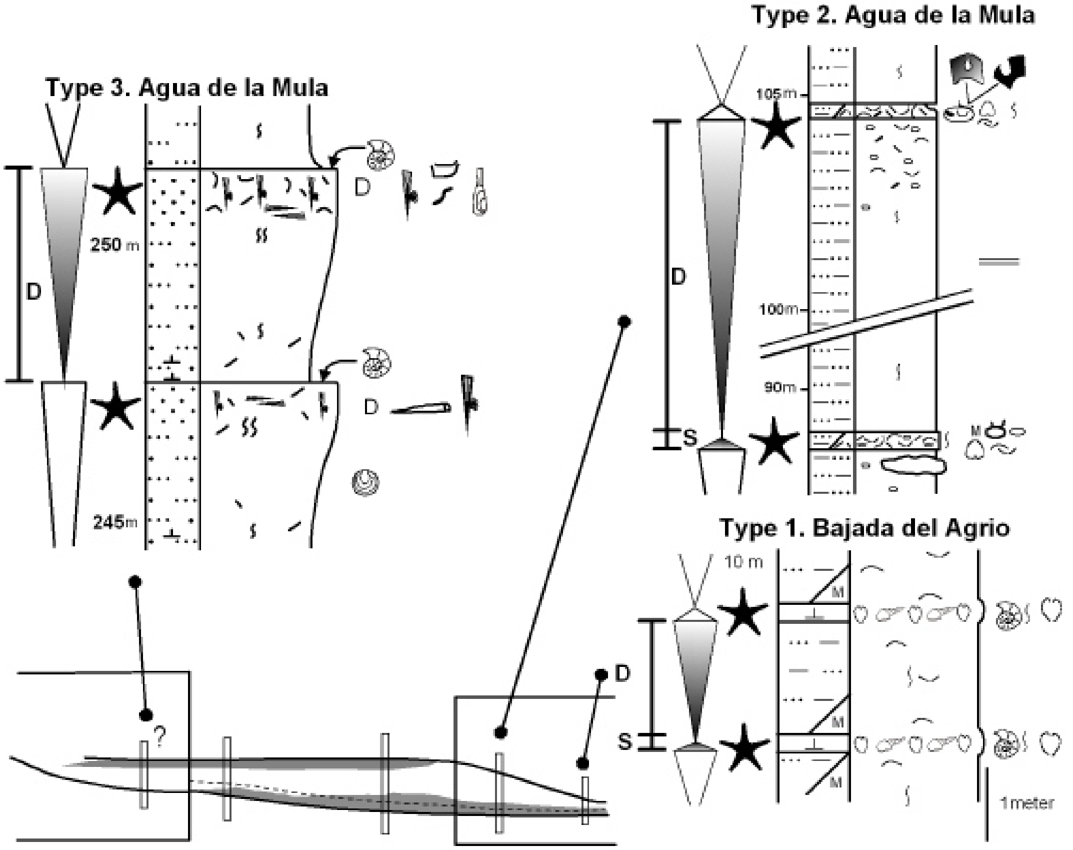

Text-Fig. 20. Sedimentary sequence (low left) with hypothetic condensed parts and the position envisaged for shell bed types. Shaded areas represent condensed beds. Examples of shell bed types were extracted from sections studied here. Large asterisks indicate the position of the shell beds (★). S: starvation hemisequence. D: dilution hemisequence. For references see Appendix-Fig. 3.

Type 1

Type 1 skeletal concentrations (Text-Fig. 20) consist of several loosely packed shell beds that occur in the first 50 to 100 m of the unit in both sections, in the context of TST, MFZ and early HST of the first third order sequence. These skeletal concentrations are characterized by simple tabular beds, 5 to 10 cm in thickness, of shelly marl, shelly micritic mudrock and shelly allochemic mudrock (facies Ma-R, Ma-B-R, MC1-R and MC2-R). Base and top of these concentrations are gradual. Fossils are small, dominated by gastropods and secondarily bivalves, all of which are excellently preserved. Ornamentation of shells is usually preserved unaltered and even colour patters are preserved. The articulation index is close to 100%, encrustation and microborings are rare. Phosphate and pyrite replacements of shells are common. Type 1 shell beds correspond mostly to association A, dominated by *Bathraspira* sp. A, *Bathraspira*? sp. C, *Mesomiltha argentina* and *Protohemichenopus* sp.

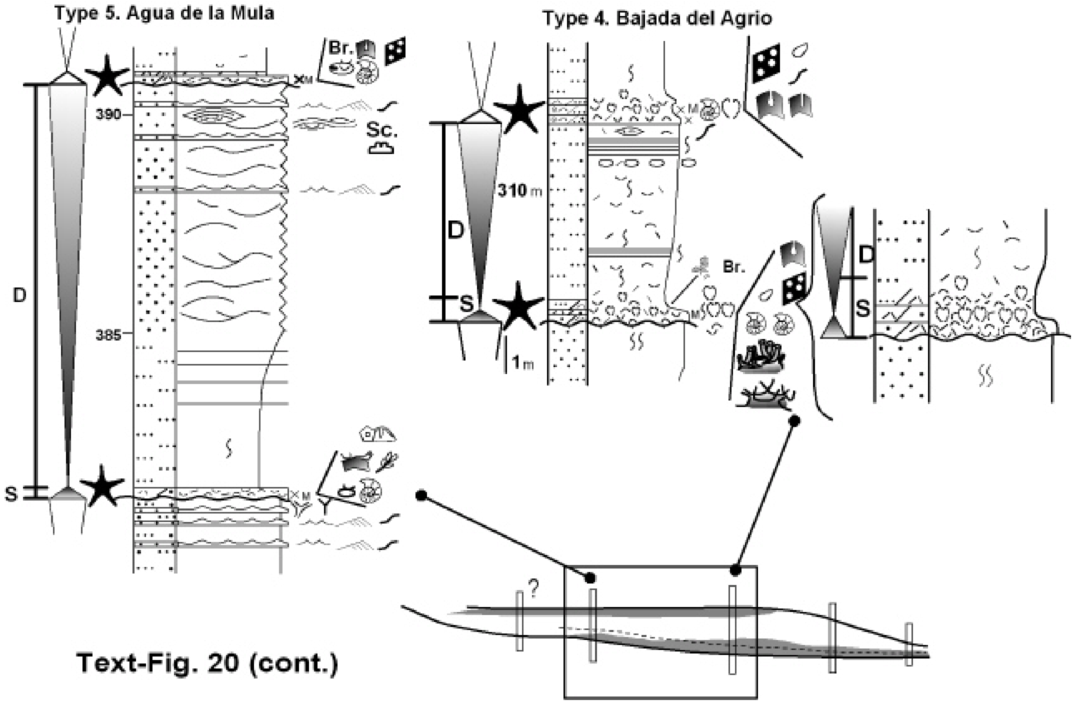

Text-Fig. 20 (cont.)

Interpretation. Type-1 shell beds are embedded in starvation hemi-sequences of starvation/dilution sequences. The fine-grained nature of the sediments that compose the matrix indicates deposition beyond the reach of fair-weather waves. Low-density concentrations of a fairly well preserved benthic fauna precludes (frequent) physical disturbance by storm waves or storm induced flows. The benthic fauna accumulated as a combined product of low net sedimentation (and hence relatively high shell production), low rate of shell destruction and high preservation potential due to pore waters supersaturated with respect to calcium carbonate. The shells were deposited in an outer ramp to basinal environment, certainly below storm wave base. Evidence of this is the excellent preservation of the fauna and the low density of the concentrations, which are biogenic in nature. Predatory drill holes are very common in *M. argentina* shells of this type of shell bed. The bivalves were killed in the sediment and remained buried. If they had been removed and exposed on the bottom, they would be found disarticulated because of the combined effect of the decay of adductor muscles and action of the ligament. This fact indicates a calm environment. Shells in the deepest facies almost completely lack microborings. This may be related to the exclusion of endolithic algae below the photic zone. However, there are several other organisms producing microborings, which do not depend on light. Differences in this feature can also be explained by a low residence time on the sea floor. In the latter case, shells never became exhumed and exposed to the activity of microborers. High turbidity related to assumed eutrophy for most of the time span represented by the section might have reduced the penetration depth of light.

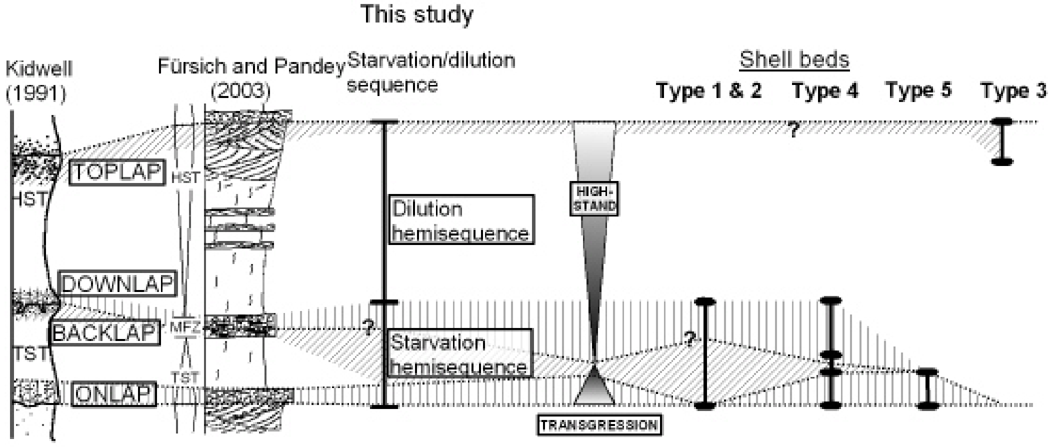

Text-Fig. 21. Comparative chart of the patterns observed in this study and models of shell bed positions in sedimentary sequences. Shaded areas represent condensed deposits.

Beds containing type 1 shell beds comprise the starvation hemisequence of sixth order sequences. They were deposited during the whole period of starvation, from the beginning of the transgression to some point already at the beginning of the regression (See Text-Fig. 11 A). If deposition of the whole sequence took approximately 20 ky, type 1 shell beds are composed by shells accumulating during a few thousand of years. Time-averaging was moderate, and as the environment did not change much during deposition of the hemisequence mixing of faunas from different habitats was not important.

Type 2

Type-2 skeletal concentrations consist of loosely- to densely-packed skeletal concentrations forming 5-20 cm thick homogeneous beds. Base and top are usually sharp. Facies are coarser than in type 1, e.g. shelly allochemic mudrocks or shelly muddy allochemic limestones (MC2-R and MB1-R facies). Strata containing these shells beds represent complete starvation hemisequences like in type-1 shell beds (Text-Fig. 11 A). They are common in intermediate positions of the HST of the first-third order sequence (DSAM-1) as well as in late TSTs and early RSTs in other sequences. The degree of articulation is moderate to low, fragmentation and abrasion are low to high, microborings are common, while macroborings are restricted to large shells of *Aetostreon* sp. and carbonate concretions. Encrustation is moderate to low. There is abundant shell hash. Type-2 shell beds characterize associations B, E, M, N, P and D. These associations are common in middle to outer ramp facies.

Interpretation. Type-2 shell beds group skeletal concentrations deposited during starvation periods of sixth order sequences deposited in outer to middle ramp settings. Physical reworking by storm waves and currents was moderate. Shells and carbonate concretions were usually reworked and exposed to the action of borers and encrusters. However, large densities of these epi and endobionts were low, probably due to the scarcity of large, stable hard substrates to settle on. Additional shell fragments were added by storm flows that brought material from shallower habitats.

If compared with type-1 shell beds, type-2 shell beds were deposited in shallower settings. Evidence of this are a higher proportion of shell fragments, a lower percentage of articulated bivalves, and a higher proportion of encrusting fauna, all of which indicate deposition under more agitated waters that resulted in disarticulation, breakage, exposure on the sea floor, and some hard substrate for attachment of cementing biota. Another directed change in the sections is the progressive decrease of the relative abundance of deposit-feeders and subsequent increment of suspension-feeders, a feature that is also associated with more agitated waters. The occurrence of microborings probably indicates deposition in the photic zone.

As with type 1, type 2 concentrations are stratigraphically homogeneous. They represent the time represented by the transgression and early regression of the starvation-dilution sequences. As such, type-2 skeletal concentrations comprise a few thousand years, the time involved in the development of the starved period of a 20,000 years sixth-order sequence. The environment did not change drastically during the deposition of the beds, so mixing of different faunal suits was probably minor. This phenomenon is apparent in the increase of encrustation on large shells and carbonate concretions, which indicates a subtle process of taphonomic feedback. Besides, in some examples deposit-feeders and chemosymbiotic lucinids and scaphopods, typical of deeper facies, characterize the top of some beds, indicating deepening. Time-averaging is then low to moderate.

In some beds, early diagenetic carbonate concretions bored and encrusted by small oysters, serpulids and corals is common. This phenomenon can be interpreted as the superposition of two cycles of sea level changes: during the first one the faunal elements were deposited, and high levels of calcium carbonate saturation led to concretionary lithification of the bed. During the second cycle more agitated (shallower) conditions winnowed the bottom. Shells were exhumed and concentrated, as well as the already lithified parts of the shell bed (i.e. the carbonate concretions), which were subsequently bored and encrusted. This last case would involve the mixing of fossils from different ages and habitats.

Type 3

Type 3 shell-beds consist of dispersed to loosely packed skeletal concentrations in a dominantly siliciclastic matrix, normally sand or silty sand. The facies containing these concentrations are fossil-rich, bioturbated, fine-grained sandstones (S-FS-R, chapter 5), which are more common at section AML than at BAL. Shells are either of originally calcitic composition such as the outer layer of *Pinna robinaldina*, serpulids (originally high-Mg-calcite), and gryphaeid oysters (originally low-Mg-calcite) or represented by internal moulds of other taxa, such as *Panopea neocomiensis*, *P*. *dupiniana*, and Veneridae sp. indet 2. Common features of most of these skeletal concentrations are a nearly complete lack of encrustation and bioerosion, low species richness, and a high proportion of both, infaunal taxa (e.g., *Panopea neocomiensis*) and the semi-infaunal *Pinna robinaldina* both articulated and in life position. In some beds, serpulids of variable morphologies are common but not attached to any shell or shell fragment (in fact, there are generally no bioclasts in this facies). Bases are transitional while tops are sharp. There is an upward increase in fossil density (Text-Fig. 20). In some cases, ammonites are particularly abundant on top of these beds. Samples of association C correspond to this type of shell bed. Type-3 skeletal concentrations occur immediately above SBAM-1 in the context of the LST-2 and the early TST-2 in the AML section (Text-Fig. 6). The sediments represent the top of dilution hemisequences.

Other disperse to loosely packed skeletal concentrations embedded in bioturbated sandstone or silty bioturbated sandstone can be found at the top of dilution hemisequences of sixth order sequences that extend into relatively shallow facies. These cases are overlain by early transgressive beds and bounded by an erosional surface. Shells are rare and the fauna is preserved as moulds.

Interpretation. There are several indications that low sedimentation rates governed deposition of the facies containing type-3 shell beds: (a) the completely bioturbated nature of the sediments, (b) the common development of skeletal concentrations, (c) the high amount of micrite, and (d) the presence of autigenic glauconite. This facies is interpreted as shoreface sandstones, which subsequently became completely bioturbated after having been flooded. Because of the absence of sedimentary structures, the environmental interpretation of this facies cannot go further. A shoreface setting for the deposition of the bioturbated sandstones is supported by the frequent position of this facies above sand-dominated CIB and HET in the same dilution hemisequence. The net rate of sedimentation was low probably due to bypassing or primary starvation, providing time for the benthic fauna to completely erase any primary sedimentary structures. Some shells were probably dissolved synsedimentarily while others early on during diagenesis.

Fossil-rich, bioturbated, fine-grained sandstones impose different constraints on the interpretation of the depositional environment compared with other skeletal concentrations. Permanent agitation by fair-weather waves does not match the widespread occurrence of the semi-infaunal *Pinna robinalina* and the infaunal *Panopea neocomiensis*, both usually articulated and in life position, and the absence of sedimentary structures. The sandstone strata could have been deposited in a shoreface setting but the colonization by the benthic community took place later on, when as a result of the transgression the sea floor occupied a greater depth. Ammonites lying on top of type-3 shell beds support the position of the maximum flooding zone at top of these sandstones.

The type-3 shell beds occur on top of dilution hemisequences. This fact plus the upward increase in shell density indicate that type 3 shell beds correspond to shell bed type I of Kidwell (1986a). It would not represent toplap condensation caused as a result of sediment bypass (Kidwell 1991a) but rather a progressive diminishing of the rate of sediment input after a fall of sea level. If this were true, type 3 shell beds would represent the time span between the end of the sea level fall and maximum flooding, although transgressive sediments are probably absent. The lack of shells of originally aragonitic composition and the dominance of calcitic ones indicate that diagenetic dissolution of shells took place. High input rates of siliciclastic sediments and the lack of erosion before deposition of the fauna did not provide good conditions for fossilization. Besides, for several examples, this feature was accentuated because of the position of these strata in siliciclastic-rich segments of high hierarchy sequences. As a result, pore waters were undersaturated with respect to calcium carbonate and only mineralogically stable shells survived.

Type 3 skeletal concentrations differ from the rest in having been preserved in regressive sediments of starvation/dilution sequences. Besides, in many examples the next (overlying) sequence lacks a transgressive bed. However, as was discussed above, most of the shell-bearing organisms lived during the transgression. A plausible interpretation for this pattern is a fast sea-level rise that did not allow reworking of late regressive sediments. As a result a tranquil environment followed on sediments deposited under a high energy regime. Another explanation would be that RST of this sixth order sequences probably received sediments while the regression lasted, i.e. HST, FSST and LST, due to high availability of accommodation space and a relatively deep setting at the beginning of the deposition of the sequence. In this way only at the end of the regression the environment was shallow and sand was deposited. The next steps were characterised by deepening and a low rate of terrigenous input. In other cases like type 4 and 5 skeletal concentrations, the RST is actually represented by an incomplete sequence of HST-FSST-LST. For instance, the RST comprises sediments deposited during the HST and perhaps during early FSST, up to reaching shoreface facies. Enhanced shallowing given by the sea-level drop led to shallower conditions and then erosion.

Type 3 skeletal concentrations preserved on top of dilution hemisequences that have transgressive strata above were probably produced as a result of starvation due to sediment bypassing (toplap condensation).

Type 4

Shell beds in starvation hemisequences developed at both, deep and shallow settings are thin, environmentally condensed simple homogeneous beds. At intermediate depths, instead, these sixth order hemisequences, i.e. type 4 shell beds are thick and complex (for a more detailed description of starvation hemisequences see chapter 5). Type 4 shell beds are well developed in the second and third third-order sequence (DSAM-2 and 3) at both localities. These skeletal concentrations are 0.5 to more than 2 m thick tabular beds. Bases are sharp and occasional erosional; tops are usually gradual. Starvation hemisequences containing type 4 shell beds can be subdivided into three components, the basal starvation bed, middle horizon and the upper starvation bed (see Text-Fig. 20), each with a taphonomically distinct skeletal concentration.

Type 4A. Shell concentrations of type 4A occur in the basal starvation bed (Pl. 6, Fig. 7). They are characterised by high degrees of fragmentation and disarticulation, and high proportions of thick-shelled specimens. Shells do not exhibit any orientation pattern indicative of sedimentary structures. It is thus assumed that all physical sedimentary structures were erased by the action of infaunal species. Species diversity is moderate. Type 4 shell beds contain fossil associations F, H, J and O. The basal starvation beds are inferred to represent high-energy early transgressive deposits usually composed of coarse mixed-rocks i.e. mixtures of fine sand, small bioclasts and physically altered normally disarticulated shells (facies MB2 and MD2, chapter 5).

Type 4B. Type 4B skeletal concentrations are found at mid-starvation horizons. These horizons consist of a level with a higher density of well-preserved bivalve shells, many of them articulated. Encrustation and borings reach high levels on semi-infaunal bivalves and ammonites (see for instance Pl. 3, fig. 7). Ammonites usually reach high densities only at this level. At this horizon the highest levels of encrustation and autigenic glauconite occur. Small and large oyster and serpulid buildups (section AML at 281 m, App.-Fig. 2) as well as coral patch reefs (section BAL at 503 m, App.-Fig. 1) are also found at this level. The mid-starvation horizon is usually composed of carbonate-dominated coarse mixed facies. From the mid-starvation horizon upwards, there is an increase in the proportion of siliciclastic mud, which progressively gives way to still muddier facies of the upper starvation bed. Fossil associations G, I, J, L and M occur in this type of shell bed.

Type 4C. The outstanding taphonomic feature of this subtype is the high proportion of articulated bivalves which are in many cases in life position. Large mollusc shells like those belonging to *Ptychomya* sp. A aff. *P. koeneni* and *Eriphyla argentina* are very well preserved without any signs of erosion. Small shells are usually partially dissolved (e.g. *Disparilia elongata*). The upper-starvation bed is characterized by a fining upward trend, with a decreasing density of shells and increasing content of siliciclastic mud (Pl. 3, Fig. 8). The subtype can reach thicknesses of up to 2 m with the development of thick accumulations of agglutinating foraminiferal constructions (see for instance section AML at 330 m, App.-Fig. 2 and Pl. 8, fig. 3). These protists are inferred to have been well adapted to cope with moderate sedimentation rates. Associations L and M are found in shell bed type 4C.

Interpretation. Together with sedimentological and paleoecological information, taphonomic aspects of skeletal concentrations helped to discern the position of the maximum flooding zone in complex starvation hemisequences (see discussion in section 6.4). Basal starvation beds show evidence of high levels of water energy and contain skeletal concentrations subtype 4A characterized by a low degree of articulation, and a high degree of breakage, and of physical and biological erosion, as well as an enrichment in large and thick shells. Middle starvation horizons show the highest levels of encrustation, hard-substrate related species, and relative abundance of carbonate particles, a better preservation of the fauna and high levels of glauconite. All this evidence indicates lowest levels of terrigenous input and deepening with respect of basal starvation beds, which places subtype 4B shell beds in the maximum flooding zone. Above the maximum flooding zone subtype 4C accompanies the resumption of the terrigenous input already in the offshore, with a higher proportion of infaunal species, low levels of borings and encrustation, and other evidence of low energy and a higher burial rate. In some examples, detritivorous species appear in these sediments. It is important to indicate that these three levels are not usually easily discerned. More often than not a basal, high-energy and the upper mud rich starvation beds can be distinguished in these complex starvation hemisequences. The middle starvation horizon cannot be easily separated from the other two components.

Type 4 shell beds formed during a period of terrigenous starvation, under depths that fluctuated from lower shoreface to outer ramp. In type 4A, the admixture of shells with different degrees of taphonomic alteration indicates that some of them could have been reworked from underlying regressive deposits by erosion. These cases represent transgressive lag deposits (Kidwell 1991a). In other instances, it is not possible to identify shells older than the sequence boundary and these can simply be considered as early transgressive deposits subject to high water energy (fair-weather and storm waves). In all cases, the poor preservation of the benthic fauna and the abundance of autigenic glauconite and iron replacements indicate low terrigenous input and high energy conditions (Archuby 2005). They represent skeletal concentrations in the context of onlap condensation (see Text-Fig. 19) partly related to ravinement processes. The mid-starvation shell bed type 4B, judging from several lines of evidence, correspond to the level with the lowest input of terrigenous sediments of the sequence (i.e. highest starvation). This is supported by the lowest levels of terrigenous sediments, highest concentrations of skeletal material, autigenic glauconite, iron impregnation, encrustation, and the development of oysters and serpulids patch reefs. The absence of terrigenous mud due to winnowing can be discarded because in many instances carbonate mud is present. From a sequence stratigraphic point of view, type 4B shell beds are equivalent to the mid-cycle shell beds and were deposited in the context of backlap and early downlap condensation. Shells in type 4B accumulated first as a consequence of reduction in the rate of sediment input and of shell destruction, the latter associated with deposition in deeper settings. Storms played a role in concentrating the infauna and taphonomic feedback added epifaunal elements. Although it represents a less time-averaged shell concentration than type 1 and 2, fidelity is in this case moderate to low due to mixing of early infaunal-dominated and late epifaunal-dominated community relicts. Type 4C represents the autochthonous relict of a community that colonized the outer ramp when the input of terrigenous mud restarted. Time-averaging is low and fidelity high.

Type 5

This type of shell bed occurs at late HSTs of third order sequences. It consists of loosely to densely-packed (matrix-supported) skeletal concentrations occuring in planar beds with erosional lower and sharp upper surfaces (Text-Fig. 20 and Pl. 3, Figs. 3 and 4). The matrix is composed of sand and iron-rich calcareous cement. Associations E, G, O, L and C occur in this type of shell bed. In the case of type 5 shell-beds a simple starvation bed is overlain by regressive sediments.

The most common facies containing this type of shell bed is the MD2 (allochemic sandstones, see section 7.2.2 in Chapter 5). Allochemic sandstones are bioturbated mixtures of usually poorly sorted, very fine- to fine-grained sandstones with some shells, shell fragments, echinoderm ossicles, and ooids. Allochemic sandstones are always found at the base of starvation hemi-sequences. This facies is typically underlain by an erosional surface corresponding to a minor sequence boundary (= transgressive surface).

In type 5 skeletal concentrations shells show evidence of a high degree of physical reworking, i.e. disarticulation, abrasion, breakage, and size sorting. Large and thick shells that are usually bored dominate the assemblages. Encrustation by oysters and/or serpulids may be locally abundant. Occasionally, the serpulid *Parsimonia antiquata* forms small buildups or occurs reworked in great abundance. Bioerosion levels are usually very high and characterized by borings such as *Gastrochaenolites*, *Meandropolydora*, *Trypanites*, *Caulostrepsis*, *Entobia*, cirripedian borings, and microborings. The bored substrate consists mainly of shells. Ammonites may be locally present.

Interpretation. Type 5 shell beds were deposited in high-energy environments, above the fair-weather wave-base, on the inner ramp. During deposition of these shell beds, fair- and storm-weather waves acted on the sea floor precluding sedimentation of fine-grained material. With advancing of transgression, shoreface erosion reworked the top of the former dilution hemisequence. The reworked pebbles already described (section 7.2.2 in Chapter 5) are clear evidence of a ravinement process, although in general the nature of the components of this shell-bed type (whether a product of ravinement or not) is usually not clear. Destruction of thin-shelled faunal elements in the high-energy environment resulted in mechanical sorting in favour of large and thick shells. The activity of infaunal organisms erased sedimentary structures as well as mixed sediments, thus producing the heterogeneous and highly bioturbated fabric.

Type 5 skeletal concentrations are interpreted as onlap shell beds, deposited in shallow, high-energy environments, with little accommodation space. High levels of water energy, together with low net input of sediments (low burial rate), were responsible for the high rate of shell destruction. The lack of middle and late starvation deposits may be due to the lack of accommodation space, the high water energy at the end of the transgression, or both. These skeletal concentrations share many features with subtype 4A, and indicate a similar genetic process. The main difference is that type 5 lacks middle to late starvation-type skeletal concentrations. This fact may be related with the position of type 5 close to major sequence boundaries, where accommodation space is at a minimum, and deposition of most of the starvation hemisequence took place in a high-energy shoreface setting. The lack of accommodation also explains why lag components are found in type 5 more often than in type 4A.

Taphonomic patterns and trends along starvation/dilution sequences

Trends in shell preservation occur in both starvation and dilution hemisequences. The first case refers to complex starvation hemisequences composed by basal, maximum flooding and upper starvation shell beds (skeletal concentrations subtypes 4A, B and C). In an upward direction, water energy decreases as a result of the change from shoreface settings at the base to an offshore position at the top. Fragmentation and disarticulation decrease tracing the energy gradient. Terrigenous input is low in the basal starvation beds, at minimum in the middle horizon, and increases upward. At the base, a low burial rate together with high destruction rate made shell destruction the main process. In Text-Fig. 22 the results of a quantitative sample in terms of articulation (a) and breakage (b) degree, taken from three shellbeds of the same starvations hemisequence (section BAL at 312 m) are shown. In other examples differences between lower (early starvation bed) and upper (middle to late starvation beds) are more pronounced. For instance, in section AML at 281 and 330 m two different starvation hemisequences were quantitatively sampled at their basal early starvation bed and at their upper middle to late starvation beds. The results are presented in Text-Fig. 23. At the position of maximum flooding, depth and hence water energy was lower and destruction rate was low although the burial rate was lower. The last feature produced the highest levels of encrustation. In the upper starvation bed restoration of the terrigenous input increased the burial rate. As a consequence, the fauna is best preserved at this level. However, there is an upward tendency to higher levels of shell dissolution possibly related to lower concentrations carbonates ions in the pore water.

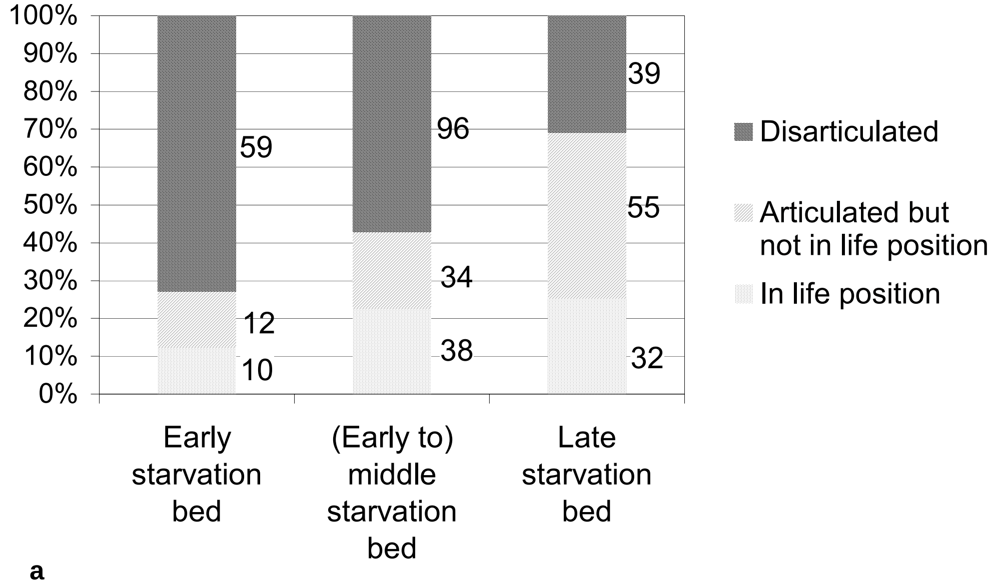

a

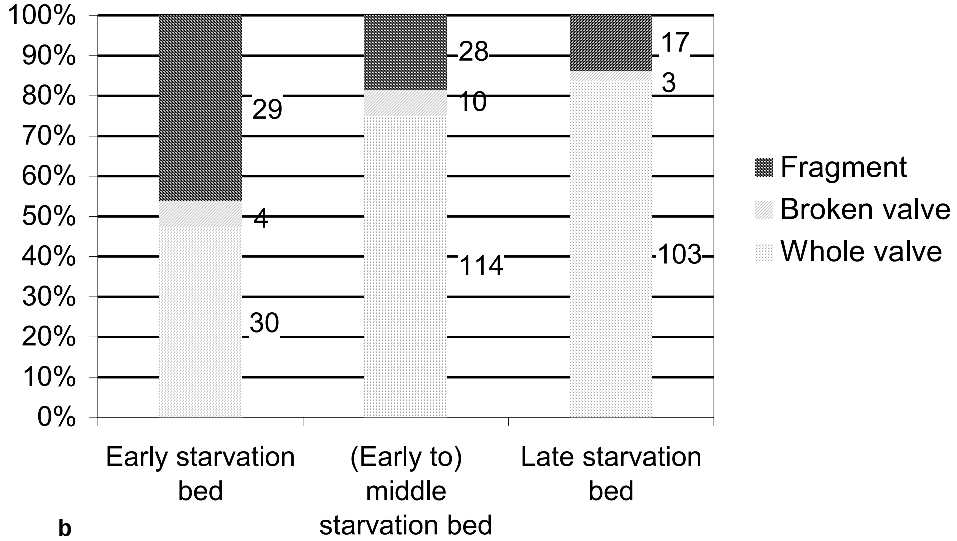

b

Text-Fig. 22. Stacked percentages column graphs showing articulation (a) and breakage (b) degrees of three shell beds of the same starvation hemisequences at different positions (section BAL at 312 m). The scale represents the percentages. Labels correspond to absolute counts.

In the case of dilution hemisequences, upward trends are as rare as skeletal concentrations. When present, as is the case in the majority of type 3 skeletal concentrations, the trend is to an upward increment in shell density. This can be explained by both, a rise in the saturation level with respect to calcium carbonate, which increased the probability of mineralization of the shells, and a decrease in the availability of accommodation space towards the end of the regression.

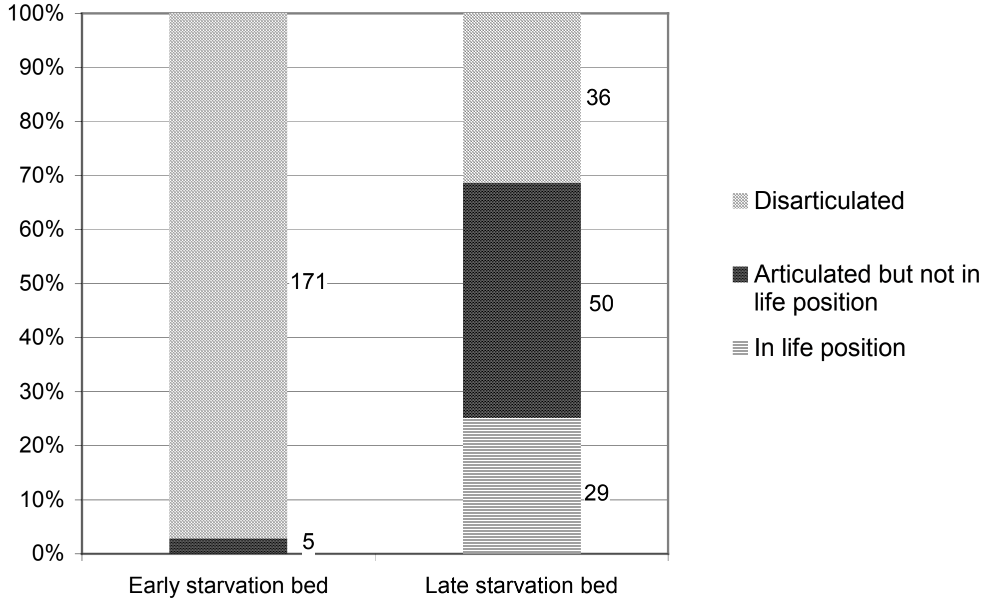

a. Section AML at 281 m

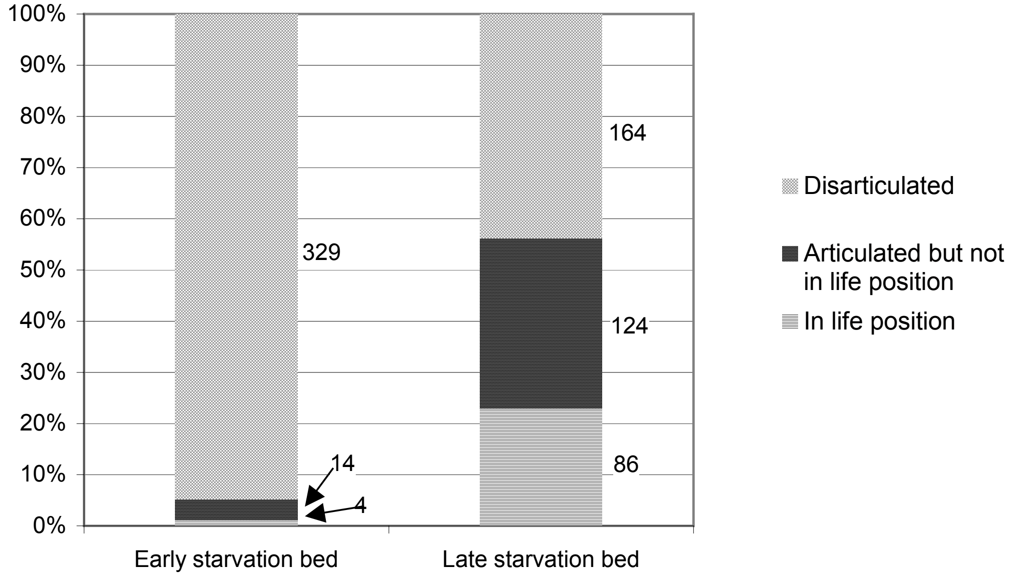

b. Section AML at 330 m

Text-Fig. 23. Stacked percentages column graphs showing articulation degrees of early vs. late starvation shell beds of the same starvation hemisequences at two different positions. b. Section AML at 281 m. b. Section

AML at 330 m. The scale represents the percentages. Labels correspond to absolute counts.

Taphonomic trends in higher hierarchy sequences

Tracing depth (as a proxy of the energy level) and terrigenous input changes, different taphonomic trends occur within medium and major sedimentary sequences. For instance, shell-bed types described in the previous sections are characteristic of particular portions of high hierarchy sedimentary sequences. Three different patterns of shell bed trends occur in the section. One of them is found in DSAM-1, characterized by high availability of accommodation space and relatively high input of terrigenous sediments. The second occurs in DSAM-2, 3 and 4, which are thinner due to smaller accommodation space and higher sediment starvation. In DSAM-5 to 9, although not always well developed, a particular trend can be envisaged. In these three groups of sequences, the pattern of succession of shell-bed types differs.

In the first major depositional sequence (DSAM-1) type 1 skeletal concentrations characterize starvation hemisequences of major MFZ-1 and early major HST-1, where sediments were deposited in basinal settings, beyond the reach of storm flows, storm waves, or fair-weather waves. In HST-1, type 1 shell beds are replaced upward by type 2, which are replaced in turn by type 4. Type 4 shell beds are, however, rare in DSAM-1, probably due to the higher rate of terrigenous input that characterizes this sequence. Type 5 shell beds are characteristic of few starvation hemisequences completely developed in the shoreface. This situation happens around the first major sequence boundary.

The second type of trend is exemplified by DSAM-2, 3 and 4. In these cases high-energy shell beds that characterize starvation hemisequences close to sequence boundaries are either of type 5 or type 4, and formed in inner to middle ramp settings. In the vicinity of MFZs, type 2 of the outer (to middle) ramp are common, while at intermediate positions type 4 skeletal concentrations are the rule. The middle to late starvation deposits of these latest Hauterivian type 4 shell beds are highly fossiliferous. Well-preserved shells of *Eriphyla argentina*, *Ptychomya koeneni*, *Pterotrigonia coihuicoensis* and crioceratitid ammonites are extremely abundant.

DSAM-5 to 9 are characterized by a very low availability of accommodation space (possibly linked to a decrease in the rate of subsidence) and evidence of very low input of terrigenous sediments (for more details see discussion in Chapter 5). These features probably constrained the development of distinct trends in the fossil concentrations. Around the shoreface deposits of SBs-5 to 9 bio-oo grainstones are developed, in which complete shells are rare and bioclasts show high degrees of abrasion and breakage. Close to MFZs of these topmost sequences, type 2 shell beds with well preserved benthic fauna are present. These cases are, however, restricted to two particular shell beds that cluster together in the fossil association D. Micritic beds with dispersed skeletal concentrations are also present.

Other phenomena detected in hierarchies higher than starvation-dilution sequences are the following:

- Amalgamation of starvation-dilution sequences. One example can be observed at the position of the MFZ-3 (352 m above the base in section BAL and 396 m in section AML). There, a low energy micritic rudstone bed, a few meters thick, changes up-section into offshore mudrocks, alternating with thin, fine-grained, mixed carbonate-siliciclastic or carbonate rocks. The same facies is found at equivalent positions in both sections, only once with this thickness, regardless of the sedimentological differences detected between the two localities. These beds are interpreted as the expression of the Faraoni global anoxic event. Other possible examples are the “Taphonomic Cycles” and 2, already described in the section of high frequency sequences of Chapter 6. In these cases, taphonomic features of starvation hemisequences exhibit a cyclic pattern and are evidence of cycles of eccentricity. In Taphonomic Cycles type 1 amalgamation is inferred from different stratigraphical and taphonomic features. These include thickly developed starvation hemisequences, internal surfaces of erosion, and the presence of early diagenetic concretions that are bored and encrusted by serpulids and oysters. However, it must be stated that none of the features used to infer amalgamation is conclusive.

- In some cases, enhanced starvation related to fifth or fourth order cyclicity caused the stacking of two or more starvation hemisequences, almost completely lacking sediments of the dilution component. Examples are found in section BAL at 225 and 282 m; in section AML at 239, 280, 343 and 350 m (Text-Fig. 6; Appendix-Figures 1 and 2). See also Pl. 9, Fig. 2.

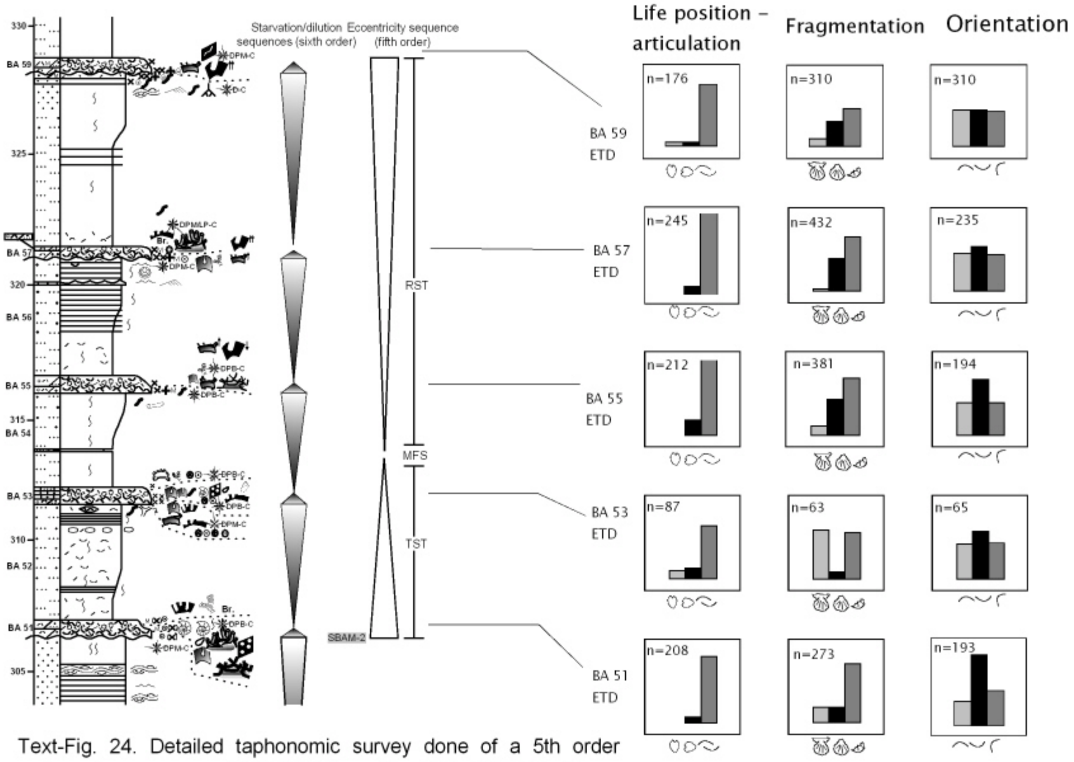

Text-Fig. 24. Detailed taphonomic survey done of a 5th order sedimentary sequence (DSAM-3/1 in section BAL, 305-329 m).

A detailed taphonomic survey was done from base to top of a 5th order sedimentary sequence (DSAM-3/1 in section BAL, developed from 305 to 329 m). The sequence comprises four S/D sequences (levels 51 to 59) and the first starvation hemisequence of the overlying sequence (see Text-Fig. 24). In every one of the five starvation hemisequences several taphonomic features were counted, in the different shell beds, whenever it was possible. Results are shown only for the early transgressive shell beds (Text-Fig. 24). Shell concentrations in early TST and late RST show the lowest preservation quality, whereas those placed in middle positions (late TST and early RST) show higher percentages of articulation, life position, and little fragmentation and abrasion. These results coincide with Fürsich and Pandey (2003a). The absence of a clear orientation pattern of shells is interpreted as due to bioturbation. Strong differences between taphonomic counts of different levels were not detected probably due to originally similar depositional settings. In turn, the surveyed fifth order sequence is inserted into a major TST, which probably influenced the results.

A general rule found in this study is that environmental changes in terms of water energy driven by S/D hemisequences are greater than those generated by higher hierarchy cycles. The consequence of this is that in most examples, regardless whether a shell bed was deposited in a fifth or fourth order sequence, if the precession cycle started with shoreface conditions at the base of the starvation hemisequence, the taphonomic signature and the biofabric of the different fossil concentrations will be similar. In other words, the imprint of precession cycles on the taphonomic features of skeletal concentrations is more relevant than the effect of other cycles.

The taphonomic “windows”

Fossil shells passed through a chain of steps from death of the individual to the fosilized end product. Every step has a particular combination of states under which a shell fossilizes. This “combination of states” can be viewed as a window that a shell has to pass before facing the next step.

The first step relates to the environmental conditions that operated during deposition of the sediments. The “environmental window” consists of a combination of the environmental factors that allowed the development of a benthic community with shelled specimens, i.e., oxygen availability and suitable water temperature and salinity. The second step, once the first has produced shells, comprises the destruction processes. Shells that do not pass through this “destruction window” are those that are destroyed before burial by means of high water energy, synsedimentary dissolution, and biogenic-driven destructive processes such as boring and grazing. The next step, connected to the second one, is the final burial of shells (possibly after one or more phases of reworking). This “burial window” is associated with high burial rates, which are in turn related with high rates of sediment input that increase the probability of a shell to become fossilized. The fourth and last step is diagenesis. Hard parts already buried are exposed to diagenetic processes. The “diagenetic window” is associated with high levels of calcium carbonate saturation of pore waters, which leads to rapid replacement of originally aragonitic shells and the lithification of the shell beds.

Every step and hence, every window, can be related to the development of sedimentary sequences in different ways. Analyses performed in this study suggest the following connections between sequence stratigraphy and taphonomy:

- Environmental window

In closed basins with little bottom circulation anoxia can be expected in deep settings during late transgression, periods of maximum flooding and early regressions. In turn, during regressions (normal or forced regressions) epicontinental basins may become totally or partially isolated from the ocean and turn hypo- or hypersaline. High water energy associated with shoreface settings are not suitable for the development of bottom communities. In turn, in supratidal habitats shelly biocoenoeses are usually not stored. High-energy shoreface and supratidal habitats are more common during regressions. Oxygen depletion, hypo- or hypersalinity, high energy and supratidal conditions may result in low density and/or low diversity communities with little chances of becoming fossilized. In the Agua de la Mula Member there are few signs of oxygen reduction during major MFZs. Under these oxygen-reduced conditions a moderately diverse community developed. Stenohaline species present in every shell bed rule out changes in salinity throughout the succession. Bioturbated sandstones suspected to have been deposited under shoreface settings contain a fossil fauna of low diversity. However, it is not clear whether the shells lived under these high energy conditions or colonized the sea floor afterwards.

- Destruction window

Shells that passed through the environmental window faced high levels of water agitation and may have become destroyed by mechanical reworking (close to major SBs, i.e. late HSTs, FSSTs, LSTs and early TSTs), may have become dissolved due to pore waters undersaturated with respect to $CaCO_3$ (dilution hemisequences in major regressions), or become destroyed by the action of bioeroders (starvation in late HSTs, and early TSTs) combined with high water energy (similar settings but close to SBs).

- Burial window

Those fossils that escaped the surficial destructive processes, after the final burial stood a greater chance of becoming fossilized. The burial window is associated with high rates of (terrigenous) sediment input, a setting observed during dilution hemisequences in major HSTs, FSSTs and LSTs. However, high rates of terrigenous input reduces the saturation of calcium carbonates in pore waters so that shells may not pass through the next, diagenetic window. It becomes clear from the data of this study that whenever terrigenous input is relatively high and constant, as is the case during dilution hemisequences, shells do not pass through the diagenetic window. Nevertheless, when the high rate of terrigenous input occurs immediately after a period of sediment starvation shells are preserved in high density, because the concentration of calcium carbonate, although diminishing, is still high. This setting allows quickly buried specimens to pass through the next window. This situation typically characterizes late stages of starvation hemisequences, which correspond to early RSTs. These facts explains why in many cases the starvation hemisequence exceeds the transgressive period: the changes in the diagenetic environment, i.e. the content of calcium carbonate in the pore water, is out of phase with respect to the sea-level changes.

- Diagenetic window

Although operating after the other three, this window shaped the preservation pattern in the Agua de la Mula Member of the Agrio Formation. Fossils become preserved almost exclusively during starved periods associated with the transgression and early regression of sixth order sequences (i.e. starvation hemisequences). Around deposition of starved sediments the saturation of calcium carbonate in pore waters is at its maximum and the probability of early lithification highest.

The sequence stratigraphic model predicts changes in sedimentation rates and turbulence levels from eustatic sea-level changes, and can also predict the positions in which syndepositional and diagenetic dissolution cannot completely remove calcareous shells from the fossil record (Fürsich and Pandey 2003).

Two contrasting types of deposits with respect to preservation of calcareous fauna are recognised in this study: well lithified, terrigenous-starved starvation hemisequences and poorly lithified, siliciclastic-dominated dilution hemisequences. A similar pattern was described by Fürsich (1982). In the first case the originally unstable, aragonitic and the more stable originally calcitic shells are preserved. Conversely, in the second type fossils are not preserved at all or only by their moulds. This pattern can be explained with the model described in Fürsich and Pandey (2003), in which high saturation of pore water with respect to calcium carbonate during the transgression results in early lithification and corresponding preservation of the skeletal concentrations. The calcium carbonate stems from the dissolution of shells that colonized the bottom during the regression phase and at the beginning of the transgression. Carbonate is migrating from the more argillaceous layers, where skeletal matter is dissolved, to the layers richer in carbonate, where calcite cement is precipitated. As a result, the layers initially richest in carbonate are further enriched (Fischer 1986). The two sides of the process are dissolution of skeletal elements during regression and preservation during transgression.

Further evidence of this model can be obtained from intermediate cases that do not fit typical starvation or dilution hemisequences. One example are the shell beds in dilution hemisequences that clustered in fossil association C (for more detail see Chapter 8). Shell concentrations are dominated by mineralogically more stable calcitic elements such as pinnids (only the outer layer), serpulids, and oysters. Species with originally aragonitic shells are present as moulds. Cementing serpulids with different morphologies are abundant although not attached to any hard substrate, which was probably synsedimentarily dissolved. All this evidence indicates some sort of selective dissolution of originally aragonitic shells. In this case, carbonate saturation was high enough to preserve part of the shelled community, although not every calcareous shell. The plausible reason of this intermediate case is the exceptionally high availability of carbonate in a dilution hemisequence. This setting is associated with deposition in a third order LST.

Samples M74P and M75 correspond to “calcite-enriched” and fully lithified parts of the same starvation hemisequence. Although both samples cluster together in the same fossil association (K), they exhibit statistically significant differences in the proportion of originally aragonitic and calcitic shells. The calcite-enriched sample was taken in a place where the bed was poorly lithified. There the matrix was fine- grained and marly with a low density of originally aragonitic shells and moulds. Selective dissolution of aragonitic shells due to low availability of calcium carbonate is inferred. This feature may be a consequence of the formation of this bed during a major HST, characterized by a general high input of terrigenous sediments and hence carbonate dilution. In this way, early lithification and preservation of the complete fossil assemblage occurred only patchily. An alternative explanation for these calcite-enriched beds is that shell concentrations were exposed to dissolution below the aragonite lysocline (ALy) which occurs at relatively shallow depths (Flügel 2004: 50).

10. General remarks and conclusions

The relationship between sequence stratigraphy, paleoecology and taphonomy was demonstrated for the Agua de la Mula Member of the Agrio Formation. A detailed facies analysis was the first step, in order to get a reliable and precise environmental interpretation. Stratigraphy was assessed from different lines of evidence, sequence stratigraphy, biostratigraphy and event stratigraphy. Then stratigraphic, paleoecologic and taphonomic analysis were developed with a high degree of integration.

A detailed macro and micro facies analyses provided strong bases to the stratigraphic interpretation. It allowed the recognition of different types of facies characteristic of the sedimentary environments in which fossils were deposited. Abundant evidence from the facies analysis and other sections of this study indicate that the Agua de La Mula Member of the Agrio Formation was deposited in an open marine ramp rather than a restricted one. There are no indications of departures from normal salinity. Oxygen was lowered during some periods but total depletion, if happened, occurred shortly. Nutrient levels were probably high during the deposition of the member, with the exception of some segments in the upper 150 m in which low input of terrigenous sediments allowed the development of oligotrophic communities.

The Agua de La Mula Member was deposited in a basin with a homoclinal ramp morphology. The first aproximately 250 m were characterized as a “siliciclastic ramp” in which mixed carbonate/siliciclastic facies are rare, restricted to starvation hemisequences, and dominated by siliciclastic components. Between 250 and 400 m the sedimentary environment was designated as a “mixed and siliciclastic ramp”, whose S/D sequences are shorter, and bioclast-dominated mixed facies are very common. At late major HST positions, shallow starvation hemi-sequences consist of mixtures of sand and bioclasts. In major TSTs of shallow settings, ooids are an important proportion of the allochems. Enhanced terrigenous starvation is evident in the stacking of several starvation hemi-sequences without the respective dilution hemi-sequences. In the upper 150 m a “carbonate-siliciclastic ramp” developed, characterized by a well developed calcareous starvation-hemisequence and a variably developed siliciclastic dilution hemisequence. Only in the RSTs of fifth or fourth order sequences dilution hemisequences show vertical changes in in facies (upward coarsening and shallowing facies successions). The carbonate ramp share features with those deposited in cool waters. The diversity of deposits with mixed siliciclastic and carbonate materials is described and their depositional environment inferred.

The ammonite biostratigraphy of the Agua de la Mula Member has been improved based on bed-by-bed collecting. The already defined biozones were detected and a further refinement was reached. Nevertheless, a detailed study of the taxonomy of crioceratitid ammonites and other, newly found cephalopods from the top of the section will substantially further improve the knowledge of the stratigraphy of this unit.

The change from uncoiled to coiled crioceratitid shells in the Neuquén Basin, previously placed between the *schlagintweiti* and *diamantensis* zones is here proposed to be shifted to the latter biozone, after the finding of uncoiled specimens of cf. *Crioceratites bederi*. Another important contribution of this study is the building of a combined biostratigraphic-sequence stratigraphic scheme. Sequence boundaries described here and already mentioned in the literature have been linked to ammonite biozones, and biozones are described in terms of sedimentological features and sequence-stratigraphic aspects.

The benefits of applying multi-facetted stratigraphic approaches to the study of a sedimentary unit could be demonstrated. For example, the beds containing the ammonite *Paraspiticeras groeberi* were previously provisionally placed at the boundary between the Hauterivian and Barremian (Aguirre Urreta and Rawson 1993). It was inferred in this study that the *P. groeberi* biozone has an Early Barremian age, after having found specimens of the species above the Faraoni Anoxic Event of latest Hauterivian age. The major sequence boundary SBAM-3, equivalent to the BARR-1 of European basins (Hardenbol et al. 1998) confirms the earliest Barremian and younger age for the last 150 m of the sections. With less certainty, the ammonite-barren sediments above the *P. groeberi* Zone were dated by correlating sequence boundaries with the already mentioned chart of European basins. The combination of different stratigraphic tools, e.g. biostratigraphy, anoxic events, and sequence stratigraphy, proved to be a very powerful approach.

The Faraoni Event, an important stratigraphic marker that indicates the top of the Hauterivian was probably detected and related to other stratigraphic features, i.e. sedimentary sequences and ammonite biozones. Apart from the Faraoni AOE, two more anoxic events were detected in the course of the study: the basal “Spitidiscus” black shale of earliest Hauterivian age, and a series of dark mudrock beds that occur at different positions in the last 100 m.

The sequence-stratigraphic analysis resulted in the division of the lower part of the member into three main depositional sequences (DSAM-1 to 3), and an upper part that was subdivided into six main sequences (DSAM-4 to 9). In this study, main sequences are not strictly related to a particular order of cyclicity but represent packages not included into higher order sequences. They are inferred to represent sequences of third-, fourth-, and perhaps fifth-order. Previously published sequence-stratigraphic charts of the Neuquén Basin did not relate sedimentary sequences to biozones, and are hence not comparable to the scheme presented here.

There is a good agreement between the sequence-chronostratigraphic scheme developed in this study and the chart that records sedimentary sequences of European basins (Hardenbol et al. 1998). A latest Early Barremian age is proposed for the almost ammonite-barren upper part of the Agrio Formation, based on correlations of sequence boundaries. Agreement with the chart of Haq et al. (1987) is less.

Cyclicity patterns are confidently explained by sequence-stratigraphic models, which consider eustatic sea-level changes as the main factor driving the development of sedimentary sequences. Here, the depositional-sequence model (Hunt and Tucker 1992; Van Wagoner et al. 1990; Van Wagoner et al. 1987; Van Wagoner et al. 1988) cannot be strictly followed, because it is not possible to detect the features and surfaces that define the three regressive systems tracts (falling stage, lowstand and highstand). Besides, the most important surface, the sequence boundary, is not easily distinguishable when this model is used. The depositional-sequence model is only applicable in the first main depositional sequence (DSAM-1). In the other major and in all high-frequency sequences the systems tracts and sequence boundaries cannot be identified. Conversely, the transgressive-regressive sequence model (Embry 1993) is more appropriate to describe most of the sequences studied here, with the exception of the lowest hierarchy (sixth-order) starvation/dilution sequences. Sixth order sequences were denominated in this work as “starvation/dilution sequences” based on the only two components that can be unequivocally distinguished: the lower starvation hemisequence and the upper dilution hemisequence. It was proposed that the starvation hemisequence is not equivalent to the transgressive systems tract, based on sedimentological, taphonomic and paleoecologic evidence. The middle starvation shell bed, equivalent to the mid-cycle shell bed of Abbott (1997), is found in the middle of complex starvation hemisequences (type 4 shell beds). This shell bed marks the boundary between transgression and regression (MFZ). For these types of shell beds it is possible to distinguish between TST and HST. Shell beds deposited in shallower settings lack the late starvation shell beds and are completely transgressive. For the remaining sixth order sequences, the boundary between TST and HST cannot be detected and then none of the sequence stratigraphic models be strictly applied.

A complex array of sequences of multiple orders composes the Agua de la Mula Member. Four orders of cyclicity (third-, fourth-, fifth-, and sixth-) were described. At least a part of this cyclicity is linked to orbitally-driven climatic cycles. Based on the duration and relative frequency of occurrence, the presence of precession, obliquity, and short- and long-eccentricity cycles was demonstrated.

There is a strong correlation between the features of the sixth-order sequences and their position with respect to higher hierarchy sequences and/or depth. Interference between different orders of cyclicity is inferred in many cases. Sixth-order sequences are made of sediments deposited during different segments of the sea-level curve, according to the depth at which they formed.

Trace fossils were detected to be linked to sedimentary cycles. While identifiable traces in soft substrates (bioturbation) are common in dilution hemisequences, high density skeletal concentrations preculded its development in starvation hemisequences, where bioerosion dominates.

Four ichnoassemblages were identified and linked to sedimentary cycles. Ichnoassemblage A was found in highly bioturbated fine sandstones on top of dilution hemisequences developed in relatively high energy parts of major sedimentary sequences. It has features of the Skolithos ichnofacies (Seilacher 1967) as well as of deeper settings. Ichnoassemblage B is typical of intermediate parts of dilution hemisequences into mejor HSTs, under high input of terrigenous sediments. It has high diversity although this can be due to the relatively higher probability of preservation in this type of sediment alternating facies. It fits Cruziana ichnofacies (Seilacher 1967). Ichnoassemblage C consists of Chondrites and other ill defined burrows that characterize sediments poor on oxygen content, found in the basinal dark mudrocks of the first major MFZ and HST, and in many other positions, some decimeters below the sediment/water interface. Ichnoassemblage D corresponds to the Trypanites ichnofacies. Further refinement can be done: the Entobia ichnosubfacies is present in the early part of starvation hemisequences developd under high energy, as well as starvation hemisequences developed in proximal offshore settings when large pieces of hard substrate were available. Gnathichnus ichnosubfacies in Agua de la Mula Member characterizes late starvation sediments, with increasing terrigenous input, or offshore starvation hemisequences without large hard substrates. Bioerosion in shells deposited in offshore settings apparently depends not only on depth but also on the position within sedimentary sequences which, in turn, governs the rate of sedimentation, and finally on the availability of large pieces of hard substrates for the settling of macroboring fauna. *Spongeliomorpha suevica* occurs usually just below transgressive surfaces, on the top of dilution hemisequences in which a low sedimentation rate is expected to produce a firm substrate. Association between sequence stratigraphy and trace fossils was thus demonstrated for both, burrows in siliciclastic sediments and borings in shell-rich starvation hemisequences.

112 samples with 22,572 individuals were grouped in fifteen fossil associations and a single assemblage. The benthic associations and the assemblage reflect the interaction of different factors, the most important being age, position in major, medium and sixth order (starvation/dilution) sequences and, relation to sequence stratigraphic position, depth, oxygen availability, rate of terrigenous input, water agitation, and substrate conditions, in particular density of hard parts on the seafloor. These fossil associations represent the first paleosynecologic approach for the Lower Cretaceous of the Neuquén Basin. Delicate evidence of biotic interactions, e.g. drilling predation, crab marks, fish bite, nestling, etc., were recorded in the excelently preserved fossil remains studied here.

The Agua de la Mula Member in the center of Neuquén Province does not have evidence of long-term anoxia. This fact is based on the analysis of facies (chapter 5), trace fossils (chapter 7) and paleoecology (chapter 8). Two important packages of bituminous black-shales were described. It is proposed here that the “Spitidiscus” black shale (Tyson et al. 2005) was not deposited under anoxic to dysoxic conditions as is considered in the literature (Spalletti et al. 2001b). Evidence (i.e. bioturbation, presence of benthic macrofauna) put forth in the present study indicates that the so-called “Spitidiscus” black shale probably did not experience oxygen depletion at any time. Instead, dysoxia and anoxia a few centimetres below the sediment-water interface can be deduced from the organic-rich nature of the sediments, the scarcity of infaunal species and the presence of lucinid bivalves, adapted to live in anoxic sediments.

Diffetent types of organic build-ups were described in this study: oyster, oyster/serpulid, serpulid, foraminifer and coral reefs. A common factor to all them is the availability of hard substrates, related to a reduced rate of sedimentation. Conversely, availability of nutrients, depth and water agitation varied among the different examples. Agglutinating foraminifers identified as *Placopsilina* sp. built small constructions at some levels, usually in high densities, originating tabular accummulations, always in the late starvation hemisequence. Characteristically, they develop in the mixed-siliciclastic ramp system of Chapter 5. Moderate mud input and low energy, and hence high availability of nutrients on the seafloor seem to have played a role in the growth of these constructions.

Neocomian oyster and serpulid patch reefs of the Neuquén Basin are inferred to have been deposited in marine habitats with normal salinity, after careful observation of the sedimentologic, paleoecologic and stratigraphic evidence associated to build-ups studied in this work, as well as observations of examples from the Valanginian Middle Member of the Mulichinco Formation made by the author of this dissertation. This is in spite of the classical actualistic view of the development of these type of biocenoses under reduced salinity conditions (Lazo 2004; Damborenea et al. 1979). Besides, a new model for the development of this type biogenic constructions is proposed here: the factors that favoured the population explosions of oysters and serpulids were probably the high availability of stable hard substrates and nutrients, situation that occurs at the base of starvation hemisequences, especially when this contact is characterized by moderate levels of energy (like in offshore transition settings).

Small coral patch reefs inferred to have developed at middle ramp position occur close to the top of the section. These colonies grew under very low to absent terrigenous input, in medium or major MFZs.

Eutrophic conditions, inferred for the Neuquén Basin during the deposition of the Agua de la Mula Member, seem to be a plausible explanation for the lack of well-developed reef complexes. This pattern fits the global dominance of carbonate ramps observed for the Early Cretaceous. For some periods, nutrient supply seems to have been especially high, as shown by the spread of opportunistic strategies demonstrated by oyster, serpulid and foraminifer buildups. The almost complete lack of typical oligotrophic and autotrophic communities such as coral reefs represents another indication of high nutrient levels that prevailed in the Neuquén Basin during deposition the Agua de la Mula Member. Only at the top of the unit, when the basin was almost completely filled the depositional system turned into a carbonate ramp on which a coral patch-reef complex developed.

Vertical pattern of benthic faunal replacement have been documented, most of them correlated with the sedimentary sequences. This pattern is somewhat distorted by the presence of lower hierarchy sequences nested into the major ones, that provoked zigzagging depth and habitat changes. Smaller scale, middle hierarchy sequences and starvation/dilution sequences also develop expectable patterns of faunal replacement. Besides, the detection of an alternation of starvation/dilution sequences interpreted as the expression of obliquity and preccesion cycles of the Milankovitch band is also followed by an alternation of different benthic associations.

Sediments in the Agua de la Mula Member are of two kinds: siliciclastic-dominated (dilution hemisequences) and condensed (limestones or mixed siliciclastic-carbonate, i.e. starvation hemisequences). Siliciclastic facies are barren or have only scarce remains of partially dissolved shells. Very exceptionally skeletal concentrations are found on top of dilution hemisequences in siliciclastic facies. In turn, condensed facies usually contain abundant fossil invertebrates. The primary absence of marine shelly fauna in the siliciclastic sediments can be discarded.

The majority of the skeletal concentrations in the Agua de La Mula Member of the Agrio Formation are restricted to the base of the starvation/dilution (sixth order) sequences. These concentrations are always more or less amalgamated. Thin shell pavements, single tempestites, etc, are completely absent. Shells belong mainly to molluscs, secondarily to serpulid polychaetes, and subordinately to foraminifers, bryozoans, scleractinian corals, echinoderms, and rare crustaceans. Among the molluscs, the bivalves are far the most abundant element. Gastropods are abundant in particular beds. Ammonites and scaphopods are third in rank abundance.

Taphonomic evidence indicate that almost all the shell beds are mostly composed by autochthonous or parautochthonous fossils, product of variable degree of reworking, but little transport. Mixing of faunal elements from probably unrelated communities was detected in a few cases of transgressive lag materials, restricted to early starvation beds deposited close to major sequence boundaries.

The time needed for the deposition of every shell bed surveyed in this study was measured with precission. The degree of time-averaging of these shell beds is inferred to be moderate to low, like in the case of the "within-habitat assemblages" of Kidwell and Bosence (1991). Skeletal concentrations of associations A, B, D, E, K, N, and P, correspond to complete starvation hemisequences. Considering a 20,000 years for the deposition of a complete sixth-order (or starvation-dilution) sequence, the starvation hemisequences and the skeletal concentrations embedded into them comprise no more than a few thousand years (from the beginning of the transgression up to the early part of the next regression). Nevertheless, little environmental change is envisaged to have happened during the period involved, based on the paleoenvironmental interpretation. The remaining associations and assemblage comprise less than that amount of time as was proved the strata containing the shell beds correspond to parts of a single starvation hemisequence (i.e. associations C, F, G, H, I, J, L, M, and O).

Based on taphonomic and taxonomic features of the fossils, as well as on stratigraphic and sedimentologic observations, the skeletal concentrations of the Agua de la Mula section were classified into five types. In type 1 shell beds loosely packed skeletal concentrations accumulated in the context of TST, MFZ and early HST of the first third order sequence, in basinal to outer ramp settings. The shells are excellently preserved. The coquinas comprise complete starvation hemi-sequences of the fossil association A. The benthic fauna accumulated as a combined product of low net sedimentation, low rate of shell destruction and high preservation potential. Type 2 shell beds differ from the former in having proofs of deposition in more agitated, distal offshore settings, at late TSTs and early HSTs of major sequences. These shellbeds are very common in the section, usually comprise complete starvation hemisequences, are moderate time-averaged and have evidence of little environmental condensation. Type 3 shell-beds consist of disperse- to loosely-packed skeletal concentrations embedded in dilution hemisequences, inferred to correspond to communities that lived during the transgression in regressive sediments. Shells are either of originally calcitic composition or internal moulds, lack encrustation and bioerosion, and are usually articulated and in life position. Samples mostly correspond to association C, and were deposited in the LST-2 and early TST-2 in the section AML. The facies holding the shell beds are shoreface sandstones, which subsequently became completely bioturbated after having been flooded. Type 3 shell beds correspond to shell bed type I of Kidwell (1985). It is inferred that diagenetic dissolution of shells took place due to pore waters undersaturated with respect to calcium carbonate. Type 4 shell beds are more complex and give the chance of refining aspects of the environmental and stratigrapchic context of its genesis. Two different hypothesis were proposed for the depositon of this type of shell bed. While types 1 and 2 are common in outer ramp to basinal settings, and type 5 in shoreface (inner ramp) ones, type 4 shell beds characteristically develped in intermediate scenarios, in which vertical changes in environmental prameters (chiefly water energy) were significant as were also taphonomic and paleoecologic aspects of the fossils. Most of the remaining fossil associations correspond to one of the suptypes of type 4 shell beds. As a whole, type 4 shell beds comprise the complete starvation hemisequence and can be subdivided into three parts. Type 4A or early starvation shell bed deposited under the influence of fair weather and storm waves, and present high degrees of breakage and disarticulation, and enrichment in large and thick-shelled elements. Type 4B correspond to the maximum flooding of the starvation-dilution sequence, equivalent to the Abbott’s mid-cycle condensed shell bed (Abbott 1997). Highest degrees of bioerosion and encrustation are found at this subtype. Build-ups of serpulids, oyster and corals are especially common at this position. The environment inferred for the deposition of type 4B is the middle ramp. Type 4C is the late starvation shell bed, deposited already in the regression systems tract of the starvation-dilution sequence. High densities of articulated and very well preserved fossils characterise these shell beds, inferred to have been deposited in the middle to outer ramp, under increasing input of siliciclastic sediments, although in an environment still rich in calcium carbonate. Type 5 shell beds correspond to starvation hemisequences completely deposited in high energy inner (to middle) ramp settings. The skeletal concentrations correspond to the early, and in some cases, poorly developed middle starvation shell beds. The preservation of the fossils is the worst in this type of shell bed.

Vertical patterns of shell bed types are described and interpreted in terms of inferred settings of the sequence stratigraphic model, that is usually very well fitted. The fossilization process of the marine calcareous shells is modelize as a series of steps, each of one figured as a window that a particular shell must pass to be exposed to the factors associated with the next step. These windows are the “environmental window”, the “destruction window”, the “burial window” and finally the “diagenetic window”. The diagenetic window is in this process crucial for being the last one.

Evidence from this study supports stating carbonate dissolution as the primary control on the development of shell beds. Dissolution/lithification of carbonates is indirectly controlled by sequence stratigraphy at different levels: in sixth order sequences there is an alternation of well-lithified, starvation hemisequences and poorly-lithified dilution hemisequences. Higher hierarchy cyclicity imposes other biases generating partial dissolution conditions even in starvation hemisequences. This pattern can be explained with the model described in Fürsich and Pandey (2003) and already mentioned in Fürsich (1982), in which high saturation of pore water with respect to calcium carbonate during the transgression results in early lithification and corresponding preservation of the skeletal concentrations. The calcium carbonate stems from the dissolution of shells that colonized the bottom during the regression phase and at the beginning of the transgression. Carbonate is migrating from the more argillaceous layers, where skeletal matter is dissolved, to the layers richer in carbonate, where calcite cement is precipitated. As a result, the layers initially richest in carbonate are further enriched (Fischer 1986). The two sides of the process are dissolution of skeletal elements during regression and preservation during transgression.

A complexive understanding of the development of life in the geological past and all the fenomena involved in the formation of a fossil deposit, i.e., paleoecology and taphonomy, implies the survey of every kind of evidence at hand. Organisms are affected by biotic factors like temperature, oxygen and nutrients availability, sedimentation and water energy. In turn, the fossilization of hard parts depend on the biostratinomic and diagenetic history of the deposits holding the fossils. Last but not least, the fidelity of the fossil record of past communities is linked to the degree of post mortem distortion (transport and destruction) and the time involved in the deposition of the bed. All these factors, those affecting living communities as well as those influencing the formation of shell beds are directly or indirectly linked to the processes called to explain the sequence stratigraphic model. Frequently during the writing of this dissertation the author found himself troubled with finding the place into the text to describe and interpret sedimentological, stratigraphic, icnologic, taphonomic and paleosinecologic aspects of the sedimentary succession. The order of the different chapters were changed several times, following the need of using evidence written in other chapters as a base to write a particular section. This fact shows that all these sources of evidence complement each other in the interpretation of the geobiohistory of a particular geological unit and, if all together, the task of developing in separated chapters is hard and no natural.

Plates

Plate 1.

Fig. 1. *Lockeia siliquaria* and *Protovirgularia* isp. Section BAL at 215 m. x 1. Fig. 2. Burrows indet. Section BAL at 215 m. x1. Fig. 3. *Gyrochorte* isp. And unidentified trails. Section BAL at 215 m. x 1. Fig. 4. *Gyrochorte* isp. And unidentified trails. Section BAL at 215 m. x 1. Fig. 5. *Bolonia lata*. Section BAL at *ca*. 400 m. x ½. Fig. 6. Upper surface of a carbonate concretion encrusted with serpulids, small oysters and scleractinian corals. Borings are not visible. Section AML at 128 m. x 1.5. 7. Carbonate concretion with two *Gastrochaenolites* isp. Section BAL at 142 m. x 1. Fig. 8. Shell fragment of *Cucullaea gabrielis* with two specimens of *Gastrochaenolites* isp. In both cases shells of inhabitants of the holes were preserved. The boring at the right shows shells of at least two generations. Section BAL at 277 m. Scale in mm.

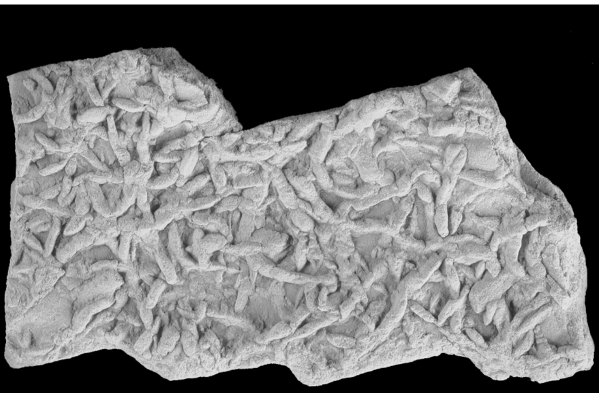

1

2

3

4

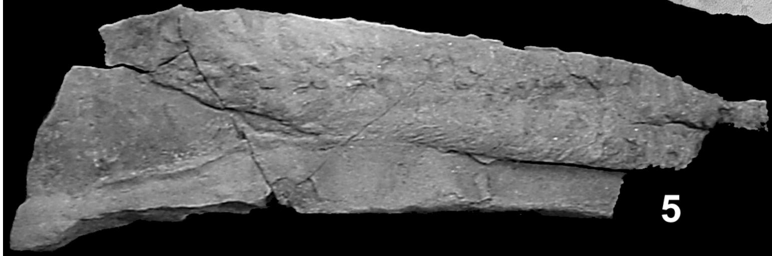

5

7

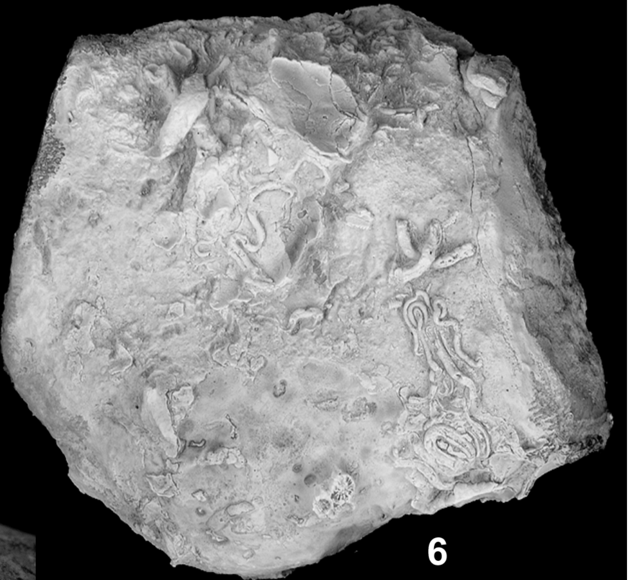

6

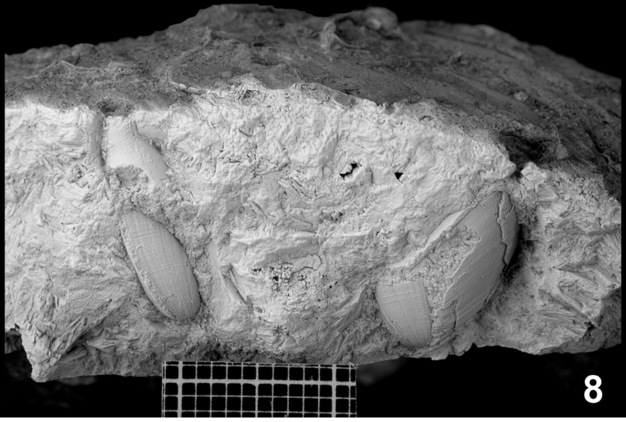

8

Plate 2.

Fig. 1. *Chondrites* isp. on upper surface of medium scale symmetrical wave ripples (facies S-FS-W). Section BAL at *ca*. 400 m. Coin diameter = 23 mm. Fig. 2. *Skolithos* isp. in bioturbated fine-grained sandstones (facies S-FS). Section AML at *ca.* 237 m. Scale segments = 10 mm. Fig. 3. *Spongeliomorpha suevica* in bioturbated fine-grained sandstones (S-FS facies). Agrio del Medio locality, close to section BAL. Lens cap diameter = 50 mm. Fig. 4. Paired openings of *Arenicolites*? isp. in bioturbated fine-grained sandstones (S-FS facies). Section BAL at 210 m. Lens cap diameter = 50 mm. Fig. 5. *Bergaueria* isp. Lower surface of a fine-grained sandstone level of facies S-FS-W. Section BAL at 390 m. Lens cap diameter = 50 mm. Fig. 6. *Spongeliomorpha suevica*. Regular maze at the lower surface of a bioturbated fine-grained sandstone tempestitic bed at 395 m. Section BAL. Lens cap diameter = 50 mm. Fig. 7. *Diplocraterion saxicava*? developed between two storm beds. Section BAL at 395 m. Lens cap diameter = 50 mm. Fig. 8. Thick burrow indet, connecting two fine-grained sandstone tempestitic beds. Section BAL at 395 m. Lens cap diameter = 50 mm.


1


2


3


4

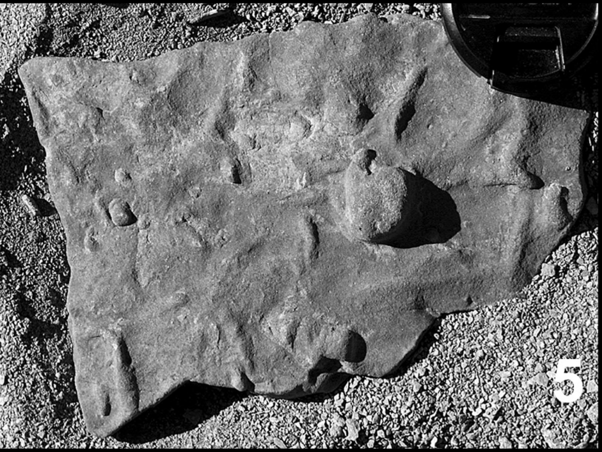
5


6


7


8

Plate 3.

Fig. 1. Fine-grained sandstone with large-scale low-angle cross stratification (S-FS-C facies). Section BAL at 510 m. Black bar length *ca*. 50 cm. Fig. 2. Bioturbated fine-grained sandstone (S-FS facies). Hammer head marks the boundary between the top of a dilution hemisequence (with S-FS facies) and the base of the subsequent starvation hemisequence. Section BAL at 251 m. Hammer length = 33,5 cm. Fig. 3. Heavily bored shell of *Cucullaea gabrielis*, with *Gastrochaenolites* isp., *Trypanites* isp. and other borings. Section AML at 269 m. Scale segments = 10 mm. Fig. 4. *Steinmanella vacaensis* shell with abundant *Gastrochaenolites* borings. *Ceratostreon* specimens attach the shell at different places. Section BAL at 368 m. Lens cap diameter = 50 mm. Fig. 5. Contact between the Avilé and the Agua de la Mula members. Section BAL. Fig. 6. Contact between the Agrio and the Huitrín formations. Section BAL. Fig. 7. *Myoconcha transatlantica* specimen with a serpulid and oyster buildup on each valve. Bar length = 1 cm. Section BAL, loose material. Fig. 8. Section BAL at 328 m. The lower part of the photography corresponds to the top of the middle starvation deposit. Hammer length = 33,5 cm.


1


2

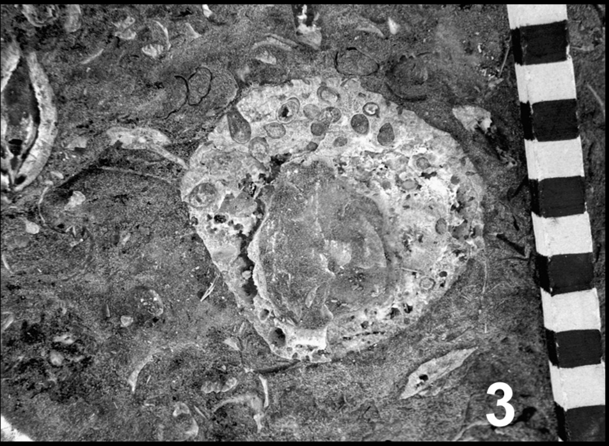
3


MINOLTA
4

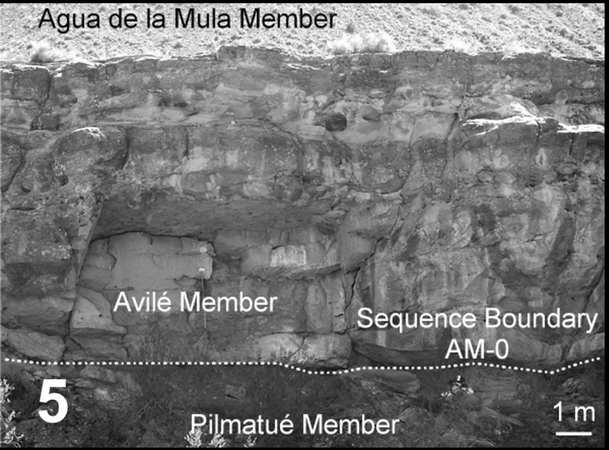
Agua de la Mula Member
Avilé Member
Sequence Boundary AM-0
5
Pilmatué Member
1 m

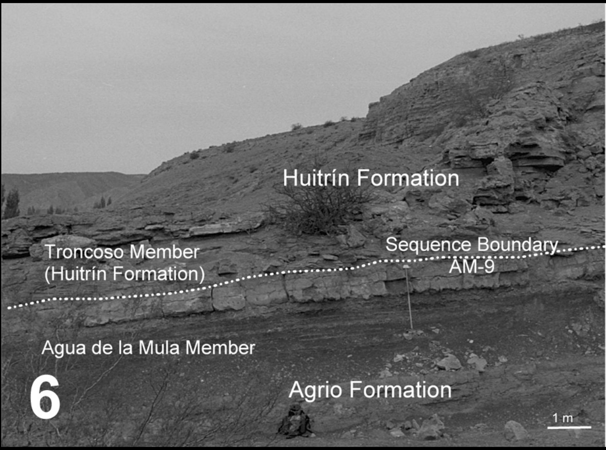
Huitrín Formation
Troncoso Member (Huitrín Formation)
Sequence Boundary AM-9
Agua de la Mula Member
6
Agrio Formation
1 m


7


8

Plate 4.

Fig. 1. *Bolonia lata* on top of a bioturbated fine-grained sandstone. Section BAL at 210 m. Lens cap diameter = 50 mm. Fig. 2. *Protovirgularia* isp. and *Lockeia siliquaria*. Lower surface of sandstone bed with ripples on top (S-HET 2-3 facies). Section BAL at 428 m. Lens cap diameter = 50 mm. Fig. 3. *Spongeliomorpha suevica* at the base of a major transgressive surface. Section BAL at 403 m. Lens cap diameter = 50 mm. Fig. 4. Small desiccation cracks close to the base of section BAL. Lens cap diameter = 50 mm. Fig. 5. Large desiccation cracks close to the base of BAL section. Lens cap diameter = 50 mm. Fig. 6. Rib and furrow structures in fine sandstone beds at the base of BAL section. Lens cap diameter = 50 mm. Fig. 7. Mudrocks (Facies 1.1) with large carbonate concretions. Section AML at 129 m. Hammer length = 33,5 cm. Fig. 8. Sandy siltstones facies (S-SaS). The sharp surface separates the top of a dilution hemisequence composed of S-SaS facies (below) and the base of the following starvation hemisequence with *Aetostreon* sp. shells concentrated (above). Section BAL at 141 m. Hammer length = 33,5 cm.


1


2


3


4


5


6


7


8

Plate 5.

Fig. 1. Coarsening/shallowing-upwards facies succession, from mud- to sand-dominated coarsely interlayered bedding (S-CIB facies). BAL section from 170 to 210 m from base. Black bar length *ca*. 3 m. Fig. 2. Mud-dominated coarsely interlayered bedding facies. BAL at *ca*. 170 m. Hammer length = 33,5 cm. Fig. 3. coarsely interlayered bedding facies type 4. BAL at 180 m. Hammer length = 33,5 cm. Fig. 4. Heterolithic bedding types 1 to 3 from base to top of the picture. Intercalations of S-FS-W and S-FS-H towards the top. BAL section at 400 m. Hammer length = 33,5 cm. Fig. 5. Fine-grained sandstone with wave ripples (S-HET-2 facies). BAL section 400 m from base. Hammer length = 33,5 cm. Fig. 6. S-HET-1 facies with low-angle cross-lamination (S-FS-H facies) and S-FS-W facies on top. Hammer length = 33,5 cm. Fig. 7. Hummocky cross stratification. BAL section at *ca*. 205 m. Scale segments = 10 mm. Fig. 8. Fine-grained sandstone with climbing ripples. BAL section at *ca*. 510 m. Lens cap diameter = 50 mm.


1


2

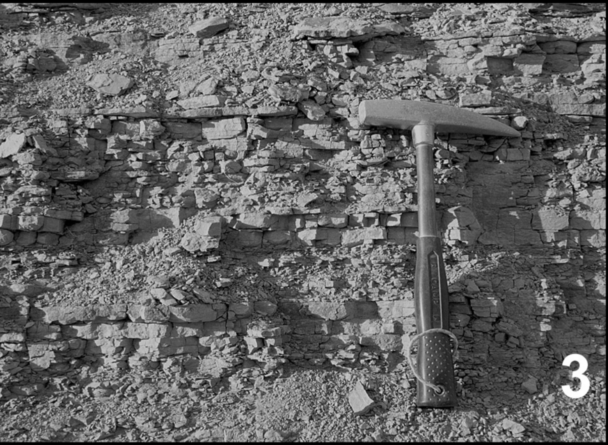
3


4


5


6


7

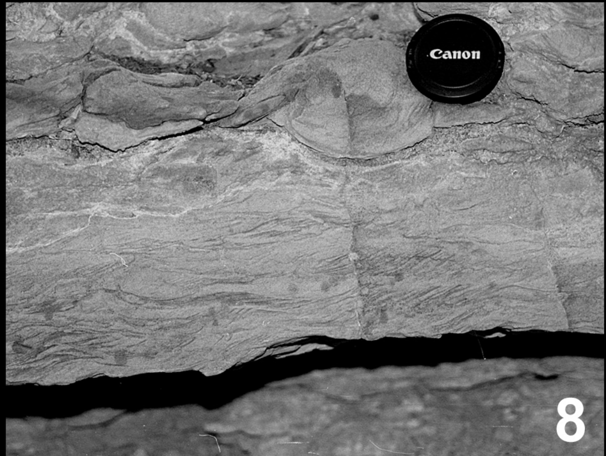

8

Plate 6.

Fig. 1. Large unidentified galleries. 465 m in section BAL. Hammer length = 33,5 cm. Fig. 2. *Skolithos*? isp. openings in fine sandstones with desiccation cracks at the base of BAL section. Bedding plane view. Lens cap diameter = 50 mm. Fig. 3. Small channel filled with medium to coarse-grained sandstone (left) cutting fine sandstones with small ripples. Base of section BAL. Lens cap diameter = 50 mm. Fig. 4. *Spongeliomorpha suevica*? Irregular maze at the lower surface of a medium sequence boundary. Section BAL at 485 m. Lens cap diameter = 50 mm. Fig. 5. Scleractinian patch reefs developed above an early transgressive bed. Patches diameter around 3 to 4 meters. Section BAL at 503 m. Fig. 6. *Planolites* isp. on top of a bioturbated fine-grained sandstone. Section BAL at 251 m. Lens cap diameter = 50 mm. Fig. 7. Section BAL at 321 m. Note the early starvation bed (onlap shellbed), dark coloured and with abundant disarticulated bivalve shells, overlying the top of the dilution hemisequence of the previous starvation/dilution sequence. Fig. 8. Section AML ca. 250 (dark-red bed to the left of the photography) to 350 m (to the right) showing high frequency of starvation-dilution sequences.


1


2


3


4


5


6


7


8

Plate 7.

Fig. 1. Large oyster and serpulid patch reef in section AML at 281 m. a. View of the reef. Dashed line outlines the buildup. b. Detail of the contact between the middle starvation hemisequence below, and the encrusting fauna. Scale segments = 10 mm. c. Segment of the section corresponding to the reef. For key of symbols see Appendix-Fig. 3.

Fig. 2. Stacking of several incomplete starvation-dilution sequences indicating enhanced starvation in section AML. a. Photograph of five starvation hemisequences stacked in a few meters. Sequence of TSTs and RSTs proposed indicated with triangles at the left. b. Segment of the section corresponding to the stacked beds. Note another stacking of incomplete starvation-dilution sequences a few meters below. For key of symbols see Appendix-Fig. 3.

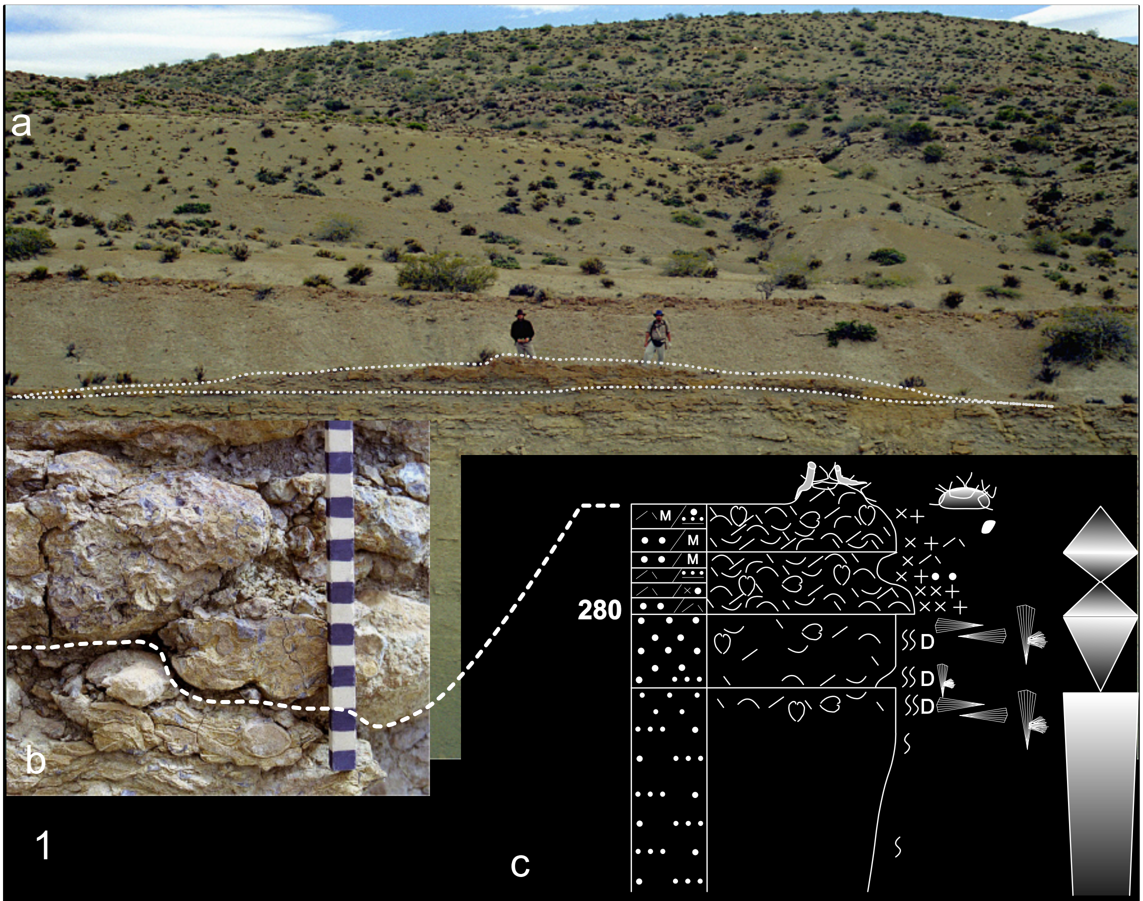
a
b
c
280
M
D
1

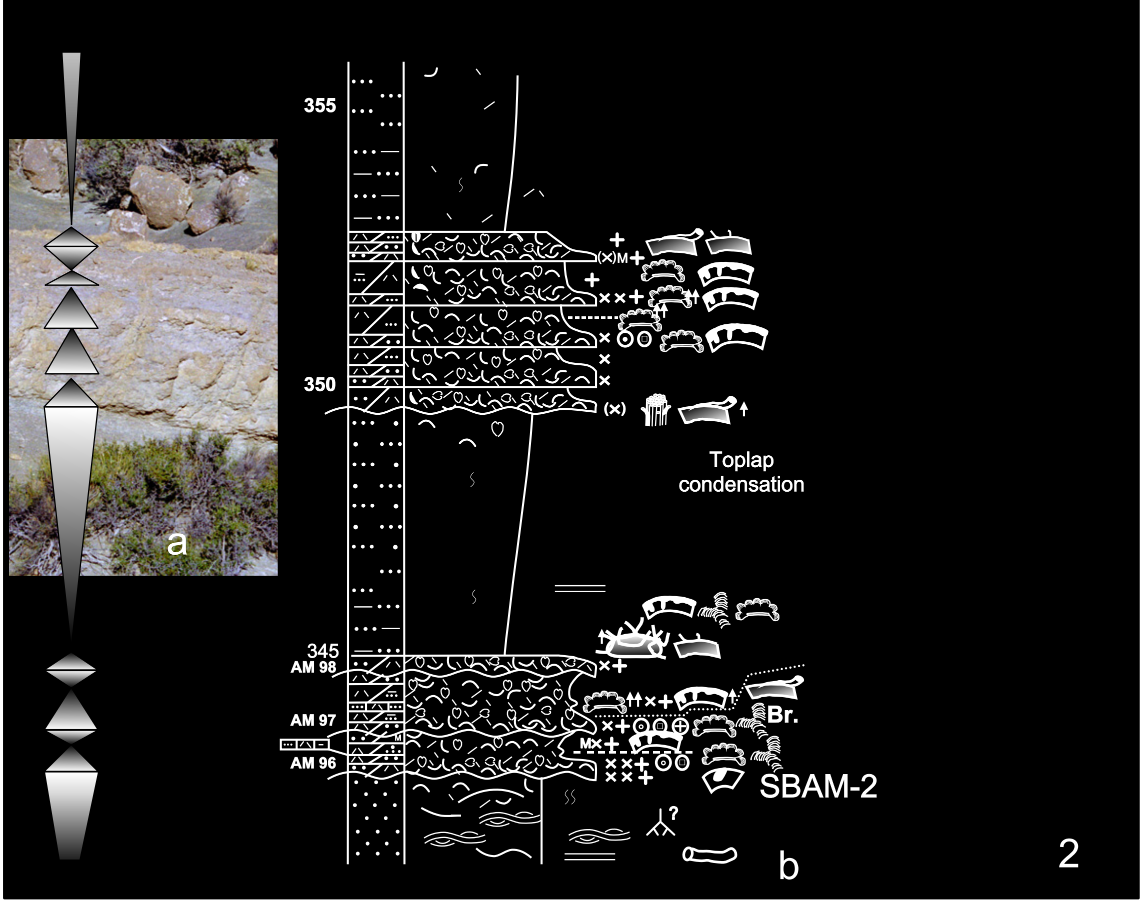
355
350
345
AM 98
AM 97
AM 96
M
Toplap
condensation
Br.
SBAM-2
a
b
2

Plate 8. All figures in natural size unless indicated. All bivalve specimens articulated except figs. 20, 21 and 23-25.

Fig. 1, *Placopsilina* sp. (x 2). Section AML at 390 m. Fig. 2, *Placopsilina* sp. growing on *Ptychomya* sp. A. Section BAL at 295 m. Fig. 3, *Placopsilina* sp. Buildup. Section AML at 371 m. Fig. 4, Small coral colony growing on a carbonate concretion. Section AML at 128 m. Fig. 5, *Cerithium* sp. A. Section BAL at 498 m. Fig. 6, *Cerithium* sp. B. Section BAL at 498 m. Fig. 7, *Rhabdocolpus* sp. A. Section BAL at 109 m. Fig. 8, *Poasia* sp. B. Section BAL at 498 m. Fig. 9, *Protohemichenopus neuquensis* (Camacho, 1953). Section BAL at 35 m. Fig. 10, *Dimorphosoma* sp. Section BAL at 402 m. Fig. 11, *Pictavia* sp. A. Section BAL at 43 m. Fig. 12, *Pictavia* sp. B. Section BAL at 505 m. Fig. 13, *Confusiscala* sp. Section BAL at 14 m. Fig. 14, *Bathraspira* sp. A. Section BAL at 20 m. Fig. 15, *Bathraspira* sp. C. Section AML at 69 m. Fig. 16, *Palaeonucula* sp., left valve view. Section AML at 128 m. Fig. 17, *Cucullaea gabrielis* (Leymerie, 1842), left valve view. Section AML, loose specimen. Fig. 18, *Grammatodon securis* (Leymerie, 1842), left valve view. Section AML at 69 m. Fig. 19, *Grammatodon* (*G.*) sp., left valve view. Section BAL at 402 m. Fig. 20, Grammatodontinae sp. A, right valve. Section BAL at 123 m. Fig. 21, Crenellinae sp. A, left valve. Section BAL at 166 m. Fig. 22, *Modiolus ligeriensis* (d'Orbigny, 1943), left valve view. Section BAL at 414 m. Fig. 23, *Mimachlamys robinaldina* (d'Orbigny, 1847), left valve. Section BAL at 306 m. Fig. 24, Anomiidae sp. x 2., left valve. Section BAL at 369 m. Fig. 25, *"Chlamys" puzoziana* (Matheron, 1842), left valve. Section BAL at 374 m. Fig. 26, *Isognomon lotenoensis* (Weaver, 1931); a, left valve, b, hinge of left valve and incomplete right valve. Section BAL at 361 m.

1

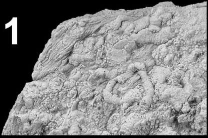

3

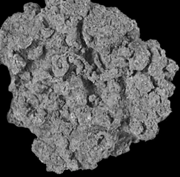

4

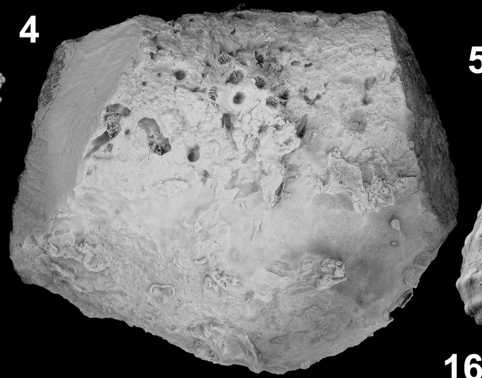

5

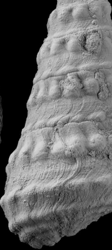

6

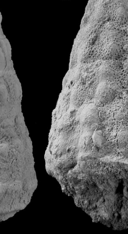

2

10

12

16

18

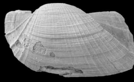

7

8

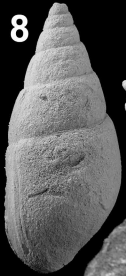

9

11

14

15

13

19

20

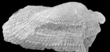

21

22

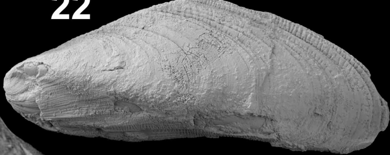

23

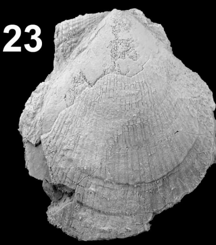

17

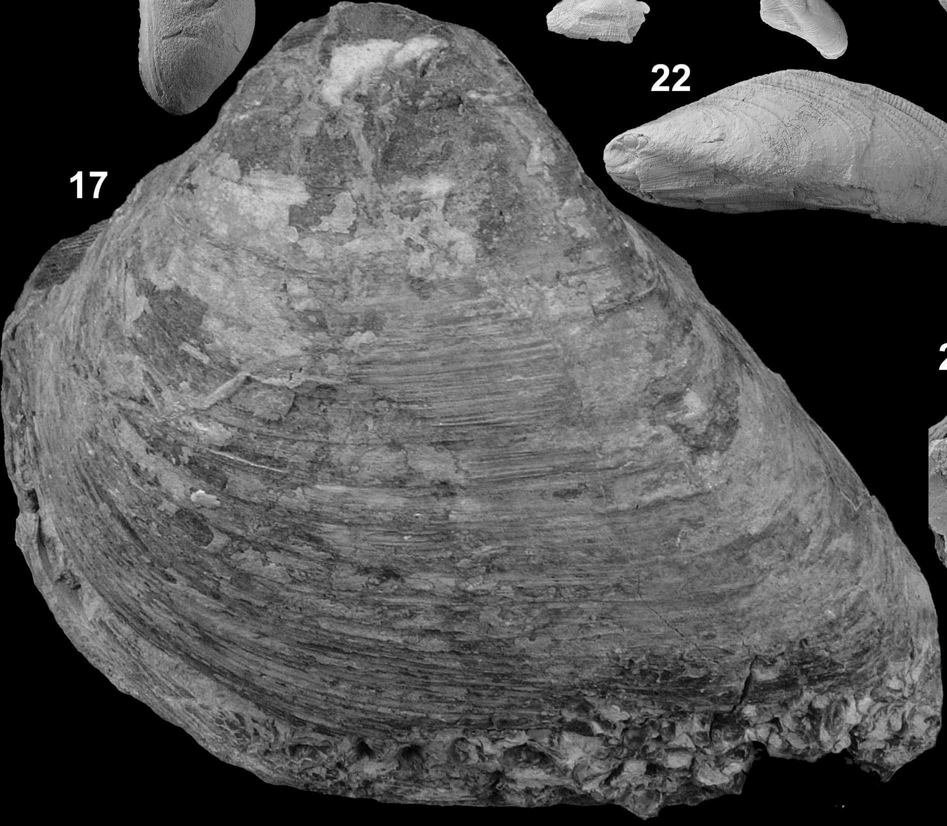

24

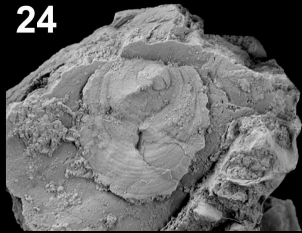

26a

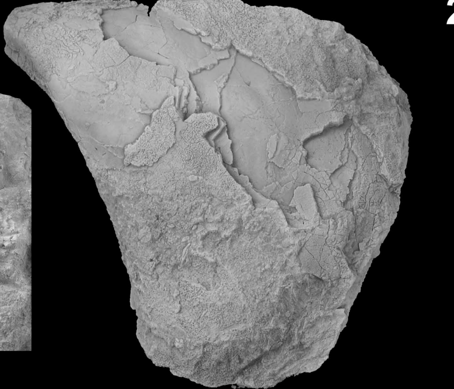

26b

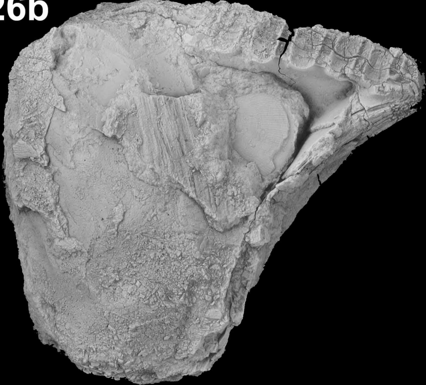

25

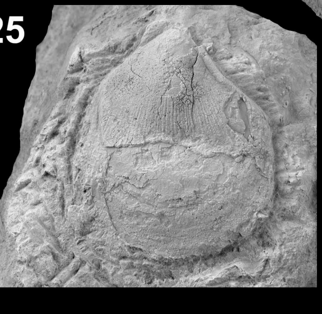

Plate 9. All figures in natural size unless indicated. All specimens articulated.

Fig. 1, *Pinna robinaldina* (d'Orbigny, 1844). Section AML at 251 m. Fig. 2, *Gervillella aviculoides* (J. Sowerby, 1814), right valve view. Section BAL at 277 m. Fig. 3, *Acesta* sp., left valve view. Section BAL, loose specimen. Fig. 4, *Inoceramus curacoensis* (Weaver, 1931), left valve view. Section BAL at 252 m. Fig. 5, *Isognomon* sp. A., right valve view. Section BAL at 361 m. Fig. 6, *Ceratostreon minos* (Coquand, 1869); a, right valve view. Section BAL, loose specimen; b, small *Ceratostreon* buildup on ammonite fragment. Section BAL at 349 m.

1

2

3

4

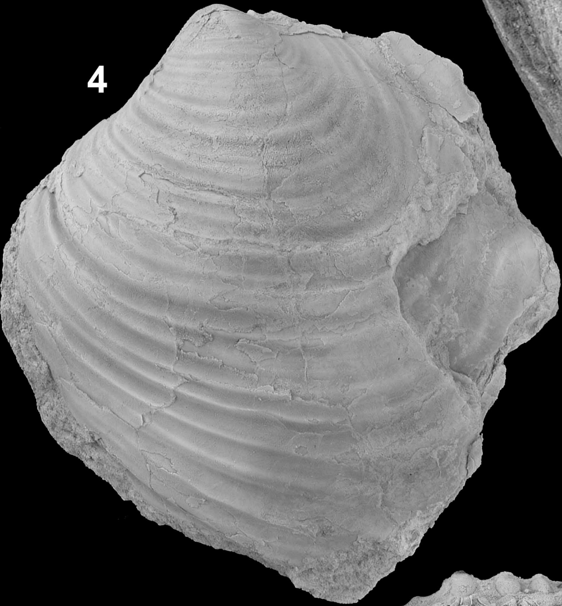

5

6a

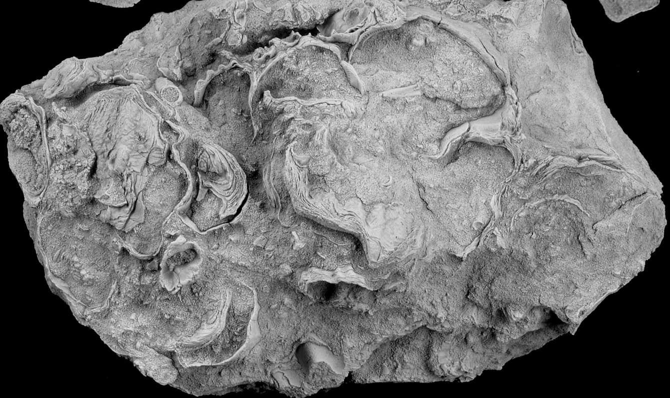

6b

Plate 10. All figures in natural size unless indicated. All specimens articulated.

Fig. 1, *Aetostreon* sp.; a, posterior view, b, upper view of right valve. Section BAL at 124 m. Fig. 2, *Gryphaeostrea* sp. 1, dorsoposterior view. Section AML, loose specimen. Fig. 3, *Gryphaeostrea* sp. 2, upper view of right valve. Section BAL at 124 m. Fig. 4, *Pterotrigonia (Rinetrigonia) coihuicoensis* (Weaver, 1931), right valve view. Section BAL at 306 m. Fig. 5, *Pterotrigonia (Rinetrigonia)* sp. A, right valve view. Section BAL at 505 m. Fig. 6, *Rutitrigonia agrioensis* (Weaver, 1931), left valve view. Section BAL at 369 m. Fig. 7, *Steinmanella (Macrotrigonia) vacaensis*, left valve view. Section BAL, loose specimen. Fig. 8, *Mesomiltha*? *Argentina* (Behrendsen, 1891), left valve view; observe multiple predatory drill holes. Section BAL at 295 m. Fig. 9, *Mesomiltha*? sp A, left valve view. Section AML at 139 m. Fig. 10, *Neocrassina (Coelastarte*?*)* sp., right valve view. Section AML at 384 m. Fig. 11, *Pholadomya gigantea* (J. de C. Sowerby, 1836), left valve view. Section BAL, loose specimen. Fig. 12, *Myoconcha transatlantica* (Burckhardt, 1900), right valve view. Section BAL, loose specimen. Fig. 13 a-c, *Disparilia elongata* (d'Orbigny, 1843), different morphologies, left valves views. Section BAL at 155 m.

1a

1b

2

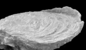

3

4

5

6

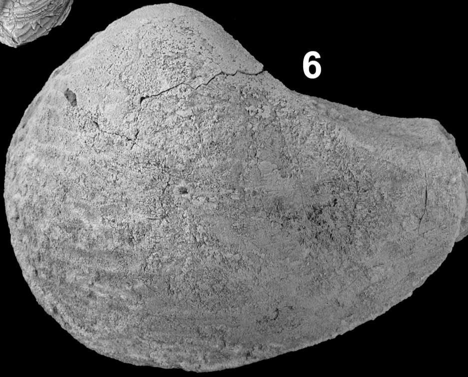

7

8

9

10

11

12

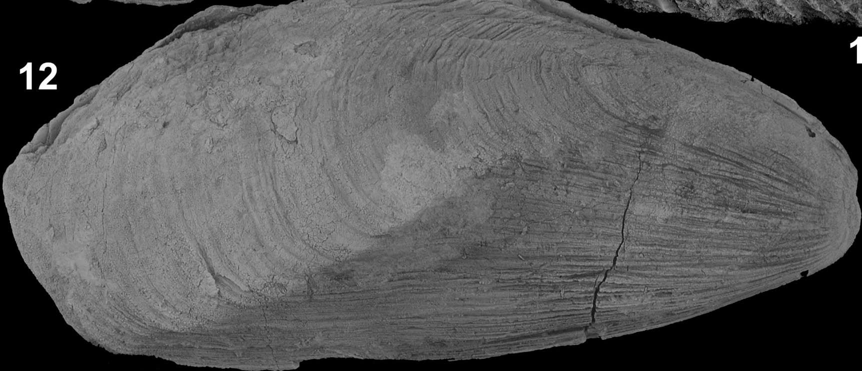

13b

13a

13c

Plate 11. All figures in natural size unless indicated. All specimens articulated.

Figs. 1-4, *Eriphyla argentina* (Burkhardt, 1900); 1, typical morphotype, right valve view. Section BAL at 231 m. 2-4 other morphologies. 2, section AML at 186 m. a, right valve view; b, left valve view. 3, section AML at 186 m. a, right valve view; b, left valve view. 4, section AML at 186 m. a, right valve view; b, left valve view. Fig. 5, Astartidae sp. A, right valve view. Section AML at 56.2 m. Fig. 6, *Protocardia* sp., left valve view. Section BAL at 505 m. Fig. 7, *Solecurtus*? *Neuquensis* (Weaver, 1931). Section BAL at 251 m. Figs. 8-13, *Ptychomya* sp A cf. *P. koeneni*. 8, left valve view. Section BAL at 295 m. 9, left valve view. Section BAL at 231 m. 10, left valve view. Section BAL at 312 m. 11, left valve view. Section BAL at 334 m. 12, left valve view. Section BAL at 361 m. 13, left valve view. Section BAL at 369 m. Fig. 14, *Ptychomya* sp. B; a, left view; b, right valveview; encrusted by serpulids. Section BAL at 505 m. Fig. 15, "*Cyprina*" sp., left valve view. Section BAL at 347 m. Fig. 16, Veneridae sp. 1, right valve view. Section BAL at 166 m. Fig. 17, Veneridae sp. 2, right valve view. Section BAL at 283 m. Fig. 18, Veneridae sp. 3, right valve view. Section BAL at 266 m. Fig. 19, *Corbulomima bodenbenderi* (Behrendsen, 1892), left valve view. Section BAL at 35 m. Fig. 20, Corbulidae sp. A, left valve view. Section BAL at 84 m. Fig. 21, *Panopea dupiniana* (d'Orbigny, 1843), right valve view. Section AML, loose specimen. Fig. 22, *Panopea gurgitis* (Brongniart, 1822), right valve view. Section AML, loose specimen. Fig. 23, *Machomya*? sp., right valve view. Section BAL 404 m.

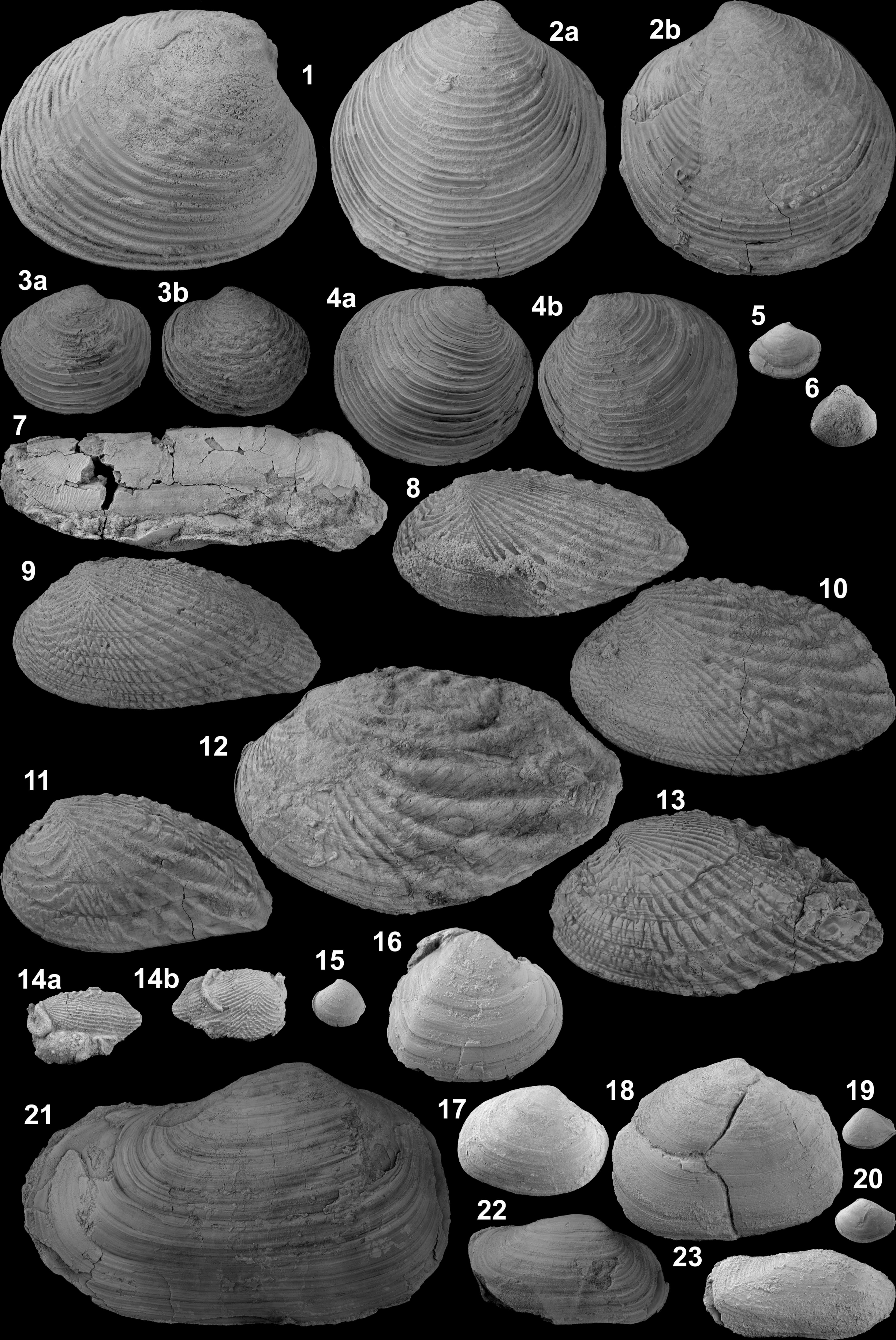
1
2a
2b
3a
3b
4a
4b
5
6
7
8
9
10
11
12
13
14a
14b
15
16
17
18
19
20
21
22
23

Acknowledgements

The acknowledgement section would be the largest of the PhD work if I wrote about the amount and quality of help I received from whom I want to acknowledge.

I am deeply indebted to my wife Marien for her continuous support of my work and her faith in me.

To Fermina, Iñaki and Arancha, my preferred projects.

My parents, César Archuby and Liliana Gliemmo who always believed in me and helped in all possible ways to develop my profession and ideals.

To Dr. Prof. Franz T. Fürsich whose patience, knowledge, and predisposition for the teaching activity made this project possible.

To Dr. Prof. Héctor Leanza who introduced me the marine mesozoic world and guided me through this project.

DAAD (Deutsche Akademischer Austausch Dienst) and CONICET (Argentinian National Council of Technologic and Scientific Research) provided grants to develop this PhD project.

To Santiago González, Martín Alarcón, Diego Balseiro, Hipólito González, whose help in the field and and lab tasks are greatly appreciated.

Dr. Prof. Carlos Cingolani, who kindly hosted my reaserach activities in the Historical Geology Chair of Natural Sciencies Faculty of the University of La Plata, Argentina.

To the Institut für Paläontologie who hosted my research and its staff who helped and enriched my work, and gave us their friendship: Markus Wilmsen, (Birgit) Sarah Niebuhr, Adam Tomasovyc, Michael and Silke Schlirf and Michael Heinze.

Daniel Poiré, Luis Spalletti, Ernesto Schwarz and Gonzalo Veiga of the Geological Research Center (Natural Sciencies Faculty of the University of La Plata, Argentina) helped in discussions about sedimentological topics of the thesis.

Valsamma and Franz Fürsich, Michael and Silke Schlirf, Markus Wilmsen and Sarah Niebuhr made our stay in Germany an exciting and enjoyable experience.

To family Mikuletz (Franky, Ale, Celes and Valen), Daniela Rais, Jeff and Carmen and Javi Schafer from Würzburg who gave us their kind friendship during our stay in Germany.

To family Roces, family Bonetto, Goethe Institut, that helped us in different way during our stay in Germany.

Everybody not explicitly named here (whom I might have forgotten) but who has contributed to the success of this study is also wholeheartedly thanked.

Reference List

Abbott, S. T. 1997. Mid-cycle condensed shellbeds from mid-Pleistocene cyclothems, New Zealand: implications for sequence architecture. *Sedimentology* **44**: 805-824.

Abbott, S. T. 1998. Transgressive systems tracts and onlap shellbeds from mid-Pleistocene sequences, Wanganui Basin, New Zealand. *Journal of Sedimentary Research* **68** (2): 253-268.

Abbott, S. T. and Carter, R. M. 1997. Macrofossil Associations from Mid-Pleistocene Cyclothems, Castlecliff Section, New Zeland: Implications for Sequence Stratigraphy. *Palaios* **12**: 188-210.

Aguirre Urreta, M. B. 1993. Neocomian ammonite biostratigraphy of the Andean Basins of Argentina and Chile. *Revista Española de Paleontología* **8** (1): 57-74.

Aguirre Urreta, M. B. 1995. *Spitidiscus riccardii* Leanza y Wiedmann (Ammonoidea) en el Hauteriviano del Neuquén. *Ameghiniana* **32** (4): 407-410.

Aguirre Urreta, M. B., Gutiérrez Pleimling, A., and Leanza, H. A. 1993. La posición estratigráfica del género *Spitidiscus* (Ammonoidea) en el Cretácico inferior de la Cuenca Neuquina. In: *XII Congreso Geológico Argentino - II Congreso de*

Exploración de Hidrocarburos Actas II, 333-338pp., Mendoza, Argentina.

Aguirre Urreta, M. B. and Rawson, P. F. 1993. The Lower Cretaceous Ammonite *Paraspiticeras* from the Neuquén Basin, west-central Argentina. *Neues Jahrbuch für Geologie und Paläontologie, Abhandlungen* **188**: 51-69.

Aguirre Urreta, M. B. and Rawson, P. F. 1997. The ammonite sequence in the Agrio Formation (Lower Cretaceous), Neuquén Basin, Argentina. *Geological Magazine* **134** (4): 449-458.

Aguirre Urreta, M. B., Rawson, P. F., Concheyro, G. A. , Bown, P. R., and Ottone, E. G. 2005. Lower Cretaceous (Berriasian-Aptian) biostratigraphy of the Neuquén Basin. In: *The Neuquén Basin, Argentina: A Case Study in Sequence Stratigraphy and Basin Dynamics*, G. D. Veiga, L. A. Spalletti, J. A. Howell, and E. Schwarz (eds.). Geological Society Special Publications, **252**, 57-81pp., London.

Archuby, F. M. 2005. Significación estratigráfica de las concentraciones esqueletales en las sedimentitas marinas del Hauteriviano- Barremiano (Cretácico Inferior). Cuenca Neuquina, Argentina. In: *16° Congreso Geológico Argentino*, E. Llambías, R. de Barrio, P. González, and P. Leal (eds.). Actas, **3**, 457-464pp., La Plata.

Bandel, K. 1999. On the origin of the carnivorous gastropod group Naticoidea (Mollusca) in the Cretaceous with description of some convergent but unrelated groups. *Greifswalder Geowissentschaftliche Beiträge* **6**: 143-175.

Barnard, T. 1958. Some Mesozoic adherent foraminifera. *Palaeontology* **1** (2): 116-124.

Behrendsen, O. 1891. Zur Geologie des Ostabhanges der argentinischen Cordillere. Part I. *Zeitschrift der Deutschen geologischen Gessellschaft*: 369-420 + 3 Pl.

Behrendsen, O. 1892. Zur Geologie des Ostabhanges der argentinischen Cordillere. Part II. *Zeitschrift der Deutschen geologischen Gessellschaft*: 1-42 + 4 Pl.

Berger, A. and Loutre, M. F. 1989. Pre-Quaternary Milankovitch frequencies. *Nature*

342: 133.

Brenchley, P. J. and Harper, D. A. T. 1998. *Paleoecology. Ecosystems, environments and evolution.* Chapman & Hall, 402pp.; London, UK.

Bromley, R. G. 1994. The palaeoecology of bioerosion. In: *The Palaeobiology of Trace Fossils*, S. K. Donovan (ed.). John Wiley & Sons, 134-154pp., UK.

Bromley, R. G. and Ekdale, A. A. 1984. Chondrites: a trace fossil indicator of anoxia in sediments. *Science* **224**: 878-874.

Burchette, T. P. and Wright, V. P. 1992. Carbonate ramp depositional systems. *Sedimentary Geology* **79**: 3-57.

Burkhardt, C. 1900. Profils geologiques transversaux de la Cordillere Argentino-Chilienne. *Museo de La Plata. Anales, Sección Geología y Mineralógica* **2**: 1-136.

Camacho, H. H. 1953. Algunas consideraciones sobre los "Aporrhaidae" fósiles argentinos. *Revista de la Asociación Geológica Argentina* **8**: 183-194.

Camacho, H. H. and Riccardi, A. C. 1978. Invertebrados. Megafauna. *Relatorio Geología y recursos minerales de Neuquén* **Relatorio**.

Casey, R. 1952. Some genera and subgenera, mainly new, of Mesozoic heterodont lamellibranchs. *Proceedings of the Malacological Society of London* **29** (4): 121-176.

Catuneanu, O. 2002. Sequence stratigraphy of clastic systems: concepts, merits, and pitfalls. *Journal of African Earth Sciences* **35**: 1-43.

Cecca, F., Marini, A., Pallini, G., Baudin, F., and Begouen, V. 1994. A guide-level of the uppermost Hauterivian (Lower Cretaceous) in the pelagic succession of Umbria-Marche Appennines (Central Italy): the Faraoni Level. *Rivista Italiana di Paleontologia e Stratigrafia* **99** (4): 551-568.

Chavan, A. 1969. Superfamily Lucinacea Fleming, 1828. In: *Treatise on invertebrate paleontology*, R. C. Moore and C. Teichert (eds.). University of Kansas Press &

Geological Society of America, N491-N518pp., Lawrence.

Coe, A. L. and Church, K. D. 2003. Sequence Stratigraphy. In: *The Sedimentary Record of Sea-Level Change*, A. L. Coe (ed.). Cambridge University Press, 57-98pp., Cambridge.

Cox, L. R. and Hertlein, L. G. 1969. Superfamily Pinnacea Leach, 1819. In: *Treatise on invertebrate paleontology*, R. C. Moore and C. Teichert (eds.). University of Kansas Press & Geological Society of America, N281-N285pp., Lawrence.

Damborenea, S., Manceńido, M. O., and Riccardi, A. C. 1979. Estudio paleontológico de la Formación Chachao. Informe inédito. Y.P.F. Buenos Aires

Dodd, J. R. and Stanton, R. J. Jr. 1981. *Paleoecology, Concepts and Applications*. John Wiley & Sons, 559pp.; New York.

Dott, R. H. and Bourgeois, J. 1982. Hummocky stratification: Significance of its variable bedding sequences. *Geological Society of America, Bulletin* **93**: 663-680.

Duke, W. L. 1985. Hummocky cross-stratification, tropical hurricanes, and intense winter storms. *Sedimentology* **32**: 167-194.

Duke, W. L. 1987. Discussion. Hummocky cross-stratification, tropical hurricanes, and intense winter storms. *Sedimentology* **34**: 333-359.

Dunham, R. J. 1962. Classification of carbonate rocks according to depositional texture. In: *Classification of carbonate rocks. A symposium.*, W. E. Ham (ed.). Amer. Ass. Petrol. Geol. Memoir, 108-121pp., USA.

Einsele, G., Ricken, W., and Seilacher, A. 1991. *Cycles and events in stratigraphy*. Springer, 956pp.; Germany.

Embry, A. F. 1993. Transgressive-regressive (T-R) sequence analysis of the Jurassic succession of the Sverdrup Basin, Canadian Arctic Archipelago. *Canadian Journal of Earth Sciences* **30**: 301-320.

Embry, A. F. and Klovan, J. E. 1971. A late Devonian reef tract on northeastern Banks

Island Nordwest Territories. *Bulletin of Canadian Petroleum Geology* **19**: 730-781.

Fischer, A. G. 1986. Climatic rhythms recorded in strata. *Annual Review of Earth Planetary Science* **14**: 351-376.

Flügel, E. 1982. *Microfacies Analysis of Limestones*. Springer-Verlag, 633pp.

Flügel, E. 2004. *Microfacies of Carbonate Rocks. Analysis, Interpretation and Application*. Springer-Verlag, 976pp.; Heidelberg.

Frey, R. W. and Seilacher, A. 1980. Uniformity in marine invertebrate ichnology. *Lethaia* **13**: 183-207.

Föllmi, F. B. and Grimm, K. A. 1990. Doomed pioneers: Gravity flow deposition and bioturbation in marine oxygen-deficient environments. *Geology* **18** (11): 1069-1072.

Fürsich, F. T. 1973. A revision of the trace fossils *Spongeliomorpha*, *Ophiomorpha* and *Thalassinoides*. *Neues Jahrbuch für Geologie und Paläontologie, Monathefte* **1973**: 719-735.

Fürsich, F. T. 1974. Corallian (Upper Jurassic) trace fossils from Ebgland and Normandy. *Stuttgarter Beiträge zur Naturkunde. Serie B (Geologie und Paläontologie)* **13**: 1-52.

Fürsich, F. T. 1975. Trace fossils as environmental indicators in the Corallian of England and Normandy. *Lethaia* **8**: 151-172.

Fürsich, F. T. 1982. Rhythmic bedding and shell bed formation in the upper Jurassic of East Greenland. In: *Cyclic and Event Stratification*, G. Einsele and A. Seilacher (eds.)., 209-222 pp.

Fürsich, F. T. 1995. Shell concentrations. *Eclogae geol. Helv* **88** (3): 643-655.

Fürsich, F. T. 1998. Environmental distribution of trace fossils in the Jurassic of Kachchh (Western India). *Facies* **39**: 243-272.

Fürsich, F. T., Berndt, R., Scheuer, T., and Gahr, M. 2001. Comparative ecological analysis of Toarcian (Lower Jurassic) benthic funas from southern France and east-central Spain. *Lethaia* **34**: 169-199.

Fürsich, F. T., Hautmann, M., Senowbari-Daryan, B., and Seyed-Emami, K. 2005 . The Upper Triassic Nayband and Darkuh formations of east-central Iran: Stratigraphy, facies patterns and biota of extensional basins on an accreted terrane. *Beringeria* **35**: 53-133.

Fürsich, F. T. and Oschmann, W. 1993. Shell beds as tools in basin analysis: the Jurassic of Kachchh, western India. *Journal of the Geological Society, London* **150**: 169-185.

Fürsich, F. T., Oschmann, W., Jaitly, A. K., and Singh, I. B. 1991. Faunal response to transgressive-regresive cycles: example from the Jurassic of western India. *Palaeogeography, Palaeoclimatology, Palaeoecology* **85**: 149-159.

Fürsich, F. T., Oschmann, W., Pandey, D. K., Jaitly, A. K., Singh, I. B., and Liu, C. 2004. Palaeoecology of Middle to Lower Jurassic macrofaunas of the Kachchh Basin, western India: an overview. *Journal of The Palaeontological Society of India* **49**: 1-26.

Fürsich, F. T. and Pandey, D. K. 2003. Sequence stratigraphic significance of sedimentary cycles and shell concentrations in the Upper Jurassic - Lower Cretaceous of Kachchh, western India. *Palaeogeography, Palaeoclimatology, Palaeoecology* **193**: 149-159.

Gale, A. S. 1998. Cyclostratigraphy. In: *Unlocking the Stratigraphical Record: Advances in Modern Stratigraphy*, P. Doyle and M. R. Bennett (eds.). John Wiley & Sons Ltd., 195-220pp., New York.

Gerth, E. 1925. La fauna Neocomiana de la Cordillera Argentina en la parte meridional de la provincia de Mendoza. *Actas de la Academia Nacional de Ciencias* **9** (2): 57-132. Argentina.

Giovine, A. T. J. 1950. Algunos cefalópodos del Hauterivense de Neuquén. *Revista de* *la Asociación Geológica Argentina* **5** (2): 35-76.

Greiner, G. O. G. 1969. Recent benthonic foraminifera: environmental factors controlling their distribution. *Nature* **223** (5202): 168-170.

Groeber, P. 1946. Observaciones geológicas a lo largo del Meridiano 70°. Hoja Chos Malal. *Revista de la Sociedad Geológica Argentina* **1**: 177-208.

Haq, B. U., Hardenbol, J., and Vail, P. R. 1987. Chronology of fluctuating sea levels since the Triassic. *Science* **235**: 1156-1167.

Hardenbol, J., Thierry, J., Farley, M. B., Jaquin, T., de Graciansky, P., and Vail, P. R. 1998. Mesozoic and Cenozoic sequence chronostratigraphic framework of European basins - Chart 4: Cretaceous sequence chronostratigraphy. In: *Mesozoic and Cenozoic sequence stratigraphy of European basins*, P. de Graciansky, J. Hardenbol, T. Jaquin, and P. R. Vail (eds.). The Society of Economic Paleontologists and Mineralogists. Special Publication, **60**.

Harms, J. C., Southard, J. B., and Walker, R. G. 1982. *Structures and sequences in clastic rocks*. Society for Economic Paleontologists and Mineralogists, Lecture Notes, Short Course, 249pp.

Haupt, O. 1907. Beiträge zur Fauna des oberen Malm und der unteren Kreide in der Argentinische Cordillere. *Neues Jahrbuch für Mineralogie, Geologie und Paläontologie, Beilage Band* **23**: 187-236, Plates VII to X.

Howell, J. A., Schwarz, E., Spalletti, L. A., and Veiga, G. D. 2005. The Neuquén Basin: an overview. In: *The Neuquén Basin, Argentina: A Case Study in Sequence Stratigraphy and Basin Dynamics*, G. D. Veiga, L. A. Spalletti, J. A. Howell, and E. Schwarz (eds.). Geological Society Special Publications, **252**, 1-14pp., London.

Hunt, D. and Tucker, M. E. 1992. Stranded parasequences and forced regressive wedge sytems tract: deposition during base-level fall. *Sedimentary Geology* **81**: 1-9.

Hägele, G. 1997. *Juraschnecken*. Quelle & Meyer Verlag, Fossilien, Sonderband **11**, 144pp.; Wiebelsheim.

Kase, T. and Ishikawa, M. 2003a. Mystery of naticid predation history solved: Evidence from a "living fossil" species. *Geology* **31** (5): 403-406.

Kase, T. and Ishikawa, M. 2003b. Mystery of naticid predation history solved: Evidence from a "living fossil" species. Reply. *Geology* **Online Forum**: e35.

Keen, M. and Casey, R. 1969. Family Arcticidae Newton, 1891. In: *Treatise on invertebrate paleontology*, R. C. Moore and C. Teichert (eds.). University of Kansas Press & Geological Society of America, N645-N650pp., Lawrence.

Kidwell, S. M. 1985. Palaeobiological and sedimentological implications of fossil concentrations. *Nature* **318**: 457-460.

Kidwell, S. M. 1986a. Models for fossil concentrations: paleobiologic implications. *Paleobiology* **12** (1): 6-24.

Kidwell, S. M. 1986b. Taphonomic feedback in Miocene assemblages: Testing the role of dead hardparts in benthic communities. *Palaios* **1**: 239-255.

Kidwell, S. M. 1991a. Condensed deposits in siliciclastic sequences: expected and observed features. In: *Cycles and Events in Stratigraphy*, G. Einsele, W. Ricken, and A. Seilacher (eds.). Springer Verlag, 682-695pp., Berlin-Heidelberg.

Kidwell, S. M. 1991b. The stratigraphy of shell concentrations. In: *Taphonomy: Releasing the data locked in the fossil record*, P. A. Allison and D. E. G. Briggs (eds.). Plenum Press Topics in Geobiology, **9**, 211-290pp., New York.

Kidwell, S. M., Best, M. M. R., and Kaufman, D. S. 2005. Taphonomic trade-offs in tropical marine death assemblages: Differential time-averaging, shell loss, and probable bias in siliciclastic vs. carbonate facies. *Geology* **33** (9): 729-732.

Kidwell, S. M. and Bosence, D. W. J. 1991. Taphonomy and time-averaging of marine shelly faunas. In: *Taphonomy: Releasing the data locked in the fossil record*, P. A. Allison and D. E. G. Briggs (eds.). Plenum Press Topics in Geobiology, **9**, 115-209pp., New York.

Kidwell, S. M. and Holland, S. M. 1991. Field description of coarse bioclastic fabrics. *Palaios* **6**: 426-434.

Klein, G. d. V. and Marsaglia, K. M. 1987. Discussion. Hummocky cross-stratification, tropical hurricanes, and intense winter storms. *Sedimentology* **34**: 333-359.

Kollmann, H. A. 2005. *Gastropodes Crétacés*. Backhuys Publishers, Révision critique de la Paléontologie françese d'Alcide d'Orbigny. **Volume III**, 235pp.; Leiden.

Kondo, Y., Abbott, S. T., Kitamura, A., Kamp, P. J. J., Naish, T. R., Kamataki, T., and Saul, G. S. 1998. The relationship between shellbed type and sequence architecture: examples from Japan and New Zealand. *Sedimentary Geology* **122**: 109-127.

Lazo, D. 2004. *Análisis de concentraciones fósiles del Cretácico Inferior de cuenca Neuquina*. Facultad de Ciencias Exactas y Naturales, Universidad de Buenos Aires, Unpublished Ph.D. Thesis. 337.

Lazo, D. 2005. Análisis preliminar de las facies de corales del techo de la Formación Agrio, cretácico inferior de la Cuenca Neuquina. In: *16° Congreso Geológico Argentino*, E. Llambías, R. de Barrio, P. González, and P. Leal (eds.). XVI Congreso Geológico Argentino. La Plata Actas CD ROM, 457-464pp., La Plata.

Leanza, A. F. 1945. Ammonites del Jurásico superior y del Cretácico inferior de la Sierra Azul, en la parte meridional de la provincia de Mendoza. *Anales del Museo de La Plata N.S.* **1**: 1-99.

Leanza, A. F. and Castellaro, H. A. 1955. Algunos fósiles cretácicos de Chile. *Revista de la Asociación Geológica Argentina* **X [1]**: 179-213.

Leanza, H. A. 1981. The Jurassic-Cretaceous boundary beds in west central Argentina and their ammonite zones. *Neues Jahrbuch für Geologie und Paläontologie, Abhandlungen* **161**: 62-92.

Leanza, H. A. 1993. Jurassic and Cretaceous Trigoniid Bivalves from West-Central

Argentina. *Bulletins of American Paleontology* **105** (343): 95.

Leanza, H. A. 2003. Las sedimentitas huitrinianas y rayosianas (Cretácico inferior) en el ámbito central y meridional de la Cuenca Neuquina, Argentina. SEGEMAR, Serie Contribuciones Técnicas, Geología 2, 1-31.

Leanza, H. A., Hugo, C. A., and Repol, D. 2001. *Hoja Geológica 3969-I - Zapala, provincia del Neuquén.* Instituto de Geología y Recursos Naturales, SEGEMAR, Boletín **275**, 128 pp.; Buenos Aires.

Leanza, H. A., Repol, D., Hugo, C. A., and Sruoga, P. 2006. *Hoja Geológica 3769-31, Chorriaca, provincia del Neuquén. Programa Nacional de Cartas Geológicas de la República Argentina a escala 1 : 100000. Instituto de Geología y Recursos Minerales*. SEGEMAR, Boletín **354**, 93 pp.; Buenos Aires, Argentina.

Leanza, H. A. and Wiedmann, J. 1992. Nuevos Holcodiscidae (Cephalopoda - Ammonoidea) del Barremiano de la Cuenca Neuquina, Argentina, y su significado estratigráfico. *Neues Jahrbuch für Geologie und Paläontologie, Monatshefte* **1992**: 24-38.

Legarreta, L. and Gulisano, C. A. 1989. Análisis estratigráfico secuencial de la Cuenca Neuquina (Triásico superior - Terciario inferior). *Cuencas Sedimentarias Argentinas*: 221-243.

Legarreta, L., Gulisano, C. A., and Uliana, M. A. 1993. Las secuencias sedimentarias jurásico-cretácicas. In: *XII° Congreso Geológico Argentino y II° Congreso de Exploración de Hidrocarburos. Geología y Recursos Naturales de Mendoza. Relatorio*, 87-114 pp., Argentina.

Legarreta, L. and Uliana, M. A. 1991. Jurassic-Cretaceous marine oscillations and geometry of back arc basin fill, central Argentine Andes. In: *Sea level changes at active plate margins: process and product*, D. I. M. Macdonald (ed.). International Association of Sedimentologists Special Publication, **12**, 429-450 pp.

Legendre, L. and Legendre, P. 1983. *Numerical Ecology*. Elsevier Scientific

Publishing, Developments in Environmental Modelling **3**, 405pp.; Amsterdam, NL.

Leighton, L. R. and Aronowsky, A. 2003. Mystery of naticid predation history solved: Evidence from a "living fossil" species. Comment. *Geology* **Online Forum**: e34-e35.

Ludbrook, N. H. 1960. Scaphopoda. In: *Treatise on Invertabrate Paleontology. Part I Mollusca 1*, R. C. Moore (ed.). Geol. Soc. of America and The Univ. of Kansas, I37-I41pp., Kansas, USA.

MacNaughton, R. B., Dalrymple, R. W., and Narbonne, G. M. 1997. Multiple orders of relative sea-level change in an earliest Cambrian passive margin succession, Mackenzie Mountains, Northwestern Canada. *Journal of Sedimentary Research* **67**: 622-637.

Miller, K. G., Kominz, M. A., Browning, J. V., Wright, J. D., Mountain, G. S., Katz, M. E., Sugarman, P. J., Cramer, B. S., Christie-Blick, N., and Pekar, S. F. 2005. The Phanerozoic record of global sea-level change. *Science* **310**: 1293-1298.

Mitchum, R. M. and Uliana, M. A. 1985. Seismic Stratigraphy of Carbonate Depositional Sequences, Upper Jurassic-Lower Cretaceous, Neuquén Basin, Argentina. In: *Seismic Stratigraphy, II: an Integrated Approach.* R. O. Berg and D. G. Woolverton (eds.). American Association of Petrololeum Geologists, Memoir , **39**, 255-274pp., Tulsa.

Mitchum, R. M. and Van Wagoner, J. C. 1991. High-frequency sequences and their stacking patterns: sequence-stratigraphic evidence of high-frequency eustatic cycles. *Sedimentary Geology* **70**: 131-160.

Mount, J. 1985. Mixed siliciclastic and carbonate sdiments: a proposed first-order textural and compositional classification. *Sedimentology* **32**: 435-442.

Nummedal, D. 1991. Shallow marine storm sedimentation - the oceanographic perspective. In: *Cycles and events in stratigraphy*, G. Einsele, W. Ricken, and A. Seilacher (eds.). Springer, 227-248pp., Germany.

Odin, G. S. and Matter, A. 1981. De glauconarium origine. *Sedimentology* **28**: 611-641.

Ogg, J. G., Agterberg, F. P., and Gradstein, F. M. 2004. The Cretaceous Period. In: *A Geologic Time Scale 2004*, F. M. Gradstein, J. G. Ogg, and A. G. Smith (eds.). Cambridge University Press, 344-383pp., Cambridge, USA.

Pemberton, S. G., MacEachern, J. A., and Frey, R. W. 1992. Chapter 4. Trace Fossils Facies Models: Environmental and Allostratigraphic Significance. In: *Facies Models. Response to sea level change*, R. G. Walker and N. P. James (eds.). Geological Association of Canada, 47-72pp., Ontario, Canada.

Ramos, V. 1977. Estructura. In: *Geología y recursos naturales de la provincia del Neuquén*, E. O. Rolleri (ed.). VII Congreso Geológico Argentino, Actas, **1**, 9-24pp., Buenos Aires.

Reading, H. G. 1996. *Sedimentary Environments: Processes, Facies and Stratigraphy*. Blackwell Science, 688pp.; Oxford.

Reid, R. G. B. and Brand, D. G. 1986. Sulfide-oxidizing symbiosis in lucinaceans: implications for bivalve evolution. *The Veliger* **29**: 3-24.

Reineck, H. E. and Singh, I. B. 1980. *Depositional sedimentary environments*. Springer-Verlag, 549pp.; Berlin.

Reineck, H. E. and Wunderlich, F. 1968. Classification and origin of flaser and lenticular bedding. *Sedimentology* **11**: 99-104.

Riccardi, A. C. 1988. The Cretaceous System of Southern South America. *Memoir Geological Society of America* **168**: 161pp.

Sagasti, G. 2000. La sucesión rítmica de la Formación Agrio (Cretácico inferior) en el sur de la provincia de Mendoza, y su posible vinculación con los Ciclos de Milankovitch. *Revista de la Asociación Argentina de Sedimentología* **7** (1-2): 1-22.

Sagasti, G. 2001. *Estudio sedimentológico y de estratigrafía secuencial de las* *sedimentitas carbonáticas de la Formación Agrio [Cretácico inferior], en el sector surmendocino de la Cuenca Neuquina, República Argentina*. Tesis Doctoral. Facultad de Ciencias Naturales y Museo, Universidad Nacional de La Plata. Tesis No. 764, La Plata. 280.

Sagasti, G. 2005. Hemipelagic record of orbitally-induced dilution cycles in Lower Cretaceous sediments of the Neuquén Basin. In: *The Neuquén Basin, Argentina: A Case Study in Sequence Stratigraphy and Basin Dynamics*, G. D. Veiga, L. A. Spalletti, J. A. Howell, and E. Schwarz (eds.). Geological Society Special Publications, **252**, 231-250pp., London.

Schlirf, M. 2000. Upper Jurassic trace fossils from the Boulonnais (northern France). *Geologica et Palaeontologica* **34**: 145-213.

Schlirf, M. 2003a. Palaeoecologic significance of Late Jurassic trace fossils from the Boulonnais, N France. *Acta Geologica Polonica* **53** (2): 123-142.

Schlirf, M. 2003b. Taxonomic reassessment of *Bolonia* Meunier, 1886 (trace fossil) based on new material from the type area in Boulonnais, northern France. *Paläontologische Zeitschrift* **76**: 331-338.

Schlirf, M. 2005. *Revision and description of Keuper (Middle Ladinian to Rhaetian) invertebrate trace fossils from the southern part of the Germanic Basin and studies of related material*. University of Würzburg, Würzburg. 300.

Schwarz, E., Archuby, F. M., and Simanauskas, T. 2001. Sedimentology, Palaeoecology and Taphonomy of Valanginian Shellbeds of the Neuquén Basin (Argentina): Palaeoenvironmental and Sequence Stratigraphic Implications. *21st IAS Meeting of Sedimentology, Davos* 86-87 (abstract).

Scrutton, C. T. 1975. Hydroid-serpulid symbiosis in the Mesozoic and Tertiary. *Palaeontology* **18 Part 2**: 255-274.

Seilacher, A. 1967. Bathymetry of trace fossils. *Marine Geology* **5**: 413-428.

Seilacher, A. and Aigner, T. 1991. Storm Deposition at the Bed, Facies and Basin

Scale: the Geologic Perspective. In: *Cycles and events in stratigraphy*, G. Einsele, W. Ricken, and A. Seilacher (eds.). Springer, 249-267pp., Germany.

Skelton, P. W. 2003. Fluctuating sea-level. In: *The Cretaceous World*, P. W. Skelton, R. A. Spicer, S. P. Kelley, and I. Gilmour (eds.). Cambridge University Press, 67-83pp., Cambridge, UK.

Soot-Ryen, T. 1969. Superfamily Mytilacea Rafinesque, 1815. In: *Treatise on invertebrate paleontology*, R. C. Moore and C. Teichert (eds.). University of Kansas Press & Geological Society of America, N271-N281pp., Lawrence.

Spalletti, L. A. 1980. Paleoambientes sedimentarios en secuencias silicoclásticas. *Asociación Geológica Argentina - Serie "B", Didáctica y Complementaria* (8): 175.

Spalletti, L. A., Del Valle, A., and Kielbowicz, A. 1990. Análisis cicloestratigráfico del intervalo Hauteriviano superior-Barremiano en el área de Filo Morado, Cuenca Neuquina. In: *IIIa Reunión Argentina de Sedimentología Actas*, 253-259pp., Argentina.

Spalletti, L. A., Franzese, J. R., Matheos, S. D., and Schwarz, E. 2000. Sequence stratigraphy of a tidally dominated carbonate-siliciclastic ramp; the Tithonian-Early Berriasian of the Southern Neuquén Basin, Argentina. *Journal of the Geological Society* **157**: 433-446.

Spalletti, L. A., Poiré, D. G., Pirrie, D., Matheos, S. D., and Doyle, P. 2001a. Respuesta sedimentológica a cambios en el nivel de base en una secuencia mixta clástica - carbonática del cretácico de la Cuenca Neuquina, Argentina. *Revista de la Sociedad Geológica de España* **14** (1-2): 57-74.

Spalletti, L. A., Poiré, D. G., Schwarz, E., and Veiga, G. D. 2001b. Sedimentologic and sequence stratigraphic model of a Neocomian marine carbonate-siliciclastic ramp: Neuquén Basin, Argentina. *Journal of South American Earth Sciences* **14**: 609-624.

ten Hove, H. A. and van der Hurk, P. 1993. A review of Recent and fossil serpulid 'reefs', actuopalaeontology and the 'Upper Malm' serpulid limestones in NW Germany. *Geologie en Mijnbouw* **72**: 23-67.

Tomasovych, A., Fürsich, F. T., and Olszewski, T. D. 2006. Modelling shelliness and alteration in shell beds: variation in hard part input and burial rates leads to opposing predictions. *Paleobiology* **32** (2): 278-298.

Tracey, S., Todd, J. A., and Erwin, D. H. 1993. Mollusca: Gastropoda. In: *The Fossil Record 2*, M. J. Benton (ed.). Chapman & Hall, 131-167pp., London.

Tucker, M. E. 1985. Shallow-marine carbonate facies and facies models. In: *Sedimentology. Recent developments and applied aspects*, P. J. Brenchley and B. P. J. Williams (eds.). Blackwell, 147-169pp., Oxford.

Tyson, R. V., Esherwood, P., and Pattison, K. 2005. Organic facies variations in the Valanginian-mid-Hauterivian interval of the Agrio Formation (Chos Malal area, Neuquén, Argentina): local significance and global context. In: *The Neuquén Basin, Argentina: A Case Study in Sequence Stratigraphy and Basin Dynamics*, G. D. Veiga, L. A. Spalletti, J. A. Howell, and E. Schwarz (eds.). Geological Society Special Publications, **252**, 251-266pp., London.

Uliana, M. A. and Legarreta, L. 1993. Hydrocarbons habitat in a Triassic-to-Cretaceous sub-Andean setting: Neuquén Basin, Argentina. *Journal of Petroleum Geology* **16**: 397-420.

Van Wagoner, J. C., Mitchum, R. M., Campion, K. M., and Rahmanian, V. D. 1990. *Siliciclastic sequence stratigraphy in well logs, cores and outcrops*. American Association of Petroleum Geologists, Methods in Exploration Series **7**, 55pp.; USA.

Van Wagoner, J. C., Mitchum, R. M. JR., Posamentier, H. W., and Vail, P. R. 1987. Key definitions of sequence stratigraphy. In: *Atlas of Seismic Stratigraphy*, A. W. Bally (ed.). **American Association of Petroleoum Geology, Studies in Geology** 27, 11-14pp., Tulsa.

Van Wagoner, J. C., Posamentier, H. W., Mitchum, R. M. , Vail, P. R., Sarg, J. F., Loutit, T. S., and Hardenbol, J. 1988. An overview of the fundamentals of sequence stratigraphy and key definitions. In: *Sea Level Changes- An integrated Approach*, C. K. Wilgus, B. S. Hastings, C. G. S. C. Kendall, H. W. Posamentier, C. A. Ross, and J. C. Van Wagoner (eds.). The Society of Economic Paleontologists and Mineralogists. Special Publication, **42**, 39-45pp., Tulsa.

Veiga, G. D., Howell, J. A., and Strömbäck, A. 2005. Anatomy of a mixed- non-marine lowstand wedge in a ramp setting. The record of a Barremian-Aptian complex relative sea-level fall in the Central Neuquén Basin, Argentina. In: *The Neuquén Basin, Argentina: A Case Study in Sequence Stratigraphy and Basin Dynamics*, G. D. Veiga, L. A. Spalletti, J. A. Howell, and E. Schwarz (eds.). Geological Society Special Publications, **252**, 139-162pp., London.

Veiga, G. D., Spalletti, L. A., and Flint, S. 2002. Aeolian/fluvial interactions and high-resolution sequence stratigraphy of a non-marine lowstand wedge: the Avilé Member of the Agrio Formation (Lower Cretaceous), central Neuquén Basin, Argentina. *Sedimentology* **49**: 1001-1019.

Veiga, G. D. and Vergani, G. D. 1993. Depósitos de nivel bajo: nuevo enfoque sedimentológico y estratigráfico del Miembro Avilé en el norte del Neuquén. In: *XII Congreso Geológico Argentino y II Congreso de Exploración de Hidrocarburos, Actas*, 55-65pp., Mendoza.

Vergani, G. D., Tankard, A. J., Belotti, H. J., and Welsink, H. J. 1995. Tectonic evolution and paleogeography of the Neuquén Basin, Argentina. In: *Petroleum Basins of South America*, A. J. Tankard, R. Suárez, and H. J. Welsink (eds.). American Association of Petroleum Geologists, Memoir, **62**, 383-402pp., Tulsa.

Villamil, T., Kaufman, E. G., and Leanza, H. A. 1998. Epibiont habitation pattern and their implications for life habits and orientation among trigoniid bivalves. *Lethaia* **31**: 43-56.

Walker, R. G. and James, N. P. 1992. *Facies models. Response to sea level change*. Geological Association of Canada, 454pp.; Newfoundland, Canada.

Weaver, C. W. 1931. *Palaeontology of the Jurassic and Cretaceous of West Central Argentina*. University of Washington, Memoir **1**, 595pp.; Seattle.

Wilmsen, M. 2003. Sequence stratigraphy and palaeoceanography of the Cenomanian Stage in northern Germany. *Cretaceous Research* **24**: 525-568.

Wilson, M. A. and Taylor, P. D. 2001. Palaeoecology of hard substrate faunas from the Cretaceous of Qahlah Formation of the Oman Mountains. *Palaeontology* **44** (1): 21-41.

Wright, V. P. and Burchette, T. P. 1996. Shallow water carbonate environments. In: *Sedimentary Environments: Processes, Facies and Stratigraphy*, H. G. Reading (ed.). Blackwell Science, 325-391pp., London.

Zapata, T. and Folguera, A. 2005. Tectonic evolution of the Andean Fold and Thrust Belt of the southern Neuquén Basin, Argentina. In: *The Neuquén Basin, Argentina: A Case Study in Sequence Stratigraphy and Basin Dynamics*, G. D. Veiga, L. A. Spalletti, J. A. Howell, and E. Schwarz (eds.). Geological Society Special Publications, **252**, 37-56pp., London.

Appendix A. Taxonomic list

In the following the taxa included in the multivariate analysis are listed. For problematic and/or not yet described species a brief description and a discussion on possible taxonomic affinities is included. Although the study of the Neocomian fauna of the Neuquén Basin began more than a century ago (Behrendsen 1891; Behrendsen 1892; Burkhardt 1900; Haupt 1907) it turn out that it is very poorly known and that the available information is restricted to the most abundant and/or stratigraphically relevant groups. Besides, several taxa have been studied only superficially and important morphological differences were not properly assessed. The taxonomic revision of the fauna is beyond the scope of this study.

Kingdom Protista

Order **FORAMINIFERIDA**

Placopsilina sp. (Pl. 8, fig. 1-3)

Test attached, wall arenaceous, composed of silt-sized particles in a calcareous cement. The test consists of an initial spire followed by a uniserial arrangement of the chambers. The features of the initial spire were not properly seen in the specimens from the Neuquén Basin. The chambers of later growth stages abut directly against one another, with no well-marked constrictions along the septa. A tendency to crowding of several individuals is common as noted by Wilson and Taylor (2001) for species of the same genus (Pl. 8, fig. 2). The uniserial part of the test is long (several mm) and soon after the initial spire the width becomes more or less constant. All these features coincide with Barnard's description of *Placopsilina* in Barnard (1958).

In the Neuquén Basin *Placopsilina* specimens were found living epifaunally associated with semi-infaunal bivalve species such as *Ptychomya koeneni* and *Steinmanella vacaensis* (see Chapter 9, autoecology).

At several levels in both sections *Placopsilina* constructs small semi-sphaerical buildups around shell fragments (see Pl. 8, fig. 3). These constructions accumulated to form up to 2 m thick late starvation deposits. Individual foraminifers are difficult to identify, although they share all morphological features and are probably the same species.

Kingdom Animalia

Phylum ***Cnidaria***

Class Anthozoa

Order **SCLERACTINIA**

Scleractinia sp. A

Small colonies encrusting carbonate concretions (Pl. 8, fig. 4).

Scleractinia sps. indet.

Scleractinian corals are rare throughout the sections except at 503 m from the base in section BAL, where a few metres thick coral patch reefs are developed. Branching corals are present at other levels as fragments. All coral remains are reworked and strongly recrystallized.

Phylum ***Echinodermata***

Class Echinoidea

Articulated echinoderms are rare although their ossicles are common and abundant at some levels. The three irregular echinoid taxa found were already mentioned by Weaver (1931). Echinoderm remains are more common towards the top of the Agrio Formation.

Irregularia

aff. *Pygaster gerthi* (Weaver 1931)

Eight weakly calcified specimens were collected from muddy sediments in a starvation hemisequence (RST) of the Agua de la Mula section. Their preservation does not allow an unambiguous identification.

Holectypus cf. planatus (Roemer)

The specimens agree with Weaver's description and figures (Weaver 1931: Pl. 12, figs. 20-22).

Holectypus sp.

Two specimens correspond to Pl. 12, figs. 23-24 of Weaver (1931). This taxon has not been described in that work but only mentioned in the captions of plate 12.

Regularia

Regularia sp. indet. A

Only a single, small specimen (1 cm in diameter) has been recovered It bears wide bases for spines and very narrow ambulacral areas.

Class Crinoidea

Crinoidea ossicles observed in thin-sections and samples, and rare stems fragments consisting of several articulated ossicles were included in the analysis. In all cases one or more remains were included in the analysis as a single count.

Phylum ***Annelida***

Fam. **SERPULIDAE**

Serpulid tubes were grouped into four categories, two of them based on the diameter of the tube: small (1 mm or less) and medium (2 to 5 mm); the other two are recognized taxa: *Parsimonia* cf. *antiquata* (larger than 5 mm) and *Sarcinella occidentalis*. This classification was used because of its simplicity and also because most morphological features of serpulid tubes are not diagnostic (ten Hove and van der Hurk 1993): Two different Recent serpulid species may have identical tubes and tubes of different specimens of the same species may show different morphological features. Thus any identification based on them would result in a distorted picture of serpulid diversity.

Parsimonia cf. antiquata (J. de C. Sowerby, 1829)

Large tubes that may reach diameters of more than 10 mm. External surface smooth, with more or less distinct growth lines. *Parsimonia* tubes are normally found conforming small buildups with other *Parsimonia* individuals and/or with the gryphaeid oyster *Ceratostreon*.

Sarcinella occidentalis (Leanza and Castellaro, 1955)

Originally described as *Serpula occidentalis* (Leanza and Castellaro, 1955) this serpulid species is characterized by boundles of hundreds of tiny tubes of small and regular diameter (around 1 mm). The bundles are several cm long and usually bifurcate. In this study only reworked bunches were found.

Small-sized serpulids.

Diameter around 1 mm or less. Probably more than one species is involved. Normally tubes occur isolated.

Medium-sized serpulids.

Diameter between 2 and 5 mm. Probably more than one species is involved. Normally tubes occur isolated.

Phylum Mollusca

Class Scaphopoda

Dentalium sp.

Scaphopods are common in shell beds deposited in fine-grained, muddy deep facies of the Agrio Formation. Despite their relative abundance in some facies they have not been mentioned in previous studies of similar age and geographic positions (Camacho and Riccardi 1978; Damborenea et al. 1979; Lazo 2004; Weaver 1931). The scaphopods found in the Agrio Formation belong to a single species characterized by a smooth, gently curved shell of up to 7-8 cm length. The diameter increases gently towards the anterior end. The shell is usually thick. Unfortunately, almost all scaphopod specimens are fragmented and there are only few more or less complete ones. In no case the posterior end was found. According to Ludbrook (1960) the specimens from the Neuquén Basin most probably belong to the genus *Dentalium*.

Class Gastropoda

(Classification of higher taxa after Tracey et al. 1993).

Subclass **STREPTONEURA**
  Order **ARCHAEOGASTROPODA**
    Suborder **VESTIGASTROPODA**
      Superfam. **TROCHOIDEA**
      Fam. **TROCHIDAE**

Trochidae sp. A

Trochidae? sp. B

Only three trochid were collected, two of them large-sized, the third minute. So far, no trochids have been described in the literature from the Neocomian of the Neuquén Basin.

Order **APOGASTROPODA**

Suborder **CAENOGASTROPODA**

Superfam. **CERITHIOIDEA**

Fam. **CERITHIIDAE**

Cerithium sp. A (Pl. 8, fig. 5)
Cerithium sp. B (Pl. 8, fig. 6)

Two cerithiid species were found. Both are restricted to Lower Barremian (or younger) beds at the top of the section. *Cerithium* sp. A resemble *Cerithium* cf. *heeri* (Pictet and Renevier 1854-58), re-described and figured by Weaver (1931). However, there are relevant differences in the ornamentation between Weaver's species and the one described here.

Cerithium sp. B has strong radial ribs with two tubercules per whorl. The ribs are not completely in phase between two contiguous whorls, a feature that is accentuated between the last two whorls.

Fam. **PROCERITHIIDAE**

- ***Rhabdocolpus* sp. A**
- ***Rhabdocolpus* sp. B**

Rhabdocolpus sp. A is figured in Pl. 8, fig. 7. Species B resembles *Promathilda (Turritelloidea)* of Hägele (1997, p. 117). It is similar in size with respect to species A, and is quantitatively rare (only four specimens).

Superfam. **PSEUDOMELANIOIDEA**

Fam. **PSEUDOMELANIIDAE**

Poasia sp. A
Poasia sp. B cf. *amphora* (d'Orbigny, 1942)
Poasia sp. C

To date no Pseudomelaniidae have been described from the Lower Cretaceous of the Neuquén Basin. The three species were found in a couple of inconspicuous transgressive beds close to the top of the section, in sediments considered to be Lower Barremian or younger. *Poasia* sp. B (Pl. 8, fig. 8) is relatively abundant in one of these levels. It is similar to the Turonian species *Poasia amphora* (d'Orbigny, 1842) figured in Kollmann (2005, Pl. 2, figs. 11-12). The other two species differ in size and morphology and are represented by a single specimen each.

Superfam. **STROMBOIDEA**
Fam. **APORRHAIDAE**

- ***Protohemichenopus neuquensis*** (Camacho, 1953) (Pl. 8, fig. 9)

Protohemichenopus neuquensis was found restricted to the first major maximum flooding zone of earliest Upper Hauterivian age. In these beds it is abundant and represents an important component of a fossil association. Among the specimens counted and collected few of them are preserve with two long spines pointing upwards and downwards. A third extension is normally preserved. It extends upward in contact with the spire.

- ***Dimorphosoma* sp.**

This aporrhaid closely resembles *Dimorphosoma? acuta* (d'Orbigny, 1843 of Kollmann (2005, Pl. 13, fig. 20a, b), and is figured in Fig. 10 of Pl. 8. The specimens of this taxon occur close to the uppermost Hauterivian major maximum flooding zone, associated to the Faraoni anoxic event (see Section 6.3 and Text-Fig. 6). This genus is present again in a MFZ of Barremian age.

- **Aporrhaidae sp. B**

A few poorly preserved aporrhaid specimens belong to a different species. They resemble *Anchura "Dicroloma*" described in Hägele (1997 pp. 99-100).

Superfam. **NATICOIDEA**
Fam. **AMPULLOSPIRIDAE**

- ***Pictavia* sp. A**

- ***Pictavia* sp. B**

One of these two species was probably briefly described by Weaver (1931) as naticid *Amauropsis* Moersch sp. indet. Weaver's description is short and based on casts and broken fragments, and lacks figures. *Pictavia* sp. A is figured in Pl. 8, fig. 11, and sp. B in Pl. 8, fig. 12. *Tylostoma jaworski* (Weaver, 1931) was found in the sections studied, but none of the specimens are from beds sampled for this work.

Superfam. **JANTHINOIDEA**

Fam. **EPITONIIDAE**

- ***Confusiscala* sp.** (Pl. 8, fig. 13)

The specimens are very similar although smaller than *Confisiscala dupiniana* (d'Orbigny, 1842) of Kollmann (2005, Pl. 2, fig. 4 a,b). Haupt (1907, p. 206; Pl. 10, fig. 5 a, b) described and figured a Neocomian-Aptian gastropod similar to this species which he named *Cerithium* sp.

Suborder **HETEROSTROPHA**

Superfam. **PYRAMIDELLIOIDEA**

Fam. **MATHILDIDAE**

- ***Bathraspira* sp. A** cf. ***B. neocomiensis*** (d'Orbigny, 1843)

Bathraspira sp. A (Pl. 8, fig. 14) is a very common species in the fossil assemblages in the first 150 m of the sections (lowermost Upper Hauterivian). It is comparable to *B. neocomiensis* d'Orbigny of Kollmann (2005, Pl. 17, figs. 16-17).

- ***Bathraspira* sp. B**

This species resembles *Bathraspira neocomiensis* (d'Orbigny, 1843) in general shape (Kollmann 2005, Pl. 17, figs. 16-17). The two species differ in the number of carinas around the suture: one in *Bathraspira* sp. B and two in *B. neocomiensis* (d'Orbigny, 1843).

- ***Bathraspira*? sp. C**

This taxon constitutes almost 10 % of all the individuals included in the analysis (Pl. 8, fig. 15). It is present only in the lower fourth of the section (lowermost Upper Hauterivian). Although the general shape of the specimens resembles *Bathraspira tecta* (d'Orbigny, 1843) figured in Kollmann (2005, Pl. 7, fig. 13 a, b) there are important differences in the ornamentation.

Subclass **EUTHYNEURA**
Superorder **OPISTOBRANCHIA**
Order **CEPHALASPIDEA**
Superfam. **RINGUICULOIDEA**
Fam. **RINGICULIDAE**

- ***Ringinella* sp. A**

The specimens from the Neuquén Basin look like *Ringinella clementina* (d'Orbigny, 1842) figured by Kollmann (2005; Pl. 6, figs. 11-12). However, the last whorl is distinctly wider in the Argentinan species. Haupt described *Acteon andinus* (Haupt, 1907) that resembles the present specimens (Haupt 1907, p. 206; Pl. 10, fig. 4 a, B).

- ***Ringinella* sp. B**

There is a single specimen of a tiny, fusiform Ringuiculidae, whose last whorl is large and has a much reduced spire. It is comparable to *Ringinella ringens* (d'Orbigny, 1842) figured by Kollmann (2005, Pl. 6, fig. 9 a, b).

Superfam. **ACTEONOIDEA**
Fam. **ACTEONIDAE**

- ***Tornatellaea* sp.**

This species of *Tornatellaea* is represented by a single specimen, characterised by its elongated nature, a feature that is common to both spire and last whorl. It resembles *Tornatellaea albensis* (d'Orbigny, 1842) in Kollmann (2005, Pl. 6, fig. 6a, b).

Class Pelecypoda

Subclass **PALEOTAXODONTA**

Order **NUCULOIDA**

Superfam. **NUCULOIDEA**

Fam. **Nuculidae**

- ***Paleonucula* sp.** (Pl. 8, fig. 16)

A single articulated specimen and a valve with a poorly preserved nuculoid hinge.

Subclass **PTERIOMORPHIA**

Order **ARCOIDA**

Superfam. **ARCOIDEA**

Fam. **ARCIDAE**

- ***Barbatia* (*Barbatia*) sp. A**

A single articulated specimen 4.5 cm long and 2.5 cm height, found a few tens of meters below the contact between Hauterivian and Barremian strata.

Fam. **CUCULLAEIDAE**

- ***Cucullaea gabrielis*** (Leymerie, 1842) (Pl. 8, fig. 17)

Fam. **PARALLELODONTIDAE**

Subfam. **GRAMMATODONTINAE**

- ***Grammatodon securis*** (Leymerie, 1842)

This species, very common in the lower 100 m of the section, is illustrated in Pl. 8, fig. 18.

- ***Grammatodon* (*G.*) sp.**

Grammatodon (*G.*) sp. is restricted to a couple of levels that correspond to the MFZ of DSAM-4 of the Lower Barremian (Pl. 8, fig. 19).

- **Grammatodontinae sp. A** (Pl. 8, fig. 20)

This species resembles the pre-Cretaceous genus *Parallellodon*.

- **Grammatodontinae sp. B**

Grammatodontinae sp. B was found only in Barremian sediments close to the top of the section. It is small and similar to Grammadontinae sp. A in outline and inflation, but lacks radial ornamentation. Abundance is low and preservation poor.

Order **MYTILOIDA**

Superfam. **MYTILOIDEA**

Fam. **MYTILIDAE**

Mytilids are rare in the Agrio Formation. In this study they represent less than 0.23 % of all specimens counted. Two species have previously been mentioned in the literature: *Modiolus* cf. *M. ligeriensis* (d' Orbigny, 1843) and *Modiolus* cf. *M. subsimplex* (d'Orbigny, 1843) (Burkhardt 1900; Camacho and Riccardi 1978; Weaver 1931). The remaining species are rare. In Crenellinae sp. A and B beaks are situated more or less behind the anterior end (Soot-Ryen 1969). Crenellinae sp. B is represented by three relatively complete valves approximately 4 cm long and 2 cm high. It fits the description of *Musculus* (Soot-Ryen 1969), although the preservation does not allow a trustable generic determination. Crenellinae sp. A is smaller, 1.5 cm long and less than 1 cm high, lacks radial ornamentation and has a pronounced carena that runs from the beak to the ventral margin of the shell (Pl. 8, fig. 21). A single articulated specimen of the Mytilinae was found. It has a typical mytiliform shape with the beaks anteriorly placed. Shells are weathered and very little of a radial ribbing can be seen. It has a length of 3.69 cm and a height of 2.48 cm.

- **Mytilinae sp. A**
- **Crenellinae sp. A** (Pl. 8, fig. 21)
- **Crenellinae sp. B**
- ***Modiolus* cf. *M. ligeriensis*** (d'Orbigny, 1943) (Pl. 8, fig. 22)
- ***Modiolus* cf. *M. subsimplex*** (d'Orbigny, 1844)

Superfam. **PINNOIDEA**

Fam. **PINNIDAE**

- ***Pinna robinaldina*** (d'Orbigny, 1844) (Pl. 9, fig. 1)
- **Pinnidae sp.**

A single incomplete valve with strong radial ribs that does not fit any of the pinnid genera described in Cox and Hertlein (1969).

Order **PTERIOIDA**

Suborder **PTERIINA**

Superfam. **PTERIOIDEA**

Fam. **BAKEVELLIIDAE**

- ***Gervillaria alatior*** (Imlay, 1940)
- ***Gervillella aviculoides*** (J. Sowerby, 1814) (Pl. 9, fig. 2)
- **Bakevelliidae sp. aff. *Cuneigervillia* sp.**

Few disarticulated, fragmented valves of a medium-sized backevelliid species. The shell is inequivalved, posterior wing well developed, hinge axis straight, the ligament carries multiple pits, and there is no ornamentation or merely consisting on smooth growth lines. The specimens resemble the genus *Cuneigervillia*, although preservation does not allow a generic identification.

- **Pterioida sp. A**

Poorly preserved pterioids. All remains have similar sizes and features, although preservation is so poor that the presence of different species cannot be ascertained.

Fam. **INOCERAMIDAE**

- ***Inoceramus* sp. A aff. *curacoensis*** (Weaver, 1931) (Pl. 9, fig. 4)
- ***Inoceramus* sp. *B***

Few small, poorly preserved fragments found in a couple of levels in the Agua de la Mula locality.

Fam. **ISOGNOMONIDAE**

One or possibly two species of *Isognomon* were found. Most of the specimens can be assigned to *I. lotenoensis* (Weaver, 1931) despite the generally poor preservation of the outer layers. The shape of some specimens differs somewhat from that of Weaver’s species. These specimens were identified as *Isognomon* sp. A.

- ***Isognomon (I.) lotenoensis*** (Weaver, 1931) (Pl. 8, fig. 26 a, b)
- ***Isognomon* sp. A aff. *I. lotenoensis*** (Weaver, 1931**)** (Pl. 9, fig. 5)

Superfam. **PECTINOIDEA**

Fam. **PECTINIDAE**

Pectinids are not abundant in the two sections, with the exception of a few shell beds, in which they reach moderate percentages. These beds are characteristically calcareous with few terrigenous grains. Preservation is usually poor due to abrasion, bioerosion, disarticulation, and fragmentation. Wings are almost never preserved. Five different species were detected, four of them already described in the literature and a fifth (Pectinidae sp. 1) is characterised by its small size (< 30 mm), orbicular shape and thin, regular, and radial ribs, the remaining features not being preserved.

- ***Mimachlamys robinaldina*** (d'Orbigny, 1847) (Pl. 8, fig. 23)
- **"*Chlamys*" *puzoziana*** (Matheron, 1842) (Pl. 8, fig. 25)
- **"*Pecten*" *vacaensis*** (Weaver, 1831)
- **cf. *Eopecten covuncoensis*** (Weaver, 1831)
- **Pectinidae sp. A**

Superfam. **ANOMIOIDEA**

Fam. **ANOMIIDAE**

- **Anomiidae sp.** (Pl. 8, fig. 24)

Superfam. **LIMOIDEA**

Fam. **LIMIDAE**

- **aff. *Acesta*** sp. (Pl. 9, fig. 3)
- **aff. *Pseudolimea*** sp.

Suborder **OSTREINA**

Superfam. **OSTREOIDEA**

Fam. **GRYPHAEIDAE**

Subfam. **EXOGYRINAE**

Gryphaeid oysters are both diverse and abundant in the Neocomian of the Neuquén Basin. There taxonomy is currently under study (Rubilar 2007, pers. comm.). *Aetostreon latissimum* (Defrance, 1821) and *Ceratostreon minos* (Coquand, 1869) show an enormous morphological variation and wide stratigraphical distribution (from the Early Valanginian to the Late Hauterivian).

- ***Aetostreon* sp. (aff. *A. latissimum*)** (Defrance 1821) (Pl. 9, fig. 6 a, b)
- ***Ceratostreon minos*** (Coquand 1869) (Pl. 10, fig. 2 a, b)
- ***Gryphaeostrea* sp. 1** (Pl. 10, fig. 2)
- ***Gryphaeostrea* sp. 2** (Pl. 10, fig. 3)
- **Exogyrinae sp.**

Fam. **OSTREIDAE**

Subfam. **LOPHINAE**

Two quantitatively rare species of Lophinae were found. Species A is preserved with highly bioeroded, although articulated, specimens. It is large (80 mm high, 55 mm long and 40 mm wide), and the attachment area is large and concave. Left valve with a curved carena. The margin has strong corrugations. With chomata. Species B is represented by a single small incomplete left valve (< 20 mm long and high).

- **Lophinae sp. A**
- **Lophinae sp. B**

Subclass **PALEOHETERODONTA**

Order **TRIGONOIDA**

Suborder **TRIGONIINA**

Superfam. **TRIGONIACEA**

Fam. **TRIGONIIDAE**

Trigoniids are very common, diverse and well known in the Neuquén Basin. They were studied extensively since the nineteenth century and revised by Leanza (1993).

Subfam. **MYOPHORELLINAE**

- ***Myophorella (Haidaia) volkheimeri*** (Leanza and Garate, 1987)

- ***Myophorella (Promyophorella) garatei*** (Leanza, 1981)

Subfam. **STEINMANELLINAE**

- ***Steinmanella (Transitrigonia) raimondii*** (Lisson, 1930)
- ***Steinmanella (Macrotrigonia) vacaensis*** (Weaver, 1931) (Pl. 10, fig. 7)

Subfam. **RUTITRIGONIINAE**

- ***Rutitrigonia agrioensis*** (Weaver, 1931) (Pl. 10, fig. 6)

Subfam. **PTEROTRIGONIINAE**

- ***Pterotrigonia (Rinetrigonia) coihuicoensis*** (Weaver, 1931) (Pl. 10, fig. 4)

Pterotrigonia (Rinetrigonia) coihuicoensis (Weaver, 1931) is the most abundant and temporally widespread trigonid species of the fauna. It has an important variation in size and morphology.

- ***Pterotrigonia (Rinetrigonia)* sp. A aff. *coihuicoensis*** (Weaver, 1931) (Pl. 10, fig. 5)

Smaller and less inflated than *P. coihuicoensis*. Umbones more anteriorly placed, ribs present on the anterior part of the escutcheon. This species is abundant only in the two youngest shell beds analysed in this study. They are Early Barremian or younger in age.

Subclass **HETERODONTA**

Order **VENEROIDA**

Superfam. **LUCINOIDEA**

Fam. **LUCINIDAE**

- ***Mesomiltha? argentina*** (Behrendsen, 1891) (Pl. 10, fig. 8)

The species is very similar to *Lucina argentina* (Behrendsen, 1891). However, Behrendsen's description is very short and the figures are drawings. More than 95 % of the 751 specimens included in this study are articulated. Among the disarticulated specimens only one could be prepared to observe internal structures of the shell. The closest genus to the Argentinian species is *Mesomiltha*. However, this genus is characterised by an anterior muscle scar which is curved and distally detached, and by a shell margin which is smooth on the inside (Chavan 1969). The present specimens have a straight muscle scar, which is proximally detached, and an inner margin which is crenulated. Both, size and external morphology are variable in this species.

- ***Mesomiltha*? sp. A** (Pl. 10, fig. 9)

Mesomiltha? sp. A is less abundant than *M.*? *argentina*. It differs from the former in having a larger and more elongated shell. Concentric ribs are more abundant (i.e. less spaced) and less irregularly placed. *Mesomiltha*? *argentina* reaches its maximum width towards its dorsal margin, its shape being more drop-like shape in cross-section than *M*. sp. A.

- ***Lucina corbisoides*** (d'Orbigny, 1845)
- ***Lucina neuquensis*** (Haupt, 1907)
- **Lucinidae sp. A**

Medium sized, moderately inflated, elongated lucinids (length= 2.70 cm; height= 2.24 cm). Very fine, abundant, concentric ribs and thread-like radial ornamentation. It differs from the lucinids mentioned above and from those formed in the literature.

Superfam. **CARDITOIDEA**

Fam. **PERMOPHORIDAE**

Subfam. **MYOCONCHINAE**

- ***Myoconcha transatlantica*** (Burckhardt, 1900) (Pl. 10, fig. 12)

This species is particularly large and abundant in the two sections. It is highly variable in size and shape.

Superfam. **CRASSATELLOIDEA**

Fam. **ASTARTIDAE**

Subfam. **ERIPHYLINAE**

- ***Eriphyla argentina*** (Burkhardt, 1900) (Pl. 11, figs. 1-4)

Eriphyla argentina (Burkhardt, 1900) is one of the most abundant species found in the Neocomian of the Neuquén Basin (Weaver 1931). The preservation of the specimens of this species is usually excellent. Among the more than 1500 specimens studied a very wide variation in shape and outline could be detected. As there are no morphological gaps amongst the specimens studied, it is believed that all these morphs correspond to the same species. In this way, *Eriphyla argentina* as conceived in this study includes *Eriphyla lotenoensis* (Weaver, 1931), *Eriphyla agrioensis* (Weaver, 1931) and *Eriphyla argentina* Burckhardt var. *picunleufuensis* (Weaver, 1931). Nevertheless, a systematic morphological analysis is needed to elucidate this problem. As some morphs appear at particular levels in the section, morphological changes may be related to sedimentary sequences.

- ***Disparilia elongata*** (d'Orbigny, 1843)

This species is relatively common throughout the sections. Morphology varies even in the same bed (e.g. Pl. 10, fig. 13 a, b). Less elongated specimens that are roughly similar to the Tithonian *Astarte aequilatera* (Behrendsen, 1891) were found in different shell beds (Pl. 10, fig. 13 c). The latter species is always small and probably represents young individuals of *D. elongata*. Because of this and the fact that in poorly preserved specimens it is nearly impossible to differentiate both species, *A. aequilateral* was included in *D. elongata*. Considering all *Disparilia* specimens this taxon also varies considerably in size and shape.

Subfam. **ASTARTINAE**

- ***Neocrassina (Coelastarte?)* sp.** (Pl. 10, fig. 10)

The shells are moderately large and always articulated, but morphological features are not well seen because of compactional flattening and fracturing and usual heavy encrustation by the foraminifer *Placopsilina* sp. A second *Neocrassina* species, characterized by a more equilateral shell, is possibly present.

- **Astartidae sp. A** (Pl. 11, fig. 5)

Shells small (< 20 mm), prosogyre, slightly inequilateral. Ribs comarginal, fine, widely spaced. Anterodorsal margin concave, and posterodorsal margin convex. Lunule ill defined, escutcheon well defined.

Superfam. **CARDIACEA**

Fam. **CARDIIDAE**

- ***Protocardia* sp.** (Pl. 11, fig. 6)

Superfam. **TELLINACEA**

Fam. **SOLECURTIDAE?**

- ***Solecurtus? neuquensis*** Weaver, 1931 (Pl. 11, fig. 7)

The external features fit Weaver's (1931) species very well. The hinge and other internal characteristics could not be observed. The specimens closely resemble *Solecurtus neuquensis* Weaver but the species most probably belongs to a different genus and possibly even family.

Superfam. **ARCTICACEA**

Fam. **PTYCHOMYIDAE**

- ***Ptychomya* sp A** cf. *P. koeneni* Behrendsen, 1892 (Pl. 8, fig. 2, Pl. 11, figs. 8-13)

This is one of the most abundant species of the Neocomian of the Neuquén Basin. It is extremely variable in outline and ornamentation. Weaver (1931) defined several morphotypes which he described as subspecies. There is no clear stratigraphical pattern in the change of morphotypes. These "subspecies" are recurrent in time, occasionally there are intermediate forms between recognized morphotypes. Hence, pre-Barremian *Ptychomya* is regarded as a single taxon in this study, although the presence of more than one species cannot be discarded. The taxonomic situation of this taxon needs to be assessed taking into account both morphology and stratigraphy in detail.

- ***Ptychomya* sp. B** (Pl. 11, fig. 14 a, b)

This small species is not mentioned in the literature. It appears in the last two fossiliferous beds investigated in this study, of Early Barremian or younger age. It is probably related with *Ptychomya koeneni*.

Fam. **ARCTICIDAE**

- **Arcticidae sp.**

This is another not yet described heterodont bivalve. It is medium-sized (maximum length 40 mm, height 30 mm), slightly inequilateral, trigonal to suboval, with concentric growth lines, a blunt posterior ridge, and hinge teeth like in Arcticidae, similar to the Albian-Rc *Arctica* (Keen and Casey 1969) and the Jurassic *Pronoella* (Casey 1952).

- ***"Cyprina"* (?) sp.** (Pl. 11, fig. 15)

This species is represented only by four articulated individuals which resemble the genus *Cyprina* Lamarck.

Superfam. **VENEROIDEA**

Fam. **VENERIDAE**

At least three venerid species were found in this study. Hinges indicate that the species are venerid, although they do not fit descriptions of other Neocomian venerid like heterodonts of the Neuquén Basin (e.g. *Cyprina argentina* Behrendsen, 1892, *Thracia aequilatera* Behrendsen, 1892 and *Meretrix quintucoenis* Weaver, 1931). Species 1 (Pl. 11, fig. 16) is characterised by a shorter shell than species 2 and a well marked posterior carena (Pl. 11, fig. 17). Species 3, in contrast, is larger and less inequilateral (Pl. 11, fig. 18).

- **Veneridae sp. 1** (Pl. 11, fig. 16)
- **Veneridae sp. 2** (Pl. 11, fig. 17)
- **Veneridae sp. 3** (Pl. 11, fig. 18)

Order **MYOIDA**

Suborder **MYINA**

Superfam. **MYOIDEA**

Fam. **CORBULIDAE**

- ***Corbulomima bodenbenderi*** (Behrendsen, 1892) (Pl. 11, fig. 19)

- **Corbulidae sp. A** (Pl. 11, fig. 20)

Slightly inquivalved, with escutcheon and corbulid hinge.

- **Corbulidae sp. B**

Similar to Corbulidae sp. A but smaller, more compressed, and anterior part shorter.

Represents a younger species found in the Barremian beds of the upper part of the unit.

Superfam. **HIATELLOIDEA**

Fam. **HIATELLIDAE**

- ***Panopea dupiniana*** (d'Orbigny, 1843) (Pl. 11, fig. 21)
- ***Panopea gurgitis*** (Brongniart, 1822) (Pl. 11, fig. 22)

Three quantitatively rare, poorly preserved, shallow infaunal heterodont bivalves were collected. Poor preservation and low abundance precluded a proper identification of these species.

- **Heterodonta sp. A**
- **Heterodonta sp. B**
- **Heterodonta sp. C**

Subclass **ANOMALODESMATA**

Order **PHOLADOMYOIDA**

Superfam. **PHOLADOMYOIDEA**

Fam. **PHOLADOMYIDAE**

- ***Pholadomya gigantea*** (J. de C. Sowerby, 1836) (Pl. 10, fig. 11)
- ***Machomya*? sp.** (Pl. 11, fig. 23)

Similar to *Solenomya neocomiensis* (Haupt, 1907). However, Haupt's species lacks the posterior carena observed in the present specimens.

Phylum **Bryozoa**

Poorly preserved fragments of bryozoan colonies are rare but present in several shell beds. At least four species were detected, based on the morphology of the zooids. These species were named Bryozoa sp. A to D. Taxonomic identifications were not performed as the material is rare and poorly preserved. Bryozoans were neglected in recent (Lazo 2004) and past (Weaver 1931) scientific studies on the Neocomian of the Neuquén Basin.

Appendix B: Taxonomic counts section BAL

The following Table lists the species included in the multivariate analysis.

	Samples																																
Taxa	M1	M2	M3	M4	M5	M6	M7	M8	M9	M10	M11	M12	M13	M14	M15	M16	M17	M18	M19	M20	M21	M22	M23	M24	M25	M26	M27	M28	M29	M30	M31	M32	M33
Placopsilina sp.	0	0	0	0	0	0	0	0	0	0	0	0	0	0	0	0	0	0	0	0	0	0	0	0	0	0	0	0	0	0	0	0	0
Scleractinia sp. A	0	0	0	0	0	0	0	0	0	0	0	0	0	0	0	0	0	0	0	0	0	0	0	0	0	0	0	0	0	0	0	0	1
Scleractinia spp. indet.	0	0	0	0	0	0	0	0	0	0	0	0	0	0	0	0	0	0	0	0	0	0	0	0	0	0	0	0	0	0	0	0	0
Pygaster gerthi	0	0	0	0	0	0	0	0	0	0	0	0	0	0	0	0	0	0	0	0	0	0	0	0	0	0	0	0	0	0	0	0	0
Holectypus cf. *H. planatus*	0	0	0	0	0	0	0	0	0	0	0	0	0	0	0	0	0	0	0	0	0	0	0	0	0	0	0	0	0	0	0	0	0
Holectypus sp.	0	0	0	0	0	0	0	0	0	0	0	0	0	0	0	0	0	0	0	0	0	0	0	0	0	0	0	0	0	0	0	0	0
Regularia sp. A	0	0	0	0	0	0	0	0	0	0	0	0	0	0	0	0	0	0	0	0	0	0	0	0	0	0	0	0	0	0	0	0	0
Echinoidea spines	0	0	0	0	0	0	0	0	0	0	0	0	0	0	0	0	0	0	0	0	0	0	0	0	0	0	0	0	0	0	0	0	0
Crinoidea spp. indet.	0	0	0	0	0	0	0	0	0	0	0	0	0	0	0	0	0	0	0	0	0	0	0	0	0	0	0	0	0	0	0	0	0
bryozoa sp. A	0	0	0	0	0	0	0	0	0	0	0	0	0	0	0	0	0	0	0	0	0	0	0	0	0	0	0	0	0	0	0	0	0
bryozoa sp. B	0	0	0	0	0	0	0	0	0	0	0	0	0	0	0	0	0	0	0	0	0	0	0	0	0	1	0	0	0	0	0	0	0
bryozoa sp. C	0	0	0	0	0	0	0	0	0	0	0	0	0	0	0	0	0	0	0	0	0	0	0	0	0	0	0	0	0	0	0	0	0
bryozoa sp. D	0	0	0	0	0	0	0	0	0	0	0	0	0	0	0	0	0	0	0	0	0	0	0	0	0	0	0	0	0	0	0	0	0
Parsimonia antiquata	0	0	0	0	0	0	0	0	0	0	0	0	0	0	0	0	0	0	0	0	0	0	0	0	0	0	0	0	0	0	0	0	0
Sarcinella occidentalis	0	0	0	0	0	0	0	0	0	0	0	0	0	0	0	0	0	0	0	0	0	0	0	0	0	0	0	0	0	0	0	0	0
Serpulidae small	2	6	0	2	0	4	0	2	0	4	2	2	0	4	6	0	0	4	8	2	16	48	2	2	16	24	0	0	22	20	0	0	13
Serpulidae middle	0	0	0	0	0	0	0	0	0	0	0	0	0	0	0	0	0	0	0	0	0	0	0	0	0	0	0	0	0	0	0	0	1
Decapoda (fragments)	0	0	0	0	0	0	0	0	0	0	0	0	0	0	0	0	0	0	1	1	0	0	0	0	1	0	0	0	0	0	0	0	0
Trochidae sp. A	0	0	0	0	0	0	0	0	0	0	0	0	0	0	0	0	0	0	0	0	0	0	0	0	0	0	0	0	0	0	0	0	0
Trochidae? sp. B	0	0	0	0	0	0	0	0	0	0	0	0	0	0	0	0	0	0	0	0	0	0	0	0	0	0	0	0	0	0	0	0	1
Cerithium sp. A	0	0	0	0	0	0	0	0	0	0	0	0	0	0	0	0	0	0	0	0	0	0	0	0	0	0	0	0	0	0	0	0	0
Cerithium sp. B	0	0	0	0	0	0	0	0	0	0	0	0	0	0	0	0	0	0	0	0	0	0	0	0	0	0	0	0	0	0	0	0	0
Rhabdocolpus sp. A	0	1	0	0	0	0	0	0	0	0	0	0	0	1	0	0	0	0	0	5	0	0	0	1	1	0	0	1	0	0	2	1	18
Rhabdocolpus sp. B	0	0	0	0	0	0	0	0	0	0	0	0	0	0	0	0	0	0	0	0	0	0	0	0	0	0	0	0	0	0	0	0	0
Poasia sp. A	0	0	0	0	0	0	0	0	0	0	0	0	0	0	0	0	0	0	0	0	0	0	0	0	0	0	0	0	0	0	0	0	0
Poasia sp. B	0	0	0	0	0	0	0	0	0	0	0	0	0	0	0	0	0	0	0	0	0	0	0	0	0	0	0	0	0	0	0	0	0
Poasia sp. C	0	0	0	0	0	0	0	0	0	0	0	0	0	0	0	0	0	0	0	0	0	0	0	0	0	0	0	0	0	0	0	0	0
Protohemichenopus sp.	20	25	25	9	13	28	2	5	3	13	18	11	20	22	19	20	23	52	14	52	62	40	6	3	17	3	6	6	7	17	3	2	5
Dimorphosoma sp.	0	0	0	0	0	0	0	0	0	0	0	0	0	0	0	0	0	0	0	0	0	0	0	0	0	0	0	1	0	0	0	0	0
Aporrhaeidae sp. B	0	0	0	0	0	0	0	0	0	0	0	0	0	0	0	0	0	0	0	0	0	1	0	0	0	0	0	0	0	0	0	0	0
Pictavia sp. A	0	1	0	0	0	0	0	0	0	0	0	0	0	0	0	1	1	0	1	2	6	2	0	18	3	0	0	2	26	12	0	4	0
Pictavia sp. B	0	0	0	0	0	0	0	0	0	0	0	0	0	0	0	0	0	0	0	0	0	0	0	0	0	0	0	0	0	0	0	0	0
Confusiscala sp.	0	0	1	0	0	0	0	0	0	0	0	0	1	0	0	0	0	0	0	0	0	0	0	0	0	0	0	2	0	1	0	0	0
Bathraspira sp. A	19	76	44	23	25	37	9	39	24	108	76	61	134	43	76	37	37	110	43	152	57	115	7	0	53	19	0	0	0	0	1	0	0
Bathraspira sp. B	0	0	0	0	1	0	0	0	0	0	0	0	0	0	2	0	0	1	0	0	0	0	0	0	0	0	0	0	0	0	0	0	0
Bathraspira? sp. C	8	26	29	4	4	29	9	10	8	15	49	12	20	53	40	26	27	62	35	64	50	229	20	202	166	17	49	17	242	156	12	24	0
Ringinella sp. A	0	0	1	0	0	0	0	0	0	0	0	0	0	0	0	0	0	0	0	0	0	0	0	0	0	0	0	0	0	1	0	0	0
Ringinella sp. B	0	0	0	0	0	0	0	0	0	0	0	0	0	0	0	0	0	0	0	0	0	0	0	0	0	0	0	0	0	0	0	0	0
Tornatellaea sp.	0	0	0	0	0	0	0	0	0	0	0	0	0	0	0	0	0	0	0	0	0	0	0	0	0	0	0	0	0	1	0	0	0
Nuculoma sp.	0	0	0	0	0	0	0	0	0	0	0	0	0	0	0	0	0	0	0	0	0	2	0	0	0	0	0	0	1	0	0	0	0
Barbatia (*Barbatia*) sp.	0	0	0	0	0	0	0	0	0	0	0	0	0	0	0	0	0	0	0	0	0	0	0	0	0	0	0	0	0	0	0	0	0
Cucullaea gabrielis	0	0	0	0	0	0	0	0	0	0	0	0	0	0	0	0	0	0	0	0	0	0	0	0	0	0	0	0	0	0	0	0	0
Grammatodon securis	4	13	4	1	3	7	2	2	2	4	3	1	5	2	2	4	4	7	3	8	2	9	2	4	3	2	10	12	2	9	3	1	3
Grammatodon (*G*) sp.	0	0	0	0	0	0	0	0	0	0	0	0	0	0	0	0	0	0	0	0	0	0	0	0	0	0	0	0	0	0	0	0	0
Grammatodontinae sp. A	0	0	0	0	0	0	0	0	0	0	0	0	0	0	0	0	0	0	0	0	0	0	0	0	0	0	0	0	0	0	0	0	0
Grammatodontinae sp. B	0	0	0	0	0	0	0	0	0	0	0	0	0	0	0	0	0	0	0	0	0	0	0	0	0	0	0	0	0	0	0	0	0
Mytilinae sp. A	0	0	0	0	0	0	0	0	0	0	0	0	0	0	0	0	0	0	0	0	0	0	0	0	0	0	0	0	0	0	0	0	0
Crenellinae sp. A	0	0	0	0	0	0	0	0	0	0	0	0	0	0	0	0	0	0	0	0	0	0	0	0	0	0	0	0	0	0	0	0	0
Crenellinae sp. B	0	0	0	0	0	0	0	0	0	0	0	0	0	0	0	0	0	0	0	0	0	0	0	0	0	0	0	0	0	0	0	0	0
Modiolus cf. *M. ligeriensis*	0	0	0	0	0	0	0	0	0	0	0	0	0	0	0	0	0	0	0	0	0	0	0	0	0	0	0	0	0	0	0	0	0
Modiolus aff. *M. subsimplex*	0,00	0	0	0	0	0	0	0	0	0	0	0	0	0	0	0	0	0	0	0	0	0	0	0	0	0	0	0	0	0	0	0	0
Pinna robinaldina	0	0	0	0	0	0	0	0	0	0	0	0	0	0	0	0	0	0	0	0	0	0	0	0	0	0	0	0	0	0	0	0	0
Pinnidae sp.	0	0	0	0	0	0	0	0	0	0	0	0	0	0	0	0	0	0	0	0	0	0	0	0	0	0	0	0	0	0	0	0	0
Gervillaria alatior	0	0	0	0	0	0	0	0	0	0	0	0	0	0	0	0	0	0	0	0	0	0	0	0	0	0	0	0	0	0	0	0	0
Gervillella aviculoides	0	0	0	0	0	0	0	0	0	0	0	0	0	0	0	0	0	0	0	0	0	0	0	0	0	0	0	0	0	0	0	0	0
aff. *Cuneigervillia*	0	0	0	0	0	0	0	0	0	0	0	0	0	0	0	0	0	0	0	0	0	0	0	0	0	0	0	0	0	0	0	0	0
Pteriorida sp. A	0	0	0	0	0	0	0	0	0	0	0	0	0	0	0	0	0	0	0	0	0	0	0	0	0	0	0	0	0	0	0	0	0
Inoceramus sp. A	0	0	0	0	0	0	0	0	0	0	0	0	0	0	0	0	0	0	0	0	0	0	0	0	0	0	0	0	0	0	0	0	0
Inoceramus sp. B	0	0	0	0	0	0	0	0	0	0	0	0	0	0	0	0	0	0	0	0	0	0	0	0	0	0	0	0	0	0	0	0	0
Isognomon lotenoensis	0	0	0	0	0	0	0	0	0	0	0	0	0	0	0	0	0	0	0	0	0	0	0	0	0	0	0	0	0	0	0	0	0
Isognomon sp. A	0	0	0	0	0	0	0	0	0	0	0	0	0	0	0	0	0	0	0	0	0	0	0	0	0	0	0	0	0	0	0	0	0
Mimachlamys robinaldina	0	0	0	0	0	0	0	0	0	0	0	0	0	0	0	0	0	0	0	0	0	0	0	0	0	0	0	1	0	0	0	0	0
"Chlamys" puzoziana	0	0	0	0	0	0	0	0	0	0	0	0	0	0	0	0	0	0	0	0	0	0	0	0	0	0	0	0	0	0	0	0	0
"Pecten" vacaensis	0	0	0	0	0	0	0	0	0	0	0	0	0	0	0	0	0	0	0	0	0	0	0	0	0	0	0	0	0	0	0	0	0
cf. *Eopecten covuncoensis*	0	0	0	0	0	0	0	0	0	0	0	0	0	0	0	0	0	0	0	0	0	0	0	0	0	0	0	0	0	0	0	0	0
Pectinidae sp. A	0	0	0	0	0	0	0	0	0	0	0	0	0	0	0	0	0	0	0	0	0	0	0	0	0	0	0	0	0	0	0	0	0
Anomiidae sp. A	0	0	0	0	0	0	0	0	0	0	0	0	0	0	0	0	0	0	0	0	0	0	0	0	0	0	0	0	0	0	0	0	0
Aff. *Acesta* sp.	0	0	0	0	0	0	0	0	0	0	0	0	0	0	0	0	0	0	0	0	0	0	0	0	0	0	0	0	0	0	0	0	0
Aff. *Pseudolimea* sp.	0	0	0	0	0	0	0	0	0	0	0	0	0	0	0	0	0	0	0	0	0	0	0	0	0	0	0	0	0	0	0	0	0
Aetostreon sp.	0	0	0	0	0	0	0	0	0	0	0	0	0	0	0	0	0	0	0	0	0	0	0	0	0	0	0	0	0	1	0	1	9
Ceratostreon sp.	0	0	0	0	0	0	1	0	0	0	0	0	0	0	0	0	0	0	0	0	0	0	0	0	0	33	2	0	0	1	0	0	0
Gryphaeostrea sp. 1	8	5	0	3	3	8	9	3	1	2	2	5	7	3	0	1	2	1	0	4	3	7	0	3	1	1	0	0	0	6	0	2	4
Gryphaeostrea sp. 2	0	0	4	5	7	0	0	0	0	0	0	3	0	1	4	0	0	0	0	0	2	11	3	0	0	1	0	0	2	0	0	0	16
Exogyrinae sp. indet.	0	0	0	0	0	0	0	0	0	0	0	0	0	0	0	0	0	0	0	0	0	0	0	0	0	0	0	0	0	0	0	0	4
Lophinae sp. A	0	0	0	0	0	0	0	0	0	0	0	0	0	0	0	0	0	0	0	0	0	0	0	0	0	0	0	0	0	0	0	0	0
Lophinae sp. B	0	0	0	1	0	0	0	0	0	0	0	0	0	0	0	0	0	0	0	0	0	0	0	0	0	0	0	0	0	0	0	0	0
Myophorella volkheimeri	0	0	0	0	0	0	0	0	0	0	0	0	0	0	0	0	0	0	0	0	0	0	0	0	0	0	0	0	0	0	0	0	0
Myophorella garatei	0	0	0	0	0	0	0	0	0	0	0	0	0	0	0	0	0	0	0	0	0	0	0	0	0	0	0	0	0	0	0	0	0
Steinmanella raimondii	0	0	0	0	0	0	0	0	0	0	0	0	0	0	0	0	0	0	0	0	0	0	0	0	0	0	0	0	0	0	0	0	0
Steinmanella vacaensis	0	0	0	0	0	0	0	0	0	0	0	0	0	0	0	0	0	0	0	0	0	0	0	0	0	0	0	0	0	0	0	0	0
Rutitrigonia agrioensis	0	0	0	0	0	0	0	0	0	0	0	0	0	0	0	0	0	0	0	0	0	0	0	0	0	0	0	0	0	0	0	0	0
Pterotrigonia coihuicoensis	0	0	0	0	0	0	0	0	0	0	0	0	0	0	0	0	0	0	0	0	0	0	0	0	0	0	0	0	0	0	0	0	0
Pterotrigonia sp. A	0	0	0	0	0	0	0	0	0	0	0	0	0	0	0	0	0	0	0	0	0	0	0	0	0	0	0	0	0	0	0	0	0
Mesomiltha argentina	32	41	27	6	6	45	6	2	1	3	31	9	8	16	47	37	30	33	32	39	60	69	19	1	24	4	7	27	3	3	0	2	3
Mesomiltha sp. A	0	0	0	0	0	0	0	0	0	0	0	0	0	0	0	0	0	0	0	0	0	0	0	0	0	0	0	0	0	0	0	0	30
Lucina corbisoides	0	0	0	0	0	0	0	0	0	0	0	0	0	0	0	0	0	0	0	0	0	0	0	0	0	0	0	0	0	0	0	0	0
Lucina neuquensis	0	0	0	0	0	0	0	0	0	0	0	0	0	0	0	0	0	0	0	0	0	0	0	0	0	0	0	0	0	0	0	0	0
Lucinidae sp. A	0	0	0	0	0	0	0	0	0	0	0	0	0	0	0	0	0	0	0	0	0	0	0	0	0	0	0	0	0	0	0	0	0
Myoconcha transatlantica	0	0	0	0	0	0	0	0	0	0	0	0	0	0	0	0	0	0	0	0	0	0	0	0	0	0	0	0	0	0	0	0	0
Eriphyla argentina	0	0	0	0	0	0	0	0	0	0	0	0	0	0	0	0	0	0	0	0	0	0	0	1	1	0	0	0	0	1	0	1	0
Disparilia elongata	0	0	0	0	0	0	0	0	0	0	0	0	0	0	0	0	0	0	0	0	0	1	0	0	1	0	1	0	0	0	0	0	7
Neocrassina (*Coelastarte*) sp.	0	0	0	0	0	0	0	0	0	0	0	0	0	0	0	0	0	0	0	0	0	0	0	0	0	0	0	0	0	0	0	0	0
Astartidae sp. A	0	0	0	0	0	0	0	0	0	0	0	0	0	0	0	0	0	0	0	0	0	4	0	0	0	0	25	0	0	0	0	0	3
Protocardia sp.	0	0	0	0	0	0	0	0	0	0	0	0	0	0	0	0	0	0	0	0	0	0	0	0	0	0	0	0	0	0	0	0	0
"*Solecurtus*" *neuquensis*	0	0	0	0	0	0	0	0	0	0	0	0	0	0	0	0	0	0	0	0	0	0	0	0	0	0	0	0	0	0	0	0	0
Ptychomya sp. A (cf. *P. koeneni*)	0	0	0	0	0	0	0	0	0	0	0	0	0	0	0	0	0	0	0	0	0	0	0	0	1	0	0	0	0	0	0	0	1
Ptychomya sp. B	0	0	0	0	0	0	0	0	0	0	0	0	0	0	0	0	0	0	0	0	0	0	0	0	0	0	0	0	0	0	0	0	0
Arcticidae sp.	0	0	0	0	0	0	0	0	0	0	0	0	0	0	0	0	0	0	0	0	0	0	0	0	0	0	0	0	0	0	0	0	0
"*Cyprina*"	0	0	0	0	0	0	0	0	0	0	0	0	0	0	1	0	0	0	0	0	0	0	0	0	0	0	0	0	0	2	0	0	0
Veneridae sp. 1	0	0	0	0	0	0	0	0	0	0	0	0	0	0	0	0	0	0	0	0	0	0	0	0	0	0	0	0	0	0	0	0	0
Veneridae sp. 2	0	0	0	0	0	0	0	0	0	0	0	0	0	0	0	0	0	0	0	0	0	0	0	0	0	0	0	0	0	0	0	0	0
Veneridae sp. 3	0	0	0	0	0	0	0	0	0	0	0	0	0	0	0	0	0	0	0	0	0	0	0	0	0	0	0	16	0	0	0	0	0
Corbulomima "*bodenbenderi*"	0	0	1	0	0	0	0	0	0	0	1	1	1	0	0	0	2	0	0	0	2	12	0	9	12	0	23	9	16	17	20	11	10
Corbulidae sp. A	0	0	0	0	0	0	0	0	0	0	0	0	0	1	0	1	1	1	0	0	1	10	0	1	4	3	0	6	2	0	0	1	2
Corbulidae sp. B	0	0	0	0	0	0	0	0	0	0	0	0	0	0	0	0	0	0	0	0	0	0	0	0	0	0	0	0	0	0	0	0	0
Panopea neocomiensis	0	0	0	0	0	0	0	0	0	0	0	0	0	0	0	0	0	0	0	0	0	0	0	0	0	0	0	0	0	0	0	0	0
Panopea dupiniana	0	0	0	0	0	0	0	0	0	0	0	0	0	0	0	0	0	0	0	0	0	0	0	0	0	0	0	0	0	0	0	0	0
Pholadomya gigantea	0	0	0	0	0	0	0	0	0	0	0	0	0	0	0	0	0	0	0	0	0	0	0	0	0	0	0	0	0	0	0	0	0
Machomya? sp.	0	0	0	0	0	0	0	0	0	0	0	0	0	0	0	0	0	0	0	0	0	0	0	0	0	0	0	0	0	0	0	0	0
Heterodonta sp. indet. A	0	0	0	0	0	0	0	0	0	0	0	0	0	0	0	0	0	0	0	0	0	0	0	0	0	0	0	0	0	0	0	0	0
Heterodonta sp. indet. B	0	0	0	0	0	0	0	0	0	0	0	0	0	0	0	0	0	0	0	0	0	0	0	0	0	0	0	0	0	0	0	0	0
Heterodonta sp. indet. C	0	0	0	0	0	0	0	0	0	0	0	0	0	0	0	0	0	0	0	0	0	0	0	0	0	0	0	0	0	0	0	0	0
Dentallium ?	0	1	0	2	0	2	0	0	0	0	0	0	0	2	3	0	0	0	0	1	2	10	2	2	6	2	3	12	3	7	0	1	13
Sample size	93	195	136	56	62	160	38	63	39	149	182	105	196	148	200	127	127	271	137	330	263	570	61	247	310	110	126	112	326	255	41	51	144

	Samples																													
Taxa	M34	M35	M36	M37	M38	M39	M40	M41	M42	M43	M44	M45	M46	M46P	M47	M48	M49	M49P	M50	M51	M52	M53	M54	M54P	M55	M55P	M56	M57	M57P	M58
Placopsilina sp.	0	0	0	0	0	2	4	0	0	0	0	0	10	10	0	0	0	0	0	0	0	0	10	10	5	5	0	30	30	1
Scleractinia sp. A	0	0	0	0	0	2	1	0	0	0	0	0	0	0	0	0	0	0	0	0	0	0	0	0	0	0	0	0	0	0
Scleractinia spp. indet.	0	0	0	0	0	0	0	0	0	0	0	0	0	0	0	0	0	0	0	0	0	0	0	0	0	0	0	0	0	0
Pygaster gerthi	0	0	0	0	0	0	0	0	0	0	0	0	0	0	0	0	0	0	0	0	0	0	0	0	0	0	0	0	0	0
Holectypus cf. *H. planatus*	0	0	0	0	0	0	0	0	0	0	0	0	0	0	0	0	0	0	0	0	0	0	0	0	0	0	0	0	0	0
Holectypus sp.	0	0	0	0	0	0	0	0	0	0	0	0	0	0	0	0	0	0	0	0	0	0	0	0	0	0	0	0	0	0
Regularia sp. A	0	0	0	0	0	0	0	0	0	0	0	0	0	0	0	0	0	0	0	0	0	0	0	0	0	0	0	0	0	0
Echinoidea spines	0	1	1	0	1	1	0	0	0	0	0	0	2	2	0	0	0	0	0	0	0	0	0	0	0	0	0	0	0	0
Crinoidea spp. indet.	0	0	0	0	0	0	0	0	0	0	0	0	0	0	0	0	0	0	0	0	0	0	0	0	0	0	0	0	0	0
bryozoa sp. A	0	0	0	0	0	1	0	0	0	0	0	0	0	0	0	0	0	0	0	0	0	0	0	0	1	1	0	0	0	0
bryozoa sp. B	0	0	0	0	0	0	0	0	0	0	0	0	0	0	0	0	0	0	0	0	0	0	0	0	0	0	0	0	0	1
bryozoa sp. C	0	0	0	0	0	0	0	0	0	0	0	0	0	0	0	0	0	0	0	0	0	0	0	0	0	0	0	0	0	0
bryozoa sp. D	0	0	0	0	0	0	0	0	0	0	0	0	0	0	0	0	0	0	0	0	0	0	0	0	0	0	0	0	0	0
Parsimonia antiquata	0	0	0	0	0	0	0	0	0	0	0	0	29	29	0	0	1	30	0	0	0	0	1	33	1	31	0	0	0	0
Sarcinella occidentalis	0	0	0	0	0	0	0	0	0	0	0	0	0	0	0	0	0	0	0	0	0	0	0	0	0	0	0	0	0	0
Serpulidae small	0	23	7	0	0	3	20	0	0	0	0	0	18	18	3	5	5	5	1	5	0	10	24	24	9	9	4	24	24	17
Serpulidae middle	0	3	0	0	0	0	0	0	0	0	0	0	0	0	0	0	1	244	0	0	0	0	0	0	0	0	0	38	78	1
Decapoda (fragments)	0	0	0	0	0	0	0	0	0	0	0	0	0	0	0	0	0	0	0	0	0	0	0	0	0	0	0	0	0	0
Trochidae sp. A	0	0	0	0	0	0	0	0	0	0	0	0	0	0	0	0	0	0	0	0	0	0	0	0	0	0	0	0	0	0
Trochidae? sp. B	0	0	0	0	0	0	0	0	0	0	0	0	0	0	0	0	0	0	0	0	0	0	0	0	0	0	0	0	0	0
Cerithium sp. A	0	0	0	0	0	0	0	0	0	0	0	0	0	0	0	0	0	0	0	0	0	0	0	0	0	0	0	0	0	0
Cerithium sp. B	0	0	0	0	0	0	0	0	0	0	0	0	0	0	0	0	0	0	0	0	0	0	0	0	0	0	0	0	0	0
Rhabdocolpus sp. A	2	12	21	1	38	9	5	0	0	0	0	0	0	0	0	0	0	0	0	0	0	0	0	0	0	0	3	0	0	0
Rhabdocolpus sp. B	0	0	0	0	0	0	0	0	0	0	0	0	0	0	0	0	0	0	0	0	0	0	0	0	0	0	0	0	0	0
Poasia sp. A	0	0	0	0	0	0	0	0	0	0	0	0	0	0	0	0	0	0	0	0	0	0	0	0	0	0	0	0	0	0
Poasia sp. B	0	0	0	0	0	0	0	0	0	0	0	0	0	0	0	0	0	0	0	0	0	0	0	0	0	0	0	0	0	0
Poasia sp. C	0	0	0	0	0	0	0	0	0	0	0	0	0	0	0	0	0	0	0	0	0	0	0	0	0	0	0	0	0	0
Protohemichenopus sp.	3	0	0	0	1	0	1	0	0	0	0	0	0	0	0	0	0	0	0	0	0	0	0	0	0	0	0	0	0	0
Dimorphosoma sp.	0	1	1	0	0	0	0	0	0	0	0	0	0	0	0	0	0	0	0	0	0	0	4	4	0	0	0	0	0	0
Aporrhaeidae sp. B	0	0	0	0	0	0	0	0	0	0	0	0	0	0	0	0	0	0	0	0	0	0	0	0	0	0	0	0	0	0
Pictavia sp. A	0	0	0	0	0	0	0	0	0	0	0	0	0	0	0	0	0	0	0	0	0	0	0	0	0	0	0	0	0	0
Pictavia sp. B	0	0	0	0	0	0	0	0	0	0	0	0	0	0	0	0	0	0	0	0	0	0	0	0	0	0	0	0	0	0
Confusiscala sp.	0	0	0	0	0	0	0	0	0	0	0	0	0	0	0	0	0	0	0	0	0	0	0	0	0	0	0	0	0	0
Bathraspira sp. A	0	1	1	0	0	0	0	0	0	0	0	0	0	0	0	0	0	0	0	0	0	0	0	0	0	0	0	0	0	0
Bathraspira sp. B	0	0	0	0	0	1	0	0	0	0	0	0	0	0	0	0	0	0	0	0	0	0	0	0	0	0	0	0	0	0
Bathraspira? sp. C	0	0	1	0	0	0	0	0	0	0	0	0	0	0	0	0	0	0	0	0	0	0	0	0	0	0	0	0	0	0
Ringinella sp. A	0	0	0	0	0	0	0	0	0	0	0	0	0	0	0	0	1	1	0	0	0	0	0	0	0	0	0	0	0	0
Ringinella sp. B	0	1	0	0	0	0	0	0	0	0	0	0	0	0	0	0	0	0	0	0	0	0	0	0	0	0	0	0	0	0
Tornatellaea sp.	0	0	0	0	0	0	0	0	0	0	0	0	0	0	0	0	0	0	0	0	0	0	0	0	0	0	0	0	0	0
Nuculoma sp.	0	0	0	0	0	0	0	0	0	0	0	0	0	0	0	0	0	0	0	0	0	0	0	0	0	0	0	0	0	0
Barbatia (*Barbatia*) sp.	0	0	0	0	0	0	0	0	0	0	0	0	0	0	0	0	0	0	0	0	0	0	0	0	0	0	0	0	0	0
Cucullaea gabrielis	0	0	0	0	0	0	0	0	0	0	78	0	2	2	0	11	28	28	0	7	0	2	30	30	4	4	0	3	3	5
Grammatodon securis	3	4	3	0	5	0	0	1	0	0	0	0	0	0	2	0	0	0	0	0	0	0	4	4	0	0	0	0	0	0
Grammatodon (*G*) sp.	0	0	0	0	0	0	0	0	0	0	0	0	0	0	0	0	0	0	0	0	0	0	0	0	0	0	0	0	0	0
Grammatodontinae sp. A	0	2	1	0	2	0	1	1	0	1	0	0	0	0	0	0	0	0	0	0	0	0	1	1	0	0	0	0	0	0
Grammatodontinae sp. B	0	0	0	0	0	0	0	0	0	0	0	0	0	0	0	0	0	0	0	0	0	0	0	0	0	0	0	0	0	0
Mytilinae sp. A	0	0	0	0	0	0	0	0	0	0	0	0	0	0	0	0	0	0	0	0	0	0	0	0	0	0	0	0	0	0
Crenellinae sp. A	0	0	0	0	0	0	0	5	0	2	0	0	0	0	0	0	0	0	0	0	0	0	7	0	0	0	0	0	0	0
Crenellinae sp. B	0	0	0	0	0	0	0	0	0	0	0	0	0	0	0	0	0	0	2	0	0	0	0	0	0	0	1	0	0	0
Modiolus cf. *M. ligeriensis*	0	0	0	0	0	0	0	1	0	0	0	0	0	0	0	0	0	0	0	0	0	0	0	7	0	0	0	6	6	0
Modiolus aff. *M. subsimplex*	0	0	0	0	0	0	0	0	0	0	0	0	0	0	0	0	0	0	0	0	0	0	0	0	0	0	0	0	0	0
Pinna robinaldina	0	0	0	0	0	0	0	1	0	0	18	134	1	1	0	28	0	0	0	0	0	2	0	0	0	0	0	0	0	0
Pinnidae sp.	0	0	0	0	0	0	0	0	0	0	0	0	0	0	0	0	0	0	0	0	0	0	0	0	0	0	0	0	0	1
Gervillaria alatior	0	0	0	0	0	0	0	0	0	0	0	0	0	0	0	0	0	0	0	0	0	0	0	0	0	0	0	0	0	0
Gervillella aviculoides	0	0	0	0	0	0	0	0	0	0	0	0	16	16	0	0	1	1	0	1	0	20	78	78	43	43	24	1	1	10
aff. *Cuneigervillia*	0	0	0	0	0	0	0	0	0	0	0	0	0	0	0	0	0	0	0	0	0	0	0	0	0	0	0	0	0	0
Pteriorida sp. A	0	0	0	0	0	0	0	0	0	0	0	0	0	0	0	0	3	3	2	0	0	0	0	0	0	0	0	0	0	0
Inoceramus sp. A	0	0	0	0	0	0	0	7	0	0	0	0	0	0	1	0	0	0	0	0	0	0	0	0	0	0	0	0	0	0
Inoceramus sp. B	0	0	0	0	0	0	0	0	0	0	0	0	0	0	0	0	0	0	0	0	0	0	0	0	0	0	0	0	0	0
Isognomon lotenoensis	0	0	0	0	0	0	0	0	0	0	0	0	2	2	0	0	0	0	0	0	0	0	4	4	2	2	0	4	4	0
Isognomon sp. A	0	0	0	0	0	0	1	0	0	0	0	0	0	0	0	0	0	0	0	0	0	0	0	0	0	0	0	0	0	0
Mimachlamys robinaldina	0	0	0	0	0	1	1	0	0	0	0	0	13	13	2	0	8	8	5	0	2	24	0	0	1	1	1	0	0	6
"Chlamys" puzoziana	0	0	0	0	0	0	0	0	0	0	0	0	0	0	0	0	0	0	0	0	0	0	0	0	0	0	0	0	0	0
"Pecten" vacaensis	0	0	0	0	0	0	0	2	2	2	0	0	0	0	0	0	0	0	0	0	0	30	0	0	0	0	0	0	0	0
cf. *Eopecten covuncoensis*	0	0	0	0	0	0	0	0	0	0	0	0	0	0	0	0	0	0	0	0	0	0	0	0	0	0	0	0	0	0
Pectinidae sp. A	0	0	0	0	0	0	0	0	0	0	0	0	1	1	0	0	0	0	1	0	0	4	0	0	0	0	0	0	0	0
Anomiidae sp. A	0	0	0	0	0	2	0	0	0	0	0	0	0	0	0	0	0	0	0	0	0	0	0	0	0	0	0	0	0	0
Aff. *Acesta* sp.	0	0	0	0	0	0	0	0	0	0	0	0	0	0	0	0	0	0	0	0	0	0	8	8	0	0	0	0	0	0
Aff. *Pseudolimea* sp.	0	0	0	0	0	0	0	2	0	0	0	0	0	0	0	0	0	0	0	0	0	0	0	0	0	0	0	0	0	0
Aetostreon sp.	2	15	15	14	12	91	117	7	108	1	16	0	1	1	0	2	4	4	0	0	0	0	0	0	0	0	0	0	0	0
Ceratostreon sp.	0	5	0	2	0	13	12	5	0	0	0	0	12	144	2	7	6	6	6	0	0	0	30	71	41	87	27	17	65	13
Gryphaeostrea sp. 1	0	0	6	1	0	0	0	0	0	0	0	0	0	0	0	0	0	0	0	0	0	0	0	0	0	0	0	0	0	0
Gryphaeostrea sp. 2	3	15	4	0	1	2	3	3	0	0	0	0	0	0	0	0	0	0	0	0	0	0	0	0	0	0	0	0	0	0
Exogyrinae sp. indet.	0	0	0	0	0	0	0	0	0	0	0	0	0	0	0	0	0	0	0	0	0	0	0	0	0	0	0	0	0	0
Lophinae sp. A	0	0	0	0	0	0	0	0	0	0	0	0	0	0	0	0	0	0	0	0	0	0	0	0	0	0	0	0	0	0
Lophinae sp. B	0	0	0	0	0	0	0	0	0	0	0	0	0	0	0	0	0	0	0	0	0	0	0	0	0	0	0	0	0	0
Myophorella volkheimeri	0	0	2	0	0	2	1	19	4	3	2	0	22	22	13	15	12	12	11	8	0	4	16	16	11	11	31	6	6	26
Myophorella garatei	0	0	0	0	0	0	0	0	0	0	0	0	0	0	0	0	0	0	0	0	0	0	0	0	0	0	0	0	0	0
Steinmanella raimondii	0	0	0	0	0	0	0	0	0	0	0	0	0	0	0	0	4	4	0	0	0	0	0	0	0	0	0	0	0	0
Steinmanella vacaensis	0	0	0	0	0	0	0	0	0	0	8	0	0	0	0	0	4	4	0	0	0	0	5	5	4	4	0	0	0	5
Rutitrigonia agrioensis	0	0	0	0	0	0	0	0	0	0	10	0	1	1	0	0	9	9	0	0	0	0	0	0	0	0	0	0	0	1
Pterotrigonia coihuicoensis	0	0	0	0	0	1	1	0	0	0	0	0	0	0	0	6	1	1	2	0	0	2	1	1	2	2	0	14	14	126
Pterotrigonia sp. A	0	0	0	0	0	0	0	0	0	0	0	0	0	0	0	0	0	0	0	0	0	0	0	0	0	0	0	0	0	0
Mesomiltha argentina	0	0	6	0	0	0	2	0	0	0	0	0	0	0	0	0	0	0	0	0	0	0	0	0	0	0	0	0	0	0
Mesomiltha sp. A	2	4	0	2	9	0	0	0	0	0	0	0	0	0	1	0	0	0	0	0	0	0	0	0	0	0	0	0	0	0
Lucina corbisoides	0	0	0	0	0	0	2	1	0	0	0	0	0	0	0	0	0	0	0	0	0	0	0	0	0	0	0	0	0	0
Lucina neuquensis	0	0	0	0	0	0	0	0	0	0	0	0	0	0	0	0	2	2	0	0	0	0	0	0	0	0	0	0	0	0
Lucinidae sp. A	0	0	0	0	0	0	0	0	0	0	0	0	0	0	0	0	1	1	0	0	0	0	0	0	0	0	0	0	0	2
Myoconcha transatlantica	0	0	0	0	0	4	14	0	0	0	0	0	21	21	0	0	0	0	0	0	0	0	56	56	1	1	0	30	30	31
Eriphyla argentina	0	0	0	0	0	0	3	15	2	2	3	0	144	144	4	65	5	5	3	7	0	2	40	40	63	63	64	134	134	51
Disparilia elongata	14	30	30	2	54	14	3	20	3	9	0	0	2	2	16	0	9	9	9	0	0	0	23	23	2	2	11	0	0	0
Neocrassina (*Coelastarte*) sp.	0	0	0	0	0	0	0	0	0	0	0	0	0	0	0	0	0	0	0	0	0	0	0	0	0	0	0	0	0	0
Astartidae sp. A	0	10	2	0	2	3	0	2	0	2	0	0	0	0	0	0	0	0	0	0	0	0	0	0	0	0	0	0	0	0
Protocardia sp.	0	0	0	0	0	0	0	0	0	0	0	0	0	0	0	0	0	0	5	0	0	0	0	0	0	0	0	0	0	0
"*Solecurtus*" *neuquensis*	0	0	0	0	0	0	0	0	0	0	0	0	2	2	0	0	16	16	0	1	0	0	0	0	0	0	6	0	0	0
Ptychomya sp. A (cf. *P. koeneni*)	2	9	2	0	0	2	2	2	0	0	0	0	25	25	9	17	23	23	7	18	0	0	82	82	11	11	12	75	75	5
Ptychomya sp. B	0	0	0	0	0	0	0	0	0	0	0	0	0	0	0	0	0	0	0	0	0	0	0	0	0	0	0	0	0	0
Arcticidae sp.	0	0	0	0	0	0	0	0	0	0	0	0	0	0	0	0	0	0	0	0	0	0	0	0	0	0	0	0	0	0
"*Cyprina*"	0	0	0	0	0	0	0	0	0	0	0	0	0	0	0	0	0	0	0	0	0	0	0	0	0	0	0	0	0	0
Veneridae sp. 1	0	0	0	0	0	0	0	87	0	21	0	0	0	0	0	0	0	0	7	0	0	0	0	0	0	0	0	0	0	0
Veneridae sp. 2	6	0	2	0	0	0	0	44	9	10	0	0	3	3	20	29	15	15	17	13	19	0	6	6	2	2	3	0	0	1
Veneridae sp. 3	0	0	0	0	0	0	0	0	0	0	0	0	0	0	0	0	27	27	96	32	7	0	11	11	1	1	3	0	0	0
Corbulomima "*bodenbenderi*"	3	10	6	0	4	0	0	7	1	2	0	0	0	0	0	0	0	0	0	0	0	0	0	0	0	0	0	0	0	0
Corbulidae sp. A	0	0	0	0	0	0	0	1	0	0	0	0	0	0	0	0	0	0	0	0	0	0	0	0	0	0	0	0	0	0
Corbulidae sp. B	0	0	0	0	0	0	0	0	0	0	0	0	0	0	0	0	0	0	0	0	0	0	0	0	0	0	0	0	0	0
Panopea neocomiensis	0	0	0	0	0	0	0	0	0	0	5	0	0	0	0	4	6	6	4	3	20	0	9	9	7	7	4	0	0	4
Panopea dupiniana	0	0	0	0	0	0	0	2	0	0	2	0	12	12	0	10	77	77	2	8	0	6	9	9	36	36	18	0	0	2
Pholadomya gigantea	0	0	0	0	0	0	0	0	0	0	0	0	3	3	0	4	0	0	0	0	0	0	0	0	4	4	2	0	0	18
Machomya? sp.	0	0	0	0	0	0	0	0	0	0	0	0	0	0	0	0	0	0	0	0	0	0	0	0	0	0	0	0	0	0
Heterodonta sp. indet. A	0	0	0	0	0	0	0	0	0	0	0	0	0	0	0	0	0	0	0	0	0	0	0	0	0	0	0	0	0	0
Heterodonta sp. indet. B	0	0	0	0	0	0	0	0	0	0	0	0	0	0	0	0	0	0	0	0	0	0	0	0	0	0	0	0	0	0
Heterodonta sp. indet. C	3	0	1	0	1	0	0	0	0	1	0	0	0	0	1	0	2	2	0	0	0	0	0	0	0	0	0	0	0	0
Dentallium ?	14	11	9	0	3	2	0	5	0	0	0	0	0	0	3	0	0	0	0	0	0	0	0	0	0	0	1	0	0	0
Sample size	57	157	121	22	133	156	194	240	129	56	142	134	342	474	77	203	271	543	180	103	48	106	459	532	251	327	215	382	470	327

	Samples																														
Taxa	M58P	M58R	M59	M60	M61	M62	M63	M63P	M64	M65	M66	M67	M68	M69	M70	M71	M72	M73	M74	M74P	M75	M76	M77	M78	M79	M80	M81	M82	M83	M84	M85
Placopsilina sp.	1	0	0	0	4	2	3	3	2	0	0	12	7	0	0	0	0	0	0	0	0	1	0	0	0	0	0	0	2	4	0
Scleractinia sp. A	0	0	0	0	0	0	0	0	0	0	0	0	0	0	0	0	0	0	0	0	0	0	0	0	0	0	0	0	0	0	0
Scleractinia spp. indet.	0	0	0	0	0	0	0	0	0	0	0	0	0	0	0	0	0	0	0	0	0	0	0	0	0	0	0	0	0	0	0
Pygaster gerthi	0	0	0	0	0	0	0	0	0	0	0	0	0	0	0	0	0	0	0	0	0	0	0	0	0	0	0	0	0	0	0
Holectypus cf. *H. planatus*	0	0	0	0	0	0	0	0	0	0	0	0	0	0	0	0	0	0	0	0	0	0	0	0	0	0	0	0	0	0	1
Holectypus sp.	0	0	0	0	0	0	0	0	0	0	0	0	0	0	0	0	0	0	0	0	0	0	0	0	0	0	1	0	0	0	0
Regularia sp. A	0	0	0	0	0	0	0	0	0	0	0	0	0	0	0	0	0	0	1	1	0	0	0	0	0	0	0	0	0	0	0
Echinoidea spines	0	0	0	0	0	0	0	0	0	0	0	0	0	0	0	0	0	0	0	0	0	0	0	0	1	0	0	0	0	0	0
Crinoidea spp. indet.	0	0	0	0	0	0	0	0	0	0	0	0	0	0	0	0	0	0	0	0	0	0	0	0	1	0	0	0	1	1	0
bryozoa sp. A	0	0	2	1	0	2	1	1	0	0	2	6	3	0	0	0	0	0	0	0	0	1	0	0	0	0	0	0	0	0	0
bryozoa sp. B	1	0	0	0	2	0	0	0	0	0	0	1	0	0	0	0	0	0	0	0	0	0	0	0	1	0	0	0	0	0	0
bryozoa sp. C	0	0	0	0	0	0	0	0	0	0	0	0	0	0	0	0	0	0	0	0	0	0	0	0	0	0	0	0	3	0	1
bryozoa sp. D	0	0	0	0	0	0	0	0	0	0	0	2	0	0	0	0	0	0	0	0	0	0	0	0	0	0	0	0	0	0	0
Parsimonia antiquata	0	0	0	0	0	0	0	0	0	0	0	0	0	0	0	0	0	0	0	0	0	0	0	0	0	0	0	0	0	0	0
Sarcinella occidentalis	0	0	0	0	0	0	0	0	0	0	0	0	0	0	0	0	0	0	0	0	0	0	0	0	0	0	0	0	26	1	0
Serpulidae small	17	10	20	7	8	18	0	0	5	0	0	15	15	0	6	1	6	0	3	3	12	1	1	0	11	1	11	0	22	2	7
Serpulidae middle	62	62	0	0	2	0	1	37	13	0	0	0	0	0	0	0	0	0	0	0	0	0	0	0	0	0	0	0	0	0	0
Decapoda (fragments)	0	0	0	0	0	0	0	0	0	0	0	0	0	0	0	0	0	0	0	0	0	0	0	0	0	0	0	0	0	0	0
Trochidae sp. A	0	0	0	0	0	0	0	0	0	0	0	0	0	0	0	0	0	0	0	0	0	0	0	0	0	0	0	0	0	0	0
Trochidae? sp. B	0	0	0	0	0	0	0	0	0	0	0	0	0	0	0	0	0	0	0	0	0	0	0	0	0	0	0	0	0	0	0
Cerithium sp. A	0	0	0	0	0	0	0	0	0	0	0	0	0	0	0	0	0	0	0	0	0	0	0	0	0	0	0	0	0	0	0
Cerithium sp. B	0	0	0	0	0	0	0	0	0	0	0	0	0	0	0	0	0	0	0	0	0	0	0	0	0	0	0	0	0	0	0
Rhabdocolpus sp. A	0	0	0	0	0	0	0	0	0	0	0	0	0	0	0	0	0	0	0	0	0	0	0	0	0	0	0	0	0	0	0
Rhabdocolpus sp. B	0	0	0	0	0	0	0	0	0	0	0	0	0	0	0	0	0	0	0	0	0	0	0	0	0	0	0	0	0	0	0
Poasia sp. A	0	0	0	0	0	0	0	0	0	0	0	0	0	0	0	0	0	0	0	0	0	0	0	0	0	0	0	0	0	0	0
Poasia sp. B	0	0	0	0	0	0	0	0	0	0	0	0	0	0	0	0	0	0	0	0	0	0	0	0	0	0	0	0	0	0	0
Poasia sp. C	0	0	0	0	0	0	0	0	0	0	0	0	0	0	0	0	0	0	0	0	0	0	0	0	0	0	0	0	0	0	0
Protohemichenopus sp.	0	0	0	0	0	0	0	0	0	0	0	0	0	0	0	0	0	0	0	0	0	0	0	0	0	0	0	0	0	0	0
Dimorphosoma sp.	0	0	0	0	0	0	0	0	0	0	0	0	0	0	0	0	3	2	1	1	0	18	0	6	0	0	0	1	0	0	0
Aporrhaeidae sp. B	0	0	0	0	0	0	0	0	0	0	0	0	0	0	0	0	0	0	0	0	0	0	0	0	0	0	0	0	0	0	0
Pictavia sp. A	0	0	0	0	0	0	0	0	0	0	0	0	0	0	0	0	0	0	0	0	0	0	0	0	0	0	0	0	0	0	0
Pictavia sp. B	0	0	0	0	0	0	0	0	0	0	0	0	0	0	0	0	0	0	0	0	0	0	0	0	0	0	0	0	0	0	0
Confusiscala sp.	0	0	0	5	0	0	0	0	0	0	0	0	0	0	0	0	0	0	0	0	0	0	0	0	0	0	0	0	0	0	0
Bathraspira sp. A	0	0	0	0	0	0	0	0	0	0	0	0	0	0	0	0	0	0	0	0	0	0	0	0	0	0	0	0	0	0	0
Bathraspira sp. B	0	0	0	0	0	0	0	0	0	0	0	0	0	0	0	0	0	0	0	0	0	0	0	0	0	0	0	0	0	0	0
Bathraspira? sp. C	0	0	0	0	0	0	0	0	0	0	0	0	0	0	0	0	0	0	0	0	0	0	0	0	0	1	0	0	0	0	0
Ringinella sp. A	0	0	0	0	0	0	0	0	0	0	0	0	0	0	0	0	0	2	0	0	0	0	0	0	0	0	0	0	0	0	0
Ringinella sp. B	0	0	0	0	0	0	0	0	0	0	0	0	0	0	0	0	0	0	0	0	0	0	0	0	0	0	0	0	0	0	0
Tornatellaea sp.	0	0	0	0	0	0	0	0	0	0	0	0	0	0	0	0	0	0	0	0	0	0	0	0	0	0	0	0	0	0	0
Nuculoma sp.	0	0	0	0	0	0	0	0	0	0	0	0	0	0	0	0	0	0	0	0	0	0	0	0	0	0	0	0	0	0	0
Barbatia (*Barbatia*) sp.	0	0	0	0	1	0	0	0	0	0	0	0	0	0	0	0	0	0	0	0	0	0	0	0	0	0	0	0	0	0	0
Cucullaea gabrielis	5	0	4	0	0	2	8	8	4	2	6	0	3	0	1	0	0	0	0	0	0	0	2	0	1	0	0	0	7	10	2
Grammatodon securis	0	0	0	0	0	0	0	0	0	0	0	0	0	0	0	0	0	0	0	0	0	0	0	0	0	0	0	0	0	0	0
Grammatodon (*G*) sp.	0	0	0	0	0	0	0	0	0	0	0	0	0	0	0	0	0	0	0	0	0	0	0	0	0	0	0	0	0	0	0
Grammatodontinae sp. A	0	0	0	0	0	0	0	0	0	0	0	0	0	0	0	0	0	1	0	0	0	0	0	0	0	0	0	0	0	0	0
Grammatodontinae sp. B	0	0	0	0	0	0	0	0	0	0	0	0	0	0	0	0	0	0	0	0	0	0	0	0	0	0	0	0	0	0	0
Mytilinae sp. A	0	0	0	0	0	0	0	0	0	0	0	0	0	0	0	0	0	0	0	0	0	0	0	0	1	0	0	0	0	0	0
Crenellinae sp. A	0	0	0	0	0	0	0	0	0	0	0	0	0	0	0	0	0	0	0	0	0	0	0	0	0	0	0	0	0	0	0
Crenellinae sp. B	0	0	0	0	0	0	0	0	0	0	0	0	0	0	0	0	0	0	0	0	0	0	0	0	0	0	0	0	0	0	0
Modiolus cf. *M. ligeriensis*	0	0	0	1	2	0	0	0	0	0	0	0	0	2	0	3	0	0	0	0	0	0	0	0	5	0	0	0	0	0	0
Modiolus aff. *M. subsimplex*	0	0	0	0	0	0	0	0	0	0	0	0	0	0	0	0	0	0	0	0	0	0	0	0	0	0	0	0	2	0	0
Pinna robinaldina	0	0	0	0	0	0	0	0	0	0	0	0	0	0	0	0	0	0	0	0	0	0	0	0	1	0	0	0	0	0	0
Pinnidae sp.	1	0	0	0	0	0	0	0	0	0	0	0	0	0	0	0	0	0	0	0	0	0	0	0	0	0	0	0	0	0	0
Gervillaria alatior	0	0	0	0	0	0	0	0	0	0	0	0	0	0	0	0	0	0	0	0	0	0	0	0	0	0	0	0	0	0	0
Gervillella aviculoides	10	0	2	2	4	2	0	0	0	1	2	0	0	0	0	0	0	0	0	0	1	0	0	0	0	0	0	0	0	0	6
aff. *Cuneigervillia*	0	0	0	0	0	0	0	0	0	0	0	0	0	0	0	0	0	0	0	0	0	0	0	0	0	0	0	0	0	0	0
Pteriorida sp. A	0	0	0	0	0	0	0	0	0	11	0	1	0	0	0	0	0	0	0	0	0	0	0	0	0	0	0	0	0	0	0
Inoceramus sp. A	0	0	0	0	0	0	0	0	0	0	0	0	0	0	1	0	0	0	0	0	0	0	0	0	0	0	0	0	0	0	0
Inoceramus sp. B	0	0	0	0	0	0	0	0	0	0	0	0	0	0	0	0	0	0	0	0	0	0	0	0	0	0	0	0	0	0	0
Isognomon lotenoensis	0	0	0	0	0	0	0	0	0	0	0	0	0	0	0	0	0	0	0	0	0	0	0	0	35	12	4	0	0	0	0
Isognomon sp. A	0	0	0	0	0	0	0	0	0	0	0	0	0	0	0	0	0	0	0	0	0	0	0	0	0	0	0	0	0	0	0
Mimachlamys robinaldina	6	0	0	0	5	0	1	1	0	3	0	0	1	0	0	0	0	0	7	7	12	0	1	0	0	0	2	0	3	0	1
"Chlamys" puzoziana	0	0	0	0	0	0	0	0	0	0	0	0	0	0	0	0	0	0	6	6	5	0	1	0	0	0	1	0	1	0	0
"Pecten" vacaensis	0	0	0	1	0	0	0	0	0	4	0	0	0	0	0	0	0	0	11	11	7	0	0	0	0	0	1	0	0	0	0
cf. *Eopecten covuncoensis*	0	0	0	0	0	0	0	0	0	0	0	0	0	0	0	0	0	0	0	0	0	0	0	0	1	0	0	0	0	0	0
Pectinidae sp. A	0	0	0	0	0	0	0	0	0	0	0	0	0	1	0	0	0	0	0	0	0	0	0	0	0	0	0	0	0	0	0
Anomiidae sp. A	0	0	0	0	0	0	0	0	0	0	0	0	0	0	0	0	0	0	1	1	0	11	0	0	0	0	0	0	0	2	0
Aff. *Acesta* sp.	0	0	0	0	0	0	0	0	0	1	0	0	0	0	0	0	0	0	0	0	0	0	0	0	4	0	0	0	0	0	0
Aff. *Pseudolimea* sp.	0	0	0	0	0	0	0	0	0	0	0	0	0	0	0	0	0	0	0	0	0	0	0	0	0	0	0	0	0	0	0
Aetostreon sp.	0	0	0	0	0	0	0	0	0	0	0	0	0	0	0	0	0	0	0	0	0	0	0	0	0	0	0	0	0	0	0
Ceratostreon sp.	246	233	24	42	49	63	23	23	25	40	22	44	49	51	92	168	28	4	109	223	96	11	62	0	10	15	43	3	199	110	13
Gryphaeostrea sp. 1	0	0	0	0	0	0	0	0	0	0	0	0	0	0	0	0	0	0	0	0	0	0	0	0	0	0	0	0	0	0	0
Gryphaeostrea sp. 2	0	0	0	0	0	0	0	0	0	0	0	0	0	0	0	0	0	0	0	0	0	0	0	0	0	0	0	0	0	0	0
Exogyrinae sp. indet.	0	0	0	0	0	0	0	0	0	0	0	0	0	0	0	0	0	0	0	0	0	0	0	0	0	0	0	0	0	0	0
Lophinae sp. A	0	0	0	0	0	0	0	0	0	0	0	0	0	0	0	0	0	0	0	0	0	0	0	0	0	0	0	0	0	0	0
Lophinae sp. B	0	0	0	0	0	0	0	0	0	0	0	0	0	0	0	0	0	0	0	0	0	0	0	0	0	0	0	0	0	0	0
Myophorella volkheimeri	26	0	0	1	0	0	0	0	8	1	12	0	0	0	6	0	2	0	0	0	1	0	0	0	0	5	1	0	0	0	0
Myophorella garatei	0	0	0	1	0	0	0	0	0	0	0	0	0	0	0	0	0	0	0	0	0	0	0	0	0	0	0	0	0	0	0
Steinmanella raimondii	0	0	0	0	0	0	0	0	0	0	0	0	0	0	0	0	0	0	0	0	0	0	0	0	0	0	0	0	0	0	0
Steinmanella vacaensis	5	0	2	1	0	0	2	2	2	0	3	0	0	2	14	10	2	0	0	0	1	3	0	0	4	0	0	0	3	5	24
Rutitrigonia agrioensis	1	0	0	0	0	0	0	0	2	0	0	0	0	0	0	0	0	0	0	0	0	0	0	0	0	0	0	0	1	2	15
Pterotrigonia coihuicoensis	126	0	20	5	6	2	15	15	57	39	81	2	6	0	29	0	12	1	4	4	11	0	5	0	74	70	88	0	20	25	166
Pterotrigonia sp. A	0	0	0	0	0	0	0	0	0	0	0	0	0	0	0	0	0	0	0	0	0	0	0	0	0	0	0	0	0	0	0
Mesomiltha argentina	0	0	0	0	0	0	0	0	0	0	0	0	0	27	0	0	0	0	0	0	0	0	0	0	0	0	0	0	0	0	0
Mesomiltha sp. A	0	0	0	0	0	0	0	0	0	0	0	0	0	0	0	0	5	3	0	0	0	0	0	0	0	0	0	0	0	0	0
Lucina corbisoides	0	0	0	0	0	0	0	0	0	0	0	0	0	0	0	0	0	0	0	0	0	0	0	0	0	0	0	0	0	0	0
Lucina neuquensis	0	0	0	0	0	0	0	0	0	0	0	0	0	0	0	0	0	0	0	0	0	0	0	0	0	0	0	0	0	0	0
Lucinidae sp. A	2	0	0	0	0	0	0	0	0	0	0	0	0	0	0	0	0	0	0	0	0	0	0	0	0	0	0	0	0	0	0
Myoconcha transatlantica	31	0	17	3	17	39	47	47	25	0	2	0	0	0	1	0	0	0	5	5	6	0	0	0	4	29	9	0	0	2	2
Eriphyla argentina	51	0	73	20	26	52	9	9	57	12	11	34	39	11	53	0	52	0	11	11	37	0	20	0	9	10	16	0	12	15	19
Disparilia elongata	0	0	0	2	5	4	0	0	0	0	3	2	2	22	6	0	19	47	1	1	0	27	1	0	0	0	0	0	0	1	0
Neocrassina (*Coelastarte*) sp.	0	0	0	0	0	0	0	0	0	0	0	1	0	1	0	0	0	0	0	0	0	0	0	0	11	0	0	0	0	0	0
Astartidae sp. A	0	0	0	0	0	0	0	0	3	0	0	2	0	0	0	0	0	0	0	0	0	2	0	0	0	0	0	0	0	0	0
Protocardia sp.	0	0	1	2	0	0	0	0	0	3	1	0	3	0	0	0	0	0	0	0	0	0	0	3	0	0	0	0	0	0	0
"*Solecurtus*" *neuquensis*	0	0	0	2	0	0	0	0	2	15	0	0	0	0	0	0	0	0	0	0	0	0	0	0	0	0	0	0	0	6	0
Ptychomya sp. A (cf. *P. koeneni*)	5	0	29	3	27	64	7	7	39	4	3	30	27	2	11	0	46	2	6	6	5	0	7	0	5	3	6	0	5	46	6
Ptychomya sp. B	0	0	0	0	0	0	0	0	0	0	0	0	0	0	0	0	0	0	0	0	0	0	0	0	0	0	0	0	0	0	0
Arcticidae sp.	0	0	0	0	0	0	0	0	0	0	0	0	0	0	0	0	0	0	0	0	0	0	0	0	0	0	0	15	0	0	0
"*Cyprina*"	0	0	0	0	0	0	0	0	0	0	0	0	0	0	0	0	0	0	0	0	0	0	0	1	0	0	0	0	0	0	0
Veneridae sp. 1	0	0	0	0	0	0	0	0	0	0	0	0	0	0	0	0	0	0	0	0	0	0	0	0	2	0	2	4	0	0	0
Veneridae sp. 2	1	0	0	0	3	0	0	0	0	2	1	0	0	8	0	0	0	0	0	0	0	24	2	73	0	0	0	34	2	2	2
Veneridae sp. 3	0	0	0	0	0	0	0	0	0	0	0	0	0	0	0	0	0	0	0	0	0	0	0	0	0	0	0	0	0	0	0
Corbulomima "*bodenbenderi*"	0	0	0	0	0	0	0	0	0	0	0	0	0	9	0	0	0	1	0	0	0	30	0	11	0	0	0	0	0	0	0
Corbulidae sp. A	0	0	0	0	0	0	0	0	0	0	0	0	0	3	0	0	0	0	0	0	0	12	0	6	0	0	0	0	0	0	0
Corbulidae sp. B	0	0	0	0	0	0	0	0	0	0	0	0	0	0	0	0	0	0	0	0	0	0	0	0	0	0	0	0	0	0	0
Panopea neocomiensis	4	0	2	0	0	0	0	0	0	2	9	0	0	3	2	6	0	0	3	3	0	8	1	3	4	2	2	5	4	8	2
Panopea dupiniana	2	0	28	4	0	0	0	0	4	3	4	0	0	2	20	2	0	0	0	0	0	0	0	8	0	0	0	0	2	10	4
Pholadomya gigantea	18	0	30	4	0	0	0	0	4	2	6	0	4	0	2	0	0	0	0	0	0	0	4	0	0	0	0	0	4	0	2
Machomya? sp.	0	0	0	0	0	0	0	0	0	0	0	0	0	0	0	0	0	0	0	0	0	0	0	0	0	0	0	0	0	0	0
Heterodonta sp. indet. A	0	0	0	0	0	0	0	0	0	0	0	0	0	0	0	0	0	0	0	0	0	0	0	0	2	0	0	0	0	0	0
Heterodonta sp. indet. B	0	0	0	0	0	0	0	0	0	0	0	0	0	0	0	0	0	0	0	0	0	4	0	2	0	0	0	0	0	0	0
Heterodonta sp. indet. C	0	0	0	0	0	0	0	0	0	0	0	0	0	2	0	0	0	0	0	0	0	0	0	0	0	0	0	0	0	0	0
Dentallium ?	0	0	0	0	0	0	0	0	0	0	0	0	0	3	0	0	0	0	0	0	0	234	0	5	0	0	0	0	0	0	0
Sample size	621	305	254	107	161	250	117	153	252	145	168	152	159	149	244	190	175	63	169	283	194	387	107	118	187	148	187	62	319	252	273

Taxa	M86	M87	M88	M89	M90	M91	M92	M93
Placopsilina sp.	0	0	0	0	0	0	0	0
Scleractinia sp. A	0	0	0	0	0	0	0	0
Scleractinia spp. indet.	0	0	0	0	2	0	0	0
Pygaster gerthi	0	0	0	0	0	0	0	0
Holectypus cf. *H. planatus*	0	0	0	0	0	2	0	0
Holectypus sp.	0	0	0	0	0	0	0	1
Regularia sp. A	0	0	0	0	0	0	0	0
Echinoidea spines	0	0	0	0	0	0	0	5
Crinoidea spp. indet.	0	0	0	0	0	1	0	1
bryozoa sp. A	0	0	0	0	0	2	0	0
bryozoa sp. B	0	0	0	0	0	0	9	15
bryozoa sp. C	0	0	0	0	0	0	0	0
bryozoa sp. D	0	0	0	0	0	0	0	0
Parsimonia antiquata	0	0	0	0	0	0	1	0
Sarcinella occidentalis	0	0	0	0	0	0	0	0
Serpulidae small	1	17	16	5	1	9	19	40
Serpulidae middle	0	0	0	0	0	0	0	0
Decapoda (fragments)	0	0	0	0	0	0	0	0
Trochidae sp. A	0	0	0	0	0	0	0	2
Trochidae? sp. B	0	0	0	0	0	0	0	0
Cerithium sp. A	0	0	0	0	0	0	9	3
Cerithium sp. B	0	0	0	0	0	0	3	5
Rhabdocolpus sp. A	0	0	0	0	0	0	0	0
Rhabdocolpus sp. B	0	0	0	0	0	0	0	4
Poasia sp. A	0	0	0	0	0	0	1	0
Poasia sp. B	0	0	0	0	0	0	1	54
Poasia sp. C	0	0	0	0	0	0	0	1
Protohemichenopus sp.	0	0	0	0	0	0	0	0
Dimorphosoma sp.	0	0	0	1	0	0	1	7
Aporrhaeidae sp. B	0	0	0	0	0	0	0	0
Pictavia sp. A	0	0	0	0	0	0	0	0
Pictavia sp. B	0	0	0	0	0	0	0	56
Confusiscala sp.	0	0	0	0	0	0	0	0
Bathraspira sp. A	0	0	0	0	0	0	0	0
Bathraspira sp. B	0	0	0	0	0	0	0	0
Bathraspira ? sp. C	0	0	0	0	0	0	0	0
Ringinella sp. A	0	0	0	0	0	0	0	0
Ringinella sp. B	0	0	0	0	0	0	0	0
Tornatellaea sp.	0	0	0	0	0	0	0	0
Nuculoma sp.	0	0	0	0	0	0	0	0
Barbatia (*Barbatia*) sp.	0	0	0	0	0	0	0	0
Cucullaea gabrielis	10	19	2	1	3	0	0	0
Grammatodon securis	0	0	0	0	0	0	0	0
Grammatodon (*G*) sp.	0	0	0	32	0	1	0	0
Grammatodontinae sp. A	0	0	0	0	0	0	0	0
Grammatodontinae sp. B	0	0	0	0	0	0	0	12
Mytilinae sp. A	0	0	0	0	0	0	0	0
Crenellinae sp. A	0	0	0	0	1	0	0	0
Crenellinae sp. B	0	0	0	0	0	0	0	0
Modiolus cf. *M. ligeriensis*	0	0	0	0	2	6	0	0
Modiolus aff. *M. subsimplex*	0	0	0	0	0	0	0	0
Pinna robinaldina	0	2	0	0	2	0	0	0
Pinnidae sp.	0	0	0	0	0	0	0	0
Gervillaria alatior	0	0	0	0	3	4	0	0
Gervillella aviculoides	0	0	0	0	0	0	0	0
aff. *Cuneigervillia*	0	0	0	0	0	0	0	19
Pteriorida sp. A	0	0	0	0	0	0	0	0
Inoceramus sp. A	0	0	0	0	0	0	0	0
Inoceramus sp. B	0	0	0	0	0	0	0	0
Isognomon lotenoensis	0	0	0	0	10	4	0	0
Isognomon sp. A	0	0	0	0	3	0	0	0
Mimachlamys robinaldina	1	0	0	0	9	1	0	0
"Chlamys" puzoziana	0	0	0	0	4	0	0	0
"Pecten" vacaensis	0	0	0	0	5	0	0	0
cf. *Eopecten covuncoensis*	0	0	0	0	0	0	0	0
Pectinidae sp. A	0	0	0	0	0	0	0	0
Anomiidae sp. A	0	0	0	0	0	0	0	0
Aff. *Acesta* sp.	0	0	0	0	0	0	0	0
Aff. *Pseudolimea* sp.	0	0	0	0	0	0	0	0
Aetostreon sp.	0	0	0	0	0	0	0	0
Ceratostreon sp.	48	179	67	129	11	60	25	0
Gryphaeostrea sp. 1	0	0	0	0	0	0	0	0
Gryphaeostrea sp. 2	0	0	0	0	0	0	0	0
Exogyrinae sp. indet.	0	0	0	0	0	0	0	0
Lophinae sp. A	0	0	0	0	2	1	0	0
Lophinae sp. B	0	0	0	0	0	0	0	0
Myophorella volkheimeri	0	1	0	0	0	0	17	0
Myophorella garatei	0	0	0	0	0	0	0	0
Steinmanella raimondii	0	0	0	0	0	0	2	0
Steinmanella vacaensis	19	3	10	1	5	14	14	3
Rutitrigonia agrioensis	3	0	21	0	0	1	7	0
Pterotrigonia coihuicoensis	93	19	4	0	0	7	0	0
Pterotrigonia sp. A	0	0	0	0	0	0	105	203
Mesomiltha argentina	0	0	0	0	0	0	0	0
Mesomiltha sp. A	0	0	0	0	0	0	0	0
Lucina corbisoides	0	0	0	0	0	0	0	0
Lucina neuquensis	0	0	0	1	0	0	0	0
Lucinidae sp. A	0	0	0	0	0	0	0	0
Myoconcha transatlantica	0	0	0	0	107	24	0	0
Eriphyla argentina	20	10	0	0	2	0	0	0
Disparilia elongata	0	1	0	0	0	0	0	2
Neocrassina (*Coelastarte*) sp.	1	2	0	0	0	0	0	0
Astartidae sp. A	0	0	0	0	0	0	0	0
Protocardia sp.	1	0	0	0	0	0	2	26
"*Solecurtus*" *neuquensis*	8	5	0	0	4	0	13	2
Ptychomya sp. A (cf. *P. koeneni*)	27	4	0	17	8	34	0	0
Ptychomya sp. B	0	0	0	0	0	0	2	28
Arcticidae sp.	2	1	0	1	2	21	15	5
"*Cyprina*"	0	0	0	0	0	0	0	0
Veneridae sp. 1	0	0	0	0	0	0	0	0
Veneridae sp. 2	0	9	0	0	2	5	2	0
Veneridae sp. 3	0	0	0	5	0	0	0	0
Corbulomima "*bodenbenderi*"	0	0	0	5	0	2	0	0
Corbulidae sp. A	0	0	0	0	0	0	0	0
Corbulidae sp. B	0	0	0	0	0	0	6	5
Panopea neocomiensis	6	2	0	3	0	0	0	0
Panopea dupiniana	4	34	0	0	15	4	0	0
Pholadomya gigantea	0	4	0	0	10	0	0	0
Machomya ? sp.	0	0	0	3	0	0	0	0
Heterodonta sp. indet. A	0	0	0	0	0	4	0	0
Heterodonta sp. indet. B	0	0	0	0	0	1	0	0
Heterodonta sp. indet. C	0	4	0	0	0	0	0	0
Dentallium ?	0	0	0	0	0	0	0	2
Sample size	244	316	120	204	213	208	254	501

Appendix C: Taxonomic counts section AML

The following Table lists the species included in the multivariate analysis.

	Samples																							
Taxa	M94	M95	M96	M97	M98	M99	M100	M101	M102	M103	M104	M105	M105P	M105R	M106	M107	M108	M109	M109P	M110	M111	M111P	M112	M112P
Placopsilina sp.	0	3	0	0	0	0	0	0	0	0	0	1	1	0	0	0	0	0	0	1	1	1	6	6
Scleractinia sp. A	0	3	0	0	0	0	0	0	0	0	0	0	0	0	0	0	0	0	0	0	0	0	0	0
Scleractinia spp. indet.	0	0	0	0	0	0	0	0	0	0	0	0	0	0	0	0	0	0	0	0	0	0	0	0
Pygaster gerthi	0	0	8	0	0	0	0	0	0	0	0	0	0	0	0	0	0	0	0	0	0	0	0	0
Holectypus cf. *H. planatus*	0	0	0	0	0	0	0	0	0	0	0	0	0	0	0	0	0	0	0	0	0	0	0	0
Holectypus sp.	0	0	0	0	0	0	0	0	0	0	0	0	0	0	0	0	0	0	0	0	0	0	0	0
Regularia sp. A	0	0	0	0	0	0	0	0	0	0	0	0	0	0	0	0	0	0	0	0	0	0	0	0
Echinoidea spines	0	0	0	0	0	0	0	0	0	0	0	0	0	0	0	0	0	0	0	0	0	0	0	0
Crinoidea spp. indet.	0	0	0	0	0	0	0	0	0	0	0	0	0	0	0	0	0	0	0	0	0	0	0	0
bryozoa sp. A	0	2	0	0	0	0	0	0	0	0	0	0	0	0	0	0	0	0	0	0	0	0	0	0
bryozoa sp. B	0	0	0	0	0	0	0	0	0	0	0	0	0	0	0	0	0	0	0	0	0	0	0	0
bryozoa sp. C	0	0	0	0	0	0	0	0	0	0	0	0	0	0	0	0	0	0	0	0	0	0	0	0
bryozoa sp. D	0	0	0	0	0	0	0	0	0	0	0	0	0	0	0	0	0	0	0	0	0	0	0	0
Parsimonia antiquata	0	0	0	0	0	0	0	0	0	0	0	1	96	96	0	0	0	0	0	0	1	113	1	105
Sarcinella occidentalis	0	0	0	0	0	0	0	0	0	0	0	0	0	0	0	0	0	0	0	0	0	0	0	0
Serpulidae small	34	5	0	3	2	11	0	12	16	1	0	0	0	0	0	0	0	0	0	0	0	0	4	4
Serpulidae middle	0	0	0	0	0	0	0	0	0	0	0	0	0	0	0	0	0	0	0	0	0	0	0	0
Decapoda (fragments)	0	0	0	0	0	0	0	0	0	0	0	0	0	0	0	0	0	0	0	0	0	0	0	0
Trochidae sp. A	0	0	0	0	0	0	0	0	0	0	0	0	0	0	0	0	0	0	0	0	0	0	0	0
Trochidae? sp. B	0	0	0	0	0	0	0	0	0	0	0	0	0	0	0	0	0	0	0	0	0	0	0	0
Cerithium sp. A	0	0	0	0	0	0	0	0	0	0	0	0	0	0	0	0	0	0	0	0	0	0	0	0
Cerithium sp. B	0	0	0	0	0	0	0	0	0	0	0	0	0	0	0	0	0	0	0	0	0	0	0	0
Rhabdocolpus sp. A	0	0	0	0	0	0	0	0	0	0	0	0	0	0	0	0	0	0	0	0	0	0	0	0
Rhabdocolpus sp. B	0	0	0	0	0	0	0	0	0	0	0	0	0	0	0	0	0	0	0	0	0	0	0	0
Poasia sp. A	0	0	0	0	0	0	0	0	0	0	0	0	0	0	0	0	0	0	0	0	0	0	0	0
Poasia sp. B	0	0	0	0	0	0	0	0	0	0	0	0	0	0	0	0	0	0	0	0	0	0	0	0
Poasia sp. C	0	0	0	0	0	0	0	0	0	0	0	0	0	0	0	0	0	0	0	0	0	0	0	0
Protohemichenopus sp.	111	0	0	0	0	0	0	0	0	0	0	0	0	0	0	0	0	0	0	0	0	0	0	0
Dimorphosoma sp.	0	0	0	0	0	0	0	0	0	0	0	0	0	0	0	0	0	0	0	0	0	0	0	0
Aporrhaeidae sp. B	0	0	0	0	0	0	0	0	0	0	0	0	0	0	0	0	0	0	0	0	0	0	0	0
Pictavia sp. A	0	0	0	0	0	0	0	0	0	0	0	0	0	0	0	0	0	0	0	0	0	0	0	0
Pictavia sp. B	0	0	0	0	0	0	0	0	0	0	0	0	0	0	0	0	0	0	0	0	0	0	0	0
Confusiscala sp.	0	0	0	0	0	0	0	0	0	0	0	0	0	0	0	0	0	0	0	0	0	0	0	0
Bathraspira sp. A	0	1	7	3	0	0	0	0	0	0	0	0	0	0	0	0	0	0	0	0	0	0	0	0
Bathraspira sp. B	0	0	0	0	0	0	0	0	0	0	0	0	0	0	0	0	0	0	0	0	0	0	0	0
Bathraspira ? sp. C	526	0	0	0	0	0	0	0	0	0	0	0	0	0	0	0	0	0	0	0	0	0	0	0
Ringinella sp. A	0	0	0	0	1	0	0	0	0	0	0	0	0	0	0	0	0	0	0	0	0	0	0	0
Ringinella sp. B	0	0	0	0	0	0	0	0	0	0	0	0	0	0	0	0	0	0	0	0	0	0	0	0
Tornatellaea sp.	0	0	0	0	0	0	0	0	0	0	0	0	0	0	0	0	0	0	0	0	0	0	0	0
Nuculoma sp.	0	0	0	0	0	0	0	0	0	0	0	0	0	0	0	0	0	0	0	0	0	0	0	0
Barbatia (*Barbatia*) sp.	0	0	0	0	0	0	0	0	0	0	0	0	0	0	0	0	0	0	0	0	0	0	0	0
Cucullaea gabrielis	0	0	0	0	0	14	0	0	0	41	3	34	34	0	0	4	0	23	23	15	8	8	0	0
Grammatodon securis	14	1	0	2	0	0	0	0	0	0	0	0	0	0	0	0	0	0	0	0	0	0	0	0
Grammatodon (*G*) sp.	0	0	0	0	0	0	0	0	0	0	0	0	0	0	0	0	0	0	0	0	0	0	0	0
Grammatodontinae sp. A	0	0	0	0	0	0	0	0	0	0	0	0	0	0	0	0	0	0	0	0	0	0	0	0
Grammatodontinae sp. B	0	0	0	0	0	0	0	0	0	0	0	0	0	0	0	0	0	0	0	0	0	0	0	0
Mytilinae sp. A	0	0	0	0	0	0	0	0	0	0	0	0	0	0	0	0	0	0	0	0	0	0	0	0
Crenellinae sp. A	0	0	0	0	0	0	0	0	0	0	0	0	0	0	0	0	0	0	0	0	0	0	0	0
Crenellinae sp. B	0	0	0	0	0	0	0	0	0	0	0	0	0	0	0	0	0	0	0	0	0	0	0	0
Modiolus cf. *M. ligeriensis*	0	0	0	0	0	0	0	0	0	0	0	0	0	0	0	0	0	0	0	0	0	0	0	0
Modiolus aff. *M. subsimplex*	0	0	0	0	0	0	0	0	0	0	0	0	0	0	0	0	0	0	0	0	0	0	0	0
Pinna robinaldina	0	0	0	0	0	7	6	28	62	9	2	0	0	0	0	0	0	2	2	0	0	0	2	2
Pinnidae sp.	0	0	0	0	0	0	0	0	0	0	0	0	0	0	0	0	0	0	0	0	0	0	0	0
Gervillaria alatior	0	0	0	0	0	0	0	0	0	0	0	0	0	0	0	0	0	0	0	0	0	0	0	0
Gervillella aviculoides	0	0	0	0	0	0	0	0	0	11	71	6	6	0	0	0	2	2	2	0	8	8	12	12
aff. *Cuneigervillia*	0	0	0	0	0	0	0	0	0	0	0	0	0	0	0	0	0	0	0	0	0	0	0	0
Pteriorida sp. A	0	0	0	0	0	0	0	0	0	0	0	0	0	0	0	0	0	0	0	0	0	0	0	0
Inoceramus sp. A	0	0	11	0	0	0	0	0	0	0	2	5	5	0	0	0	0	0	0	0	0	0	0	0
Inoceramus sp. B	0	0	0	0	0	0	0	0	0	0	0	0	0	0	4	0	2	0	0	0	0	0	0	0
Isognomon lotenoensis	0	0	0	0	0	0	0	0	0	0	0	0	0	0	0	0	0	0	0	0	0	0	12	12
Isognomon sp. A	0	0	0	0	0	0	0	0	0	0	0	0	0	0	0	0	0	0	0	0	0	0	0	0
Mimachlamys robinaldina	0	0	0	0	0	0	0	0	0	1	0	0	0	4	0	0	0	4	4	0	0	0	7	7
"Chlamys" puzoziana	0	0	0	0	0	0	0	0	0	0	0	0	0	0	0	0	0	0	0	0	0	0	0	0
"Pecten" vacaensis	0	0	0	0	0	0	0	0	0	0	0	0	0	0	0	0	0	0	0	0	0	0	0	0
cf. *Eopecten covuncoensis*	0	0	0	0	0	0	0	0	0	0	0	0	0	0	0	0	0	0	0	0	0	0	0	0
Pectinidae sp. A	0	1	0	0	0	0	0	0	0	0	0	1	1	0	0	0	1	0	0	0	0	0	0	0
Anomiidae sp. A	0	0	0	0	0	0	0	0	0	0	0	0	0	0	0	0	0	0	0	1	0	0	0	0
Aff. *Acesta* sp.	0	0	0	0	0	0	0	0	0	0	0	0	0	0	0	0	0	0	0	0	0	0	0	0
Aff. *Pseudolimea* sp.	0	0	0	0	0	0	0	0	0	0	0	0	0	0	0	0	0	0	0	0	0	0	0	0
Aetostreon sp.	0	48	0	6	10	84	84	3	2	7	0	1	1	0	0	0	0	0	0	0	0	0	1	1
Ceratostreon sp.	0	4	0	0	18	91	0	0	0	0	0	2	212	210	0	32	30	4	116	0	9	99	10	313
Gryphaeostrea sp. 1	0	0	0	0	0	0	0	0	0	0	0	0	0	0	0	0	0	0	0	0	0	0	0	0
Gryphaeostrea sp. 2	7	0	0	0	0	0	0	0	0	0	0	0	0	0	0	0	0	0	0	0	0	0	0	0
Exogyrinae sp. indet.	0	0	0	0	0	0	0	0	0	0	0	0	0	0	0	0	0	0	0	0	0	0	0	0
Lophinae sp. A	0	0	0	0	0	0	0	0	0	0	0	0	0	0	0	0	0	0	0	0	0	0	0	0
Lophinae sp. B	0	0	0	0	0	0	0	0	0	0	0	0	0	0	0	0	0	0	0	0	0	0	0	0
Myophorella volkheimeri	0	0	0	12	5	0	0	0	2	2	22	28	28	0	0	0	0	0	0	0	0	0	29	29
Myophorella garatei	0	0	0	0	0	0	0	0	0	0	0	0	0	0	0	0	0	0	0	0	0	0	0	0
Steinmanella raimondii	0	0	0	0	0	0	0	0	0	0	0	0	0	0	0	0	0	0	0	0	6	6	0	0
Steinmanella vacaensis	0	0	0	0	0	0	0	0	0	37	9	6	6	0	0	0	0	6	6	4	66	66	0	0
Rutitrigonia agrioensis	0	0	0	0	0	0	0	0	0	0	1	0	0	0	0	0	0	0	0	0	0	0	0	0
Pterotrigonia coihuicoensis	0	0	0	0	0	0	0	0	0	4	0	2	2	0	0	0	0	0	0	0	3	3	40	40
Pterotrigonia sp. A	0	0	0	0	0	0	0	0	0	0	0	0	0	0	0	0	0	0	0	0	0	0	0	0
Mesomiltha argentina	43	0	0	0	0	0	0	0	0	0	0	0	0	0	0	0	0	0	0	0	0	0	0	0
Mesomiltha sp. A	0	37	1	3	0	0	0	0	0	0	0	0	0	0	0	0	0	0	0	0	0	0	0	0
Lucina corbisoides	0	0	0	0	0	0	0	0	0	0	0	0	0	0	0	0	0	0	0	0	0	0	0	0
Lucina neuquensis	0	0	0	0	0	0	0	0	0	0	0	0	0	0	0	0	0	0	0	0	0	0	0	0
Lucinidae sp. A	0	0	0	0	0	0	0	0	0	0	0	0	0	0	0	0	0	0	0	0	0	0	0	0
Myoconcha transatlantica	0	0	0	0	0	0	0	0	0	19	0	0	0	0	0	0	0	0	0	2	0	0	160	160
Eriphyla argentina	0	0	0	29	6	13	0	0	2	72	9	50	50	0	6	1	1	0	0	0	0	0	117	117
Disparilia elongata	0	2	82	24	15	0	0	0	0	0	0	1	1	0	0	3	0	0	0	0	0	0	0	0
Neocrassina (*Coelastarte*) sp.	0	0	0	0	0	0	0	0	0	0	0	0	0	0	0	0	0	0	0	0	0	0	0	0
Astartidae sp. A	0	0	0	0	0	0	0	0	0	0	0	0	0	0	0	0	0	0	0	0	0	0	0	0
Protocardia sp.	0	1	0	0	0	0	0	0	0	0	0	0	0	0	0	0	0	0	0	0	0	0	0	0
"*Solecurtus*" *neuquensis*	0	0	0	0	0	0	0	0	0	0	0	0	0	0	0	0	0	0	0	0	0	0	0	0
Ptychomya sp. A (cf. *P. koeneni*)	0	1	0	9	3	0	0	0	0	3	1	55	55	0	0	6	1	0	0	0	0	0	226	226
Ptychomya sp. B	0	0	0	0	0	0	0	0	0	0	0	0	0	0	0	0	0	0	0	0	0	0	0	0
Arcticidae sp.	0	0	0	0	0	0	0	0	0	0	0	0	0	0	0	0	0	0	0	0	0	0	0	0
"*Cyprina*"	0	0	0	0	0	0	0	0	0	0	0	0	0	0	0	0	0	0	0	0	0	0	0	0
Veneridae sp. 1	0	0	0	0	0	0	0	0	0	0	0	0	0	0	0	0	0	0	0	2	0	0	0	0
Veneridae sp. 2	0	0	0	3	0	0	0	0	1	0	0	12	12	0	70	0	0	11	11	37	0	0	1	1
Veneridae sp. 3	0	0	0	0	0	0	0	0	0	0	0	0	0	0	4	0	0	3	3	0	0	0	0	0
Corbulomima "*bodenbenderi*"	2	1	7	0	0	0	0	0	0	0	0	0	0	0	0	0	0	0	0	0	0	0	0	0
Corbulidae sp. A	0	0	0	0	0	0	0	0	0	0	0	0	0	0	0	0	0	0	0	0	0	0	0	0
Corbulidae sp. B	0	0	0	0	0	0	0	0	0	0	0	0	0	0	0	0	0	0	0	0	0	0	0	0
Panopea neocomiensis	0	0	0	0	0	0	0	6	11	0	0	8	8	0	23	8	1	81	81	0	0	0	0	0
Panopea dupiniana	0	0	0	0	0	8	0	0	2	15	66	58	58	0	22	2	0	30	30	2	4	4	0	0
Pholadomya gigantea	0	0	0	0	0	0	0	0	0	0	10	6	6	0	0	0	0	0	0	0	0	0	0	0
Machomya ? sp.	0	0	0	0	0	0	0	0	0	0	0	2	2	0	0	3	0	0	0	0	0	0	0	0
Heterodonta sp. indet. A	0	0	0	0	0	0	0	0	0	0	0	0	0	0	0	0	0	0	0	0	0	0	0	0
Heterodonta sp. indet. B	0	0	0	0	0	0	0	0	0	0	0	0	0	0	0	0	0	0	0	0	0	0	0	0
Heterodonta sp. indet. C	0	0	0	0	0	0	0	0	0	0	0	0	0	0	0	0	0	0	0	0	0	0	0	0
Dentallium ?	0	6	1	0	0	0	0	0	0	0	0	0	0	0	0	0	0	1	1	0	0	0	0	0
Sample size	737	116	117	94	60	228	90	49	98	222	196	279	584	310	129	59	38	167	279	64	106	308	628	1035

Appendix D: samples per cluster, section BAL

Appendix D. Samples per cluster. (1) For more information see Chapter 8. (2) Refers to position within starvation/dilution sequences as decribed in Chapter 5: 0, sample taken from beds without internal stratigraphy; 1, base of complex starvation hemisequences; 2, middle starvation horizon; 3, upper starvation horizon; 4, samples taken from complex starvation hemisequences regardless of internal stratigraphy; 5, samples from dilution hemisequences. Intermediate cases possible (e.g. 1-2 for samples taken fron lower and middle parts of complex starvation hemisequences). (3) As discussed in Chapter 9. For statistics see Chapter 8.

Sample	Cluster (1)	Section	Position within S/D seq. (2)	Shell bed Type (3)	m above base	Sample size (N)	Species Richness (S)	Shannon's diversity (H')	Evenness index (E)
M1	A	BA	0	Type 1	2,1	93	7	1,66	85,41
M2	A	BA	0	Type 1	3,1	195	10	1,69	73,39
M3	A	BA	0	Type 1	4	136	9	1,64	74,77
M4	A	BA	0	Type 1	4,3	56	10	1,84	79,97
M5	A	BA	0	Type 1	4,9	62	8	1,70	81,87
M6	A	BA	0	Type 1	5	160	8	1,74	83,85
M8	A	BA	0	Type 1	5,9	38	7	1,72	88,42
M7	A	BA	0	Type 1	5,9	63	7	1,26	64,94
M9	A	BA	0	Type 1	7,3	39	6	1,16	64,81
M10	A	BA	0	Type 1	9,2	149	7	1,01	51,80
M11	A	BA	0	Type 1	10,8	182	8	1,44	69,43
M12	A	BA	0	Type 1	13,8	105	9	1,42	64,67
M13	A	BA	0	Type 1	13,8	196	8	1,12	53,99
M14	A	BA	0	Type 1	14,7	148	11	1,64	68,60
M15	A	BA	0	Type 1	16,6	200	10	1,62	70,29
M16	A	BA	0	Type 1	17,1	127	8	1,56	74,91
M17	A	BA	0	Type 1	20	127	9	1,65	75,31
M18	A	BA	0	Type 1	22,3	271	9	1,50	68,05
M19	A	BA	0	Type 1	29,4	137	8	1,61	77,26
M20	A	BA	0	Type 1	30	330	11	1,52	63,51
M21	A	BA	0	Type 1	34,8	263	12	1,80	72,52
M22	A	BA	0	Type 1	41	570	16	1,86	66,92
M23	A	BA	0	Type 1	44	61	8	1,69	81,26
M25	A	BA	0	Type 1	48,5	310	16	1,61	57,92
M26	A	BA	0	Type 2	56,2	110	12	1,88	75,50
M24	B	BA	0	Type 2	56,2	247	12	0,82	32,88

M27	B	BA	0	Type 2	56,2	126	9	1,70	77,30
M28	B	BA	0	Type 2	72,1	112	13	2,17	84,68
M29	B	BA	0	Type 2	72,1	326	11	1,03	43,08
M30	B	BA	0	Type 2	72,1	255	16	1,53	55,21
M31	B	BA	0	Type 2	72,1	41	6	1,33	74,25
M32	B	BA	0	Type 2	75	51	12	1,73	69,57
M34	E	BA	0	Type 2	109,4	144	19	2,53	85,78
M33	E	BA	0	Type 2	109,4	57	12	2,17	87,39
M35	E	BA	0	Type 2	123,8	157	18	2,50	86,51
M36	E	BA	0	Type 2	123,8	121	20	2,43	81,01
M37	E	BA	0	Type 2	140	22	6	1,22	68,23
M38	E	BA	1	Type 2	141	133	13	1,71	66,70
M39	E	BA	0	Type 2	142	156	19	1,70	57,78
M40	E	BA	0	Type 2	142	194	19	1,60	54,35
M41	E	BA	1	Type 5	166	240	23	2,20	70,24
M42	E	BA	0	Type 2	166	129	7	0,70	35,80
M43	E	BA	1	Type 4/5	166	56	12	1,94	77,94
M44	O	BA	1	Type 5	210	142	9	1,51	68,50
M45	C	BA		Type 5	211	135	2	0,04	6,31
M47	E	BA	3	Type 4	232	77	13	2,09	81,41
M46	M	BA	2	Type 4	232	342	22	2,18	70,37
M46P	M	BA	2	Type 4	232	474	22	2,07	67,09
M48	M	BA	0	Type 2	243	203	13	2,13	83,20
M49	N	BA	0	Type 2	252	271	26	2,58	79,05
M49P	N	BA	0	Type 2	252	543	26	2,13	65,33
M50	N	BA	0	Type 2	253	180	17	1,85	65,45
M51	M	BA	0	Type 2	258	103	11	2,03	84,72
M52	P	BA	0	Type 2	266	48	4	1,14	82,58
M53	O	BA	1	Type 4	276	106	11	1,94	80,92
M54	M	BA	2-3	Type 4	277	459	23	2,59	82,52
M54P	M	BA	2-3	Type 4	277	532	23	2,63	83,78
M55	M	BA	2-3	Type 4	283	251	21	2,26	74,13
M55P	M	BA	2-3	Type 4	283	327	21	2,23	73,35
M56	M	BA	2-3	Type 4	283	215	17	2,21	78,06
M57	I	BA	2-3	Type 4	295	382	13	1,98	77,26
M57P	I	BA	2-3	Type 4	295	470	13	2,03	79,04
M58R	G	BA	2	Type 4	307	305	3	0,64	58,40
M58	L	BA	2-3	Type 4	307	327	21	2,12	69,56
M58P	L	BA	2-3	Type 4	307	621	21	1,96	64,33
M59	L	BA	2-3	Type 4	311	254	14	2,15	81,29
M60	L	BA	2-3	Type 4	311	107	19	2,15	73,05
M61	I	BA	2	Type 4	316	161	15	2,13	78,79
M62	I	BA	2-3	Type 4	316	250	11	1,76	73,45
M63	I	BA	1-2	Type 4	321	117	11	1,78	74,41
M63P	I	BA	1	Type 4	321	153	11	1,88	78,40
M64	L	BA	2	Type 4	328	252	16	2,16	78,03
M65	L	BA	1	Type 4	333	145	17	2,12	74,94
M66	L	BA	1-2	Type 4	333	168	16	1,90	68,66

M67	I	BA	3	Type 4	334	152	13	1,90	73,99
M68	I	BA	3	Type 4	334	159	12	1,90	76,33
M69	P	BA	4	Type 4	337	149	16	2,07	74,67
M70	L	BA	4	Type 4	346	244	14	1,88	71,28
M71	G	BA	0	Type 2	349	190	6	0,51	28,68
M73	E	BA	2-3	Type 4	351	63	9	1,06	48,45
M72	I	BA	1	Type 4	351	175	10	1,82	79,00
M74	K	BA	4	Type 4	354	169	14	1,46	55,50
M74P	K	BA	4	Type 4	354	283	14	1,00	38,00
M75	K	BA	4	Type 4	354	194	12	1,67	67,15
M76	P	BA	0	Type 2	356	387	15	1,55	57,31
M77	L	BA	4	Type 4	357	107	12	1,44	58,00
M78	P	BA	0	Type 2	359	118	10	1,43	62,27
M79	J	BA	2	Type 4	361	187	21	2,13	70,03
M80	J	BA	1-2	Type 4	361	148	10	1,61	69,94
M81	J	BA	1-2	Type 4	361	187	14	1,67	63,12
M82	P	BA	0	Type 2	364	62	6	1,27	70,64
M83	L	BA	2	Type 4	368	319	19	1,55	52,71
M84	L	BA	3	Type 4	368	252	18	1,93	66,61
M85	L	BA	2	Type 4	374	273	17	1,57	55,47
M86	L	BA	0	Type 2	381	244	15	1,92	70,90
M87	L	BA	4	Type 2	391	316	18	1,69	58,62
M88	G	BA	0	Type 5	401	120	6	1,29	71,87
M89	G	BA	0	Type 2	402	204	13	1,31	51,25
M90	H	BA	1	Type 4	403	213	23	2,09	66,74
M91	H	BA	1	Type 4	414	208	22	2,35	76,05
M92	D	BA	0	Type 2	498	254	20	2,16	72,22
M93	D	BA	0	Type 2	505	501	24	2,16	67,81

Appendix E: samples per cluster, section AML

Appendix E. Samples per cluster. (1) For more information see Chapter 8. (2) Refers to position within starvation/dilution sequences as decribed in Chapter 5: 0, sample taken from beds without internal stratigraphy; 1, base of comples starvation hemisequences; 2, middle starvation horizon; 3, upper starvation horizon; 4, samples taken from complex starvation hemisequences regardless of internal stratigraphy; 5, samples from dilution hemisequences. Intermediate cases possible (e.g. 1-2 for samples taken fron lower and middle parts of complex starvation hemisequences). (3) As discussed in Chapter 9. For statistics see Chapter 8.

Sample	Cluster (1)	Section	Position within S/D seq. (2)	Shell bed Type (3)	m above base	Sample size (N)	Species Richness (S)	Shannon's diversity (H')	Evenness index (E)
M94	B	AM	0	Type 2	67,1	737	7	0,97	49,80
M95	E	AM	4	Type 2	129	116	15	1,71	63,12
M96	E	AM	5	Type 2	185	117	7	1,07	55,15
M97	E	AM	0	Type 2	186	94	10	1,90	82,35
M98	E	AM	0	Type 2	186	60	8	1,78	85,37
M99	O	AM	1	Type 4	239	228	7	1,44	73,99
M100	E	AM	2	Type 4	239	90	2	0,24	35,34
M101	C	AM	5	Type 3	247	49	4	1,09	78,81
M102	C	AM	5	Type 3	251	98	8	1,20	57,49
M103	O	AM	1	Type 5	269	222	13	1,98	77,10
M104	O	AM	2	Type 4	281	196	11	1,63	67,81
M105	M	AM	2-3	Type 4	281	279	19	2,21	74,92
M105P	M	AM	2-3	Type 4	281	584	19	2,04	69,32
M105R	G	AM	2	Type 4	281	310	3	0,68	62,17
M106	P	AM	5	Type 3	293	129	6	1,30	72,49
M107	G	AM	0	Type 2	297	59	8	1,50	72,35
M108	G	AM	4	Type 4	306	38	7	0,88	45,20
M109	P	AM	0	Type 2	312	167	11	1,62	67,50
M109P	P	AM	0	Type 2	312	279	11	1,58	65,90
M110	P	AM	0	Type 2	315	64	8	1,28	61,80
M111	F	AM	1	Type 4	329	106	9	1,37	62,33
M111P	F	AM	1	Type 4	329	308	9	1,45	65,96
M112	I	AM	2-3	Type 4	330	628	16	1,74	62,90
M112P	I	AM	2-3	Type 4	330	1035	16	1,90	68,66

Appendix-figures 1-3

Appendix-Fig.1. Bajada del Agrio section of the Agua de la Mula Member. Key in Appendix-Fig. 3

Bajada del Agrio Section (1)

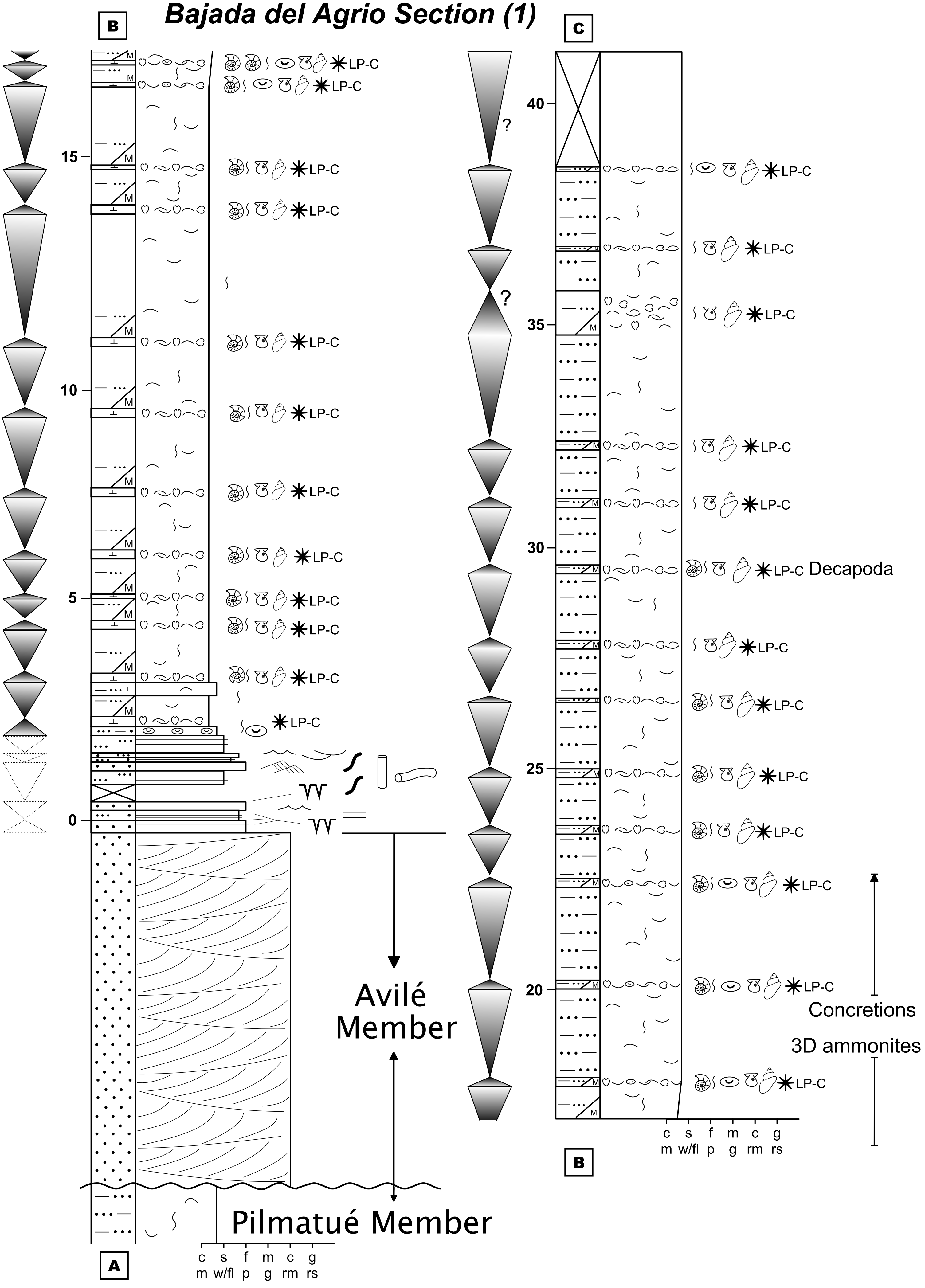

Bajada del Agrio Section (2)

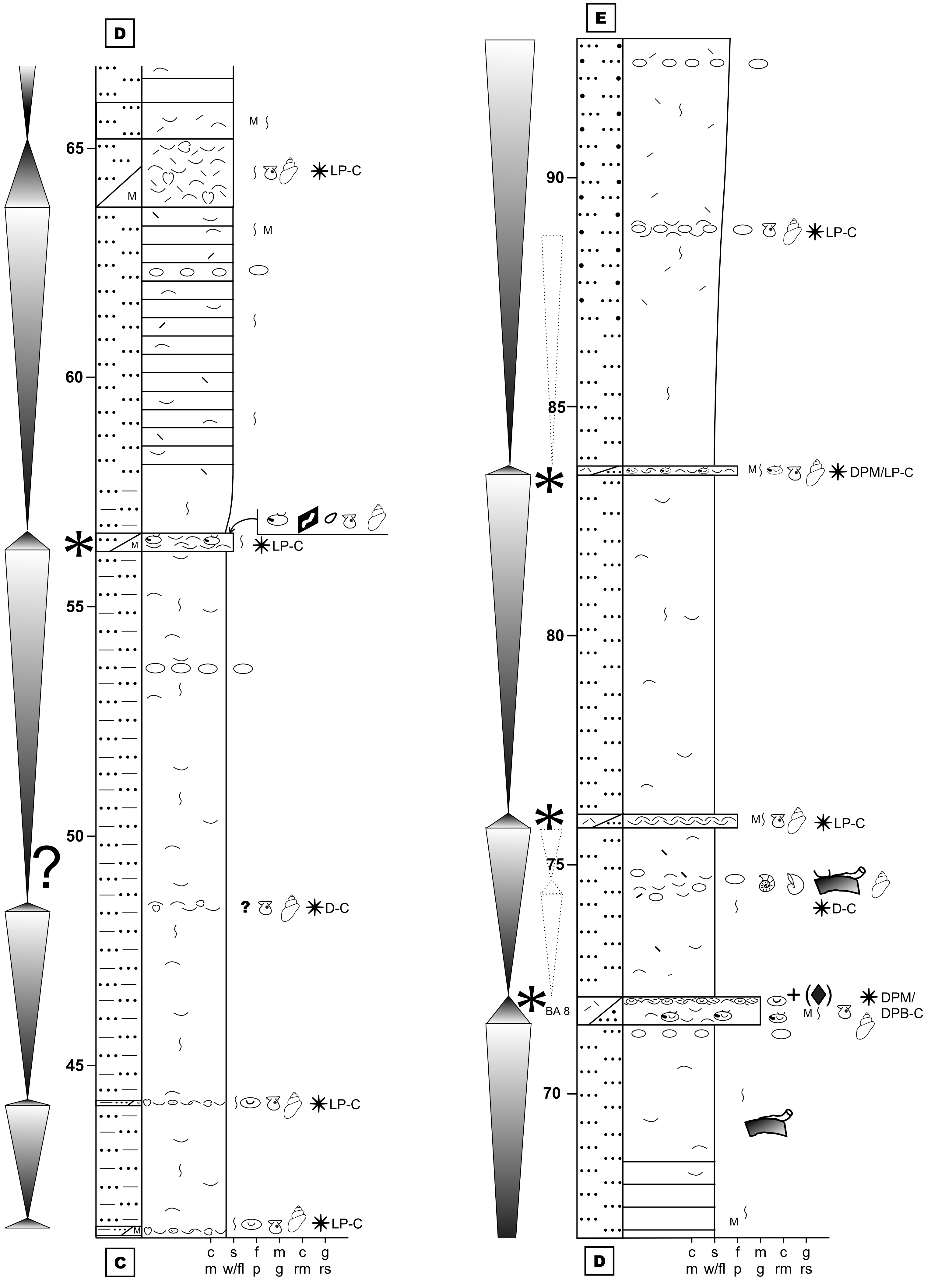

Bajada del Agrio Section (3)

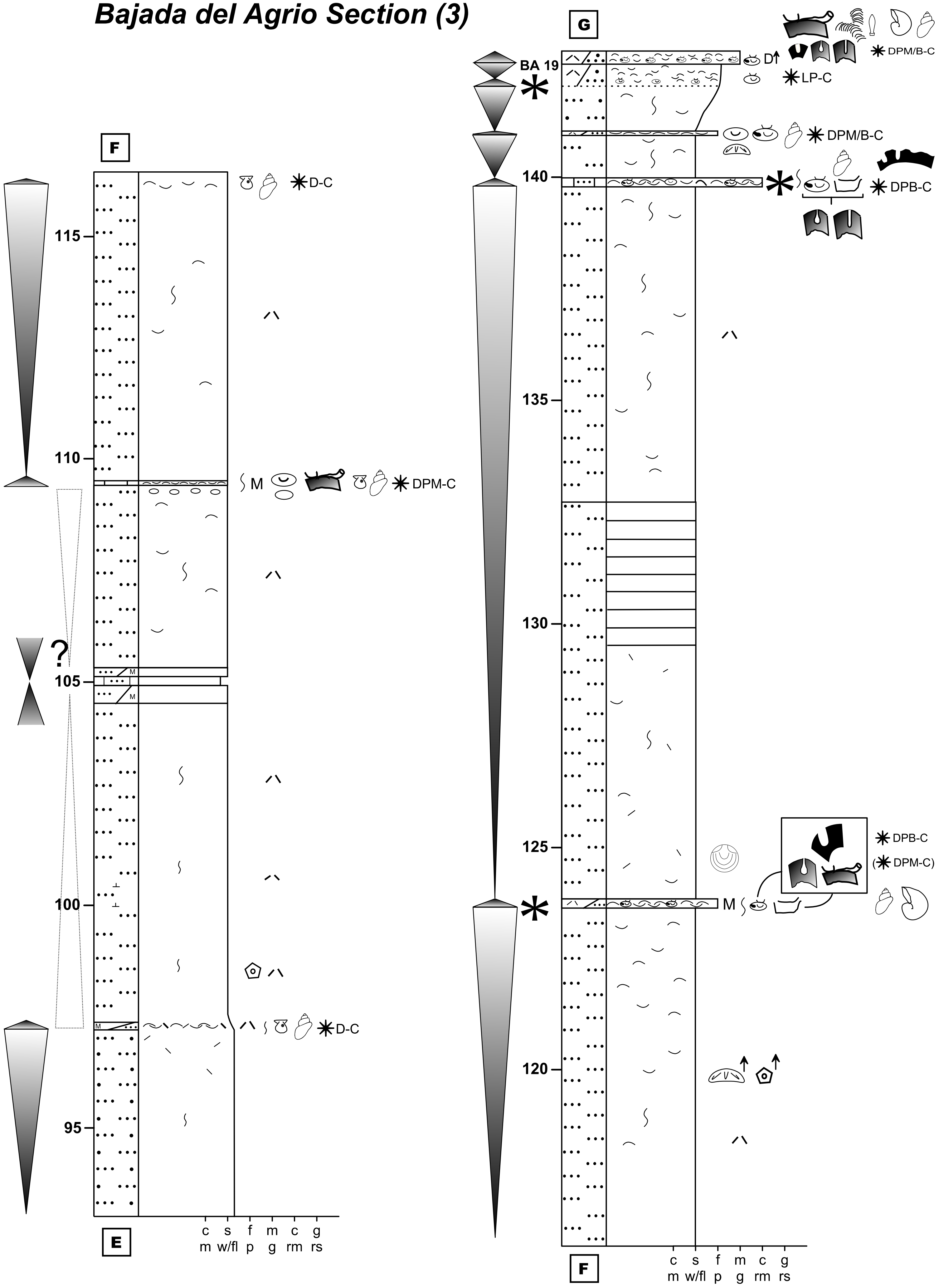

Bajada del Agrio Section (4)

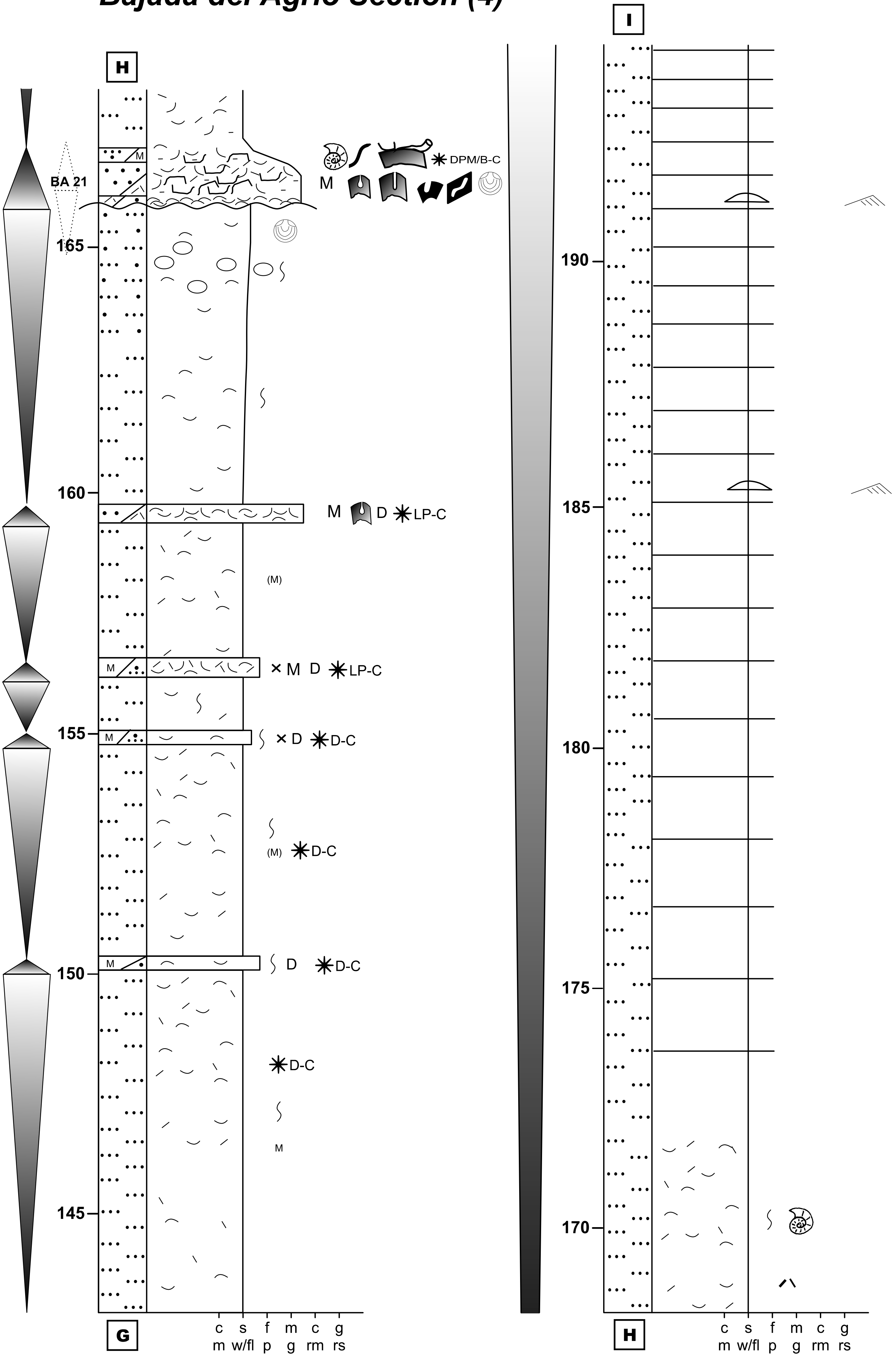

Bajada del Agrio Section (5)

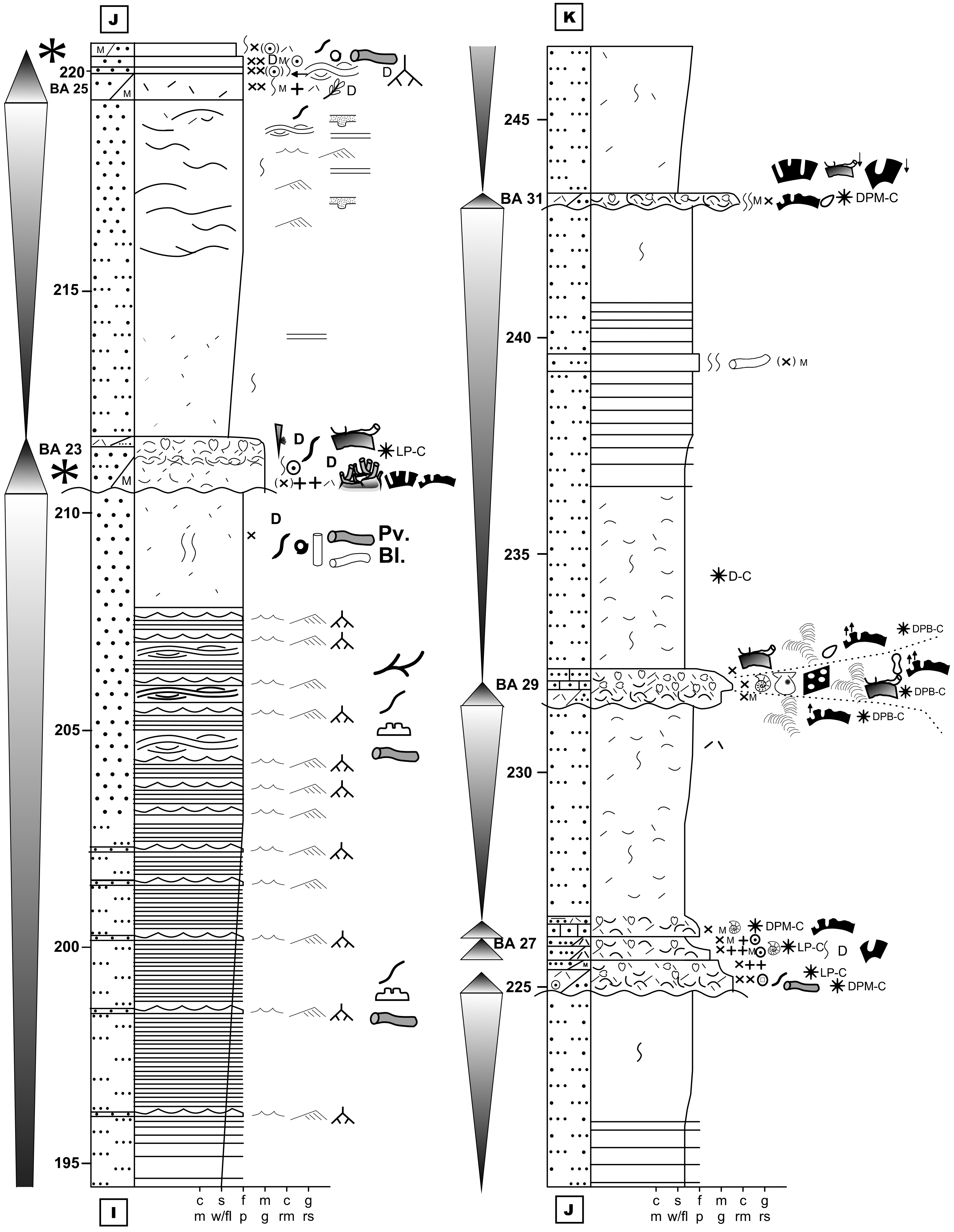

Bajada del Agrio Section (6)

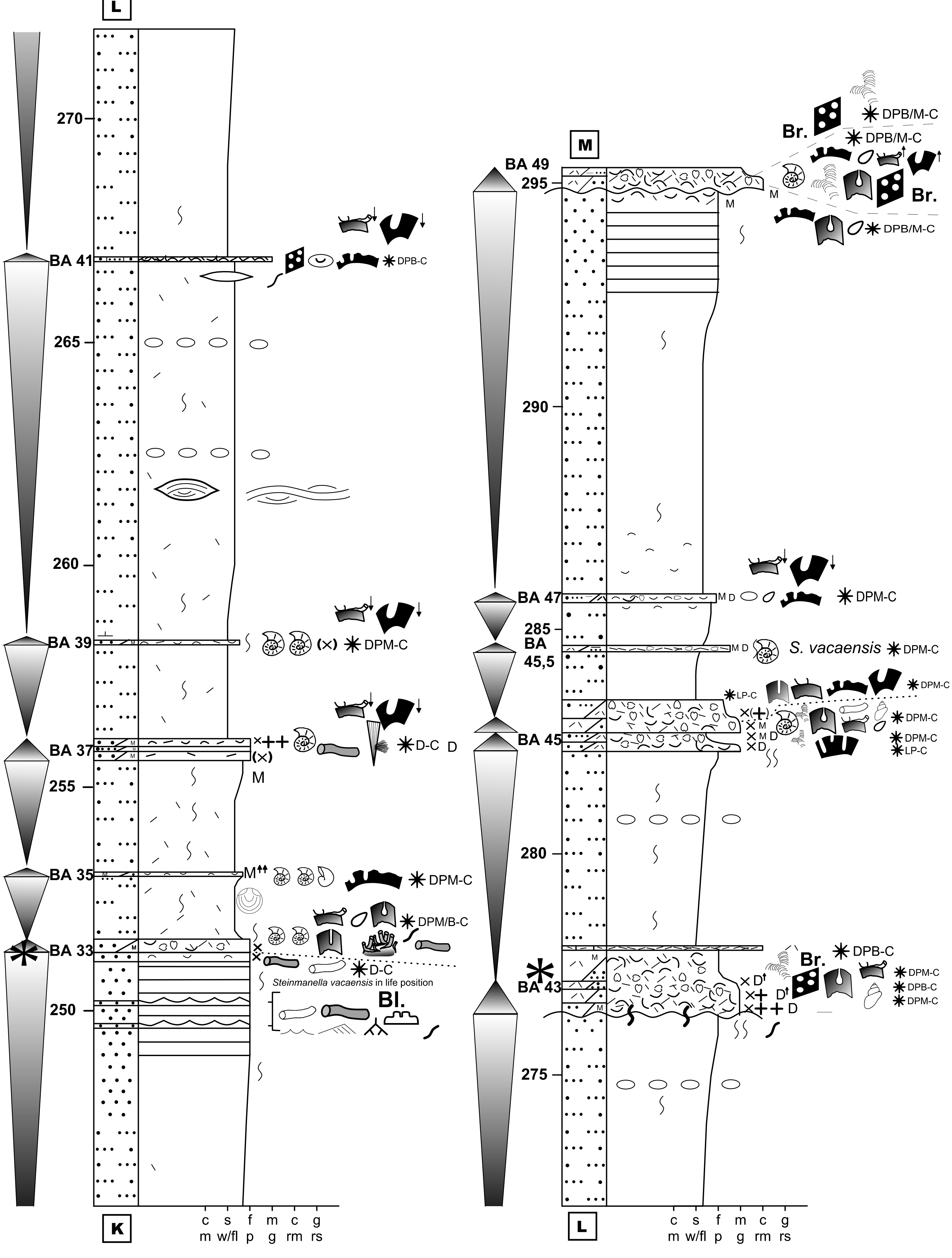

Bajada del Agrio Section (7)

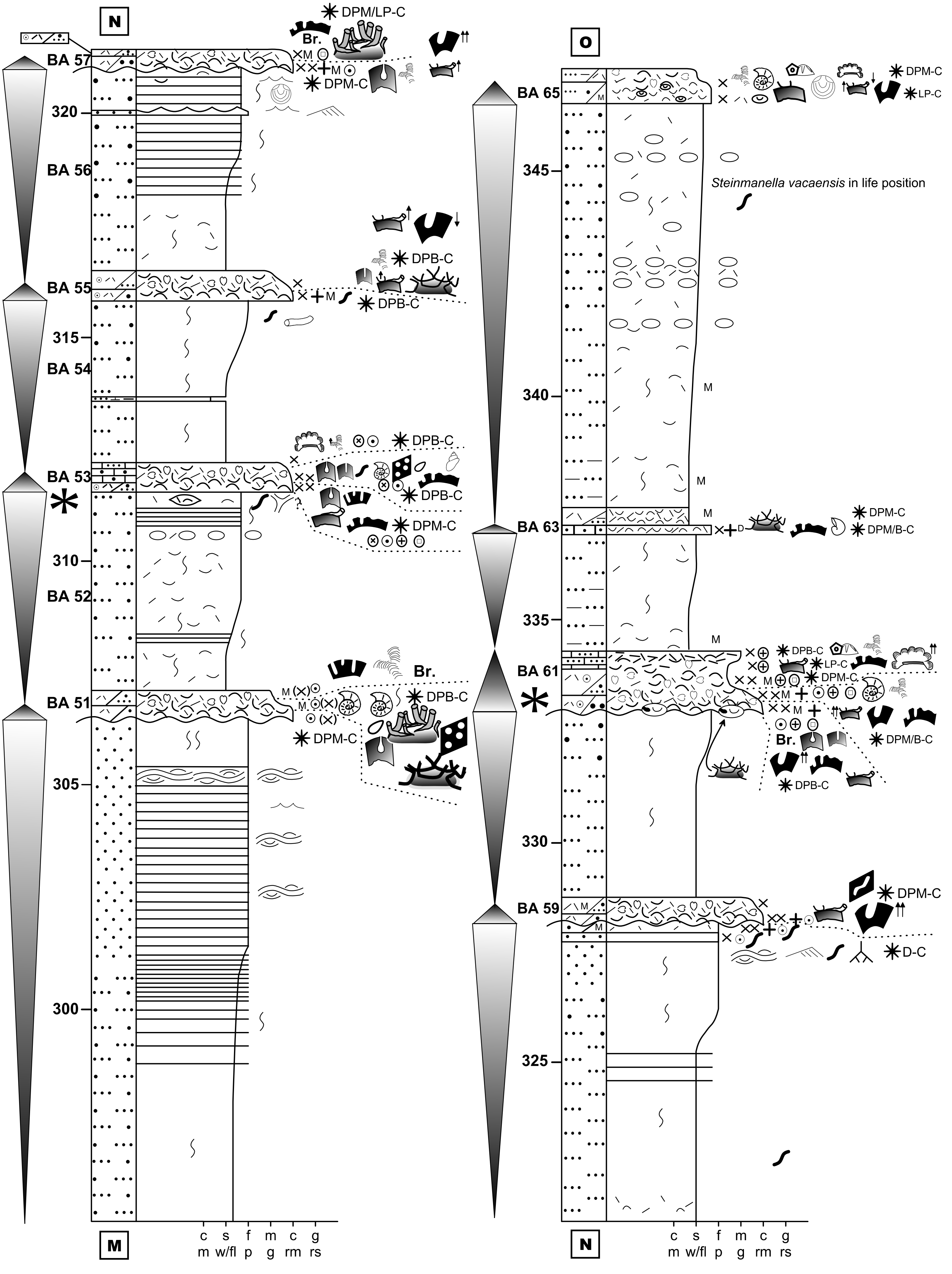

Bajada del Agrio Section (8)

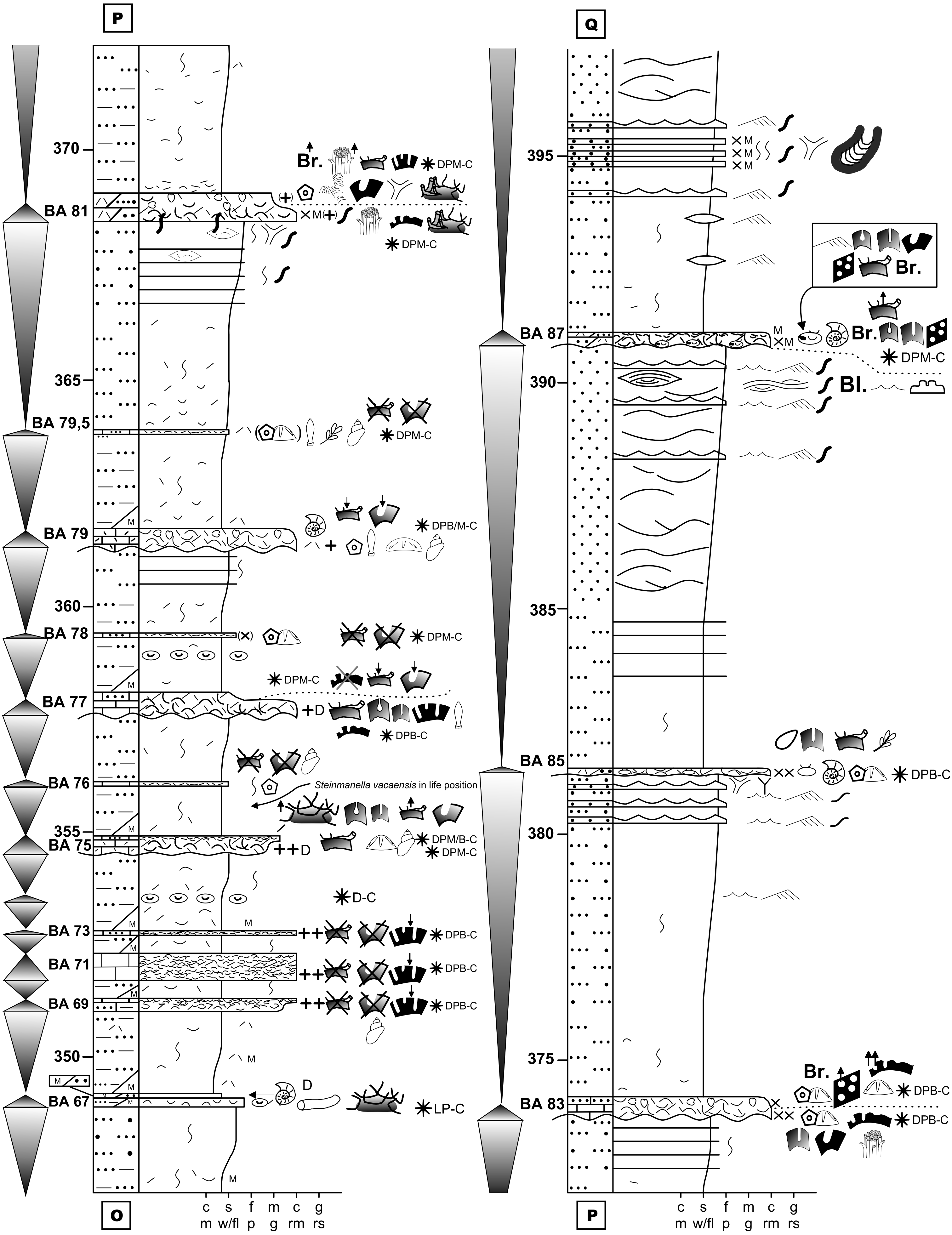

Bajada del Agrio Section (9)

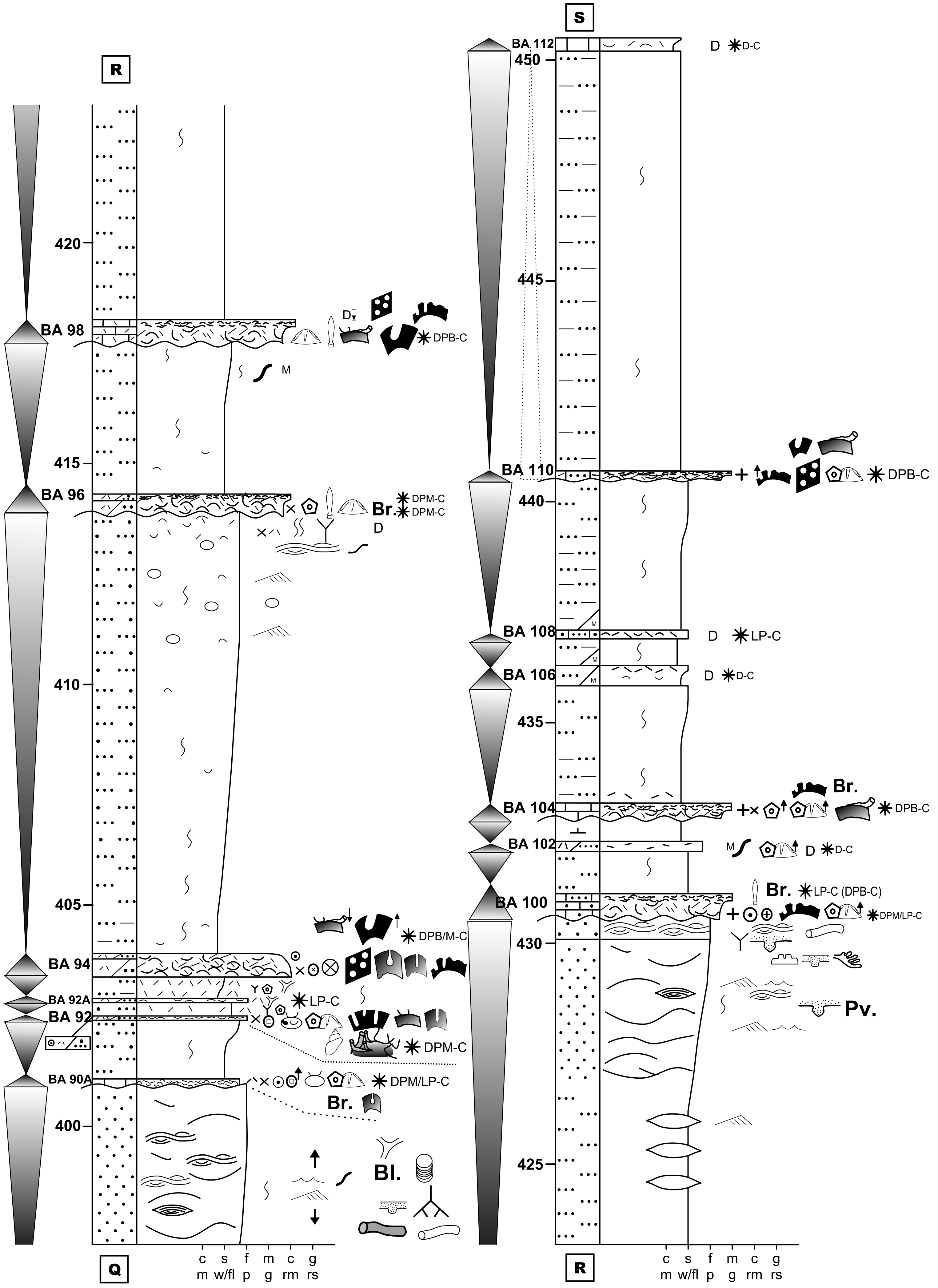

Bajada del Agrio Section (10)

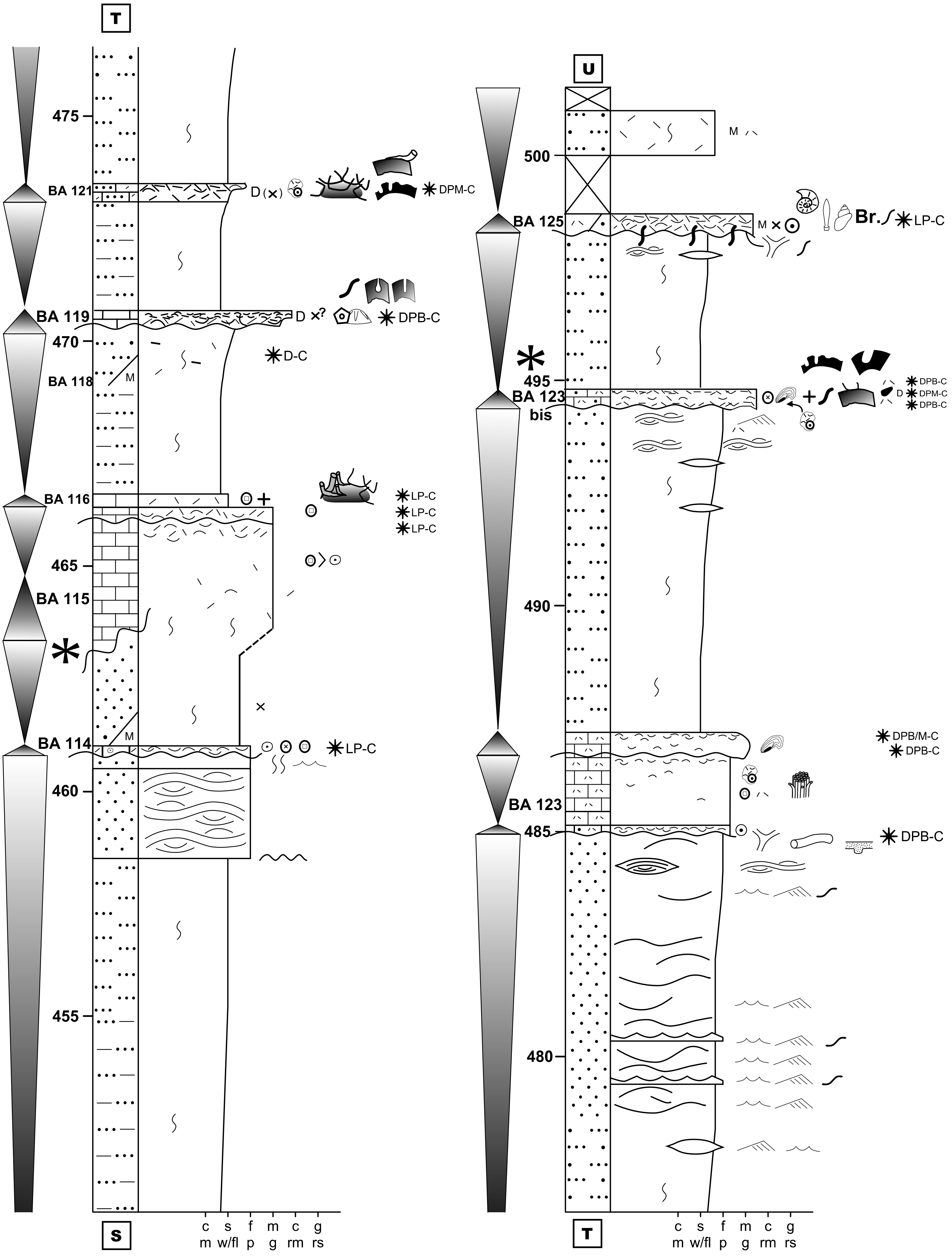

Bajada del Agrio Section (11)

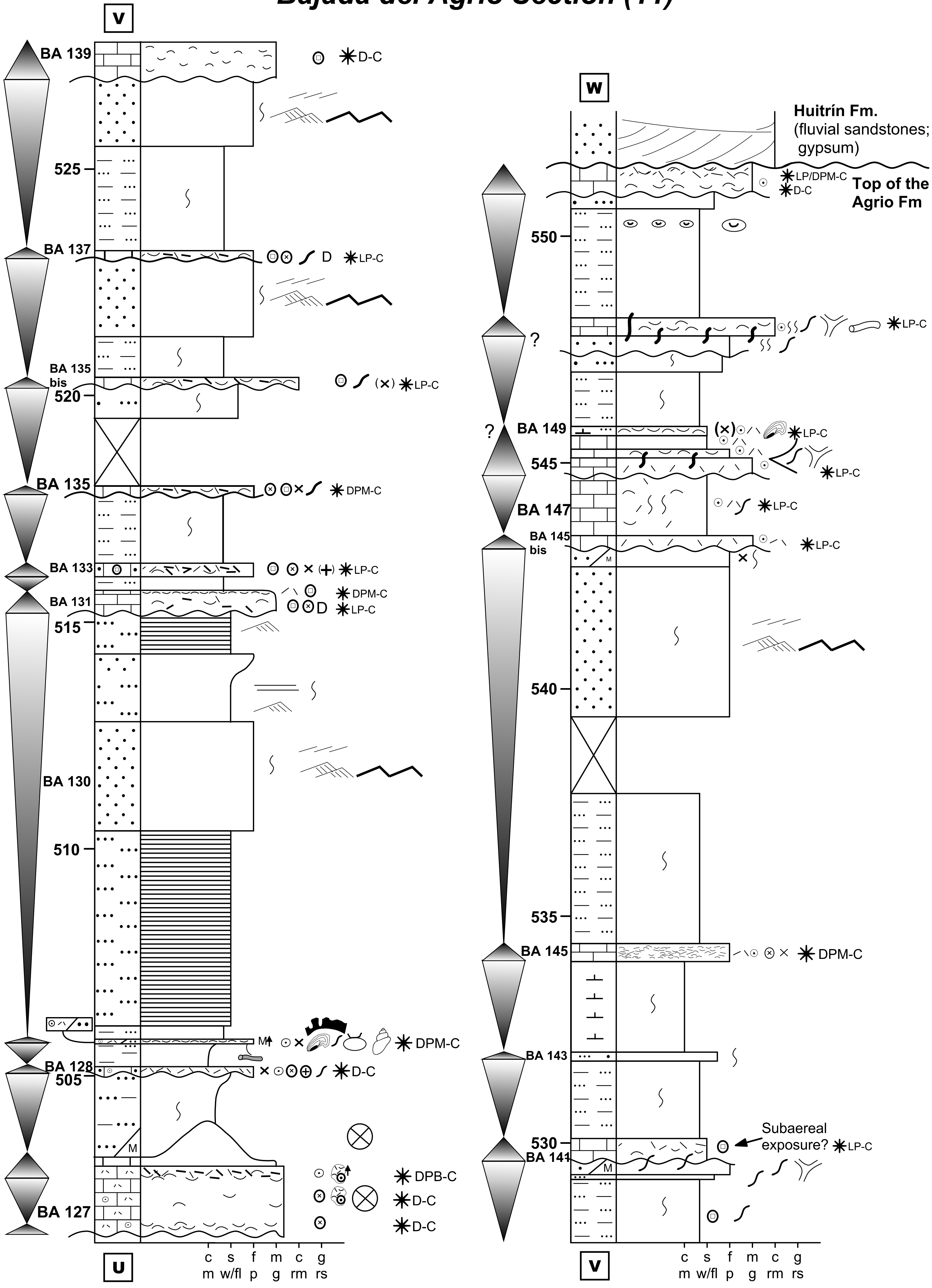

Appendix-Fig.2. Agua de la Mula section of the Agua de la Mula Member. Key in Appendix-Fig. 3

Agua de la Mula Section (1)

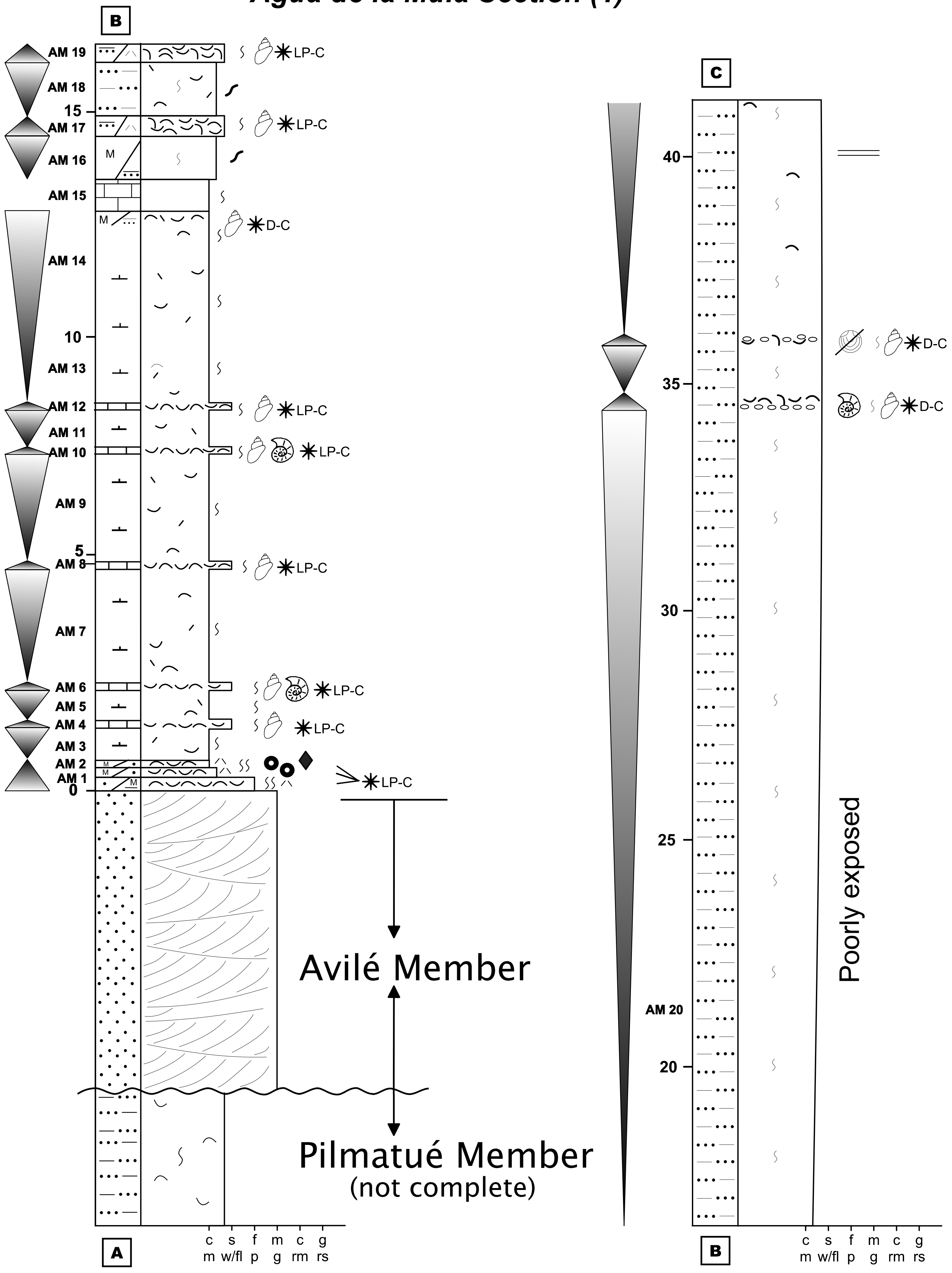

Agua de la Mula Section (2)

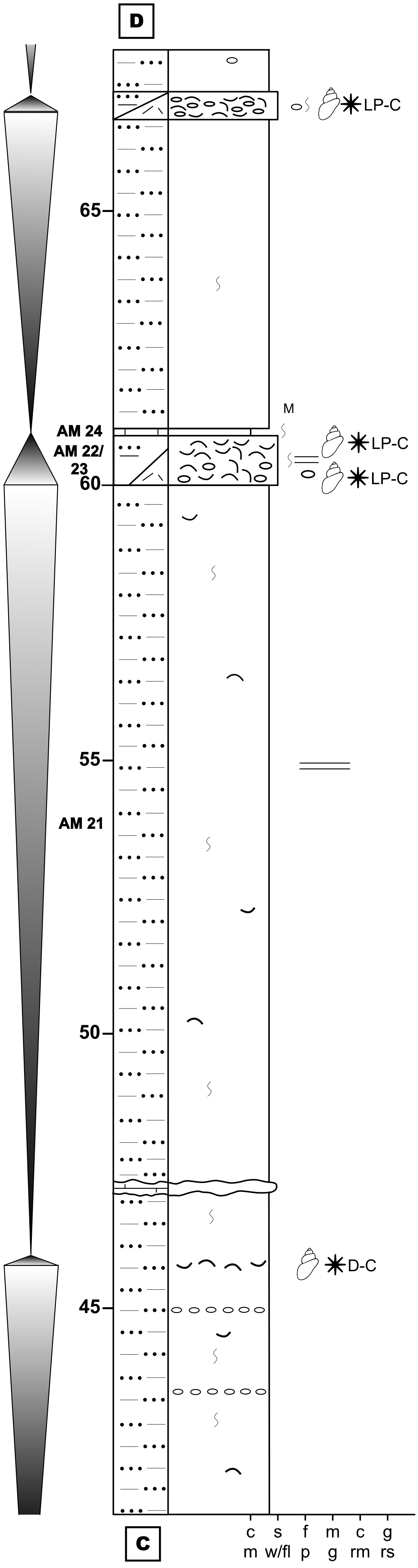

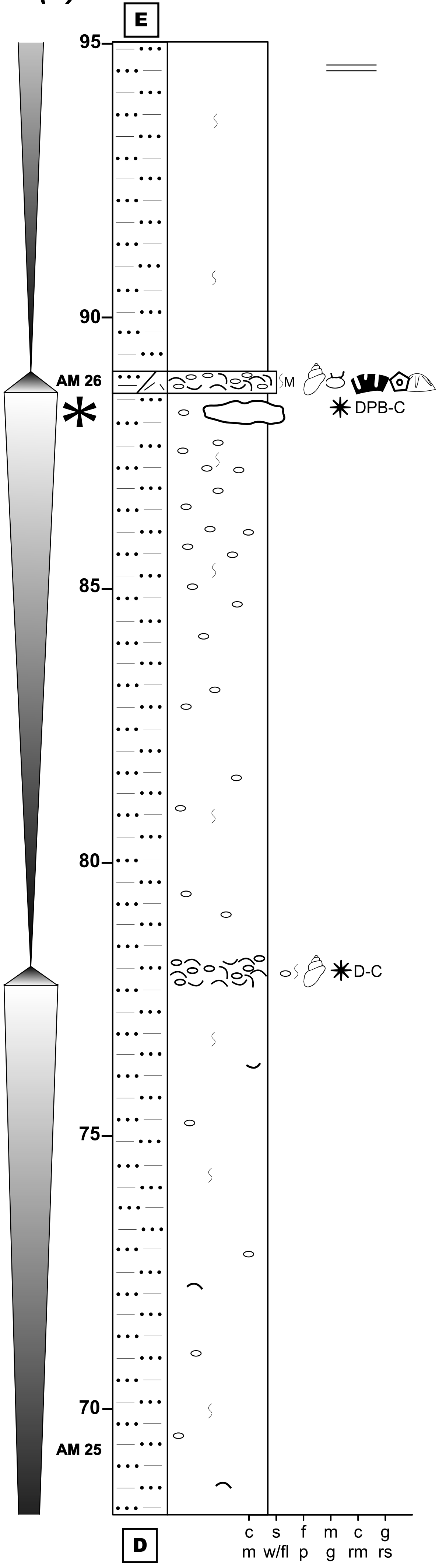

Agua de la Mula Section (3)

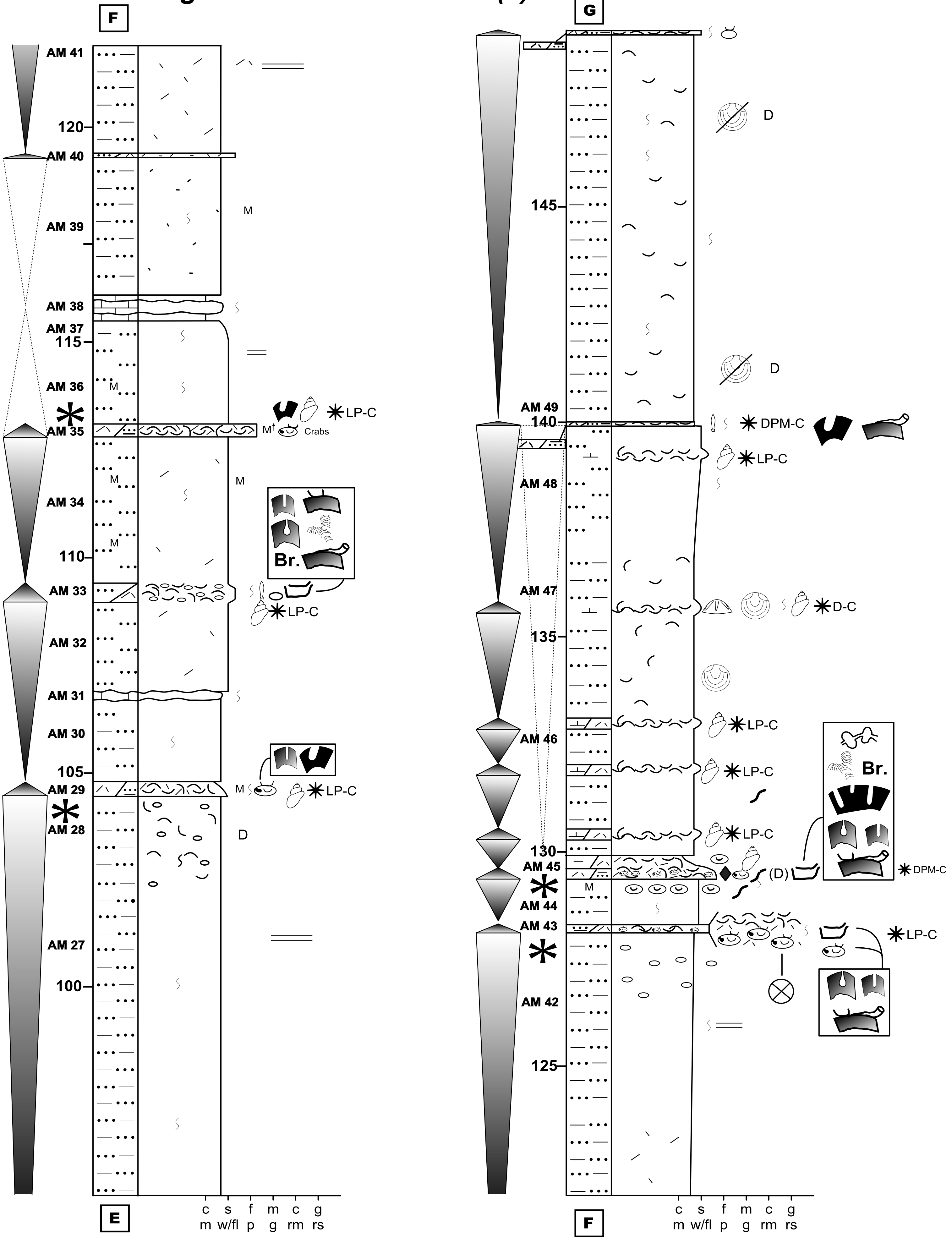

Agua de la Mula Section (4)

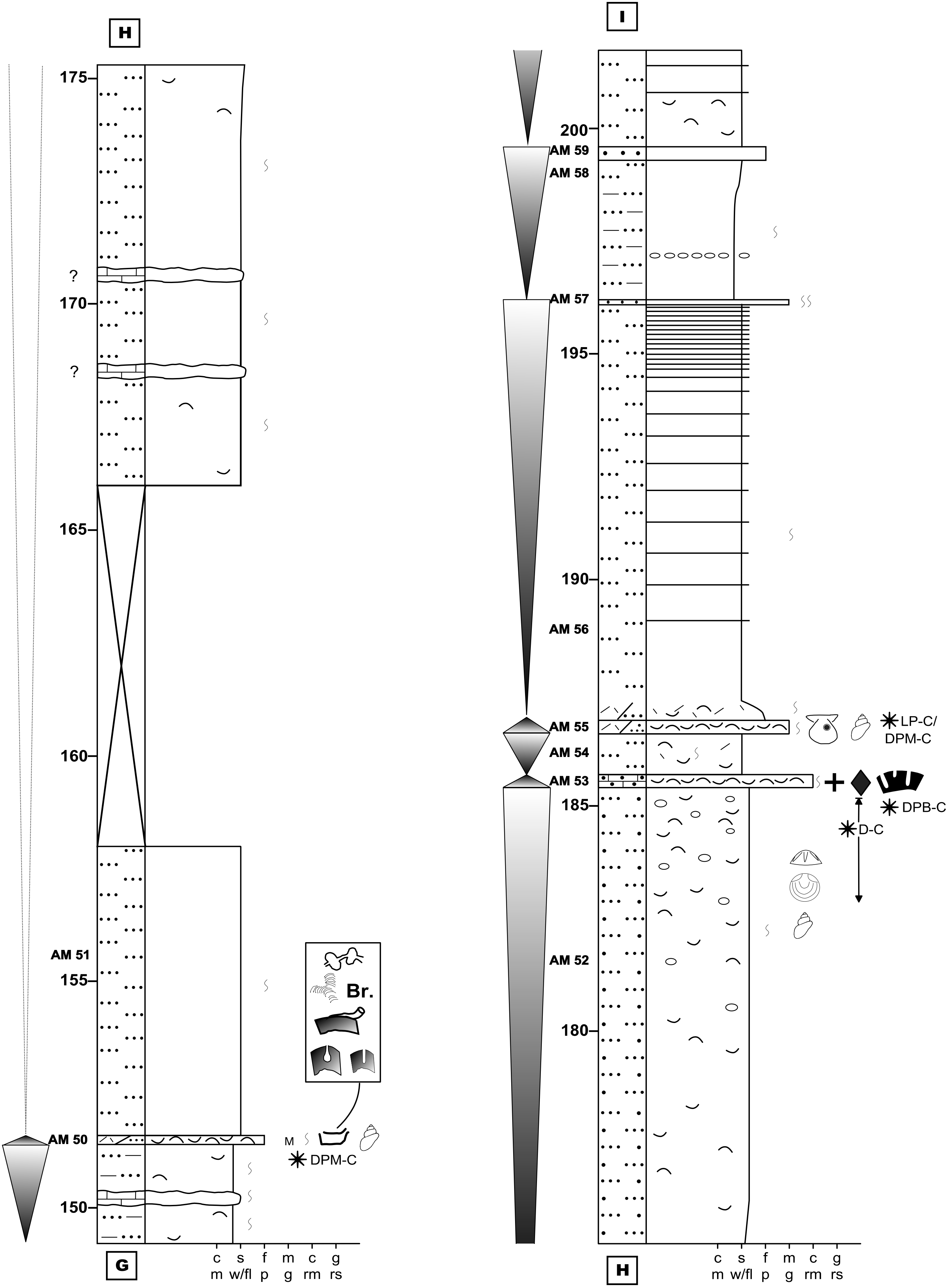

Agua de la Mula Section (5)

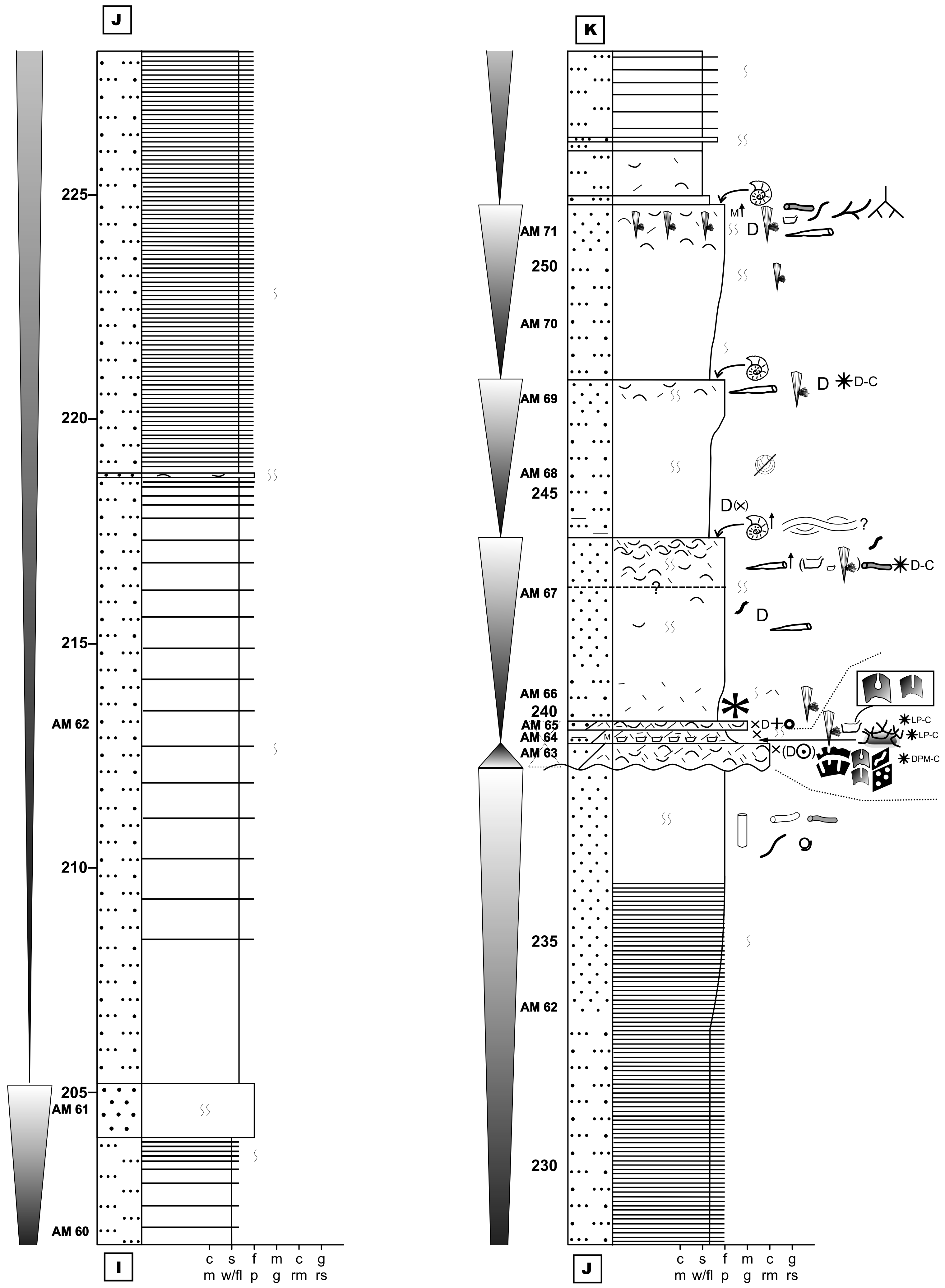

Agua de la Mula Section (6)

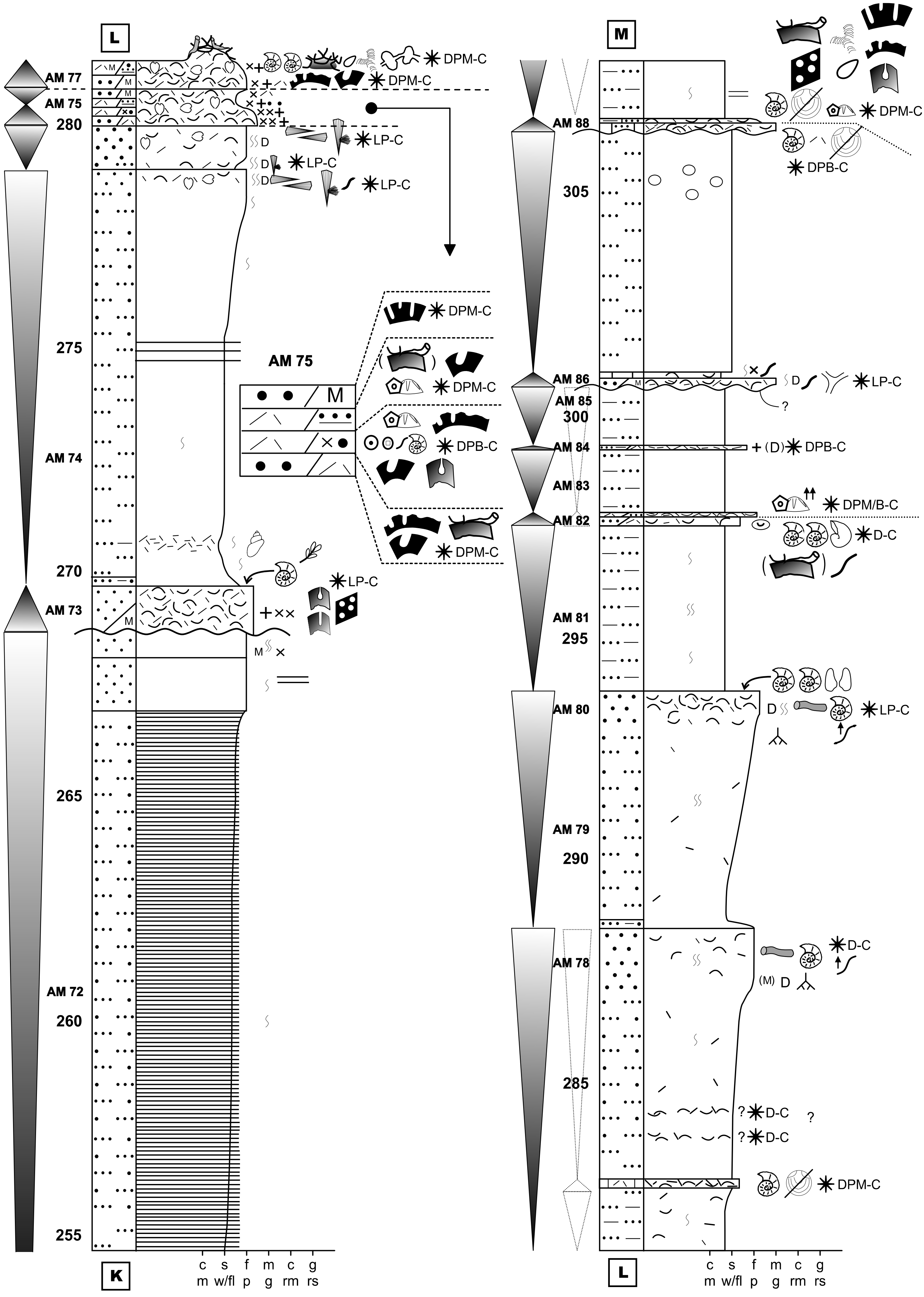

Agua de la Mula Section (7)

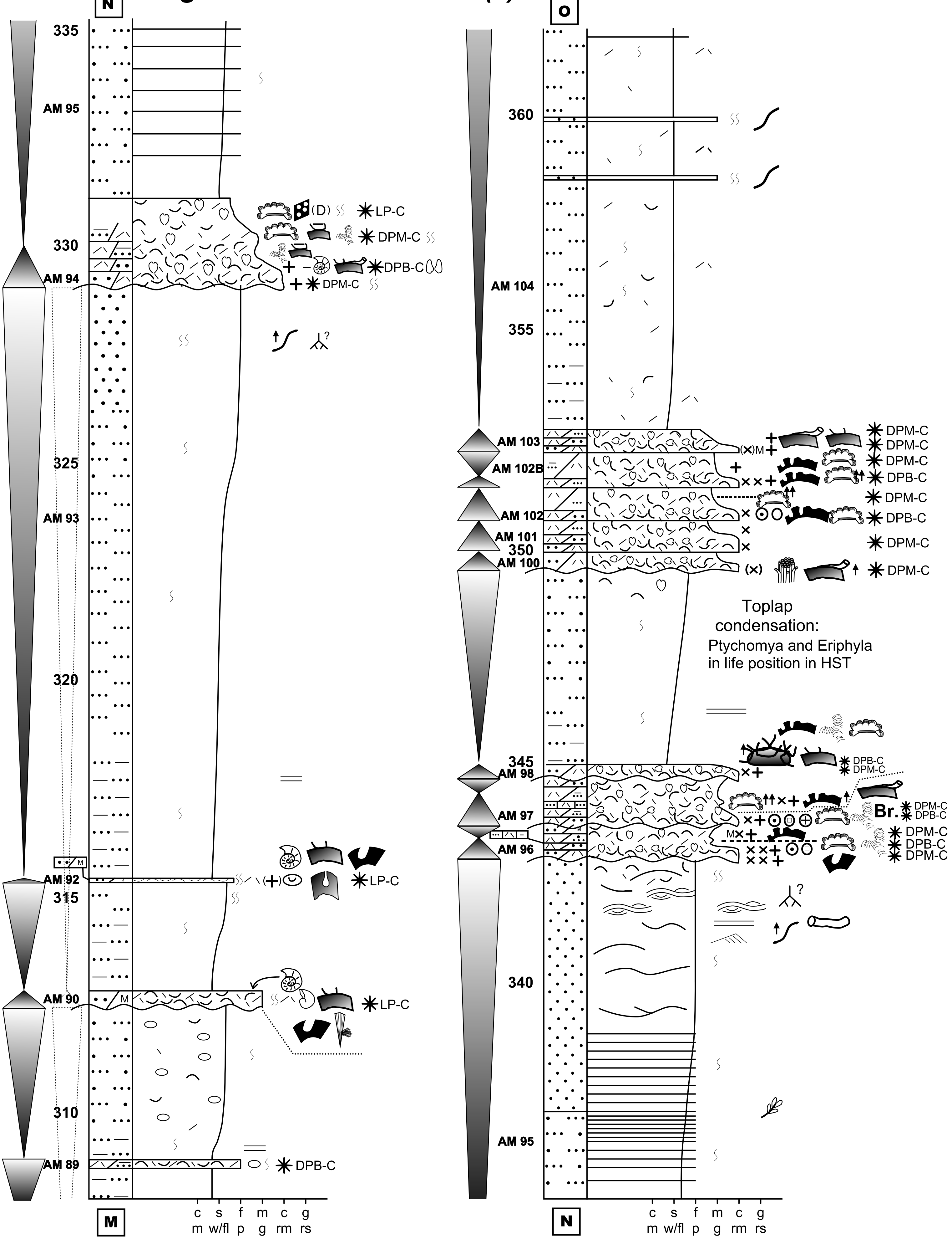

Toplap condensation: Ptychomya and Eriphyla in life position in HST

Agua de la Mula Section (8)

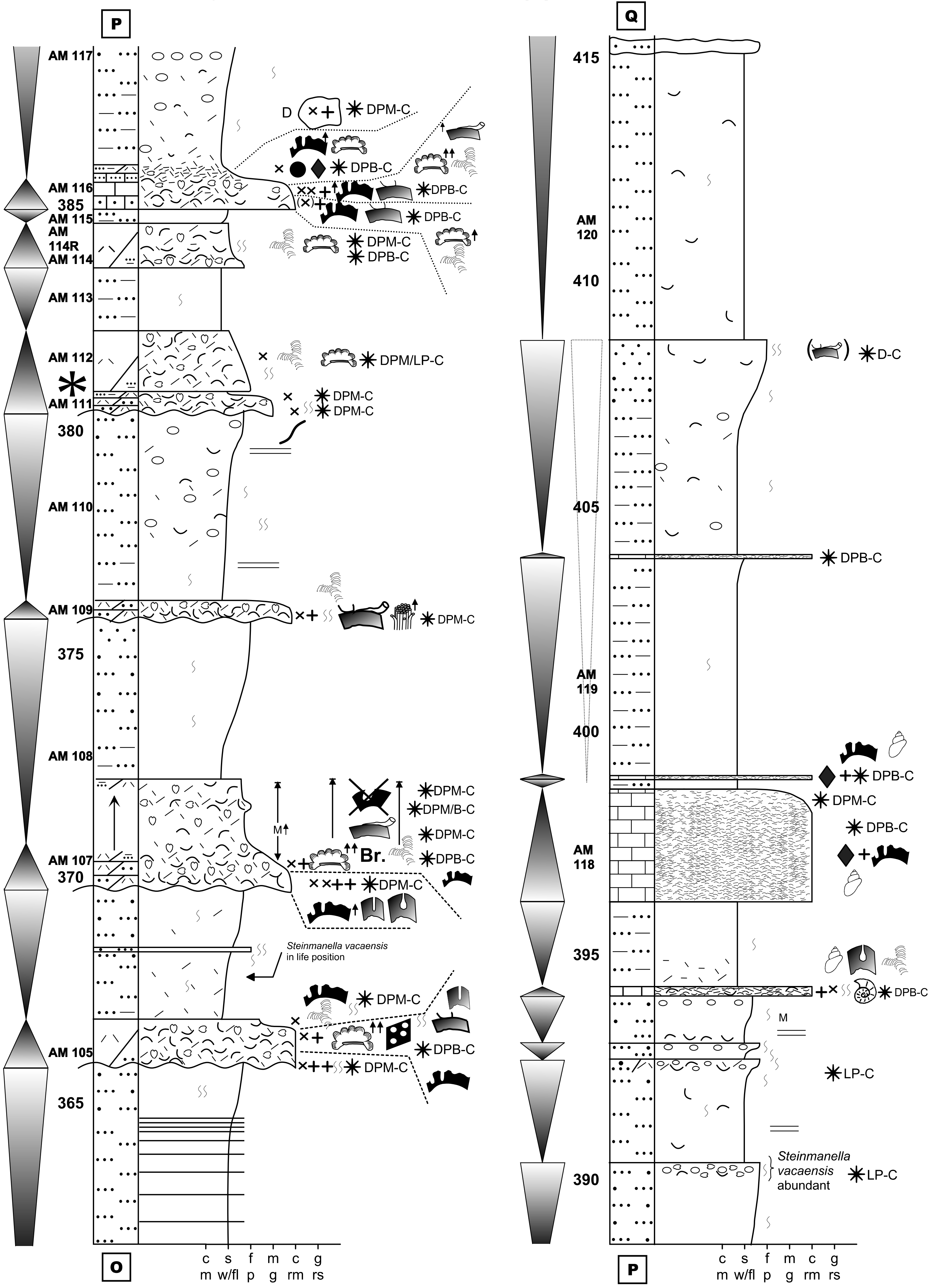

Agua de la Mula Section (9)

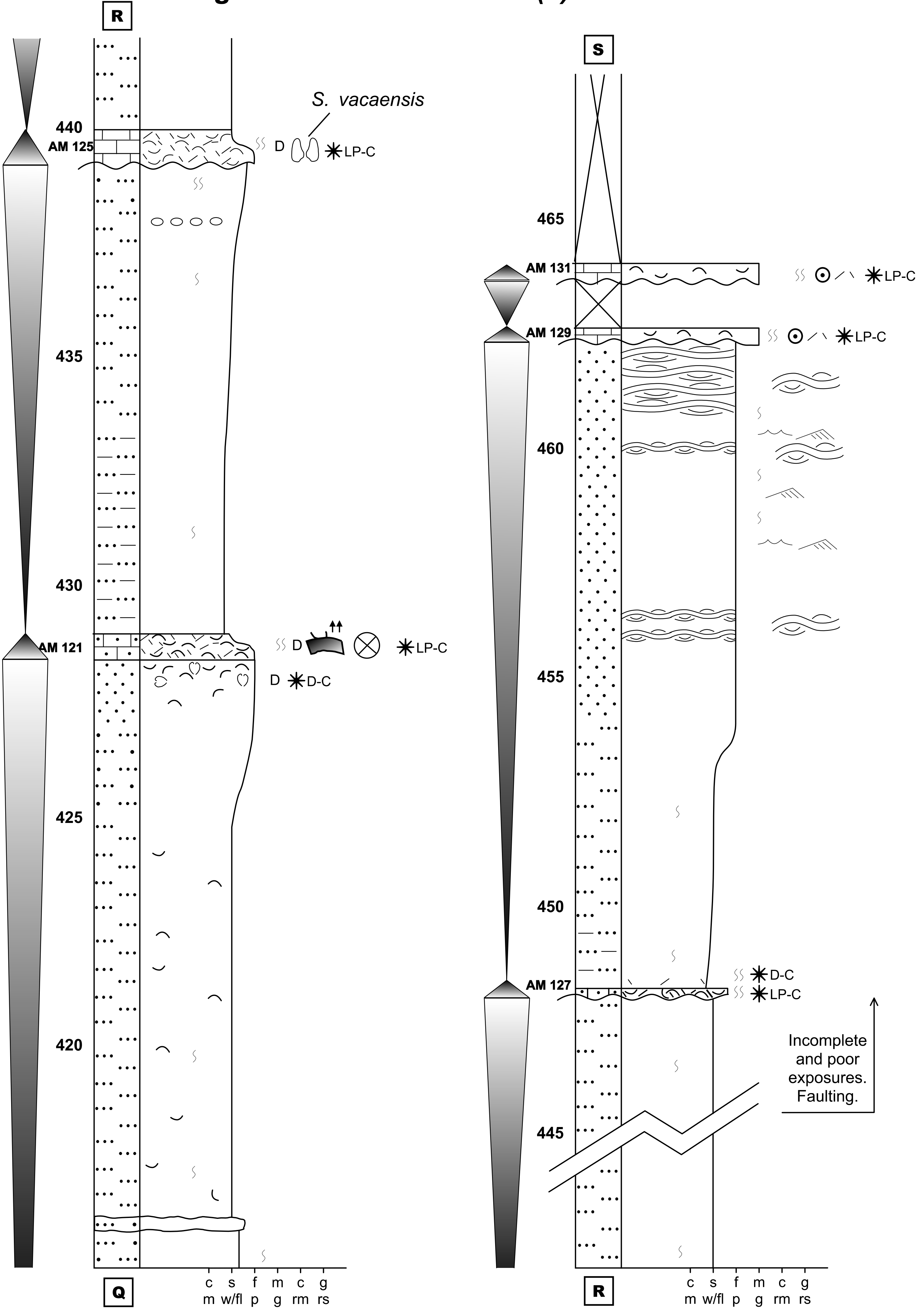

Agua de la Mula Section (10)

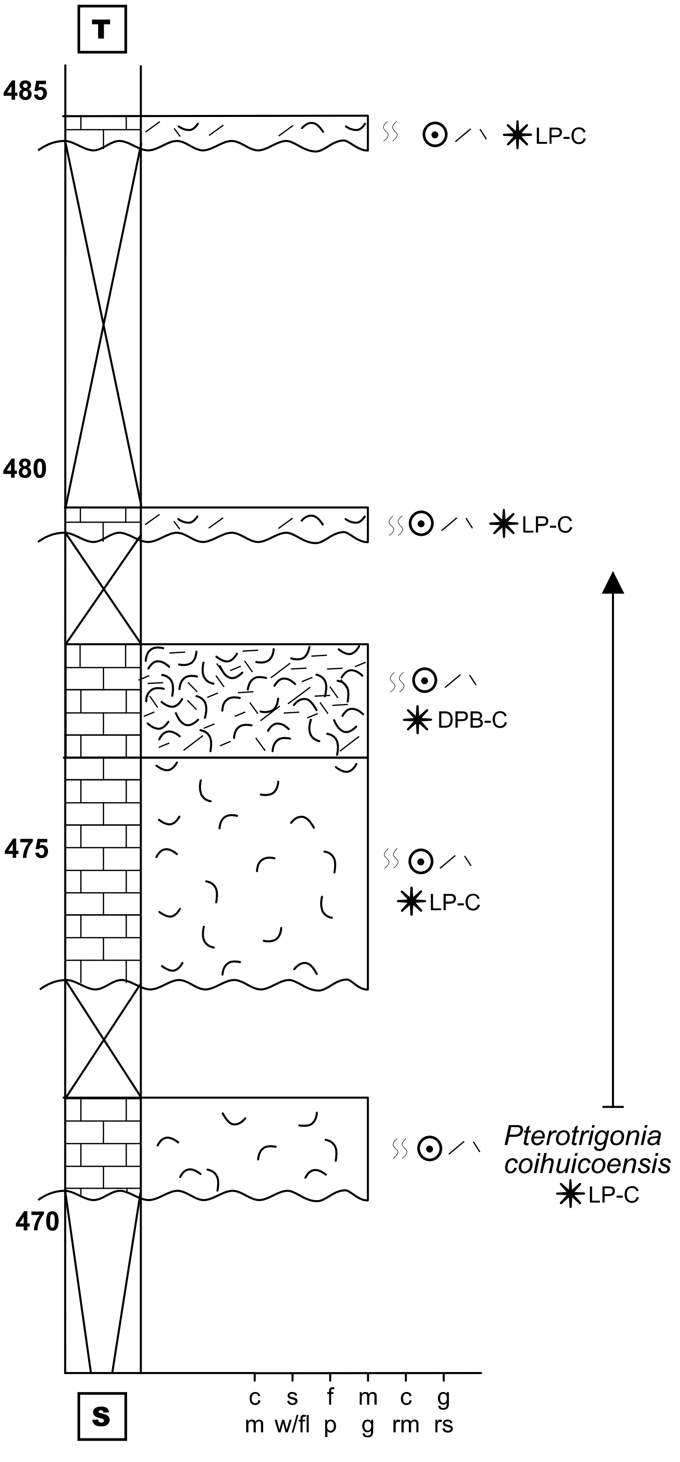

Appendix-Fig. 3. Key of the profiles in Appendix-Fig.1 and 2.

Legend (1)

Lithological, sedimentoogical and stratigraphical features

- sandstone
- siltstone
- clay
- limestone
- marl
- marlstone
- bioclasts
- shells
- × glauconite
- M micrite
- D disolution
- ◆ pyrite
- + ferruginous replacements
- ● pellets
- ◉ phosphate
- Intraclasts
- Microbial crust

- dessication cracks
- cross lamination
- oscillation ripples
- climbing ripples
- asymmetrical ripples
- trough crossbedding
- tabular crossbedding
- hummocky cross-bedding
- parallel stratification
- erosive base
- sharp base
- shell bed

c/m = clay/mudstone
s/w/fl = siltstone/wackestone/floatstone
f/p = fine sst./packstone
m/g = medium sst./grainstone
c/rm = coarse sst./micritic rudstone
g/rs = gravel/sparitic rudstone

Heterolithic stratification:

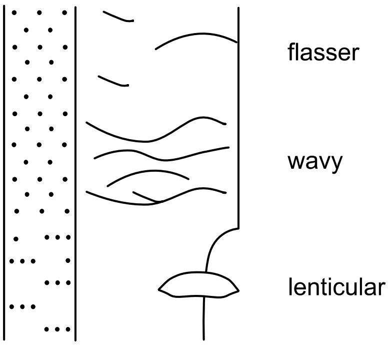

Coarsely interlayered bedding (CIB):

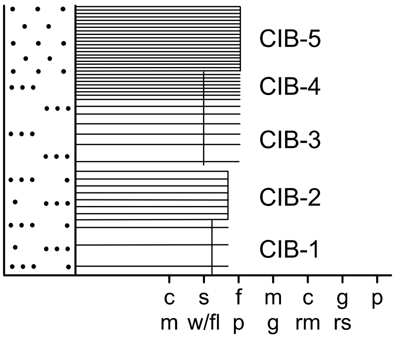

Ooids:

- ⊙ sandy-nucleus
- ▣ allochemic-nucleus
- ⊗ glauconitic-nucleus
- ⊕ ferruginous ooids

Carbonate concretions:

- of early diagenesis
- reworked (bored)
- reworked (encrusted)
- reworked (bored and encrusted)

Mixed rocks nomenclature:

1/2 1: main component
2: main antithetic component

E.g.:

Allochemic (bioclastic) sandstone

- regression
- transgression
- alternative interpretation of the cyclicity pattern
- possible amalgamation of cycles

NOTE: upward or downward pointing arrows indicate respectively high or low levels of the feature. For some features an ordinal scale was used. Repetition of icons indicate high degrees. Brackets () are used when the presence of a feature is rare. For instance, for the glauconite:

(×) Very low levels (a few grains in a whole sample)
× Low levels (few grains per field, 12X)
×× High levels (abundant grains, but never above 5%)

Appendix-Fig.3. Key of symbols used in this work.

Legend (2)

Fossil remains and taphonomic features

- ⊗ corals
- plant remains
- **Br.** briozoans
- irregular echinoids
- regular echinoids
- crinoid ossicles
- echinoid spines
- echinoderm ossicles (undifferentiated)
- serpulids
- *Sarcinella* sp. branches
- encrusting-agglutinating foraminifers
- encrusting-agglutinating foraminifers build-ups
- encrusting foraminifers?
- ammonites
- nautiloids
- *Inoceramus sp.*
- *Pinna robinaldina*
- *Aetostreon* sp.
- *Ceratostreon* sp.
- gastropods

bivalves:
- in life position
- articulated
- disarticulated

- valves in butterfly position
- deep burrowing bivalves
- *Ceratostreon* sp. encrustation
- oysters,serpulids or mixed build-ups
- undiferentiated encrustation
- fragments of *Inoceramus sp.*
- D partial or complete dissolution of shells

Borings

- *Gastrochaenolythes*
- *Trypanites*
- *Meandropolydora*
- *Entobia*
- Cirripaedian boring
- *Caulostrepsis*?
- *Oichnus simplex*
- undiferentiated macroborings
- microborings
- micritization /alteration

Shell packing of skeletal concentrations

(modified after KIDWELL & HOLLAND 1991; for further explanation see the text):

- ✱D-C: disperse - concentration
- ✱LP-C: loosely packed - concentration
- ✱DPM-C: : densely packed matrix-supported
- ✱DPB-C: densely packed bioclast-supported

Burrows

- *Skolithos*
- *Arenicolites*? openings
- *Diplocraterion saxonica?*
- *Spongeliomorpha suevica* (large)
- *Spongeliomorpha suevica* (small)
- *Planolites*
- *Paleophycus*
- **Bl.** *Bolonia lata*
- *Bergaueria*
- *Lockeia siliquaria*
- **Pv.** *Protovirgularia*
- *Phycodes*
- *Treptichnus*
- *Chondrites*
- *Gyrochortes*
- *Teichichnus*
- bioturbation
- Undifferentiated burrows

Erklärung

Hiermit erkläre ich, dass ich die vorliegende Arbeit selbständig und nur unter Verwendung der genannten Quellen und Hilfsmittel angefertigt habe.

Würzburg, den **Fernando M. Archuby**

CURRICULUM VITAE

I. PERSONAL INFORMATION

Name:	**ARCHUBY Fernando Miguel**
Address:	Calle 115 Nro. 424 1900 – La Plata Argentina Tel: 0054 – 221- 4220308
e-mail:	farchuby@fcnym.unlp.edu.ar
Date and place of birth:	28-August-1973, La Plata, Argentina
Nationality:	Argentine
Marital status:	married (two children)

Present Positions

- Graduate Teaching Assistant in Statistics. FCNyM, UNLP (see “Notes” below)
- Head of the office in charge of protecting the paleontological heritage in Buenos Aires Province
- Representant in the Professional Council of Natural Sciences of Buenos Aires Province

Abbreviations

UNLP: Universidad Nacional de La Plata (La Plata National University), La Plata, Argentina.
FCNyM: Facultad de Ciencias Naturales y Museo (Faculty of Natural Sciences and Museum, part of UNLP), La Plata, Argentina.
FCE: Facultad de Ciencias Exactas (Faculty of Exact Sciences, part of UNLP), La Plata, Argentina.
MLP: Museo de La Plata (La Plata Museum, part of FCNyM), La Plata, Argentina.
CONICET: Consejo Nacional de Investigaciones Científicas y Técnicas (National Council of Scientific and Technological Research), Argentina.
CICPBA: Comisión de Investigaciones Científicas de la Provincia de Buenos Aires (Scientific Research Commission of Buenos Aires Province), Buenos Aires Province, Argentina.
FCEyN, **UNC**: Facultad de Ciencias Exactas y Naturales, Universidad Nacional de Córdoba (Faculty of Exact and Natural Sciences, Córdoba National University), Córdoba, Argentina.

Notes

As a **Graduated Teaching Assistant** I teach basic Statistics weekly to a whole course of about 30 to 60 geology or biology students. I share the responsibility of the practice contents of the course. This means that I have to teach theoretical introductions, explain how to solve exercises, and evaluate and coordinate the development of a final work.

Licentiate is a degree awarded at the completion of a five-year program at university.

II.- EDUCATION

University studies:

1993 – 1999	Licentiate in Biology oriented to Zoology (see “notes” in page 3). FCNyM, UNLP. Date of degree: October 27 of 1999. Average of marks: 9.20/10

Postgraduate studies:

2003-2009	Natural Sciences Doctorate (Ph.D.). University of Würzburg, Germany. Project title: “**Taphonomy and paleoecology of benthic macroinvertebrates from the Upper Member of Agrio Formation (Lower Cretaceous), Neuquén Basin (Argentina): Sequence stratigraphic significance**”.

Post-graduated courses

- **“Predator-prey interactions. Experimental and Field Approaches in Biology and Paleontology”.** Summer Course of instruction. University of Washington (USA). Friday Harbor Laboratories. Teachers: Michal Kowalewski, Lindsey Leighton and John Huntley. Evaluation: passed. 2006

- **Regression analysis applied to biological, agrarian and environmental sciences”.** Post graduate course for the Ph. D. Program Faculty of Agrarian and Forest Sciences UNLP. Teachers: Dr. Marcelo Arturi and Dr. Luis. E. Castro. Duration: 40 hours. Evaluation: passed. 2006.

- “**Sedimentary processes and records in coastal areas and platforms**”. Post graduate course, FCNyM, UNLP Teachers: Dr. José Luis Cavallotto and Dr. Roberto Violante. Duration: 30 hours. Evaluation: passed. 2005..

- “**Paleoecology and taphonomy: basic concepts, methodologies and new approaches**”. Post graduate course for the Ph. D. Program in Geological Sciences, of the University of Córdoba. Teachers: Drs. Teresa Sánchez, Beatriz Waislfeld and Marcelo Carrera. FCEyN, UNC. Duration: 30 hours. Evaluation: passed. 2001

- “**Sedimentary rocks**”. Annual regular course of FCNyM, UNLP. Teacher: Dr. Daniel Poiré. Evaluation: practice passed. 2000

- “**Carbonatic rocks, depositional environments and petrology**”. Semi annual regular course of Natural and Exact Sciences Faculty, Buenos Aires University. Teacher: Dr. Ricardo Palma. Evaluation: practice passed. 2001

- **“Multivariate analysis”**. Teacher: Dr. Laura Pla. Duration: 40 hours. Without evaluation. April 2000. FCNyM, UNLP.

- **“Geometry of the biologic shape: theory, techniques and applications in systematics. Advanced course.”** Teacher: Dr. Diego Rasskin-Gutman. Duration: 40 hours. Evaluation: passed. September 1997. FCNyM, UNLP.

- **“Geometry of the biologic shape”**. Teacher: Dr. Diego Rasskin-Gutman. Duration: 40 hours.. September 1997, Sciences Faculty, Universidad de la República, Montevideo, Uruguay.

Courses taken at the Würzburg University

- Allgemeine Paläontologie. Professor: Dr. Franz Fürsich

- Präparative Arbeitsmethoden in der Paläontologie. Professor: Dr. Michael Heinze

- Methoden der Stratigraphie. Professor: Dr. Marcus Wilmsen

Field Trips

- Agrio Formation, Neuquén Basin. Neuquén Province, Argentina. March 2004. 25 days.
- Agrio Formation, Neuquén Basin. Neuquén Province, Argentina. April 2003. 25 days.
- Agrio Formation, Neuquén Basin. Neuquén Province, Argentina. December 2002. 10 days.
- Agrio Formation, Neuquén Basin. Neuquén Province, Argentina. March 2002. 20 days.
- Neuquén Basin, general trip. Neuquén Province, Argentina. November 2001. 10 days.
- Mulichinco Formation, Neuquén Basin. Neuquén Province, Argentina. March 2000. 10 days.
- Holocene of Buenos Aires Province. Rescue of cetacean remains. October 2008. 2 days.
- Miocene marine trace fossils in cliffs of Las Grutas, Río Negro Province. July 2008. 4 days.
- Continental cliffs in General Alvarado, Buenos Aires Province. February 2009. 2 days.
- Holocene shelly beach ridges. Buenos Aires Province. Octubre de 2007 and 2008. 2 days.

Visits to foreign Universities

- Institute of Palaeontology, University of Würzburg, Germany. June – July 2002
- Institute of Palaeontology, University of Würzburg, Germany. August 2003 – September 2004
- Institute of Palaeontology, University of Würzburg, Germany. November – December 2005
- Friday Harbor Labs, University of Washington, USA. July-August 2006.

Languages

- Foreign

English: I can speak, read and write acceptably.
German: basic knowledge of the German language after having finished a 2 months language course at the Goethe Institut in Mannheim.

- Native: Spanish.

III. AREAS OF SPECIALIZATION

- Paleoecology and taphonomy and sequence stratigraphy.
- Quantitative methods applied to natural sciencies. Teaching and research.
- Biotic interactions in recent and geologic times, with emphasis in drilling predation.
- Management of natural heritage

IV. RESEARCH SUPPORT, FELLOWSHIPS, AND AWARDS

- DAAD "Sandwich-type" scholarship. Project: "**Taphonomy and paleoecology of benthic macroinvertebrates from the Upper Member of Agrio Formation (Lower Cretaceous), Neuquén Basin (Argentina): Sequence stratigraphic significance**". German Director: Prof. Dr. Franz T. Fürsich. Institut für Paläontologie der Universität, Würzburg. Argentine Director: Prof. Dr. Héctor A. Leanza. Argentine Museum of Natural Sciences "Bernardino Rivadavia", National Geological Service and FCNyM, UNLP, Argentina. Duration: 14 months from August 2003.

- Doctoral Fellowship. CONICET. Project: "**Taphonomy and paleoecology of benthic macroinvertebrates from the Upper Member of Agrio Formation (Lower Cretaceous), Neuquén Basin (Argentina): Sequence stratigraphic significance**". Local Director: Prof. Dr. Héctor A. Leanza. Argentine Museum of Natural Sciences "Bernardino Rivadavia", National Geological Service and FCNyM, UNLP, Argentina. External Director: Prof. Dr. Franz T. Fürsich. Institut für Paläontologie der Universität, Würzburg, Germany. Local Co-director: Dr. Tristán Simanauskas, MLP -CONICET. Duration: five years from 1st of June 2001.

- FCNyM Fellowship. Project: "**Preliminary paleoecological analysis of the boundstones of oysters and serpulids of Mulichinco Formation, Lower Cretaceous, Neuquén Basin, Neuquén Province, Argentina.**" Director: Dr. Tristán Simanauskas (MLP-CONICET), Co-director: Dr. Ramiro Sarandón (Professor at FCNyM). Duration: a year from November 2000 (resigned June 2001).

- Fellowship for distinguished university students, Antorchas Foundation. Project: "**Limb bones allometry of Buenos Aires Province fossil ungulates. Locomotion and allometric models**". Director: Dr. Sergio Vizcaíno (MLP- CONICET). May 1998 to October 1999.

- Training Fellowship for students. Scientific Research Commission of Buenos Aires Province (CICPBA). Project: "**Limb bones allometry of Buenos Aires Province fossil ungulates. Implications in locomotion**". Director: Dr. Sergio Vizcaíno (MLP- CONICET). May 1997 to April de 1999.

- Award for the best article in *Psicofarmacología* 2007. Article:
"Palacios Vallejos, M.E.; Zelaschi NM, Archuby, F.; Rodríguez, J.L.; Queipo, G.; Gaitan, S., 2007. Esquizofrenia: relación entre funcionamiento neurocognitivo, calidad de vida y movimientos anormales involuntarios. Psicofarmacología 7:46, 9-11"

- **Joaquín Víctor González Award**. Municipalidad de La Plata, Argentina. Award given to the ten most distiguished graduated students of the each Faculty of the UNLP. 1999.

V. TEACHING EXPERIENCE

- May-01-05 and continues. Graduated Assistant Teacher in Statistics for Biology and Geology. FCNyM, UNLP
- April-01-00 to Jan-31-2003. Graduated Assistant Teacher in Statistics for Biology and Geology. FCNyM, UNLP
- Dec-01-96 to Jan-31-2000. Student Assistant Teacher in Statistics for Biology and Geology. FCNyM, UNLP
- Jul-01-94 to Jun-31-95.Student Assistant Teacher in Chemistry for Biology and Geology. FCNyM, UNLP
- Oct-01-92 to Mar-31-94. Student Assistant Teacher in Automatic treatment of the information (Informatics) Faculty of Humanities and Educational Sciences, UNLP

VI. OTHER PREVIOUS POSITIONS

- Web Master FCNyM – UNLP. 2003.
- Administrative activities in Postgraduate Department, FCNyM, UNLP. April-01-00 to July-31-00.
- Since July-31-2000 I have participated in seven environmental assessment evaluations in different factories around Buenos Aires and La Plata Cities with Lic. Gustavo D. Bulus Rossini.
- Web Master and Designer: Statistics regular undergraduate course at the FCNyM, UNLP 2000-2003

VII. SCIENTIFIC ACTIVITIES.

Articles and abstracts

Sedimentology, paleoecology, taphonomy.

Scientific articles

- Archuby, F. 2005. Significación estratigráfica de las concentraciones esqueletales en las sedimentitas marinas del Hauteriviano- Barremiano (Cretácico Inferior). Cuenca Neuquina, Argentina. In: Llambías, E., R. de Barrio, P. González and P. Leal (eds.). *16º Congreso Geológico Argentino, Actas* 3: 457-464. La Plata (Buenos Aires).

Abstracts

- Archuby, F. 2004. Sequence stratigraphy and skeletal concentrations in the Lower Cretaceous of the Neuquén Basin (Northern Patagonia, Argentina) *74. Jahrestagung der Paläontologischen*

Gesellschaft Gesellschaft „GEOBIOLOGIE“ (*74th Annual Meeting Of the German Palaeontological Society “Geobiology”)*, Göttingen, Germany, October 2004.

- Archuby, F. 2004. Sequence stratigraphic significance of skeletal concentrations: an example from the Lower Cretaceous of the Neuquén Basin (Northern Patagonia, Argentina) *19th Sedimentological Conference 2004 at the Rheinish Westphalian University of Technology in Aachen*. Aachen, Germany. 1-4 July 2004.

- Schwarz, E., Fernando Archuby and Tristán Simanauskas, 2001. “Sedimentology, paleoecology and Taphonomy of Valanginian Shellbeds of the Neuquén Basin (Argentina): Paleoenvironmental and Sequence Stratigraphic Implications”. *21st. I.A.S. Meeting of Sedimentology*, 3-5 September 2001, Davos, Switzerland.

- Schwarz, E., Simanauskas, T. y Archuby, F., 2000. “Sedimentología de depósitos carbonáticos en el noroeste de Neuquén, Formación Mulichinco (Valanginiano), Cuenca Neuquina, Argentina”. *Resúmenes del II Congreso Latinoamericano de Sedimentología y VIII Reunión Argentina de Sedimentología*. Mar del Plata, Argentina. pp.165-166

Allometry and Biomechanics of Pleistocene mammals (Developed during the last two year of the Licentiate. Supported by two grants).

Scientific articles

- Bargo, María S., Vizcaíno, Sergio F., Archuby, Fernando M. and Blanco R. Ernesto, 2000. “Limb bone proportions, strength and digging in some Lujanian (Late Pleistocene-early Holocene) Mylodontid ground sloths (Mammalia, Xenarthra)”. *Journal of Vertebrate Paleontology*. 20 (3):601-610.

Abstracts

- Archuby, F., 1998. “Alometría de los huesos largos de *Toxodon platensis* (Notoungulata) y *Macrauchenia patachonica* (Litopterna). Implicancias en su locomoción.”. *Resúmenes del VII Congreso Argentino de Paleontología y Bioestratigrafía*. Bahía Blanca. 1998, p.101

Unpublished works

- Archuby, F. “Alometría de los huesos largos de Toxodon platensis (Notoungulata) y Macrauchenia patachonica (Litopterna). Implicancias en su locomoción.”

Morphometry and palaeobiology of ichthyiosaurian eyes

Scientific articles

- Fernández, M.S., F. Archuby, M. Talevi and R. Ebner., 2005. The ichthyiosaurian eyes: paleobiological information content in the sclerotic ring of *Caypullisaurus* (Ichthiosauria, Ophthalmosauria) and in other Jurassic ichthyiosaurs. *Journal of Vertebrate Paleontology*, 2005, 25(2):330-337

Abstracts

- M. Fernández, R. Ebner, F. Archuby y M. Talevi, 2003. El ojo de los ictiosaurios: ¿qué ves cuando me ves?. XIX Jornadas Argentinas de Paleontología de Vertebrados. Actas. Buenos Aires, 2003.

Neuroendocrinology of schizophrenic patients. (I participated in the research group directed by Dr. Med. N.M Zelaschi. My tasks are related with the design of surveys and statistic analysis).

Scientific articles

- Palacios Vallejos, M.E.; Zelaschi NM, Archuby, F.; Rodríguez, J.L.; Queipo, G.; Gaitan, S., 2007. Esquizofrenia: relación entre funcionamiento neurocognitivo, calidad de vida y movimientos anormales involuntarios. *Psicofarmacología* 7:46, 9-11.

- Palacios Vallejos, M.E.; Zelaschi, N.M.; Rodríguez, J.L.; Gaitan, S.; Archuby F. y Zieher, L. M. 2004. Déficits neurocognitivos.en pacientes hospitalizados tratados con drogas antipsicóticas. *Psicofarmacología*. 4 (27): 15-22.
- Palacios Vallejos ME, Zelaschi NM, Rodriguez JL, Gaitan S, Zieher LM, Archuby F., 2003. "Posible mejoría del Funcionamiento Neurocognitivo en la Esquizofrenia facilitada por los tratamientos farmacológicos" *Boletin CENICOM* AÑO III, 20-30.

Abstracts

- Zelaschi NM, Queipo, G.; Archuby, F.; Gaitan, S., Rodríguez, J.L.; Zieher, L. M., 2007. Seguimiento longitudinal de niveles de prolactina en la esquizofrenia crónica tratada con ziprazidona (bloqueante D2-5HTA2). *Medicina*, 67, 3, P211. (Abstract with evaluation)
- Palacios Vallejos, M.E.; Archuby, F.; Gaitan, S., Queipo, G.; Rodríguez, J.L.; Zelaschi NM, Zieher, L. M., 2007. Bloqueantes D2-5HTA2: déficit neurocognitivo y su relación con la mejoría de la calidad de vida en la esquizofrenia crónica. *Medicina*, 67, 3, P98. (Abstract with evaluation)
- Gobbi, S.A.; Archuby, F.; Zelaschi NM, Zierher, L.M., 2007. Estudio de prevalencia de síntomas depresivos antenatales y factores de riesgo psicosociales en sectores populares. *Medicina*, 67, 3, P157. (Abstract with evaluation)
- Palacios Vallejos, M.E.; Zelaschi NM, Archuby, F.; Rodríguez, J.L.; Queipo, G.; Gaitan, S., 2007. Esquizofrenia: relación entre funcionamiento neurocognitivo, calidad de vida y movimientos anormales involuntarios. *Psicofarmacología* 7:46, P 9. (Abstract with evaluation)
- Rodríguez, J.L.; Queipo, G.; Archuby, F.; Palacios Vallejos, M.E.; Zelaschi NM, 2007. Niveles de Prolactina en pacientes psicóticos con Ziprasidona. *23° Congreso Argentino de Psiquiatría. Libro de Abstracts,* P 104. (Abstract with evaluation)
- Zelaschi, N.M.; Rodríguez, J.L.; Gaitan, S.; Panizzo, S.; Archuby, F.; Zierher, L.M., 2004. Effects of Long – Term Treatment with Atypical Antipsycohotics drugs in patients with schizophrenics Disorders; a comparative study of Clozapine, Risperidone and Olanzapine". *Cell and Molecular Neurobiology*. 24 (1):180. (Abstract with evaluation)
- Palacios Vallejos ME, Zelaschi NM, Rodriguez JL, Gaitan S, Panizzo, S., Archuby F, Zieher LM., 2003. "Neurocognitive Performance in Schizophrenic Patients Treated With Atypical Antipsychotics". *Cell and Molecular Neurobiology*. 24 (1):179. (Abstract with evaluation)
- Zelaschi NM, Rodríguez JL, Gaitán S, Palacios Vallejos ME, Panizzo S, Archuby F., Zieher LM., 2002. "Efectos comparativos del Tratamiento Prolongado con Antipsicóticos Atípicos en pacientes esquizofrénicos" *Medicina*, 62, 5, 483,2003. (Abstract with evaluation)
- Zelaschi N., Rodríguez J., Gaitán S., Panizzo S., Chiodi C. Sobrero A., Archuby F., Zieher L M., 2001. "Niveles séricos de prolactina en pacientes esquizofrénicos Hospitalizados tratados con clozapina". *Medicina*, 61, 5/2, 755, 2001. (Abstract with evaluation)
- Zelaschi N. M, Rodriguez J, Gaitan S, Panizzo S, Sobrero A, Lopez A, Archuby F., 1999. Diferencias Clínicas en la Respuesta Terapéutica de los Antagonistas D_2 – 5ht A_2 Risperidona y Clozapina, luego de la observación prolongada de Pacientes Esquizofrénicos Hospitalizados." *Medicina*, 641, 1999. (Abstract with evaluation).
- Zelaschi N. M, Rodriguez J, Gaitan S, Panizzo S, Sobrero A, Lopez A, Archuby F., 1999. "Niveles Sericos Comparativos de Prolactina en el Tratamiento Prolongado con los Antagonistas D_2–5ht A_2 Risperidona y Clozapina. En Pacientes Esquizofrenicos Hospitalizados". *Medicina*, 59, 609 - 610; 1999. (Abstract with evaluation).
- N.M. Zelaschi, S. Gaitán, S.O. Panizzo, A.B. Sobrero, A.E. López, J.L. Rodríguez y F.M. Archuby, 1998. "Efectos clínicos del cambio de Antipsicóticos Típicos a Antipsicóticos Atípicos Antagonistas D2-5HTA2. Risperidona y Clozapina en Pacientes con Trastornos Esquizofrénicos Hospitalizados". *Medicina* 1998, 58 (5/2): 634. (Abstract with evaluation).
- N.M. Zelaschi, S. Gaitán, S.O. Panizzo, A.B. Sobrero, A.E. López, J.L. Rodríguez y F.M. Archuby, 1998. "Niveles Séricos de Prolactina luego del Tratamiento Prolongado con el Antagonista D2-5HTA2,

Risperidona en Pacientes Esquizofrénicos Hospitalizados". *Medicina*. 1998, 58 (5/2): 643 (Abstract with evaluation)

- N. M. Zelaschi, J. L., Rodriguez, D. Panizzo, F. M. Archuby, M. Chiodi., 1997. "Niveles séricos de Prolactina durante la reducción progresiva de dosis de antipsicóticos típicos" *Medicina*, 57, Supp: 4, 22, 1997. (Abstract with evaluation).
- N. M. Zelaschi, J. L, Rodriguez, F. M. Archuby, 1997. "Movimientos involuntarios anormales durante la reducción progresiva de la dosis de antipsicóticos típicos". *Medicina*, 57, Supp, 4, 22, 1997. (Abstract with evaluation)
- N.M. Zelaschi, F.M. Archuby, J.L. Rodríguez, M. Semasendi y S. Pujol., 1997. "A comparison study of neurological side effects during first time exposure and long –term treatment". *Journal of the Neurological Sciences* (Abstract with evaluation). 1997 Supl.Vol 150: 5-42-09 S 334.
- N.M. Zelaschi, F.M. Archuby, J.L. Rodríguez, S.O. Panizzo y M.C. Chiodi., 1997. "Neurological side effects related to the reduction of typical antipsychotics drugs in long-term treatment" .*Journal of the Neurological Sciences* (Abstract with evaluation). 1997. Supl. Vol 150: 4-42-08 S 263
- Zelaschi NM, Rodriguez JL, Archuby FM, Pujol S, Semasendi M., 1996. "Síntomas y efectos colaterales neurológicos durante la primera hospitalización por trastornos esquizofrénicos.". *Medicina*, (Abstract with evaluation). 1996 56(5):586
- Semasendi M, Rodriguez JL, Zelaschi NM, Archuby FM, Pujol S. 1996. "Negative symtoms and tardive diskinesia" .*X World Congress of Psychiatry*. Abstracts. 1996, Vol 2:305. (Abstract with evaluation)
- Pujol S., Archuby FM, Rodriguez JL, Zelaschi NM., Semasendi M., 1996. "Clinical features in the First Hospitalization of the schizophrenia".*X World Congress of Psychiatry. Abstracts*. 1996, Vol 2: 289. (Abstract with evaluation)
- Zelaschi NM, Rodriguez JL, Delucchi GA, Pujol S., Archuby FM, Semasendi M., 1996. "Plasma PRL levels during chronic NLP treatment.". *X World Congress of Psychiatry*. Abstracts.1996, Vol 2: 118. (Abstract with evaluation)
- N.M. Zelaschi, J.L. Rodríguez, G. Delucchi, F.M. Archuby, 1995. "Hiperprolactinemia dosis-dependiente durante el tratamiento prolongado con neurolépticos típicos" (Abstract con referato). *Medicina* (Abstract with evaluation). 1995, 55 (5/2):581

Natural Heritage Protection

Books

- Archuby F. M. y F.W.P. Oliva (Editors) In Press. Proceedings of the "Cuartas Jornadas Paleontológicas Regionales". Puntal Alta, octubre de 2005. Boletín del Centro, 6; 136 pp. ISSN-1850-292X

Abstracts

- Archuby, F.M., Di Carlo U. y Acosta Hospitaleche, C., 2007. La Ley 25.743/2003 y la protección del patrimonio paleontológico bonaerense: virtudes, problemas y posibles soluciones. Libro de Resúmenes, Quintas Jornadas Paleontológicas Regionales, Santa Clara, 2007

Other fields

Abstracts

- Archuby, Fernando M.; Reynaldi, Francisco J.; Teodoroff, Tamara A.; Vizcaíno, S.; Reguero, M., 1998. "Análisis de la diversidad de taxones de seláceos (Pisces: Chondrichthyes) del Eoceno de la Isla Seymour, Antártida". *Acta Geológica Lilloana, 18(1):192.* XI Jornadas de Paleontología de Vertebrados. Universidad Nacional de Tucumán. 1995.

- Archuby, Fernando M. y Sergio F. Vizcaíno, 1996. “Análisis comparativo de la diversidad de Seláceos (Pisces, Chondrichthyes) de dos localidades del Eoceno medio de la Isla Seymour, Antártida. En *Resúmenes del Simposio de Geología y Paleontología del Paleógeno de Antártida, Congreso Paleógeno de América del Sur*. Santa Rosa, La Pampa. Actas, p.27.

Unpublished work

- Archuby, F. y Sergio Vizcaíno. “Análisis comparativo de la diversidad de Tiburones (Chondrichthyes, Elasmobranchii) de dos localidades del Eoceno medio de la Isla Seymour, Antártida”.

Scientific divulgation

- Marisa Espósito and Fernando M. Archuby, 1997. “Un trabajo interdisciplinario (sobre la reserva de Cuña pirú, Misiones)”. Revista Museo. Fundación Museo de La Plata “Francisco Pascasio Moreno”, .1997. 2 (9): 81-85.

Scientific meetings attended

- *XVI Argentine Geological Congress*, La Plata, Septiember 2005.
- *74th Annual meeting of the German Palaeontologic Society* (*74. Jahrestagung der Paläontologischen Gesellschaft* in Göttingen). October 2004.
- 19th Sedimentological Conference 2004 at the Rheinish Westphalian University of Technology in Aachen. Aachen, Germany.
- *Argentine Palaeontological Society Annual Meeting*. 2000.
- *VII Argentine Congreso of Palaeontology and Stratigraphy*, Bahía Blanca, October 1998.
- First *Regional Meeting on Natural Resources and Environment for university students*. FCN y M, UNLP, La Plata, Argentine, October 1996.
- Symposium on Geology and Palaentology of the Paleogene of Antarctica, Congress of Paleogene of South America. Santa Rosa, La Pampa, Argentine. May 1996.
- XII Argentine Meeting of Vertebrate Palaeontology. Santa Rosa, La Pampa. May 1996.
- Symposium on Antarctica, XI Vertebrate Palaeontology Meeting. Argentine Palaeontological Association. Tucumán National University, Argentine. May 1995.
- V Litoral Natural Sciences Meeting. Posadas, Misiones, Argentine. June 1994.

Research projects (participation)

- 2006-2007 “**Evaluation of the influence of tectonic and climatic processes on the Jurasic-Cretaceous sedimentation in the Neuquén Basin**”. Director: L. Spalletti.
- 2005-2006 “**Geologic controls on the development of the mesozoic sedimentary sequences in the Neuquén Basin**”. Director: L. Spalletti. UNLP.
- 2003 and continues “**Taphonomy and palaeoecology of benthic macroinvertebrates from the Upper Member of Agrio Formation (Lower Cretaceous), Neuquén Basin (Argentina): Sequence stratigraphic significance**”. Ph.D. project.
- 2000-2004 “**Sedimentology, Palaeoecology and Taphonomy of Valanginian Shellbeds of the Neuquén Basin (Argentina): Palaeoenvironmental and Sequence Stratigraphic Implications**”. With Lic. Ernesto Schwarz (UNLP - CONICET) and Dr. Tristán Simanauskas (UNLP-CONICET).
- 1997–2002 “**Fossil mammals biomechanics and palaeobiology of Buenos Aires Province**”. With Dr. Sergio F. Vizcaíno (MLP - CONICET).
- 1995 and continues. **“Clinical Effects with Long Term Treatment with Neuroleptic Drugs in psychotic patients”**. I currently belong to the Psychiatrist Norberto M. Zelaschi scientific group, where I participate in experiments design and statistical data analysis.
- 1994–1995 **“Diversity analysis of the selachii (Pisces: Chondrichthyes) from the Eocene of Seymour Island, Antarctica”.** With Dr. Sergio F. Vizcaíno (MLP - CONICET).
- 1994 – 1995 **“Biological study of the temporary ponds faunal composition”.** Faunal Reservation “Selva Marginal de Punta Lara”. Punta Lara, Buenos Aires Province. With Lic. Gustavo Bulus, Cátedra of Statistics, FCNyM, UNLP.
- 1994–1995 “**Biological population study of *Cynolebias* sp. in temporary ponds”**. Faunal Reservation “Selva Marginal de Punta Lara”. Punta Lara, Buenos Aires Province. With Lic. Gustavo Bulus, Cátedra of Statistics, FCNyM, UNLP.

VIII. POLITIC- ACADEMIC ACTIVITY

- Member of the Student Union of the National College “Rafael Hernández”, UNLP
- Student member in the FCNyM Government (1995, 1996, 1997)
- Vice-President and President in the Student Union of FCNyM, UNLP (1996 and 1997)
- Member of the University Assembly to elect University President (1995)
- Participation in other academic activities at the UNLP

IX. MEMBERSHIPS

- Argentine Paleontological Association. Since 1996

- Member of the Professional Council of Natural Sciences. Provincia de Buenos Aires. Since 2008.

Fernando Miguel Archuby